

66-992

CLEARINGHOUSE FOR FEDERAL SCIENTIFIC AND TECHNICAL INFORMATION	
Hardcopy	Microfiche
\$10.	\$2.25
5058	

ARCHIVE COPY

DESIGN HANDBOOK

FOR

SUBMERGED ENGINE COOLING SYSTEMS

AND

DUCT SYSTEMS

DDC

DEPARTMENT OF DEFENSE
SEP 12 1966
REF ID: A658116
B

PREPARED FOR THE DEPARTMENT OF THE NAVY,
BUREAU OF AERONAUTICS, WASHINGTON, D.C., BY
VERTOL AIRCRAFT CORPORATION, MORTON, PENNA.
UNDER CONTRACT NOas 56-880-f

JANUARY, 1958

DISTRIBUTION OF THIS DOCUMENT
IS UNLIMITED

<u>Section:</u>	<u>Number of Pages</u>
Title Page	1
Table of Content	1
I	11
II	20
III	85
IV (page 1V-144 is omitted)	183
V	8
VI	70
A - I	68
A - II	14
A-- III	13
A - IV	5
A - V	3
A - VI	9
Index	11

TABLE OF CONTENTS

CHAPTER	PAGE
I. INTRODUCTION TO THE HANDBOOK	I-1
II. COOLING REQUIREMENTS	II-1
III. INTERNAL AIRFLOW SYSTEMS - INLETS, DUCTS, EXITS	III-1
IV. AIR PUMPS - AXIAL FLOW FANS AND EJECTORS	IV-1
V. OIL COOLERS	V-1
VI. TESTING METHODS	VI-1

APPENDIX

I. ILLUSTRATIVE PROBLEM - DESIGN AND TEST	A-I-1
II. BIBLIOGRAPHY	A-II-1
III. GENERAL TECHNICAL DATA	A-III-1
IV. STANDARD SYMBOLS	A-IV-1
V. DESCRIPTION AND DEFINITION OF TERMS	A-V-1
VI. SAMPLE FLIGHT TEST PROGRAM	A-VI-1

INDEX

CHAPTER I
INTRODUCTION TO THE HANDBOOK

TABLE OF CONTENTS

	Page
1-1 Introductory Discussion	1-3
1-2 Scope	1-3,5
1-3.0 Helicopter and Airship Cooling Systems	1-5
1-3.1 Discussion	1-5
1-3.2 Air Flow Pressure Energy Diagrams	1-5,7,8
1-3.3.0 Outline of Design Procedure for Helicopter or Airship Cooling Systems	1-8
1-3.3.1 Cooling Requirements	1-8,9
1-3.3.2 Selection of Critical Cooling Condition. .	1-9
1-3.3.3 Air Pump Design Conditions	1-9
1-3.3.4 Fan or Ejector Design	1-9
1-3.4 Fan and Ejector Tests	1-9
1-3.5 Installation Tests	1-9
1-3.6 Applicable Specifications	1-9,10
1-4.0 Helicopter and Airship Ducting Systems	1-10
1-4.1 Discussion	1-10
1-4.2.0 Outline of Design Procedure for Helicopter or Airship Ducting Systems	1-10
1-4.2.1 Layout	1-10
1-4.2.2 Component Testing	1-10,11
1-5 List of Symbols	1-11

CHAPTER I

LIST OF FIGURES

<u>Figure No.</u>	<u>Description</u>	<u>Page</u>
1-1	Schematic Diagram of Submerged Power Plant Cooling Installation	1-4
1-2	Schematic Velocity Pressure Profile in a System	1-6
1-3	Schematic Static and Velocity Pressure Profile in a System	1-6
1-4	Schematic Static, Velocity and Total Pressure Profile in a System	1-6

CHAPTER I
INTRODUCTION TO THE HANDBOOK

1-1 INTRODUCTORY DISCUSSION

The submerged powerplant installations required in helicopter and airship designs result in a unique internal airflow situation. Various internal airflows must be provided for these submerged power plants, and the most distinguishing feature is that the system must operate satisfactorily from a condition of maximum forward speed to the completely un-rammed hovering flight regime.

Paramount among the required internal airflows for reciprocating engines is the cooling air with its attendant power losses. With the advent of shaft turbine engines, the induction airflow problems include a compressor face pressure distribution criterion of no minor proportions.

The Industry need for a gathering of the material required for the design and test of helicopter and airship internal flow systems into one convenient source was recognized by the Bureau of Aeronautics. Therefore, this handbook has been prepared to provide aerodynamic and thermodynamic data required in the design of helicopter or airship cooling and induction airflow systems. In addition, considerable data have been provided to assist in the physical design of the various internal flow components. A rather extensive bibliography has been presented; the most apparently useful works are catalogued with each appropriate chapter, while an additional extensive bibliography is presented as an entity in Appendix II.

It should be pointed out that this handbook has not particularly attempted to develop the aerodynamic and thermodynamic theories of heat and fluid flow; obviously essential principles must be discussed, but the basic aim of providing a useful design handbook has been the prime consideration.

The organization of this handbook has been by subject chapters. It is hoped that the table of contents and the index will provide easy usage.

In order to clarify the steps required in the design of the internal flow systems for helicopters and airships, an extensive illustrative problem has been prepared in Appendix I. This illustrative problem presents a cooling system design from the heat rejection, through cooling airflow requirements, to fan design and test.

1-2 SCOPE

The intent of this handbook is to provide a basis for the design of internal flow components such as ducts, fans and ejectors so that an optimum cooling or duct system may be selected for helicopters or airships. Certain limits to the extent of the data were therefore defined; where applicable the following general limits apply:

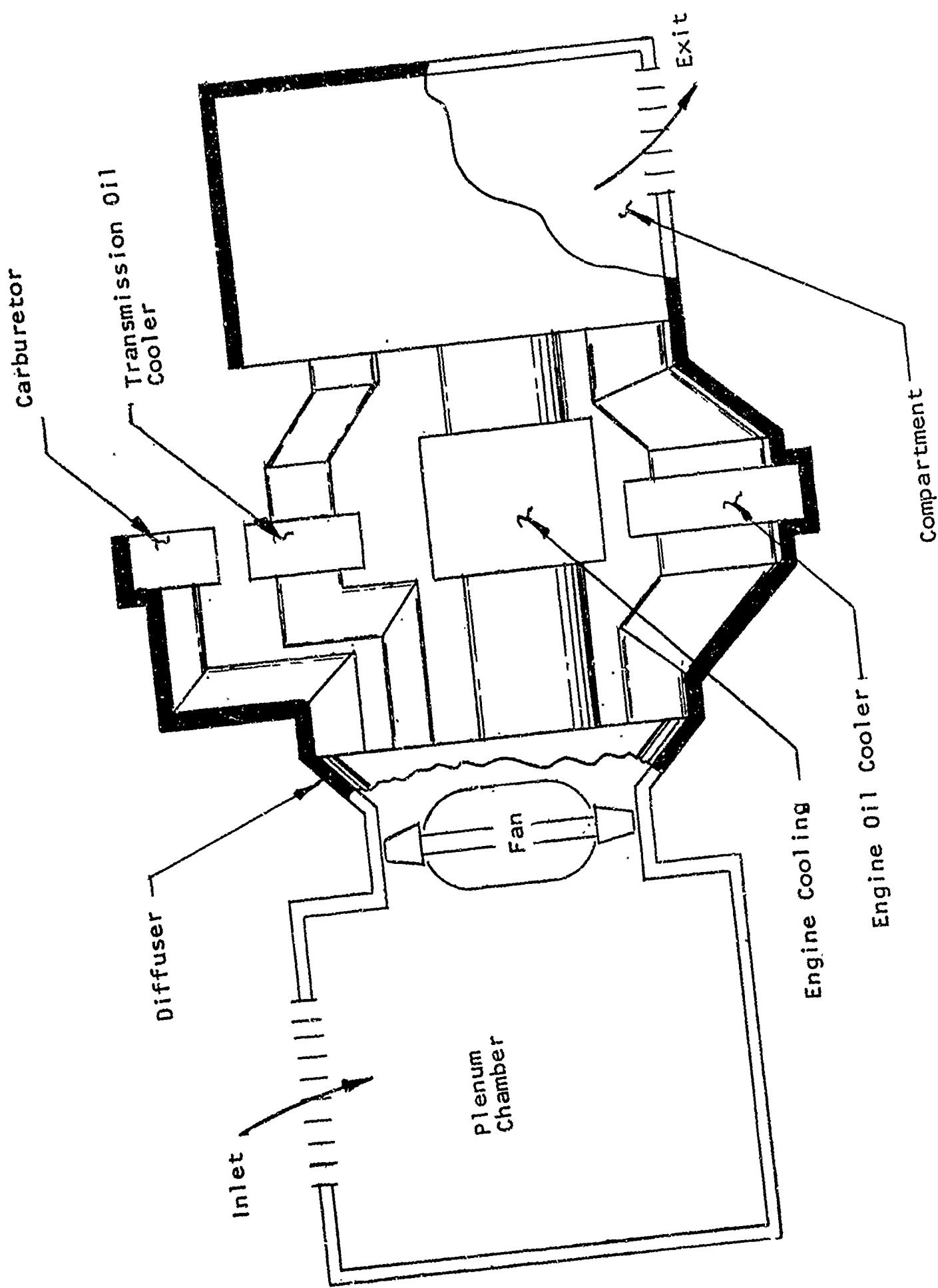


FIGURE 1-1. Diagram of Submerged Cooling Installation.

Mach Number	0 to .5
Pressure Altitude	0 to 35,000 ft.
Internal Air Flow Quantities	0 to 50,000 cfm
Air Pump Pressure Rise	Maximum of 20" H ₂ O

1-3.0 HELICOPTER AND AIRSHIP COOLING SYSTEMS

1-3.1 Discussion

To satisfy the requirement of cooling at zero forward speed, the helicopter or airship cooling system requires an air pump. This may be an ejector but is most often a fan. The cooling system is typically an air inlet, ducting to the fan, ducting to the air using components (such as the engine cylinder cooling fins and baffling, oil coolers, and accessories), a collection chamber, and ducting to the air exit. Figure 1-1 schematically presents such a cooling system for a reciprocating power plant.

Turbine cooling installations are similar except for the almost negligible external cooling required for the engine. A turbine installation is, therefore, essentially an oil cooling problem. Unlike reciprocating engine installations where oil cooler pressure drop is dictated by the engine baffle pressure drop, oil cooling air pressure drop may be optimized in a turbine installation. This is discussed in Chapters II and V.

As shown in Figure 1-1, the cooling airflow is supplied by one fan. Often, components may be cooled individually by a separate system. This is an advantage when:

- (a) Large distances between cooler locations exist (requiring either extensive air ducting or lengthy oil lines).
- (b) Large differences in cooling air pressure drop occur for different coolers (relatively high pressure drops for engine cylinder fins and baffling may not be desired for oil coolers).

Whether separate cooling systems or a common system are utilized, the design data in this handbook are applicable for the components.

As with any aircraft cooling system, the intent is to provide cooling with the least power absorption and at a minimum weight. Particularly for helicopters, a minimum of cooling power requirements takes precedence over minimum weight considerations. That this can be the correct approach may be seen by remembering that current helicopter power loadings range from 10 to 15 pounds per horsepower. Each horsepower saved by efficient cooling will be worth 10 to 15 pounds of gross weight lifting capacity.

1-3.2 Airflow Pressure Energy Diagrams

The airflow energy levels and the power required for a typical helicopter cooling system may be best evaluated by construction of a pressure energy level diagram for the system. Figures 1-2, 1-3, and 1-4 present such diagrams for a typical cooling system. The construction of the

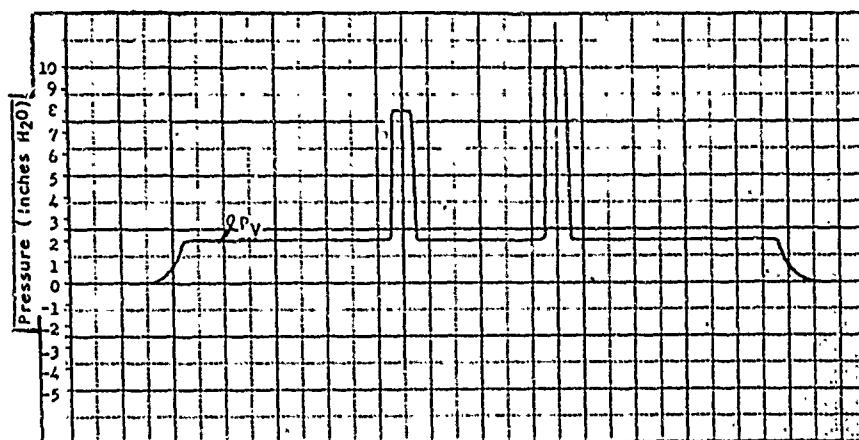
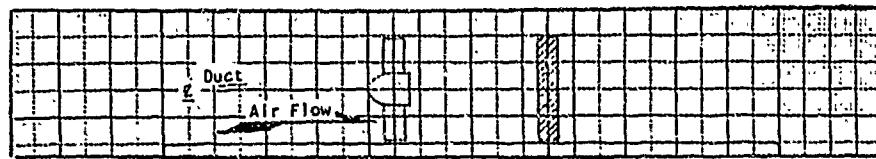


FIGURE 1-2. Duct-Fan-Resistance Schematic Showing Pressure In Transition.
Velocity Pressure Profile.

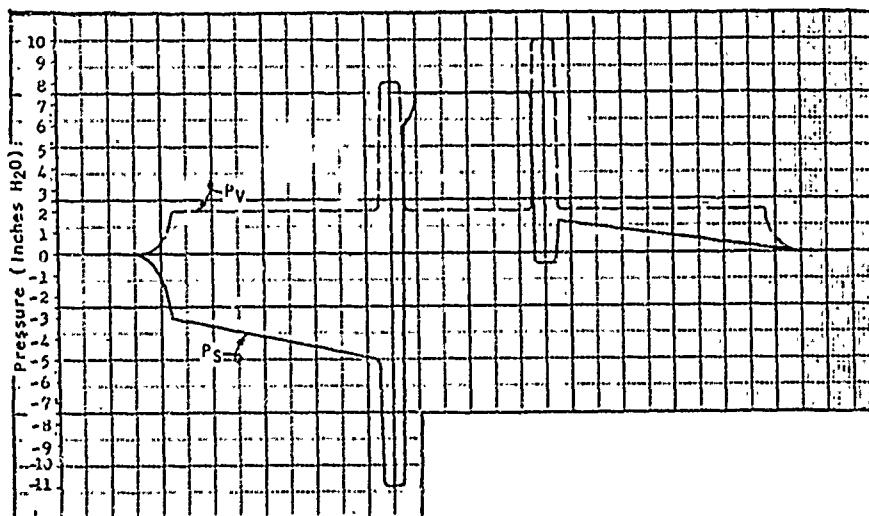


FIGURE 1-3. Velocity and Static Pressure Profiles.

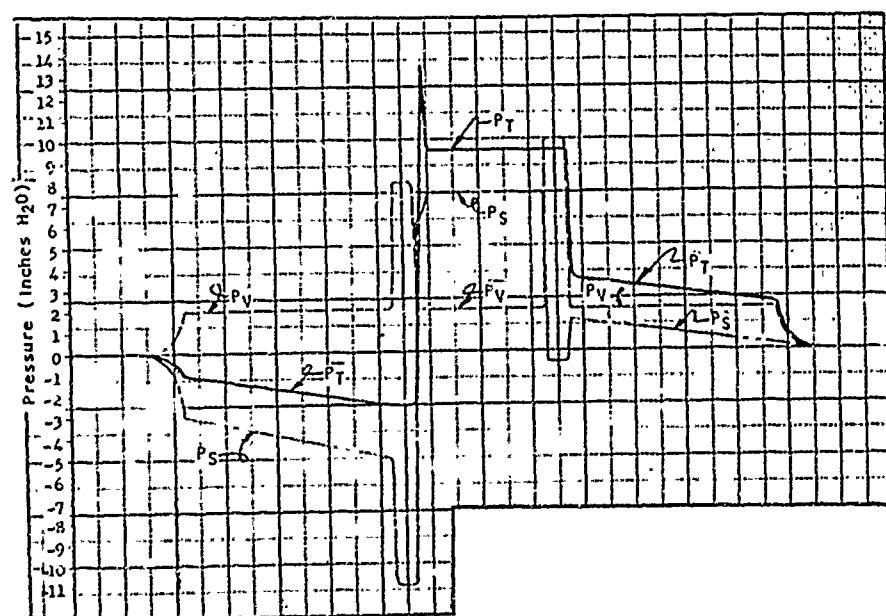


FIGURE 1-4. Velocity, Static and Total Pressure Profiles.

pressure energy diagrams is guided by the fluid flow principles of a subsonic internal flow system. Since flow may be considered incompressible, the flow continuity equation

$$Q = V_1 A_1 = V_2 A_2 = V_3 A_3 \dots \text{Equation 1-1}$$

applies. The significance of such flow continuity is that the velocity at any station of ducting (any streamtube station for the general case) is completely defined by the flowing volume and the cross-sectional area of the duct. This is the basis of the velocity pressure diagram of Figure 1-2, where

$$q = P_v = \frac{1}{2} \rho V^2.$$

Static pressures within the duct system, if there were no flow pressure energy losses, would exactly reflect the velocity pressure. That is, for a frictionless system, Bernoulli's equation is

$$q_1 + P_{s1} = q_2 + P_{s2} \text{Equation 1-2}$$

However, the friction and eddy losses which do exist add an additional term, ΔP_{loss} .

$$q_1 + P_{s1} = q_2 + P_{s2} + \Delta P_{1-2 \text{ loss}} \text{Equation 1-3}$$

If a device is inserted into the duct to provide a pressure energy increase (such as a fan)

$$q_1 + P_{s1} = q_2 + P_{s2} + \Delta P_{1-2 \text{ loss}} - \Delta P_{1-2 \text{ boost}} \text{Equation 1-4}$$

It should be noted that either the right or left side of Equation 1-4 is total pressure. Total pressure is the algebraic sum of velocity pressure plus static pressure and is the same at any duct station except for losses or additions in pressure energy between stations. Figures 1-3 and 1-4 are therefore dependent on Bernoulli's principle. Losses encountered are the subject of a complete chapter in this handbook.

Although considerable simplification of boundary layer and flow distribution principles has been made, this has been found adequate for helicopter or airship internal flow system visualization. The significant fact is that duct losses are total pressure losses. Whether the static pressure decreases or increases while such a loss occurs depends on the flow area.

Velocity pressure, static pressure and then total pressure may be constructed beginning at the inlet and exit and working toward the fan. The flow quant' must be known as well as the pressure drop of the cooling resis. and the pressure losses of the ducting. Entrance or exit pressi levels need not necessarily be zero (the hovering situation is presented on Figures 1-2, 1-3 and 1-4) but should be determined from the external flow characteristics of ram inlets or flapped exits.

It can be seen that the resistance of a typical helicopter cooling system can greatly exceed the flow resistance of the cooler itself. Levels of energy expenditure are evident from such diagrams and are found to be essentially:

- a. Inlet
- b. Ducting
- c. Fan Expansion
- d. Cooler Resistance
- e. Exit

Since the fan horsepower requirement is

$$HP = \frac{Q \Delta P_f}{\eta \cdot 550} \quad \text{Equation 1-5}$$

where

Q = airflow, ft.³/sec.

ΔP_f = fan pressure rise, lb./ft.²

η = fan efficiency,

a reduction in any of the flow path pressure losses will result in the design of a fan which would require less power.

Helicopter or airship ducting other than cooling may also be studied by pressure energy level diagrams. Regions of energy expenditure may thus be known, and if reviewed at various stages throughout the design (preliminary, layout, test, etc.), internal flow system power may be kept at a minimum.

1-3.3.0 OUTLINE OF DESIGN PROCEDURE FOR HELICOPTER OR AIRSHIP COOLING SYSTEM

The procedure required for the design of a helicopter cooling system, based on the design data detailed in the following chapters, will now be very briefly reviewed.

1-3.3.1 Cooling Requirements

The first step in cooling system design is the evaluation of the cooling requirements. This means the required quantity of airflow and the pressure drop of the system.

- (a) Engine Cylinders: The cooling air quantity and baffle pressure drop are directly specified by the engine manufacturer.
- (b) Engine Oil: The heat rejection to the engine oil, and the oil operating temperature limits are specified by the engine manufacturer. To obtain the airflow quantities, the oil heat rejection data must be referred to an oil cooler manufacturer.
- (c) Transmission Oil: The heat rejection from the gear meshes must be calculated. This heat rejection, the oil flow and oil temperature limits must then be referred to an oil cooler manufacturer to obtain airflow quantity and pressure.

(d) Accessories: Airflow quantity and/or pressure required may be obtained from military specifications for the equipment (for instance generators) or other sources (for instance the manufacturer's required blast for engine shock mounts).

1-3.3.2 Selection of Critical Cooling Condition

The above steps (a thru d) must be performed for various flight regimes. Airflow quantity and pressure should be ratioed to a common atmospheric condition and a common fan RPM to select the critical design condition. Careful compromising may be made at this point so as not to severely over design the cooling system for some improbable flight regime.

1-3.3.3 Air Pump Design Conditions

Once the critical cooling point is known, ducting, inlet and exit losses may be added to define ΔP_{fan} .

It is helpful here, as previously discussed, to construct a diagram of the pressure energy levels through the system.

1-3.3.4 Fan or Ejector Design

The fan or ejector may now be designed to provide the required ΔP and quantity airflow.

1-3.4 Fan or Ejector Test

A prototype fan or ejector should be constructed (not necessarily a flight article) and flow tested. If any redesign is required, this should be accomplished and the final design released. The final fan or ejector should be completely aerodynamically and structurally tested.

1-3.5 Installation Tests

Functional, cooling and endurance tests must be performed on the aircraft.

The steps outlined above (1-3.3.0 to 1-3.4) will result in the proper cooling system for the aircraft. Details of each step are presented in Chapters II through VI.

1-3.6 Applicable Specifications

The following specifications and drawing bear directly on the design of submerged cooling systems and duct systems in helicopters and airships:

Military Specifications

MIL-C-8678 (Aer.) "Cooling Requirements of Power Plant Installations"

MIL-G-6099 "Generators and Regulators; Aircraft, Alternating Current, General Specification for"

MIL-G-6162 "Generators, 30 Volt, Direct Current, Aircraft Engine Driven, General Specification for"

Air Force - Navy Aeronautical Bulletins

No. 421 "Atmospheric Properties - Extreme Cold And Hot: Standard For Aeronautical Design"

Drawing

Bureau of Aeronautics Drawing No. 49A1B15

1-4.0 HELICOPTER AND AIRSHIP DUCTING SYSTEMS

1-4.1 Discussion

Aerodynamic data for the design of ducting systems, either for cooling air, induction air, or even heating and ventilating systems, are contained in this handbook. Essentially, aerodynamically good ducting design is based on the three concepts of:

- (1) Minimum flow pressure losses.
- (2) Minimum contribution to external drag.
- (3) Minimum duct weight.

External drag concepts may be more important for the airship with its inherent long range and endurance requirements, while helicopter ducting is often compromised toward hovering where maximum power is required to support the aircraft.

Duct aerodynamic design data are presented primarily in Chapter III, but the significance of ducting is included throughout the handbook. Chapter VI on testing methods includes a section on duct test procedures and the illustrative problem in Appendix I includes samples of duct loss evaluations.

1-4.2.0 Outline of Design Procedure For Helicopter or Airship Ducting Systems

1-4.2.1 Layout

The usual procedure in aircraft ducting design is to follow the principles of adequate flow area, bend radii, diffusion ratios, and inlet contours as described in Chapter III. This work proceeds in unison with the layout of the aircraft so that the restrictions of space and shape may be incorporated.

1-4.2.2 Component Testing

Helicopter and airship ducting problems benefit greatly from model flow tests performed concurrently or prior to the layout stage.

Inlet compromises, which often must be made in favor of the hovering conditions, may be investigated for forward flight effects by model (or full scale) tests in conjunction with a wind tunnel. Probably the most important type of ducting for which such tests are recommended are turbine inlet ducts. Here, aside from the considerations of duct losses, a rather severe limitation to compressor face pressure distribution must usually be met.

Another type of helicopter or airship ducting which is recommended for pre-layout flow tests is the ducting often provided between the cooling fan and the carburetor. Such reciprocating engine induction ducting is used to boost the available carburetor deck pressure in an aircraft which has essentially no external ram. (Note that the cooling fan design would have to include the engine induction airflow volume.) The usual problem with the fan pressurized induction duct lies at the cowl duct entry where a very turbulent region (between the fan and the engine) exists. Cowl entry radii based on bellmouth data of Chapter III have been found to increase carburetor deck pressures by as much as thirty percent of the available fan total pressure rise.

Installations tests in the aircraft will provide the final evaluation of ducting systems. The details of duct test procedures are presented in Chapter VI.

1-5 LIST OF SYMBOLS

SYMBOLS

Q	Flow, CFM
V	Velocity, Ft/Sec
A	Area, Ft ²
	Area of Surface Exposed to Airflow, Ft ²
	Area in Plane Perpendicular to Heat Flow Path
q _p	Dynamic Pressure = $1/2 \rho V^2$
P	Power Input, HP
P	Pressure, Absolute
ρ	Density, Slugs/ft ³
Δ	Delta
HP	Horsepower
η	Efficiency
ΔP	Pressure Loss

SUBSCRIPTS

1	First Station in Direction of Flow
2	Second Station in Direction of Flow
3	Third Station in Direction of Flow
S ₁	Static (Pressure) at First Station
S ₂	Static (Pressure) at Second Station
1-2 _{loss}	Pressure Loss Between Stations 1 and 2
1-2 _{boost}	Pressure Rise Provided Between Stations 1 and 2
f	fan
fan	fan

CHAPTER 11
COOLING REQUIREMENTS
TABLE OF CONTENTS

<u>Section</u>	<u>Title</u>	<u>Page</u>
2-1	Introduction	11-3
2-2	Basic Heat Transfer Theory	11-3,4,5,6
2-3.0	Engine External Cooling	11-6
2-3.1	Reciprocating Engines	11-6,7
2-3.2	Turbine Engines	11-7
2-4.0	Oil Cooling	11-8,9,10
2-4.1	Engine Oil Cooling	11-10
2-4.2	Transmission Oil Cooling	11-10,12,13
2-5	Cooling of Accessories	11-13
2-6	Total Cooling Requirements	11-14,18
2-7	Determination of the Critical Air Pump Condition	11-18
2-8	List of References	11-19
2-9	List of Symbols	11-20

CHAPTER 11
LIST OF FIGURES

<u>Figure No.</u>	<u>Description</u>	<u>Page</u>
2-1	Reciprocating Engine Oil Heat Rejection Curves	11-11
2-2	Typical Turbine Engine Reduction Gear Loss vs. Output Power	11-11
2-3	Schematic Diagram of a Mixing Gear Box	11-12
2-4	Required Generator Cooling Air	11-15
2-5	Altitude Rating Curve for Blast Cooled Aircraft Generators	11-16
2-6	Air Film or Surface Conductance as a Function of Air Velocity for Smooth Surfaces	11-17

CHAPTER II

COOLING REQUIREMENTS

2-1 INTRODUCTION

The first step in the design of any cooling and ducting system is the establishment of the requirements to be fulfilled by that system.

The purpose of this Chapter is to set forth the heat transfer theory, discussion and analytical methods with which the cooling requirements of a helicopter or airship submerged cooling and ducting system may be determined.

The heat rejection requirements or temperature limits of the various aircraft components (such as engine cylinders, engine oil, transmissions, electrical equipment, engine dynamic mounts) must be assimilated and resolved into a total required airflow rate and required pressure drop for each component. The determination of the total cooling airflow required permits the selection of a suitable cooling configuration and the determination of the airflow path pressure losses. Finally, the total pressure rise and flow rate are obtained to form the requirements for the airflow pump design. The task is unavoidably lengthened by the necessity that these requirements be determined at various operating conditions of the aircraft so that the most critical cooling condition may be determined.

Chapter III, entitled Internal Airflow Systems, deals with the design of the ducting system through which the required air must flow.

Chapter IV, entitled Air Pumps, treats the design means to create the differential pressure required to cause the air to flow.

Chapter V, Oil Coolers, is concerned with the design of the oil cooler, one of the most important cooling resistances in the submerged or internal cooling system of a helicopter or airship.

Chapter VI treats the testing of axial flow fans and ejectors, ducting systems and submerged helicopter and airship power plants.

With the above basic procedure as a guide, the individual requirements of the various components may be approached. However, a few basic fundamentals of heat and heat transfer will first be reviewed.

2-2 BASIC HEAT TRANSFER THEORY

Thermal energy either may be stored in a mass or it may be passing from one mass to another due to a temperature difference between the two. The term heat is normally reserved to define the latter, i.e., heat is energy in transition due to a temperature difference. Likewise, the thermal energy stored in a mass is generally defined as internal energy.

Internal energy is further differentiated as internal kinetic energy or internal potential energy. A change in the internal potential energy is evidenced by a change of state, while a change in internal kinetic energy is due to a change in temperature. Therefore, the internal kinetic energy level of a mass is measured by the temperature of the mass.

The most commonly used measure of heat energy is the British Thermal Unit or BTU. The BTU is defined as 1/180 of the amount of heat required to raise the temperature of one pound of water from 32° to 212°F at a pressure of 29.92" Hg.

The same quantity of heat added to two different substances of equal mass will usually produce different changes in temperature. The heat, measured in BTU, required to raise the temperature of one pound of a substance through 1°F is the specific heat of that substance. Since the specific heat of water is unity, it, therefore, follows that specific heat is the ratio of the heat capacity of a substance compared to the heat capacity of water.

The specific heat of a compressible fluid such as air depends upon the flow process. The flow process in an aircraft cooling system is essentially a constant pressure process. Specific heat, as ordinarily used throughout this handbook, is, therefore, specific heat at constant pressure. The specific heat of air varies somewhat with the temperature of the air, but for most purposes relative to aircraft cooling system calculations, a constant value of .24 BTU/#/°F may be used.

Within the definition of specific heat lies a most useful tool for the cooling system designer. If heat is added to a substance, the internal kinetic energy of that substance will be increased by an amount depending upon its heat capacity and weight, as expressed by the following formula

$$H = W c_p \Delta t \quad \text{Equation 2-1}$$

where

H = heat in BTU

W = weight in pounds

c_p = heat capacity or specific heat - BTU/#/°F

Δt = temperature rise

If, during the process of adding heat, a change of state of the substance is evidenced, Equation 2-1 must be expanded to include the change in internal potential energy, i.e., the latent heat of vaporization or of fusion of the substance.

It will be noted that up to this point the discussion has been in terms of static bodies and absolute quantities of heat. In aircraft cooling systems, fluids in motion are encountered and heat is treated in terms of heat per unit time. However, the same basic concepts presented are applicable to flowing fluids. For example, Equation 2-1 may be used to define the heat per unit time absorbed by oil flowing through an engine or transmission, in which case the terms would represent:

H = heat absorbed BTU/min.
 W = oil flow rate pounds/min.
 c_p = specific heat of oil BTU/#/ $^{\circ}$ F
 Δt = temperature difference between oil
 into and out of the transmission -
 temperature rise $^{\circ}$ F

Heat has been defined as thermal energy in transition due to a temperature difference. The three methods by which heat may be transferred are radiation, conduction and convection. Normally heat is transferred by all three methods simultaneously; however, a temperature difference must exist before any net heat transfer will occur.

Thermal radiation is the transfer of heat from one body to another through space. Such radiant energy transfer is usually considered negligible in aircraft cooling analyses due to the relatively low surface temperatures encountered. A possible exception to this is the power plant. Of some significance, but rather difficult for quantitative evaluation, is heat radiated from the engine to the cowling in reciprocating engine installations. A more important consideration of radiated heat may be encountered in submerged turbine engine installations, not so much in the quantity of heat radiated from the engine surface, but in the amount of radiated heat which is absorbed by the surrounding structure. In this handbook, no attempt is made to present theory or methods of determining effects of radiant heat. However, various bibliography items are listed in Sections B-2, B-3 and B-4 of Appendix II.

Conduction is the transfer of heat from one part of a body to another part of the same body, or from one body to another in physical contact with it, without displacement of the particles of either body. The transfer occurs only if there is a temperature gradient within the body or between the two bodies. The rate of heat conduction is a function of the temperature difference, the conductivity of the material, the area over which the heat transfer occurs, and the distance the heat must travel. The heat transfer by conduction through a body may be determined by the expression

$$H = A \frac{X}{K} (t_1 - t_2) \quad \text{Equation 2-2}$$

where

H = heat transfer, BTU/hr
 A = area in plane perpendicular to heat flow path, ft^2
 X = thickness of body or length of flow path, inches
 K = conductivity of material, BTU/hr/ ft^2 / $^{\circ}$ F/inch
 $t_1 - t_2$ = temperature difference causing the heat transfer, $^{\circ}$ F

Thermal convection is literally the carrying of heat to or from a body due to mass movement of a fluid contacting the body. This form of heat transfer may occur either as natural convection, wherein the fluid

motion is due to a change in its density caused by a temperature change, or as forced convection, wherein the fluid motion is attained by some mechanical means.

Whenever a fluid is moved across a body there exists a thin film of stagnant fluid adjacent to the surface. Heat transfer by convection cannot occur without a motion of the fluid; therefore, the heat must be transferred through the stagnant film by conduction.

Since gases are poor heat conductors, this stagnant film produces an undesirable insulating effect on the surface in the case of air cooling. The film thickness may be reduced, with a corresponding increase of heat transfer, by increasing the speed of the air past the surface or by producing a turbulent boundary layer at the surface. The heat transfer per unit area between moving air and a surface is a function of the film heat transfer coefficient and the temperature difference between the surface and the air. The film heat transfer coefficient is in turn dependent upon the type of flow, laminar or turbulent, the flow velocity, and the mean temperature between the surface and the air. When the film transfer coefficient is known, the heat transfer is determined by

$$H = h A \Delta t \quad \text{Equation 2-3}$$

where

H = heat transfer, BTU/hr

h = film heat transfer coefficient, BTU/hr/ft²/°F

A = area of surface exposed to airflow, ft²

Δt = temperature difference between surface and air, °F

2-3.0 ENGINE EXTERNAL COOLING

The heat transfer process occurring between the combustion gases of an engine and the cooling air may now be examined. Regardless of the type of engine, whether reciprocating or turbine, some of the thermal energy released by combustion of the fuel will be transferred to the engine external surfaces. This heat must then be carried away by the engine coolant, either liquid or air. The rate of the heat transfer depends, among other things, upon the allowable temperature of the engine exterior. If, for example, the allowable temperature of the engine exterior were equal to the mean combustion gas temperature, there would be no transfer of heat to the exterior and, therefore, no need for engine external cooling. However, such factors as breakdown of the lubricating oil, strength of the engine components, and engine detonation problems limit the temperature of external surfaces surrounding the combustion chamber to 450 - 500°F for reciprocating engines and 800 - 1200°F for turbine engines.

2-3.1 Reciprocating Engines

Due to the allowable cylinder head temperature of a reciprocating engine, which is relatively low compared to the mean combustion gas temperature,

a very substantial quantity of heat is delivered to the cylinder fins. The magnitude of the thermal energy, as a matter of interest, varies from 30% to 40% of the energy delivered to the shaft in an aircraft reciprocating engine. Before being convected away by the cooling air, the heat must be conducted through the stagnant film adjacent to the cylinder cooling fins. Turbulent flow is obtained by proper cooling fin and baffle arrangements during the engine design, thus increasing the heat transfer rate. Therefore, the heat transfer process need not be considered during the design of the cooling system for an engine already equipped with proper finning and baffling.

Detailed information defining cooling characteristics for the entire range of anticipated engine operating conditions is available from the engine manufacturer. This information includes (a) baffle pressure drop, (b) cooling airflow rate, and (c) cooling air temperature rise across the engine. Also, maximum allowable temperatures for critical engine components are specified by the engine manufacturer.

Typical curves of engine manufacturer's cooling data are included in the illustrative problem of Appendix I. The required pressure drop and airflow for any flight condition for a particular engine may be determined from the manufacturer's data. This procedure is illustrated in the aforementioned Illustrative Problem.

2-3.2 Turbine Engines

As previously noted, the external surface surrounding the combustion section of aircraft gas turbine engines is at a temperature between 800° and 1200°F . The lower value may be somewhat misleading in that it occurs in a special type of turbine wherein the induction air passes through an annular section between the combustion chamber and the external surface before entering the burners. This method of pre-heating the induction air tends to lower the engine external surface temperature and effectively provide internal cooling for the engine.

The more common aircraft gas turbine, in which the induction air makes one direct pass through the engine, normally operates with an external surface temperature of between 1000° and 1200°F . This high surface temperature results in a low cooling air requirement, compared to an equivalent reciprocating engine, for two reasons. First, by virtue of the increased surface temperature, the temperature difference between the combustion gases and the external surface is decreased, thus reducing the heat transferred to the surface. Secondly, the increased surface temperature increases the temperature difference between the surface and the cooling air, thus decreasing the required film heat transfer coefficient. The combined effect reduces the required engine surface cooling to such an extent that the engine compartment usually need only be ventilated. Certain components on the engine, such as fuel pumps and the fuel control system, will most likely require cooling in order to maintain their temperatures at acceptable levels. This may be accomplished by blasting cooling air upon these components. Required blast cooling air data should be furnished by the engine manufacturer. If such data are not available for a particular component, a heat transfer analysis may be made to determine the approximate blast cooling air requirements.

2-4.0 OIL COOLING

The determination of requirements for oil cooling in terms of pressure drop and airflow is more involved than that for engine surface cooling. The oil heat rejection required must first be determined, then the allowable oil cooler air pressure drop established, a suitable oil cooler selected, and finally, the required cooling airflow rate determined. Essentially, the procedure must be undertaken for any flight condition which might be a suspected critical cooling condition.

It is normally expected, however, that the critical cooling condition for an oil cooler will occur at sea level. This is basically due to the relatively low temperature difference existing between the oil and cooling air. The temperature change with increasing altitude increases the temperature difference between the air and oil, thus tending to increase the heat rejection rate. Conversely, the density change tends to decrease the heat rejection rate for two reasons: (1) at a constant cooler air pressure drop, the decreased density decreases the cooling air mass flow rate, thus decreasing the heat rejection, and (2) the decreased density decreases the pressure rise of the air pump, causing a corresponding decrease in the available cooler pressure drop, thus further decreasing the air mass flow rate. Examination of the characteristics of a typical aircraft plate type oil cooler at a constant heat rejection rate reveals that the decreasing cooling air temperature associated with increasing altitude usually more than compensates for the effects of decreasing air density. A possible exception to this may occur with required operation at an altitude condition other than as defined by the ANA hot day, such as the familiar 95°F at 6000 feet altitude.

The transfer of heat from the oil to the air within the cooler is due to the relative temperature of the incoming air and oil. This inlet temperature difference, commonly referred to as ITD, is probably the most important single factor in oil cooler system design. For a given heat rejection, the higher the available ITD, the lower will be the cooling power and/or cooler weight.

In consideration of oil cooler design parameters, as in other cooling system design calculations, allowance should be made for the expected cooling air temperature rise upstream of the cooler. The cooling air may absorb heat by conduction through the duct walls and from compression through the air pump. The cumulative effect of these may increase the cooling air temperature to a value 5° to 15°F above ambient temperature.

The maximum allowable oil temperature in engines and transmissions varies from 175°F to 250°F. The maximum allowable oil temperatures for engines are specified by the engine manufacturer in engine model specifications. In the case of transmissions, the temperature may be limited by such factors as gear tooth loading, bearing life, oil seal life, and perhaps even the oil itself. The temperature of the oil entering the oil cooler, neglecting the heat loss in the oil lines, is equal to the temperature leaving the engine or transmission and also equal to the maximum oil temperature in the engine or transmission.

Thus the ITD for the critical oil cooler condition is equal to the maximum allowable oil temperature minus the cooling air temperature.

To restrict cooling power required and the cooler weight to minimum values (1) the highest possible oil temperature should be utilized and (2) the system should be designed to restrain the cooling air temperature rise upstream of the cooler to a minimum.

The oil cooler design air pressure drop value depends upon the type of cooling system installation. In the case of a single air pump supplying air to cool several items, that item requiring the highest pressure drop dictates the pressure drop to be available for each of the items in the system. This is illustrated in the case of a reciprocating engine installation. The engine baffle pressure drop at the critical cooling condition is specified by the engine manufacturer. Since the engine cooling air is the major portion of the total air pump flow, it should dictate the air pump pressure rise. The pump pressure rise being known and the preliminary layouts of the ducting having been made, the available oil cooler pressure drop may be determined.

In a system cooling several items, none of which requires a given pressure drop, or in a system cooling only a single item which does not require a given pressure drop, the optimum cooler pressure drop for the installation may be chosen. This is accomplished by compromising between the air pump power required and the cooling system weight. A high pressure drop will result in high air pump power requirements and low oil cooler weight, while low pressure drop coolers will be heavier but require less pumping power. In a study of this type, it is recommended that the known data (items 1 through 5, Section 5-1 of Chapter V, Oil Coolers) be presented to an oil cooler manufacturer and that he be requested to furnish cooler parameters (weight, size, airflow required) for three or four cooler air pressure drops. With this information, one pressure drop may be selected which best fits the particular installation, i.e., that which permits the lowest combination of pump power and system weight. However, at this point the available cooler space, rather than the minimum power and weight, may dictate the design cooler pressure drop.

In the design stage, the allowable cooler pressure drop has little effect upon the required cooling airflow rate. The airflow rate is more nearly a function of ITD for a given heat rejection rate. High ITD's usually reflect low required airflow rates. In the preliminary design stage, the required cooling airflow rate may be approximated by assuming an air temperaturerise across the cooler of 30 to 40°F (depending upon the ITD) and the expression $H = W_{cp} \Delta t$ solved for W , the air weight flow rate. This method should be used only for that condition representing the design condition of the cooler involved.

All cooler units mounted together in an installation will operate at the same cooler air pressure drop. This does not necessarily mean that they should each be designed for the same pressure drop, since the critical condition for each cooler may occur at different aircraft flight conditions. Rather, each cooler should be designed at the critical cooling condition for its respective unit, the design pressure drop being that pressure available at the specific flight condition. If the critical condition of each of the coolers is expected to occur at the same flight condition (which would normally be expected if the operating ITD for each cooler were approximately the same) the design pressure drop for each cooler should be the same.

A further discussion of oil cooler parameters and oil cooler design is presented in Chapter V.

2-4.1 Engine Oil Cooling

The lubricating oil of an aircraft reciprocating engine absorbs some heat from the combustion chambers by way of pistons and cylinder walls. The major portion of the heat rejected to the oil, however, is that which is released through mechanical friction, and thus is essentially a function of engine RPM. Varying the power output of a particular engine at a constant RPM has very little effect on the heat rejection to the oil, as shown by Figure 2-1.

The heat rejection of an oil cooler installation is affected by ITD, oil flow rate, and airflow rate. The effects of ITD have been discussed previously. An increase of oil flow, ITD being constant, will increase the heat rejection rate of the cooler. Likewise, an increase of airflow will slightly increase the heat rejection.

When the engine RPM is increased, the required heat rejection increases, the engine oil flow increases, and the cooling airflow rate increases for a mechanically driven air pump. The combined effect of increasing oil flow and cooling airflow rate may increase the actual cooler heat rejection to a greater extent than the required rejection is increased. For this reason, the critical engine oil cooling condition will not necessarily occur at maximum engine RPM. Since the critical condition is not readily determinable without knowledge of the particular cooler characteristics, this condition must be estimated. The other conditions may then be checked after the calculated cooler performance curves are obtained.

Turbine engine bearing oil cooling and the selection of coolers for turbine engines are essentially the same as for reciprocating engines. However, the required oil heat rejection is normally much less than that for a reciprocating engine of the same power.

Required oil heat rejection rates, oil temperatures, and oil flow rates for both turbine and reciprocating engines are obtained from the engine manufacturer. These data are usually presented in curve form so that the values may be determined at any desired engine power and RPM.

2-4.2 Transmission Oil Cooling

Required heat rejection characteristics of transmissions or engine reduction gear boxes are almost identical to those for engine oil cooling since the heat involved in both cases is primarily due to mechanical friction.

If the engine reduction gear box is provided by the engine manufacturer, the applicable cooling requirements may be obtained from that manufacturer. This is generally included with engine oil cooling in the case of reciprocating engines. In the case of turbine engines, the engine manufacturer ordinarily provides the engine bearing oil cooling system. If not, the requirements are generally included with engine reduction gear oil cooling as in the case of reciprocating engines.

The heat rejection requirements and characteristics for transmission and gear boxes designed by the airframe manufacturer must be determined by the cooling system designer.

Corrected to:
 185°F Oil Inlet Temp.
 75 PSI Oil Pressure
 These curves are estimated averages

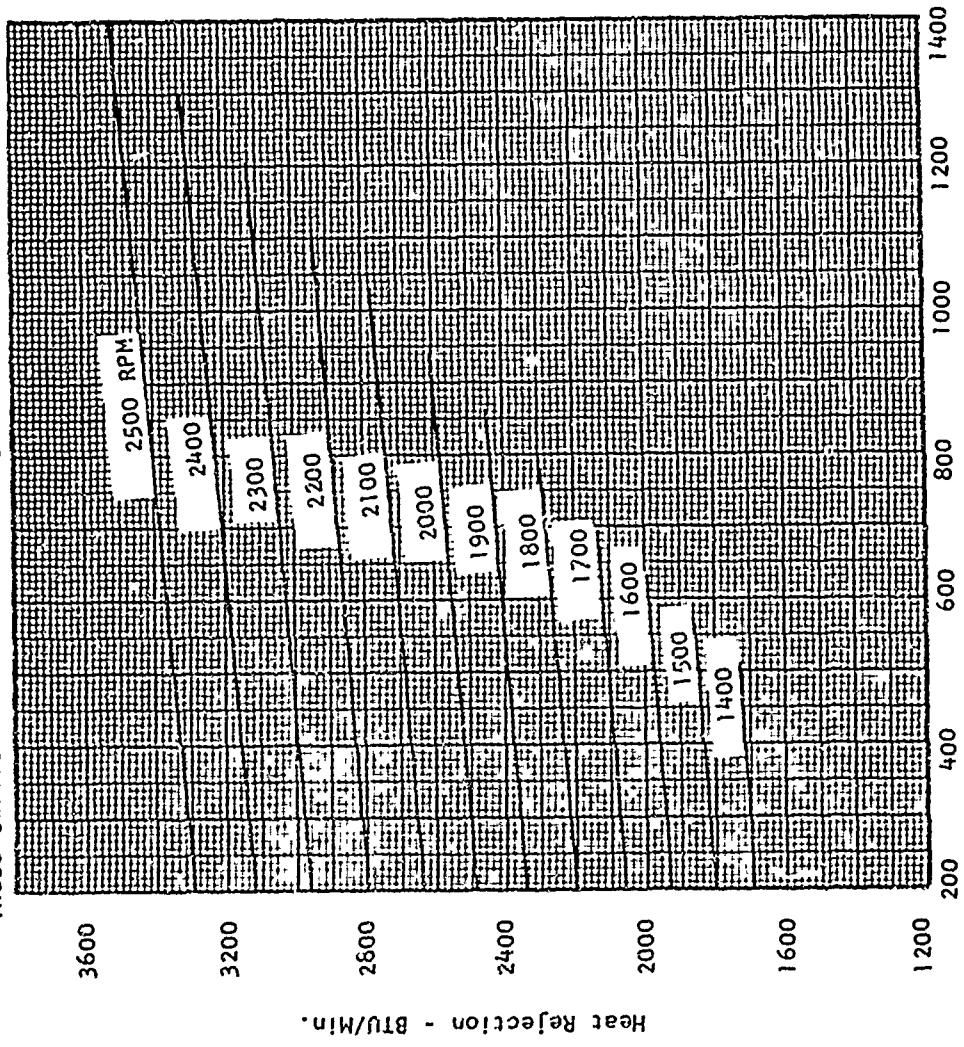


FIGURE 2-1. Typical Reciprocating Engine Oil Heat Rejection vs. Brake Horsepower.

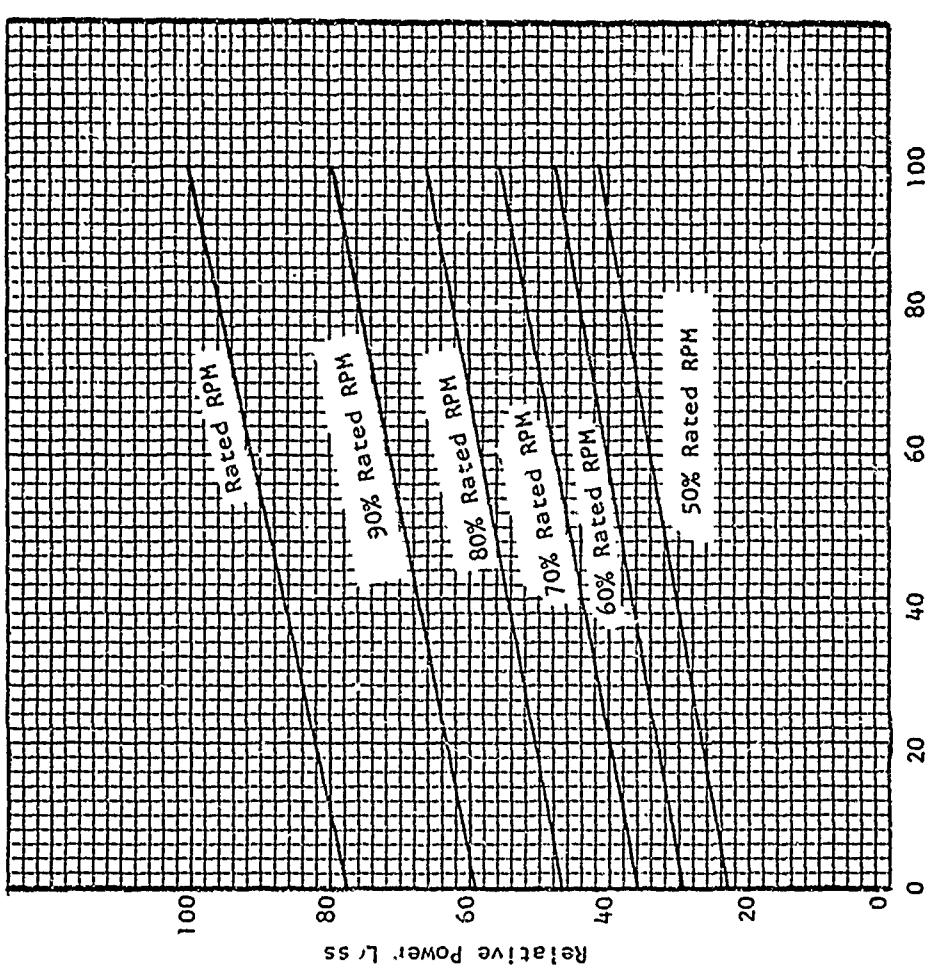


FIGURE 2-2. Typical Turbine Engine Reduction Gear Losses vs. Output Power.

Examination of Figure 2-2 reveals that, as with reciprocating engine oil cooling, the heat rejection of turbine engine reduction gear boxes is only slightly affected by variation in power transmitted, but greatly affected by RPM. This indicates that the power loss in the transmission (power loss being directly related to total required heat rejection) is more nearly a function of bearing surfaces and is, therefore, associated with the power for which the gear mesh was designed.

The total power lost in the transmission is converted to heat energy. Some of this energy is rejected by conduction, convection, and radiation by way of the transmission case and shafting. The remaining heat energy must be rejected by the oil cooler. Current practice in the helicopter industry is to use values of 0.6-per cent to 1.0 per cent of the design power transmitted per mesh for the oil cooler required heat rejection, rather than the actual power being transmitted at any specific condition. This is illustrated by the following example.

Figure 2-3 is a schematic diagram of the mixing gear box for a twin engine helicopter. Gears 1 and 2 are the input gears from each of the two engines. Gear 3 is the collector and speed reduction gear and gear 4 represents the final speed reduction and output gear for this gear box.

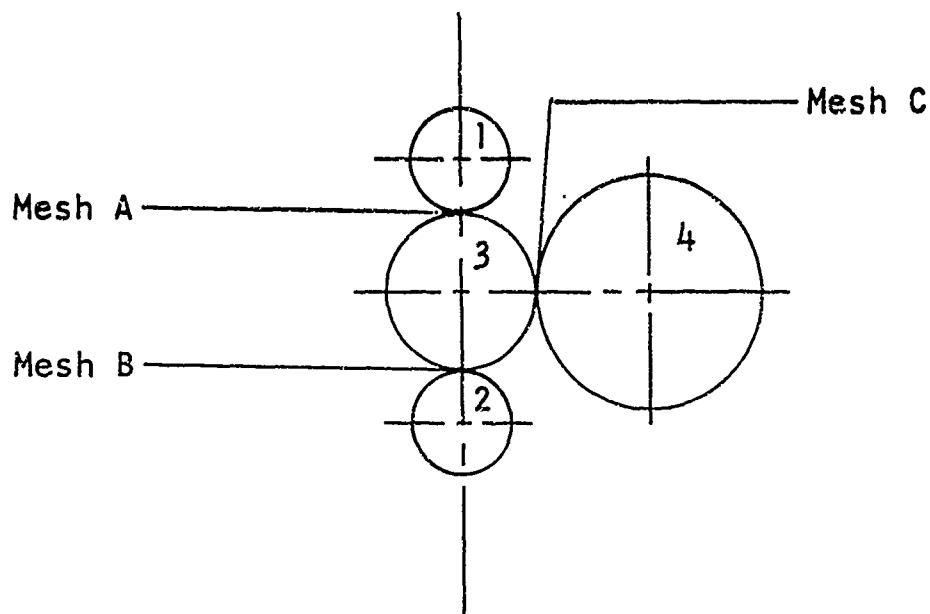


Figure 2-3
Schematic Diagram of a Mixing Gear Box

The desired gear surface finish, the location within the aircraft, and the design practice for this gear box indicated a value of 0.75 per cent of the design power transmitted per mesh for the required oil heat rejection. For this helicopter, the full engine power available is utilized only during single engine operation. For normal operation, a maximum of 3000 horsepower is used. Therefore, referring again to Figure 2-3, mesh A and mesh B were designed for the transmission of full engine power, or 2000 horsepower, and mesh C was designed for 3000 horsepower. The basic oil heat rejection for the gear box at design RPM is determined by:

Mesh A	2000 HP @ .0075	=	15 HP
Mesh B	2000 HP @ .0075	=	15 HP
Mesh C	3000 HP @ .0075	=	22.5 HP
	effective sum	=	52.5 HP
or	2230 BTU/min.		

2-5 COOLING OF ACCESSORIES

In addition to the primary power plant and drive system components, the cooling of many secondary accessory components such as generators, inverters and electronic equipment must be considered. These may be classified into three categories according to the method of cooling: (1) those which include provisions for internal blast cooling, (2) those which are cooled by external blast air, and (3) those which may be cooled by ventilation.

Aircraft generators, excepting those which have an integral cooling air pump, are cooled by internal blast air which must be provided by the aircraft cooling air pump. An inlet tube for entrance of cooling air is incorporated in the generator design. The maximum required cooling air flow rate and pressure is limited by Military Specification MIL-G-6099 or MIL-G-6162, references 2-1 and 2-2, respectively. Even though the generator which is planned to be installed may not require the maximum allowable cooling air flow, the system should be designed to provide the maximum flow in order to insure cooling of any generator of equal rating. The installation would then not be restricted to a particular generator. Rather, it would allow use of any generator of equal rating which meets the applicable Military Specification.

The sea level cooling requirements may be determined from the aforementioned Military Specifications. The required airflow rate is dependent upon the generator electrical rating. A curve of basic airflow vs. generator rating is included as Figure 2-4. The required pressure, defined as inlet total pressure minus outlet static pressure, is specified as 6 in.¹H₂O at basic airflow or 5.31 "H₂O at 130 per cent basic airflow. These somewhat odd requirements are to allow for differences in generators due to production methods. Required pressure at altitude may be determined from Figure 2-5. The pressure required at a given altitude will depend upon the cooling air temperature and the desired per cent generator rating.

Accessories such as magnetos, engine dynamic mounts, and various electrical equipment may be cooled by ventilation or, if located in a high temperature or stagnant air area, may require external blast air cooling. In order to determine whether ventilation will provide adequate cooling, the mean velocity and temperature of the air surrounding the unit must be estimated and a heat transfer analysis performed. Approximate heat transfer coefficients for this analysis may be obtained from Figure 2-6. If the analysis indicates a possible cooling deficiency, it may be desired to perform the more rigorous analysis presented in Section 4-20 of reference 2-3. In the event that ventilation will not provide adequate cooling, blast air must be supplied. An analysis similar to that for ventilation cooling will yield approximate values of blast air flow rate and velocity.

2-6 TOTAL COOLING REQUIREMENTS

At this point in the cooling study, the critical cooling condition for each component should have been estimated and applicable cooling data, including calculated oil cooler performance charts, should be available. Several flight conditions probably would have been investigated even though the same flight conditions may not have been investigated for all components.

The next step in the analysis is to determine, at each flight condition which has been investigated, the maximum pressure drop required for cooling any component in a given system. This pressure drop must be the sum of the pressure drop across the component and the pressure drop through the ducting to and from that component. The maximum required pressure drop at each flight condition represents the total pressure rise required at that condition.

The flow rate through each airflow path may now be determined for each flight condition. This flow rate must be based on the maximum pressure rise required at that flight condition, rather than on the pressure required for cooling each respective component. This means that the critical component at each condition investigated will receive just enough air to provide adequate cooling, while the other components will receive slightly more air than is required. This over supply of air cannot be amended unless it occurs for a given component at each flight condition. In this case, the ducting to that component could be restricted if it were desired to decrease the total cooling airflow rate.

After determining the airflow rate of each component, the total cooling airflow required at each flight condition is obtained by summing the individual airflow rates. This results in the total airflow rate which must be provided by the air pump.

The required air pump pressure rise is obtained by subtracting any inlet ram or exit external pressures from the previously calculated total required pressure rise.

This procedure gives the total airflow and pressure rise which must be provided by the air pump of one cooling flow system for each flight condition. If the aircraft cooling system consists of more than one air pump, the total flow and pressure requirements of each pump may be determined in the same manner.

2-7 DETERMINATION OF THE CRITICAL AIR PUMP CONDITION

The airflow and pressure rise requirements for the air pump have now been ascertained for several aircraft flight conditions. It is now desirable to determine the most critical of those requirements. This may easily be obtained if the air pump is to be a fan. For each flight condition, the following data have been determined: (1) airflow; Q , (2) pressure rise, ΔP , (3) engine RPM, and (4) air density ratio, σ . By utilizing the fan laws,

For Higher Ratings Assume Extension of Straight Line

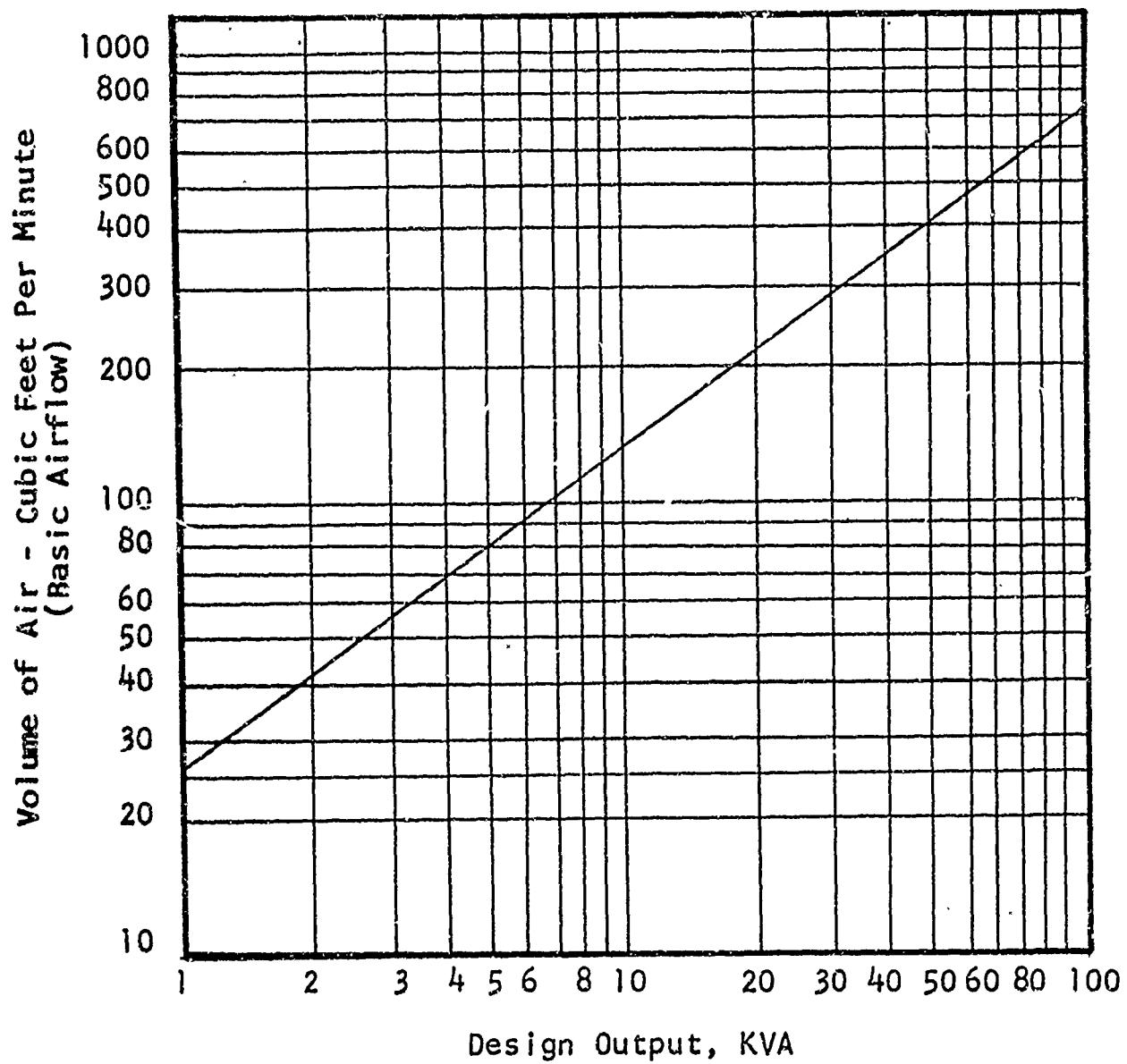


FIGURE 2-4. Required Generator Cooling Air.
(Source: Ref. 2-1)

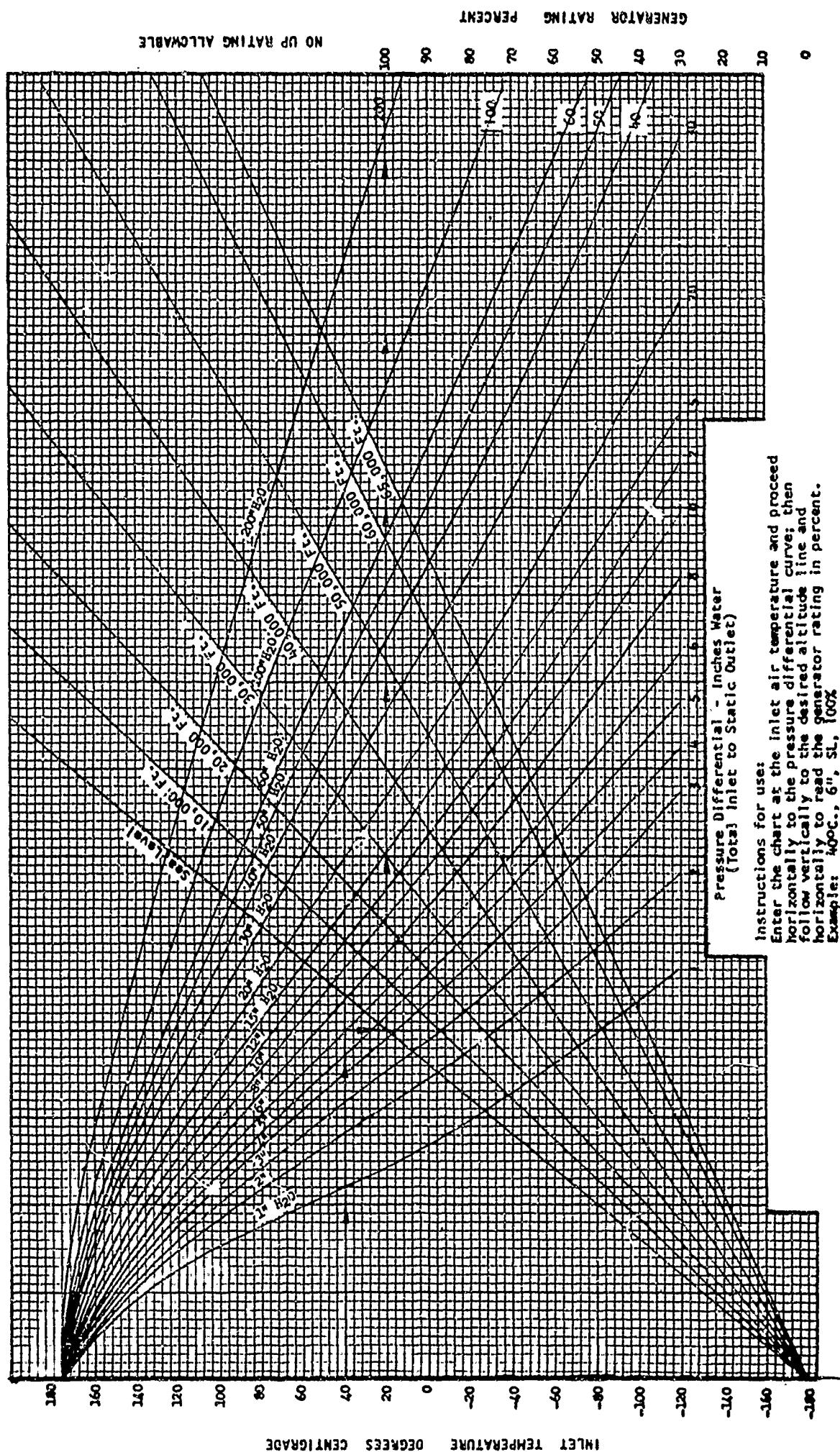


FIGURE 2-5. RATING CURVE FOR BLAST COOLED AIRCRAFT GENERATORS. (Redrawn from Bu Aer Des. No. 49A1815).

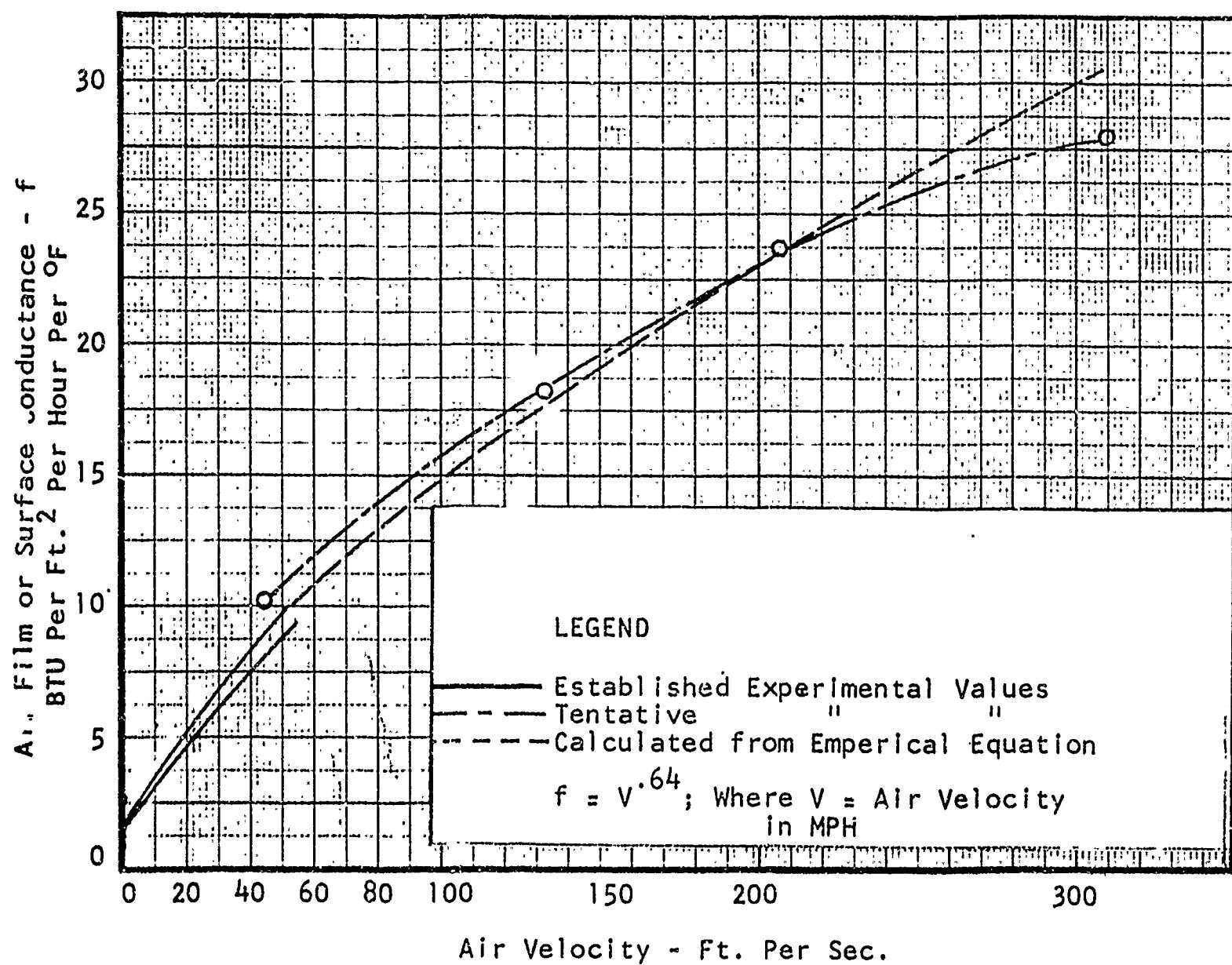


FIGURE 2-6. Air Film or Surface Conductance as a Function of Air Velocity for Smooth Surfaces. (Source: Ref. 2-9)

$$Q_2 = Q_1 \frac{RPM_2}{RPM_1}$$

and

$$\Delta P_2 = \Delta P_1 \left(\frac{RPM_2}{RPM_1} \right)^2 \frac{\sigma_2}{\sigma_1},$$

the fan requirements at each flight condition may be resolved to one common condition such as sea level, standard day, and normal engine RPM. The critical fan condition is then readily discernible.

There are no generalized laws for ejector air pumps. Therefore, if it is desired to utilize an ejector, it is necessary to estimate the most critical pump condition, select the required geometry to meet that condition and then check the operation of the ejector at the remaining conditions. The design procedure for constant area cylindrical ejectors with a primary pressure ratio greater than the critical pressure ratio for the primary fluid used is described in Section 4-3.0 in Chapter IV. Conical ejectors and cylindrical ejectors with a primary pressure ratio less than critical cannot be sensibly analyzed mathematically and must be designed by trial and error.

2-8 LIST OF REFERENCES

- 2-1 Military Specification MIL-G-6099, Generators and Regulators; Aircraft, Alternating Current, General Specification for.
- 2-2 Military Specification MIL-G-6162, Generators, 30 Volt, Direct Current, Aircraft Engine Driven, General Specification for.
- 2-3 Committee A-9, Air Conditioning Equipment, Society of Automotive Engineers, New York: Airplane Air Conditioning Engineering Data, Heat Transfer. SAE Aeronautical Information Report No. 24, February 1, 1952.
- 2-4 Military Specification MIL-C-8678 (Aer), Cooling Requirements of Power Plant Installations.
- 2-5 Bureau of Aeronautics Specification SD-24, General Specification for Design and Construction of Airplanes for the United States Navy.
- 2-6 Air Force - Navy Aeronautical Bulletin No. 421, Atmospheric Properties- Extreme Cold and Hot: Standard for Aeronautical Design.
- 2-7 Fan Engineering, An Engineer's Handbook, The Buffalo Forge Company, Buffalo, N. Y.
- 2-8 McAdams, William H., Heat Transmission, McGraw - Hill Book Company, 1942.
- 2-9 Technical Glass Bulletin Number 8, Pittsburgh Plate Glass Company, December 16, 1941.
- 2-10 Wright Cyclone Military C9HD Series Engines Installation Data AED-16, May, 1950. Wright Aeronautical Corporation, Division of Curtiss-Wright Corporation, Woodridge, N. J.

2-9 LIST OF SYMBOLS

SYMBOLS

H	Heat, BTU Heat absorbed, BTU per minute Heat transfer rate, BTU per hour
W	Weight, pounds Width of duct
	Weight flow rate, pounds per second
C	Resultant velocity vector Coefficient Blade chord, feet
Δt	Coefficient of discharge
ITD	Temperature difference, degrees Fahrenheit Inlet temperature difference between air and oil, degrees Fahrenheit
x	Thickness of body or length of flow
K	Loss factor, decimal fractional part of velocity head
h	Film heat transfer coefficient, BTU/hour/square foot/ $^{\circ}$ F
RPM	Revolutions per minute
BTU	British thermal units
H ₂ O	Water
ρ	Air density ratio (ambient density - NACA standard density at sea level)
2θ	Included angle between sides of converging or diverging duct
KVA	Kilovoltamperes

SUBSCRIPTS

p	Constant pressure
1	higher
2	lower

CHAPTER III

INTERNAL AIRFLOW SYSTEMS - INLETS, DUCTS, EXITS

TABLE OF CONTENTS

	<u>PAGE</u>
3-1	III-6,7
3-2.0	III-8,9
3-2.1	III-9
3-2.2	III-9
Selection of Cross-Sectional Shape and Transition Shapes	III-9
Duct Entrance Design	III-10
3-2.3.1.0 General Internal Airflow Duct Entrances	III-10
3-2.3.1.1 Abrupt Entry	III-10
3-2.3.1.2 Rounded Entry (Bellmouth)	III-10
3-2.3.1.3 Re-entrant Entry	III-10
3-2.3.1.4 Converging Entry	III-11
3-2.3.1.5 Straight Expanding Entry	III-11
3-2.3.1.6 Rectangular Duct Inlet with Expanding Curved Entry, 2 Walls Diverging, 2 Walls Parallel Inlet Screens	III-12
3-2.3.2	III-13
3-2.3.3	III-14,15
3-2.3.4	III-15,16,17,18
3-2.4.0	III-18
3-2.4.1	III-18
3-2.4.2	III-19
3-2.4.3	III-19
3-2.5.0	III-19
3-2.5.1	III-19,20
3-2.5.2	III-21
3-2.5.3	III-21,22
3-2.5.4	III-22
3-2.5.5	III-22,23
3-2.6	III-23,24
3-2.7.0	III-24
3-2.7.1	III-24
3-2.7.2	III-24,25
3-2.7.3	III-25
Annular Diffusers with Constant Diameter Outer Walls	III-25
3-2.7.4 Diverging Nozzle	III-25,26
3-2.7.5 Abrupt Expansions	III-26
3-2.8.0	III-26
3-2.8.1	III-26
3-2.8.2.0 Orifices and Nozzles	III-26
3-2.8.2.1.0 Discharging from a Plenum	III-26
3-2.8.2.1.1 Sharp - Edged Orifice	III-26,27
3-2.8.2.1.2 Smooth - Edged Orifice	III-27
3-2.8.2.1.3 Slots	III-29
3-2.8.2.1.4 Flow Nozzle	III-29
3-2.8.2.1.5 Short Length of Pipe (or Duct)	III-29
3-2.8.2.1.6 Re-entrant Nozzle	III-29

CHAPTER III

INTERNAL AIRFLOW SYSTEMS - INLETS, DUCTS, EXITS

TABLE OF CONTENTS (CONTINUED)

	<u>PAGE</u>
3-2.8.2.1.7	III-29
3-2.8.2.1.8	III-30
3-2.8.2.2.0	III-30
3-2.8.2.2.1	III-30
3-2.8.2.2.2	III-31
3-2.8.2.2.3	III-31
3-2.8.2.2.4	III-31, 32
3-2.8.2.2.5	III-32
3-2.9.0	III-34
3-2.9.1	III-34
3-2.9.2	III-34, 35
3-2.10.0	III-35
3-2.10.1	III-36
3-2.10.2	III-36
3-2.11	III-37, 38, 39, 40
3-2.12	III-40
3-3.0	III-71
3-3.1	III-71
3-3.2	III-71
3-3.3	III-72
3-3.4	III-73, 75
3-3.5	III-75, 78
3-3.6	III-80
3-3.7	III-80
3-4	III-81, 82
3-5	III-83, 84, 85

CHAPTER III

LIST OF FIGURES

	<u>PAGE</u>
3-1 Abrupt Entry to Duct	III-10
3-2 Rounded Entry (Bellmouth)	III-10
3-3 Reentrant or Open End Duct	III-10
3-4 Converging Entry	III-11
3-5 Straight Expanding Entry	III-11
3-6 Rectangular (Rem) Duct Inlet with Expanding Curved Entry	III-12
3-7 Abrupt Contraction in Duct	III-18
3-8 Streamlined Contraction in Duct	III-19
3-9 Conical Contraction in Duct	III-19
3-10 Elbow Terms	III-20
3-11 Diffuser, Conical Cross-Section	III-25
3-12 Diffuser, Square Cross-Section	III-25
3-13 Diverging Nozzle	III-25
3-14 Abrupt Enlargement	III-26
3-15 Sharp-Edged Orifice	III-27
3-16 Smooth-Edged Orifice	III-28
3-17 Flow Nozzle	III-28
3-18 Short Pipe	III-29
3-19 Reentrant Nozzle	III-29
3-20 Converging Nozzle	III-30
3-21 Flow Nozzle	III-30
3-22 Sharp-Edged Orifice	III-31
3-23 Short Pipe	III-31
3-24 Converging Nozzle	III-31
3-25 Orifice Plates	III-33
3-26 Venturi Tube	III-33
3-27 Gate Valve	III-36
3-28 Damper	III-36
3-29 Effect of the Included Angle in Unflanged Hoods	III-41
3-30A Abrupt Contraction	III-41
3-30B Correction Factor for Rounded Entrance	III-41
3-31 Variation of the Loss in a Straight Expanding Entry	III-42
3-32 Dependence of the Loss in a Curved Diffusion on the Rate of Expansion	III-43
3-33 Pressure Loss Factor for Inlet Screens	III-43
3-34 Inlet Conditions - Flush Circular Duct and Circular Hole in Flat Plate	III-44
3-35 Outlet Conditions - Flush Circular Duct and Circular Hole in Flat Plate	III-45
3-36 Loss of Pressure in 90° Rectangular Elbow with and without Splitters	III-46
3-37 Loss of Pressure in 90° Round Elbow	III-46
3-38 vs. C	III-47
3-39 Aspect vs. E - Aspect Ratio vs. E	III-47

CHAPTER III

LIST OF FIGURES (CONTINUED)

	<u>PAGE</u>
3-40 Effect of Aspect Ratio and Radius Ratio on Loss in Bends (Rectangular Cross-Section)	III-48
3-41	III-49
3-42	III-50
3-43 Effect of Aspect Ratio and Radius Ratio on Loss in Bends (Elliptical Cross-Section)	III-50
3-44	III-51
3-45	III-51
3-46 Rectangular and Circular Ducts - Loss Coefficient vs. Turning Angle	III-52
3-47A Loss Coefficient for a 90° Bend - of Circular Cross- Section	III-52
3-47B 90° Bend of Square Cross-Section	III-52
3-48 Typical Elbows	III-53
3-49 Loss @ End of Duct	III-54
3-50 Rectangular Compound Bends	III-55
3-51 Total Pressure Loss Coefficients Net	III-56
3-52 for Compound Rectangular Bends	III-56
3-53	III-57
3-54 Chart for Determining the Location of Elbow Splitters in Rectangular Elbows	III-58
3-55 Design of Turning Vanes	III-59
3-56 Design of Blade Elbows	III-60
3-57 Loss Coefficient of Vanes	III-61
3-58 Duct Branches	III-62
3-59A Max. Efficiency of Conical Diffusers	III-62
3-59B Max. Efficiency of Square or Rect. Diffusers	III-62
3-60 Variation of the Efficiency with the Angle of Expansion	III-63
3-61 Static Pressure Regain in Diverging Nozzle in Duct	III-63
3-62 Schematic Diagram of Diffuser	III-64
3-63 Schematic Diagram of Five Diffusers and Area Distrib- ution Curve	III-64
3-64 Inlet Pressure Ratio vs. Loss Coefficient	III-65
3-65 and Whirl Angle for Annular Diffusers	III-65
3-66 Coefficient of Discharge for Converging Nozzles Discharging from a Plenum Chamber	III-66
3-67 Static Pressure Regain in Diverging Nozzle at End of Pipe	III-66
3-68 Equivalent Diameter of Rectangular Ducts	III-67
3-69 Relation of Reynolds Number and Friction Factor for Circular Pipes	III-68
3-70 Effect of Roughness on Reynolds Number vs. Friction Factor	III-68
3-71 Absolute Viscosity vs. Temperature	III-69
3-72 Kinematic Viscosity vs. Temperature	III-69
3-73 Cooling System for Submerged Turbine Engine Installation	III-70
3-74 Cooling System for Submerged Reciprocating Engine Installation	III-70
3-75 Duct Inlets Integral with Aircraft Structure	III-72

CHAPTER III

LIST OF FIGURES (CONTINUED)

	<u>PAGE</u>
3-76 Types of Connections	III-73
3-77 Type of Duct Problem & Solution	III-74
3-78 Space Conservation for Ducting System	III-74
3-79 Branch Ducts for Parallel Requirements	III-74
3-80 Flexible Connections	III-76
3-81 Connections	III-76
3-82 Expansion and Contraction Joint	III-77
3-83 Slip Joint	III-77
3-84 Bellows Joint for High Velocity, High Temperature	III-77
3-85 Flange Designs for Self-Supporting, Laminated Glass Fabric Ducts	III-79
3-86 A Self-Supporting, Laminated Glass Fabric Duct	III-79
3-87 Metal Duct	III-79

CHAPTER III
INTERNAL AIRFLOW SYSTEMS
INLETS, DUCTS, EXITS

3-1 PRESENTATION OF AERODYNAMIC THEORY

Internal fluid flow principles required for most helicopter or airship cooling and ducting systems are based on three simple concepts:

a. Equation of Flow Continuity

$$Q = AV \quad \text{Equation 3-1}$$

(Volume Flow = Area x Velocity)

b. Equation of Pressure Energy Continuity (Bernoulli's Theorem)

$$P_1 + \frac{1}{2} \rho V_1^2 = P_2 + \frac{1}{2} \rho V_2^2 + \Delta P_T \quad \text{Equation 3-2}$$

static pressure + velocity pressure = static pressure + velocity pressure + total pressure

at station (1) at station (2) between station (1) & (2)

c. Equation of Impulse & Momentum

$$F = M (V_2 - V_1) \quad \text{Equation 3-3}$$

(Force = mass per unit time x change in velocity)

In addition, since the volume occupied per pound of fluid (or per total pounds of fluid flowing per minute) is a function of the density of the fluid, a very convenient expression for relative density for air may be expressed as

$$\sigma = \frac{\rho}{\rho_0} = .245 \frac{P}{T} \quad \text{Equation 3-4}$$

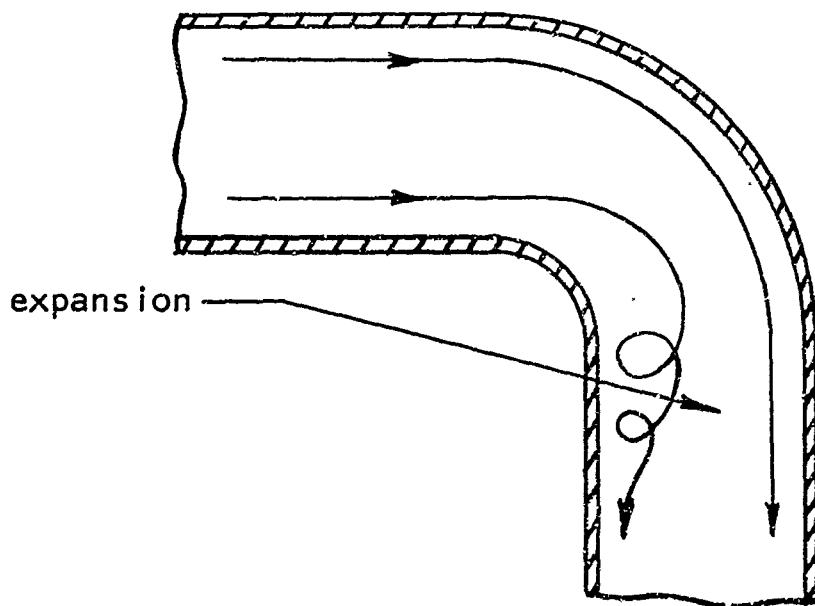
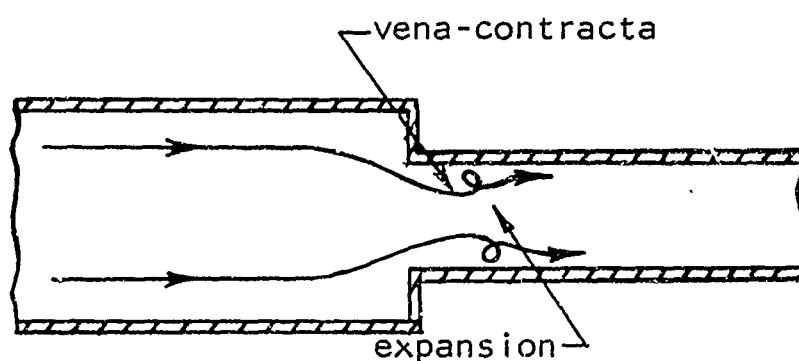
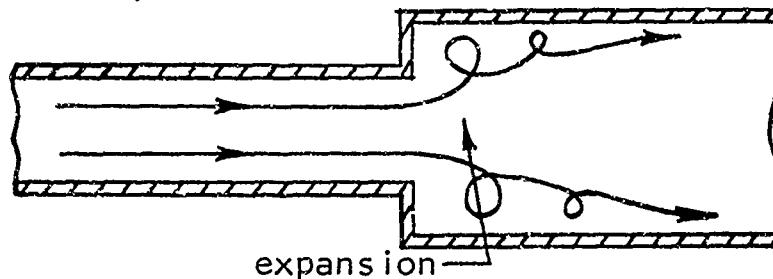
where P is lb/ft^2 , static pressure
 T is $^{\circ}\text{F}$ absolute ($^{\circ}\text{R}$)

From equation 3-1 it may be seen that the velocity is dependent on the size of the duct (for a given quantity flow)

From equations 3-2 and 3-3 a convenient development can be obtained to express the losses in pressure energy suffered through a ducting component. This principle is developed on Page 213 of Reference 8 but will only be explained in words here. The statement is made that duct losses due to an expansion of flow area may be expressed as a percentage of a velocity head associated with the expansion area, that is:

$$P_T = K \left(\frac{1}{2} \rho v_{Ref.}^2 \right) \quad \text{Equation 3-5}$$

In addition, it is postulated that all losses due to flow area changes are expansion losses. Even pressure losses due to contractions or direction changes are due to an expansion, a deceleration of the flow velocity. That this is so may be visualized from the following 3 sketches:



This concept, that pressure energy losses due to duct area or direction change are a result of a flow expansion, combined with the ability to evaluate the pressure loss as a percentage of the approaching (or some other pertinent) velocity head provides a convenient means of data presentation. The percentages of a referenced velocity head lost in an "expansion" are presented for many duct configurations in the following portions of this chapter.

As with all rules, one exception must now be made: pressure energy losses due to friction in a duct are expressed as a percentage of the velocity head but the percentage varies with velocity, or more exactly with Reynolds number. Duct frictional loss data are also presented in the following portions of this chapter.

3-2.0 Application of Theory to Design

The intent in this chapter is to provide design data for ranges of parameters as follows:

a. Duct Sizes

1. Length from zero to ten feet
2. Diameter from three inches to three feet

b. Duct Shapes

1. Straight sections with circular, elliptical and annular cross-sections with radius ratio up to 2:1, and rectangular with aspect ratio up to 3:1.
2. Transition sections between the above sections from abrupt to 10 degrees included angle and up to 4:1 area ratio.
3. Bends of simple and compound nature with radius ratio from zero (square corners) to 6 and up to 90 degrees of turn.

c. Inlets and Outlets

1. Flush and submerged inlets and outlets with air passing through at relative flow angles from zero to ninety degrees.

In most of these cases, the intended range of design parameters has been far exceeded.

A presentation has been made of physical duct design considerations in Section 3-3.0 of this chapter.

The most important criteria for the design of aircraft internal ducting systems are weight, flow losses and available space. The relative importance of these criteria depends on the particular application and installation.

In many fixed-wing aircraft, high flow losses are tolerated to reduce weight and space. In helicopters equipped with submerged power plants, flow losses must be carefully analyzed against weight and space considerations. Often, modest weight penalties are more desirable than flow losses. For a given helicopter with a power loading of 10:1, flow losses

which decrease the engine power available by one HP decrease the pay-load by 10 to 15 pounds if the helicopter is to maintain its performance. This is vividly illustrated for a particular widely-used engine, where an increase in the carburetor induction duct loss of one inch of water penalizes the full-throttle available power by approximately 4 horsepower.

Airship flow losses are minimized in designing ducting systems in order to achieve the highest possible available pressure drop across cooling resistances at critical low cooling fan rotational speeds.

For a secondary branch duct to a small oil cooler, on the other hand, there may be ample pressure available, but space and weight restrictions may be of paramount importance.

Flow losses can be minimized as follows (Reference No. 3-3):

- (a) By using minimum practicable duct velocity.
- (b) By using ducting having the smallest practicable wetted surface area.
- (c) By keeping all wetted surfaces smooth and "streamlining" all decreases in flow area.
- (d) By making all changes in direction of flow through efficient elbows.
- (e) By making all velocity reductions in accordance with efficient diffuser design requirements.
- (f) By using flow-straightening devices when serious flow disturbances are unavoidably introduced.

Rotation, or "swirl" of the fluid about an axis parallel to the mean flow path is likely to introduce abnormally high losses in elbows and turning vanes. Accordingly, when swirl exists, an effort should be made to straighten the fluid flow before turning a corner.

3-2.1 Selection of Duct Area

The duct area is chosen as that necessary to carry the required flow rate of air, plus an allowance for leakage, if required, as discussed in Chapter II. The area should be sufficient to permit the minimum practicable velocity, according to the relationship of the continuity theory $Q = VA$.

3-2.2 Selection of Cross-Sectional Shape and Transition Shapes

The following two considerations should be used to determine the cross-sectional shape, and transition shapes, within the limits of available space:

- a. The duct having the smallest practicable wetted perimeter should be designed.
- b. The cross-section should be chosen to be as uniform as possible along a duct section. If changes of cross-sectional shape must be made, transitions should be as gradual and "streamlined" as possible.

3-2.3.0 Duct Entrance Design

3-2.3.1.0 General Internal Airflow Duct Entrances

The duct entrance shape should be chosen to yield the lowest possible flow loss. However, there are times when the duct inlet is restricted to a particular design. Therefore, several inlets will be discussed with a view towards finding the factor, K, used in the equation

$$\Delta P = K \rho \frac{V^2}{2}$$

3-2.3.1.1 Abrupt Entry to Duct

There are round, square and rectangular inlets of this type as shown in Figure 3-1. Figure 3-29 gives the entrance loss, K, for these shapes at an included angle of 180°.

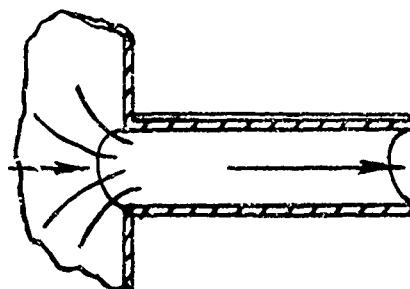


FIGURE 3-1
Abrupt Entry to Duct

3-2.3.1.2 Rounded Entry (Bellmouth)

For a well-rounded bellmouth ($R_c/D > 0.15$) shown in Figure 3-2 the flow loss may be neglected for ordinary ventilating work since K is less than 0.05. When $R_c/D < 0.15$, K can be determined by $K' \times C_c$ where $K' = 0.46$, and C_c is determined by using Figure 3-30B.

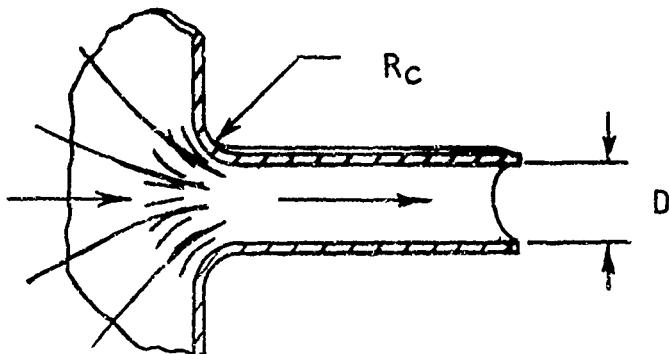


FIGURE 3-2
Rounded Entry (Bellmouth)

3-2.3.1.3 Re-Entrant or Open End Duct

This type of entrance shown in Figure 3-3 causes a large loss ($K = 0.85$ to 0.95), and should be avoided whenever possible. The aforementioned K factor is for re-entrant distances of at least 2 diameters. For shorter distances, K will be lower, approaching the values given for an abrupt entry.

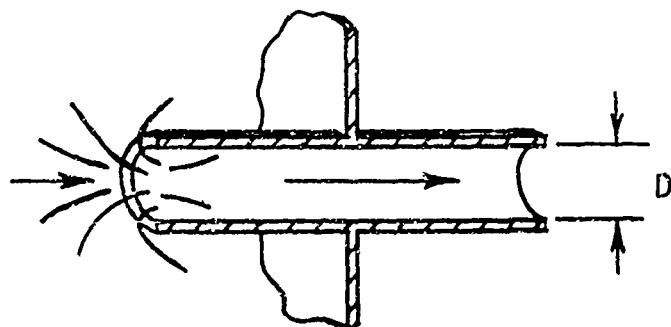


FIGURE 3-3
Reentrant or Open End Duct

3-2.3.1.4 Converging Entry

There are round, square and rectangular inlets of this type shown in Figure 3-4. Figure 3-29 gives the entrance loss, K , for these shapes as a function of the total included angle (2θ) between the sides of the hood. The ratio of the area of the hood to the area of the duct, A_1/A_2 , should be 2 to 1 or greater in order to gain the effect of a converging entry. Figure 3-29 is from tests based on a hood ratio of 5 to 1, but the values are not reduced more than 5% for hood ratios as low as 2 to 1.

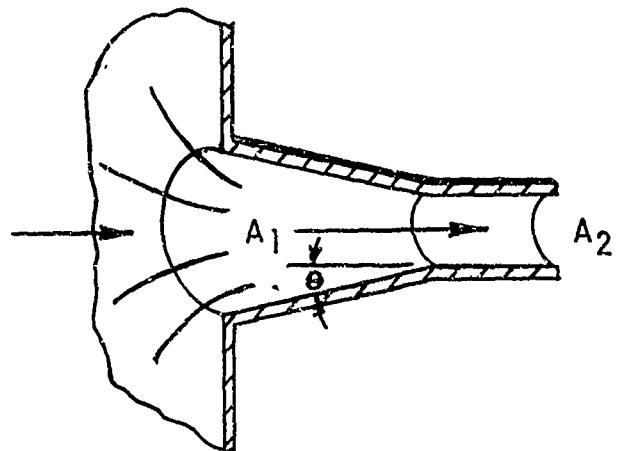


FIGURE 3-4
Converging Entry

3-2.3.1.5 Straight Expanding (Ram) Entry

The flow loss for this type of entry duct

$$= K \frac{\rho V^2}{2}, \text{ where } V > V_1 > V_2,$$

as shown in Figure 3-5. Figure 3-31 gives the factor K as a function of 2θ for V_1/V ratios of from 0.25 to 1.00. As 2θ becomes larger, K increases, until there is an angle at which it is no longer feasible to expand the entry.

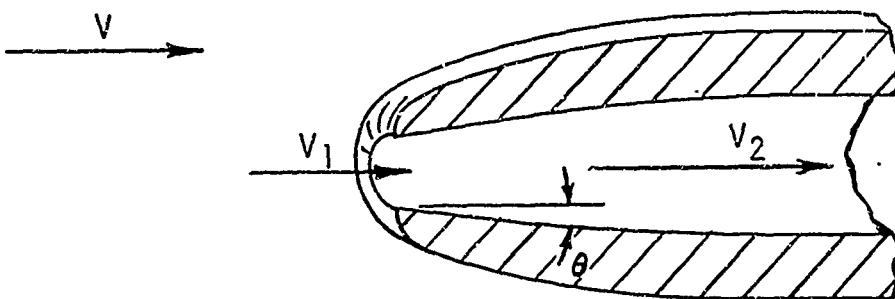


FIGURE 3-5
STRAIGHT EXPANDING ENTRY

3-2.3.1.6 Rectangular (Ram) Duct Inlet with Expanding Curved Entry.
Two Walls (Diverging and Two Walls Parallel: Figure 3-6)

The flow loss for this type of entry duct

$$= \frac{K \rho v_1^2}{2}$$

where K is presented in Figure 3-32 as a function of A_1/A_2 with R_i/d and R_o/d as parameters.

A_1 = inlet area

A_2 = final area

The values in Figure 3-32 are for an inlet aspect ratio (w/d) = 4.0. Data are available only for this aspect ratio.

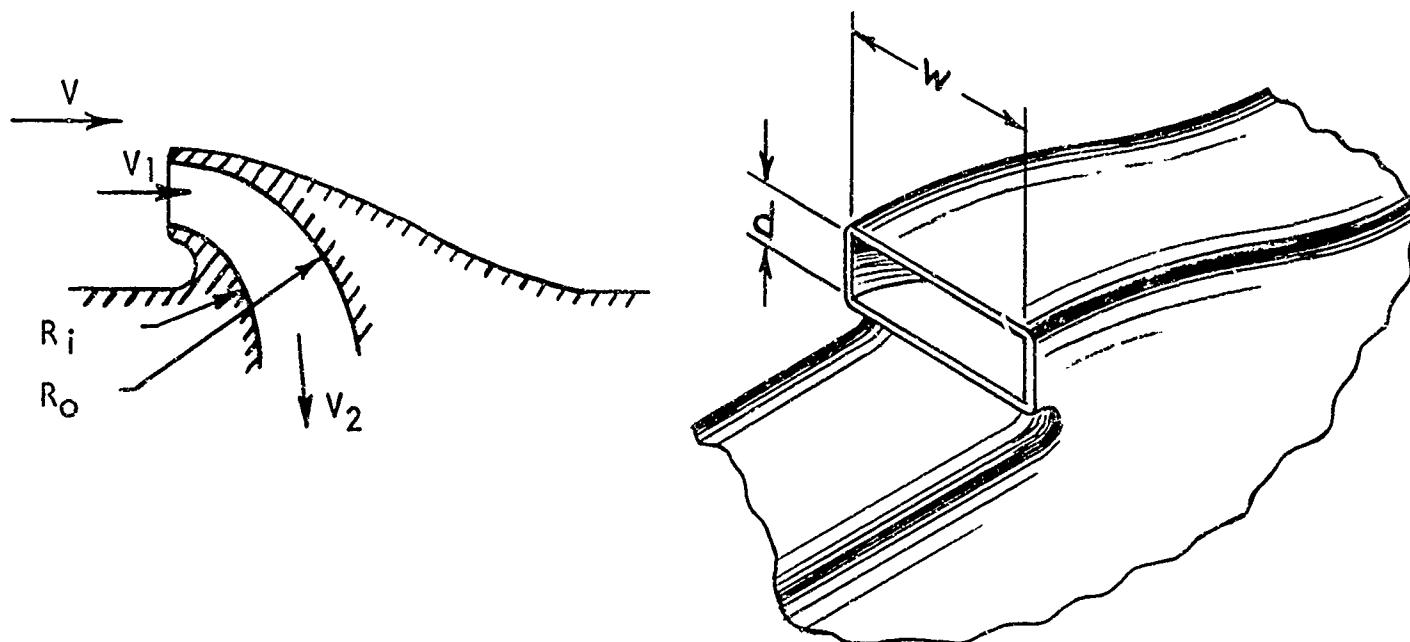


FIGURE 3-6

RECTANGULAR DUCT INLET WITH EXPANDING CURVED ENTRY, TWO WALLS DIVERGING AND TWO WALLS PARALLEL

3-2.3.2 Inlet Screens

Losses due to screen installations in duct systems require careful consideration. The flow through a screen of round wire may be considered as that through a number of nozzles arranged in parallel, wherein the stream velocity is increased passing through the screen (nozzles), then again decreased. The energy loss for a round wire screen installation was expressed by Borda as

$$K_{\text{round}} = \left(\frac{\sigma'}{1 - \sigma'} \right)^2$$

where σ' = screen solidity ratio = Projected solid area / total area

K_{round} , the loss coefficient, is equal to

$$\frac{P_1 - P_2}{\frac{1}{2} \rho V^2} = \frac{\Delta P}{q}$$

The flow through a screen or grid of sharp-edged strips is contracted to approximately two-thirds of the nozzle area, so that the solidity is effectively higher than the physical dimensions indicate. The loss coefficient may be expressed as

$$K_{\text{sharp}} = \left(\frac{0.5 + \sigma'}{1 - \sigma'} \right)^2$$

Test data for round wire screens, presented in Figure 3-33, substantiate these theoretical equations at solidity values above 0.6.

The loss for round wire screens at lower solidities may be expressed by the equation

$$K_{\text{free}} = C_d \frac{\sigma'}{(1 - \sigma')^2}$$

where C_d is the drag coefficient of the screen member shape. In the case of round wire screens of low solidity where $C_d = 1.2$ for the circular cross-sectional shape, this equation fits test data well. However, a transition occurs in test data between this equation up to solidity values of 0.2' to 0.3 and the equation $K_{\text{round}} = \left(\frac{\sigma'}{1 - \sigma'} \right)^2$ at solidities of 0.6 and above, as shown in Figure 3-33.

The losses incurred by screens or grids composed of streamlined or airfoil-shaped sections are much smaller than those for round wire screens. The loss coefficient may be based on the skin-friction drag, taking into account the average velocity increase through the grid as $V_2 = V_1 / (1 - \sigma')$:

$$K_{\text{streamline}} = \frac{2 C_f}{t/c} = \frac{\sigma'}{(1 - \sigma')^2} -$$

Test data shown in Figure 3-33 substantiate this equation to solidities of 0.5.

A high-solidity round wire screen installed in the carburetor inlet duct of an average supercharged reciprocating aircraft engine entails a loss of approximately two percent of the engine power. A grid of streamlined elements results in saving most of this loss.

3-2.3.3 Ram Recovery

The recovery of ram pressure in forward flight may be used effectively to augment the total pressure of an internal air pump for a submerged engine cooling installation. The magnitudes available are relatively small for slow-flying aircraft such as helicopters and airships. For instance, the free-stream velocity pressure at 100 miles per hour at standard sea level density is 4.92 inches of water. This pressure, of course, varies as the square of the velocity, where

$$q = 1/2 \rho V_o^2$$

The pressure recovery of an engine cooling system inlet is decreased from this value by an amount resulting from all pressure losses between the free-stream and the point under consideration within the duct. These losses may include all of the following: friction loss on duct walls, friction loss on approach surfaces (on skin ahead of entry), shock losses from flow separation caused by bends, inefficient diffusion, abrupt expansion as into a plenum chamber, or the adverse pressure gradient caused by the entry, and drag losses from objects within the duct or upstream of the entry (such as from turbine shafting in a turbine compressor inlet duct).

In airships, inlets operating essentially as wing leading edge entries are used to supply air to the engine cooling fan. In helicopters, much less efficient entry locations are commonplace. For example, some engine cooling air inlets are located on fuselage tops and sides, far from the nose of the aircraft. These entries are normally of the flush type so that entry losses in the hovering condition are minimized. In hover, the helicopter requires a large percentage of its available power and, of course, no forward speed ram pressure is available. A properly designed fixed area ram entry may often result in unnecessary flow pressure losses during hovering due to (1) excessive entry velocities and (2) an additional elbow.

Below critical altitude, such a loss may be offset by further opening the throttle so that the decrease in throttle loss is equivalent to the entry loss. Above critical altitude, the increased entry loss would result directly in an equivalent power loss. However, each design must be studied according to its own peculiarities. In several instances, helicopter submerged engine cooling systems have been supplied air through ducting having ram recovery entrances when adequate "natural" external fairings were available.

If a fan must satisfactorily cool to a very low RPM, such as in an airship operating at minimum power, ram inlet ducting may be desirable. The principle here is to prevent the slightest increase in required fan pressure output which would be multiplied by RPM^2 with considerable overcooling energy waste when operating at normal or military RPM. The large inlet areas required to recover low external ram pressures unfortunately will need or require variable area inlets so that excessive external drag is not encountered at higher aircraft speeds.

If a ram scoop is to be used, the aerodynamic design problems center on the internal flow pressure recovery. Figure 3-31 shows the basic relationship for such a subsonic inlet, and the pressure recovery effi-

ciencies to be expected. The principle, of course, is to recover the velocity energy of the external airflow by reducing the velocity during entry. This deceleration may occur externally, internally, or both. The rate of external deceleration depends on the area of the inlet, which defines V_1/V_0 for a given quantity flow. Internal deceleration is then a function of the external deceleration as shown in Figure 3-31; the more the external expansion, the greater the internal expansion may be. Maximum efficiency may be maintained with internal wall divergence as great as 20 degrees included angle if a V_1/V_0 of .25 can be utilized.

The limits to external deceleration lie in the external drag characteristics of the inlet. With large natural fairing, greater external deceleration may be used. For a typical helicopter fixed area inlet, a V_1/V_0 ratio of about .5 is usually a good compromise. Detailed duct entry design data are presented in Section 3-2.12.

Low speed (40 and 80 miles per hour) tunnel test data were obtained on a variety of inlets (and outlets) and presented in Reference 3-10~~and~~11. Side entries of flush holes, flush circular ducts, internal and external flaps, protruding scoops, submerged inlets, wing inlets of flaps, nose and 0.800C wing inlets are included, as are outlets of the same configurations. Extracted data from this source are included in Figure 3-34 for inlets and Figure 3-35 for outlets in Section 3-2.12. of this chapter.

3-2.3.4. Drag Effects of Inlets and Outlets

The drag of internal flow systems is divided into two components, the momentum drag and the external drag.

The momentum drag of a helicopter or airship internal flow system

$$D = M \Delta V \quad HP = D V$$

may be calculated, based on the inlet and exit areas of the duct system configuration. The momentum power resulting from the deceleration of a mass of air entering a fixed area internal flow system is at the greatest value at the maximum speed of the aircraft. When the helicopter is hovering $V = 0$; the momentum drag is zero. The momentum drag may be minimized by directing the exiting air in the sense opposite to the travel of the aircraft (rearward). A considerable treatment of the value of variable areas to control momentum drag losses is presented in References 3-9~~and~~11. If the air and/or gas passing through the system is heated within the aircraft and exited with a rearward component, the momentum drag may be made negative or, in other words, a thrust force realized.

An inlet protruding from a fuselage increases the total drag of the fuselage through two effects. A scoop-type inlet, for instance, not only presents its own drag but, if located in an ordinarily laminar-flow area, may cause the boundary layer flowing along the fuselage to become turbulent and this may increase the drag loss of the fuselage.

A flush inlet may be expected not to have an external drag component since it operates completely within the fuselage boundary layer. Of course, this type opening will not of itself cause internal flow to

occur if the inflow is perpendicular to the external flow across the fuselage. The pressure differential required to maintain flow must, in such a case, be produced by an air pump such as a fan or ejector or by a local positive static pressure resulting from the inlet location. Tests of various inlet scoops and flush entries in reference 10 were made in which the total drag of the scoop was measured, corrected to present total drag coefficients for the scoop only, as mounted on a flat surface.

The data are presented as plots of $\frac{P}{q}$ versus V_i/V . The total pressure in the duct or inside the entry or outlet may be computed as follows:

$$P_{T_i} = q_i + \left(\frac{P}{q_0} \right) q_0$$

where subscript i indicates a station inside the duct and subscript 0 indicates the free-stream condition.

An internal flow system operating in the propeller slip stream or in the boundary layer or the wake of an aerodynamic body such as a wing on a fuselage, in which the inlet velocity may differ from that of an isolated system, has ideal characteristics described as follows:

$$\text{Drag} \quad D = Q \rho (V_i - V_0)$$

$$\text{Drag Power} \quad DV = 2 Q \rho \left(\frac{V_i}{V} - \frac{V_0}{V} \right) \quad \text{Equation 3-6}$$

$$\text{Total Pressure Loss} \quad \Delta P_t = q \left[\left(\frac{V_i}{V} \right)^2 - \left(\frac{V_0}{V} \right)^2 \right] \quad \text{Equation 3-7}$$

$$\text{and, where } \frac{V_i}{V} = K_i \text{ and } \frac{V_0}{V} = K_o,$$

$$\text{Pump Efficiency} \eta_p = \frac{\Delta P_t Q}{DV} = \frac{K_i + K_o}{2} = \frac{K_i + (K_i^2 - \frac{P_t}{Q})^{1/2}}{2}$$

In the majority of airship and helicopter submerged engine cooling systems, the most important aspect of system performance is moving a required airflow quantity with a minimum pressure loss, not pump or propulsive efficiency.

The power loss, $DV - \Delta P_t Q$, may be used to establish a dimensionless performance parameter, the power loss coefficient

$$C_{PL} = \frac{DV - \Delta P_t Q}{Qq}$$

Equation 3-8

Substituting equations 3-6 and 3-7 in equation 3-8 yields the following simplified equation:

$$\begin{aligned} C_{PL} &= (K_o - 1)^2 - (K_i - 1)^2 \\ &= 2 \left[K_i - \left(K_i^2 - \frac{\Delta P_t}{q} \right)^{1/2} \right] - \frac{\Delta P_t}{q} \end{aligned}$$

Therefore, the minimum C_{PL} occurs when K_o equals unity and when K_i is a minimum for systems giving thrust or at a maximum for systems experiencing drag.

The relationships among the above parameters may be expressed by the following two equations:

$$\eta = \frac{1 + C_{PL}}{P_t/q}$$

$$\eta_p = \left(1 + \frac{C_{PL}}{P_t/q} \right) - 1$$

When inlets and outlets are considered separately, rather than as parts of a complete internal system, as is often the case in design analyses, the foregoing theory may be altered to show the ideal characteristics of the inlet and outlet openings. In each case alone, the aircraft mass may be considered to change at the rate $Q\dot{Q}$, which represents a change of kinetic energy at the rate qQ . The separate ideal characteristics are:

Inlets

$$D_i = Q \rho V_i$$

$$P_{T_i} = q K_i^2$$

Outlets

$$D_o = -Q \rho V_o$$

$$P_{T_o} = q K_o^2$$

$$C_{PLi} = \frac{VD_i - (P_{T_i} Q + qQ)}{qQ} = -(K_i - 1)^2 \quad C_{PLo} = \frac{VD_o - (P_{T_o} Q + qQ)}{qQ} = (K_o - 1)^2$$

$$P_i = \frac{P_{T_i} Q + qQ}{VD_i} = \frac{K_i^2 + 1}{2K_i}$$

$$P_o = \frac{-VD_o}{P_{T_o} Q + qQ} = \frac{2K_o}{K_o^2 + 1}$$

where $(P_T, Q \neq qQ)$ is the available power and $(P_{T_i}, Q \neq qQ)$ is the expanded power of the internal flow at the inlet and outlet, respectively.

In the ideal fluid theory presented thus far in this chapter, the fluid density has been considered to remain constant along the flow path and, therefore, the volume rate of flow Q is equal at inlet and outlet. When the exchange of heat or combustion changes the fluid density and quantity flow between the inlet and outlet, the above formulae may be used by adding subscripts to define the conditions at the inlet and outlet:

Inlet

$$\text{drag } D_i = \sigma_i \dot{Q}_i \rho v_i$$

Outlet

$$D_o = -\sigma_o \dot{Q}_o \rho v_o$$

$$\text{Total Pressure } P_{T_i} = \sigma_i \dot{Q} K_i^2$$

$$P_{T_o} = \sigma_o \dot{Q} K_o^2$$

The other formulae may be altered as required to account for the effects of variations of σ and Q .

Power-loss coefficients and efficiencies, as functions of the velocity ratios, are unaffected by variations of fluid density. The total drag for any particular case, however, depends upon the addition or loss of heat as well as upon the addition or loss of pressure energy within the system. Any increment of heat energy may be computed and the resulting change in volume flow used to evaluate the power loss or useful work of the internal-flow system.

The above treatment is essentially that of Reference 3-10, although not presented here in as great detail. This presentation was made in order to take full advantage of the performance data for inlets and outlets of Reference 3-10, presented in part as dimensionless parameter plots in Figure 3-34 and 3-35 in Section 3-2.12.0 of this chapter. Additional valuable data are presented in Reference 3-9.

3-2.4.0 Design of Duct Contractions

There are several types of duct contractions encountered in internal airflow systems. Contraction losses are rather small because the flow separations which cause the energy losses are minimized by the favorable pressure gradient during the static to velocity pressure transformation.

3-2.4.1 Abrupt Contraction (Figure 3-7)

The pressure loss coefficient, K , is a function of A_2/A_1 , and can be determined from Figure 3-30A.

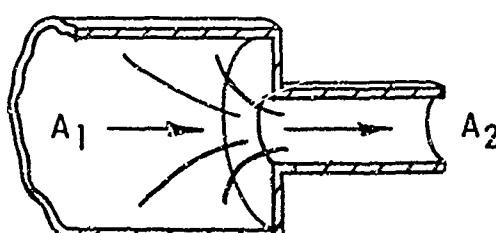


FIGURE 3-7
Abrupt Contraction
(Sharp Edged)

3-2.4.2 Streamlined Contraction (Bell-Mouth) (Figure 3-8)

A streamlined contraction is an abrupt contraction corrected by a factor for the rounded contraction. Therefore, the flow loss would equal $\frac{K \rho C_c V^2}{2}$,

where C_c is the "streamline" factor for the rounded entrance from Figure 3-30B and K is the same factor as for the abrupt contraction from Figure 3-30A.

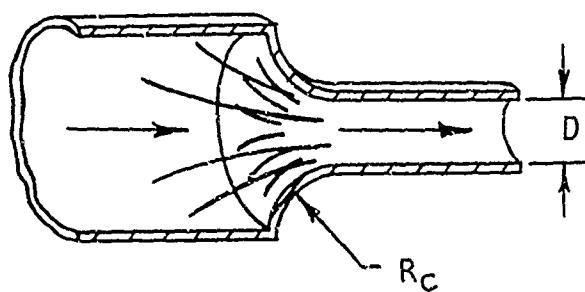


FIGURE 3-8
Streamline Contraction
(Bell Mouth)

3-2.4.3 Conical Contraction (Figure 3-9)

The converging nozzle or cross-sectional area reduction for the moderate angles ordinarily used has very little total pressure loss, the loss being mainly due to the reestablishment of the flow after the slight contraction in the small pipe. For total angles up to 45° the actual shock loss, ordinarily will not be over 4 or 5% of the velocity pressure in the smaller pipe.

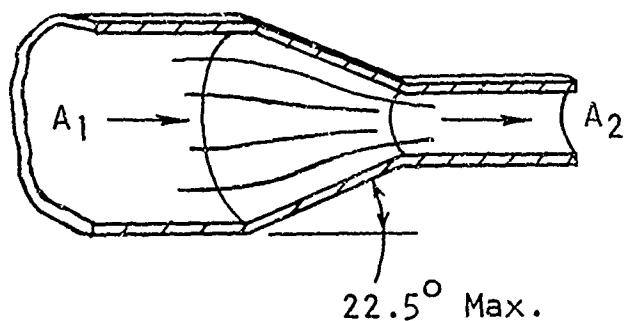


FIGURE 3-9
Conical Contraction

3-2.5.0 Design of Bends

3-2.5.1 General Discussion

The pressure loss in an elbow is of a complicated nature varying with size, shape, velocity, and even the conditions of the ducts leading to and from it. In most cases it will not be possible to take all of these factors into consideration, and a conservative analysis of elbow losses may be considered good practice.

The greatest factor influencing loss of pressure in an elbow is the curvature in relation to the depth of the duct. This may be expressed in either of two ways, curve ratio or radius ratio. The curve ratio is equal to the inside radius of the elbow divided by the outside radius R_i/R_o . The radius ratio is equal to the center line radius of the elbow depth in the plane of the bend (R/D).

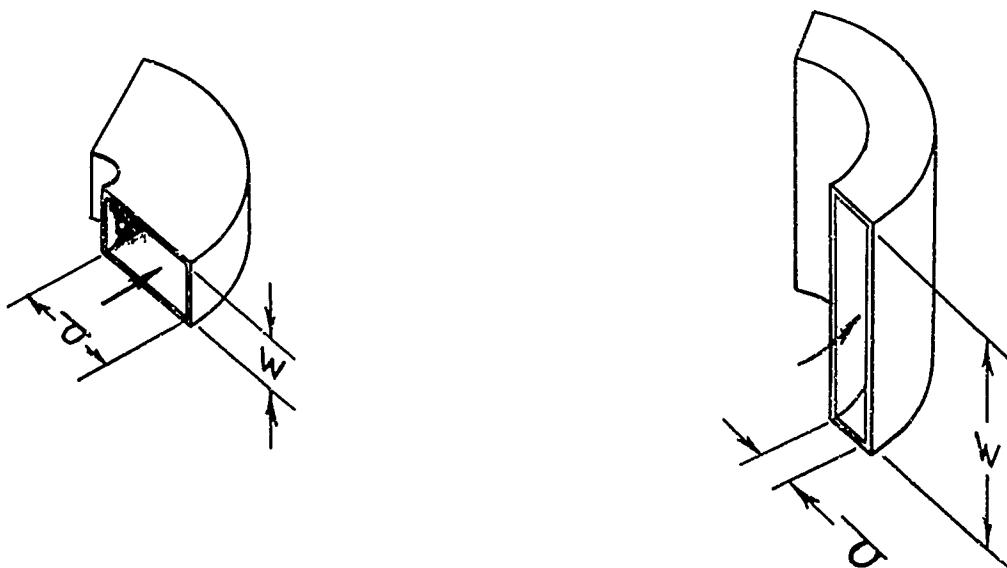


FIGURE 3-10
Elbow Terms

The loss in an elbow may be divided into two components: (1) The eddy loss or internal friction of the fluid itself due to the elbow and (2) the surface friction along the walls of the elbow.

Figures 3-36 and 3-37 show the flow loss in round and rectangular elbows as a function of the curve and radius ratios, and refer to a design in which the elbow in a duct system is followed by at least 3 or 4 diameters of straight duct. The values given are for the complete losses of the elbow including surface friction. It may be observed that the pressure loss increases as the inside radius becomes less and is at a maximum value when both the outside and inside radii are square corners. As the rate of curvature becomes less, that is the curve ratio becomes larger, the value of the elbow loss diminishes until a minimum value is reached at about 0.6 to 0.7 curve ratio. If, however, the friction of the extra length of straight duct is added to the loss of an elbow of this curvature to make the equivalent of an even greater curvature the total loss would be decreased. Elbows of very large curve ratio are not regularly used because the weight, space and cost are out of proportion of the loss saving effected. Generally, then a low loss elbow is considered to be one of 0.5 curve ratio and this has become an accepted standard for most engineering work. In aircraft applications available space is usually the limiting factor.

In rectangular ducts the effect of the cross-sectional shape has considerable bearing upon pressure loss. The term aspect ratio is used to represent this shape in relation to the bend, and is the width of elbow along the axis of the bend divided by the depth in the plane of the bend. Figure 3-47B expresses the loss in percent of the velocity head for the R/D of the bend. Figures 3-38 and 3-39 give correction factors for degree of bend and aspect ratio, respectively.

The flow loss factor $\frac{\Delta P}{q}$, for both rectangular and elliptical cross-section bends may be obtained from Figures 3-40, 3-41, and 3-42 and 3-43, 3-44, and 3-45, respectively, as a function of radius and aspect ratios. In the data for elliptical elbows, friction losses were not included in the net pressure loss coefficient.

Values of loss in per cent of velocity head for circular, square and mitered elbows are presented in Figures 3-46, 3-47A and 3-47B.

The size of an elbow has little effect on the pressure loss for elbows in the neighborhood of 0.5 curve ratio which is that ordinarily used in good designs. Figure 3-48 contains a tabulation of the elbows tested in Reference 3-5.

The velocity effect upon pressure loss in elbows depends upon the abruptness of turn.

A common misconception is that the loss in an elbow is proportional to the angle of bend for angles up to 90° . While the loss in a 45° elbow is somewhat greater than half of that for a 90° elbow, the loss in elbows greater than 90° shows less than the proportional increase in loss. For example, tests on a 180° elbow of square cross-section and 0.28 curve ratio show that the loss is 165% of the 90° loss instead of the 200% as might be supposed.

3-2.5.2 Elbows at the End of a Duct

Elbows at the end of a duct have losses which are materially higher than when the regain effect of the discharge duct is present. Figure 3-49 gives the loss factor, K, for such elbows as a function of the aspect and curve ratios.

3-2.5.3 Compound Elbows

Compound Elbows are of 3 types: U- bend, Z- bend, and the 90° - offset bend as shown in Figure 3-50. The flow loss factor for these bends without spacer, $K = \frac{\Delta P}{q}$ (excluding friction losses) can be obtained

from Figures 3-51 and 3-52, where K is expressed as a function of the aspect and radius ratios at a constant Reynold's number. Figure 3-53 shows K excluding friction losses, as a function of aspect and radius ratios for these bends with 5 foot spacer.

It is clear from these plots that the relative radius of curvature R/D is the most important of the factors affecting the net pressure drop. As compared with this factor the effect of length of spacer between elbows may be regarded as being of the nature of an interference. In general, as the length of the spacer is decreased, this interference causes a decrease of net pressure drop in the case of the U - bend, an increase in the case of the Z - bend, and almost no change in the case of 90° - offset bends.

The pressure drop across the 90° - offset bend is less than that across the corresponding U - bend or - Z - bend, but the magnitudes of the differences are small.

The test data from Reference 3-5 were cross-plotted at two different Reynolds numbers. It was found satisfactory to not differentiate among the types of compound elbows. Accuracy of K' values for the common plot is within 0.05 σ of the loss coefficients presented in the original data for the three types of compound elbows.

3-2.5.4 Splitters

Curved vanes called splitters are sometimes installed in elbows to minimize the elbow losses. One or more splitters may be used, each concentric with the inner and outer radius and extending the full arc of the elbow. The separate flow paths created have larger curve ratios and a larger aspect ratio than those of the elbow alone. The optimum arrangement is that which improves the curve ratio of each of the separate paths over the original path. The improved aspect ratio, although beneficial, is not as important as the improvement of curve ratio.

The curve ratio change due to splitters may be expressed by the following formula:

$$CR' = x \sqrt[1]{CR}$$

$$\text{and } R_1 = \frac{R_a}{CR'}, \quad R_2 = \frac{R_1}{CR'}, \quad R_3 = \frac{R_2}{CR}, \quad \text{etc.}$$

where CR' = curve ratio of component elbows formed by splitters

CR = curve ratio of the original elbow without splitters

x = number of splitters

R_a = inside radius

R_1, R_2, R_3 = radii of first, second and third splitters starting on the inside.

The placement of splitters in rectangular elbows can be determined by using Figure 3-54. Figure 3-36 shows the effect of 1, 2 and 3 splitters in square cross-section elbows. This figure may also be used for cross-sections approximating this shape.

3-2.5.5 Turning Vanes

Curved vanes of small radii placed diagonally at a uniform spacing across the corner of a mitered elbow, wherein the axes of the curvature of the bend and the vanes are parallel, are known as turning vanes. The vanes may be of constant thickness or of varying thickness in order to maintain constant flow path depth through the vaned bend.

The dimensions and spacing of turning vanes depend upon the installation under consideration, but in general the vane length should be approximately six times the spacing to derive the benefit of the aspect ratio factor.

Reference 3-1 contains information on both turning vanes and splitters.

Figures 3-55 and 3-56 show recommended vane designs. Figure 3-57 shows the loss coefficient, $\lambda = K$, for certain vanes. For a rectangular elbow with optimum design turning vanes (Figure 3-55), the loss coefficient at various bend angles, compared to bends without vanes, is as follows:

<u>Elbow Bend</u>	<u>With Vanes</u>	<u>Without Vanes</u>
90°	K = 0.13	K = 1.63
60°	= 0.15	= 1.08
45°	= 0.14	= 0.53
30°	= 0.10	= 0.15

Turning vanes in elbows may be used to reduce the pressure loss and to provide a more uniform velocity distribution downstream of the bend. Vanes and concentric splitters are recommended particularly for mitered elbows in which even the most elementary vane installation results in a substantial reduction in pressure loss.

3-2.6 Design of Duct Branches

Internal flow systems are often comprised of main ducts with individual branch ducts to divert parts of the flow. In the usual case of a duct system supplied from a common source, all branches of which exhaust to a common chamber (pressure), the pressure loss through all branches must be equal. A good aerodynamic design approach is to analyze the pressure energy losses through each path to provide the required airflow and to restrict each branch exit as required so that the velocity head dissipated will equal the total head remaining at the exit. Data on branch duct losses are sufficiently incomplete to warrant the conservative practice of designing branch duct exits with converging sections to have an exit area ten to twenty percent less than calculated. Tests may then be conducted in which the converging sections are shortened to increase the exit area and thus reduce the exit velocity pressure loss until balanced branch flow is achieved.

Branch duct system losses consist of:

1. Losses in the main duct
2. Losses in the branch ducts

Loss coefficients for mains and for branches are presented in diagrams on Figure 3-58, wherein the reference velocity pressure, q , is determined upstream of the connection.

It is stated in Reference 3-7 that the loss in the main duct is approximately 35% of that for an abrupt expansion for the same velocity ratio. The loss in the branch duct is dependent upon the velocity ratio, branch to main, and on the branch takeoff angle. The total loss is at a minimum at a given takeoff angle for each given velocity ratio. Therefore, both the main duct loss and the branch duct loss must be analyzed for a range of takeoff angle in order to determine that angle at which the total loss is at a minimum.

A tabulation of branch duct loss coefficients as a function of the take-off angle and of the velocity ratio, branch to main, "Reprinted by permission from HEATING VENTILATING AIR CONDITIONING GUIDE 1956, Chapter 32", follows:

RATIO OF PRESSURE LOSS TO BRANCH VELOCITY PRESSURE

Ratio of Velocity in Branch to Velocity in Main Duct

Take-off Angle	0.4	0.6	0.8	1.0	1.5	2.0	3.0	
90°	6.5	3.1	2.0	1.5	0.95	0.74	0.62	ΔP_{br}
60°	5.0	2.2	1.3	0.77	0.47	0.47	0.58	q_{br}
45°	3.5	1.3	0.64	0.43	0.40	0.45	0.54	

3-2.7.0 Design of Diffusers

Diffuser design practice is a highly specialized subject. In general, the problem reduces to decelerating the relative air velocity in a duct at a rate compatible with good efficiency. However, the deceleration rate that may be used varies with configuration, mach number and Reynolds number.

3-2.7.1 A Design Method

In helicopter and airship internal airflow duct systems, diffusers are often used upstream of resistances (heat exchangers, compressors, etc.). A method suggested in Reference 3-13 for their design is as follows:

Since the length of the diffuser is the most important consideration in its design, great care should be exercised in locating the various resistances so that sufficient diffuser lengths may be obtained to minimize expansion losses. If the various units can be so located that conical diffusers of approximately 7° included angle may be utilized, the system will be as efficient as possible. If the space available does not allow a 7° conical diffuser to expand the air the required amount, as is usually the case, the following layout procedure is suggested for the case where a resistance follows the diffuser:

- (1) Lay out a 7° or 8° conical diffuser, starting from the duct entrance.
- (2) Lay out a cone of about 20° using the resistance as the base and projecting the elements upstream until they intersect the 7° or 8° entrance cone.
- (3) Check ratio of duct area at resistance to that at intersection of 7° or 8° and 20° cones. If this expansion ratio is less than 3, it is considered to be satisfactory.

A certain amount of latitude may be exercised in the design details to suit the case in question. For instance, most duct passages in actual installations will not be circular in cross-section. Although a great deal is not known about the behavior of diffusers other than those with circular cross-sections, it seems reasonable that the rate of expansion should be slightly less for other cross-sections, especially for rectangular ducts where the air in the corners is actually expanding at a much greater rate than the air along the center of the sides.

3-2.7.2 Diffuser Losses (Figures 3-11 and 3-12)

Although there are numerous cross-sectional diffuser shapes the same basic equation is used to determine the total pressure loss due to this diffusion.

$$\Delta P = (1 - \eta) \frac{\rho V_1^2}{2} \left[1 - \left(\frac{A_1}{A_2} \right)^2 \right] \text{ from Ref. 3-2}$$

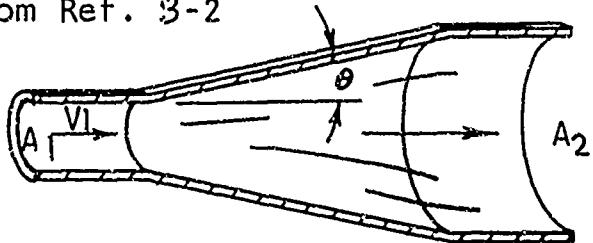


FIGURE 3-11

where $(1 - \eta) \left[1 - \left(\frac{A_1}{A_2} \right)^2 \right] = K$

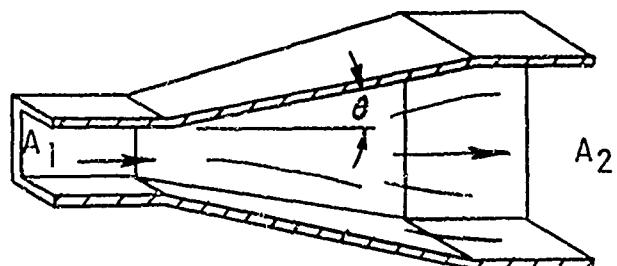


FIGURE 3-12
Diffusers, Square Cross-Section

The efficiency of diffusion, η , can be obtained from Figures 3-59A, -59B, -60 as a function of the included angle, 2θ and the area ratio A_2/A_1 for the various cross-sections (round, square, rectangular). If the cross-section is of a different shape it is best to deal with equivalent diameters. The equivalent diameter, $D = 4A/\ell$, where A is the cross-sectional area and ℓ the wetted perimeter. The angle of diffusion θ can then be determined from $\tan \theta = \frac{D_2 - D_1}{2L}$ where L is the length of diffusion, and 1 and 2 refer to stations before and after diffusion.

3-2.7.3 Annular Diffuser with Constant - Diameter Outer Walls

The general diffuser configuration and station locations for tests of Reference 3-4 are given in Figure 3-62. Performance data are compared for 5 diffusers which cover a range of equivalent conical expansion angles from 15° to 180° ; the corresponding ratios of diffuser length to center body diameter, L_d/d_2 range from 1.072 to 0. Line drawings of these 5 configurations and curves of the longitudinal variations of flow area are given in Figure 3-63; data are in Figures 3-64 and 3-65.

3-2.7.4 Diverging Nozzle (Figure 3-13)

A diverging nozzle is used in an air duct when the area is increased in order to reduce the velocity, or when moving into an enclosed space or plenum chamber.

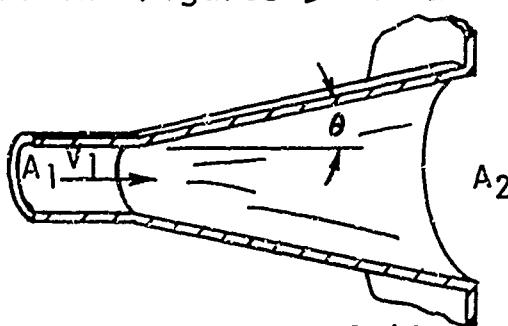


FIGURE 3-13
Diverging Nozzle

Any change from a higher to a lower velocity is accompanied by a conversion from velocity to static pressure, but inasmuch as there is always some loss in making this conversion, the total pressure is less after the velocity is reduced.

Figure 3-61 shows the per cent regain of velocity pressure as a function of the area ratio and angle of divergence (' θ '), when the diverging connection is in a section of duct with 4 to 6 diameters of straight duct following.

3-2.7.5 Abrupt Expansions

There are times in internal airflow ducting when a gradual expansion cannot be achieved and a sudden expansion is the only alternative. In this case, the flow loss coefficient, K , is equal to $(1-A_1/A_2)^2$, and the formula for the total pressure loss for a sudden expansion becomes $\Delta P = \frac{(1 - A_1/A_2)^2 \rho V_1^2}{2}$

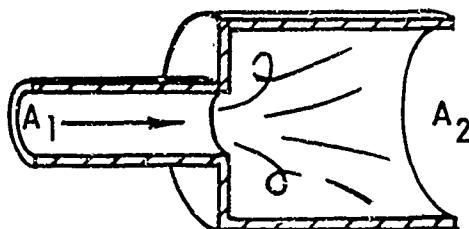


FIGURE 3-14
Abrupt Enlargement

3-2.8.0 Design of Duct Exits

3-2.8.1 Introduction

At a duct exit the entire velocity head is lost when diffusing into the atmosphere. If a certain pressure drop is required at the outlet, a method of diverging or contracting the exit to decelerate or accelerate the flow may be needed. This is accomplished with the use of nozzles or orifice plates which will be discussed in Section 3-2.8.2.2.0.

3-2.8.2.0 Orifices and Nozzles

Orifices and nozzles may be divided into 3 categories; discharging from a plenum, at the end of a pipe, and in the pipe line.

3-2.8.2.1.0 Discharging from a Plenum

3-2.8.2.1.1 Sharp Edged Orifice (Figure 3-15)

The flow characteristics of orifices make them useful for flow measurements of air or other gases. The sharp edged orifice is a thin plate in which is a carefully made hole. The inlet edge is deburred so that the flow is over a sharp 90° corner. The following plate thicknesses may be used for low pressure work: 1/16" up to 6" orifice diameter, 3/32" for 6 to 12" diameter, 1/8" for 12 to 24" diameter, and 3/16" for 24 to 48" diameter. Should high pressures dictate thicker plates, the downstream side should be beveled so that the axial constant-diameter is no more than twelve per cent of the orifice diameter.

The sharp edged orifice discharging from a plenum or installed at a pipe entry may be used over a Reynold's number range of 30,000 to 1,000,000 for the determination of flow rates within approximately one per cent accuracy, as stated in Reference 3-1 using the following coefficients:

$$\text{Coefficient of velocity } C_V = 0.97 \text{ to } 0.98$$

$$\text{Coefficient of contraction } C_C = 0.62$$

$$\text{Coefficient of discharge } C = 0.60 = C_V \times C_C$$

$$\text{Coefficient of resistance } C_r = 0.04 \text{ to } 0.06$$

The coefficient of contraction is the ratio of the vena contracta or contracted stream minimum diameter to the orifice diameter. Using the above coefficients the discharge flow rate may be determined as follows:

$$Q = 1096.5 C_C C_V A \sqrt{\frac{P}{w}} = 1096.5 C A \sqrt{\frac{P}{w}}$$

where

Q = discharge, cfm

A = area of orifice, ft.²

P = static pressure, inches H₂O

w = spec. weight of air, #/ft.³

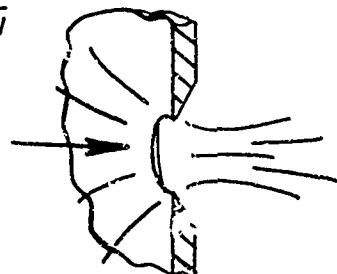


FIGURE 3-15
Sharp Edged Orifice

and the total pressure loss, which may be expressed as:

$$\Delta P = C_r P_v = \left(\frac{1}{C_V^2} - 1 \right) (P_v) = C_r w \left(\frac{V}{1096.5} \right)^2$$

where ΔP = total pressure loss, inches of H₂O

P_v = velocity pressure at the vena contracta, inches of H₂O

V = velocity at the vena contracta, fpm

w = specific weight, #/ft.³

The small frictional pressure loss of the flow through a sharp edged orifice has resulted in this orifice being described as the frictionless orifice.

3-2.8.2.1.2 Smooth Edged Orifice (Figure 3-16)

The coefficient of discharge is increased if the inlet or upstream side of the orifice is even slightly rounded. Flow nozzle characteristics are approached.

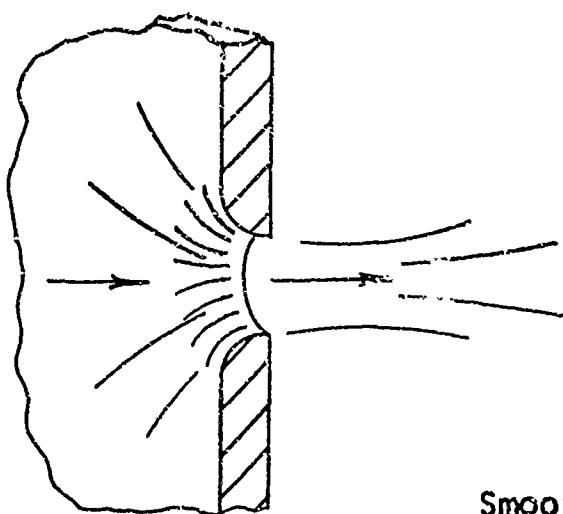
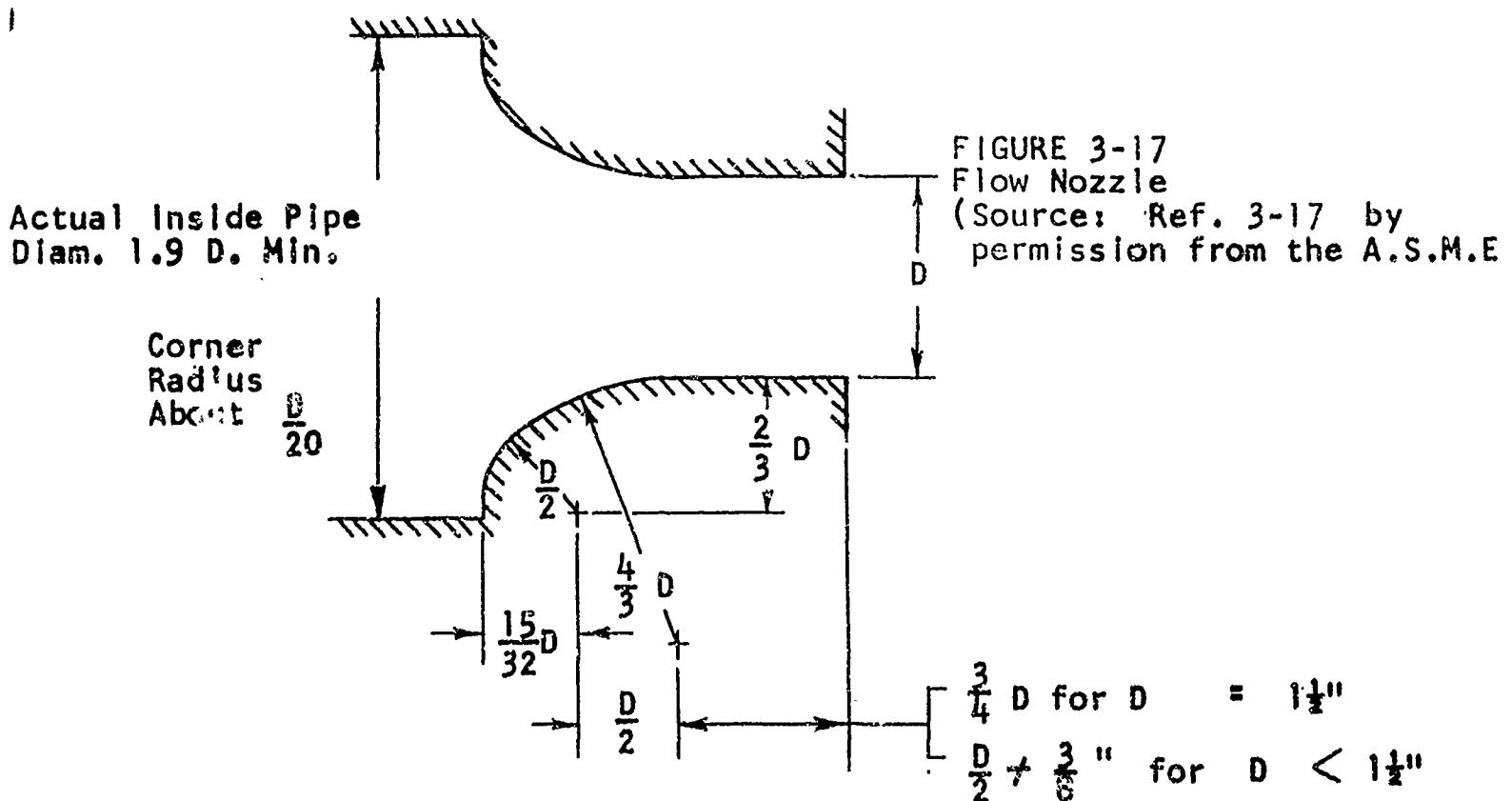


FIGURE 3-16
Smooth Edged Orifice



3-2.8.2.1.3 SLOTS

Long narrow orifices with high aspect ratios are called slots. Regardless of whether the shape of a sharp edged orifice is round or rectangular, the coefficient of discharge is approximately 0.6. The coefficient of discharge may approach 1.0 if the upstream edges are rounded.

3-2.8.2.1.4 Flow Nozzle

An accurately made flow nozzle, in which the upstream side is rounded to prevent the formation of a vena contracta, as in Figure 3-17, will have a coefficient of discharge of approximately 0.99, changing slightly with Reynold's number. Approximate coefficients for the average flow nozzle are:

$$C = 0.97 \text{ to } 0.99$$

$$C_v = 0.02 \text{ to } 0.06$$

3-2.8.2.1.5 Short Length of Pipe (Figure 3-18)

Three to four diameters in the axial direction are required for the stream to be reestablished downstream of the vena contracta. For this configuration

$$C = 0.82$$

$$C_v = 0.47$$

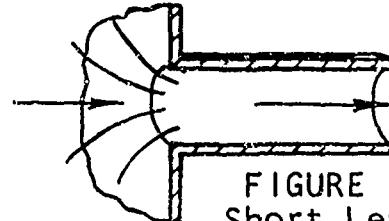


FIGURE 3-18
Short Length
of Pipe

3-2.8.2.1.6 Reentrant Nozzle (Figure 3-19)

The reentrant nozzle or Borda mouthpiece is a configuration in which the pipe entry extends approximately three diameters into a chamber or plenum. The coefficients are

$$C = 0.72$$

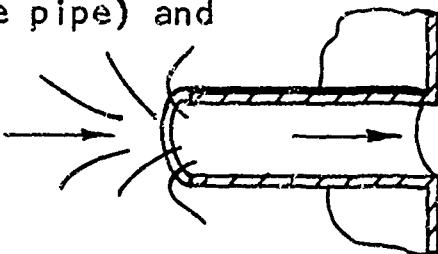
$$C_v = 0.85$$

For a reentrant pipe less than three diameters in length, contraction may occur (when the stream does not fill the pipe) and the coefficients become

$$C = 0.53$$

FIGURE 3-19
Reentrant Nozzle

$$C_v = 0.56$$



3-2.8.2.1.7 Diverging Nozzle

The diverging nozzle with a sharp edged entrance has no special application but the diverging nozzle with a rounded entry causes a flow contraction followed by an expansion. The venturi meter of Section 3-2.9.2 is based on this contraction - expansion process, test applications of which are presented in Chapter VI.

3-2.8.2.1.8 Converging Nozzle (Figure 3-20)

The loss coefficient curves for sharp edged and rounded entry converging nozzles discharging from a plenum are presented in Figure 3-66. Regardless of the entry shape, the stream contracts leaving the nozzle. The optimum included angle (A^o) for a sharp edged entry is 13^o . The nozzle length should be approximately three times the orifice diameter.

3-2.8.2.2.0 Orifices and Nozzles at the End of a Pipe

3-2.8.2.2.1 Flow Nozzle (Figure 3-21)

The differential pressure producing flow through an orifice or nozzle at the end of a pipe is the total (velocity plus static) pressure in the pipe minus the static pressure outside the pipe exit. The velocity pressure effect may be taken into account by the use of the velocity of approach factor, f , when the static pressure is measured in the pipe ahead of the orifice or nozzle.

$$f = \left(\frac{1}{1 - (A_3/A_1)^2} \right)^{1/2}$$

The discharge may be expressed as

$$Q = 1096.5 CA_2 f \sqrt{\frac{P_s}{w}} = 1096.5 CA_2 \sqrt{\frac{P_t}{w}}$$

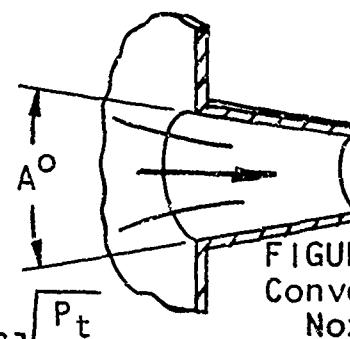


FIGURE 3-20
Converging Nozzle

Where

Q = Discharge, CFM

C = Coefficient of discharge

A_1 = Area of pipe, Sq. Ft.

A_2 = Area of orifice, Sq. Ft.

A_3 = Area of Vena Contracta, Sq. Ft.

= A_2 for flow nozzle with smooth (Bell mouthed) approach

P_s = Static pressure in pipe, inches of water

P_t = Total pressure in pipe, inches of water

w = Weight of air, lb. per cubic foot

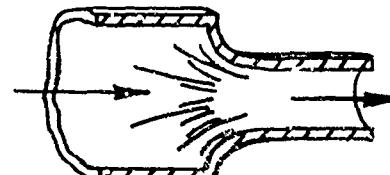


FIGURE 3-21
Flow Nozzle

In the average flow nozzle or rounded entry orifice, $A_3 = A_2$. Values of the velocity of approach factor, f , for different area ratios A_2/A_1 , are as follows:

A_2/A_1	.1	.2	.3	.4	.5	.6	.7	.8
f	1.005	1.021	1.048	1.091	1.155	1.250	1.400	1.666

3-2.8.2.2.2 Sharp Edged Orifice (Figure 3-22).

Both the coefficient of contraction and the coefficient of discharge must be considered for the sharp edged orifice at the end of a pipe because the values of the area ratio, A_2/A_1 , reflect the orifice ratio, not the actual stream to pipe area ratio. The following values of A_2/A_1 , may be used for normal air work, but more complete data should be used for unusual pipe sizes or velocities:

A_2/A_1	.1	.2	.3	.4	.5	.6	.7	.8
C	.601	.609	.618	.636	.656	.682	.708	.73
f	1.002	1.008	1.018	1.036	1.061	1.095	1.15	1.23
C_{xf}	.602	.614	.629	.659	.697	.748	.815	.90

Above values of C_{xf} are to be used in the formula:

$$Q = 1096.5 CA_2 f \sqrt{\frac{P_s}{w}}$$

FIGURE 3-22
Sharp Edged Orifice

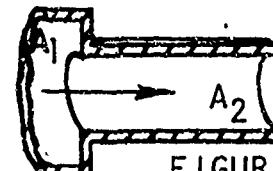
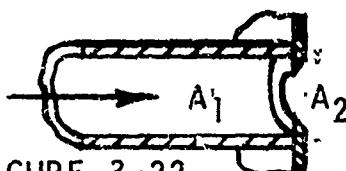


FIGURE 3-23
Short Length of Pipe

3-2.8.2.2.3 Short Length of Pipe (Figure 3-23)

The following values should be used in the formula of Section 3-2.8.2.2.2.

A_2/A_1	.1	.2	.3	.4	.5	.6	.7	.8	.9
C	.821	.827	.836	.853	.868	.893	.912	.935	.96

3-2.8.2.2.4 Converging Nozzle (Figure 3-24)

A converging nozzle at the end of a pipe causes a velocity increase. There are special applications, such as in a thrust producing device or as a flow measuring device. Pitot tube readings are taken at the center of the vena contracta, where the static pressure is zero. Therefore, the total or impact tube may be used to determine velocity pressure directly. This technique is useful for testing small capacity, high pressure fans for which only a few operating points are desired. A nozzle with a straight entrance has a very low coefficient of resistance. The pipe or fan outlet diameter should be reduced considerably at the orifice to achieve a uniform velocity distribution across the orifice cross-section. The velocity of approach factor does not apply directly because the flow total pressure is taken. Thus, the following formula is used:

$$Q = 1096.5 CA_2 \sqrt{\frac{P_t}{w}}$$

FIGURE 3-24



If a static pressure is taken inside of the pipe, the following formula is used:

$$Q = 1096.5 CA_2 f \sqrt{\frac{P_s}{w}}$$

In either case, the following values of C for various angles of convergence may be used:

Included Angle	10	12	14	16	18	20
C	.972	.965	.957	.948	.940	.932

3-2.8.2.2.5 Diverging Nozzle

Flow discharged from the end of a pipe entails the loss of the velocity head. A diverging nozzle or diffuser may be used to reduce the velocity head, that is, to convert a portion of the velocity pressure to static pressure. The curves in Figure 3-67 show the static pressure regain for diverging nozzles at the end of a pipe in terms of per cent of the inlet velocity pressure. Only a portion of the theoretical regain will be achieved depending on the nozzle diffusion angle and the area ratio. Any regain achieved in a system outlet is in effect an increased entry pressure.

The following formula may be used for the determination of the static pressure regain:

$$\text{Pipe } \Delta P_s = e \left[1 - \left(\frac{A_1}{A_2} \right)^2 \right] P_{v1} = e \left[P_{v1} - P_{v2} \right]$$

where

ΔP_s = regain or increase in static pressure in larger pipe, inches of water

P_{v1} = velocity pressure in smaller pipe, inches of water (*)
 P_{v1} and P_{v2} in same units as ΔP_s

P_{v2} = velocity pressure in larger pipe, inches of water (*)

A_1 = area of smaller pipe, square feet

A_2 = area of larger pipe, square feet

e = factor representing the efficiency of the conversion

The loss in total pressure may be found by substituting $(1 - e)$ for e in the above.

The above equation, neglecting compressibility effects (Mach Number below 0.5), may be expressed, to keep terms uniform, as in Reference 33, as

$$\Delta P_s = P_{s2} - P_{s1} = \eta \rho \frac{V_1^2}{2} \left[1 - \left(\frac{A_1}{A_2} \right)^2 \right]$$

Square or rectangular cross-section diffusers may have divergence angles between all four walls, or between only two walls. Efficiencies to be expected for such units are shown on the chart in Figure 3-59B.

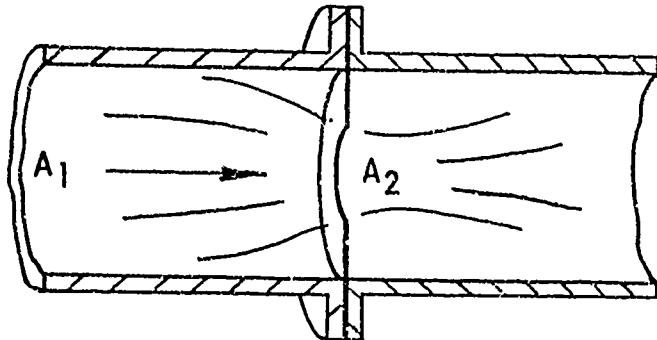


FIGURE 3-25
Orifice Plate in Duct

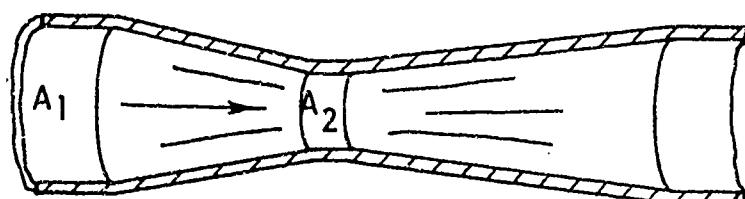


FIGURE 3-26
Venturi Tube

3-2.9.0 Flow Measuring Devices

3-2.9.1 Orifice Plates in Duct (Figure 3-25)

Orifice plates installed in a duct constitute a convenient device for measuring flow. Their application to testing is discussed in Chapter VI.

From Figure 3-25 it may be seen that the stream is subjected to an abrupt contraction followed by an abrupt expansion to the pipe diameter. In cases where the value of the area ratio, A_2/A_1 , is small, the usual orifice coefficients are used. However, as the area ratio approaches unity, the flow conditions are changed considerably.

The coefficients presented in the tabulation of this section were computed from experimental data in Reference 3-11 for pipes three to twelve inches in diameter with area ratios up to 70 percent. For this tabulation

$$\Delta P = C_r \sqrt{\frac{Q}{4005 CA}} \quad \text{and} \quad Q \text{ is cfm}$$

A_2 is orifice area, ft^2
 ΔP is total pressure loss, " H₂O

$$Q = 4005 CA \sqrt{P} \quad P \text{ is static pressure differential}$$

between main pipe ahead of ori-

fice and at vena contracta.

		A_2/A_1	0.1	0.2	0.3	0.4	0.5	0.6	0.7
	3"	C	.619	.631	.653	.684	.728	.788	.880
Pipe	Cr		.875	.773	.675	.587	.508	.425	.354
	12"	C	.610	.620	.637	.663	.700	.756	.846
Pipe	Cr		.881	.777	.674	.584	.503	.427	.359

Straight line interpolation may be used for intermediate pipe sizes. These data are only for orifices within, not at the end of, a pipe.

3-2.9.2 Venturi Meter (Figure 3-26)

The venturi meter, consisting of a gradually contracting, followed by a gradually expanding, section of piping, usually with a short constant diameter between the two, is another device for the measurement of flow through pipes. The venturi meter is treated here and further in Chapter VI.

Although the process is not completely a reversible adiabatic one because of losses due to friction and turbulence, it is nearly so. It may be considered that the gas or other fluid expands adiabatically in the converging section to a lower static pressure and contracts adiabatically in the diverging section. Actually, the losses entailed in the flow through a well-designed venturi meter are as much as approximately twelve per cent of the venturi pressure difference. The throat to pipe diameter ratio is ordinarily 1/2 to 1/3 so that the area ratio is 1/4 to 1/9. The included angle of the converging section should be approximately thirty degrees and that of the diverging section seven to eight degrees for minimum venturi losses.

The formula for flow through a venturi meter, from Reference 3-1, is:

$$Q = 1096.5 CA_2 \sqrt{\frac{P}{w}} \sqrt{\frac{1}{1 - (A_2/A_1)^2}}$$

where

Q = flow, cfm.

C = coeff. of discharge = about 0.98

A_1 = area of pipe, square feet

A_2 = area of throat, square feet

P = pressure difference between pipe and throat, inches of H_2O

w = specific weight of air, #/ft.³

3-2.10.0 Throttling Devices

When a fluid flows from a region of higher pressure into a region of lower pressure through a valve or constricted passage, it is said to be throttled or wiredrawn. Examples: steam through a pressure reducing valve, expansion valve in a refrigerator.

The general equation applicable to throttling processes is:

$$(V_2^2 - V_1^2) / 2g = (h_1 - h_2) J$$

The velocities V_2 and V_1 are practically equal, and it follows that $h_1 = h_2$; i.e., in a throttling process there is no change in enthalpy.

Usually a gas drops in temperature when throttled. This is not universally true. Hydrogen, for example, has a temperature rise for throttling processes over ordinary ranges of temperature and pressure. The inversion temperature, for every gas, is that at which no temperature change occurs during a Joule-Thomson expansion. Below this temperature a gas cools on throttling; above, its temperature rises.

Loss due to throttling - a throttling process in a cycle of operations always introduces a loss of efficiency. There are several throttling devices, two of which will be discussed.

3-2.10.1 Gate Valve

Representing a contraction-expansion throttling loss in which $\Delta P = Kq$, as shown in Figure 3-27, the loss coefficient is tabulated below.

Source: Ref. 3-3

S/D	K
1.0	.00
7/8	.07
6/8	.26
5/8	.81
4/8	2.06
3/8	5.52
2/8	17.00
1/8	97.8

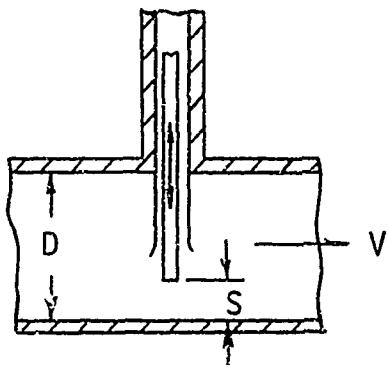
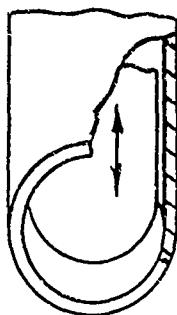


FIGURE 3-27
Gate Valve

q = is determined downstream of the valve

ΔP = pressure loss across the valve

Essentially all duct losses are throttling processes, but a throttle is usually considered for use when a loss is desired.

3-2.10.2 Damper or Butterfly as shown in Figure 3-28, is a throttling means in which: $\Delta P = Kq$, loss coefficient values are tabulated below.

Source: Ref. 3-3

a	K
5°	.24
10°	.52
15°	.90
20°	1.54
25°	2.51
30°	3.91
35°	6.22
40°	10.8
45°	18.7
50°	32.6
55°	58.8
60°	118.0
65°	256.0
70°	751.0

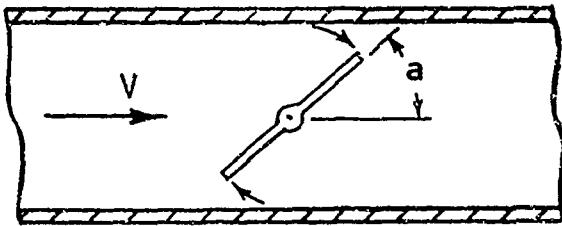


FIGURE 3-28
Damper

q is determined downstream of the damper

3-2.11 Friction Losses

A difference in static pressure is required to cause a fluid to flow through a pipe of uniform cross-section. If the pipe has changing cross-section, the energy due to velocity must also be considered so that for any conduit it can be said that a difference in total pressure is required to cause flow.

Professor Osborne Reynolds was the first to show that there are two very different conditions under which a fluid can flow through a conduit, namely, laminar flow and turbulent flow.

Reynold's explanation of the phenomenon exhibited during his experiments was that at low velocities there was no intermingling of the molecules and the fluid particles moved in parallel layers of laminae; thus, the name laminar flow. At higher velocities there was the intermingling of particles of turbulence.

Critical velocity is that velocity at which there is a transition from laminar to turbulent flow. Critical velocity varies with the fluid and other factors, but even for a specific fluid, critical velocity is a range rather than a definite value.

A dimensionless term, now called Reynolds number, can be used to define the type of flow:

$$R = \frac{VDw}{\mu} * \frac{V}{D}$$

where R = Reynolds Number, dimensionless for any homogeneous system of units

V = average fluid velocity, fps

D = internal pipe diameter, ft.

w = fluid density, lb. mass per ft.³

μ = fluid absolute viscosity, lb. mass per ft. sec.

ν = fluid Kinematic viscosity, ft. ² per sec.

Plots of absolute viscosity and kinematic viscosity for air at various temperatures are presented in Figures 3-71 and 3-72.

In aircraft internal airflow applications, laminar flow is very rarely encountered because of the high Reynold's numbers of the airflow.

Therefore, the loss of pressure caused by friction of the fluid with the walls of the pipe can be expressed as follows:

$$h_f = f \frac{L}{D} \frac{V^2}{2g} = \frac{f}{4} \frac{L}{M} \frac{V^2}{2g} \quad \text{from Reference No. 1}$$

where h_f = static pressure loss, ft. of fluid in uniform duct
 L = length of pipe, ft.
 D = diameter of pipe, ft.
 M = mean hydraulic radius, feet - A/P ; that is, the cross-sectional area divided by the perimeter of the section
 V = velocity, fps
 g = acceleration of gravity = $32.2 \text{ f}ps^2$
 f = friction coefficient, Figure 3-70

Flow losses in straight ducting may be determined with knowledge of the following factors (from References 3-2 and 3-3).

- a. Weight velocity per unit cross-sectional area
- b. Temperature of air (Stream)
- c. Shape and size of duct cross-section
- d. "Roughness factor" of duct wall
- e. Density of air flowing
- f. Length of duct
- g. Absolute fluid viscosity

In considering the duct cross-section, it is necessary to determine the "equivalent diameter". This number is used to relate losses in round ducts to those of other shapes. The hydraulic radius is defined as the area of flow cross-section divided by the wetted perimeter. In a round pipe of diameter D, the hydraulic radius

$$r = \frac{D^2/4}{D} = \frac{D}{4}$$

and $D = 4r$, where D is the hydraulic or equivalent diameter. Reference No. 3-2 presents the following formulae:

- a. For a round duct, the equivalent diameter is equal to the actual diameter,

$$\Delta P = f \rho v^2 \frac{L}{2D} = \frac{f G^2 L}{2g^2 \rho D} = \frac{.81 f W^2 L}{g^2 \rho D^5}$$

- b. For a square duct, the equivalent diameter is equal to the length of one side,

$$\Delta P = \frac{f \rho v^2 L}{2S} = \frac{f G^2 L}{2g^2 \rho S} = \frac{.50 f W^2 L}{g^2 \rho S^5}$$

c. For a rectangular duct, the equivalent diameter, plotted on Figure 3-68, is:

$$D_e = \frac{2db}{d+b} \quad \text{where } d = \text{depth of rectangle}$$

$$b = \text{width of rectangle}$$

$$\Delta P = \frac{f \rho v^2 L}{4 \left(\frac{db}{d+b} \right)} = \frac{f G^2 L}{4g^2 \rho \left(\frac{db}{d+b} \right)} = \frac{.25 f w^2 L}{g^2 \rho \left(\frac{d^3 b^3}{d+b} \right)}$$

d. For an annular duct

$$D_e = D_o - D_i \quad D_o = \text{outside dia.} \quad D_i = \text{inside dia.}$$

$$\Delta P = \frac{f \rho v^2 L}{2(D_o - D_i)} \quad \frac{f G^2 L}{2 g^2 \rho (D_o - D_i)} \quad \frac{.81 f w^2 L}{g^2 \rho (D_o - D_i)^2 (D_o - D_i)^2}$$

e. Ducts of any cross-section other than square, rectangular or circular.

r = hydraulic radius (sometimes referred to as hydraulic mean depth)

$r = \frac{A}{\ell}$ where A = cross-sectional area, ft.²
 ℓ = length of wetted perimeter, feet

The circular diameter which is hydraulically equivalent to the cross-section under consideration is equal to four times the hydraulic radius. (This diameter is hydraulically equivalent only as concerns friction. Original area must be used in computing velocity.)

$$D = 4r = \frac{4A}{\ell}$$

Therefore,

$$\Delta P = \frac{f \rho v^2 L \ell}{8A} = \frac{f G^2 L \ell}{8g^2 \rho A} = \frac{f w^2 L \ell}{8 g^2 A^3 \rho}$$

Friction factor "f" is given as a function of Reynold's Number R_e for round pipes of different diameters and roughness in Figure 3-69.

$$R_e = \frac{GD}{\mu} = \frac{4GA}{\mu \ell} = \frac{4VA \rho g}{\mu \ell}$$

$$\frac{k}{D} = \frac{k \ell}{4A}$$

Density of air is commonly expressed as a ratio, σ
 where $\sigma = \frac{\text{density of air in duct}}{\text{NACA standard sea level air}}$

and $\sigma' = \left(\frac{519.6}{29.92} \right) \left(\frac{P}{T} \right) = 17.37 \left(\frac{P}{T} \right)$

where P = pressure in inches of mercury absolute

T = temperature in $^{\circ}$ R ($^{\circ}$ F + 459.6 $^{\circ}$)

This may be expressed as

$$\sigma' = .245 \frac{P}{T}$$

where P = pressure, #/Ft.² = 2116 @ sea level

T = temperature in $^{\circ}$ R

Friction factor, f, is plotted as a function of R in Figure 3-70. R, "Reynolds Number", is a dimensionless parameter expressing the tendency toward turbulence in fluid flow. It thus serves as an indication of the types of flow losses that may be expected within any given system. The definitive equation is as follows:

$$R = \frac{GD_e}{\mu} = \frac{g \rho V D_e}{\mu} = \frac{V D_e}{\nu}$$

where G = $\frac{W}{A}$ = weight rate of flow per unit area

W = weight flow, lbs./sec.

A = duct area, square feet

D_e = equivalent diameter

μ = absolute fluid viscosity, #/sec./ft. (Figure 3-71)

ρ = fluid density, slugs/ft.³

V = fluid velocity, ft/sec.

ν = kinematic viscosity, sq. ft/sec. (Figure 3-72)

With these basic parameters determined, and the friction factor charts, the pressure loss for any configuration duct may be determined.

3-2.12 Calculation of Pressure Losses

The previous sections have dealt with the determination of the pressure loss coefficient, K to be used in the formula $\Delta P = \frac{K \rho V^2}{2}$, except where otherwise noted. In this section plots based on these determinations of K are presented in figures, the numbers of which were presented in the individual sections dealing with specific cases.

(Text continued on page III-71).

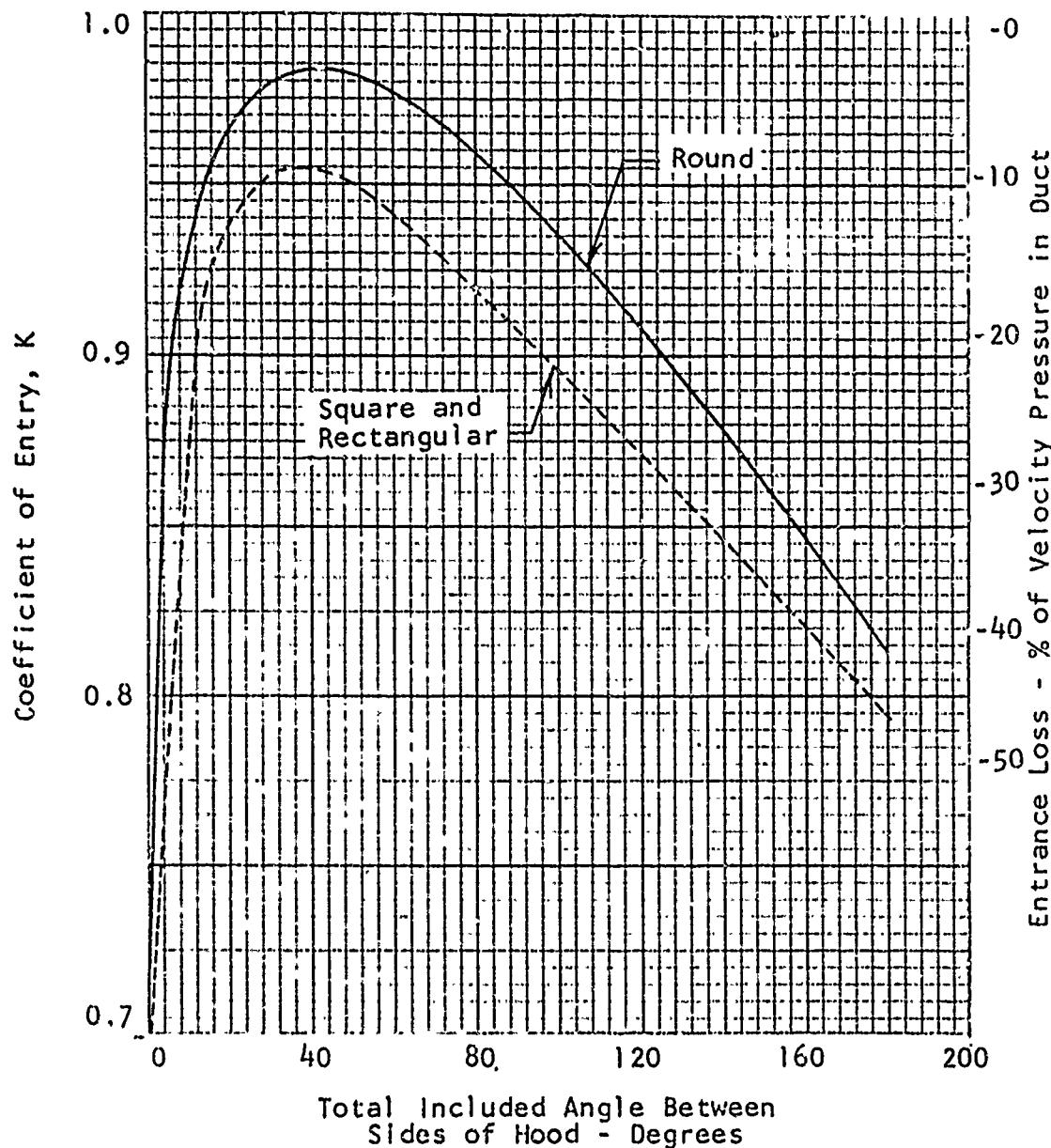


FIGURE 3-29. Effect of the Included Angle in Unflanged Hoods. (Source: Ref. 3-16 by permission from ASHAE. From Energy Losses at Suction Hoods, by Allen D. Brandt and Russell J. Steffy, ASHAE Journal Section, Heating, Piping and Air Conditioning, September 1946.)

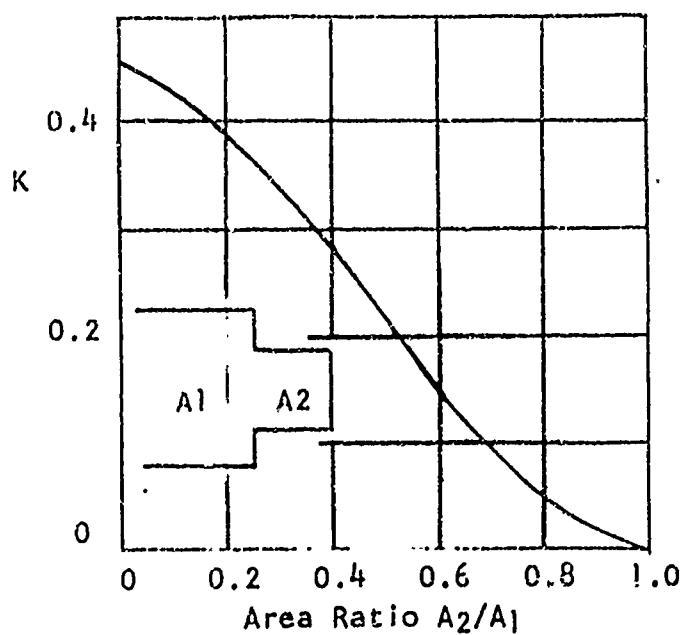


FIGURE 3-30A. Loss Coefficient for Abrupt Contractions. (Source: Ref. 3-3)

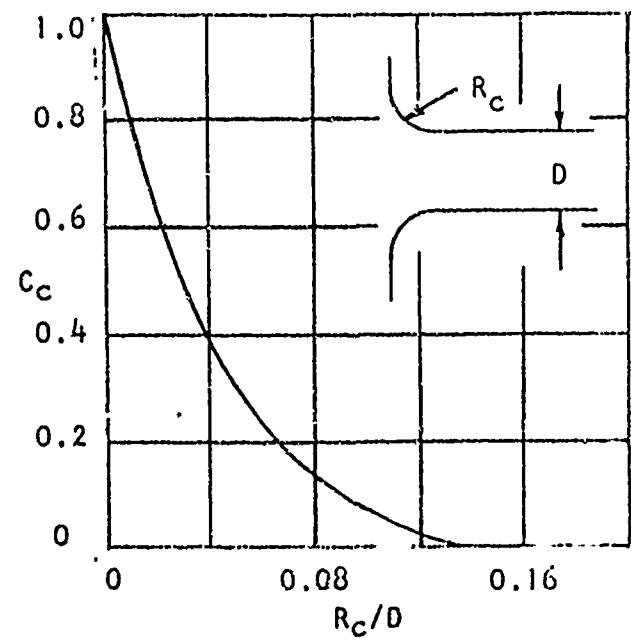
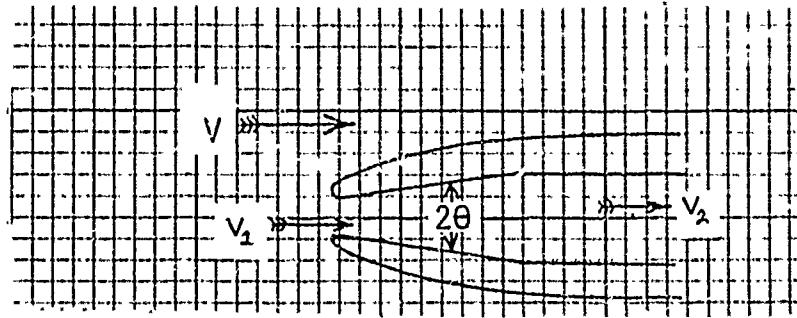


FIGURE 3-30B. Correction Factor for Rounded Entrance. (Source: Ref. 3-3)



$$v > v_1 > v_2$$

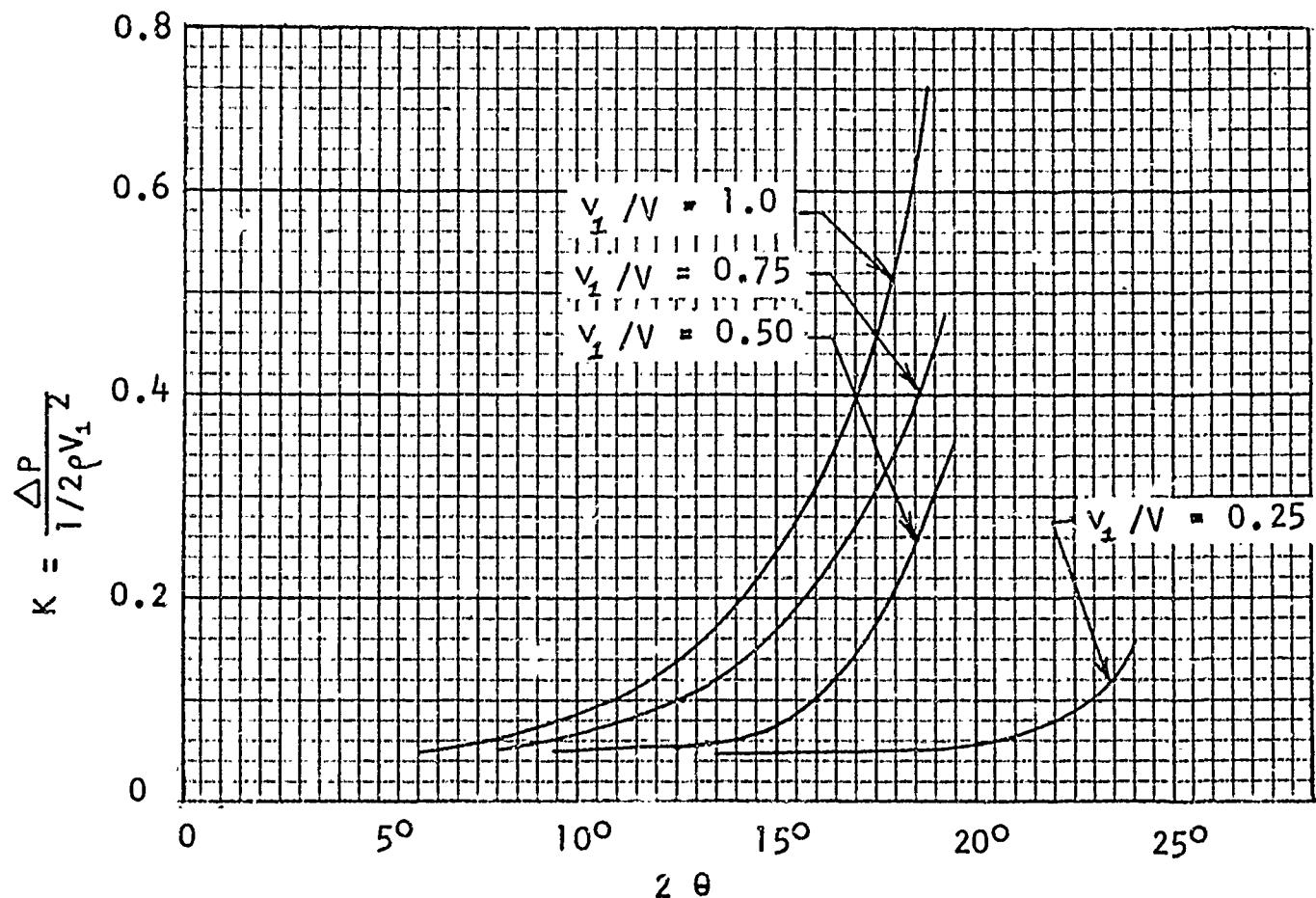


FIGURE 3-31. Variation of the Loss in a Straight Expanding Entry with the Internal (2θ) External (v_1/V) Expansion. (Source: Ref. 3-3)

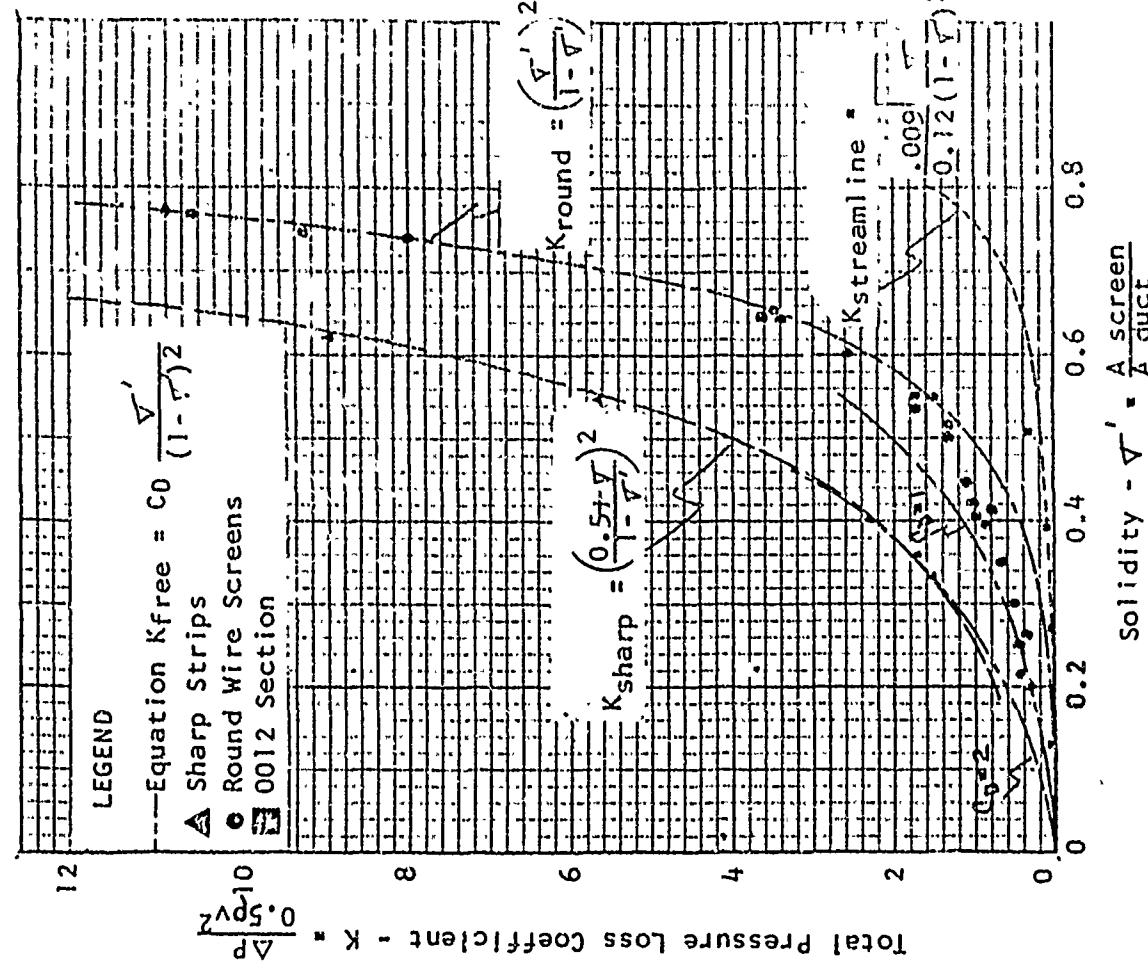
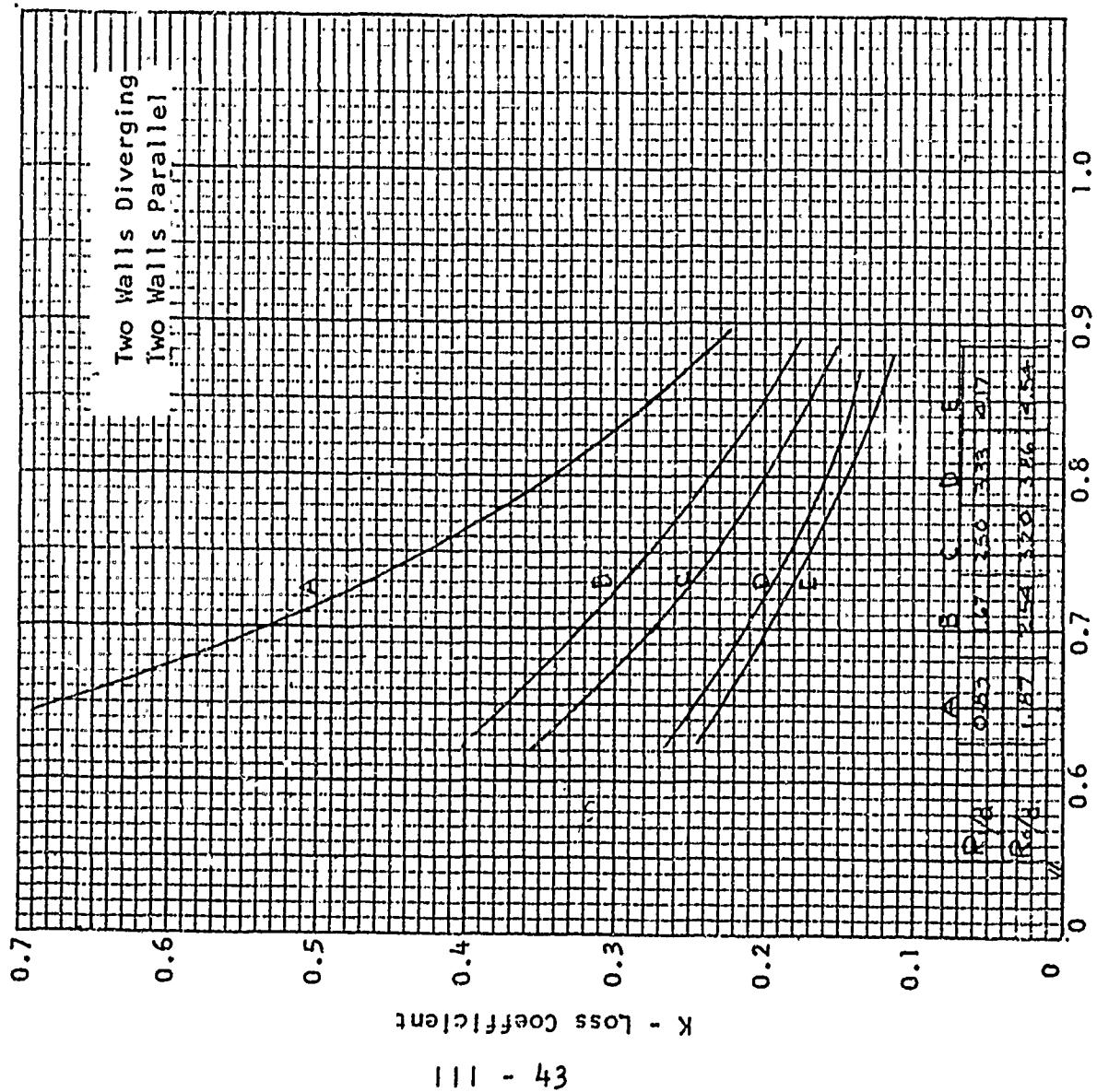
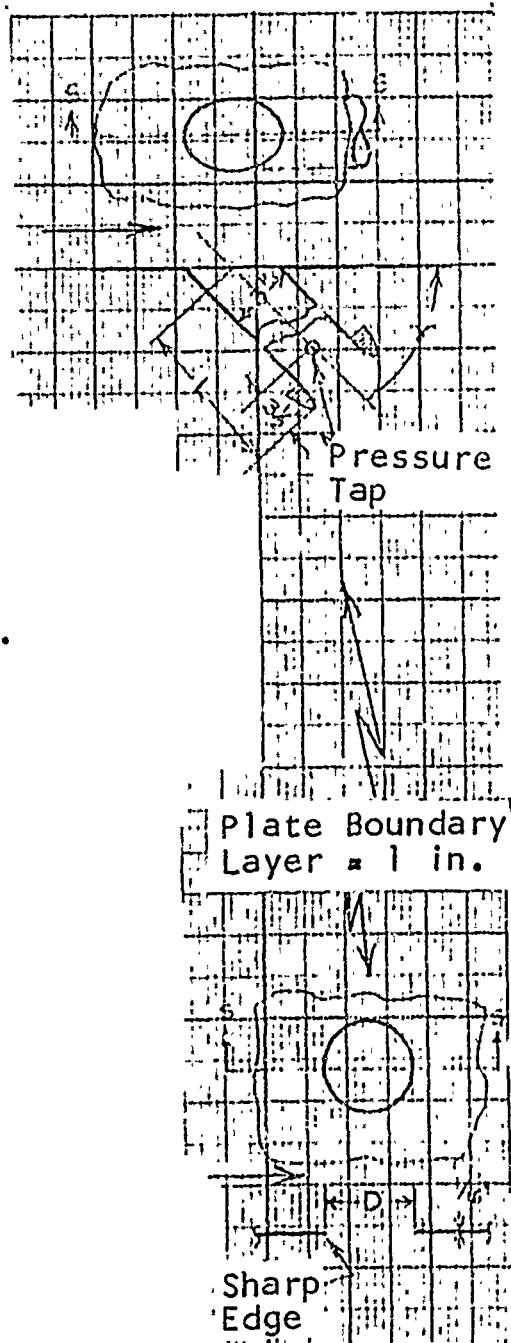
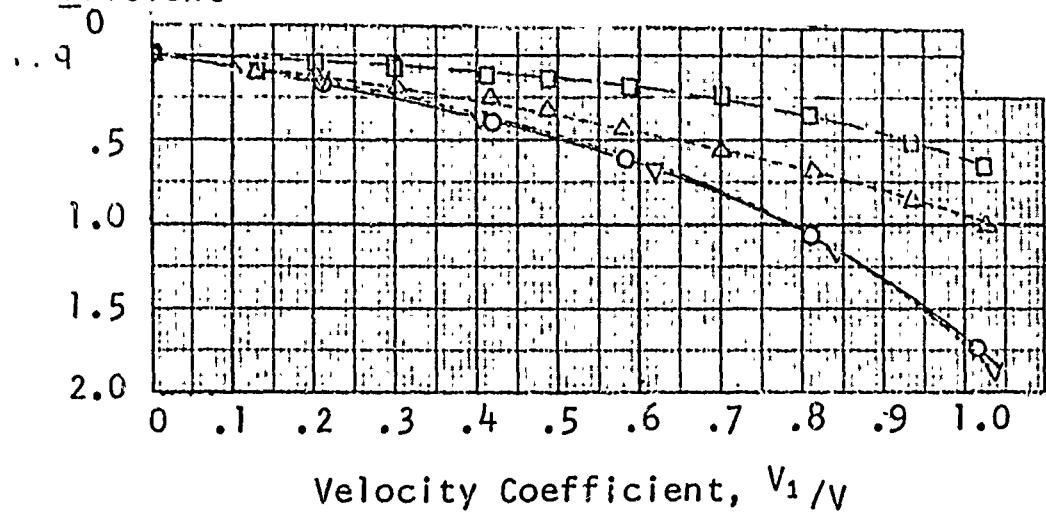


FIGURE 3-32. Dependence of the Loss in a Curved Diffusion on the Rate of Expansion. (Source: Ref. 3-3)

FIGURE 3-33. Pressure Loss Factor for Inlet Screens. (Source: Ref. 3-9 by permission from author and publisher)

	V_1 M.P.H.	A_1 SQ.FT.	$(\frac{A}{A_d})^2$	L, IN.	DEG.
○---3P30-90	40	.0441	1.000	16-3/4	90
△---3P30-60	40	.0441	1.000	13-1/2	60
□---3P30-45	40	.0441	1.000	13	45
×---3P30-90	80	.0441	1.000	16-3/4	90

Static Pressure Loss Coefficient Inlet - Flush Circular Duct in a Flat Plate



Static Pressure Loss Coefficient Inlet - Circular Hole in A Flat Plate

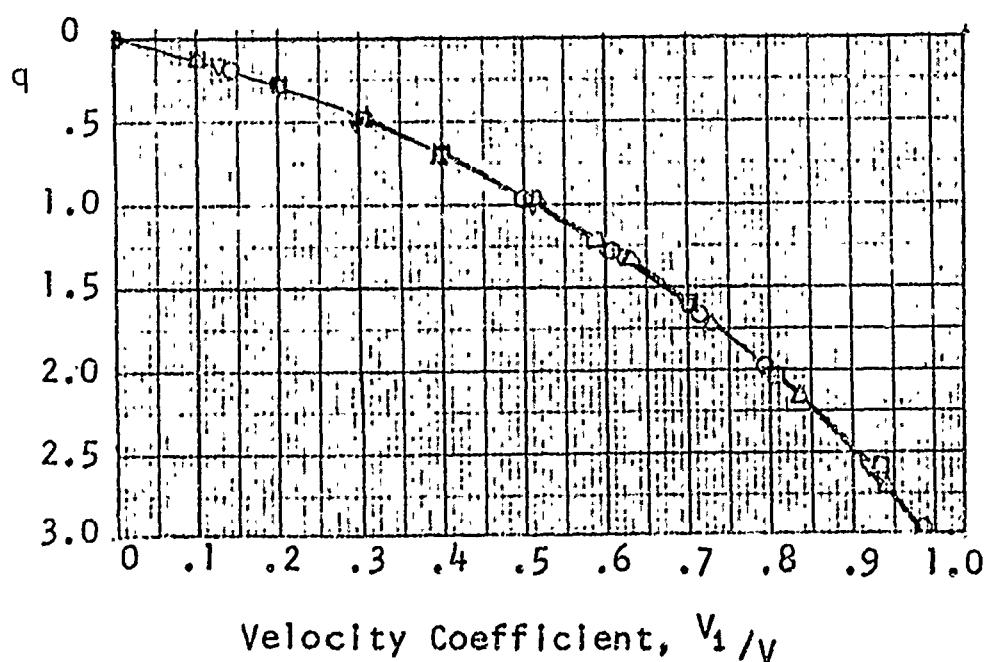
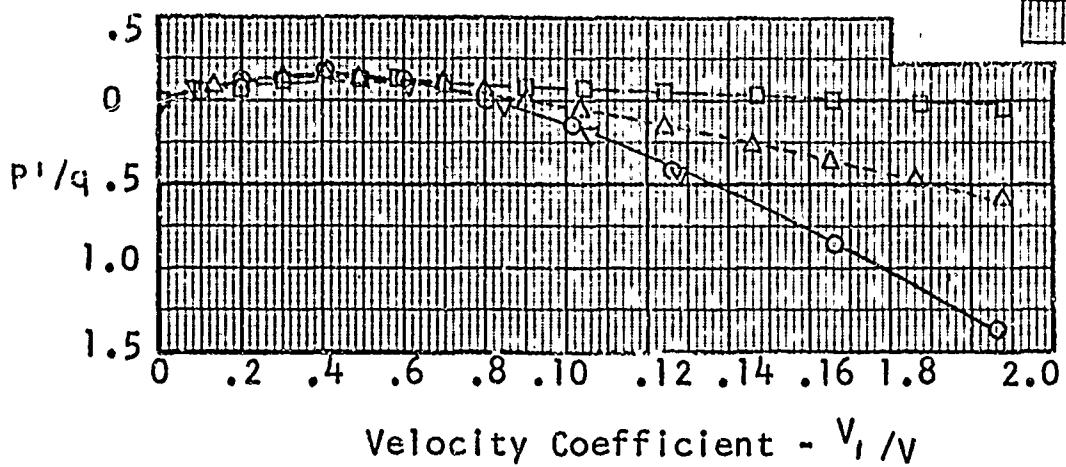


FIGURE 3-34. Inlet Loss Characteristics of a Flush Circular Duct and of a Circular Hole in a Flat Plate. (Source: Ref. 3-10)

	V M.P.H.	A SQ.FT.	$(\frac{A}{A_d})^2$	L IN.	γ DEG
O—3530-90	40	.0441	1.000	16 3/4	90
△---3530-60	40	.0441	1.000	13 1/2	60
□---3530-45	40	.0441	1.000	13	45
▽ 3530-90	80	.0441	1.000	16 3/4	90

Static
pressure
Loss
Coefficient

Outlet - Flush Circular Duct
in a Flat Plate



	V M.P.H.	A SQ.FT.	$(\frac{A}{A_d})^2$	D IN.
O—35200	40	.0229	.000	.2
▽ 35300	40	.0511	.001	.3
□---35200	80	.0229	.000	.2
△---35300	80	.0511	.001	.3

Static
Pressure
Loss
Coefficient

Outlet -
Circular Hole
in a Flat
Plate

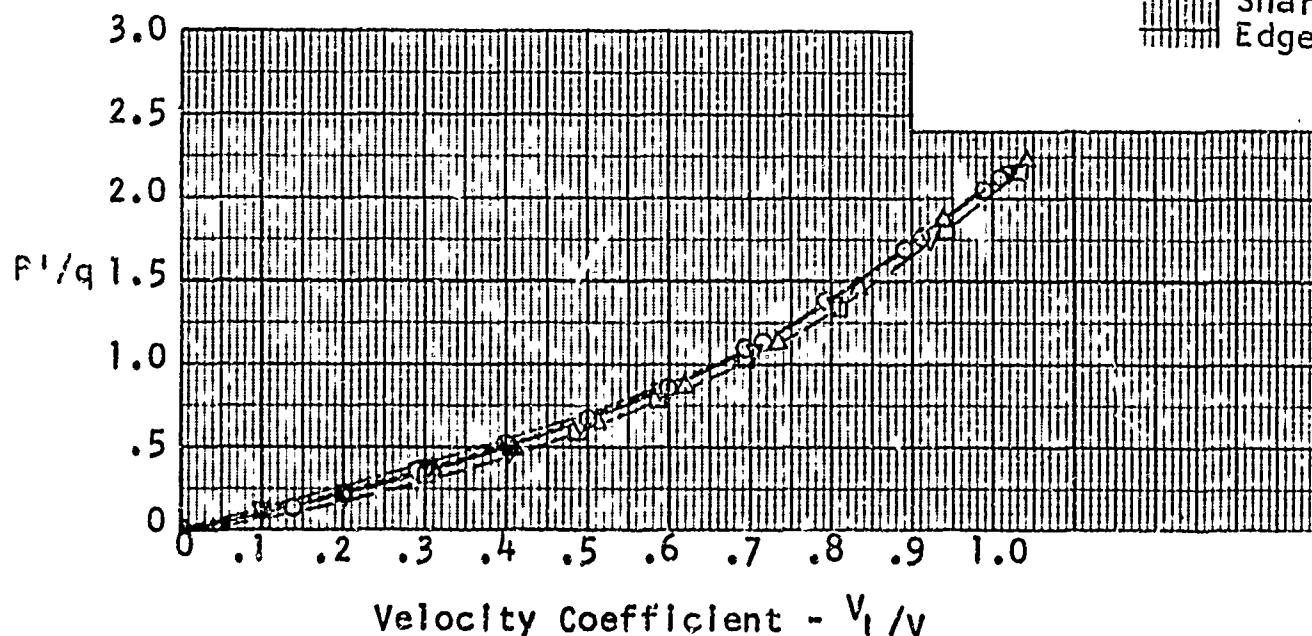


FIGURE 3-35. Outlet Loss Characteristics of a Flush Circular Duct and of a Circular Hole in a Flat Plate. (Source: Ref. 3-10)

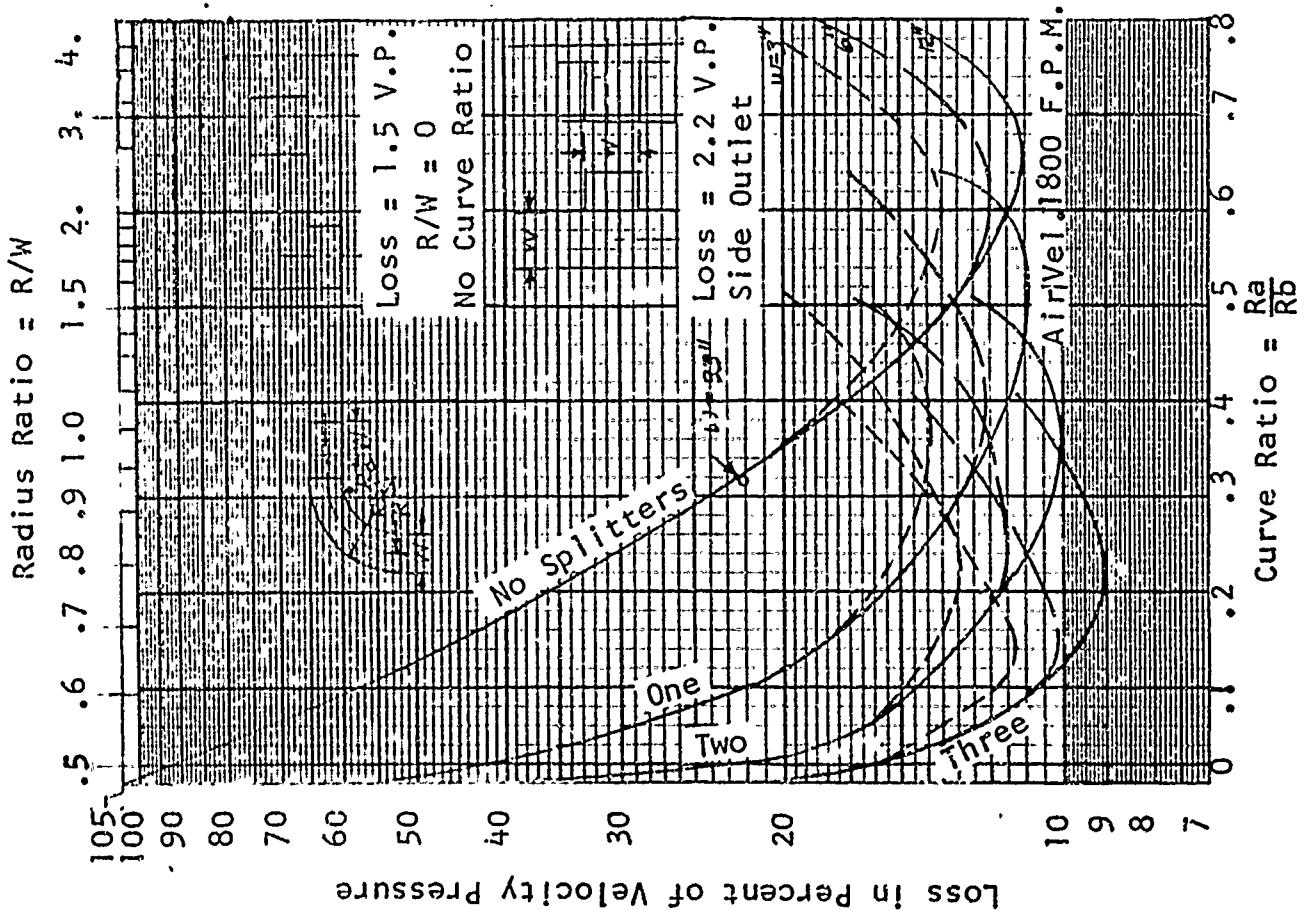


FIGURE 3-36. Loss of Pressure in 90 Degrees Rectangular Elbows With and Without Splitters.
(Source: Ref. 3-17 by permission from ASME)

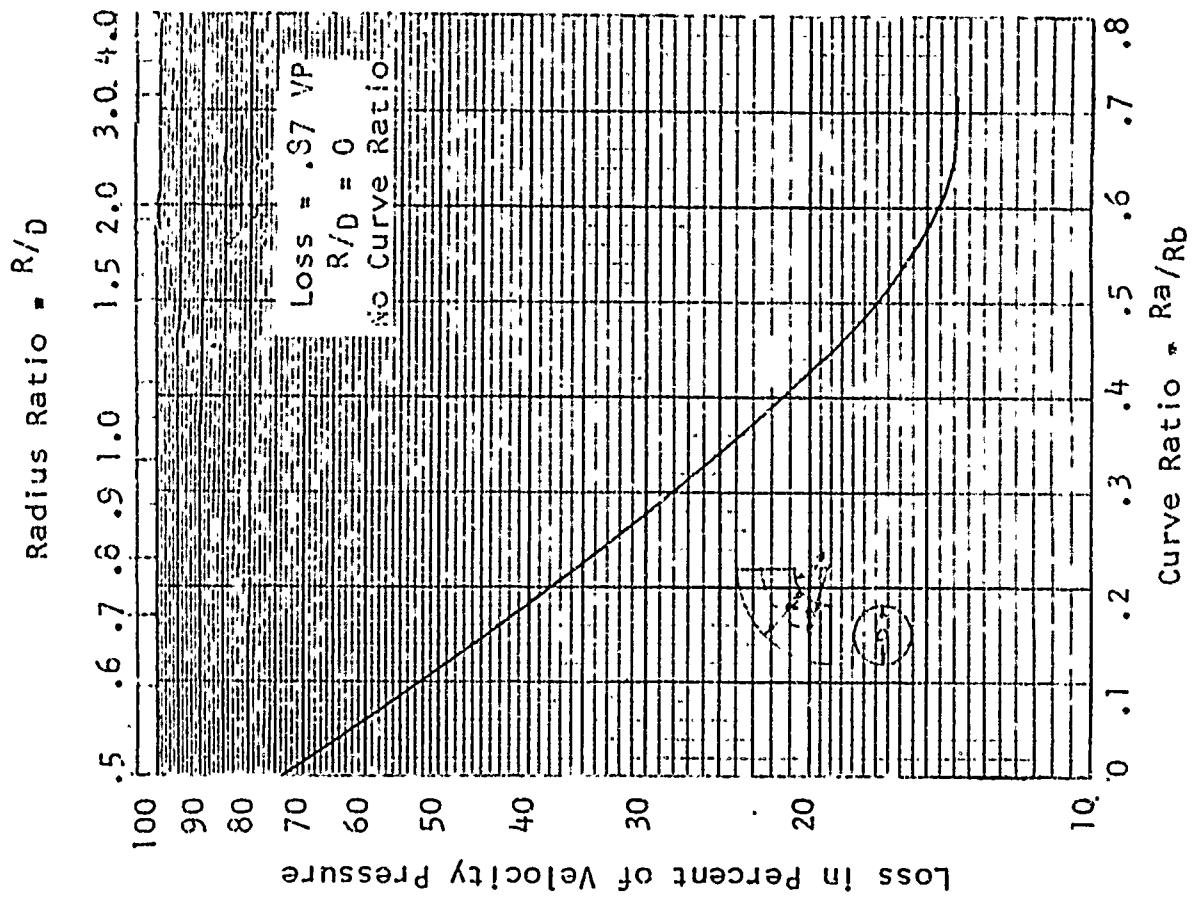


FIGURE 3-37. Loss of Pressure in 90 Degree Round Elbows. (Source: Ref. 3-18)

FIGURE 3-39. Elbow Aspect Ratio Factor vs. Aspect Ratio - w/d
 (Source: Ref. 3-19 by permission from the General Electric Company)

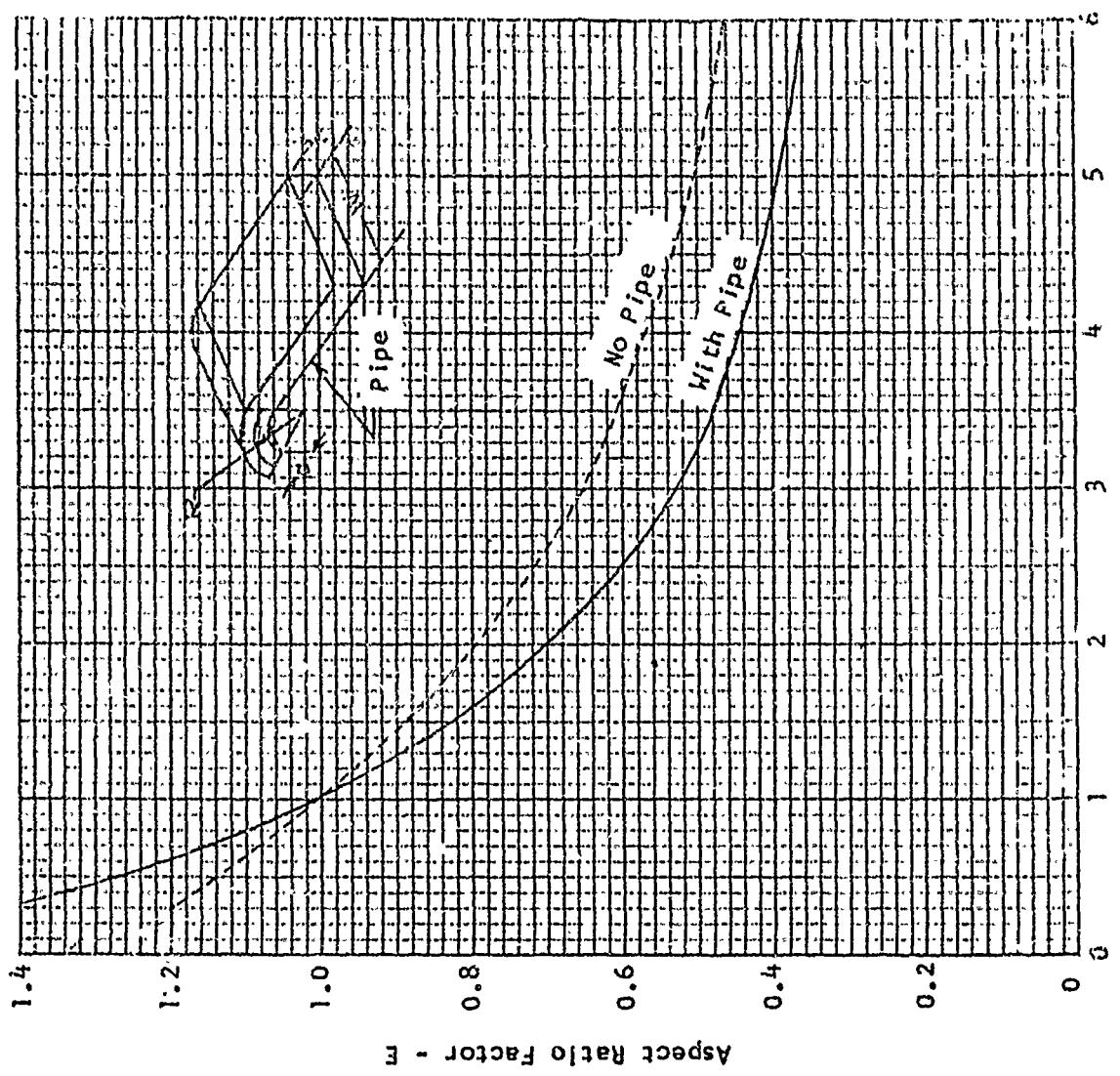
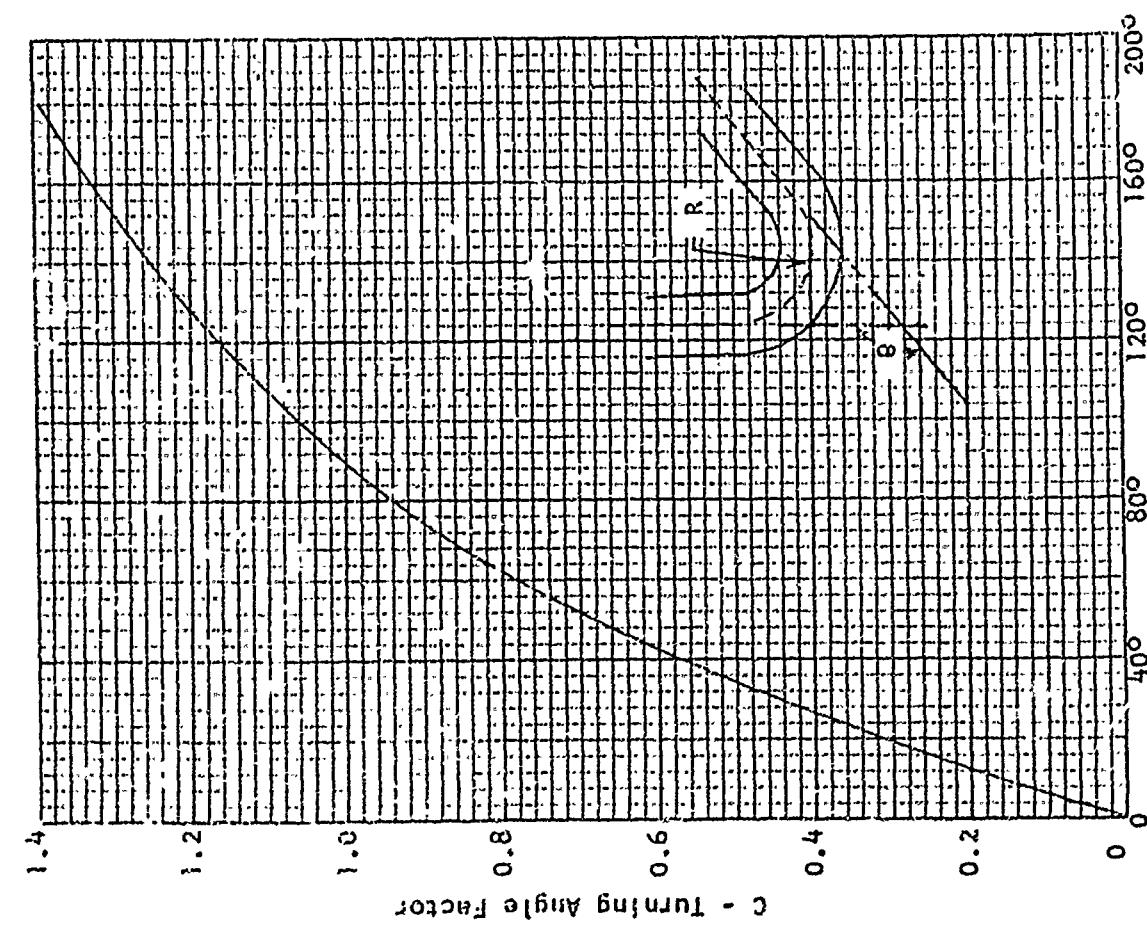


FIGURE 3-38. Elbow Turning Angle Factor vs. Turning Angle. (Source: Ref. 3-3)



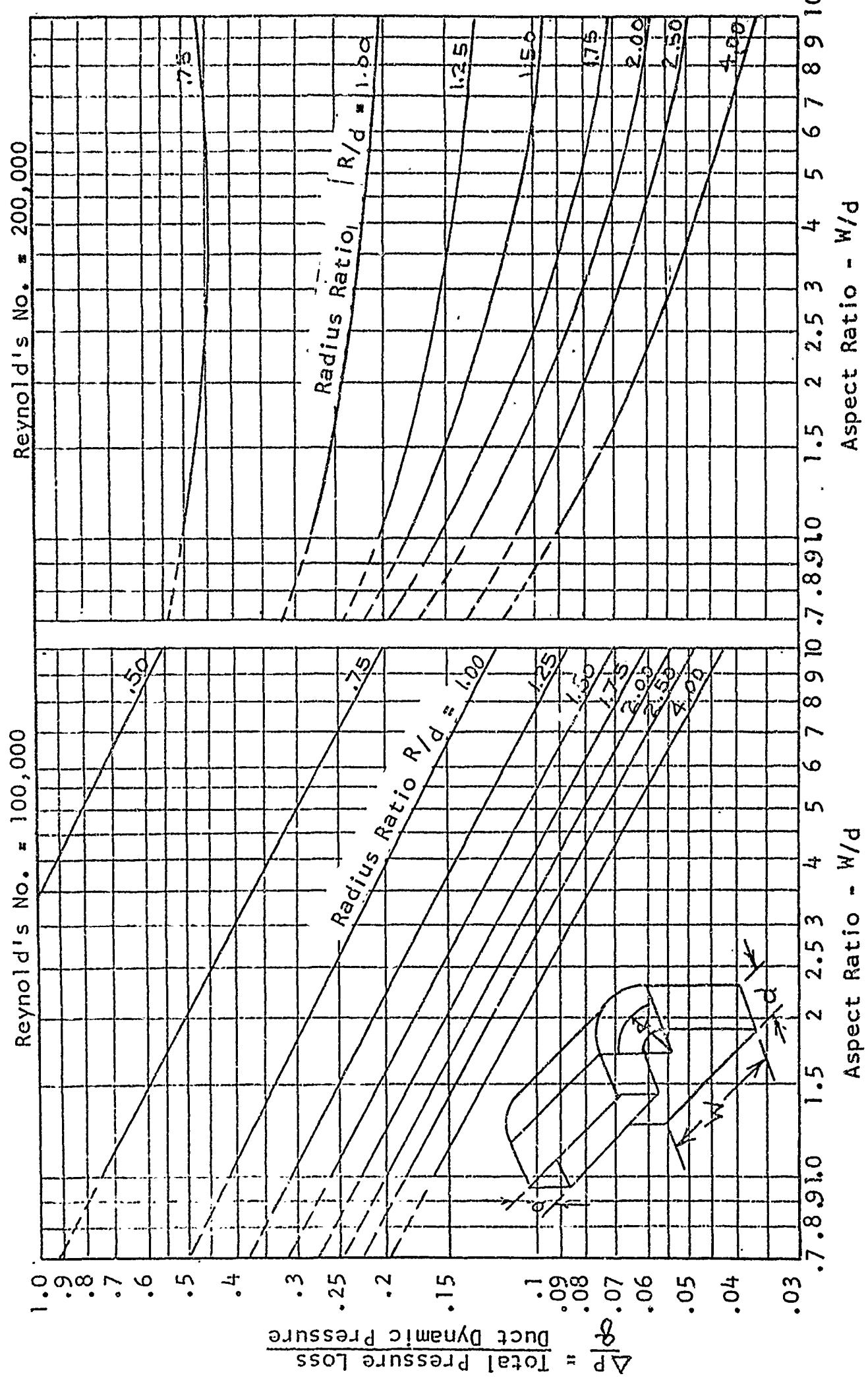


FIGURE 3-40. Total Pressure Loss Coefficients for Rectangular 90° Bends at Reynold's No. of 100,000 and 200,000. (Source: Ref. 3-3)

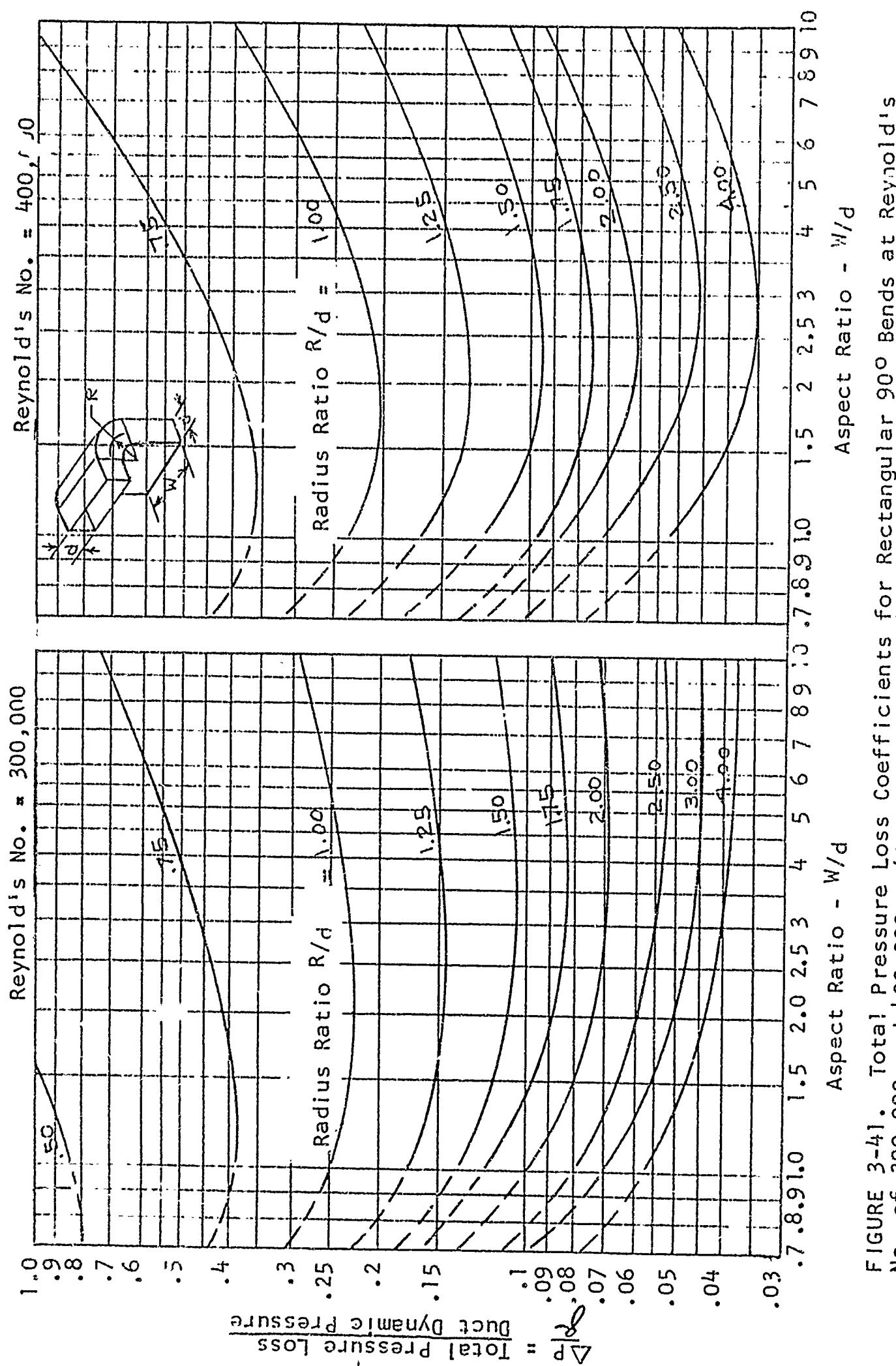


FIGURE 3-41. Total Pressure Loss Coefficients for Rectangular 90° Bends at Reynolds No. of 300,000 and 400,000. (Source: Ref. 3-3)

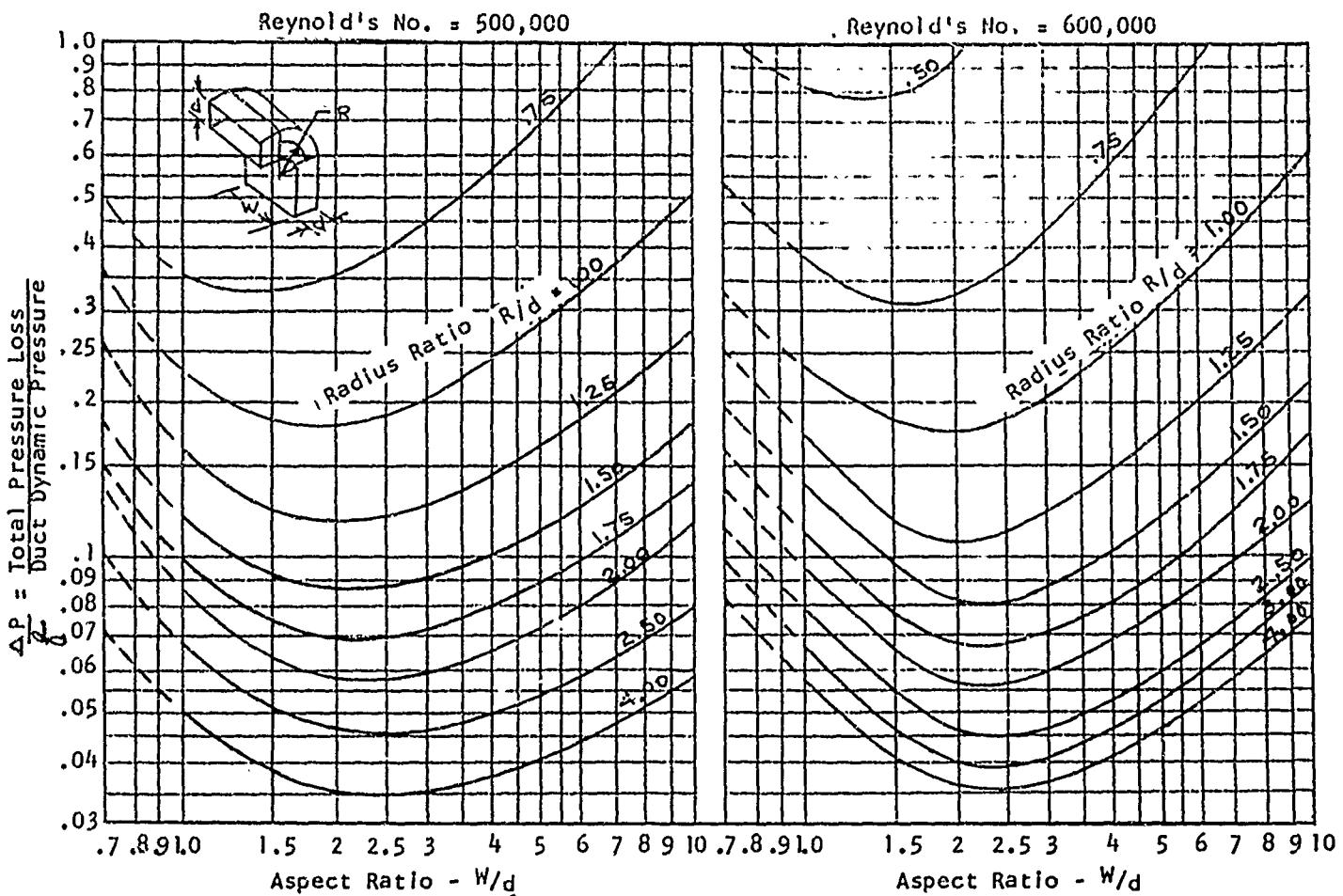


FIGURE 3-42. Total Pressure Loss Coefficients for Rectangular 90° Bends at Reynold's No. of 500,000 and 600,000. (Source: Ref. 3-3)

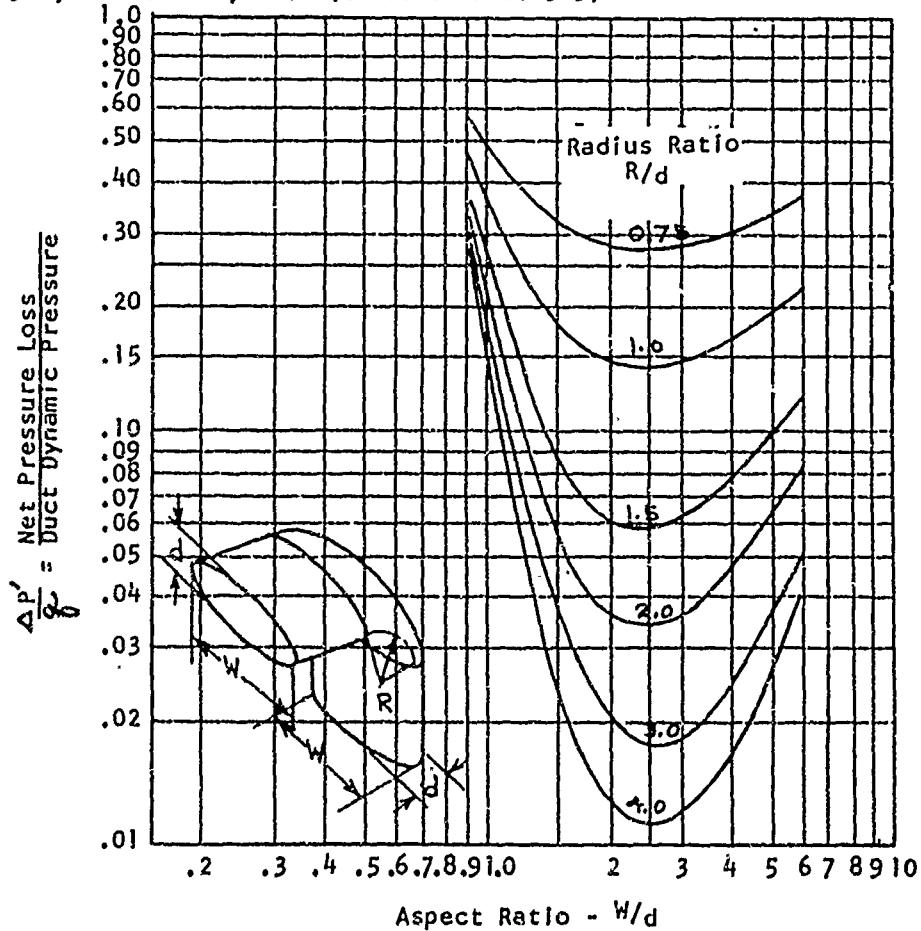


FIGURE 3-43. Net Pressure Loss Coefficients for Elliptical 90° Bends at Reynold's No. of 150,000. Friction Losses Not Included. (Source: Ref. 3-5)

DESIGN HANDBOOK FOR COOLING SYSTEMS AND DUCT SYSTEMS

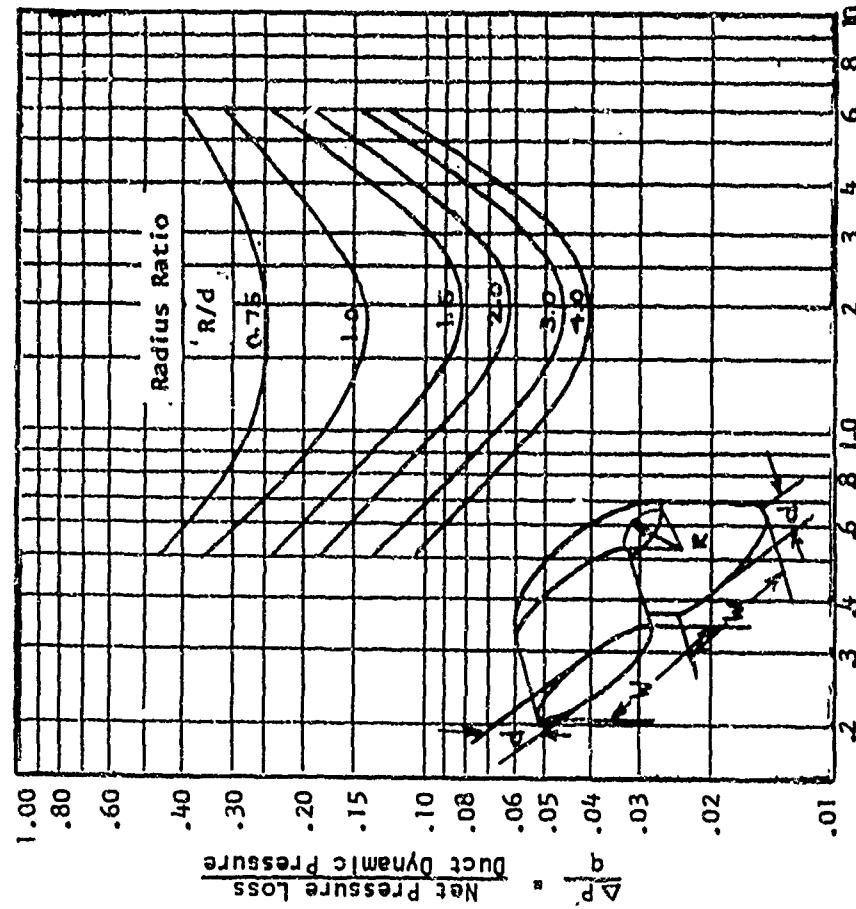


Figure 3-45. Net Pressure Loss Coefficients For Elliptical 90° Bend At Reynold's No. of 600,000. Friction Losses Not Included. (Source: Ref. 3-5)

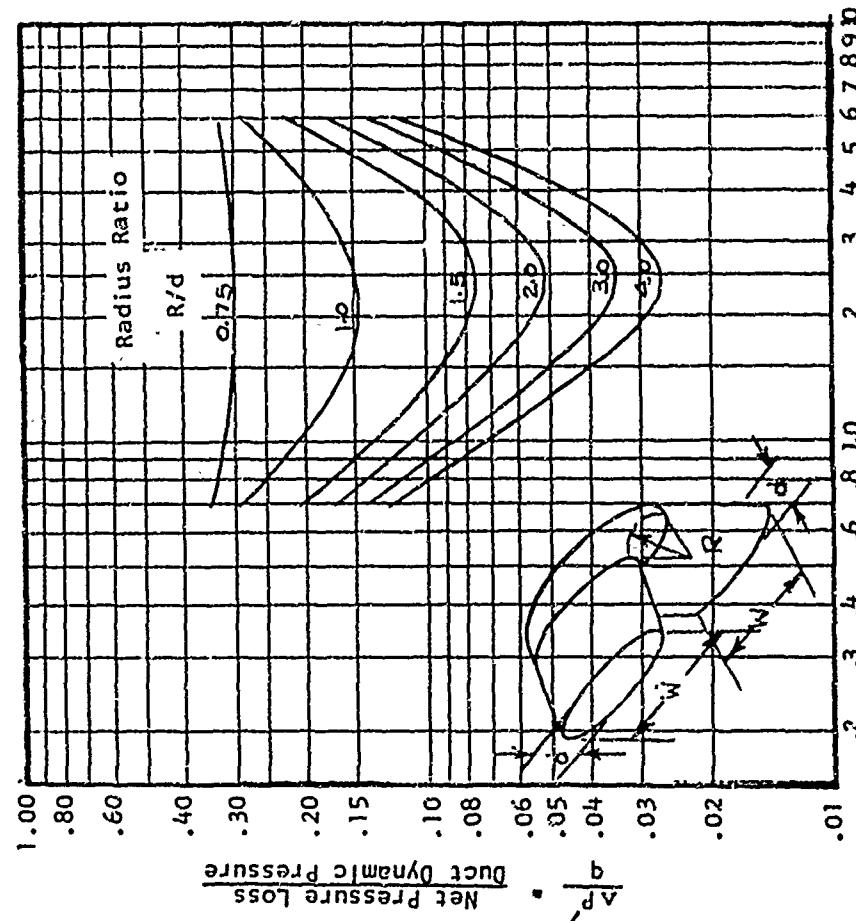


Figure 3-44. Net Pressure Loss Coefficients For Elliptical 90° Bend At Reynold's No. of 300,000. Friction Losses Not Included. (Source: Ref. 3-5)

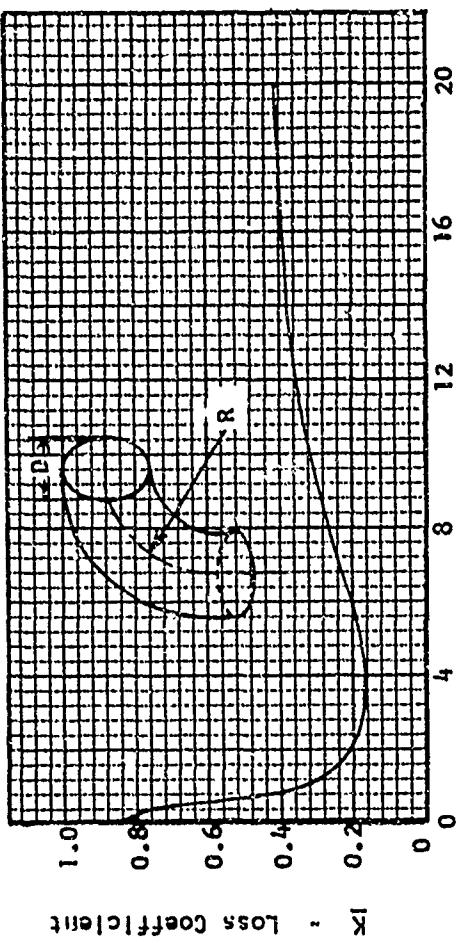


Figure 3-47A. Loss Coefficient For A 90° Bend Of Circular Cross Section
(Source: Ref. 3-3)

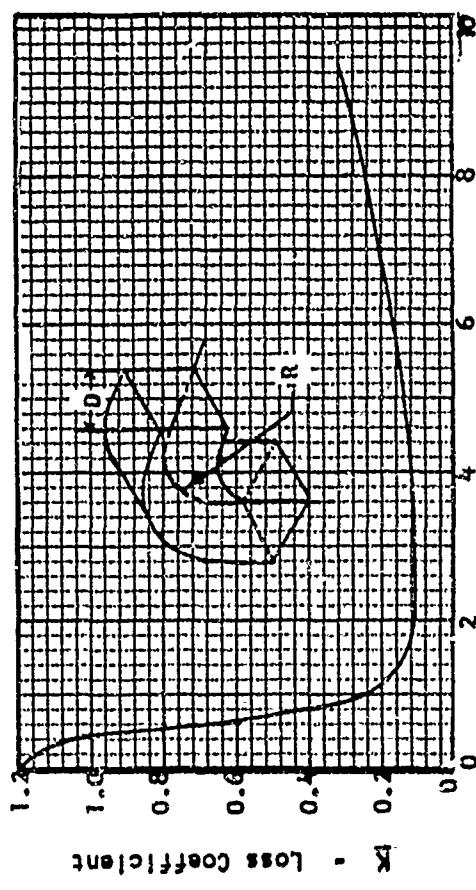


Figure 3-47B. Loss Coefficient For A 90° Bend Of Square Cross Section
(Source: Ref. 3-3)

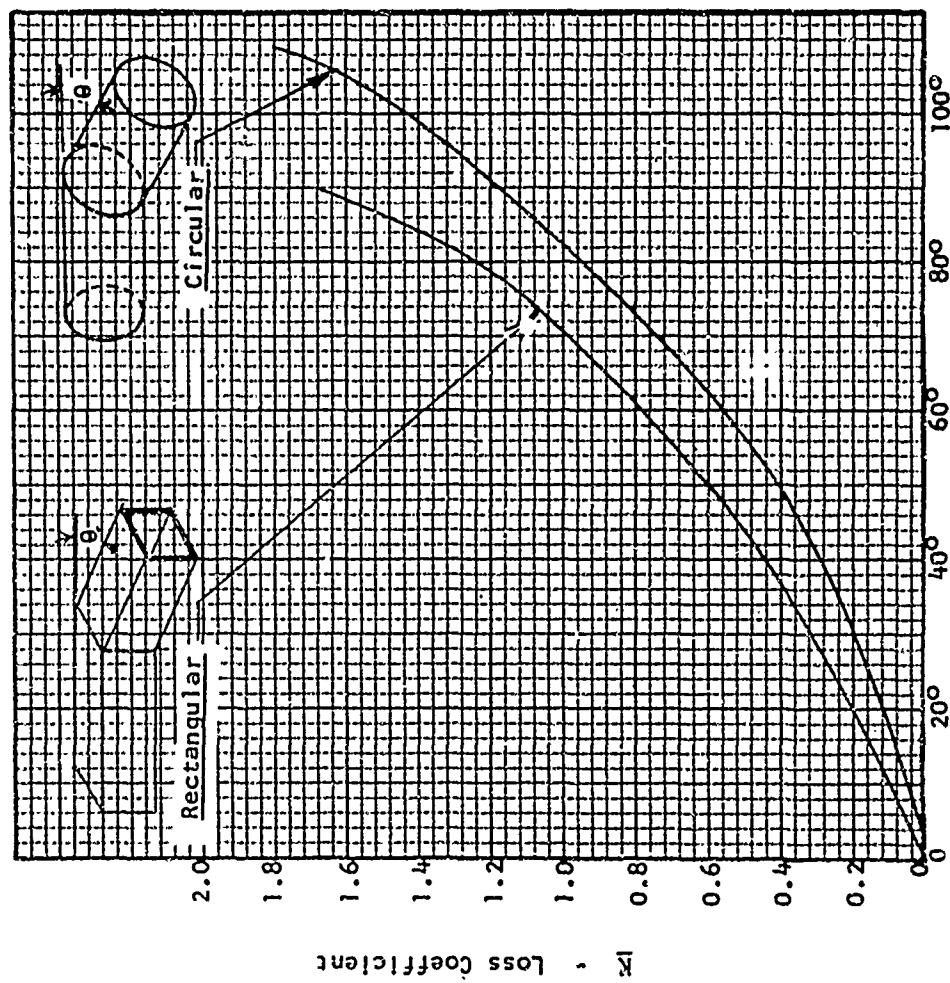


Figure 3-46. Loss Coefficient Versus Turning Angle
For Rectangular And Circular Ducts
(Source: Ref. 3-3)

Elbow	Cross Section	Width Depth	Dimensions (In.)	Area (Sq. In.)	Mean Radius (In.)	Radius Ratio
1	Circular	1	Radius 3	28.2	4.5	0.75
2					9.0	1.5
3					24.0	4.0
4	Elliptical	3	Major Axis 10.5 Minor Axis 3.5	28.2	2.65	0.75
5					5.25	1.5
6					14.0	4.0
7	Elliptical	5	Major Axis 13.25 Minor Axis 2.65	28.2	2.0	0.75
8					4.0	1.5
9					10.6	4.0
10	Square	1	Width 5.125 Depth 5.125	28.0	3.9	0.75
11					7.75	1.5
12					20.75	4.0
13	Rectangular	3	Width 9.1875 Depth 3.06	28.0	2.3	0.75
14					4.6	1.5
15					12.25	4.0
16	Rectangular	5	Width 11.875 Depth 2.375	28.0	1.8	0.75
17					3.56	1.5
18					9.5	4.0

FIGURE 3-48. Dimensions of Elbows (Typical) Tested in Reference 3-5.

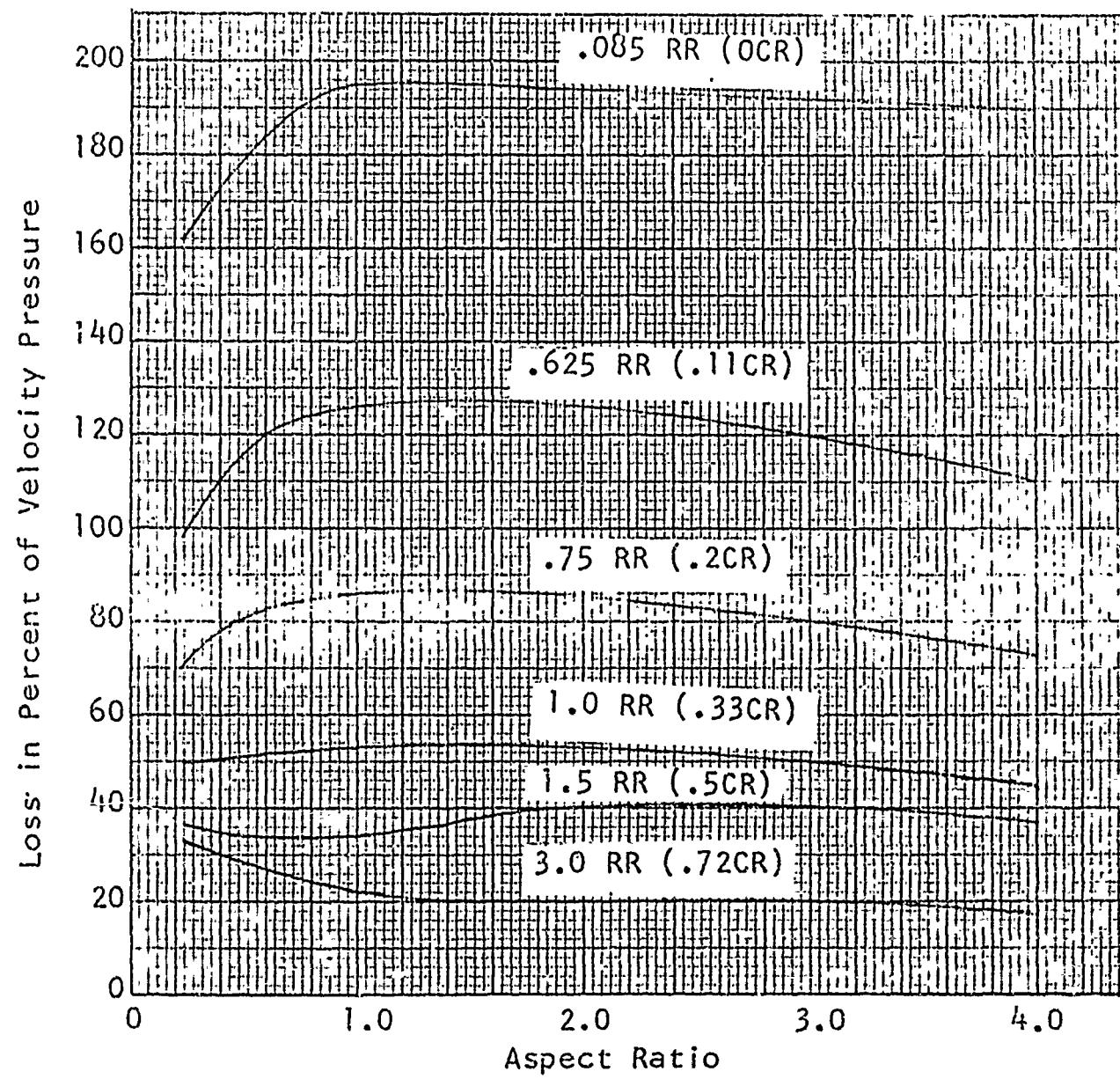


FIGURE 3-49. Pressure Losses in 90 Degree Elbow
Discharging Directly into the Air. (Source: Ref. 3-1
by permission from the editor and publisher)

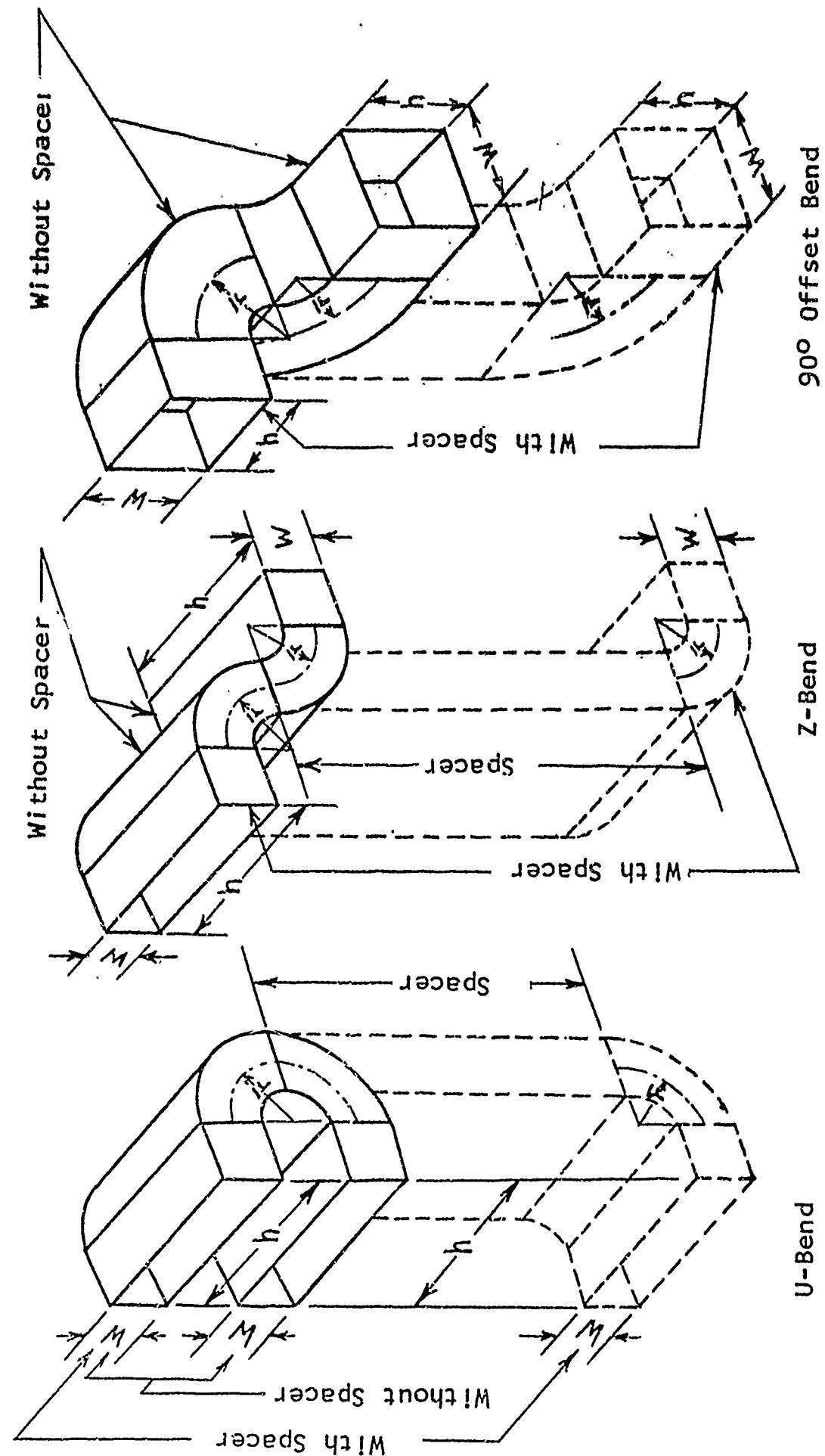


FIGURE 3-50. Sketches of Rectangular Compound Bends. (Source: Ref. 3-5)

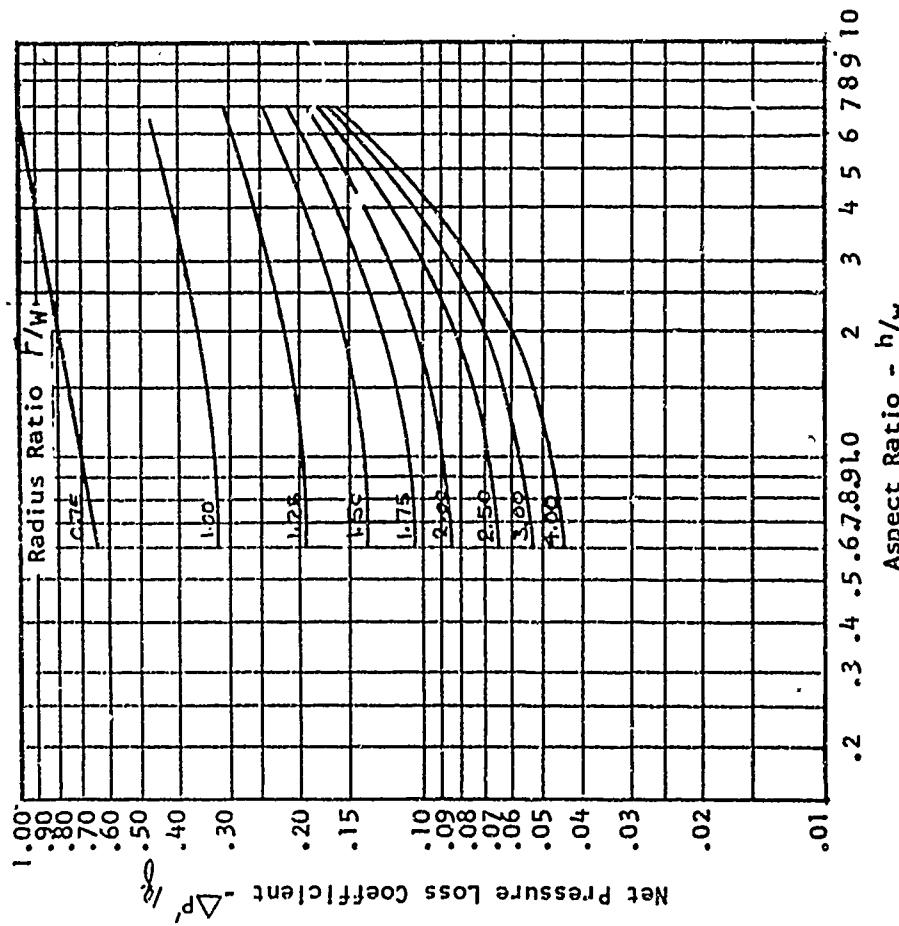
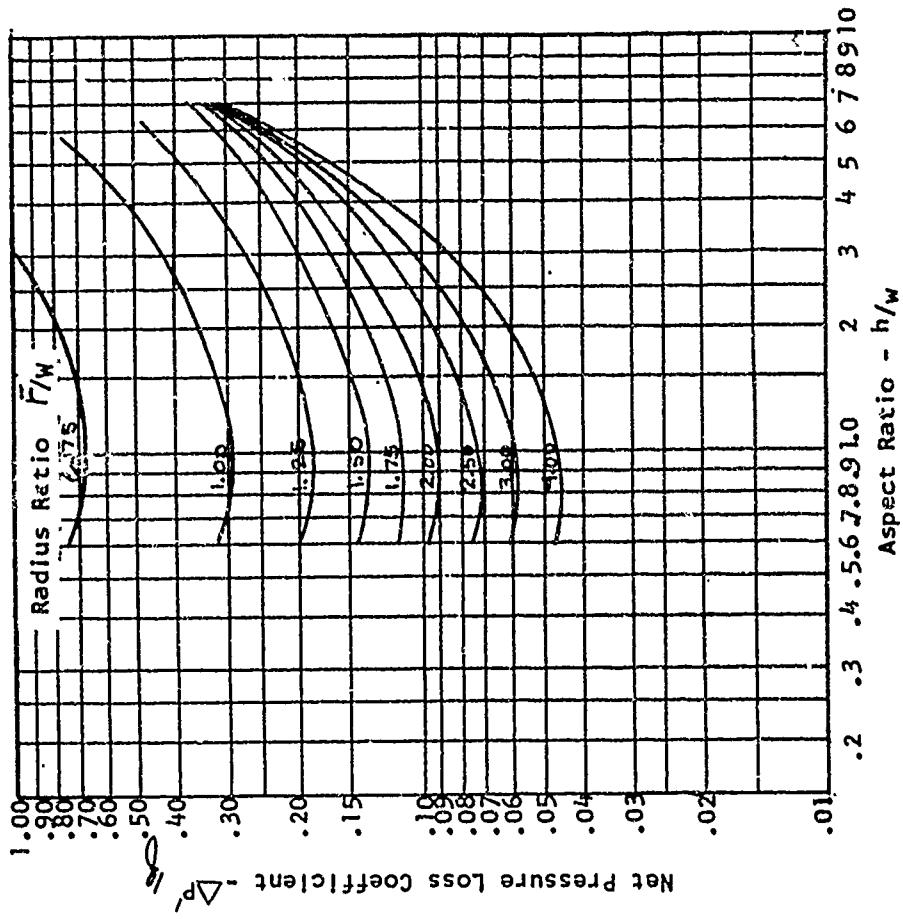


FIGURE 3-52. Net Pressure Loss Coefficients for Compound Rectangular U, Z, and 90° Offset Bends Without Spacers at Reynold's No. of 600,000. Friction Losses Not Included. (Source: Ref. 3-5)

FIGURE 3-51. Net Pressure Loss Coefficients for Compound Rectangular U, Z, and 90° Offset Bends Without Spacers at Reynold's No. of 300,000. Friction Losses Not Included. (Source: Ref. 3-5)

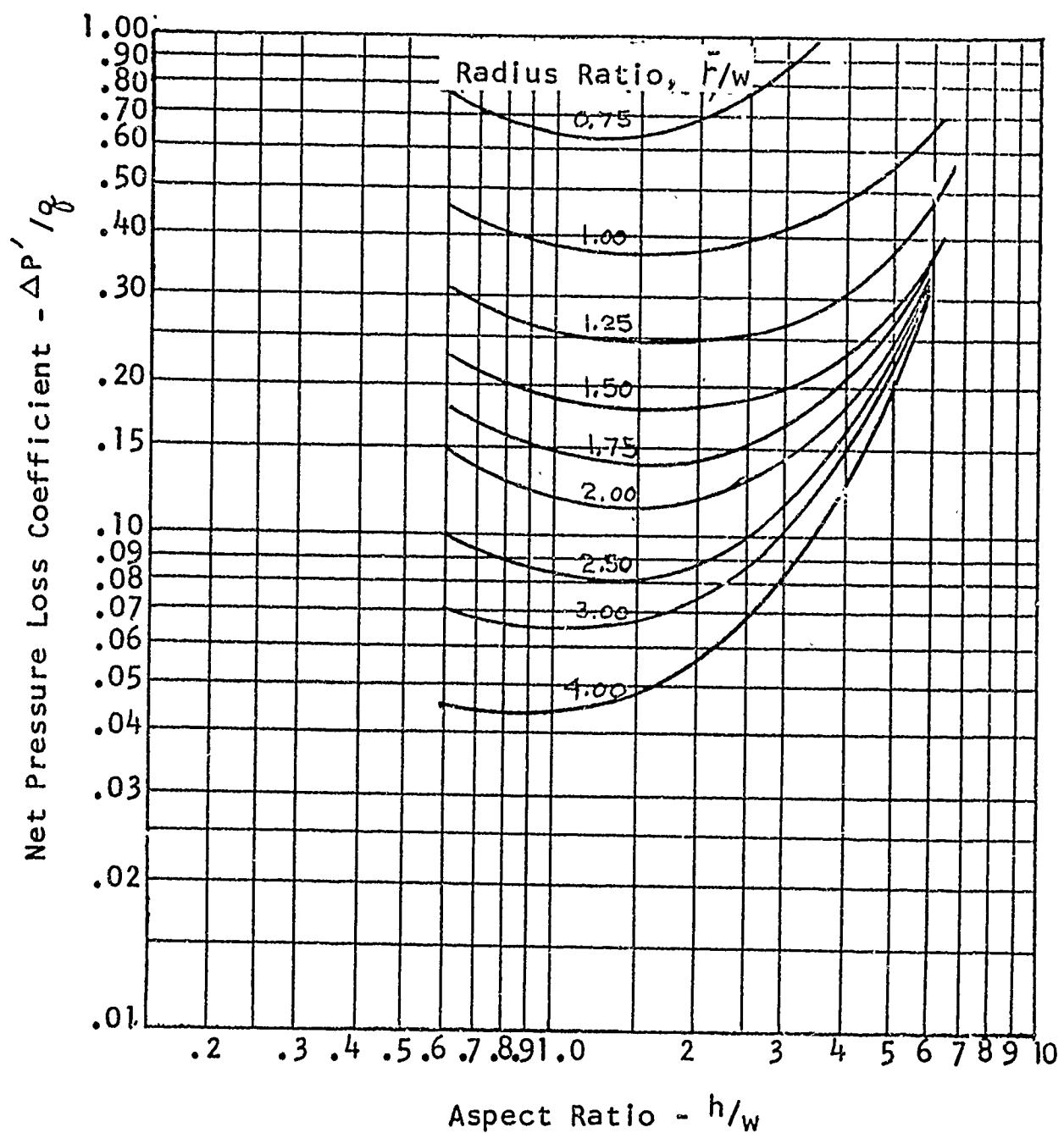


FIGURE 3-53. Net Pressure Loss Coefficients for Compound Rectangular U, Z, and 90° Offset Bends with 5-Foot Spacers at Reynold's No. of 600,000. Friction Losses Not Included. (Source: Ref. 3-5)

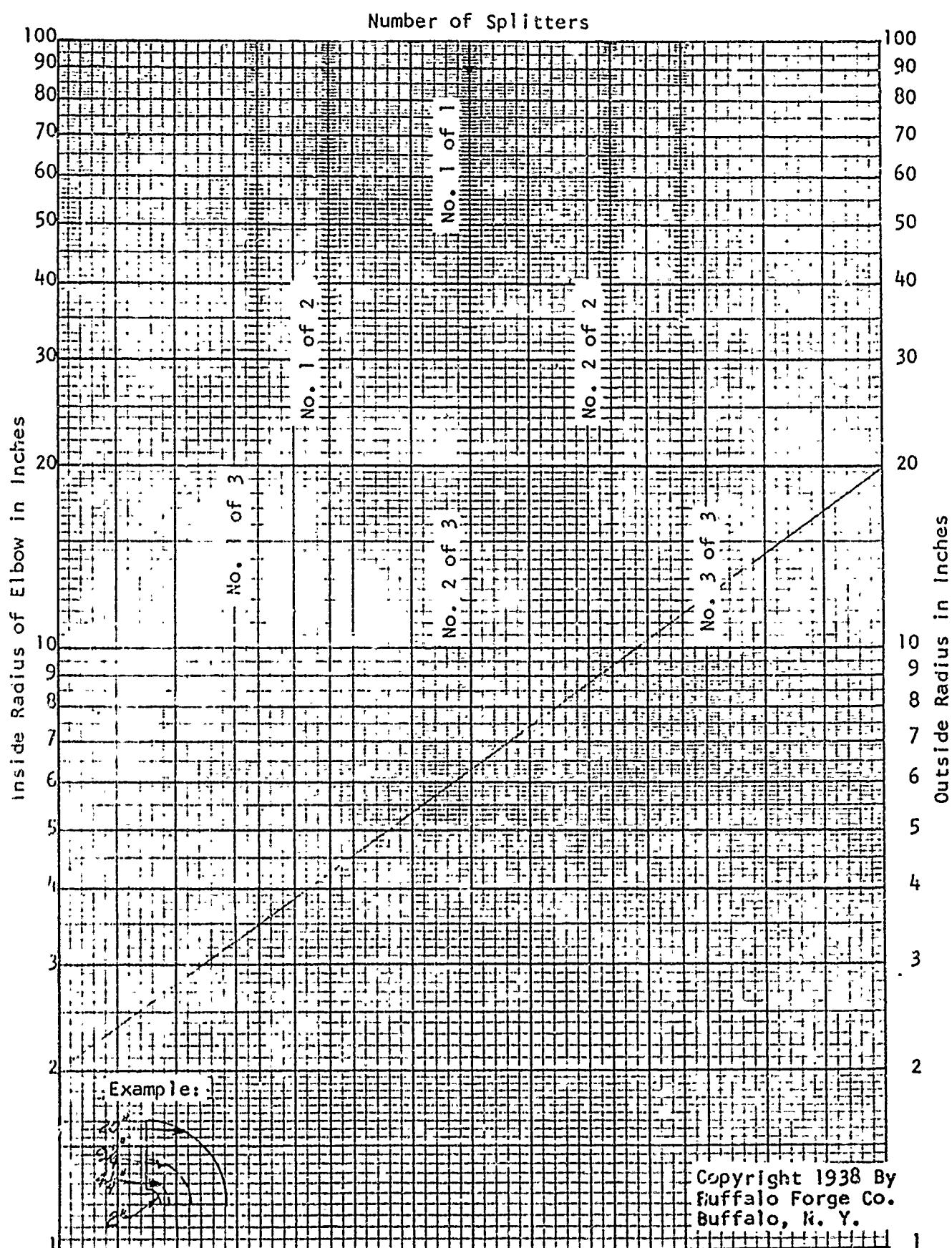


FIGURE 3-54. Chart for Determining the Location of Elbow Splitters in Rectangular Elbows. (Source: Ref. 3-1 by permission from the editor and publisher.)

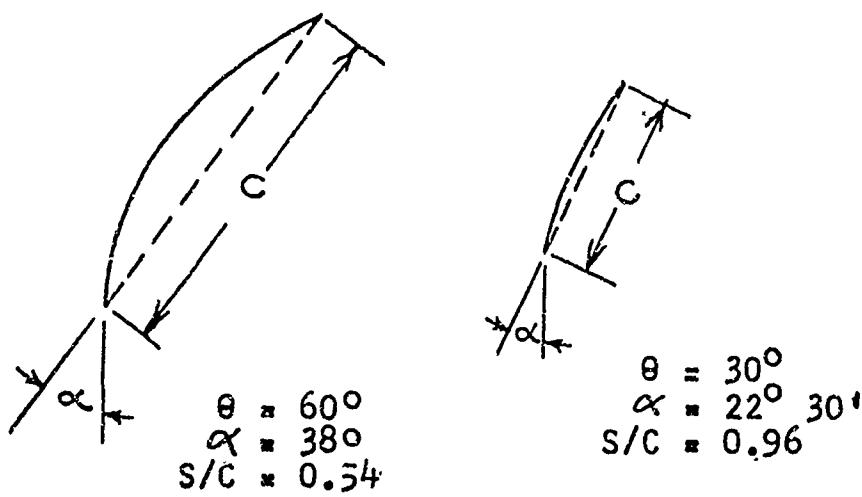
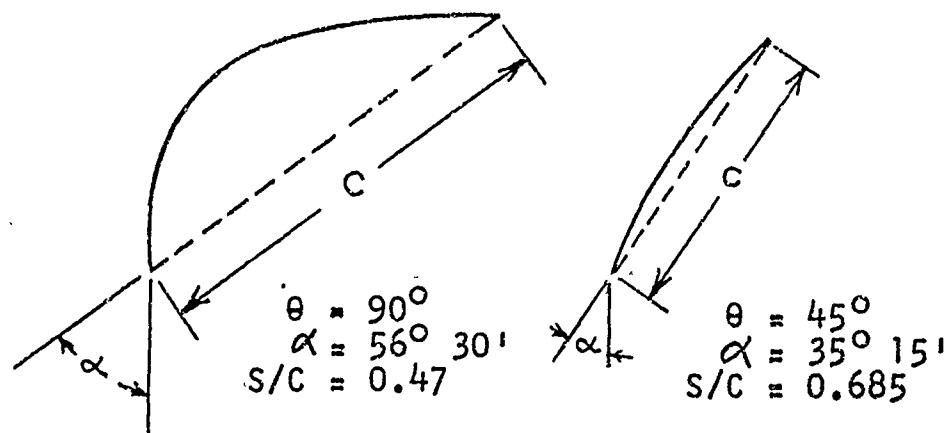
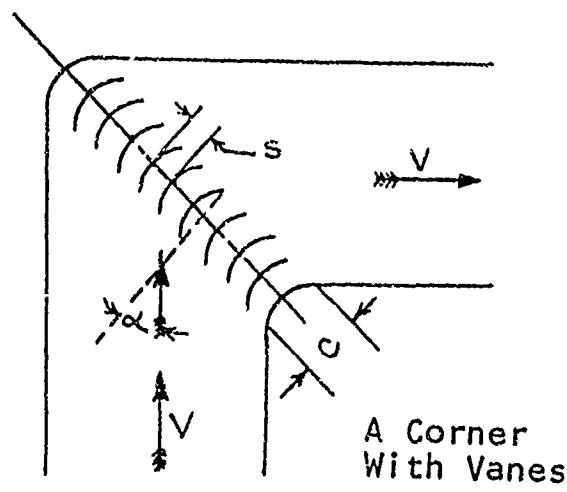
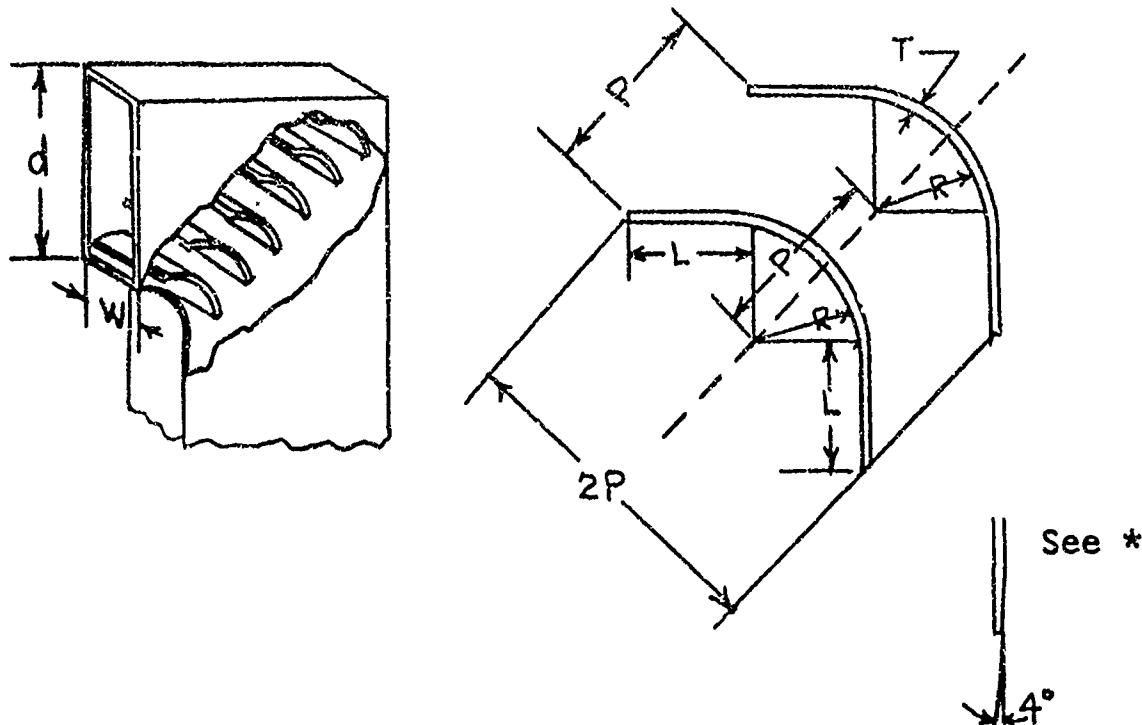


FIGURE 3-55. Design of Turning Vanes.
 (Source: Ref. 3-3)



NOTE: Thin blades are better
if they keep their shape

* Taper thick blades

d = Depth of Duct, Inches
 W = Width of Duct, Inches
 N = Number of Blades
 L = Lip on Blade

$$N = 6 \frac{d}{W} - 1, \text{ Approx.}$$

$$\text{AW} = \text{Axial Width} = \frac{d}{N^{\frac{1}{2}}}$$

$$\text{Pitch} = P = \text{AW} \times 1.41$$

$$\text{Radius} = R = \text{AW} \times 1.28$$

$$\text{Lip} = L = \text{AW} \times .75$$

$$\text{Thickness} = T = \frac{\text{AW}}{16} \text{ or Less}$$

FIGURE 3-56. Design of Blade Elbows. (Source: Ref. 3-3)

Reproduced from G. N. Patterson, Note on the Design
of Corners in Duct Systems, R & M No. 1773.

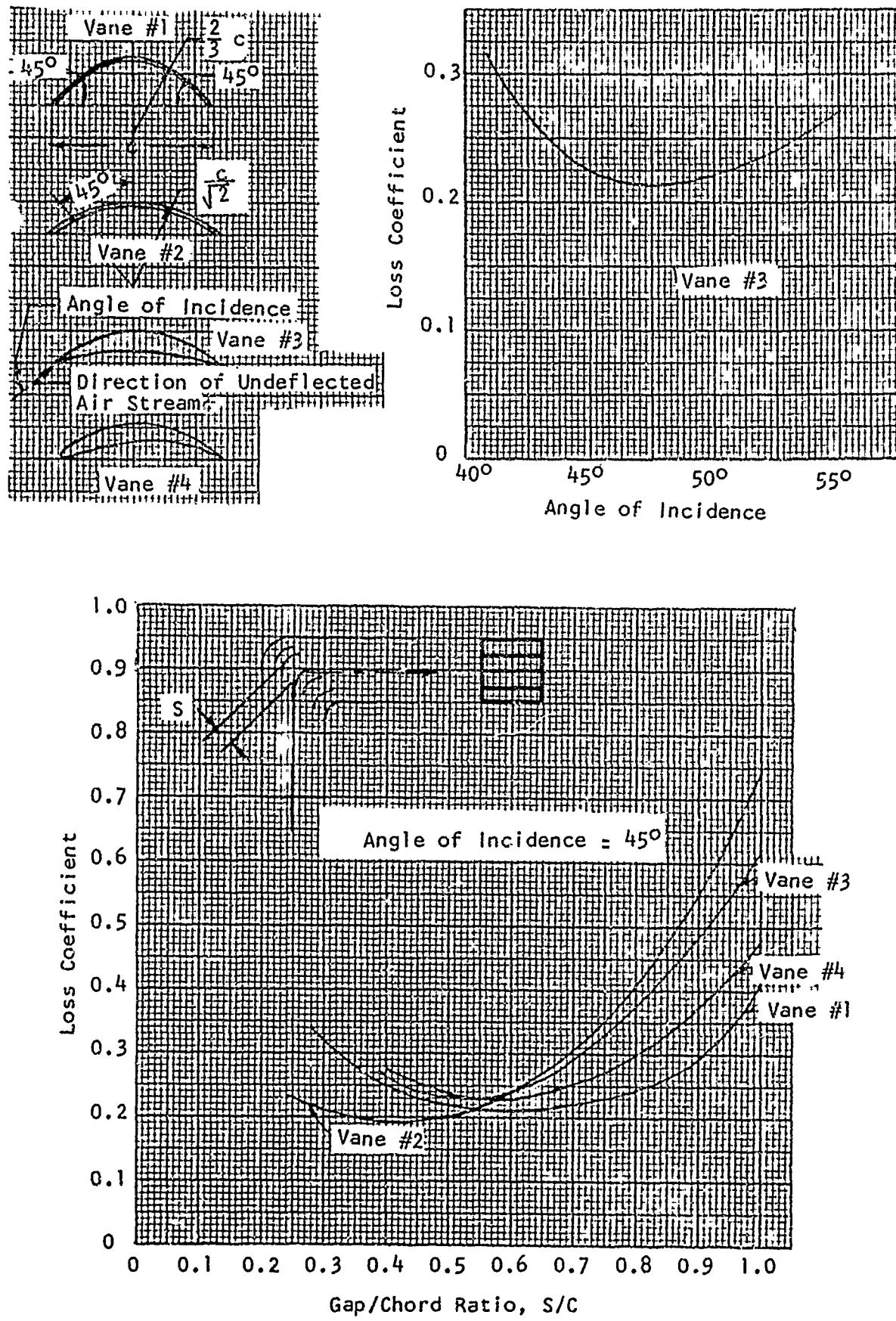
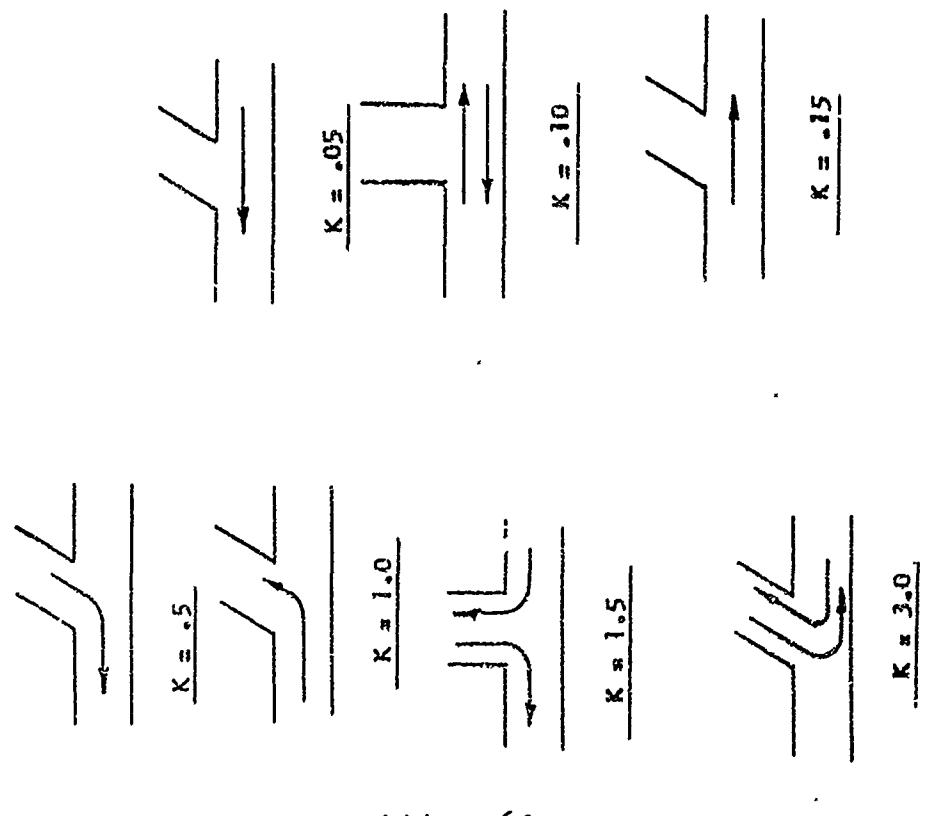


FIGURE 3-57. Loss Coefficient of Vaned Elbows.
(Source: Ref. 3-3)



- 62 -

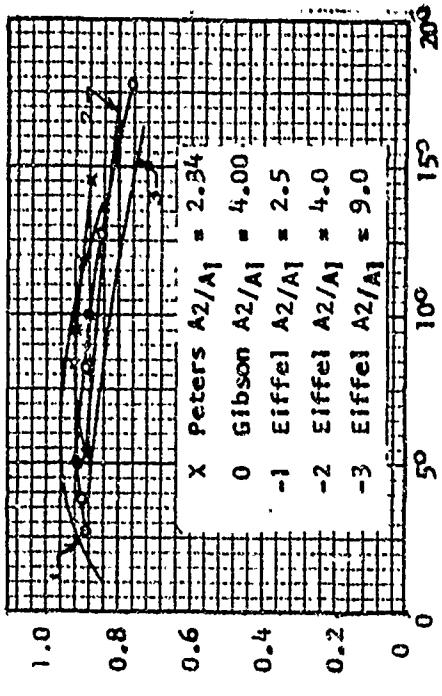


FIGURE 3-59A. Maximum Efficiency of Conical Diffusers

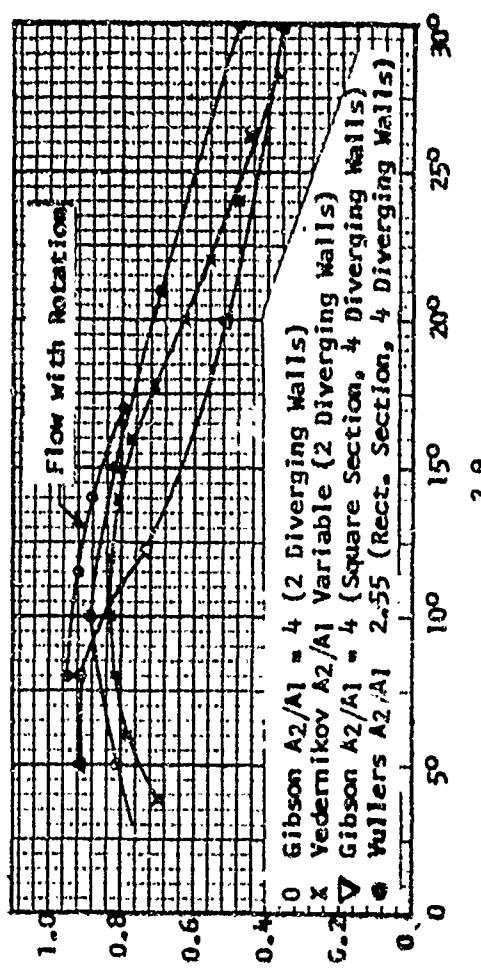


FIGURE 3-59B. Maximum Efficiency of Square Rectangular Diffusers

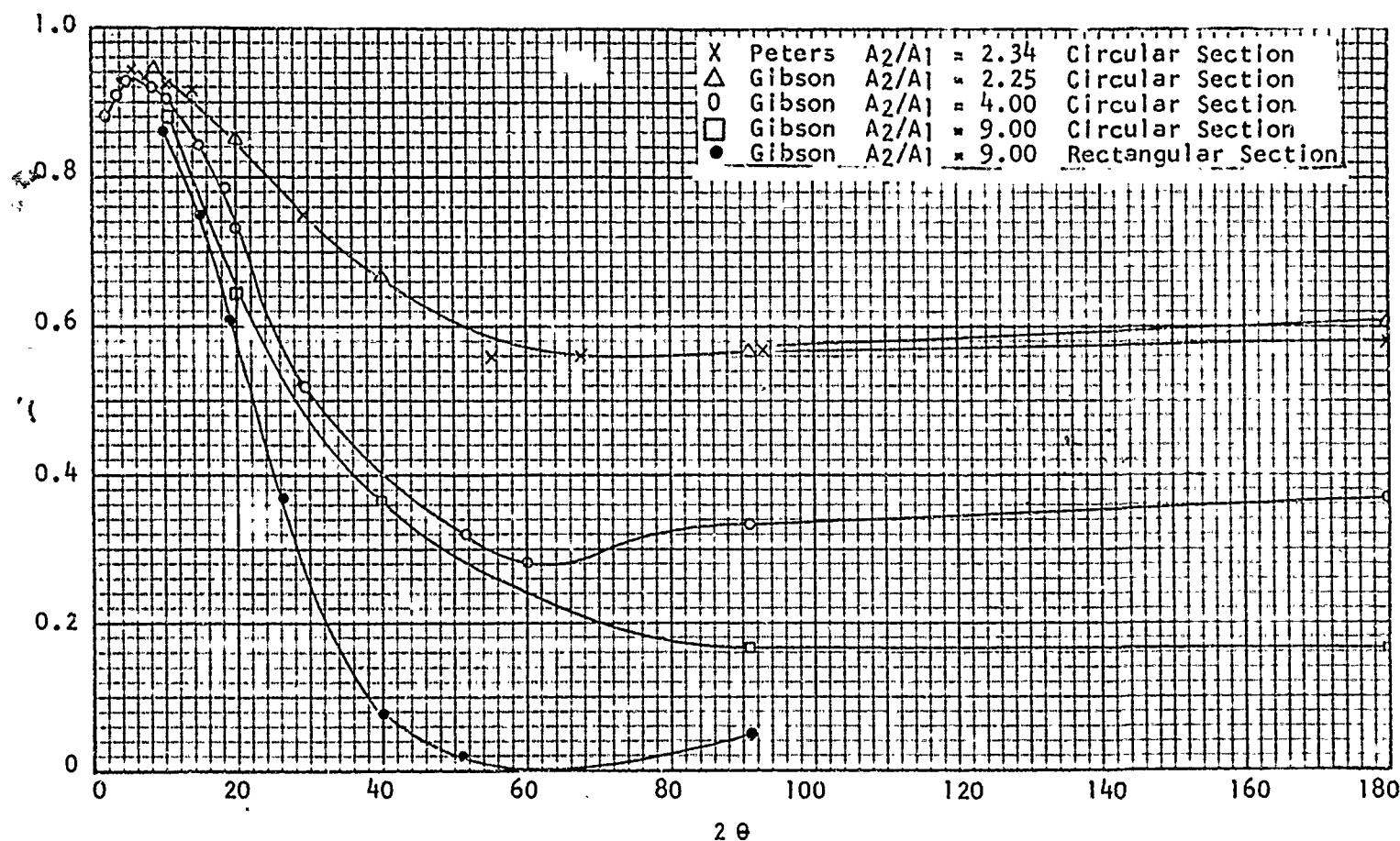


FIGURE 3-60. Variation of the Efficiency of Diffusers with the Angle of Expansion.
(Source: Ref. 3-3)

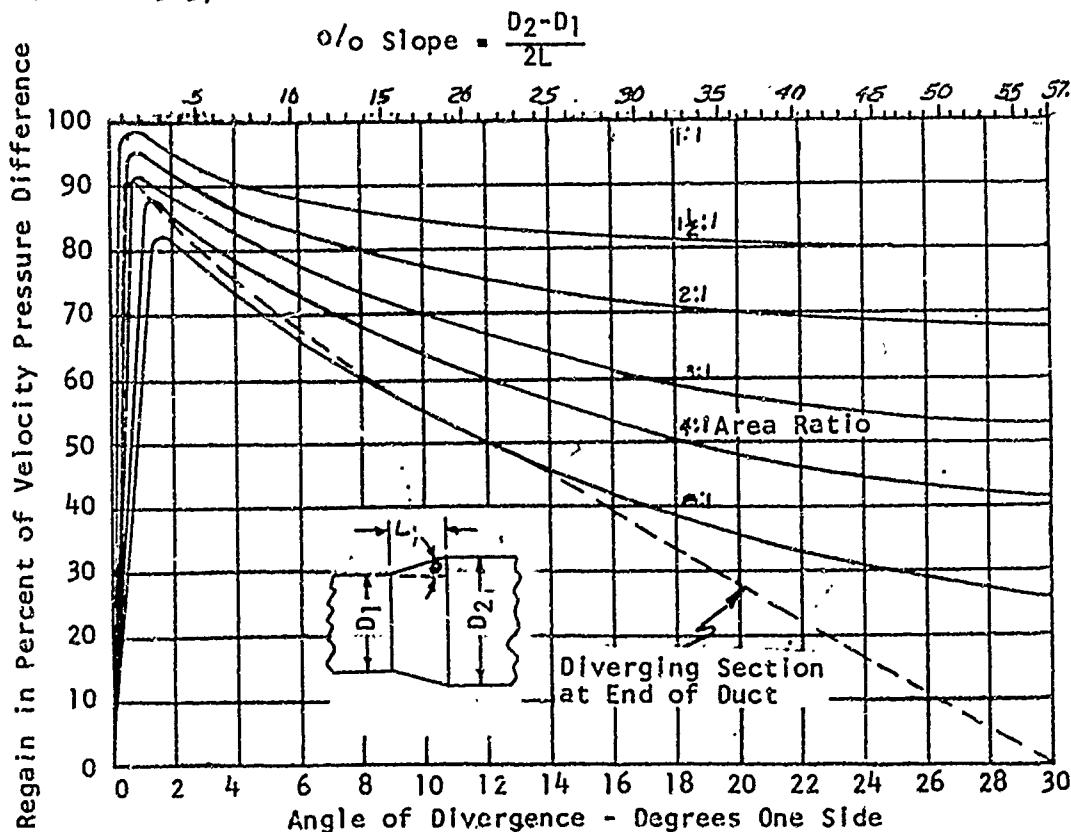


FIGURE 3-61. Static Pressure Regain in Diverging Nozzle in Duct. (Source: Ref. 3-1 by permission from the Buffalo Forge Company, Buffalo, N. Y.)

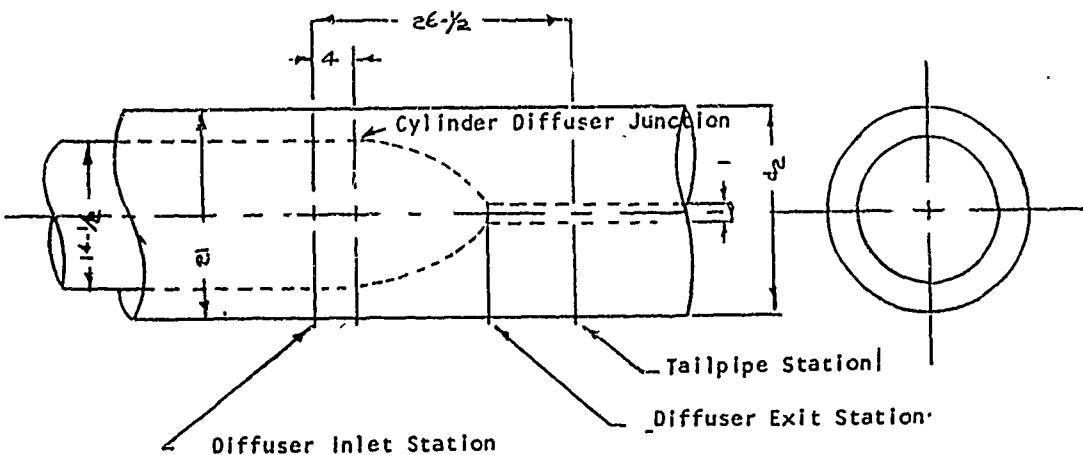


FIGURE 3-62. Schematic Diagram of Diffuser 2 of Figure 3-63. (Source: Ref. 3-4)

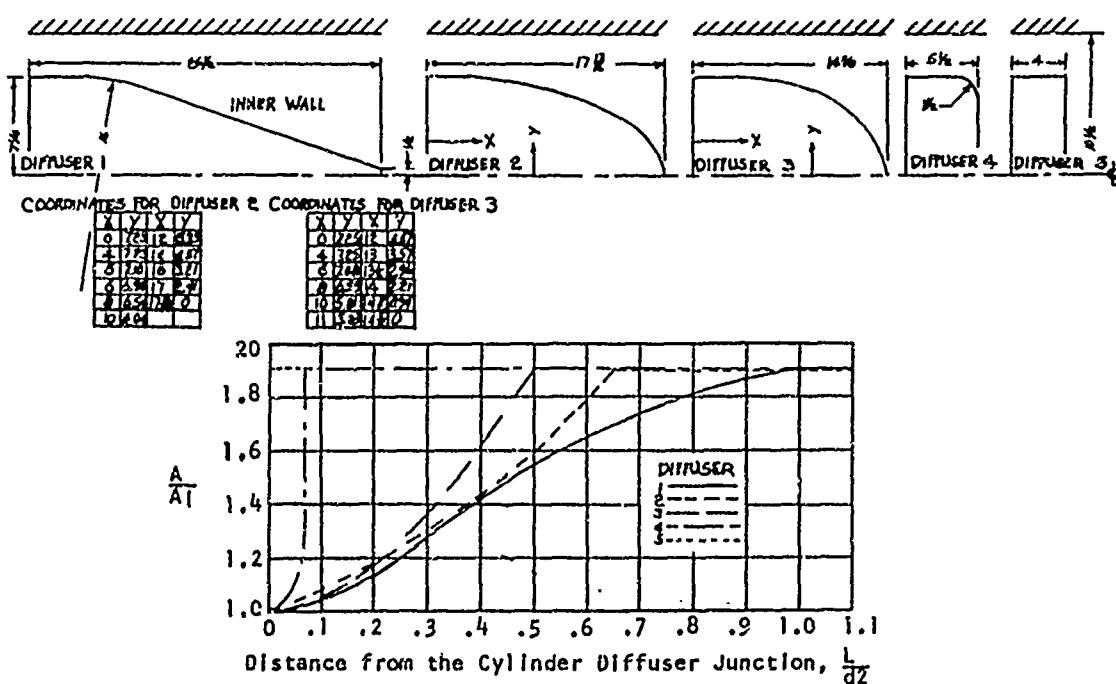


FIGURE 3-63. Schematic View and Area-Distribution Curve of Each of the Five Diffusers Investigated in Reference 3-4. All Dimensions are in Inches.

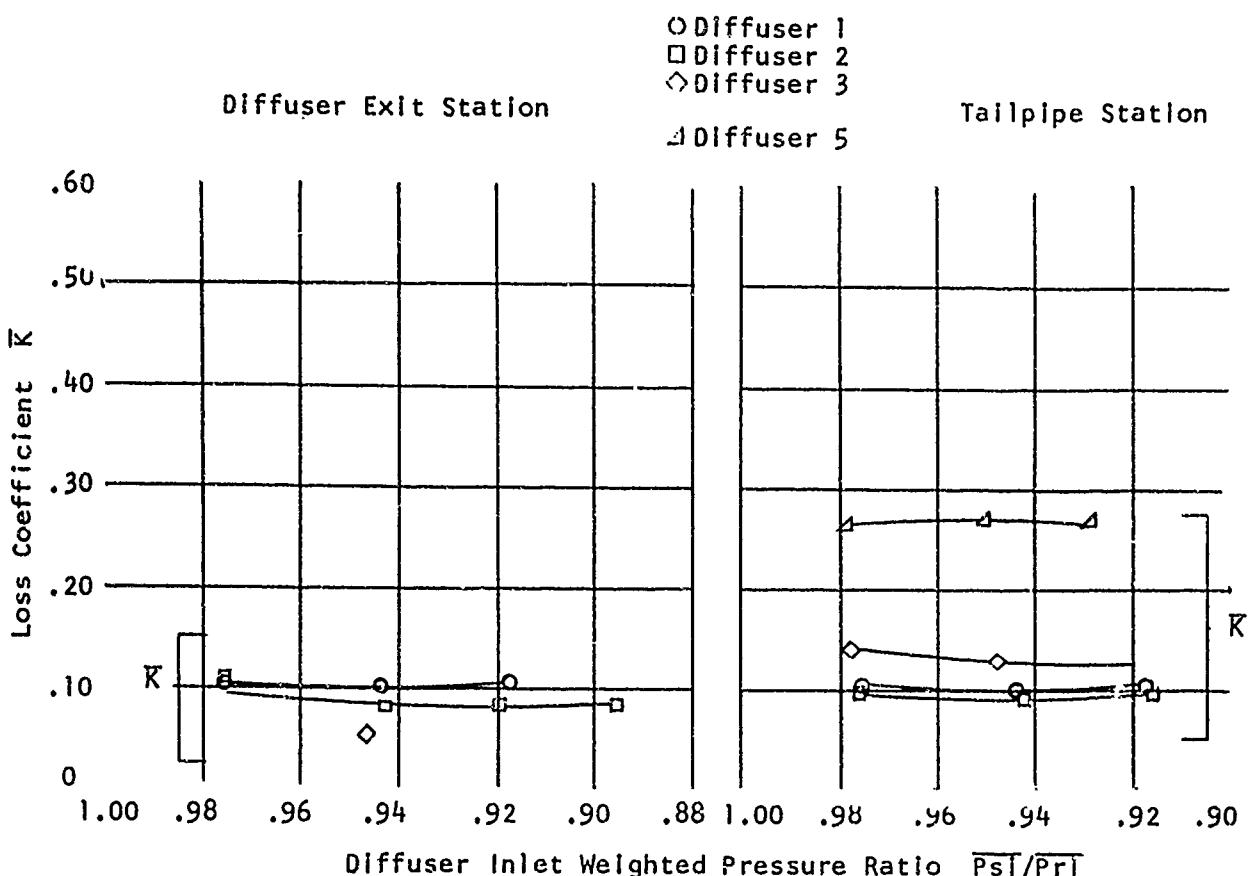


FIGURE 3-64. Variation of Loss Coefficient at the Diffuser Exit and Tailpipe Stations with Inlet Pressure Ratio for Each of the Five Diffusers of Figure 3-63 Without Vortex Generators. $X_i = 0^\circ$ (Source: Ref. 3-4)

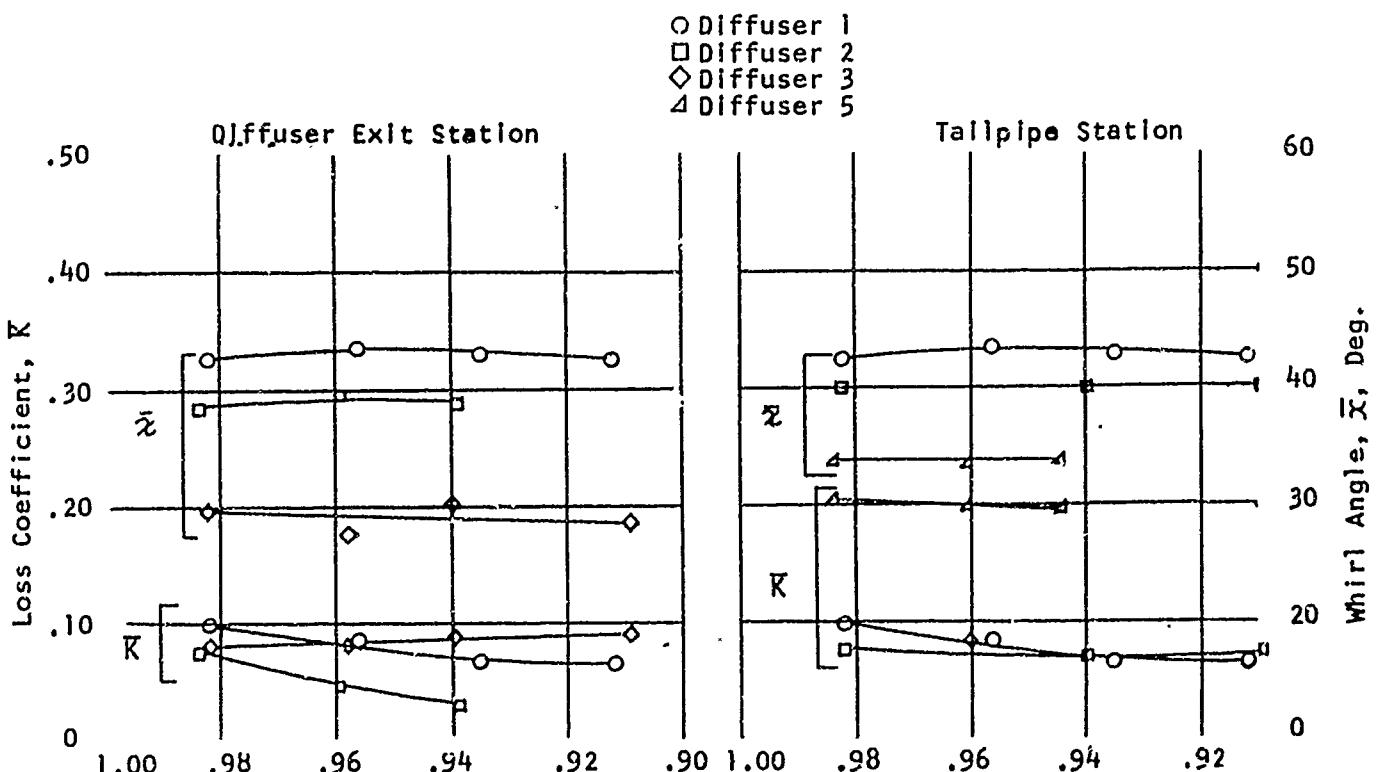


FIGURE 3-65. Variation of Loss Coefficient, and Whirl Angle at the Diffuser Exit and Tailpipe Stations with Inlet Pressure Ratio for Each of the Diffusers of Figure 3-63 without Vortex Generators $X_i = 20.6^\circ$ (Source: Ref. 3-4)

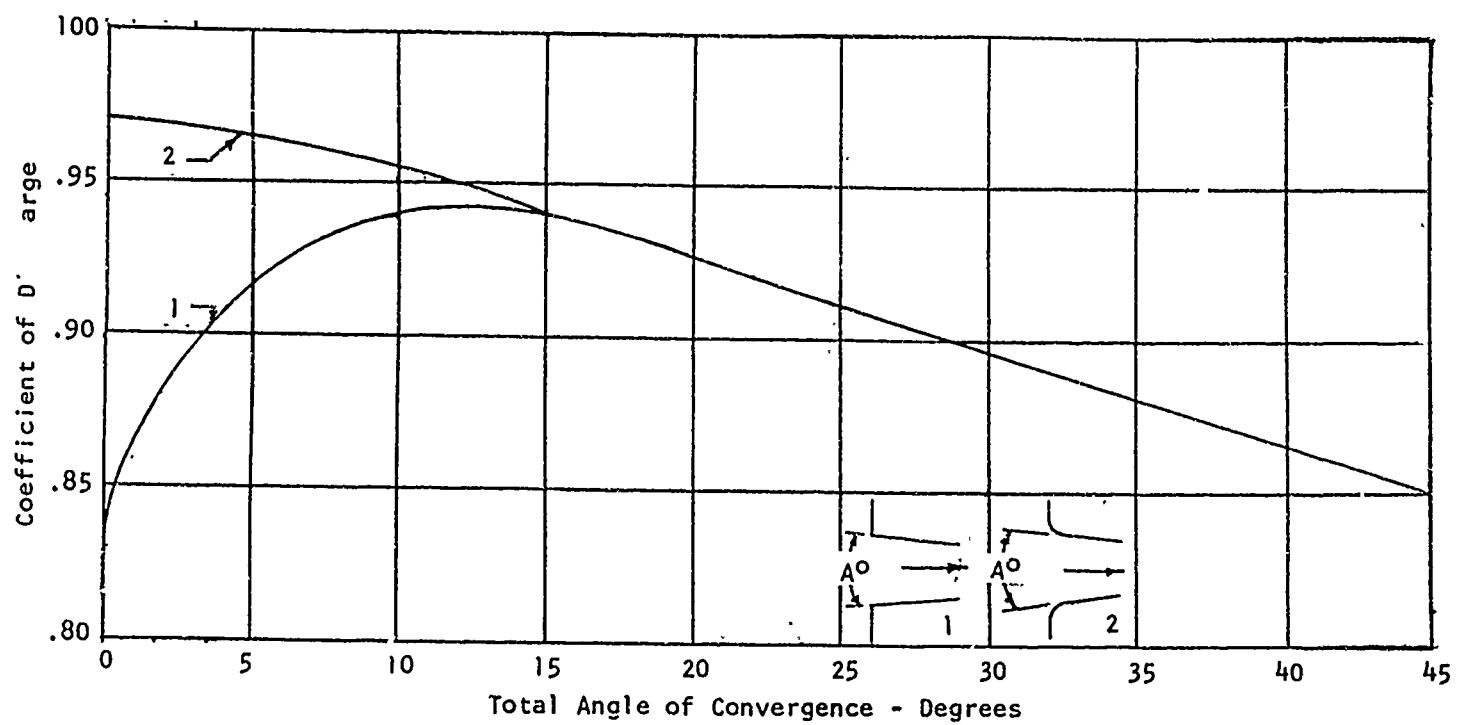


FIGURE 3-66. Coefficient of Discharge for Converging Nozzles Discharging from a Plenum Chamber. (Source: Ref. 3-1 by permission from the Buffalo Forge Company, Buffalo, N. Y.)

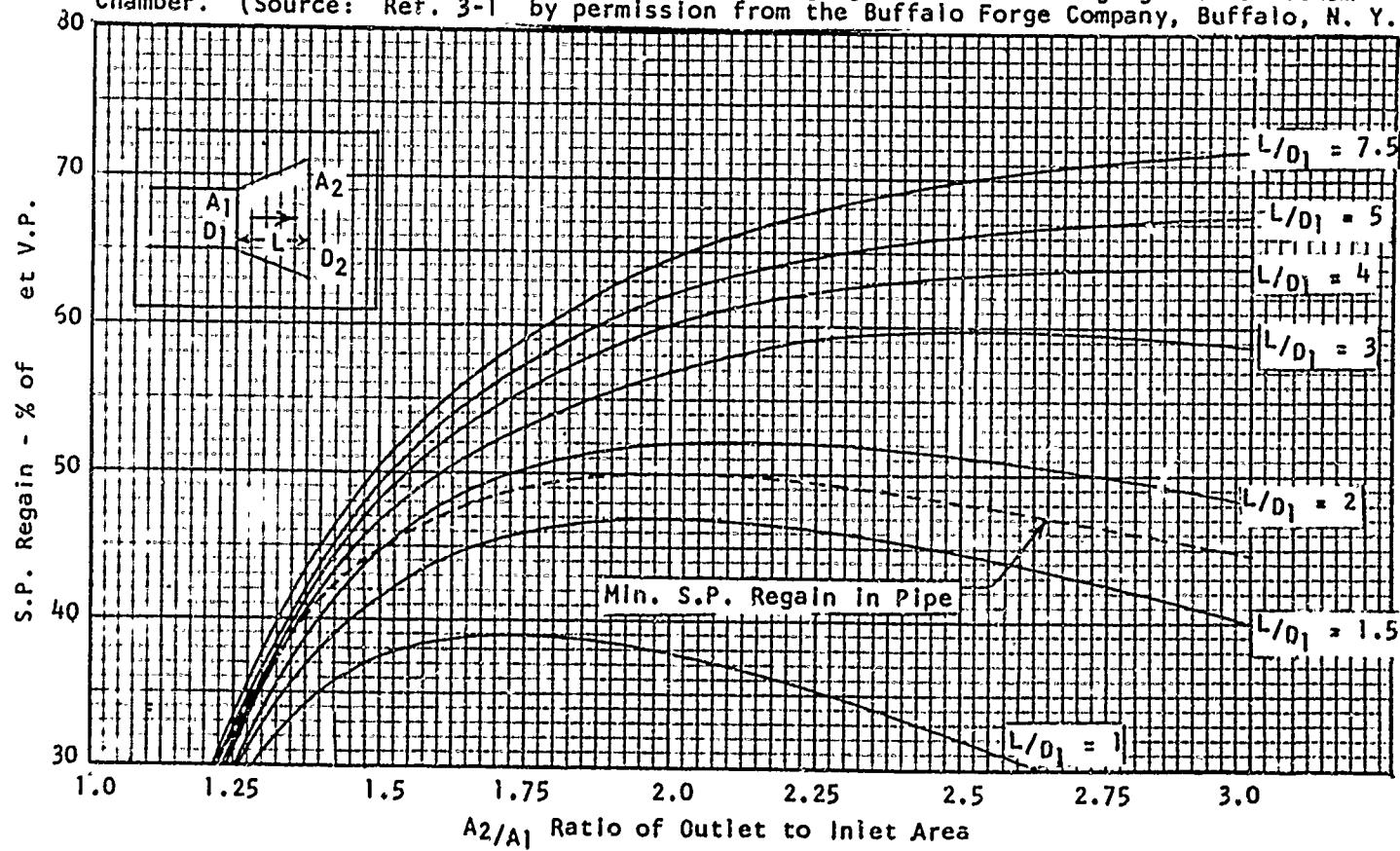


FIGURE 3-67. Static Pressure Regain in Diverging Nozzle at End of Pipe. (Source: Ref. 3-1 by permission from the Buffalo Forge Company, Buffalo, N. Y.)

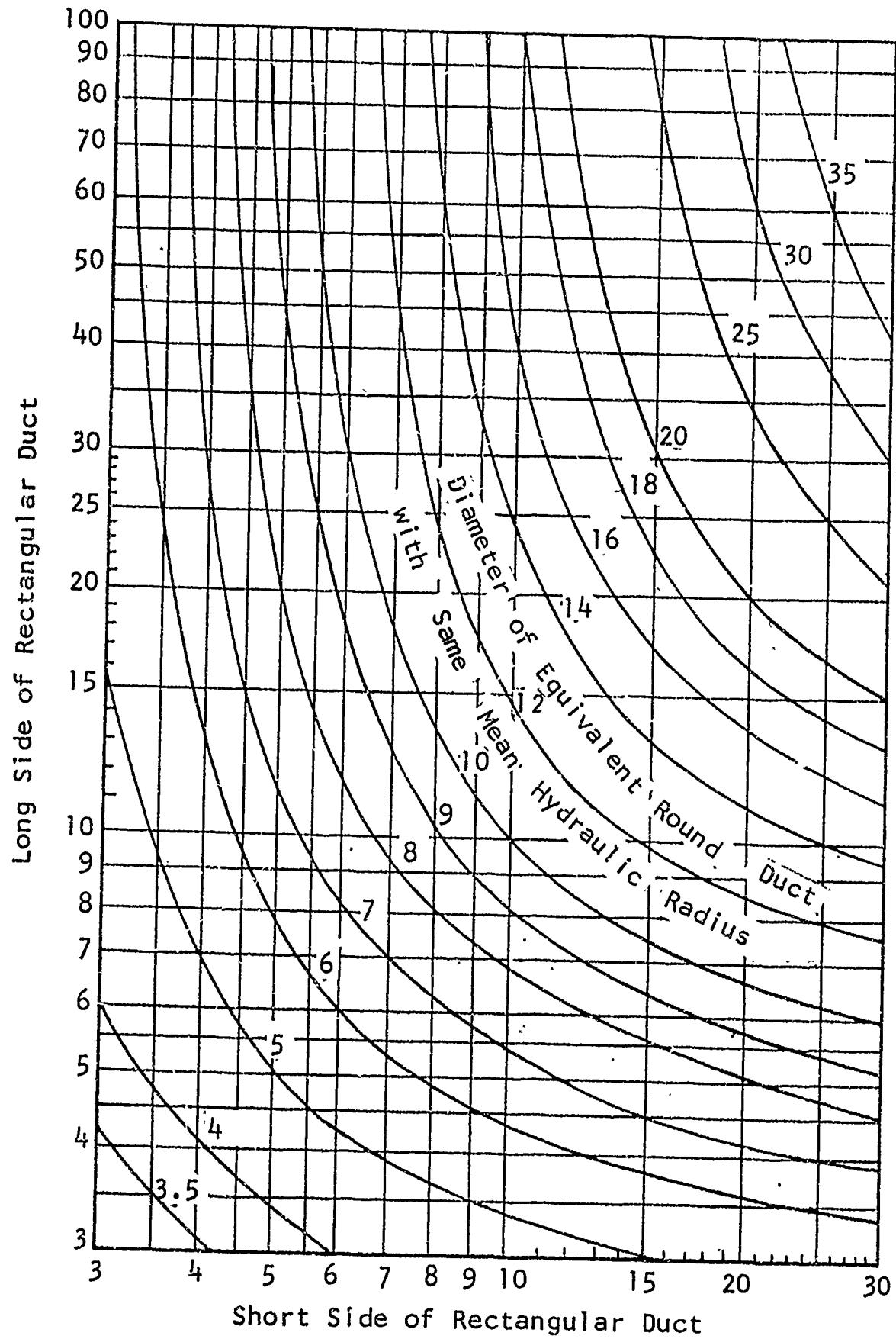


FIGURE 3-68. Equivalent Diameter of Rectangular Ducts. (Source: Ref. 3-1 by permission from the Buffalo Forge Company, Buffalo, N. Y.)

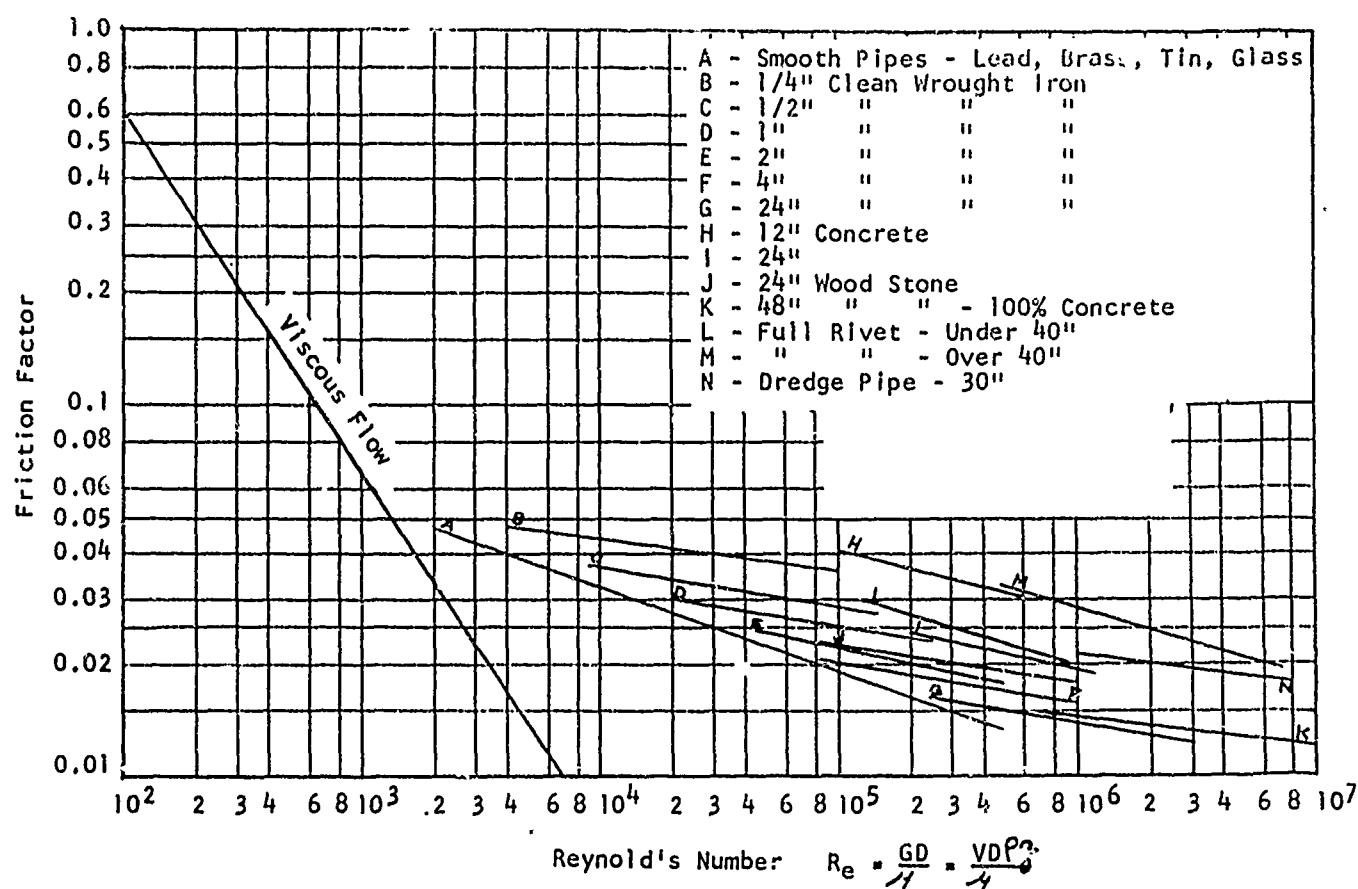


FIGURE 3-69. Relation of Friction Factor and Reynold's Number for Circular Pipes of Different Diameters and Roughnesses. (Source: Ref. 3-2)

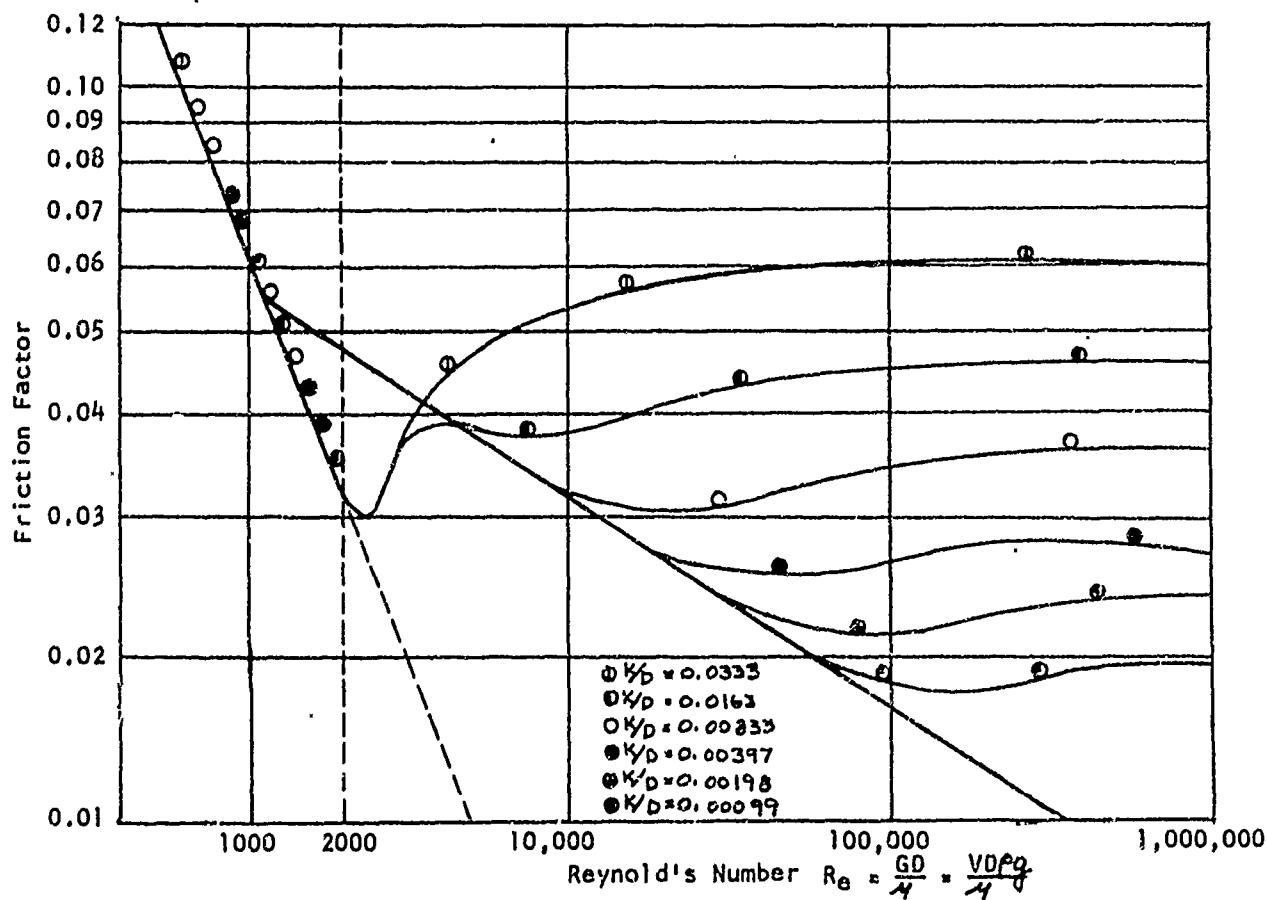


FIGURE 3-70. Nikuradse's Experiments, Showing the Effect of Roughness on the Transition from Laminar to Turbulent Flow. (Source: Ref. 3-2)

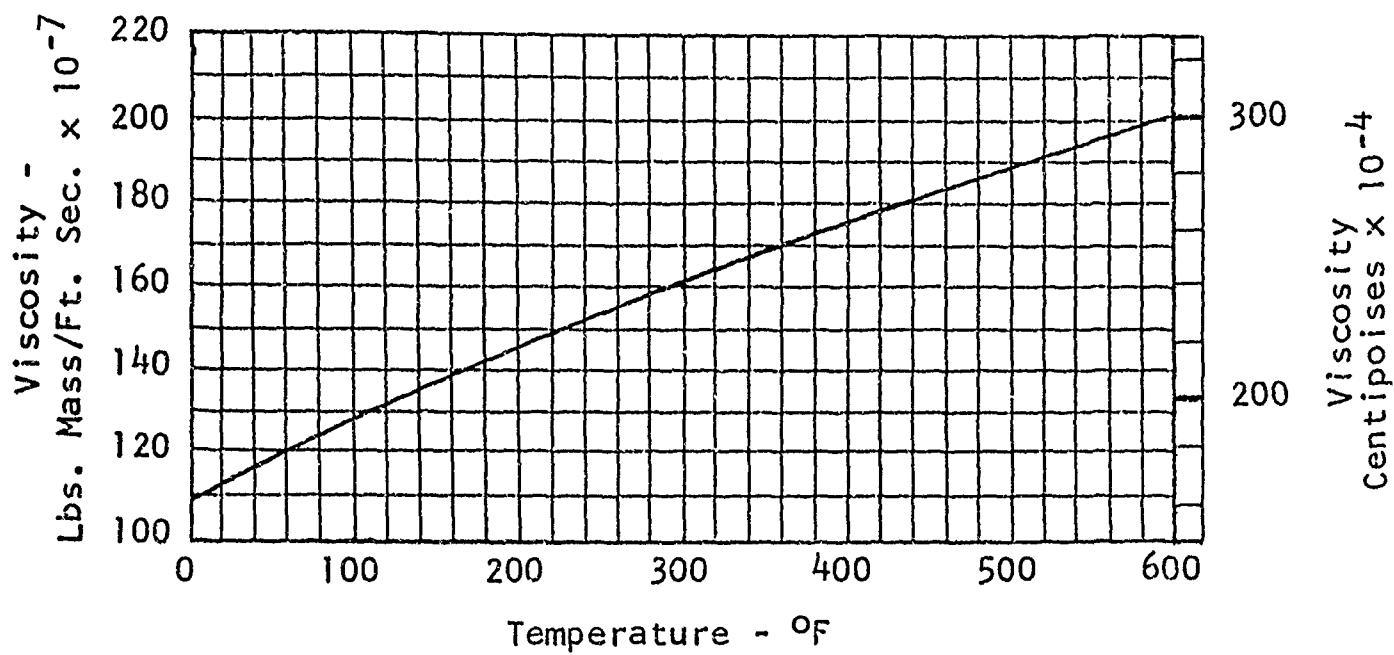


FIGURE 3-71. Viscosity of Air - Standard Atmosphere. (Source: Ref. 3-1)

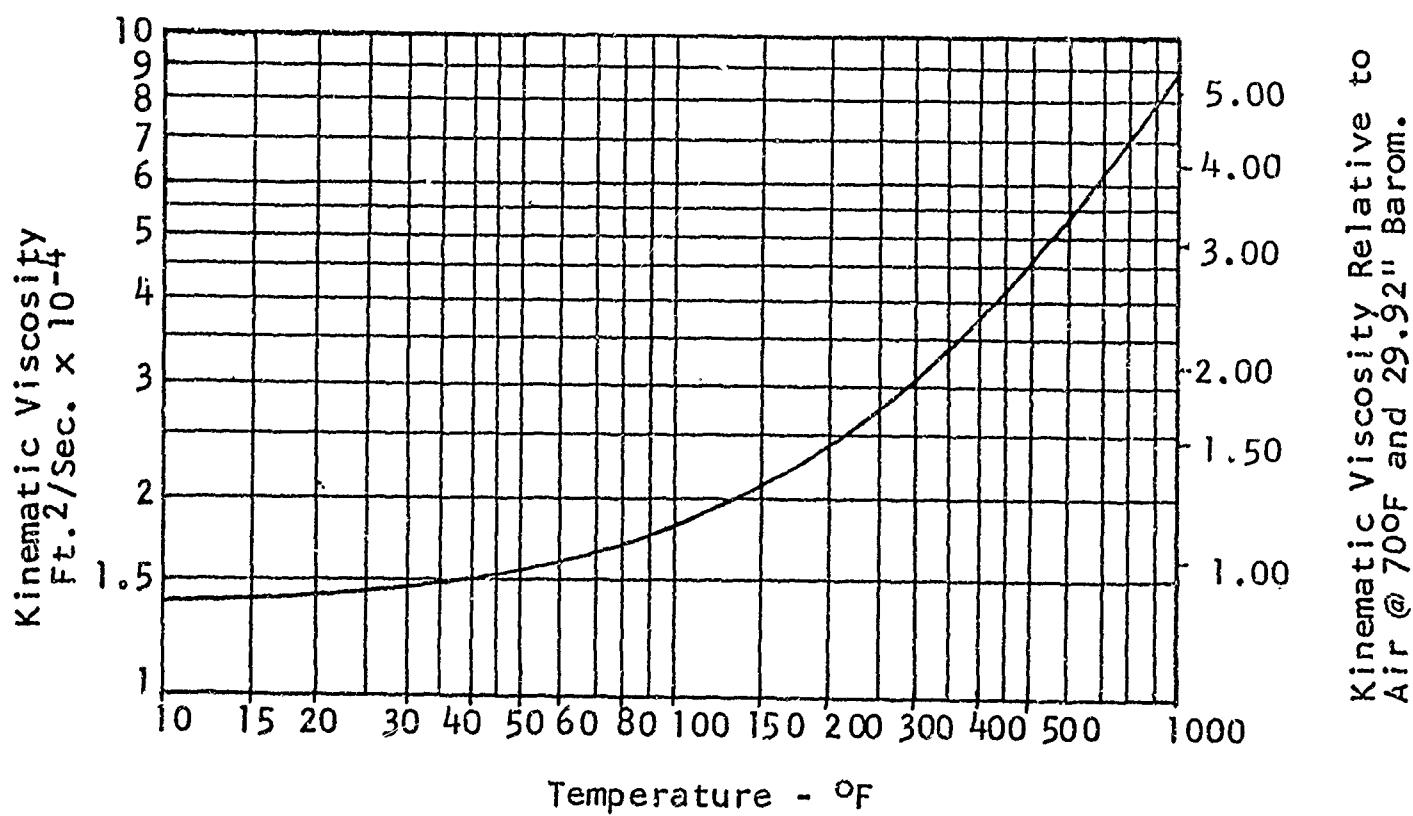


FIGURE 3-72. Kinematic Viscosity of Air - Standard Atmosphere. (Source: Ref. 3-1)

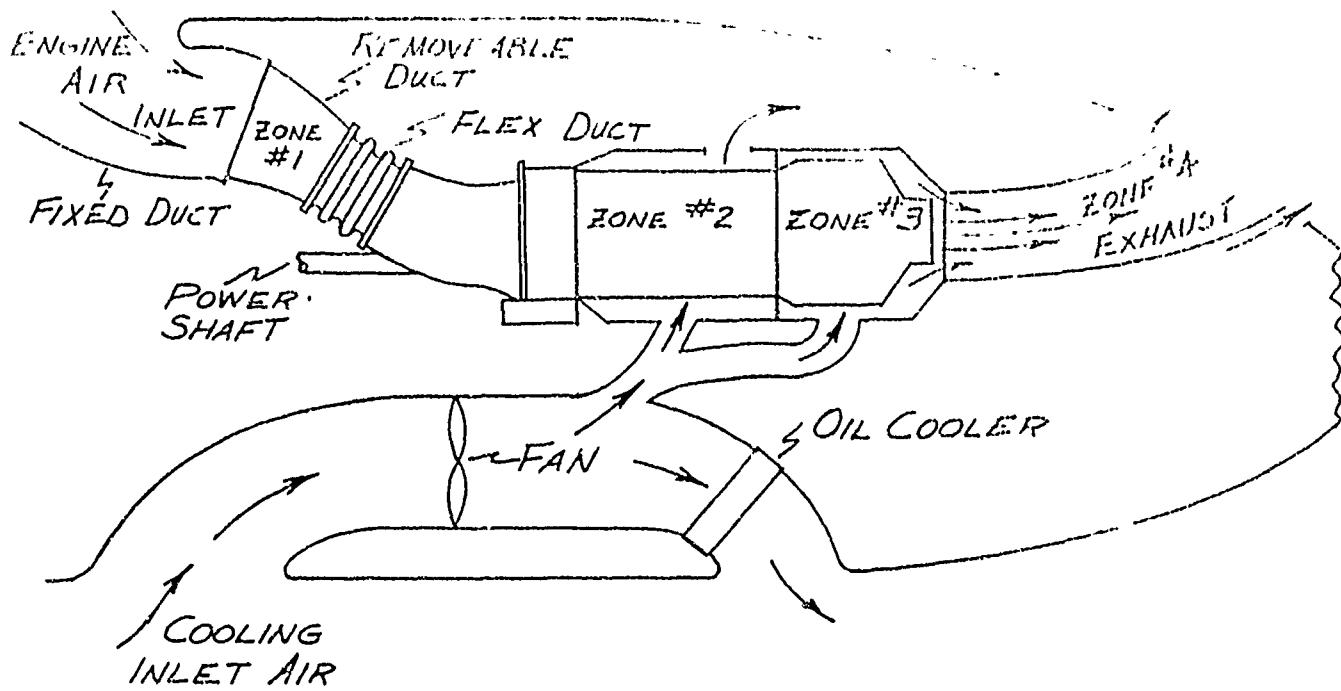


FIGURE 3-73
Cooling System for Submerged Turbine Engine Installation

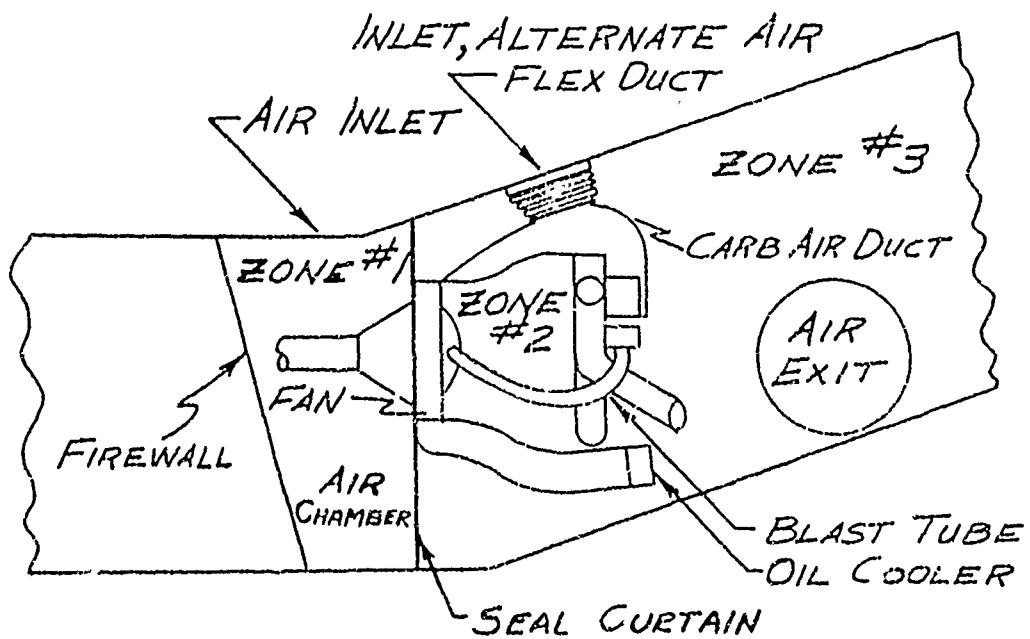


FIGURE 3-74
Cooling System for Submerged Reciprocating Engine Installation

3-3.0 Physical Duct Design Considerations

3-3.1 Introduction

There are three primary types of duct systems in an aircraft: The engine air intake system; the engine exhaust system; and the accessories duct system. The engine air intake system conducts ambient air through the aircraft into the engine. The engine exhaust system conducts products of combustion through the aircraft overboard. The accessories duct system includes all other gas conducting systems, such as heating, ventilating, anti-icing and cooling ducts, required for aircraft operation. See Figures 3-73 and 3-74 for typical installation ducting.

3-3.2 Installation Requirements

Procuring agencies always indicate certain design specifications to which the aircraft must conform. These specifications, either directly or by inference, establish some of the requirements for the duct systems. Specific materials, minimum gages, minimum performance and required routing may be described in the design specifications. In general, all ducts should be designed to the following:

- a. Minimum weight
- b. Occupy a minimum of space within the aircraft
- c. Effect a minimum of energy loss
- d. Effect a minimum of flow distortion
- e. Be easy to design, fabricate and service
- f. Be easy to install, remove and store
- g. Allow access to all other equipment
- h. Avoid all fire hazards
- i. Clear all equipment and structure
- j. Resist erosion, corrosion, abrasion
- k. Not trap liquids or foreign objects
- l. Maintain shape
- m. Must not impose loads on other parts of the aircraft
- n. Prevent leakage into or out of the duct system
- o. Doors and controls arranged to offer least resistance to flow. Control rods should be external to ducts as opposed to passing through ducts.
- p. Branch ducts designed and fabricated to provide proper flow distribution (See discussion in Section 3-2.6).

3-3.3 Support and Flexibility

Ducts which carry low pressure air at approximately ambient temperature can be incorporated, into or at least supported by, the aircraft structure. Air inlets integral with the aircraft structure are illustrated in Figure 3-75. If the duct conducts gases at elevated temperature or pressure it can be supported by the aircraft structure using attachments which allow thermal expansion and/or pressure load deflection.

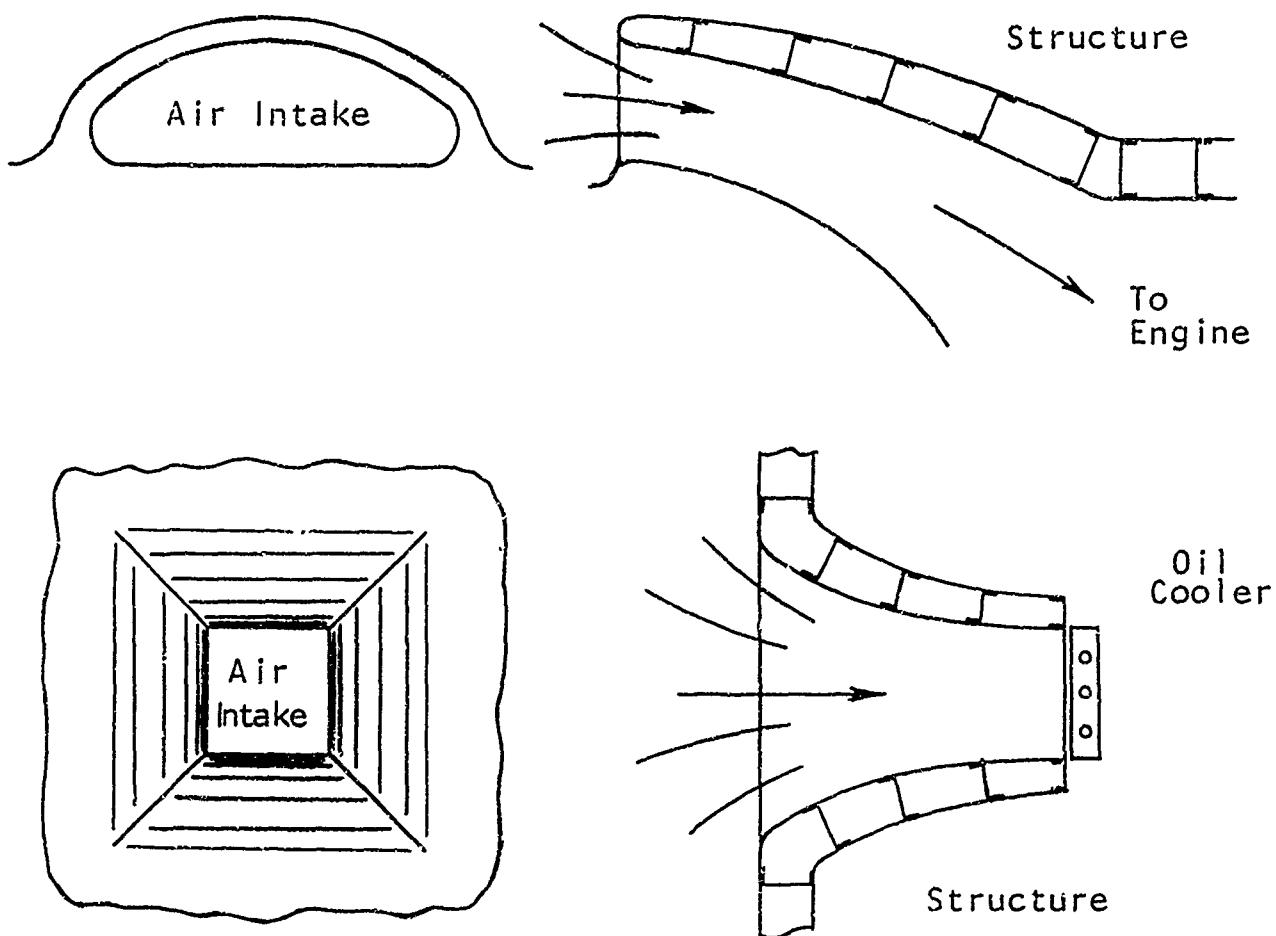


FIGURE 3-75
Duct Inlets Integral with Aircraft Structure

A duct system which bridges two or more elements having relative movement, such as the airframe and the engine, can be supported by the end attachments, providing sufficient flexibility is incorporated into the duct. The type and degree of flexibility required depends upon the deflection encountered, be it thermal expansion or a cyclic movement of vibration.

Engine specifications define a maximum load which may be imposed by the inlet and exhaust duct connections. Usually reciprocating engine exhaust systems are supported by the engine and do not bridge to the airframe.

3-3.4 Ease of Handling

All ducts must have appropriate rigidity and strength to withstand operational loading. In addition, they must be designed for rough handling during installation, removal and storage. Ducts, being considered auxiliary equipment, are subject to careless handling, and this must be considered in the selection of materials, gages, and in design.

Metal ducts are subject to denting and abrasion during handling. Any dents will adversely affect the flow performance of the reinstalled duct. Scratches received in handling might result in cracks during operation. Non-metallic ducts are subject to tearing and/or denting during handling. Glass fabric laminated ducts, being dent and abrasion resistant, are the least affected by careless handling.

Metal ducts can often be divided into sections in such a way that, when laid on a flat surface for storage, they will rest on flange edges or on reinforced areas.

All ducts which are removable for servicing should be attached by means of quick disconnect attachments such as clamps or fasteners. See Figure 3-76 for types of attachments. Band or V-clamps must fit around a convex periphery to assure a tight fit. Flat or concave segments of a periphery do not permit effective clamping action of the clamp. If fasteners are used they should be of a type which is retained on the flange to avoid loose pieces falling into the duct on disassembly. Allowance must be provided for tool clearance and for access to the clamp or fasteners.

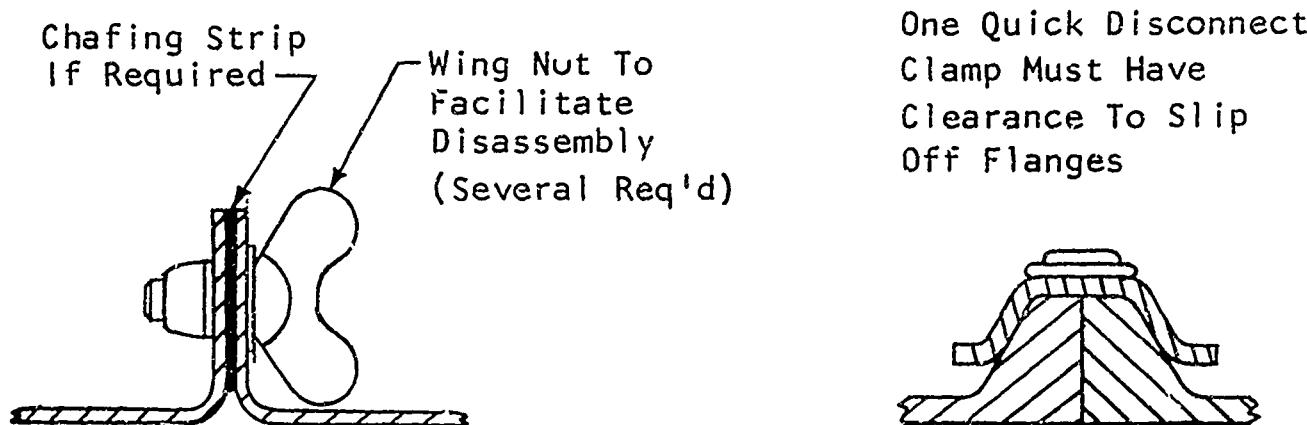


FIGURE 3-76
Types of Connections

It is possible to combine cabin ducting with hinged or removable access panels or cowls. Thus, when the panel or cowl piece is removed the duct section is removed at the same time, allowing access to the installation. See Figure 3-77. Consideration must be given to the duct section seal so that, on closing, the integrity of the duct system is maintained. Similarly, cabin heating and ventilating ducts can be combined with shafting and personnel guards. See Figure 3-78.

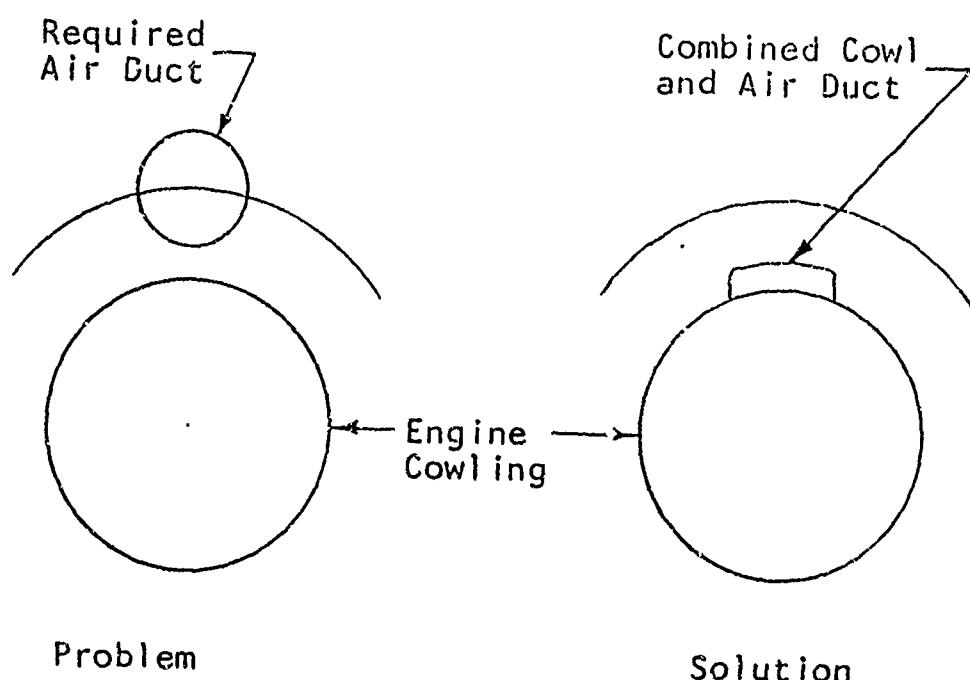


FIGURE 3-77
Type of Duct Problem and Solution

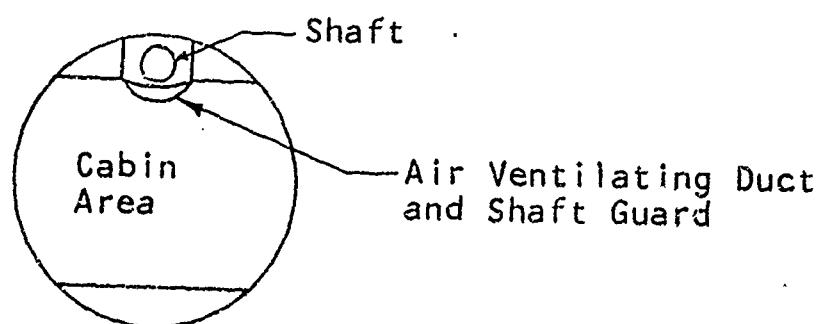


FIGURE 3-78
Space Conservation for Ducting System

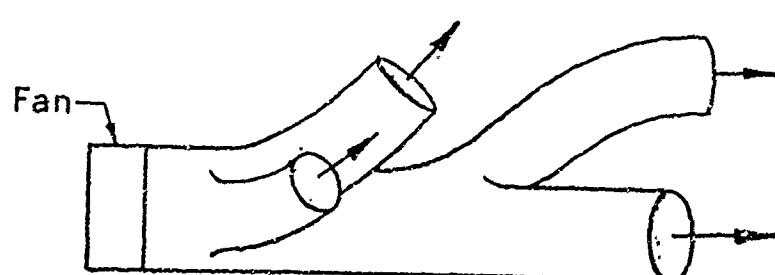


FIGURE 3-79
Branch Ducts for Parallel Requirements

When several ducts carry a common medium it is advisable to combine them into a single branched system. Figure 3-79 shows one large fan and diffuser duct as used for all accessory cooling rather than many separate systems.

Ducting, especially engine air intake and engine exhaust ducting, may be of large diameter and difficult to handle or remove. Removal in the field of duct sections should be considered, and the sections made small enough to permit handling in a high wind.

3-3.5 Materials

Ducts can be made of many suitable materials depending upon the conditions under which they are to operate. The applicable design specifications indicated by the procuring agency frequently will designate specific materials, finishes or minimum gages for certain of the duct systems. If the material is not specifically indicated then other requirements, such as fire zoning, may infer the use of a certain material. In the absence of such requirements, either explicit or implied, a variety of material is available for duct construction.

New materials are being developed continuously, and the duct designer should survey the entire materials field. However, until a new material is accepted for use by the procuring agency, standard qualified materials must be used.

Ambient air ducts can be made of practically any material suitable for ducting, depending upon the cost, weight and availability. Aluminum alloy, being the basic aircraft material, is usually used as it is available in the field for duct repair. Straight ducts can be made of any type of aluminum of a thickness commensurate with the operational loading and handling requirements. Below temperatures of 250°F 2024-T4 or 7075-T6 aluminum can be used. If welding or extensive forming is required, 5052-0, 6061-0 and 7075-0 aluminum can be used. These materials can be cold formed, but 7075-0 is extremely sensitive to scratches. 5052-0 is usually chosen for formed ducts requiring welding.

Non-metallic air ducts are becoming increasingly acceptable due to thin light weight, strength, flexibility or stiffness (as desired) and ease of fabricating into complex shapes if necessary. The use of material depends on temperature, pressure, shape and function.

Neoprene type material can be used up to temperatures of 300°F, silicone rubber up to 500°F constant and 750°F for short duration, while glass cloth will serve up to 750°F.

Ducts made of neoprene or silicone rubber material alone are limited to smaller sizes due to weight buildup and need of extensive dies. However, for odd shaped ducts needing the ability to permit large magnitudes of flexure, this type of construction is excellent.

For larger construction needs, the most prevalent material is fiberglass cloth or cotton cloth impregnated with neoprene, silicone rubber, or various resins. These are very easily laid up over simple molds with the number of plies varying to suit requirements, whether rigid or flexible.

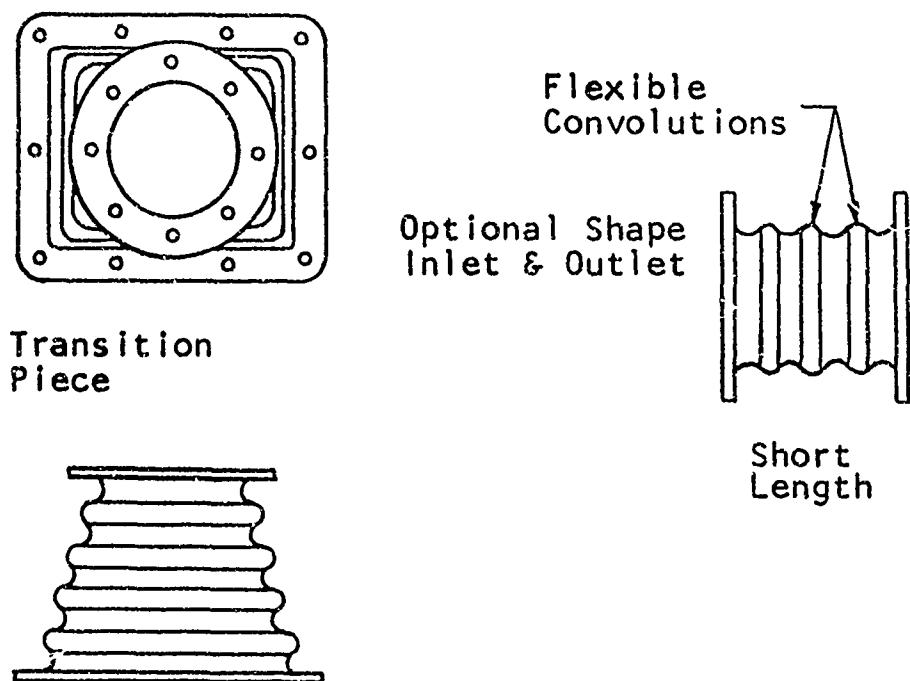


FIGURE 3-80
Flexible Connections

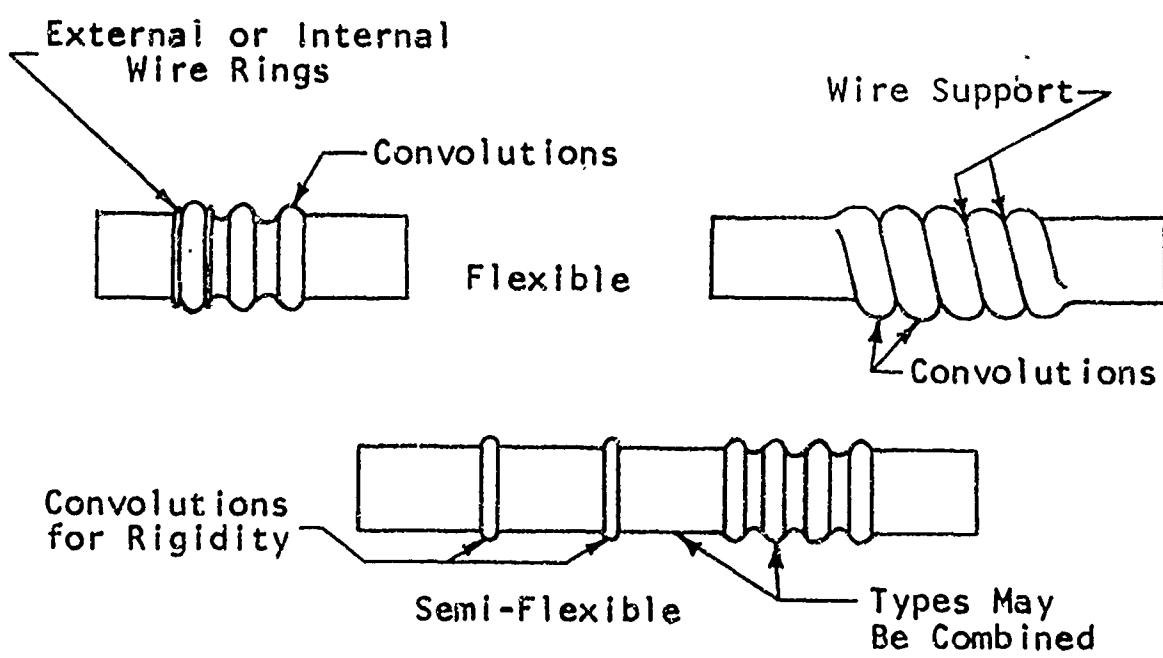


FIGURE 3-81
Connections

Neoprene or Silicone
Coated Glass Laminated
or Stainless Steel Bellows

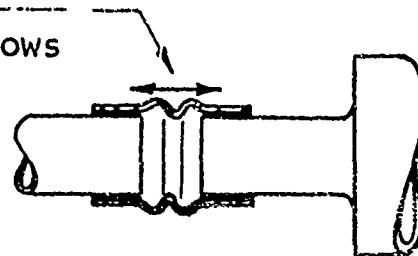


FIGURE 3-82
Expansion and Contraction Joint

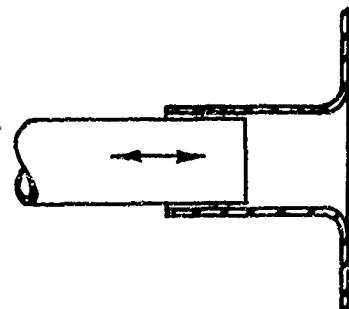


FIGURE 3-83
Slip Joint

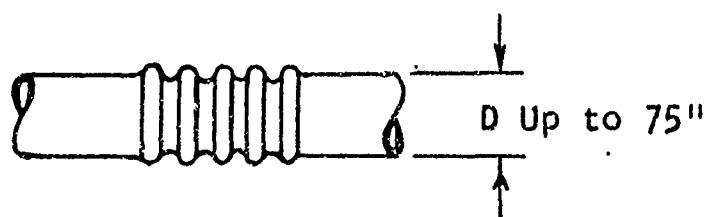


FIGURE 3-84
Bellows Joint for High Velocity
and High Temperature

Flexible segments of a duct of regular or irregular section are usually achieved by the addition of convolutions and the use of "softee" or less stiff materials.

Most ducts of this type are of constant circular section with the choice of diameter and length virtually unlimited and readily available. The construction can vary greatly depending on functional requirements. For pressure conditions approaching ambient, the ducts may not require any reinforcement. Any extremes of pressure, positive or negative, dictate reinforcement which can be achieved by the use of individual rings between each convolution or a continuous helix of wire, either internal or external. With this constant section type of duct, a single unit can be made to contain flexible and rigid segments in any combination desired by the simple expedient of selective placement of convolutions or "straight" walls (Ref. Figures 3-80 and 3-81).

Expansion provisions can be provided with non-metallic ducts as shown in Figure 3-82.

Short flexible ducts made of neoprene or silicone-coated asbestos can be used for extremely high temperature operation. This type of material has successfully withstood a temperature of 2000°F for 15 minute periods.

Most tailpipes, as well as collector rings, shrouds and exhaust tubes, are made of stainless steel, special alloy steel, inconel or titanium. Straight tailpipes for gas turbine engines can be made of stainless steel, type 320 for temperatures up to 1700°F. For temperatures up to 700°F, and for straight round section tailpipes, titanium can be used if fusion welding is not required. Titanium, in its present state of development, is difficult to form as it is extremely sensitive to scratches.

For prolonged heat exposure, stainless steel, type 321, can be used. This material can be spot welded, fusion welded and formed. The high temperature encountered requires that expansion provisions be incorporated. See Figure 3-83 for a type of expansion slip joint and Figure 3-84 for a bellows. Stainless steel bellows can be procured in diameters up to 75 inches and of almost any length.

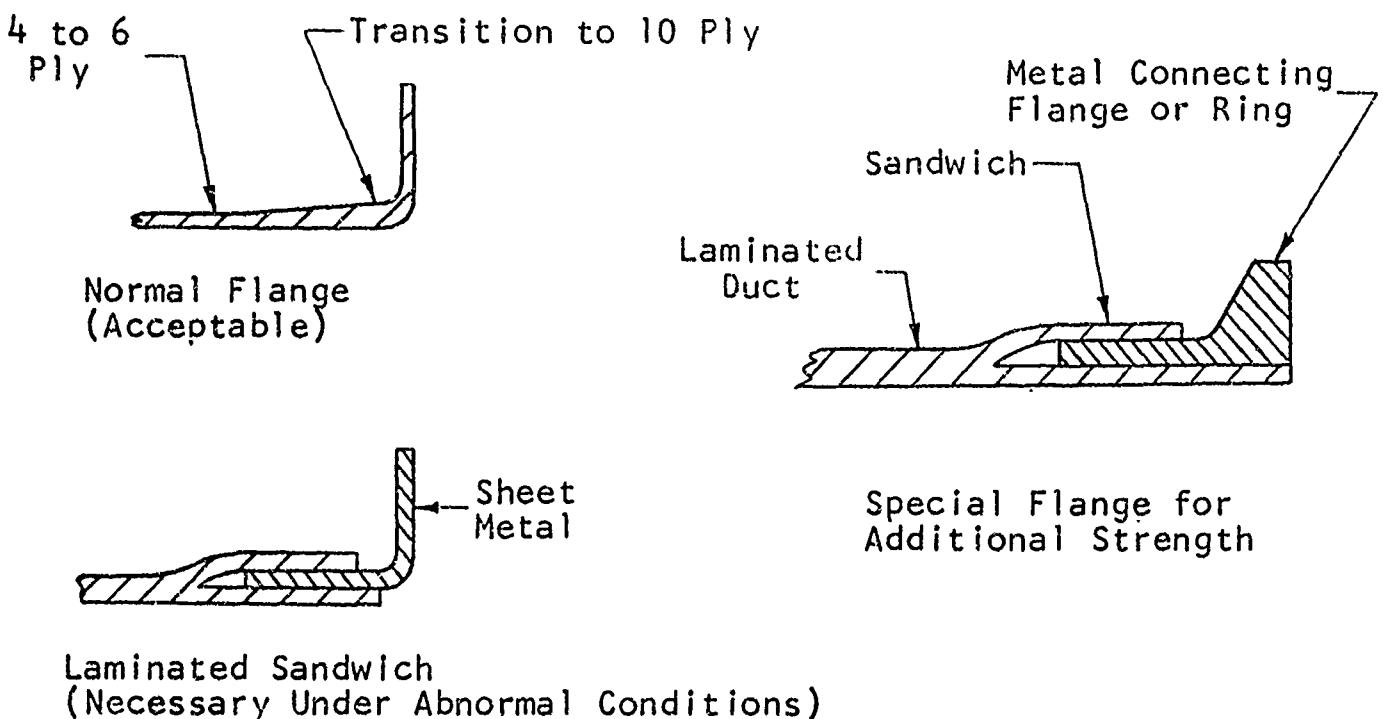


FIGURE 3-85
Flange Designs for Self-Supporting Laminated Glass Fabric Ducts

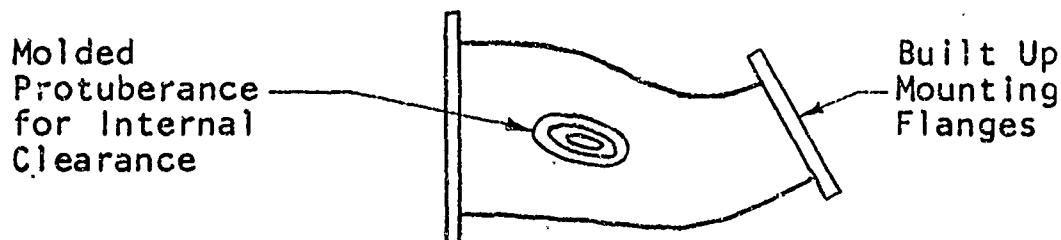


FIGURE 3-86
A Self-Supporting Laminated Glass Fabric Duct

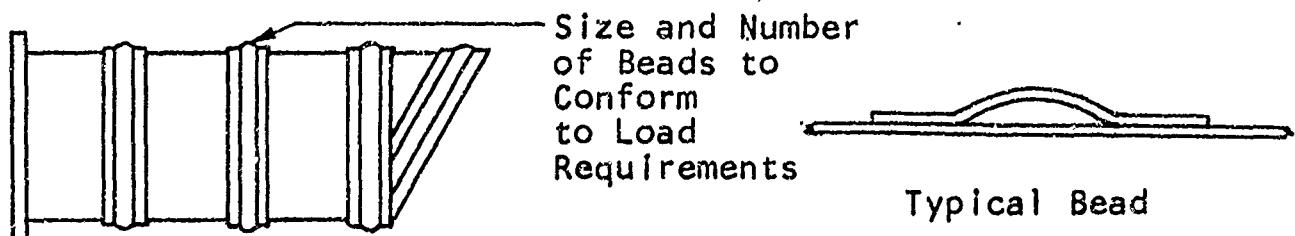


FIGURE 3-87
Metal Duct

3-3.6 Weight

All ducting material should be considered with regard to the installed weight. Proper selection of materials may allow a combination of ducting with structure which would otherwise be impractical. A comparison of the weights of the more common materials follows:

aluminum alloy	0.101	#/ in^3
glass laminate	0.00065	#/0.007" ply/ in^2
titanium	0.162	#/ in^3
stainless steel	0.284	#/ in^3

3-3.7 Ease of Fabrication

Glass laminated ducts are built up over wooden or plaster male forms. Due to the method of construction, glass laminated ducts offer important advantages. Flanges or areas of stress concentration require additional layers of glass fabric which can be applied and "feathered" out to spread the load into the rest of the duct. See Figures 3-85 for examples of fabric build-up.

For additional strength, especially at flanges or attachment points, metal can be inserted between layers of fabric and become an integral part of the finished product. It is also possible to incorporate easily any protuberance required to clear other equipment. See Figure 3-86. Any cracks or breaks can be repaired easily in the field.

Glass laminated parts can be cold cured, heat cured, or heated under pressure. For most applications heat curing is required. Cold cured products may include areas which are not properly impregnated with resin. These areas, if not detected at inspection and corrected will crack in service.

Rigid metal ducts are easy to fabricate, providing no extreme welding or forming is required. Straight metal ducts, reinforced with beads (See Figure 3-87) can be easily fabricated in the shop with semi-skilled personnel. Spotwelding or seamwelding such ducting is inexpensive. Overlapping spotwelds and seamwelding will provide gas tight joints. Fusion welding and extensive forming require special materials and skilled personnel.

Experimental metal ducts can be formed by hammering pieces over a wooden form and then fusion welding the pieces into one assembly. Production ducts should be designed for press or stretch forming.

3-4 Duct References

- 3-1 Madison, Richard D.: Fan Engineering. Buffalo Forge Company, Buffalo, N. Y., 1949.
- 3-2 Committee A-9, Aircraft Air Conditioning Equipment, Society of Automotive Engineers, New York: Airplane Heating and Ventilating Equipment Engineering Data, SAE Aeronautical Information Report No. 2 1943.
- 3-3 Committee A-9, Aircraft Air Conditioning Equipment, Society of Automotive Engineers, New York: Airplane Heating and Ventilating Equipment Engineering Data, SAE Aeronautical Information Report No. 23 1951.
- 3-4 Wood, Charles C., and Higginbotham, James T.: Effects of Diffuser and Center-Body Length on Performance of Annular Diffusers with Constant-Diameter Outer Walls and with Vortex-Generator Flow Controls. NACA Research Memorandum L54G21, 1954.
- 3-5 Weske, John R., Pressure Loss in Ducts with Compound Elbows. NACA Report W-39, 1943.
- 3-6 McLellan, Charles H., and Nichols, Mark R.: An Investigation of Diffuser-Resistance Combination in Duct Systems. NACA Report WR L-329, 1942.
- 3-7 The American Society of Heating and Ventilating Engineers: Heating, Ventilating and Air Conditioning Guide. Waverly Press, Inc., Baltimore, Maryland, 1953.
- 3-8 Dodge, Russell A. and Thompson, Milton J., Fluid Mechanics. McGraw - Hill Book Company, 1937.
- 3-9 Hoerner, Sighard F., Aerodynamic Drag. The Otterbein Press, Dayton, Ohio, 1951.
- 3-10 Rogallo, F. M., Internal-Flow Systems for Aircraft. NACA Report No. 713, 1941.
- 3-11 Mobley, Charles A., Essentials of Airplane Duct Design. Published in Aero Digest, 1944.

- 3-12 Spitzglass, Jacob M., Orifice Coefficients. Trans. A.S.M.E. Vol. 44, 1922.
- 3-13 McLellan, Charles H. and Nichols, Mark R.; An Investigation of Diffuser-Resistance Combinations. NACA WR L-329. February, 1942.
- 3-14 Seddon, J., Air Intakes for Aircraft Gas Turbines. Journal, Royal Aeronautical Society. October, 1952.
- 3-15 Winter, K. C., Comparative Tests of Thick and Thin Turning Vanes in the Royal Aircraft Establishment 4 x 3 foot Wind Tunnel. British Report R&M 2589. August, 1947.
- 3-16 Brandt, Allen D., and Steffy, Russell J., Energy Losses at Suction Hoods. ASHAE Journal Section, Heating, Piping and Air Conditioning. September 1946.
- 3-17 Madison, R. D., and Parker, J. R., Pressure Losses in Rectangular Elbows. ASME Transactions AER 58-2, April 1936.
- 3-18 Busey, F. L., Loss of Pressure Due to Elbows in the Transmission of Air through Pipes or Ducts. Transactions A.S.H. and V.E. 1913.
- 3-19 Wirt, L., New Data for the Design of Elbows in Duct Systems. General Electric Review, Issue of June, 1927.

3-5 List of Symbols

<u>Symbols</u>	<u>Subscripts</u>
Q Volume Flow Rate, C.F.M.	1 Mixing Chamber Flow
A Area - Ft. ² Area of Surface Exposed to Airflow - Ft. ² or to Fluid Flow Path	Exit - Primary Nozzle Total - Secondary Flow at Entrance to Mixing Chamber Entering Blade Row
V Velocity - Ft./Sec.	2 Exit of Diffuser Outlet Velocity
P Power Input - HP Pressure - Absolute	Lift Exit Mixing Chamber Leaving Blade Row
ρ Density - Slugs/ Ft. ³	REF. Reference
ΔP Pressure Loss	c Contraction Corrected Bellmouth Entrance
F Force	Round Screen Wire Cross-Sectional Shape
M Mass Mean Hydraulic Radius = $\frac{\text{Cross Sectional Area}}{\text{Perimeter}}$	Sharp Screen Wire Sharp-Edged Strips
σ' Density Ratio = $\frac{\text{Density of Air in Duct}}{\text{NACA Std. S.L. Air}}$	free Free-flow (screen)
K Loss Coefficient Factor - % of Velocity Head, Velocity Ratio	d Drag
R Gas Constant Reynolds Number Radius, Rankine	T _i Inlet total (pressure) in duct
D Diameter - Ft. - Equivalent Diameter, Ft. Drag - #	t Total
C Coefficient Blade Chord, Ft. Coefficient of Discharge	P Pump
K' Primary Loss Factor	PL Power Loss
θ Temperature Correction T/518.4°R Diffusion Angle, Degrees Turning Angle of Air Passing Through Blade Row - Degrees Contraction Angle - Degrees	T _o Freestream total (pressure) Outlet total (pressure)
	PL _i Inlet power loss
	PL _o Outlet power loss
	3 Station in duct system
	br Branch
	a Inner

3-5 List of Symbols (Continued)

<u>Symbols</u>	<u>Subscripts</u>
W Weight - Lbs. Width of Duct Weight Flow - #/Sec.	b Outer v Velocity
d Resultant Velocity Vector Diameter - Ft. Depth of Rectangular Duct - Ft.	r Resistance s Static
σ' Solidity Ratio = $\frac{\text{Projected Solid Area}}{\text{Total Area}}$	v_1 Velocity at Station 1 v_2 Velocity at Station 2 s_1 Static at Station 1 s_2 Static at Station 2
q Dynamic Pressure = $1/2 \rho v^2$	f Skin Friction Drag Friction Velocity of Approach Factor
t Temperature Thickness	e Equivalent
c Chord	T Throat of Primary Nozzle Total
η Efficiency	o Fan Outlet Required Ambient Outside Outer (Radius) Outlet
w Specific Weight, Lbs./ Cu. Ft.	i Induced Total - Primary Flow Rotor Inside Inlet Inner (Radius)
CR Curve Ratio of Elbow Without Splitters	
CR' Curve Ratio of Component Elbows Formed by Splitters	
X Number of Splitters	
λ Loss Coefficient	
L Lift Force - Lbs. Length of Mixing Chamber Length of Diffusion Length of Duct Section	
ℓ Wetted Perimeter	
f Friction Factor	
e Factor Representing the Efficiency of the Conversion	
h Enthalpy Film Heat Transfer Coefficient BTU/Hour/Ft. ² /OF	

3-5 List of Symbols (Continued)

Symbols

- a Damper Angular Position Relative to Duct Axis, Degrees
- η Fluid Absolute Viscosity - #/Ft.-Sec.
- ζ Fluid Kinematic Viscosity
Ft.²/Sec. = $\frac{\eta}{\rho g}$ = $\frac{\eta}{w}$
- g 32.2 feet/second²
- b Width of Rectangular Duct
- r Hydraulic Radius, Ft.
- HP Horsepower
- α Turning Vanes Incidence Angle
Contraction Angle, Degrees
- G Weight Rate of Flow
- S Spacing of Turning Vanes (Gap)
Length of Side of Square Duct
- V.P. Velocity Pressure

CHAPTER IV

AIR PUMPS

TABLE OF CONTENTS

	PAGE
4-1 Introduction	IV-1
4-2.0 Axial Flow Fans	6
4-2.1.0 Aerodynamic Theory of Axial Flow Fans	7
4-2.1.1 Development of Fan Design Formulae	8
4-2.1.2.0 Fan Losses	11
4-2.1.2.1 Profile Drag Losses	11
4-2.1.2.2 Tip Clearance Losses	11
4-2.1.2.3 Inner Wall Losses	12
4-2.1.2.4 Rotational Flow Losses	12
4-2.2.0 Application of Theory to Design	12
4-2.2.1 Air Flow and Pressure Rise Requirements	13
4-2.2.2.0 Selection of Design Parameters	13
4-2.2.2.1 Choice of Fan Rotational Speed	15
4-2.2.2.2 Selection of Fan Diameters and Axial Velocity	15
4-2.2.2.3 Choice of Rotor Inlet Angle, β_1	16
4-2.2.2.4 Rotor Outlet Velocity Magnitude and Direction, W_2 and β_2	17
4-2.2.2.5 Rotor Turning Angle, θ_R	19
4-2.2.2.6 Choice of the Rotor Cascade	19
4-2.2.2.7 Determination of Stator Root Parameters	20
4-2.2.2.8 Determination of Rotor and Stator Tip Parameters	21
4-2.2.2.9 Definition of Intermediate Spanwise Stations	22
4-2.2.3 Determination of Fan Total Pressure Rise	22
4-2.2.4 Estimation of Fan Efficiency and Power Required	23
4-2.2.5 Blade Airfoil Layout	25
4-2.2.6 Charts for Rapid Determination of Fan Diameters	32
4-2.2.7.0 Off Design Fan Operation	33
4-2.2.7.1 Variable Angle Pre-Rotation Vanes	34
4-2.2.7.2 Relief Parts for Fan Power Savings	35
4-2.2.8 Fan Entrance and Fan Diffuser Design	35
4-2.3 Fan Testing	37
4-2.4 Illustrative Fan Design	37
4-2.5.0 Physical Fan Design Considerations	145
4-2.5.1.0 General	145
4-2.5.1.1 Drawings and Procurement Specifications	145
4-2.5.1.2 Materials and Processes	146
4-2.5.2.0 Rotor Assembly	147
4-2.5.2.1.0 Wheel Assembly	150
4-2.5.2.1.1 Hub	151
4-2.5.2.1.2 Disc	151
4-2.5.2.2 Blades	151
4-2.5.2.3 Assembly of Wheels and Blades	153
4-2.5.2.4 Balancing	154
4-2.5.3 Stator and Rotor Cowling Assembly	154
4-2.6 Fan References	161

TABLE OF CONTENTS (Continued)

	<u>Page</u>
4-3.0 Ejectors	IV-163
4-3.1.0 General	163
4-3.1.1 Nomenclature	163
4-3.1.2 Definition	165
4-3.1.3 Types of Ejectors	165
4-3.1.4 Method of Establishing Secondary Flow Requirements	167
4-3.1.5 Method of Determining Primary Flow Requirements	167
4-3.2.0 Theory of Constant Area Cylindrical Ejectors	167
4-3.2.1 Design Parameters	167
4-3.2.2.0 Discussion	169
4-3.2.2.1 Area Ratio	169
4-3.2.2.2 Mixer Length Ratio	169
4-3.2.2.3 Diffuser Ratio	169
4-3.2.2.4 Primary Nozzle	170
4-3.2.2.5 Temperature Ratio	170
4-3.2.2.6 Molecular Weight Ratio	170
4-3.2.3.0 Ejector Design Chart	170
4-3.2.3.1 General	171
4-3.2.3.2 Procedure	171
4-3.3 Reciprocating Engine Exhaust Ejectors	171
4-3.4 Turbine Exhaust Ejectors	174
4-3.5 Turbine Compressor Bleed Air Ejectors	175
4-3.6.0 Ejector Design Considerations	175
4-3.6.1 General	175
4-3.6.2.0 Support	175
4-3.6.2.1 Reciprocating Engine Exhaust Ejectors	175
4-3.6.2.2 Gas Turbine Exhaust Ejectors	176
4-3.6.2.3 Compressor Air Bleed Ejectors	176
4-3.6.3 Materials	176
4-3.6.4 Service	176
4-3.6.5 Miscellaneous	176
4-3.7 Ejector References	177
4-4 List of Symbols	182

LIST OF FIGURES

<u>Figure No.</u>	<u>Title</u>	<u>Page</u>
4-1	Path of Stream Filament Through Blade Row	IV-8
-2	Fan Vector Diagrams, Velocity and Force	9
-3	Plot, Tip Clearance Losses in Percent of Ideal Pressure Rise	12
-4	Plot, ANA Standard, Hot and Cold Days	14
-5	Construction of NACA 65 - Series Compressor Blade Section	27
-6	Ordinates for NACA 65-010 Basic Thickness Forms	28
-7	Ordinates for the NACA $a = 1.0$ Mean Line	29
-8	Lower Cambered Blade Sections Tested	30
-9	Higher Cambered Blade Sections Tested	31
-10	Typical Performance Characteristics of an Axial Flow Fan	36
-11	Blade Section Characteristics for the Blade Sections	38
thru -89	Tested in Reference 4-4	thru 116
-90	Summaries of Turning Angle, θ , Angle of Attack, α	117
thru -105	Relationship for the Blade Sections tested in Reference 4-4	thru 132
-106	Variation of Design Angle of Attack with Solidity for the Sections Tested in Reference 4-4	133
-107a & b	Variation of Design Turning Angle with Solidity and Inlet Angle for the Sections Tested in Reference 4-4	134 & 135
-108	Fan Diameter vs. Axial Velocity for Various Flows at 5" H ₂ O	136
-109	Fan Diameter vs. Axial Velocity for Various Flows at 10" H ₂ O	137
-110	Fan Diameter vs. Axial Velocity for Various Flows at 15" H ₂ O	138
-111	Fan Diameter vs. Axial Velocity for Various Flows at 20" H ₂ O	139
-112	Fan Diameter vs. RPM for Various Flows at 5" H ₂ O	140
-113	Fan Diameter vs. RPM for Various Flows at 10" H ₂ O	141
-114	Fan Diameter vs. RPM for Various Flows at 15" H ₂ O	142
-115	Fan Diameter vs. RPM for Various Flows at 20" H ₂ O	143
-116	Rotor Details	148
-117	Five Typical Fan Assemblies	149
-118	Four Typical Blade Attachment Methods	152
-119	Exploded Photograph of Fan - Single Bolt Blade Mount	155
-120	Photographs of Two Types of Axial Flow Cooling Fans	156
-121	Exploded Photograph of an Axial Flow Fan Showing Keyed Blade Mounting Method	157
-122	Photograph of Fan Shown in Figure 4-12 as Assembled	158
-123	Stator Details and Assembly	159

LIST OF FIGURES (Continued)

<u>Figure No.</u>	<u>Title</u>	<u>Page</u>
-124	Diagram of Cylindrical Ejector	IV-163
-125	Diagram of Conical Ejector	163
-126	Typical Single Stage Cylindrical Ejector	164
-127	Typical Two Stage Cylindrical Ejector	164
-128	Typical Conical Ejector	164
-129	Diagram of Typical High Performance Ejector	166
-130	Ejector Design Chart, Reduced Size	166
-131	Ejector Design Chart, Full Size (Back Fly Leaf)	168

CHAPTER IV

AIR PUMPS - FANS, EJECTORS

4-1 INTRODUCTION

To define the air flow capacity and pressure rise requirements of an air pump, the individual requirements of the system must be totalled. The total required airflow is the sum of the individual requirements of all of the cooling resistances plus an allowance, if indicated, for leakage. The air pump pressure rise required is the summation of the pressure rise required by the cooler (or the maximum resistance of one cooler when several are in parallel) plus the pressure rise required to overcome the entry, friction, shock and exit losses resulting from the flow through the duct system. Should the system be such that a portion of the pressure rise is provided by some source other than the air pump being designed, the air pump pressure rise is less than the total required by this amount. Such a case exists where entry ram pressure is provided by the forward speed of the aircraft. A helicopter or airship receives no forward speed ram effect when it hovers at zero airspeed.

Submerged engine installations used in helicopters and airships often employ a single cooling air pump to provide the cooling requirements for all of the following:

- a. Cylinder cooling on reciprocating engine.
- b. Engine oil cooler.
- c. Engine accessories.
- d. Transmission oil coolers (including turboshaft gearbox coolers).
- e. Reciprocating engine induction air (not cooling, but benefit of air pump pressure rise may be utilized).
- f. Various other single components requiring cooling.

A discussion of the necessity for balancing resistances of separate branches of a branch duct system is presented in Section 3-2.6 of Chapter III.

The total required pressure rise, being partially dependent upon duct losses, may not be finally determined until the system is designed to a point where the geometry of the ducting is finalized. It is, therefore, desirable to evaluate duct losses and approximate the air pump geometry at several phases of the cooling system design, with some form of chronological log history. This will assure that the air pump requirements are finalized when the final duct configuration is reached.

The air pump is ordinarily located upstream of cooling resistances so that it may pump more dense air than would be the case where the air first passes through a cooling resistance, is heated, and expands as a result of this temperature rise. Physical considerations sometimes dictate that the air pump be located downstream of the cooling resistance. Pumping less dense air, the air pump power required may then be greater than for one located upstream of the cooling resistance.

The determination of requirements for the critical cooling condition has been discussed in Chapters II and III.

Two basic types of air pumps will be discussed in this chapter:

1. Axial flow fans in Section 4-2.0.
2. Ejectors in Section 4-3.0.

4-2.0 AXIAL FLOW FANS

In submerged helicopter and airship cooling systems single stage axial flow fans have been much more widely used than any other single type of air pump. This type of air pump provides a relatively low pressure rise to a large airflow quantity. Recovery of entry ram pressure resulting from forward speed has been utilized in both types of aircraft to enhance the air pump pressure rise. In airships, this pays greater dividends than in helicopters because of the difference in normal operating regimes of the two types. Airships often operate at the power setting providing the greatest brake mean effective pressure at the lowest possible engine speed in order to achieve the lowest possible brake specific fuel consumption. This low RPM condition is ordinarily the most critical cooling regime and a forward speed ram pressure rise of as little as two inches of water may be profitably utilized to ease the fan design criteria.

As a result of the low engine speed being the common operational regime, over-cooling results during operations at higher engine speeds, such as in take-off and climb. Airflow rate control is ordinarily provided to prevent over-cooling. This is accomplished by area control of the cooling duct inlet.

The fan pressure rise decreases with engine speed and usually at a greater rate than the required pressure drop across the engine cylinder baffling. Therefore, the low RPM (approximately 1200 for one R1300 engine airship installation) operating condition is normally the critical one. Although this is a low power, low heat rejection condition, the low fuel flow decreases fuel cooling and the low RPM decreases the fan pressure rise, which varies as the square of the RPM. Pressure drop is ordinarily expressed, in all design work, as $\sigma \Delta P$, where σ is the air density relative to standard sea level (or, where required, other reference) air density and ΔP is the pressure drop at the air density at the conditions being investigated. One advantage of using this expression is that comparative evaluations at different density conditions may be made easily, as discussed in Chapter II.

The normal engine speed operating range for helicopters is much narrower and is at the high end of the engine allowable speed range. Any ram recovery inlet design must function so that the system does not suffer from materially increased entry losses at zero airspeed, because the helicopter hovers at high engine speed and power required, often for relatively long periods of time. The critical cooling requirements of the helicopter may occur in cruise, hover, or some other condition. Therefore, a complete investigation of the cooling requirements within the operating envelope must be made to determine the critical regime and to determine whether forward speed ram pressure may be profitably utilized.

A mechanical drive system is normally employed to turn axial flow cooling fans in helicopters and airships. They may be turned at engine speed or at propeller speed when a gear-reduction engine nose section is used, or they may be driven by a separate gear train to achieve a desired speed.

In many installations, cooling is required at a number of places remote from one another, such as cooling an engine and oil in transmissions which may be at the other ends of the aircraft. Here weight and pressure losses prohibit the use of a central source with air distribution by ducting. Either a number of separate small cooling systems must be used or the oil to be cooled must be carried by long lines to a group of centrally located coolers which can all be fed from a common air source.

The axial flow fan consists essentially of one or more sets of rotating blades which may be operating in conjunction with one or more sets of stationary guide vanes. A set of rotating blades is referred to as a "rotor" and a set of stationary blades as a "stator". A rotor operating without a stator increases the static pressure and imparts kinetic energy of rotation to the air passing axially through the rotor. This kinetic energy of rotation may be converted into additional static pressure rise by using a stator downstream of the rotor to turn the rotational component into the fan axial direction. A stator mounted upstream of a rotor turns the air and decreases the static pressure upstream of the rotor. The rotor then returns the direction of the air to the axial direction and increases the pressure. The most commonly used configuration is the rotor-stator arrangement. The other arrangements, rotor only, stator-rotor, and the rotor-stator with upstream guide vanes, are possible, but only the design of a rotor-stator arrangement is treated in detail in this Section. However, a discussion of fixed and variable angle upstream guide vanes is presented in Section 4-2.2.7.1.

The detailed treatment of the rotor-stator arrangement in this Section 4-2.0 is comprised of the following items, which yields and assumes the use of an NACA 65-series compressor blade section:

- a. Aerodynamic theory.
- b. Selection of fan parameters and design details.
- c. Cascade data.

4-2.1.0 Aerodynamic Theory of Axial Flow Fans

Various theoretical treatments, including those of references 1 and 2, have fully developed fan design based on single airfoil theory. Current practice for the design of single stage axial flow fans for submerged cooling applications in helicopters and airships is to utilize cascade test data, rather than single-airfoil theory. These data were presented in Reference 4 for two-dimensional cascade tests of NACA 65-series compressor blades at low speed. Plots of the data required for fan design have been reproduced in this Handbook.

The presentation of aerodynamic theory in this section is limited to that amount required: (1) for the complete fan design; and (2) for an understanding of fan capabilities to provide the required pressure rise to the air being pumped through the system by the fan.

The basis of any fan design is a vector diagram. Figure 4-1 shows the path of a stream filament through a blade cascade and Figure 4-2, the velocity vector diagrams for this flow, at a given radial station of the cascade of blades. Fan symbols are presented in Appendix IV and fan design formulae in Section 4-2.1.1 of this Chapter.

4-2.1.1 Development of Fan Design Formulae

Referring to Figure 4-1, the path of one stream filament through a blade cascade is shown, as is the blade wake A_B , the thickness of which decreases as the flow continues downstream.

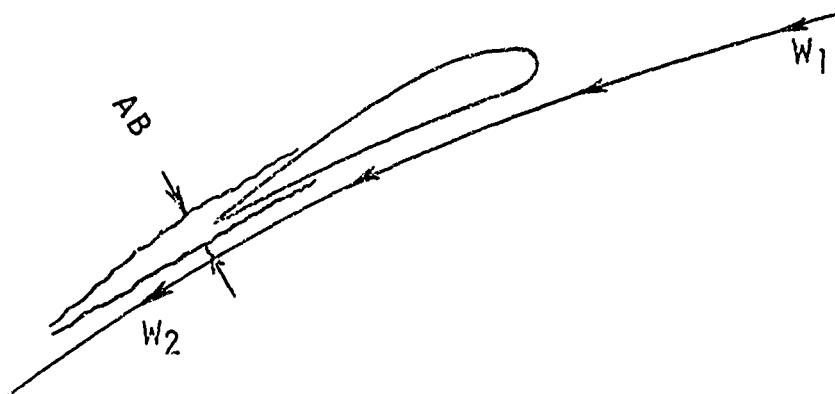


FIGURE 4-1. Path of Stream Filament Past Cascade Blade and Wake Downstream of Blade

Figure 4-2 shows the construction of both velocity and force diagrams.

Generally, at blade solidity values of C/S greater than 0.5, the series of airfoil sections is considered to be a cascade. At solidity values below 0.5, the airfoils are better treated individually, with conventional propeller in-flow corrections. For helicopter and airship axial cooling fans, cascades are usually employed to provide the static pressure ratios required.

Because the velocity vector diagram, as is shown in Figure 4-2, is the basis for the fan design, the construction of such a vector diagram is the first step in the fan design. The terms in the following equations are defined in Figure 4-2.

The selection of the parameters of the fan root and tip diameters, rotational speed and airflow rate permit the determination of the vectors

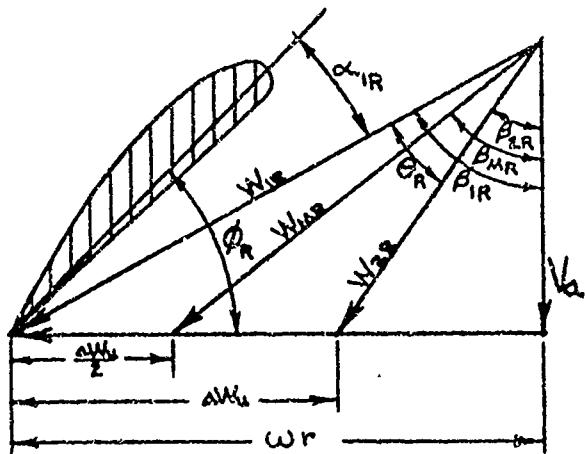
V_a and ωr

$$V_a = \frac{0}{\frac{\pi}{4}(D_T^2 - D_R^2)} \quad \text{Equation 4-1}$$

$$\omega r = \frac{(RPM)(D)\pi}{60} \quad \text{Equation 4-2}$$

RELATIVE VELOCITY
VECTOR DIAGRAMS

ROTOR
(AIRFOIL SECTION)



TRUE VELOCITY
VECTOR DIAGRAMS

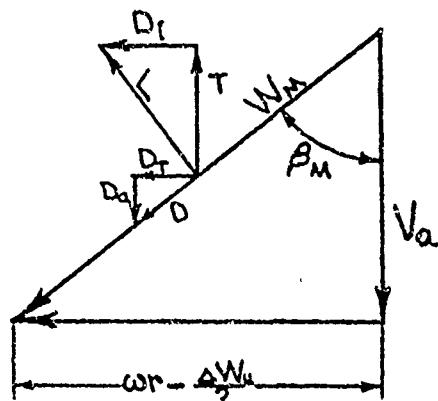
ENTERING
ROTOR

V_a

RELATIVE FORCE
VECTOR DIAGRAM

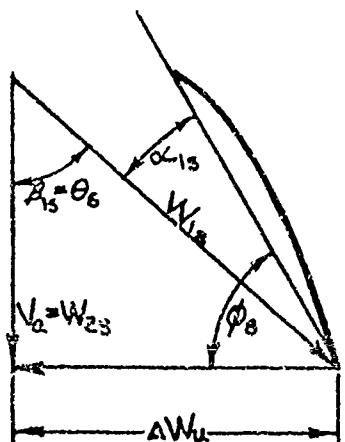
LEAVING ROTOR
ENTERING STATOR

$V_a + \Delta W_u$



STATOR

(CONSTANT THICKNESS
BLADE FORMED TO
MEAN LINE)



ROTATION

LEAVING
STATOR

V_a

DEFINITIONS

V_a	Air Axial Velocity Component
ωr	Rotor Rotational Velocity Component
ΔW_u	Rotational Velocity Component Imparted to Air by Rotor
W	Resultant Relative Velocity of Air
β_{IR}	Air Inlet Angle to Rotor with Respect to Axial Direction
θ	Air Turning Angle
ϕ	Incidence Angle
α	Angle of Attack
L	Lift
D	Drag
T	Thrust

SUBSCRIPTS

1	Entering
2	Leaving or Exiting
M	Mean
R	Rotor
S	Stator
a	Axial
u	Rotational
i	Induced
t	Tangential

FIGURE 4-2. Typical
Fan Vector Diagrams

The resultant inlet velocity vector is then known:

$$W_1 = \left(V_a^2 + (\omega r)^2 \right)^{1/2} = \frac{\omega r}{\sin \beta_i} \quad \text{Equation 4-3}$$

where $\beta_i = \tan^{-1} \frac{\omega r}{V_a}$ Equation 4-4

The required fan pressure rise, determined according to the procedures of Chapters II and III, is known and the principle of obtaining this pressure rise may be visualized most easily as the increase in static pressure which occurs as the stream filament velocity pressure is decreased from

$$q_1 = \frac{1}{2} \rho W_1^2 \quad \text{Equation 4-5}$$

entering the cascade, to

$$q_2 = \frac{1}{2} \rho W_2^2 \quad \text{Equation 4-6}$$

leaving the cascade.

$$\text{Then } \Delta P_{\text{Fan}} = \frac{1}{2} \rho (W_1^2 - W_2^2), \quad \text{Equation 4-7}$$

which expression clearly defines the transformation of a portion of the velocity pressure into an equal amount of static pressure, losses being neglected for the moment. These losses are discussed in the following section. It is to be noted that the blocking effect of the airfoil, evidenced as the blade wake area, A_B , in Figure 4-1, which reduces the flow area, is negligible for helicopter and airship cooling fan design purposes. Therefore, equation 4-7 is considered valid.

The means of accomplishing this required reduction of the inlet relative velocity vector W_1 to the existing relative velocity vector W_2 in order to achieve the fan static pressure rise is discussed in detail in Section 4-2.2.0 of this chapter.

The presentation in Section 4-2.2.0 includes the following:

1. Fan parameter selection details.
2. Calculation of power, efficiency, and losses.
3. Cascade data.

Stated briefly, the requirement is to select a cascade which will provide the required turning angle, $\theta = \beta_1 - \beta_2$, based on the values of the various parameters. Several possibilities will be available as combinations of low solidity and large angle of attack or high solidity and smaller angle of attack.

4-2.1.2.0 Fan Losses

Three main kinetic energy losses and one potential source of energy loss arise in the action of a rotor: (1) the profile-drag losses on the blades, (2) the tip-clearance losses, (3) the inner-wall losses, and (4), the rotational kinetic energy of the flow downstream of the rotor.

4-2.1.2.1 Profile Drag Losses

The profile-drag losses, the quantitative determination of which is discussed in Section 4-2.2.3 of this chapter, are based on values of coefficient of drag, C_d , presented in plot form with other blade section characteristics in Figures 4-11 to 4-89, inclusive. In Reference 4-4, resultant blade force coefficients were calculated from test data. These coefficients were resolved into components perpendicular and parallel to the mean velocity vector, W_m , to obtain the lift coefficient C_l , and the drag coefficient C_d , respectively, shown in the above Figures. The mean velocity was calculated as the vector average of the velocities far upstream and far downstream of the test cascade. These coefficients derive, of course, from the drag and lift forces shown on the force diagram in Figure 4-2.

4-2.1.2.2 Clearance Losses

From Reference 4-1, the tip clearance losses are usually much greater than the profile-drag losses. They are caused by flow leakage from the high-pressure to the low-pressure side around the blade tip. The loss in efficiency due to tip clearance is evidenced as a reduction in pressure rise of the fan, the power taken by the fan remaining about the same for all clearances. This effect is probably largely caused by turbulent mixing in the axial direction.

In Reference 4-2, the tip clearance losses were determined experimentally for an eight-blade rotor-stator combination with rotor solidity varying from 0.79 at the hub to 0.52 at the tip section. The hub diameter was 9.85 inches and the outer wall diameter was 19.7 inches. Figure 4-3 presents the mean of curves determined for three different blade loadings. The separate curves depart from the mean by approximately 1 percent. The reduction in pressure due to tip clearance is large, about 7.5 percent for a clearance of only 2 percent of the blade span. The variation of tip clearance loss as a function of the ratio of tip clearance to blade span in percent, resulting from this test, was extracted from Reference 1 and is presented in Figure 4-3.

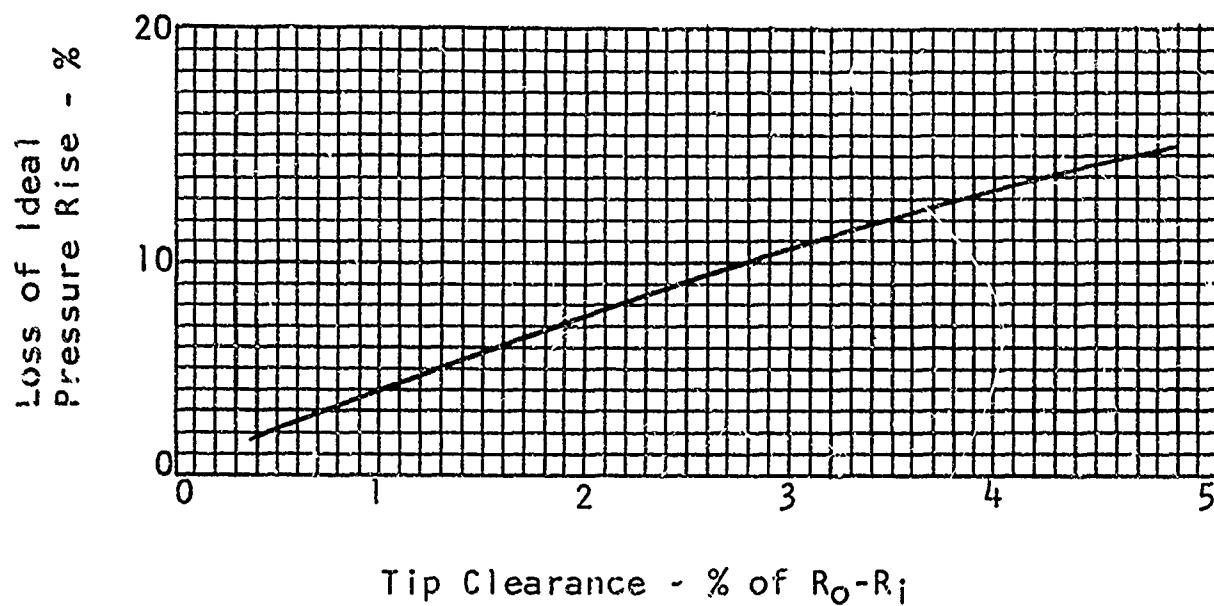


FIGURE 4-3. Tip-Clearance Losses in Percent of Ideal Pressure Rise.

4-2.1.2.3 Inner Wall Losses

Again from Reference 4-1, the inner-wall losses are caused by the boundary layer on the inner wall of the rotor. By the same argument as previously given, these losses should also manifest themselves as a reduction in pressure rise. The air at the hub, however, is swept to the tip by the centrifugal force of rotor rotation, with the result that these losses may be largely included in the tip-clearance losses.

Some measurements of wall losses in a stationary cascade are given in Reference 4-5. The results are not directly applicable to a rotor, however, because the span-wise flow of air just mentioned was not present in these tests. Because these inner wall losses for rotating cascades cannot be determined analytically or measured, no direct correction can be applied for them. Since they are manifested largely as tip clearance losses, no correction other than for the tip clearance losses is required. This is true because the Reference 4-1 tip clearance loss data in Figure 4-3 include the effect of inner wall losses.

4-2.1.2.4 Rotational Kinetic Energy of Flow Downstream of Rotor

The rotational kinetic energy of the downstream flow will be dissipated and thus lost if it is not transformed to pressure energy by a set of stationary guide vanes or by other means. Primarily for this reason, present helicopter and airship axial cooling fans are designed with a rotor and a stator to turn all rotational components into the axial direction.

4-2.2.0 Application of Theory to Design

4-2.2.1 Airflow and Pressure Rise Requirements

The cooling requirements for the cooling system are determined in terms of total pressure rise and cooling air flow rate required, as discussed in Chapters II and III.

In order to determine these requirements, the various flight regimes are investigated to arrive at the most severe cooling requirements. The assumed ambient temperature for this study is ordinarily that of an ANA Hot Day (Figure 4-4) for the particular altitude in question.

The pressure rise required for a given engine cooling installation is the sum of the following:

- a. *Pressure drop across the engine cylinder baffles or oil cooler.
- b. Pressure drop through ducting (including fan upstream losses, shock and friction losses and all exit losses).
- c. Fan velocity pressure loss, a part of the ducting loss, but the only loss which is a function of fan axial velocity.

*For a system with several branches, the design pressure will be determined by the branch where this total is highest.

The cooling airflow requirement is the sum of the following:

- a. Airflow across the engine cylinder baffles.
- b. Airflow across all oil coolers (engine, transmissions).
- c. Leakage allowance.
- d. Engine induction air, if supplied by common system.
- e. Airflow ducted directly to accessories.

For convenience in evaluating the Q and ΔP required at various points within the operating envelope of the aircraft being designed, the fan requirements may be most easily compared by reducing the requirement at each flight condition to a common atmospheric condition and RPM. Sea level standard atmospheric conditions and normal RPM are usually chosen for this comparison point (Figure 4-4). This reduction to a common operating point follows the fan laws, wherein:

$$Q = f \text{ (RPM)}$$

$$\Delta P = f (\sigma^*, \text{RPM}^2)$$

Thus, the cooling airflow and the pressure rise to be supplied by the air pump at standard conditions are known.

4-2.2.2 Selection of Design Parameters

This section presents a step-by-step procedure to design a rotor-stator cooling fan arrangement. The selection of various parameters is discussed herein at the point where each parameter is considered in the design procedure. This procedure is tailored to the selection of an NACA 65-series compressor blade for both the rotor and stator, which form is most widely used in the field under discussion.

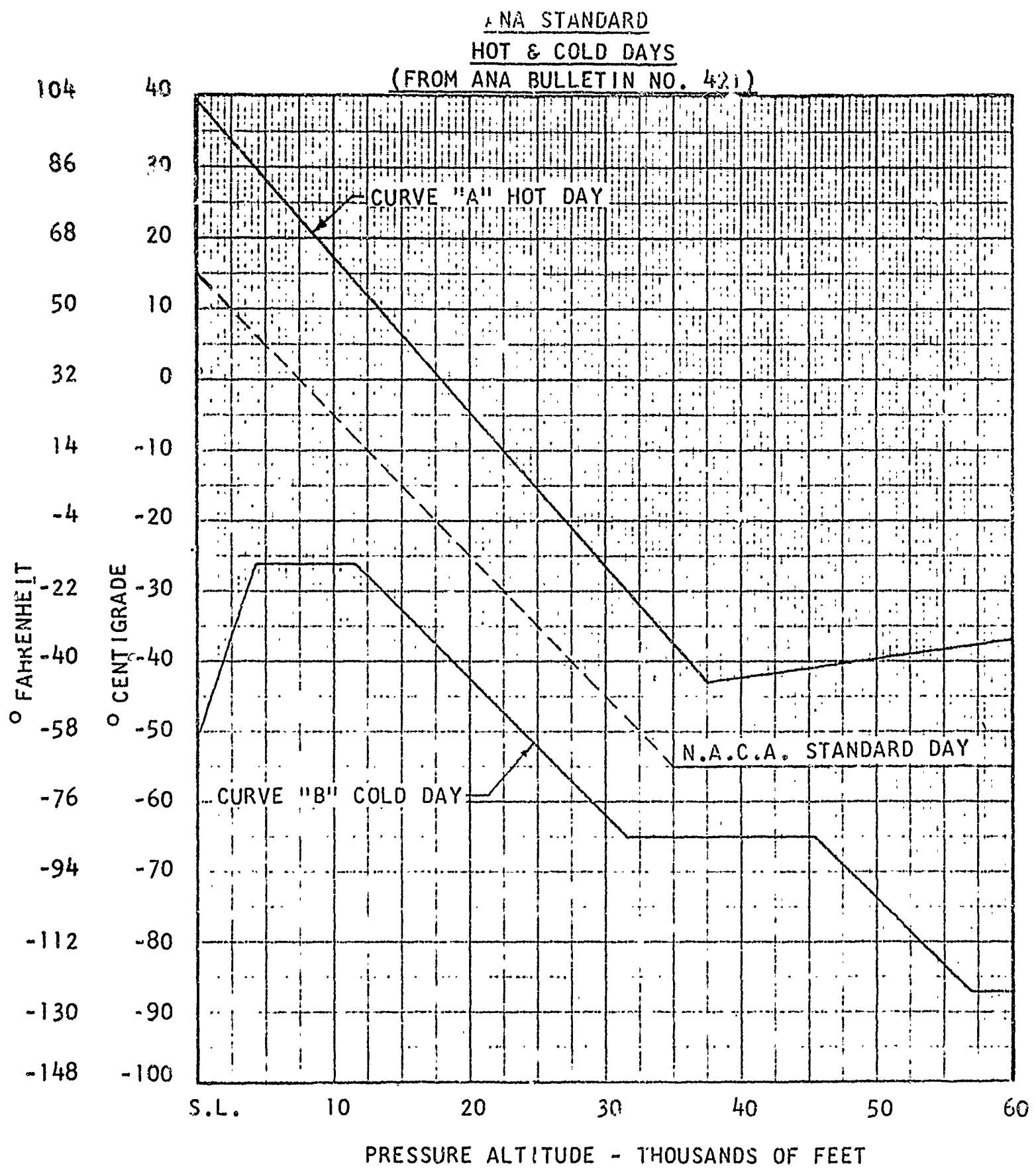


FIGURE 4-4. ANA Standard Hot and Cold Days
(From ANA Bulletin No. 421)

The National Advisory Committee for Aeronautics performed systematic two-dimensional cascade tests of NACA 65-series compressor blades and reported the results in Reference 4-4. In this investigation blade sections of camber from C_{l_0} of 0 to C_{l_0} of 2.7 were tested over the useable angle of attack range for various combinations of inlet angle β_1 of 30° , 45° , 60° and 70° , and solidity σ' of 0.50, 0.75, 1.00, 1.25 and 1.50. Design points are indicated in this reference for each combination of these parameters on the basis of optimum high-speed operation. Interpolation and limited extrapolation are possible.

Because of the systematic test results of Reference 4-4, the procedure herein, based on these data, permits the accurate determination of fan performance, whereas no other design method yielding the same accuracy has been found. However, considerable and valuable theoretical and design discussions are presented in References 4-6 and 4-7.

A preliminary study of axial velocity, RPM, and fan diameter should be made for the required flow and pressure rise. The preliminary fan design charts should prove helpful in conducting this study (in Section 4-2.2.6 and in Figures 4-116 to 4-123, inclusive).

4-2.2.2.1 Choice of Fan Rotational Speed

Ordinarily, the fan rotational speed for a reciprocating engine cooling installation is defined by the operating speed of the engine, since an engine cooling fan is usually mounted on the engine shaft or propeller shaft. A choice of rotational speed is ordinarily available to the fan designer for application on a turbine installation. Successful fans have been designed to operate over at least part of the range from 1000 to 8000 RPM for helicopters and airship engine and transmission cooling applications.

4-2.2.2.2 Selection of Fan Diameters and Axial Velocity

The following considerations determine the fan outside diameter. A maximum value may be expected to be dictated by available space and weight considerations. The outside and inside diameters must be chosen to provide the cross-sectional annular area required for the cooling air moving at a chosen velocity. The axial velocity of the air is ordinarily established at as low a value as possible in order to keep downstream fan diffuser losses at a minimum.

The minimum axial velocity V_a may be determined as a value which results in θ , the turning angle, a function of V_a , becoming so large that the fan operation range is severely limited. This occurs when the design turning angle of some blade station must approach the maximum turning angle possible.

Depending on the cascade chosen, turning angles as high as 40° to 50° are possible; however, a turning angle of 25° has been found to provide sufficient operating range for nearly all conditions. A limit to turning angle for helicopter cooling fans is therefore recommended to be 25° .

The upper limit of V_a may be taken to be that which would result in W_{1T} becoming 600 feet per second.

One other consideration in choosing the relationship between the inner and outer diameter is that, as the inner, or hub, diameter becomes larger in relation to the outer, or tip, diameter, the blade span becomes shorter. For a given blade tip clearance value, then, the ratio of tip clearance to blade span increases and, as a result, the tip clearance loss increases, resulting in a decreased blade row (rotor) pressure rise. It is stated in Reference 4-6 that an increase in the ratio of the root diameter to tip diameter above 0.85 causes a marked decrease in the efficiency of an axial flow compressor. One consideration that may influence the minimum size of the hub is that the blade attachment to the hub becomes more difficult with decreasing hub size.

In summation, then, the relationship among the required airflow rate (Q), axial velocity (V_a), and fan inner (D_i) and outer (D_o) diameters may be expressed as

$$Q = V_a A$$
$$= V_a \frac{\pi}{4} (D_o^2 - D_i^2)$$

4-2.2.2.3 Choice of Rotor Inlet Angle, I

The inlet angle, β_1 , is a function of the axial velocity, V_a , and the rotational velocity, ω_r , as shown in the velocity diagram of Figure 4-2. Whereas the choice of a low value of V_a is desirable to minimize downstream losses, and high ω_r values may be expected in an aircraft application, a limiting ratio of ω_r to V_a is established by the upper value of β_1 of 70° tested in Reference 4-4 (for 65-series compressor blades). Extrapolation not exceeding 5° above this value has been undertaken successfully in fan design applications. Since the maximum β_1 occurs at the tip for uniform axial velocity fans, this limits the fan diameter-RPM combination for a given V_a .

The angles defining the rotor and stator blading at root and tip may now be determined. General practice is to proceed entirely through the stage at one limit radial station, i.e., root or tip. It is emphasized that the blade vector diagrams and resulting cascades are different for the root and for the tip. Certain of the parameters may be expected to be encountered at limiting magnitudes at the root and others at the tip. Briefly, the inlet angle is greatest at the tip, the incidence angle and the turning angle are greatest at the root. Approximate practical limits are:

$$\theta_{\text{Root Max.}} = 25^\circ, \theta_{\text{Tip Min.}} = 4^\circ, \beta_1 \text{ Tip Max.} = 70^\circ \\ (75^\circ \text{ extrapolated}).$$

At this point, the following parameters have been chosen:

Q Airflow, cfm.

v_a Axial velocity through fan, fps.

r_o Fan rotor tip radius, feet.

r_i Fan rotor hub radius, feet.

A_f Annular cross-sectional area through fan, square feet.

ωr Velocity in plane of rotation, fps.

s Blade span, feet.

β_1 Rotor inlet velocity direction, degrees, at root or tip.

w_1 Rotor inlet velocity magnitude, fps, at root or tip.

Somewhat arbitrarily the flow path through the root section will first be investigated.

A trial and error approach is now taken to provide the required fan pressure rise. The desired, or ideal rotor pressure rise is chosen as described in Section 4-2.2.2.4. The rotor pressure rise is primarily a function of the difference between the rotor inlet and outlet velocity magnitudes squared, which magnitudes define turning angles when combined vectorially (Figure 4-2).

4-2.2.2.4 Rotor Outlet Velocity Magnitude and Direction, w_2 and β_2

The ideal pressure rise of the rotor, neglecting losses, referring to Figure 4-2, is

$$\Delta P_{ir} = \frac{1}{2} \rho (w_{1r}^2 - w_{2r}^2)$$

where $w_{1r}^2 = v_a^2 + (\omega r)^2$

and $w_{2r}^2 = v_a^2 + (\omega r - \Delta w_u)^2$ Equation 4-8

Substituting the terms for w_{1r}^2 and w_{2r}^2 in the equation 4-8 results in the following:

$$\Delta P_{ir} = \frac{1}{2} \rho (2\omega r \Delta w_u - \Delta w_u^2) \quad \text{Equation 4-9}$$

Similarly, the ideal pressure rise of the stator, neglecting losses, is

$$\Delta P_{is} = \frac{1}{2} \rho (w_{1s}^2 - w_{2s}^2) \quad \text{Equation 4-10}$$

where

$$w_{1s}^2 = v_a^2 + \Delta w_u^2$$

and

$$w_{2s}^2 = v_a^2$$

Substituting the terms for w_{1s}^2 and w_{2s}^2 in equation 4-10 for the ideal pressure rise of the stator, above, gives

$$\Delta P_{is} = \frac{1}{2} \rho \Delta w_u^2. \quad \text{Equation 4-11}$$

Then

$$\begin{aligned} \Delta P_{ifan} &= \Delta P_{ir} + \Delta P_{is} \\ &= \rho \omega r \Delta w_u \end{aligned} \quad \text{Equation 4-12}$$

An analysis of equations 4-9, 4-11 and 4-12 for any given fan design problem will determine the ideal relationship between the rotor and the stator pressure rise. The analysis of this ideal relationship is essential so that the trial and error design method does not become too lengthy by virtue of poor assumptions of the ΔP_{ir} .

The rotor outlet velocity magnitude, then, is expressed by equation 4-8 above, the direction of which is expressed by

$$\beta_{2r} = \cos^{-1} \frac{v_a}{w_{2r}}$$

It is reiterated that the cascade is theoretically different for each radial station because ωr increases linearly from the blade root to the blade tip. At least these two extreme positions, i.e., root and tip, should be investigated and defined. Intermediate stations usually should be defined when the blade span exceeds three inches. This necessity to investigate and finally to define the cascade for two or more radial stations is discussed further in the illustrative problem of Appendix I.

4-2.2.2.5 Rotor Turning Angle, θ_R

The turning of the air through the rotor results in a decrease of the tangential, or rotor plane, component of the air velocity relative to the rotor, as seen in Figure 4-2.

$$\Delta W_u = \omega r - W_2 \sin \beta_2$$

$\theta_R = \beta_1 - \beta_2$, the rotor turning angle, which, before the design is carried further, should be investigated for a possible approach to θ_{\max} . Twenty-five degrees at the critical root section is an approximate limit for the NACA 65-series compressor blade sections.

It may be noted that V_a and ΔW_u define the stator entry velocity conditions. The stator design presentation begins in Section 4-2.2.2.7.

4-2.2.2.6 Choice of the Rotor Cascade

The requirements and the operating conditions for the cascade have now been chosen. That is, the inlet angle and the turning angle have been determined. It is now necessary to choose the cascade of blades which will produce the required air turning angle when the cascade operates at the design conditions.

The cascade is defined by solidity, blade camber and operating angle of attack. These three parameters are interdependent so that any two define the third, and therefore, the cascade, for a given design requirement. Normally the solidity and the camber are selected, thereby defining the design angle of attack, α_{design} .

The solidity, σ' , is defined here, as in Reference 4-4, at a given radius, as:

$$\sigma' = \frac{c}{S} = \frac{bc}{2\pi r}$$

where c = blade chord, feet,

b = number of blades

S = peripheral spacing between like points on adjacent blades, feet

The use of Figures 4-90 through 4-105 permits a selection of σ' , α_{design} , and the airfoil contour necessary to obtain the required θ at β_1 . For an inlet angle β_1 of 70° , solidities of $\sigma' = 1.0, 1.25$, and 1.5 were tested in Reference 4-4. Interpolation of this parameter is satisfactory. A root solidity should be chosen which will not result in this parameter being reduced below $\sigma' = 1.0$ at the tip, in order to eliminate the necessity to extrapolate below 1.0 if high β_1 values (approximately 70°) are used.

The blade chord and number of blades, interdependent parameters, may now be chosen for the rotor, but this step need not be undertaken until the trial-and-error procedure has progressed to the final step which produces the required fan pressure rise.

For the rotor only, at this point, the relationship is:

$$bc = 2\pi r \sigma'$$

Space, weight and cost considerations enter into the choice of the blade chord and number of blades. The rotor hub becomes thicker axially as the blade chord increases. Axial space limitations will ultimately define a limit. The stator depth, to be discussed later, must be sufficient to provide structural integrity and may limit the rotor axial depth.

The number of blades is ordinarily limited by space considerations, as well as by weight and cost considerations. Blade attachment hardware may dimensionally limit the number of blades.

It may be pointed out that reciprocating engine cooling fans in helicopters are ordinarily designed to provide the fly wheel inertia requirement for the aircraft engine and this consideration may enter into blade geometry choices, although it is more likely that the required weight will be provided primarily by the thickness of the hub faces or discs, rather than by attempting to provide this weight by an increased number of blades and attendant hardware.

The design rotor blade root angle of attack α , which was determined for the chosen cascade, is now used to define the incidence angle, or angle that the rotor blade chord line is inclined to the rotor plane of revolution. The incidence angle, θ , is established as:

$$\theta = 90^\circ - \beta_1 + \alpha$$

4-2.2.2.7 Determination of Stator Root Parameters

The stator root section may now be designed in the same fashion as the rotor root. The rotor root exit velocity conditions define the entry conditions to the stator root. In order to recover kinetic energy losses of rotation downstream of the fan, the stator is designed to have exit velocity components in the axial direction only.

Some difficulty is often encountered in visualizing the airflow through the fan, so that a short review discussion of the situation may be helpful. In the case of the rotor stator arrangement, although the cascade is considered stationary in the analysis, with relative air-flow velocities, the air actually approaches the rotor in a purely axial direction at a velocity of V_a feet per second. The rotor, turning at ω radians per second, imparts a tangential velocity component to the air stream. This component, ΔW_u , is in the direction of fan rotation. For the purpose of the analytical rotor design, the rotor blade is considered stationary and both the entry and exit velocity vectors are acting relative to the blade at the respective angles of β_{1r} and β_{2r} ; whereas, when the turning rotor is considered, the air retains its axial velocity component and, in addition, receives the tangential or rotational component imparted by the rotor.

These two components, V_a and ΔW_u , determine the magnitude and direction of the velocity vector entering the stator section. The inlet angle to the stator is

$$\beta_{1s} = \tan^{-1} \frac{\Delta W_u}{V_a}$$

and the magnitude is

$$W_{1s} = \left(V_a^2 + (W_u)^2 \right)^{\frac{1}{2}}.$$

The stator turning angle is defined as the difference between the stator inlet and exit angles or

$$\theta_s = \beta_{1s} - \beta_{2s}.$$

However, because it is desired to release the air at the stator exit with no rotational velocity, the stator exit angle β_{2s} , should be zero. The stator turning angle at the design condition is then equal to the stator inlet angle, or

$$\theta_s = \beta_{1s}$$

The stator thus removes the ΔW_u velocity component from the air, producing a rise in static pressure. The ideal pressure rise for the stator is then

$$\Delta P_{ideal\ stator} = 1/2 \rho \left(W_{1s}^2 - V_a^2 \right)$$

or

$$\Delta P_{ideal\ stator} = 1/2 \rho \Delta W_u^2$$

The design procedure will now be resumed, with the stator root section being considered. The inlet angle, β_{1s} , turning angle, θ_s , and exit angle $\beta_{2s} = 0^\circ$, are determined as described in the preceding paragraphs. The parameters of stator root solidity, blade chord, number of blades, camber, angle of attack and incidence angle are chosen as described in Section 4-2.2.2.5.

4-2.2.2.8 Determination of Rotor and Stator Tip Parameters

The preceding steps in Sections 4-2.2.2.4 to 4-2.2.2.7, inclusive, may now be repeated to define the rotor and stator tip parameters. One note of caution, however, is that the parameters of each section through the stage, i.e., rotor and stator, should be so chosen as to provide an average total pressure rise within one to two percent of the ideal pressure rise with due consideration for losses, as discussed in the following sections, to provide spanwise equilibrium of total pressure rise.

Such constant pressure blading has been suggested to reduce spanwise flow effects. The criterion of constant spanwise axial velocity requires that the rotor tip inlet angle β_1 be greater than at any other spanwise station. It is to be remembered that providing equal spanwise total pressure rise through the rotor will tend to prevent the formation of radial velocity components. Removing all radial velocity components from the airflow leaving the stator will stabilize the downstream flow, as discussed previously. As at the root, the inlet angle β_1 at the tip is a function of the axial velocity V_a and the rotational velocity ωr . The design is then carried on in the manner already described, so that equal total pressure rise is accomplished from root to tip of the rotor with the stator exit velocity being V_a with no rotational component. The rotor tip turning angle should have at least a slight positive value (previously mentioned as arbitrarily 4°).

4-2.2.2.9 Definition of Intermediate Spanwise Stations

If the blade span is less than three inches in length, satisfactory performance may usually be achieved by defining the full blade with straight lines joining the root and tip sections, i.e., leading edge, trailing edge and upper and lower surfaces with due consideration for chord differences, if any. For longer blades, intermediate spanwise stations should be investigated, based on the constant spanwise total pressure rise criterion, to produce the required airfoil section at one or more intermediate stations. Lines should then be lofted to define the spanwise variations of like points of the cross-sections.

4-2.2.3 Determination of Fan Total Pressure Rise

Although the pressure rise for each spanwise station of both the rotor and stator can be determined as each of those sections is investigated, the discussion of this parameter has been introduced here because the proper treatment may now be discussed in relation to over-all fan performance.

The determination of the pressure rise through one blade row is now undertaken. For the rotor,

$$\Delta P_{i\text{Rotor}} = \frac{1}{2} \rho (w_{1r}^2 - w_{2r}^2)$$

and for the stator

$$\Delta P_{i\text{Stator}} = \frac{1}{2} \rho (w_{is}^2 - V_a^2) - \frac{1}{2} \rho (\Delta w_u)^2.$$

Neglecting for the moment the pressure loss resulting from rotor tip clearance, the actual pressure rise in each row is $\Delta P_{i\text{actual}} = \Delta P_{i\text{ideal}} - \Delta P_{i\text{pro}}$, in which the profile drag pressure loss

$$\Delta P_{i\text{pro}} = f \times c_d \times \sigma' \times \frac{W_1}{V_a} q_f$$

where c_d is the profile drag coefficient, σ' is the solidity, θ is the turning angle and α is the angle of attack of the blade form chosen,

as determined from the blade section characteristics on Figure 4-11 through 4-89 inclusive. The factor f in the above formula is included for the purpose of increasing the c_d value. The values of c_d in Reference 4-4 varied as much as 30 percent with Reynolds number and roughness. One manufacturer uses a value of $f = 1.5$ for forged and precision-cast blades and $f = 2.0$ for rough-cast blades. There are no data to indicate the accuracy of these factors. However, it may be reiterated that profile drag losses have a very small effect on the fan pressure rise. The parameters σ' , W_1 and V_a have been explained. The quantity q_f is the axial velocity pressure or $q_f = \frac{1}{2} \rho V_a^2$.

The tip clearance losses, which are presented herein in Figure 4-3, as in Reference 4-1, are expressed as a percentage reduction of fan ideal pressure rise as a function of rotor tip clearance. Therefore, the blade span

loss must be applied to both the rotor and stator. To determine the actual fan pressure rise, average ideal rises for the rotor and for the stator should be used in determining all of the losses. The actual fan pressure rise, then, is $\Delta P_{fan} = \Delta P_{ir} (1 - T.C. \text{ Loss Factor}) - \Delta P_{pror} + \Delta P_{is}$ (1-T.C. Loss Factor) - ΔP_{ros} , where the values refer to the average of all of the sections computed, first for the rotor and then for the stator. The rotor ideal pressure rise, span-wise, should be equal, while the stator ideal pressure rise for each section must be of a magnitude to remove the tangential component of velocity imparted by the rotor at that section.

The actual fan pressure rise must now be compared to the required pressure rise. If the rise achieved is greater than required, the trial and error procedure must be repeated, with the rotor ideal pressure rise requirement reduced. The change of the rotor required pressure rise, which is initially used to determine the rotor velocity inlet conditions, is magnified in that a reduction will reduce both the rotor and stator pressure rises and an increase will increase both.

4-2.2.4 Estimation of Fan Efficiency and Power Required

The discussion of tip clearance losses in Reference 4-1 included the statement that "The loss in efficiency due to tip clearance is evidenced as a reduction in pressure rise of the fan, the power taken by the fan remaining about the same for all clearances". Therefore, it is assumed that -

- the pressure rise at any blade element is equally affected by tip clearance losses (due to spanwise flow), and
- the fan power required is not affected by the fan tip clearance,

an expression to approximate the fan efficiency may be derived. Referring to the fan vector diagrams of Figure 4-2, the fan output may be written as

$$HP_{OUTPUT} = \frac{0}{550} \times [(\Delta P_s + \Delta P_r) n_{T.C.} - \Delta P_{as} - \Delta P_{ar}]$$

and the power input as

$$HP_{REQ} = \frac{D_i + D_t}{550} \omega r$$

For a given blade element, the efficiency is therefore

$$\eta_{Element} = Q \left[\frac{(\Delta P_S + \Delta P_R) \eta_{T.C.} - \Delta P_{as} - \Delta P_{ar}}{\omega r (D_i + D_t)} \right] \quad \text{Equation 4-13}$$

where

$$\Delta P_S = \frac{\rho}{2} (\Delta W_u)^2$$

$$\Delta P_R = \frac{\rho}{2} \left[2\omega r (\Delta W_u) - (\Delta W_u)^2 \right]$$

$$\Delta P_{as} = V_a w_m \sigma'_R c_{dR} \frac{\rho}{2}$$

$$\Delta P_{ar} = V_a \sigma'_S c_{ds} \frac{\rho}{2} \left[V_a^2 + (\Delta W_u)^2 \right]^{\frac{1}{2}}$$

$$D_i = A (\Delta P_R) \frac{V_a}{\omega r - \frac{\Delta W_u}{2}} = Q \rho \Delta W_u$$

$$D_t = (\omega r \frac{\Delta W_u}{2}) w_m \sigma'_R A c_{dR} \frac{\rho}{2}$$

Substituting these terms in Equation 4-13 and simplifying gives

$$\begin{aligned} \eta_{Element} &= \frac{\eta_{T.C.}}{1 + c_{dR} \sigma'_R \frac{w_m}{4 V_a} \frac{2 \omega r - 1}{\Delta W_u}} \\ &- \frac{V_a}{\omega r} \left[\frac{c_{ds} \sigma'_S \sqrt{V_a^2 + \left(\frac{\Delta W_u}{2} \right)^2} + c_{dR} \sigma'_R w_m}{2 \Delta W_u + (c_{dR} \sigma'_R w_m) \frac{\omega r - (\Delta W_u)^2}{V_a}} \right] \end{aligned} \quad \text{Equation 4-14}$$

The blade section characteristics data in Figures 4-11 to 4-69, inclusive, for the applicable cascade combination, are used for the solution of Equation 4-14. The over-all fan efficiency may be determined as the mean of the tip and root element efficiencies. The estimated fan power required may then be calculated by

$$HP_{Req.} = \frac{\Delta P_{Fan} \times Q}{33,000} \div \eta_{Fan}$$

where ΔP_{Fan} is expressed in psf and Q in cfm.

Fan efficiency and power required calculations are illustrated in the sample problem, Appendix I.

4-2.2.5 Blade Airfoil Layout

Having established the values of β_1 , θ , σ' and α_{des} , and airfoil camber, the applicable blade form is completely defined at the particular radial station under investigation. Figures 4-6, 4-7, 4-8 and 4-9, are used directly to establish the blade form. Figure 4-6 is a Table of Ordinates for NACA 65-010 Basic Thickness Forms, with stations and ordinates in percent of chord. The first column of ordinates describes the surfaces of the airfoil section tested in Reference 4-4 and the second column is a presentation of derived values. Either of these sets of ordinates may be used to design 65-series compressor blades, within the accuracy of the test results of Reference 4-4. The basic mean line, tabulated in Figure 4-7, is the $a = 1.0$ mean line given on Page 97 of Reference 4-9. The amount of camber is defined in Reference 4-9 above as design lift coefficient for the isolated airfoil, and that system was retained in Reference 4-4, as presented herein in Figure 4-7. Ordinates and slopes for the $a = 1.0$ mean line of Figure 4-7 for $C_{l_0} = 1.0$ are scaled directly to obtain other cambers. Cambered blade sections are obtained by applying the thickness of Figure 4-6 perpendicular to the mean line at stations laid out along the chord line, as illustrated in Figure 4-5. In this designation system, the camber is expressed by the first number after the dash in tenths of C_{l_0} . For example, the NACA 65-810 and NACA 65-(12)10 blade sections are cambered for $C_{l_0} = 0.8$ and $C_{l_0} = 1.2$, respectively.

Figure 4-8 shows the lower cambered sections tested in Reference 4-4 and Figure 4-9 shows the higher cambered sections tested.

Three place accuracy should be provided in blade surface determinations, so slide-rule accuracy is not sufficient.

Use of basic 65-series airfoil shapes has been found to result in fan blades with trailing edges which are difficult to fabricate and liable to damage in handling. One solution that has been successfully used without noticeably sacrificing design performance has been to thicken the trailing edge. Uniformly progressive thickness increases, with equal additional thickness on each side of the mean line, are made from no thickening at the 40% chord line to the desired amount at the trailing edge.

Both graphical and analytical solutions for increasing the thickness are satisfactory. The blade section ordinates of Figure 4-6 are expressed in percent of chord so, for layout purposes, these ordinates must be transformed into absolute dimensions (inches, etc.). An example of the analytical method of blade thickening is included in the illustrative problem, Appendix I.

For cast blades, where a root fillet is employed to prevent stress concentrations and to provide ease of die making, the blade cross-sectional shape must be defined outside but adjacent to the fillet area (For instance 1/4" away from I.D. or hub diameter for rotor when the inner fillet is 1/4" or less). All parameters, including the defining blade shape of the mean line and ordinates, incidence angle and chord, must be specified at such a point.

It is useful to plot various parameters versus blade span in an analytical design in order to be able to determine the parameter values at any spanwise or radial station.

If constant thickness (sheet-metal) stator blading is to be designed, the blade contour is formed to the mean line. This is discussed in the illustrative problem of Appendix I.

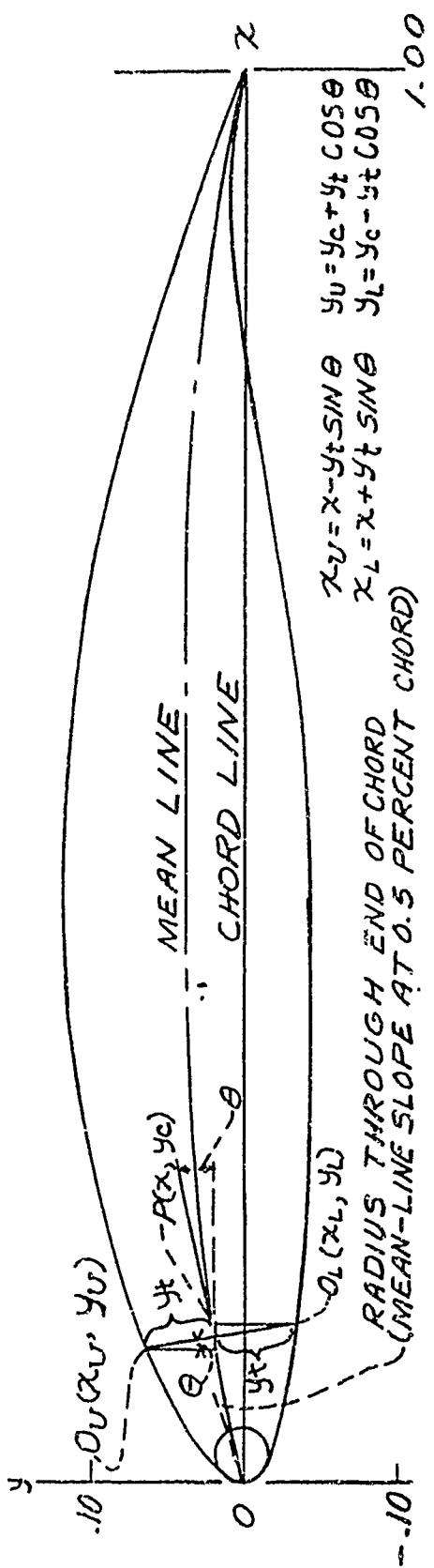


FIGURE 4-5. Construction of NACA 65 Series Compressor Blade Section

ORDINATES FOR NACA 65-010 BASIC THICKNESS FORMS

(SOURCE: REF. 4-4)

(Stations and Ordinates in Percent of Chord)

Station, x % Chord	Ordinates, $\frac{c}{2}y$	
	65(216)-010 airfoil combined with $y = 0.0015x$	Derived 65-010 airfoil
0	0	0
.5	.752	.772
.75	.890	.932
1.25	1.124	1.169
2.5	1.571	1.574
5.0	2.222	2.177
7.5	2.709	2.647
10	3.111	3.040
15	3.746	3.666
20	4.218	4.143
25	4.570	4.503
30	4.824	4.760
35	4.982	4.924
40	5.057	4.996
45	5.029	4.963
50	4.870	4.812
55	4.570	4.530
60	4.151	4.146
65	3.627	3.682
70	3.038	3.156
75	2.451	2.584
80	1.847	1.987
85	1.251	1.385
90	.749	.810
95	.354	.306
100	.150	0
L.E. Radius	.666	.687

FIGURE 4-6

ORDINATES FOR THE NACA $a = 1.0$ MEAN LINE

(Stations and Ordinates in Percent of Chord)

$C_{l_0} = 1.0$		
Station, x	Ordinate, y	Slope, dy/dx
0	0	-----
.5	.250	0.42120
.75	.350	.38875
1.25	.535	.34770
2.5	.930	.29155
5.0	1.580	.23430
7.5	2.120	.19995
10	2.585	.17485
15	3.365	.13805
20	3.980	.11030
25	4.475	.08745
30	4.860	.06745
35	5.150	.04925
40	5.355	.03225
45	5.475	.01595
50	5.515	0
55	5.475	-.01595
60	5.355	-.03225
65	5.150	-.04925
70	4.860	-.06745
75	4.475	-.08745
80	3.980	-.11030
85	3.365	-.13805
90	2.585	-.17485
95	1.580	-.23430
100	0	-----

FIGURE 4-7

(SOURCE: REF. 4-4)

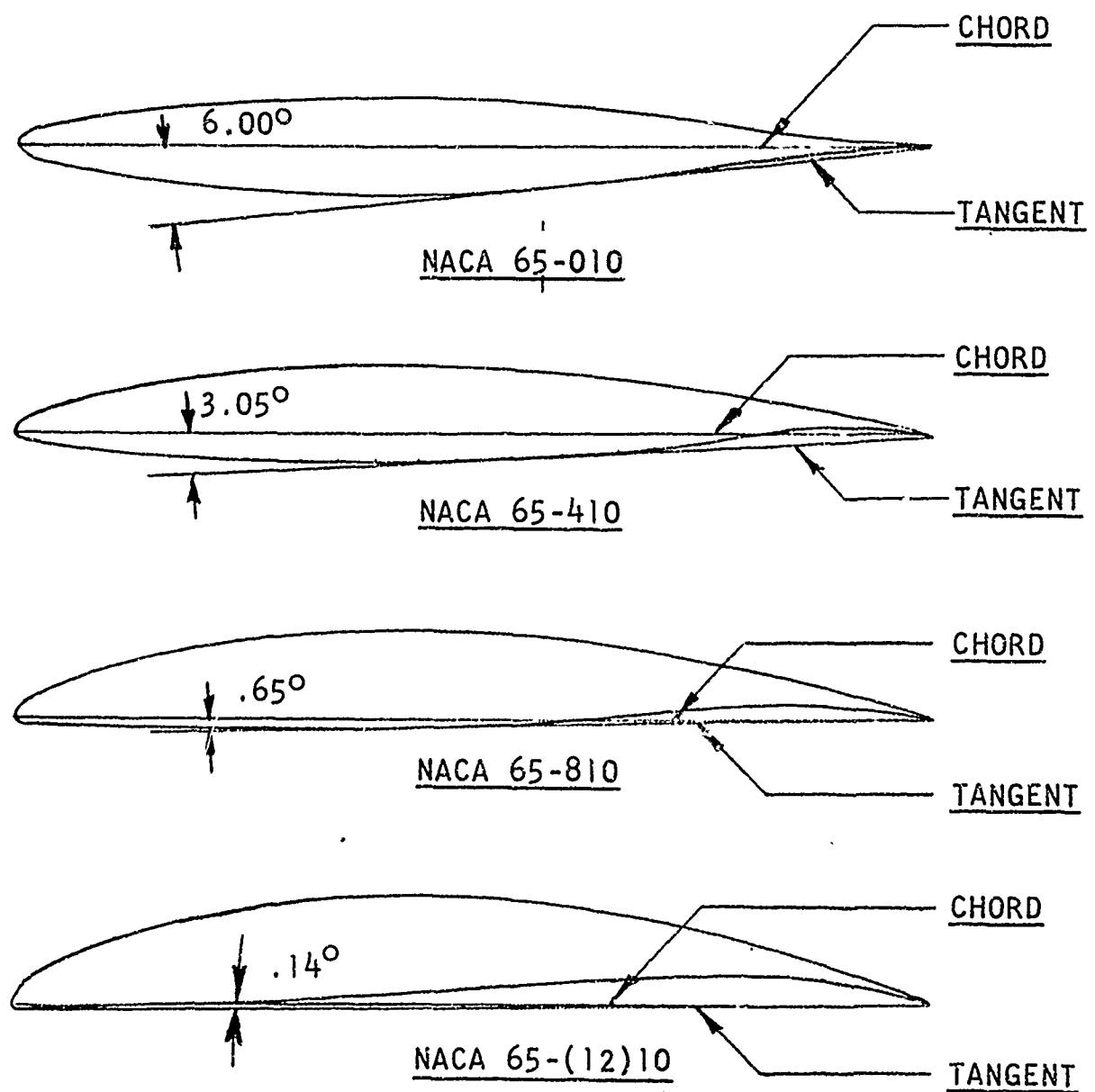


FIGURE 4-8

Lower Cambered Sections. Angle Between
Chord Line and Tangent to Lower
Surface As Shown for the Various Sections.
(Source: Ref. 4-4)

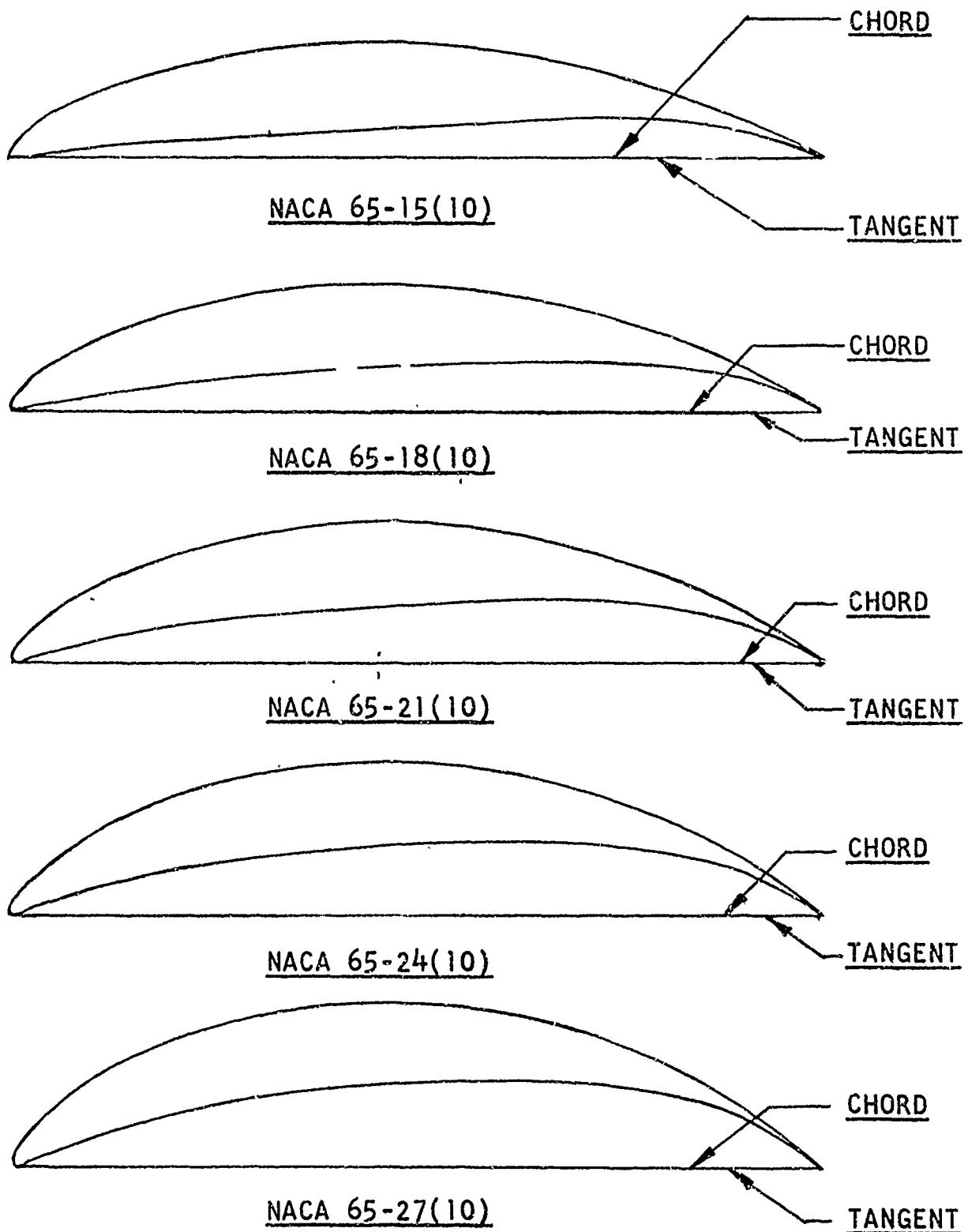


FIGURE 4-9

HIGHER CAMBERED SECTIONS. CHORD LINE
AND TANGENT LINE COINCIDENT.
(Source: Ref. 4-4)

4-2.2.6 Charts for Rapid Determination of Fan Diameters

Charts for the rapid determination of fan diameters are presented in Figure 4-108 through 4-115, inclusive. The analysis required for their preparation was based on the cascade design techniques which have been discussed in this Chapter. The calculations were performed on a digital computer; ordinary hand work could not have been considered because of the prohibitive cost.

Plots of axial velocity versus fan O.D. for a family of flow (Q) curves are presented on Figures 4-108 through 4-111, inclusive. The figures are for a pressure rise of 5, 10, 15 and 20 inches of water respectively. The tip inlet angle θ_1 from 62° to 74° in 2° increments, is indicated for each flow curve. These curves are flows from 2500 cfm to 50000 cfm. Limiting values for all data presented were $\theta_{Tip,min.} = 4^\circ$ and $\theta_{Root,max.} = 25^\circ$. In order to permit designs at lower axial velocities than would be possible without increasing θ_1 beyond 70° (the present limit of available cascade data) curves have been drawn from the θ_1 Tip = 70° point of each Q curve. These represent θ_{Tip} increasing from $\theta_{Tip} = 4^\circ$, without exceeding θ_1 Tip = 70° . In addition, θ_1 Tip values of 72° and 74° have been plotted at constant $\theta_{Tip} = 4^\circ$ which may be used if it is desired to extrapolate the 65-series compressor blade data from Reference 4 in cases where fan diameter is critical.

Plots of RPM versus fan O.D. for the same family of flow curves at the same four values of pressure rise are presented in Figure 4-112 through 4-115 inclusive.

Referring to Figure 4-108 through 4-111 as the axial velocity plots and to Figures 4-112 through 4-115 as the RPM plots, the applications may be described as follows:

- a. To design an installation in which the RPM is dictated by considerations outside of the fan design (such as in the case of a fan mounted on the shaft of a reciprocating engine), enter the RPM plot for the required pressure rise at the proper RPM. Proceed horizontally to the required Q curve and read the fan O.D. vertically downward. Then enter the axial velocity plot for the same pressure rise. Proceed vertically from the previously determined fan O.D. to the required Q curve and read the axial velocity horizontally to the left.

The fan I.D. may readily be determined by using the formula

$$Q = \pi V_a (r_o^2 - r_i^2)$$

where r_o and r_i are, respectively, the outer and inner radius.

- b. To design an installation in which the fan designer may choose the fan RPM, enter the axial velocity plot for the proper pressure rise at the desired value, of V_a , bearing in mind that lower axial velocities result in lower fan diffuser losses, but also result in greater values of fan O.D. Proceed horizontally to the required Q curve and read vertically downward the fan O.D.

Then enter the RPM plot for the same pressure rise at the same fan O.D. Proceed vertically upward to the required Q curve and read the RPM horizontally to the left.

All four axial velocity plots are at the same scales of axial velocity and fan O.D. so that pressure rise interpolation may be made by tracing overlays. All four RPM plots are at the same scales of RPM and fan OD to aid in interpolating between plots of different pressure rises in the same fashion. Interpolation of Q values is also possible.

It is to be emphasized that the parameters of fan diameters, axial velocity, RPM, $\theta_{1\text{Tip}}$ and $\theta_{2\text{Tip}}$ resulting from the use of these charts

are preliminary in nature. The charts are presented so that the designer may easily determine the range of the parameters just mentioned. The charts were constructed for rotor pressure rise only of a rotor-stator axial fan arrangement, and, therefore, are based on the assumption that the stator pressure rise is offset by blade profile and tip clearance losses. Although the preliminary values of the parameters above are approximate because of this assumption, these values describe quickly and easily an initial set of conditions with which to begin the detailed fan design. The end result of the detailed design procedure will be accurate, since both the stator pressure rise and the losses are considered in the detailed design.

4-2.2.7.0 Off Design Fan Operation

It is usually necessary to investigate the fan performance over its full range of rotational speed. If indicated, this may be done analytically during the design stage, but at least it is usually checked during testing to determine the range of parameters, specifically pressure rise, airflow rate, power required and efficiency. Variable angle blading and relief ports to effect fan power reductions are discussed in Sections 4-2.2.7.1 and 4-2.2.7.2 respectively.

The following fan design performance parameters, for series-65 compressor blades, extracted from the test results of Reference 4-4, are presented in carpet-plot form in Reference 4-10.

Blade camber	Angle of attack (Design)
Inlet angle	Entering mach. no.
Turning angle	Pressure rise coefficient
Solidity	Incidence angle
	Angle of attack (Twice minimum drag)

These plots assist the selection of blade sections required to fulfill velocity diagrams. The data presented in this summary form increase the usefulness of the subject matter by providing a simple method of interpolating the cascade data. It also aids in the investigation of off-design variation of turning angle with angle of attack.

The off-design performance may be estimated by assuming that the overall fan performance is equal to the calculated performance of the blade midspan section. The performance of the midspan section may be determined by calculating the pressure rise for various assumed values of V_a .

The fan performance of each blade section at flows other than the design flow, for a constant RPM, cannot be readily determined because the V_a is different for each section. Therefore, caution should be used in

applying the assumption of the preceding paragraph, especially if the off-design point results in inlet angles exceeding the blade incidence angles at the outer radial stations.

The application of the following fan laws permits the determination of off-design performance at various RPM's.

$$Q_1 = Q_2 \quad \frac{RPM_1}{RPM_2}$$

$$\Delta P_1 = \Delta P_2 \quad \left(\frac{RPM_1}{RPM_2} \right)^2$$

$$HP_1 = HP_2 \quad \left(\frac{RPM_1}{RPM_2} \right)^3$$

4-2.2.7.1 Variable Angle Pre-Rotation Vanes

Cooling requirements of both airflow quantity and pressure for an engine cooling system in a given aircraft vary with heat rejection required which, at different operating conditions, is a function primarily of engine power and RPM and cooling air temperature and density. In order to provide adequate cooling throughout the range of operating conditions, the cooling fan must be designed to cool at the most severe condition. Overcooling, therefore, occurs at all less severe conditions and wasted fan power results.

Variable angle rotor blades could effectively be used to vary the airflow, pressure rise, and fan power but the mechanical complexity would be considerable, if not prohibitive.

Variable angle inlet stator blades could be used to vary the airflow rate and pressure rise and, therefore, the fan power. Any anticipated application would require investigation to compare the fan power savings with the additional weight and cost of the control complexity.

One application of variable angle upstream stator blading, in conjunction with a rotor and downstream stator, is described in References 4-11 and 4-12. Reference 4-11 presents the aerodynamic design and Reference 4-12, the performance test results.

In Reference 4-11, two configurations of variable inlet stator blading were studied. The first employed a single piece symmetrical blade with the blade angle varying from plus 50° to minus 30° to the axis of rotor rotation. The second configuration employed a symmetrical blade hinged on the center line at the 50% chord line. The upstream half was mounted in the axial direction and design performance required blade angles of the movable portion varying from plus 45° to minus 30°. This second configuration was chosen as the more desirable, based on the following:

- a. The inner stator ring must be supported from the outer and if full movable stators are used, extra struts must be provided.
- b. Length must be kept as short as possible since this portion of the structure is cantilevered.

c. The stator must contain de-icing provisions and this can best be done in a stationary member.

No firm basis could be found in the literature at the time of this design (1950) to evaluate the turning angle as a function of trailing edge deflection angle in conjunction with the percentage of the airfoil turned. One report, Reference 4-15, on ailerons, indicated that turnings on the order of 20° could be accomplished by deflecting the last 20% of the airfoil.

It, therefore, appeared reasonable that a symmetrical airfoil articulated at the 50% of chord point would turn air further with less increment of drag than the aileron type of blade. This blade articulated at 50% is similar to a cambered airfoil in its deflected position.

As usual, downstream stator outlet tangential velocity components were tolerated at flight conditions off design.

The control system for the movable upstream stator blade portions introduced difficulties. For weight-saving purposes, a pulley was mounted on the shaft of each blade movable portion and a cable system actuated the blades at the pulleys. It was found to be difficult to maintain angles of the 58 blades within desirable tolerances.

There is no known case of mechanically variable angle stator blading for axial flow cooling fans having reached the flight stage, although such blading is used in turbine engines.

4-2.2.7.2 Relief Ports for Fan Power Savings

Because of the characteristic shape of the performance curves of the axial flow fan, power may be saved, as discussed in Section 4-2.2.7.1 above, by changing the airflow from that value at which the highest pressure rise occurs. Usually, the fan power required decreases more rapidly as the flow increases beyond the point of maximum pressure than it does as the flow decreases, below that point, as shown in Figure 4-10, which represents test results of an actual fan installation.

Efficiency also decreases, but may be expected to peak at a higher flow rate than that providing maximum pressure rise or power required.

Therefore, for off design conditions, a relief port(s) located between the fan and downstream cooling resistances may be utilized to increase the airflow and, therefore, to lower the fan power by venting air out of the cooling system. Flap weight and actuator weight, as well as aircraft drag if the flap is located on the aircraft exterior, must be considered.

4-2.2.8 Fan Entrance and Fan Diffuser Design

Fan entrance and downstream diffuser design should follow good design practices, limited usually by space limitations, as described in Chapter III. In general, bellmouth fan entries should be provided from the usual upstream plenum chamber. Hub spinners have been employed to achieve the best aerodynamic entrance conditions. The weight penalty, as in all aircraft design problems, must be considered against the reduction in entry pressure losses.

PERFORMANCE CHARACTERISTICS OF FAN

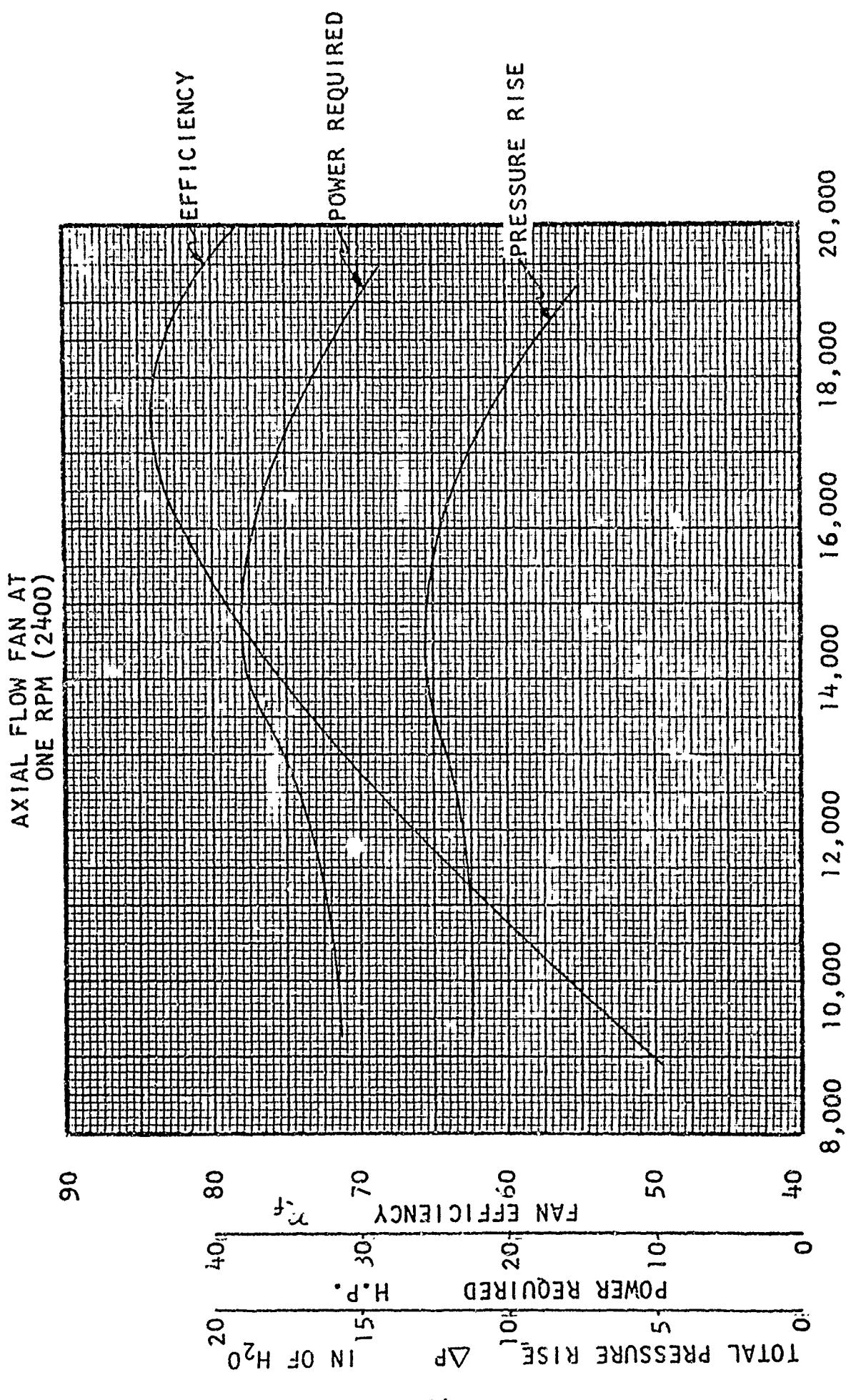


FIGURE 4-10

Fan diffuser design for reciprocating engine cooling applications is usually heavily penalized by axial space limitations between the fan and the engine cylinders. Ideally, a long gradual diffusion lessens this diffusion losses. A downstream diffusing center body, as well as the peripheral diffuser, should receive consideration.

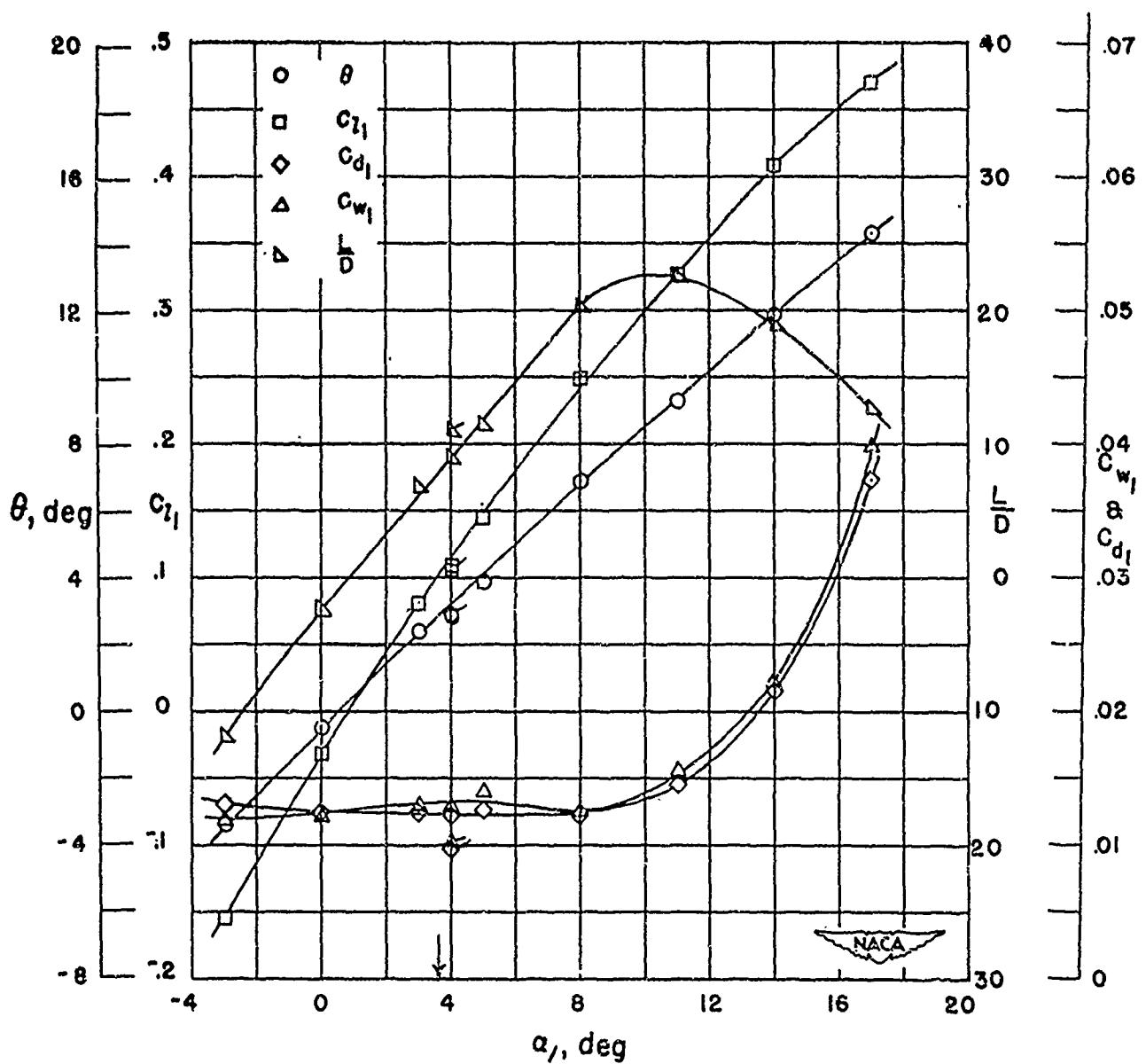
4-2.3 Fan Testing

The testing of all items, including fans, is included in Chapter VI.

4-2.4 Illustrative Fan Design

The complete design analysis, testing and sample design details from drawings are presented in the sample problem, Appendix I, for a fan that was designed, fabricated, tested and flown in a U.S. Navy helicopter submerged reciprocating engine cooling installation.

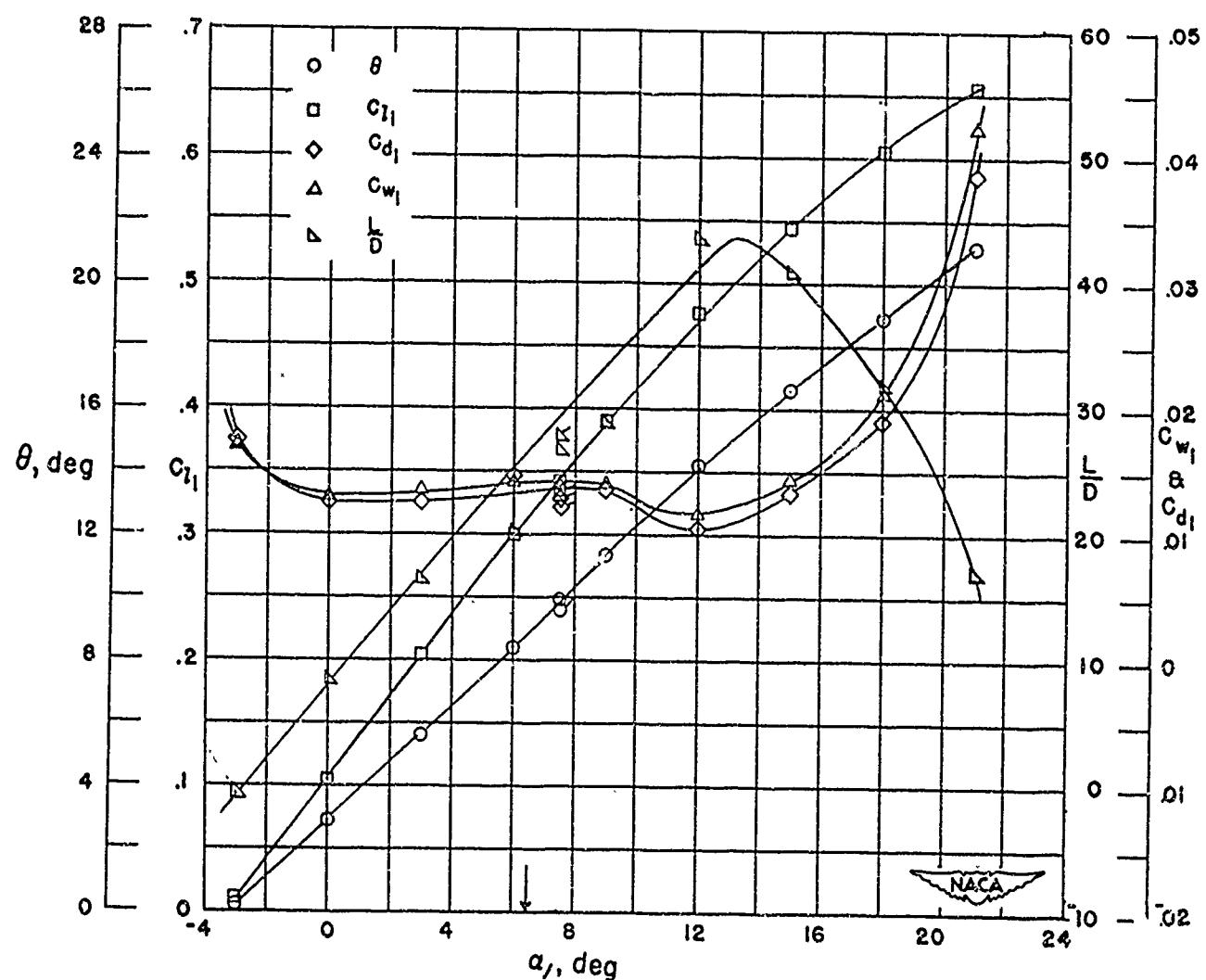
(Text continued on page IV-145).



Section characteristics; arrow shows design angle of attack,
flagged symbol indicates leading-edge roughness.

Cascade combination, $\beta_1 = 30^\circ$, $\sigma' = 1.00$
blade section, NACA 65-010

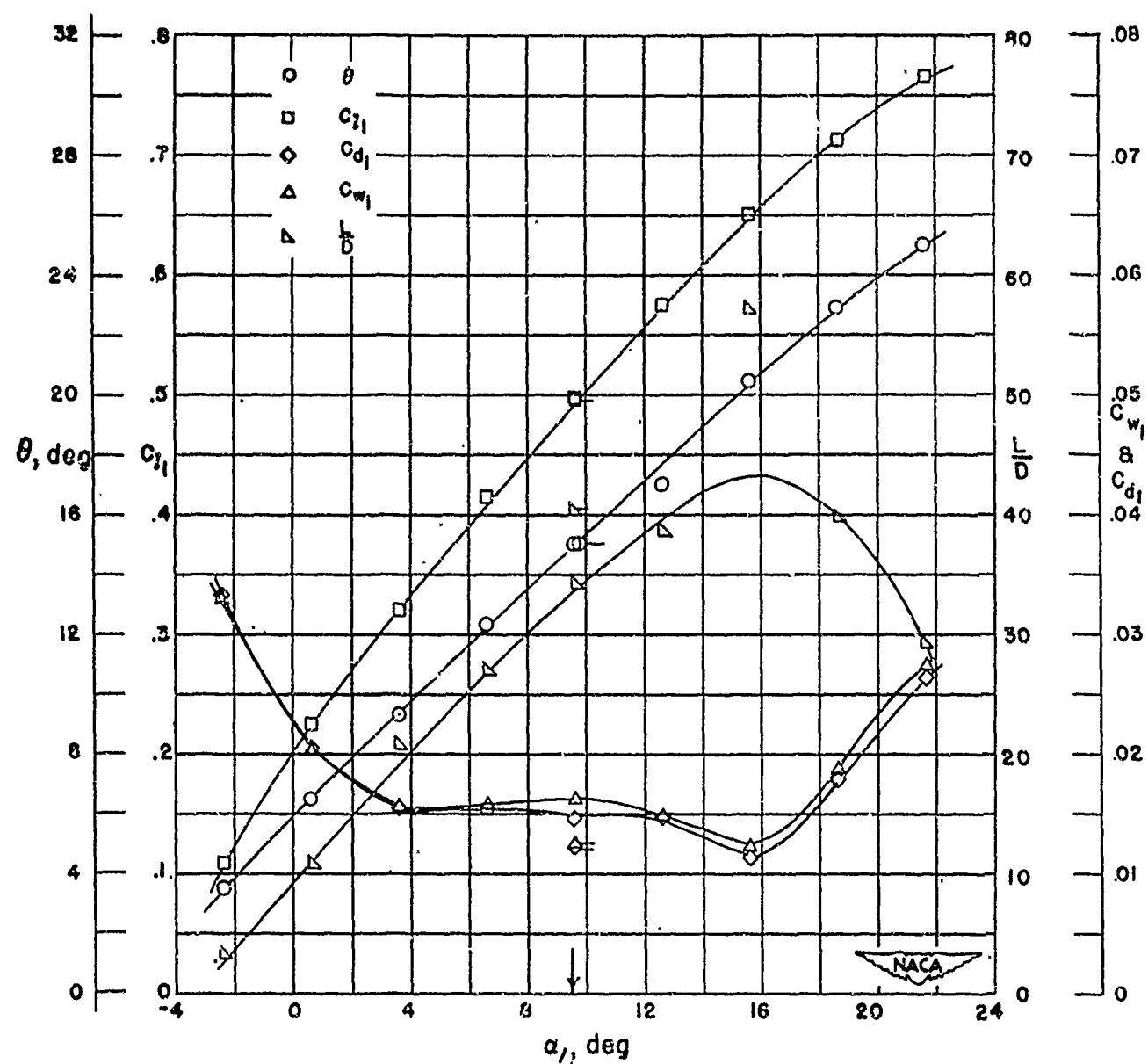
Figure 4-11
(Source: Ref. 4-4)



Section characteristics; arrow shows design angle of attack,
flagged symbol indicates leading-edge roughness.

Cascade combination, $\beta_1 = 30^\circ$, $\sigma' = 1.00$
blade section, NACA 65-410

Figure 4-12
(Source: Ref. 4-4)



Section characteristics; arrow shows design angle of attack,
flagged symbol indicates leading-edge roughness

Cascade combination, $\beta_1 = 30^\circ$, $\sigma' = 1.00$
blade section, NACA 65-810

Figure 4-13
(Source: Ref. 4-4)

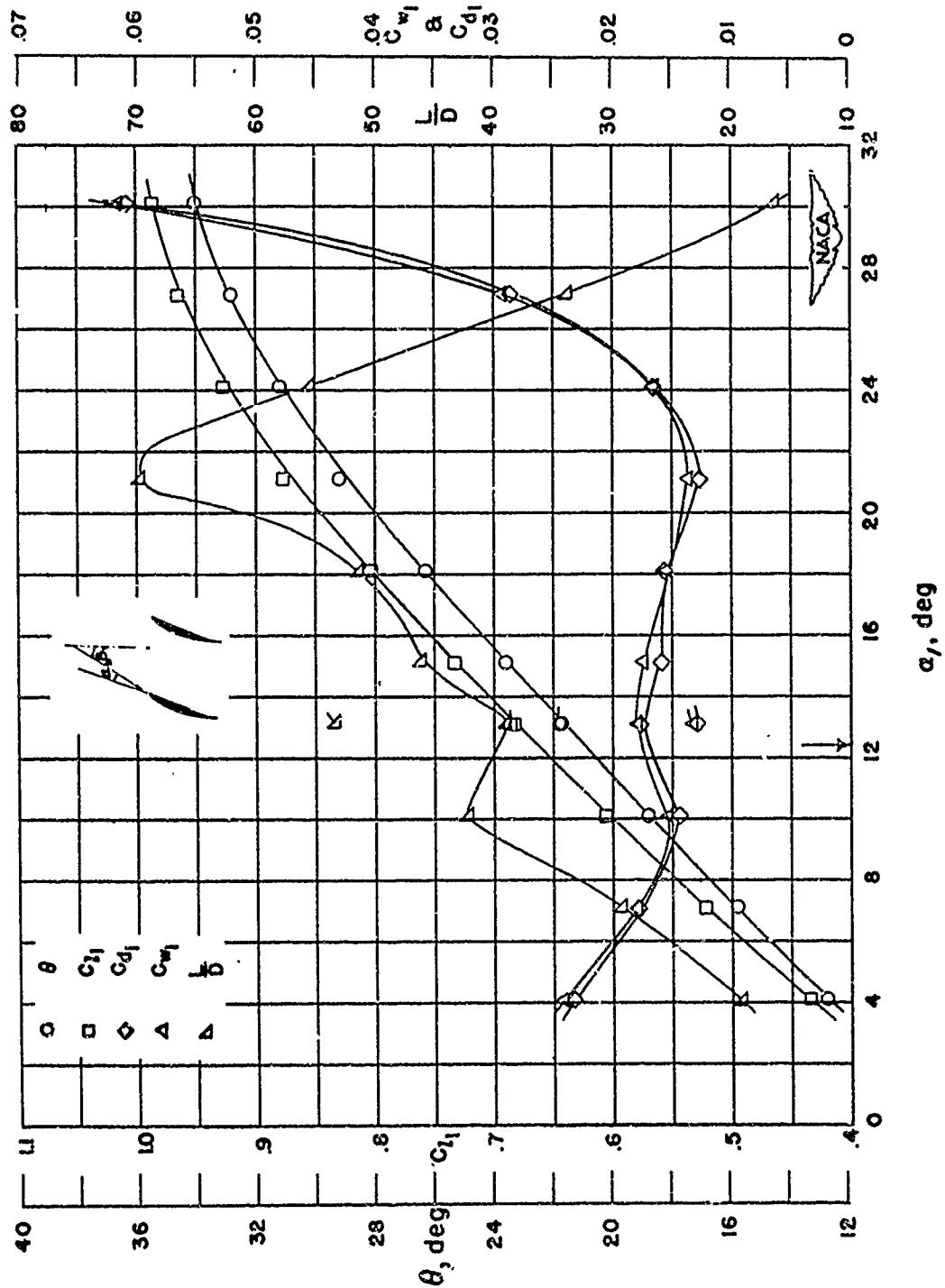
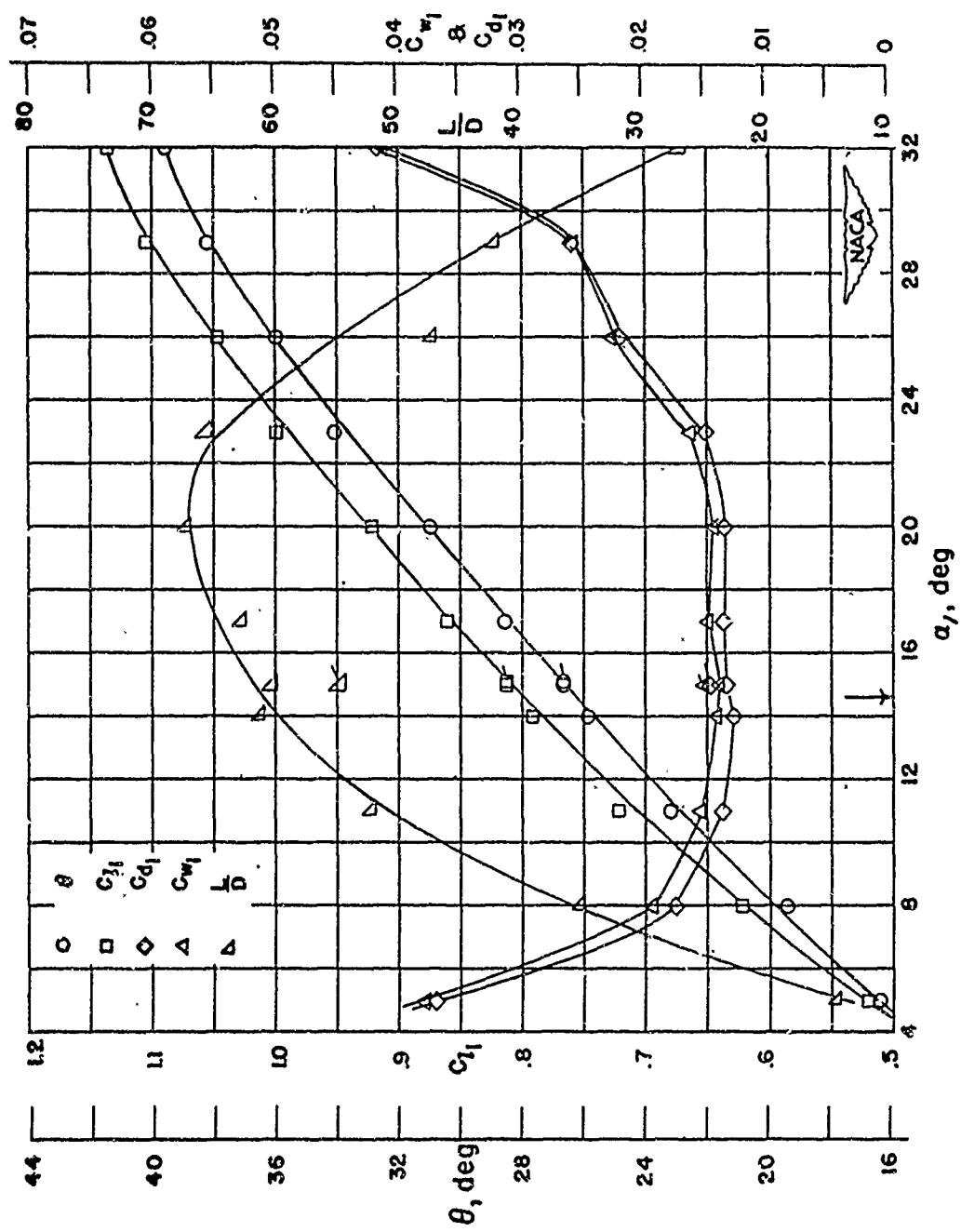


Figure 4-14
(Source: Ref. 4-4)

Section characteristics; arrow shows design angle of attack;
flagged symbol indicates leading-edge roughness.

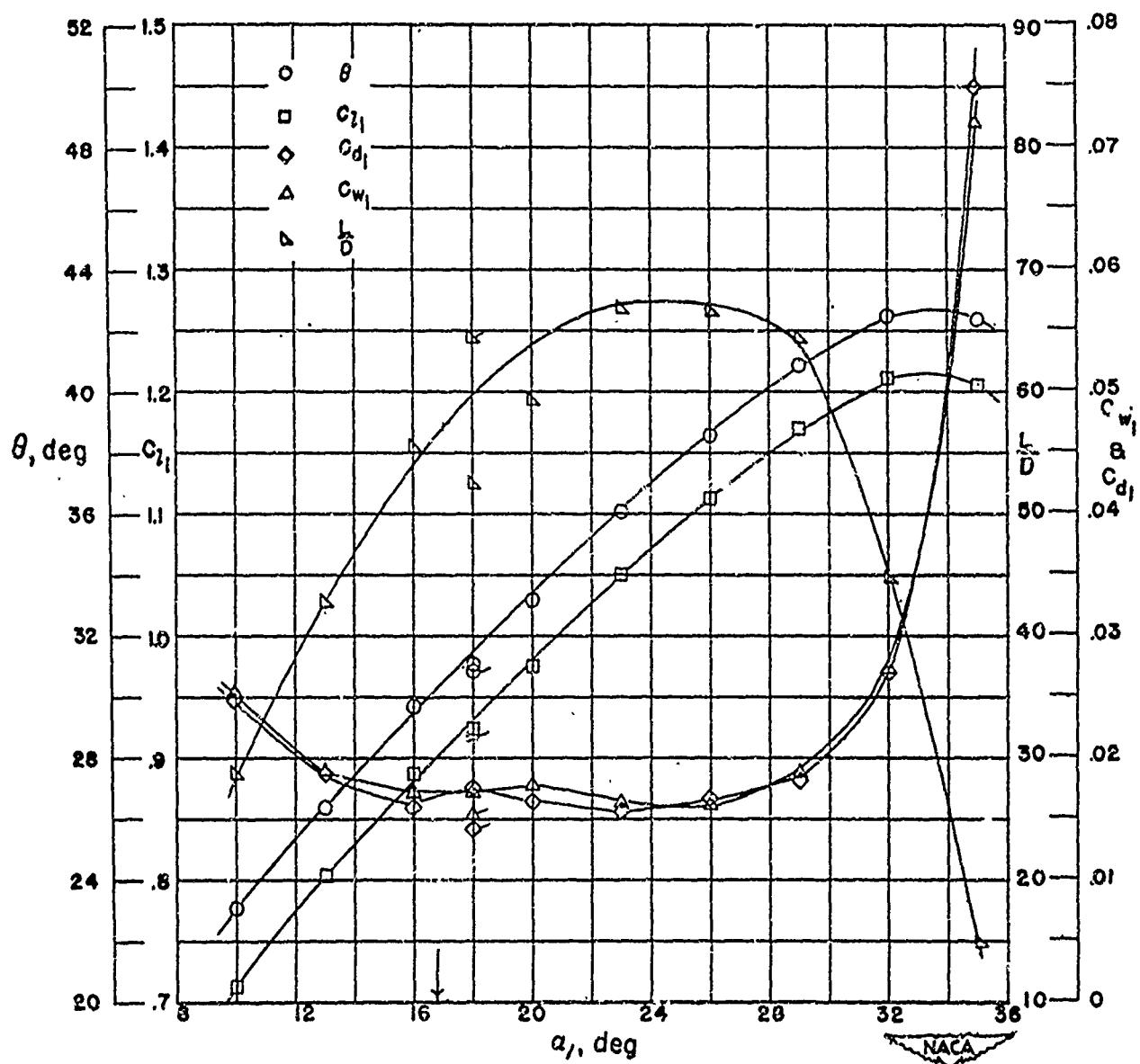
Cascade combination, $\beta_1 = 30^\circ$, $\sigma' = 1.00$
blade section, NACA 65-(12)10



Section characteristics; arrow shows design angle of attack;
flagged symbol indicates leading-edge roughness.

Cascade combination, $\beta_1 = 30^\circ$, $\sigma' = 1.00$
blade section, NACA 65-(15)10

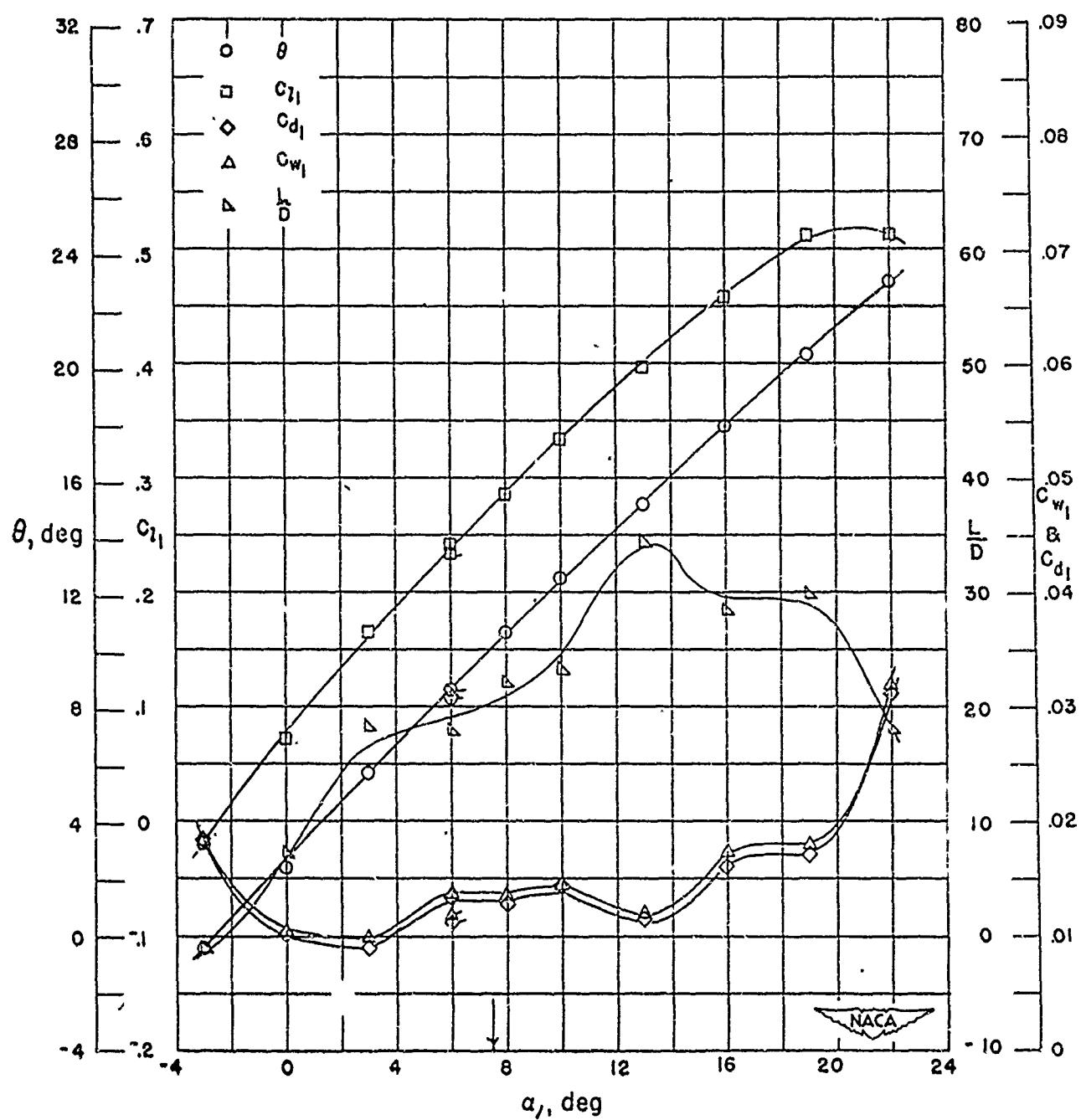
Figure 4-15
(Source: Ref. 4-4)



Section characteristics; arrow shows design angle of attack,
flagged symbol indicates leading-edge roughness.

Cascade combination, $\beta_1 = 30^\circ$, $\sigma' = 1.00$
blade section, NACA 65-(10)10

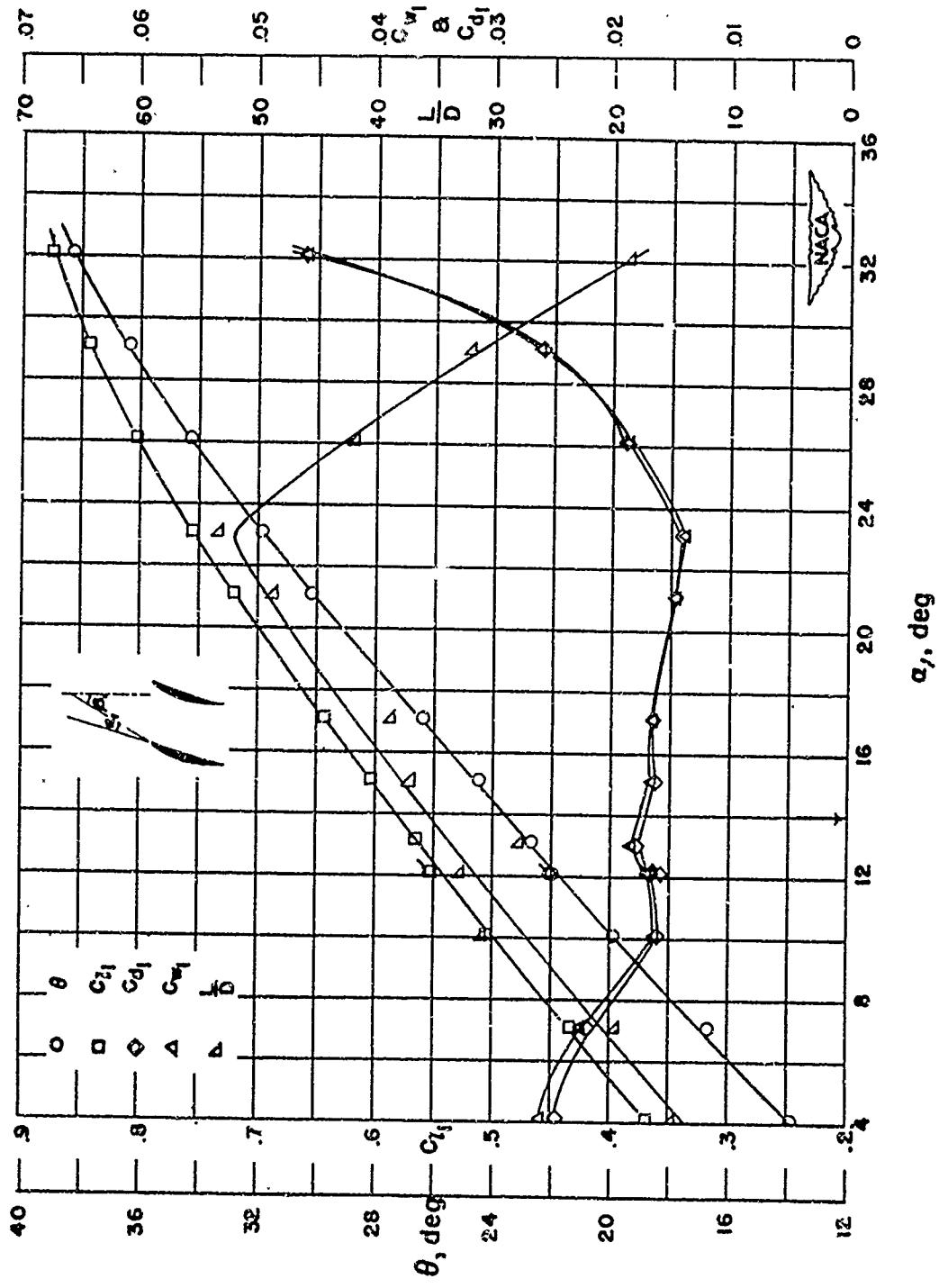
Figure 4-16
(Source: Ref. 4-4)



Section characteristics; arrow shows design angle of attack,
flagged symbol indicates leading-edge roughness.

Cascade combination, $\beta_1 = 30^\circ$, $\sigma' = 1.25$
blade section, NACA 65-410

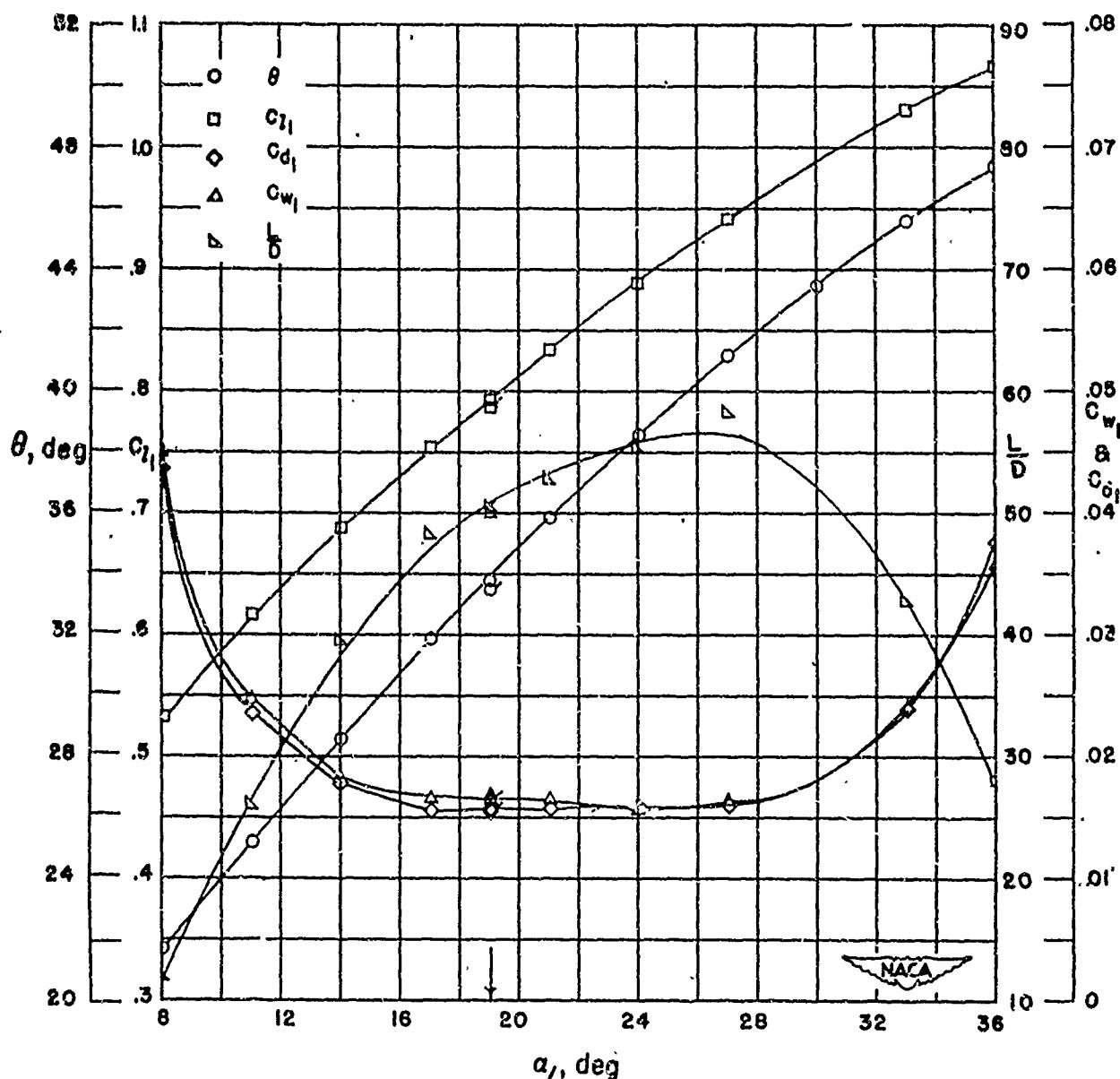
Figure 4-17
(Source: Ref. 4-4)



Section characteristics; arrow shows design angle of attack;
flagged symbol indicates leading-edge roughness

Cascade combination, $\beta_1 = 30^\circ$, $\sigma' = 1.25$
blade section, NACA 65-(12) 10

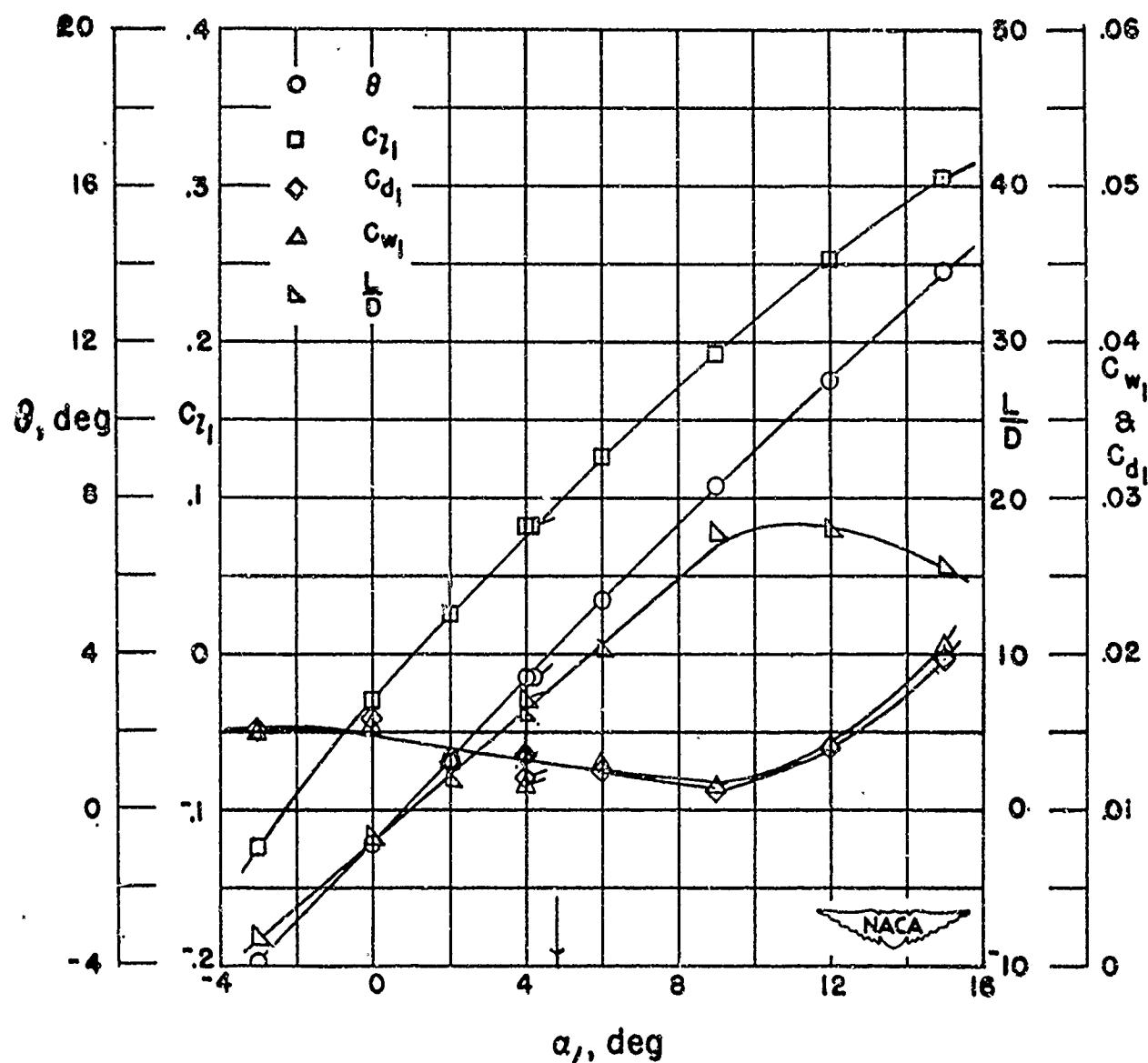
Figure 4-18
(Source: Ref. 4-4)



Section characteristics; arrow shows design angle of attack;
flagged symbol indicates leading-edge roughness.

Cascade combination, $\beta_1 = 30^\circ$, $\sigma' = 1.25$
blade section, NACA 65-(18)10

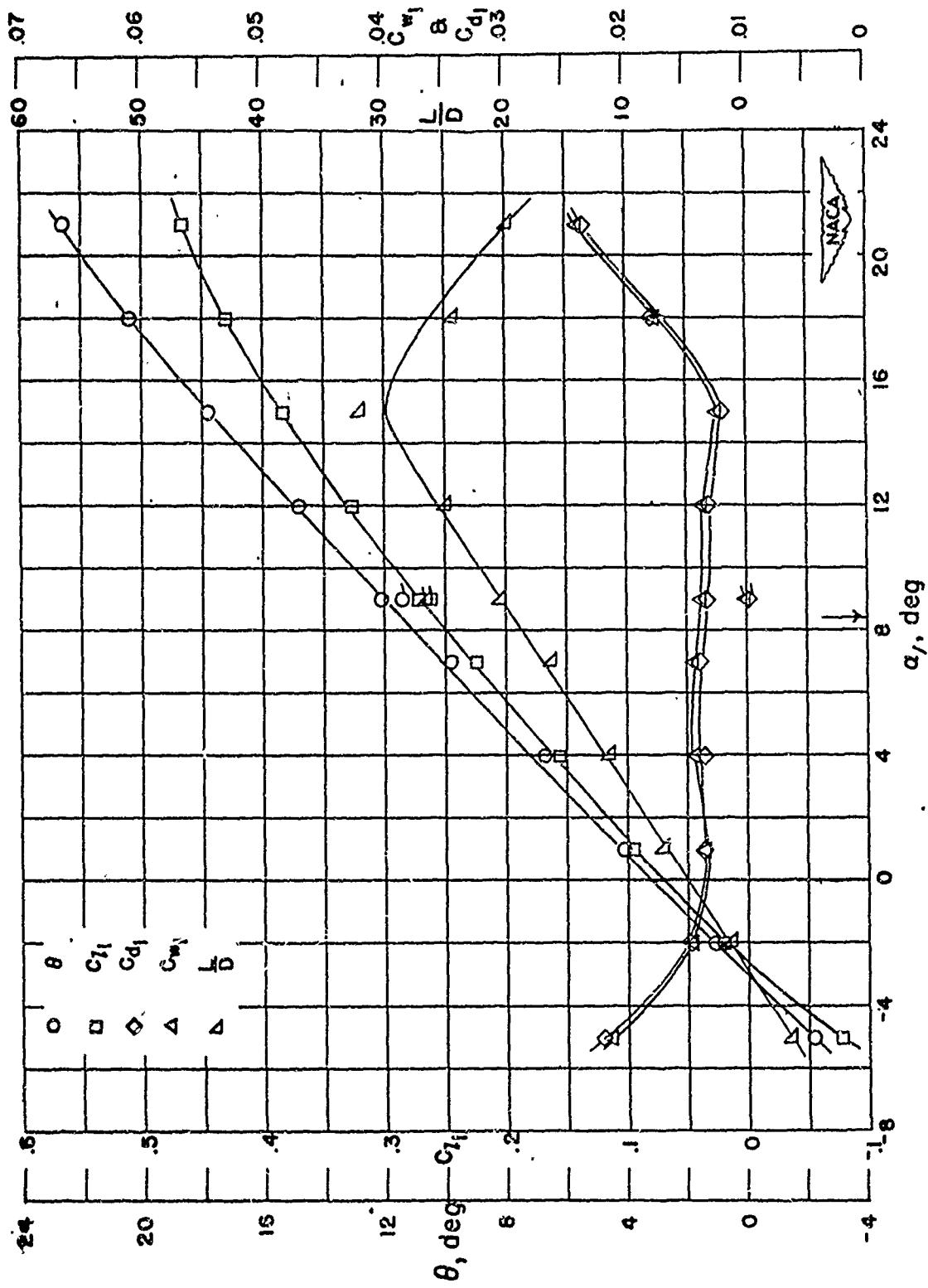
Figure 4-19
(Source: Ref. 4-4)



Section characteristics; arrow shows design angle of attack;
flagged symbol indicates leading-edge roughness.

Cascade combination, $\beta_1 = 30^\circ$, $\sigma' = 1.50$
blade section, NACA 65-010

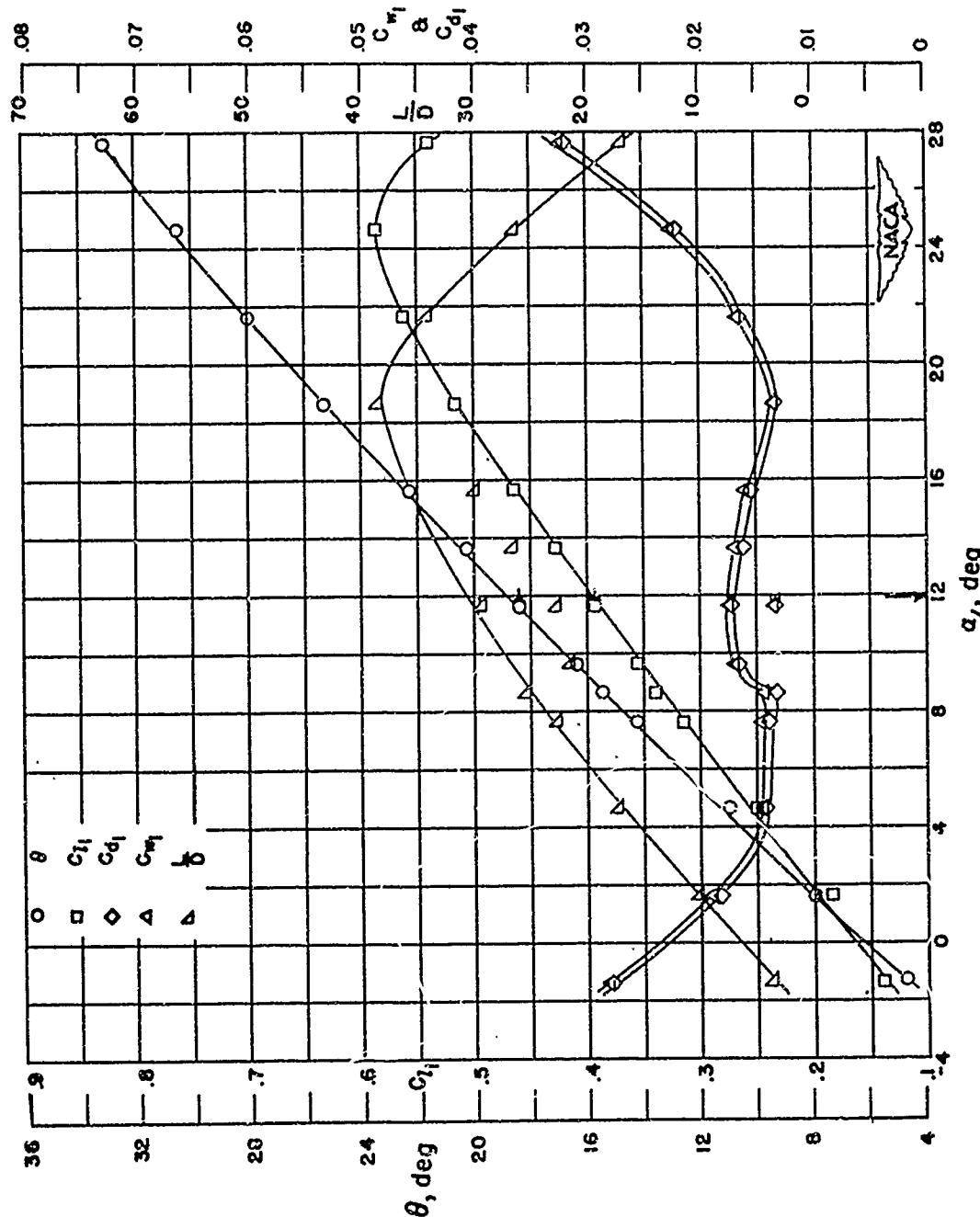
Figure 4-20
(Source: Ref. 4-4)



Section characteristics; arrow shows design angle of attack;
flagged symbol indicates leading-edge roughness

Cascade combination, $\beta_1 = 30^\circ$, $\sigma' = 1.50$
blade section, NACA 65-410

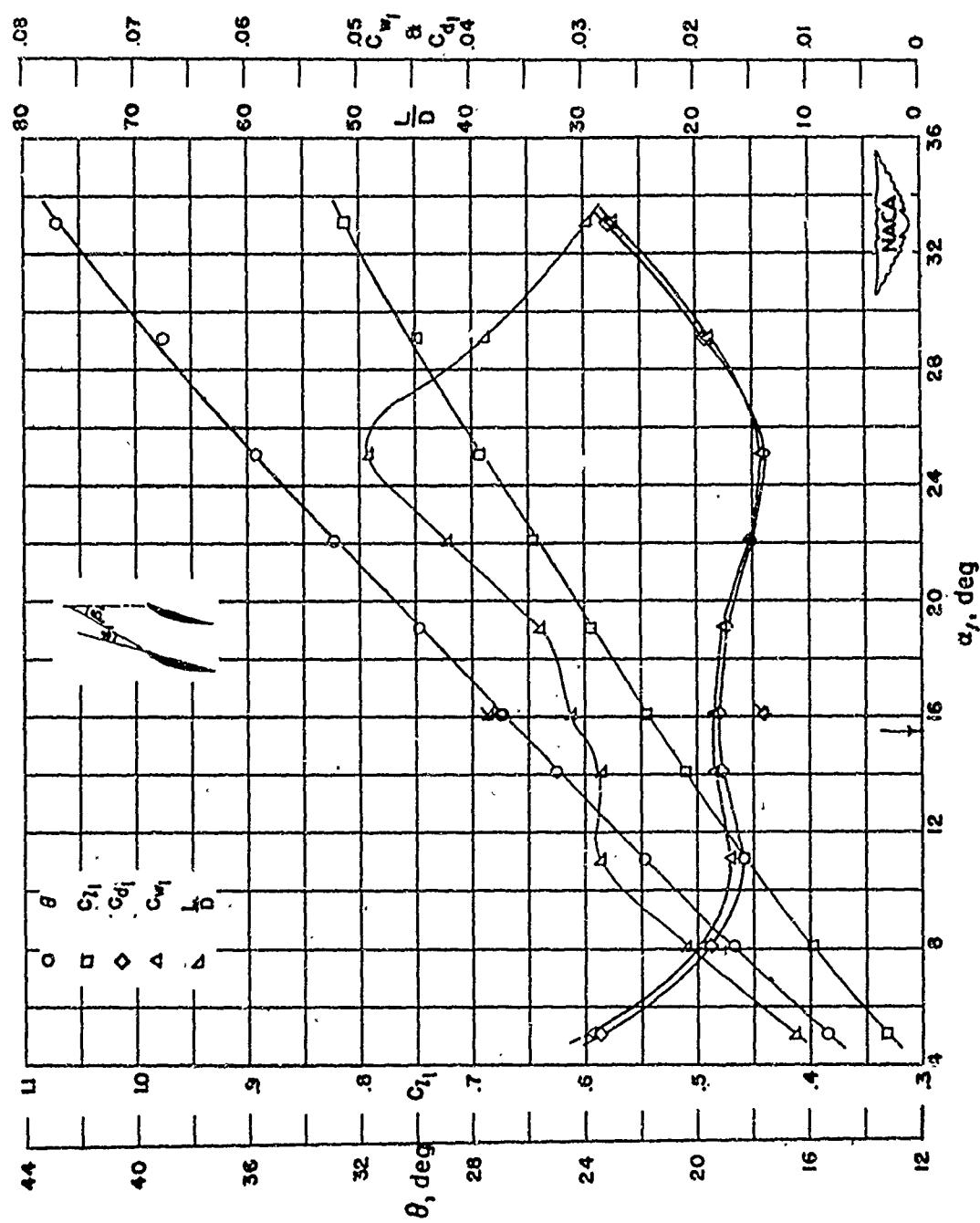
Figure 4-21
(Source: Ref. 4-4)



Section characteristics; arrow shows design angle of attack;
flagged symbol indicates leading-edge roughness

Cascade combination, $\beta_1 = 30^\circ$, $\sigma' = 1.50$
blade section, NACA 65-810

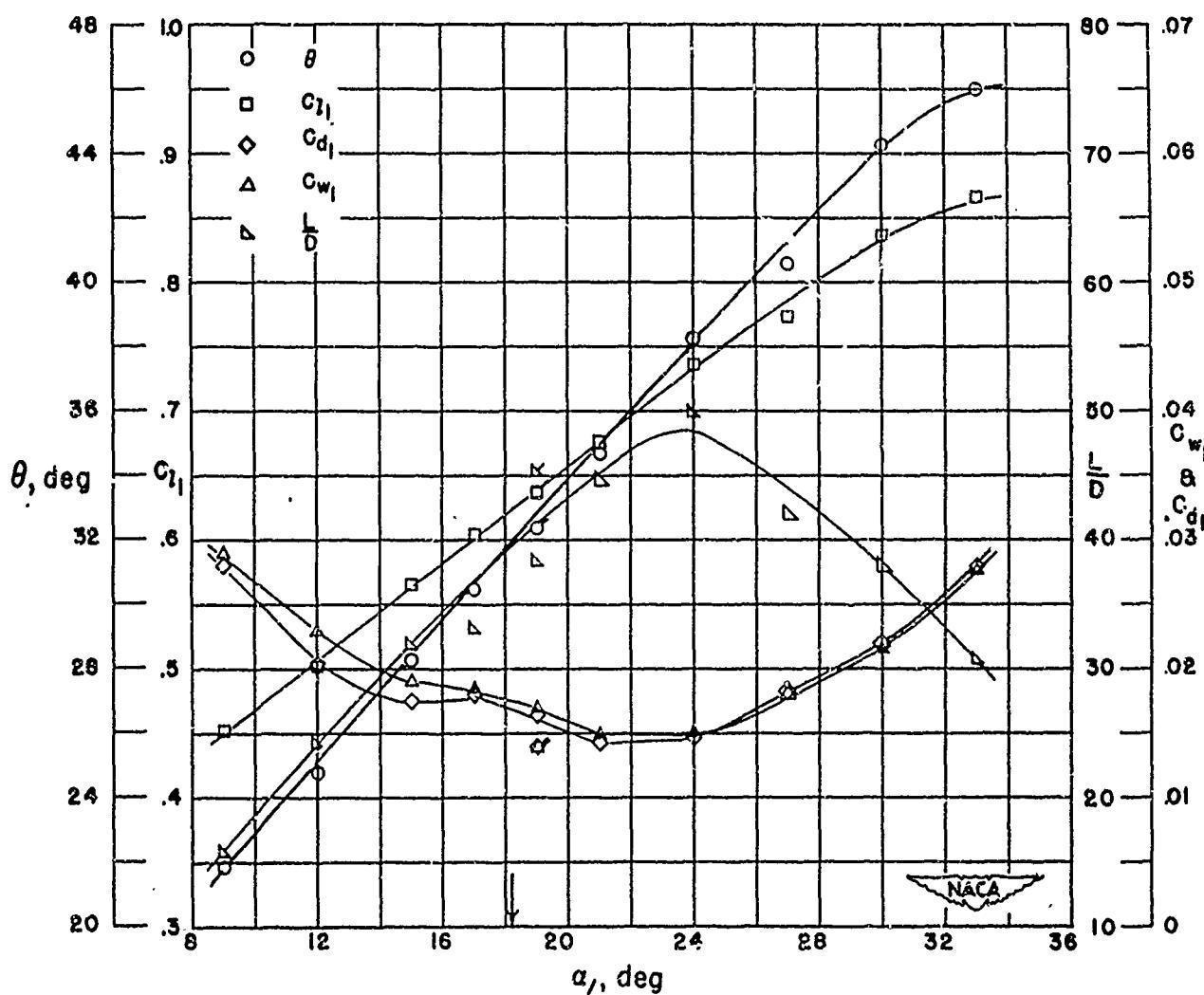
Figure 4-22
(Source: Ref. 4-4)



Section characteristics; arrow shows design angle of attack,
flagged symbol indicates leading-edge roughness.

Cascade combination, $\beta_1 = 30^\circ$, $d' = 1.50$
blade section, NACA 65-(12)10

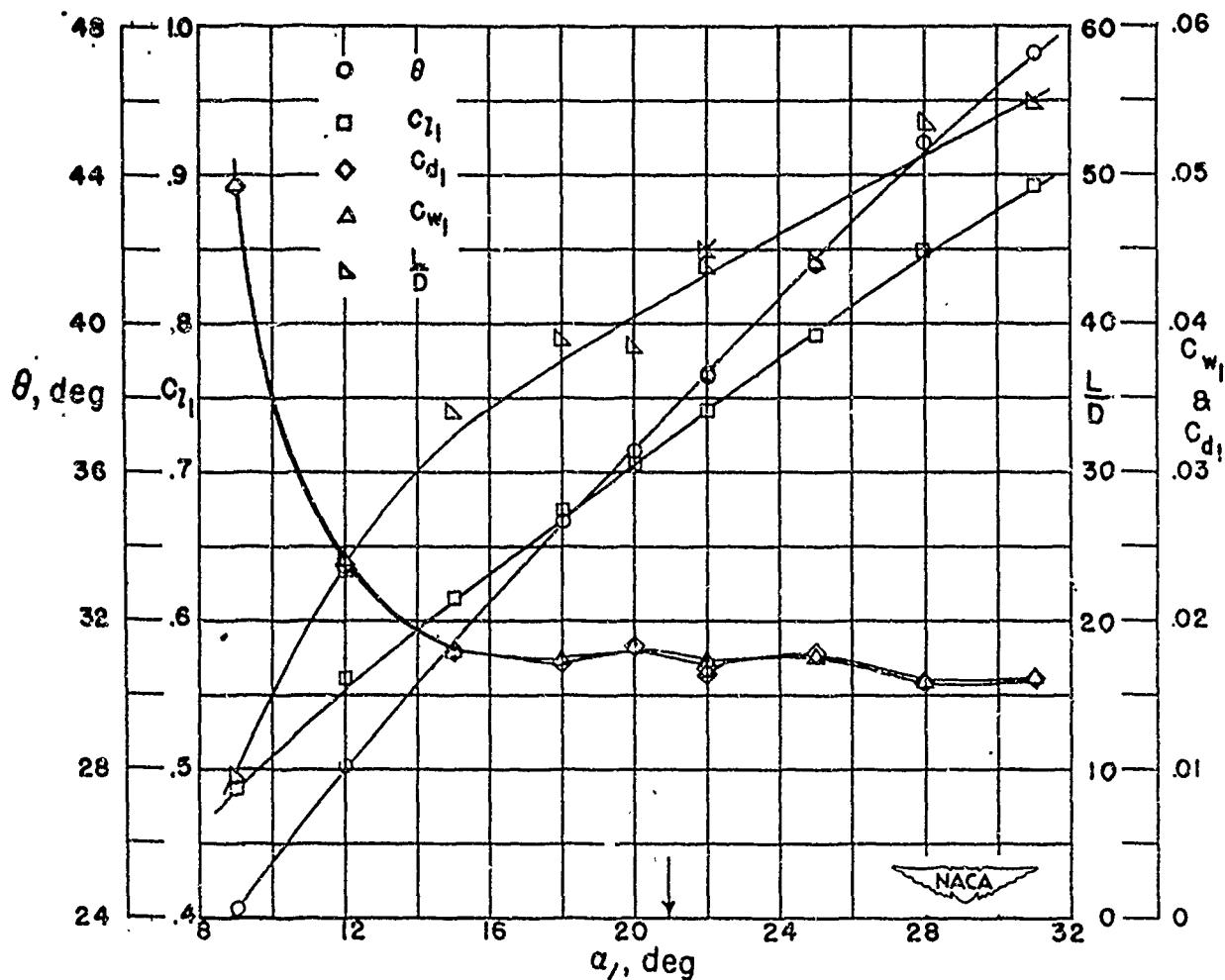
Figure 4-23
Source: Ref. 4-4)



Section characteristics; arrow shows design angle of attack,
flagged symbol indicates leading-edge roughness.

Cascade combination, $\beta_1 = 30^\circ$, $\sigma^1 = 1.50$
blade section, NACA 65-(15)10

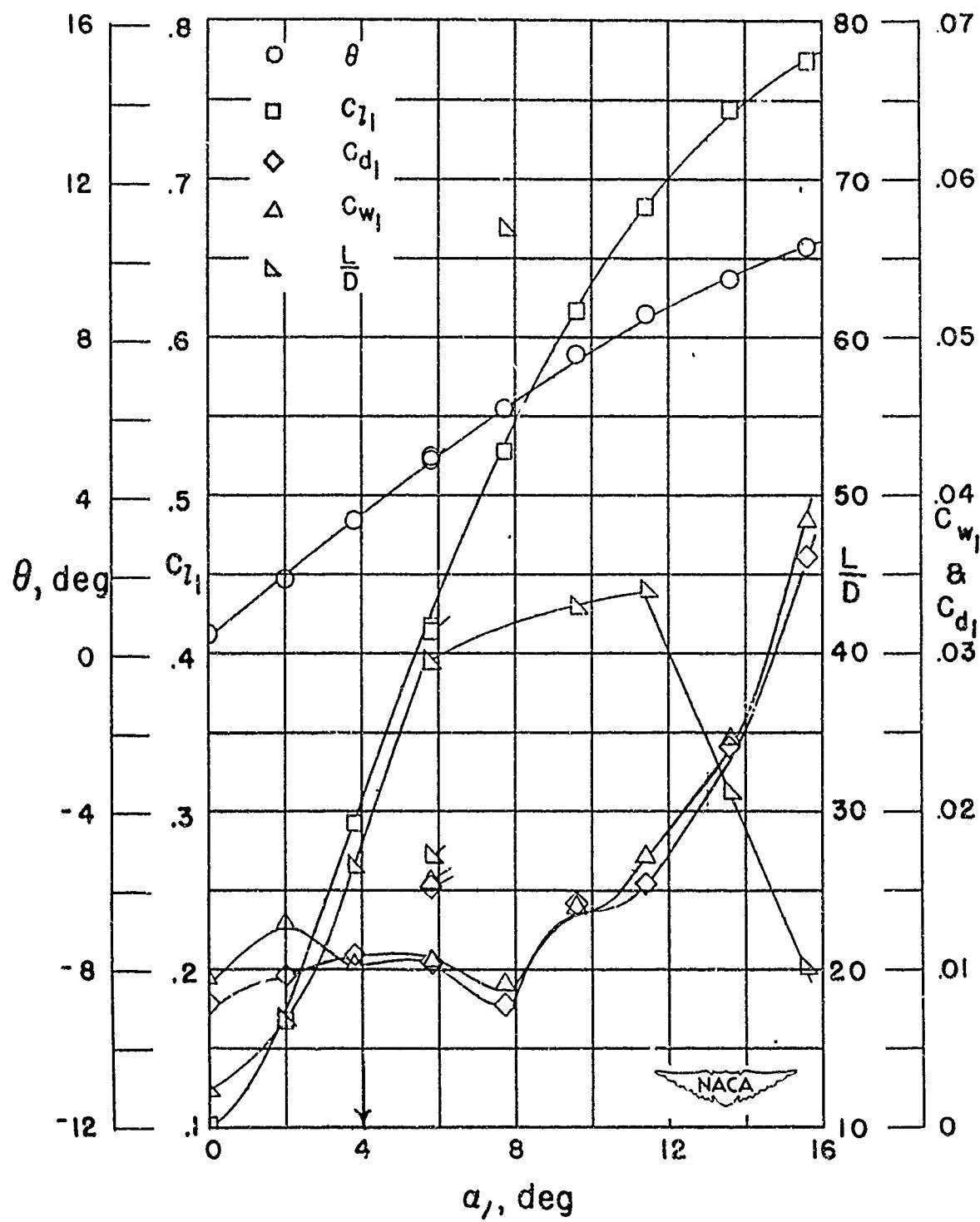
Figure 4-24
(Source: Ref. 4-4)



Section characteristics; arrow shows design angle of attack,
flagged symbol indicates leading-edge roughness.

Cascade combination, $\beta_1 = 30^\circ$, $\sigma' = 1.50$
blade section, NACA 65-(18)10

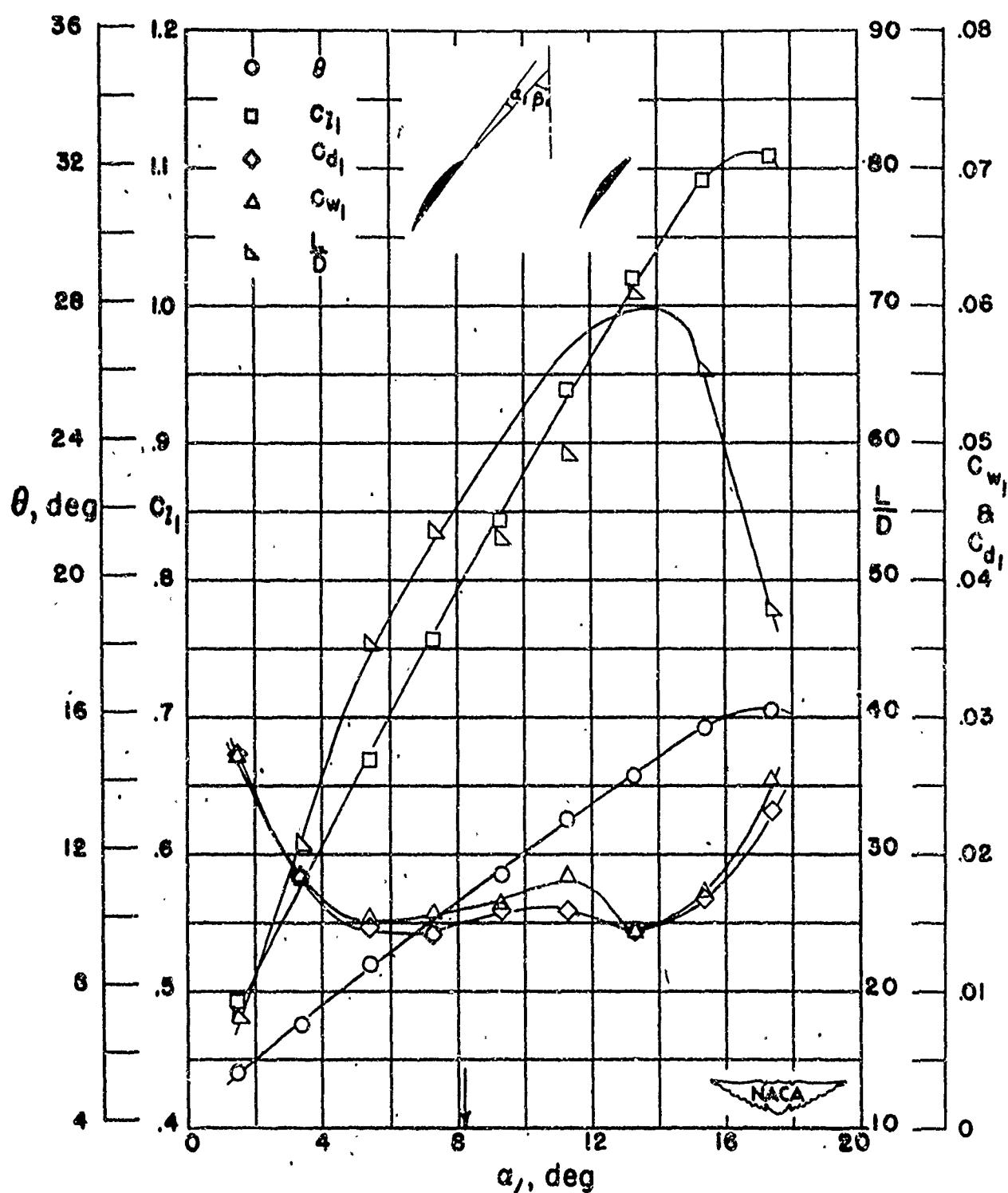
Figure 4-25
(Source: Ref. 4-4)



Section characteristics; arrow shows design angle of attack,
flagged symbol indicates leading-edge roughness

Cascade combination, $\beta_1 = 45^\circ$, $\sigma' = 0.50$
blade section, NACA 65-410

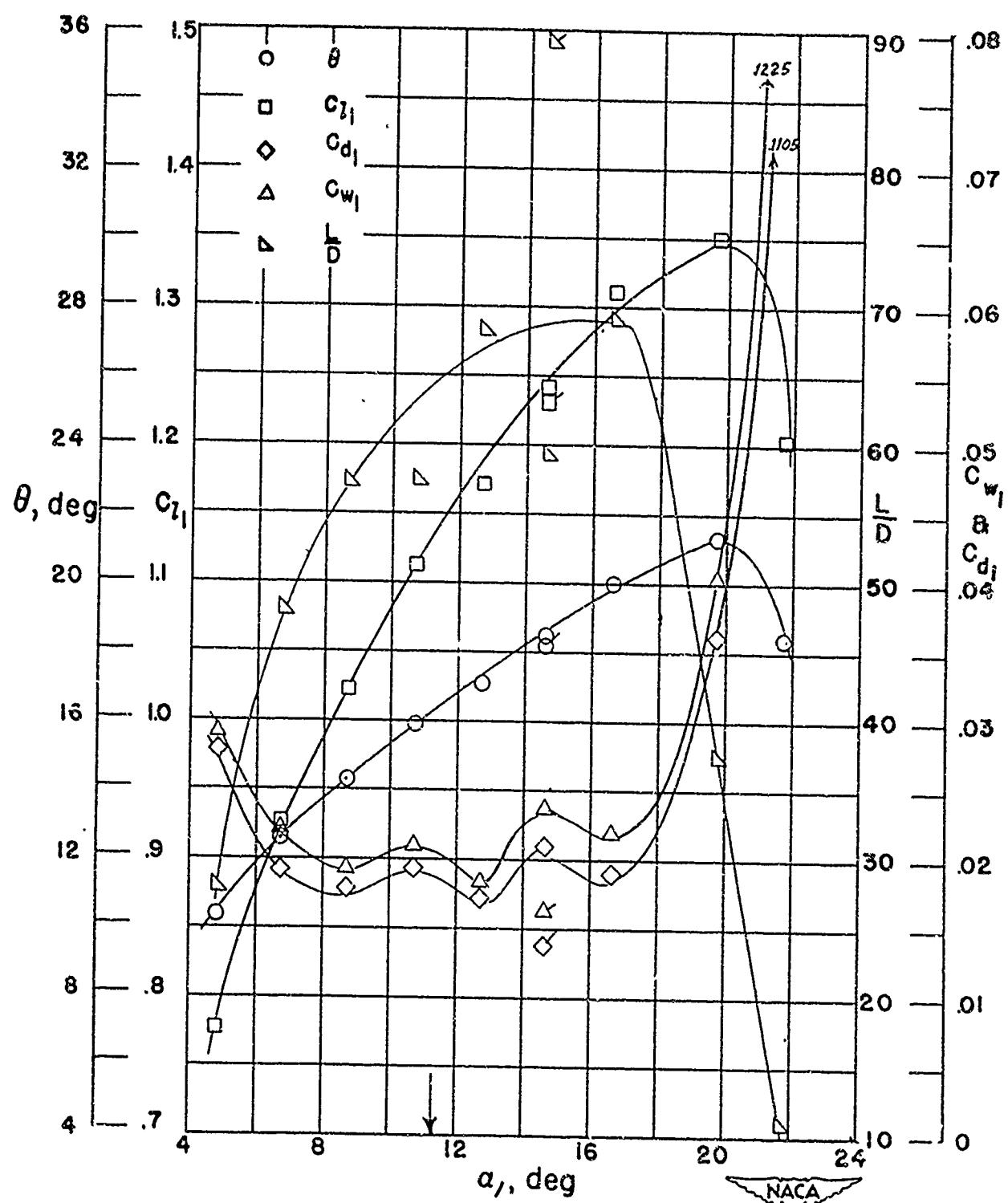
Figure 4-26
(Source: ref. 4-4)



Section characteristics; arrow shows design angle of attack.

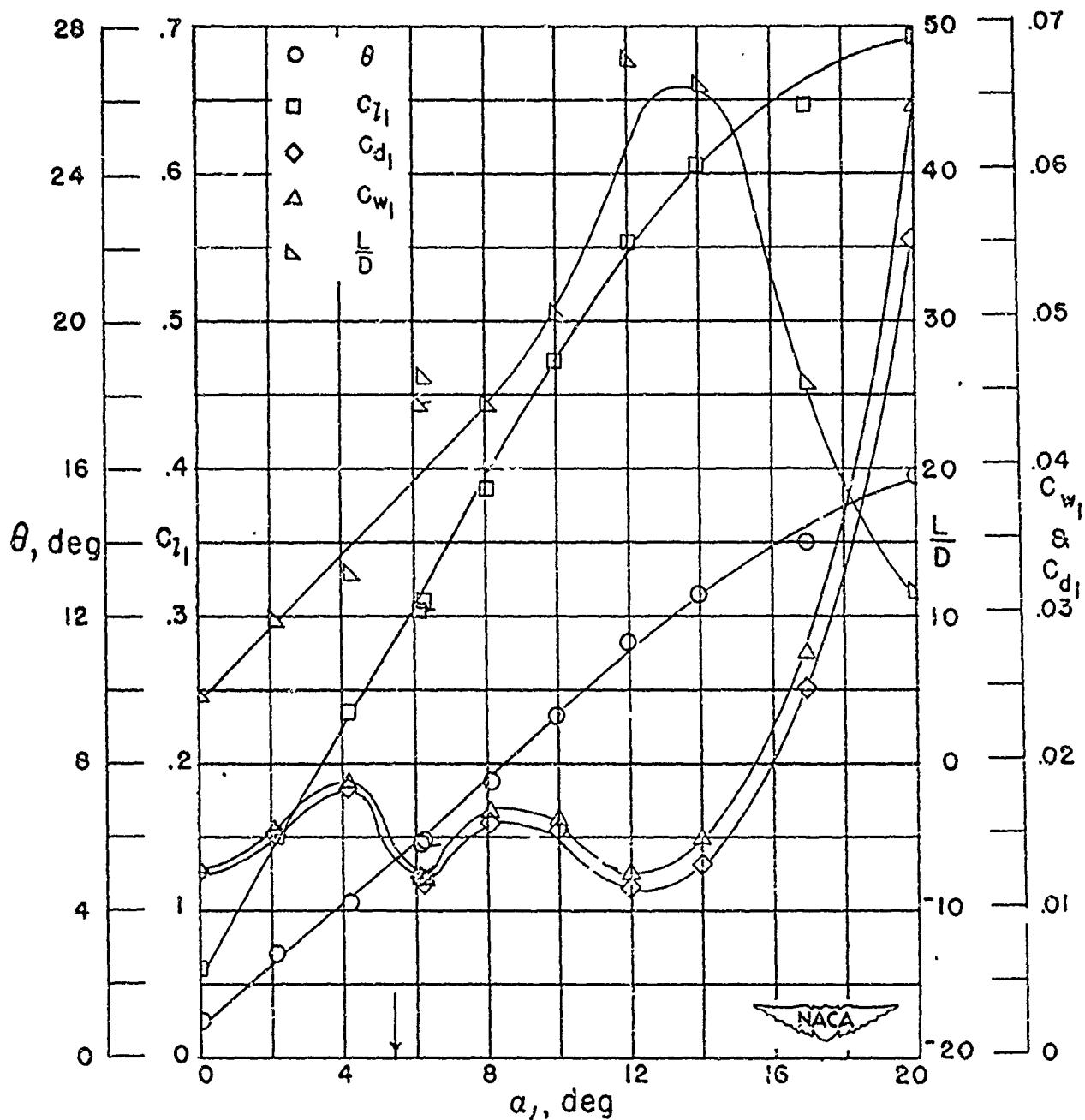
Cascade combination, $\beta_1 = 45^\circ$, $\sigma' = 0.50$
blade section, NACA 65-(12)10

Figure 4-27
(Source: Ref. 4-4)



Cascade combination, $\beta_1 = 45^\circ$, $\sigma' = 0.50$
blade section, NACA 65-(18)10

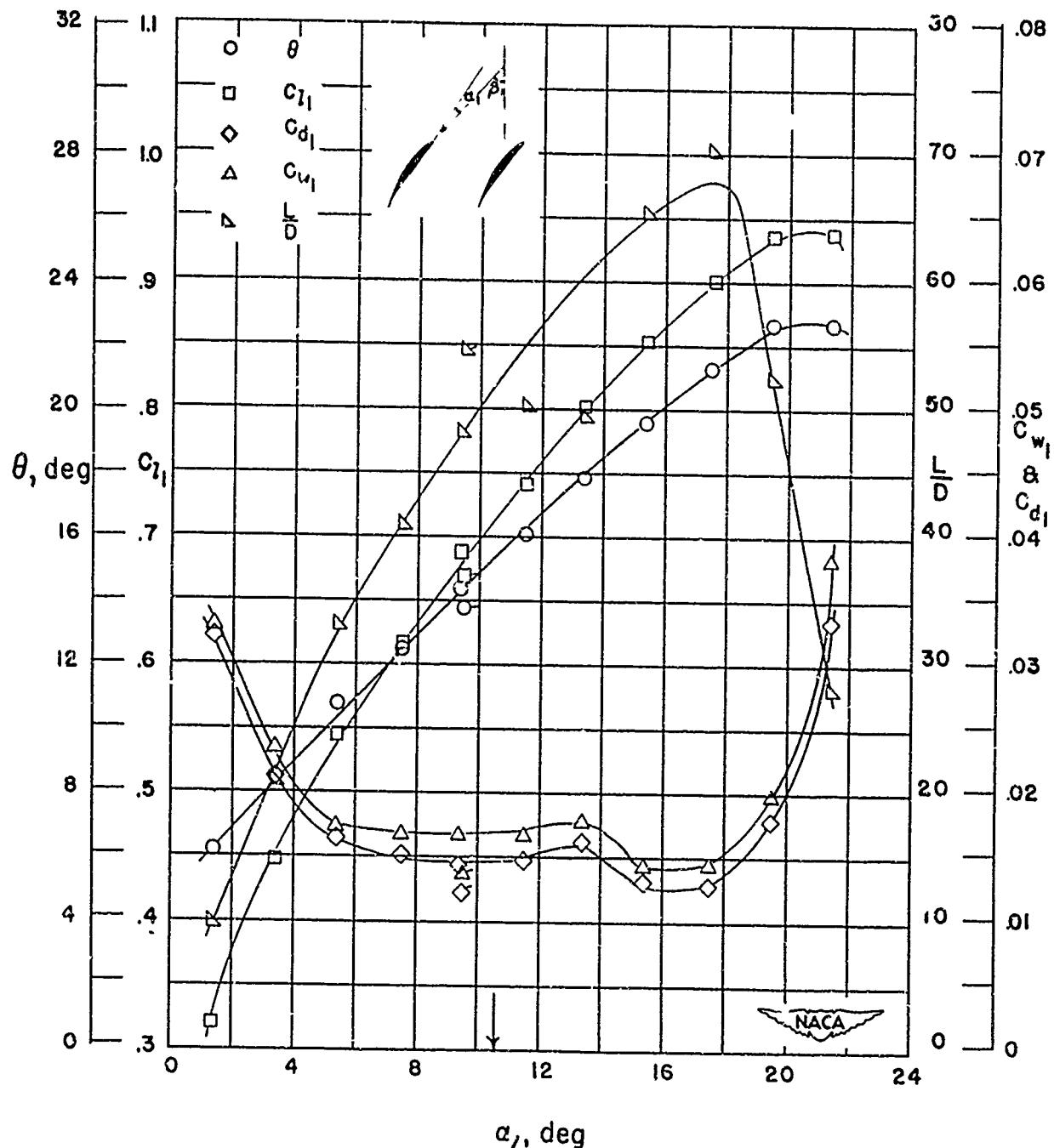
Figure 4-28
(Source: Ref 4-4)



Section characteristics; arrow shows design angle of attack;
flagged symbol indicates leading-edge roughness

Cascade combination, $\beta_1 = 45^\circ$, $\sigma' = 0.75$
blade section, NACA 65-410

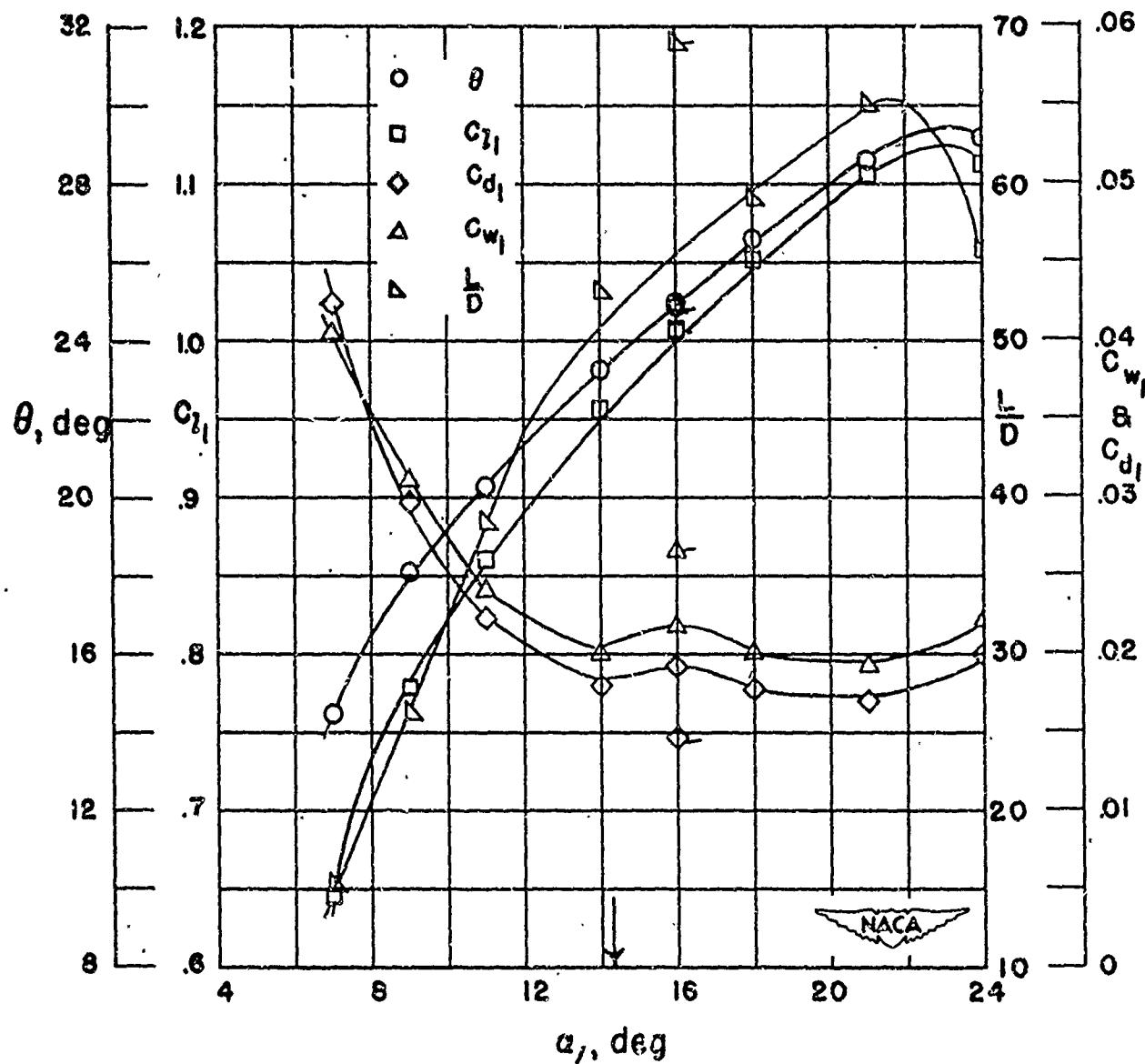
Figure 4-29
(Source: Ref. 4-4)



Section characteristics; arrow shows design angle of attack,
flagged symbol indicates leading-edge roughness

Cascade combination, $\beta_1 = 45^\circ$, $\sigma' = 0.75$
blade section, NACA 65-(12)10

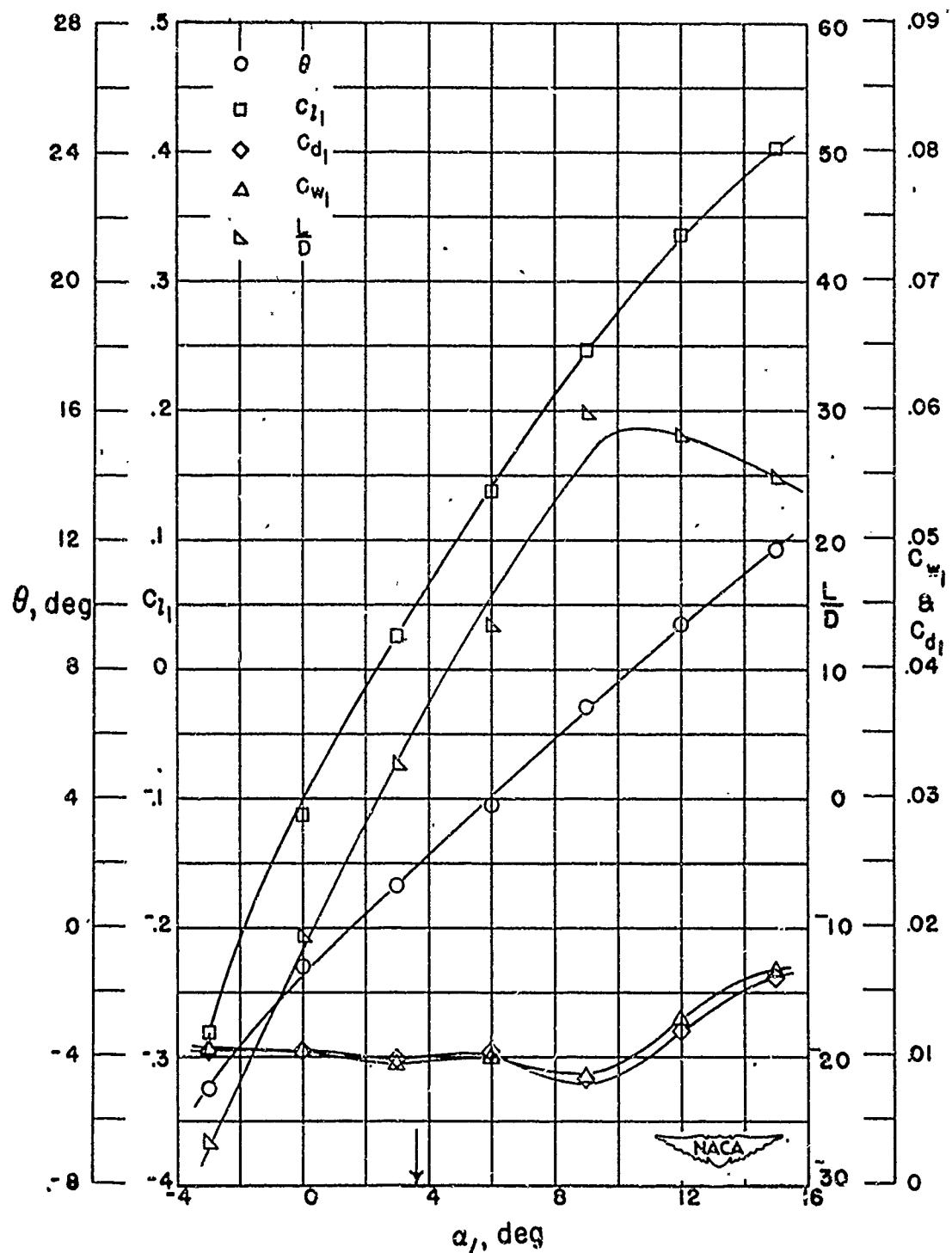
Figure 4-30
(Source: Ref. 4-4)



Section characteristics; arrow shows design angle of attack;
flagged symbol indicates leading-edge roughness.

Cascade combination, $\beta_1 \approx 45^\circ$, $\sigma' = 0.75$
blade section, NACA 65-(18)10

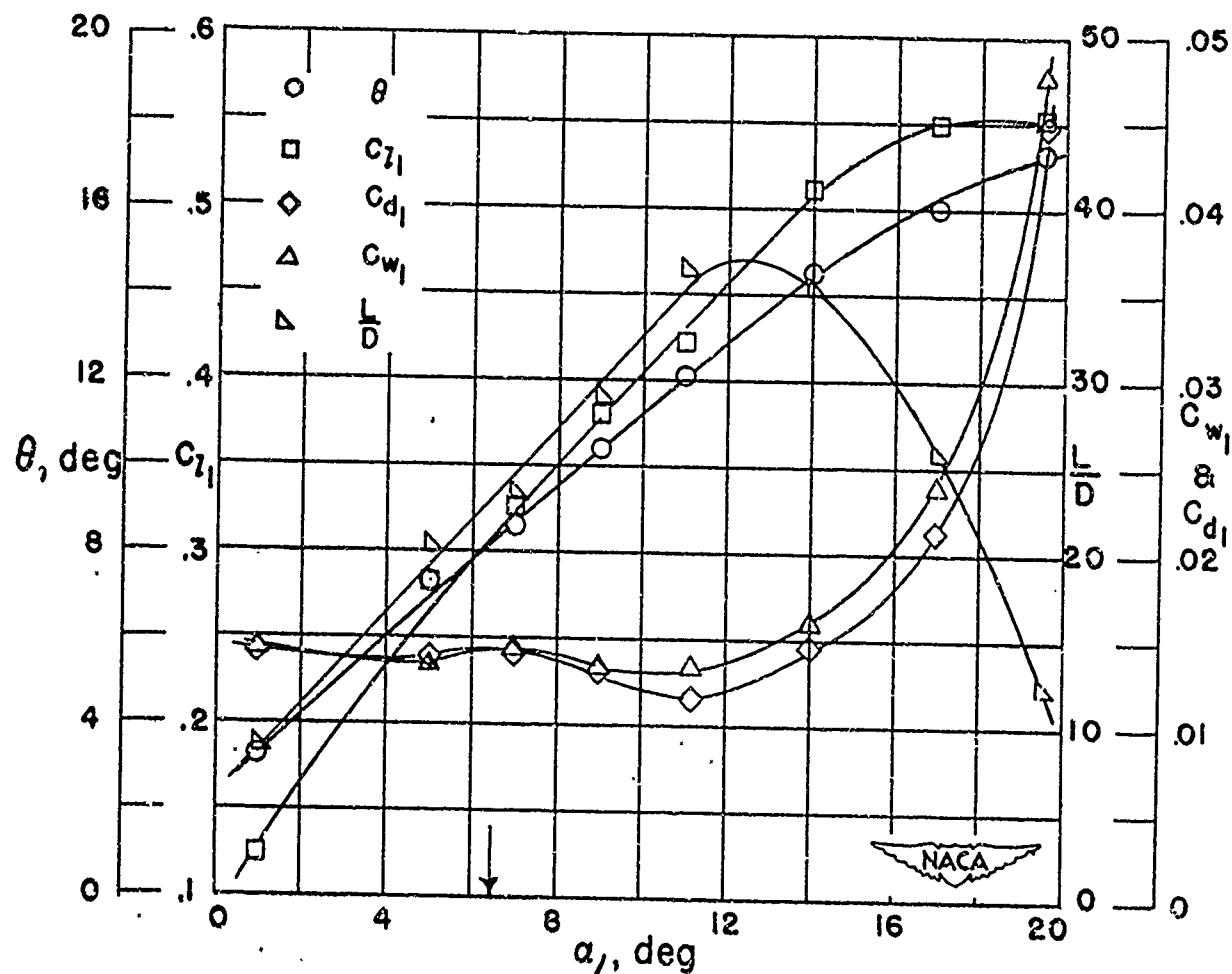
Figure 4-31
(Source: Ref. 4-4)



Section characteristics; arrow shows design angle of attack.

Cascade combination, $\beta_1 = 45^\circ$, $\sigma' = 1.00$
blade section, NACA 65-010

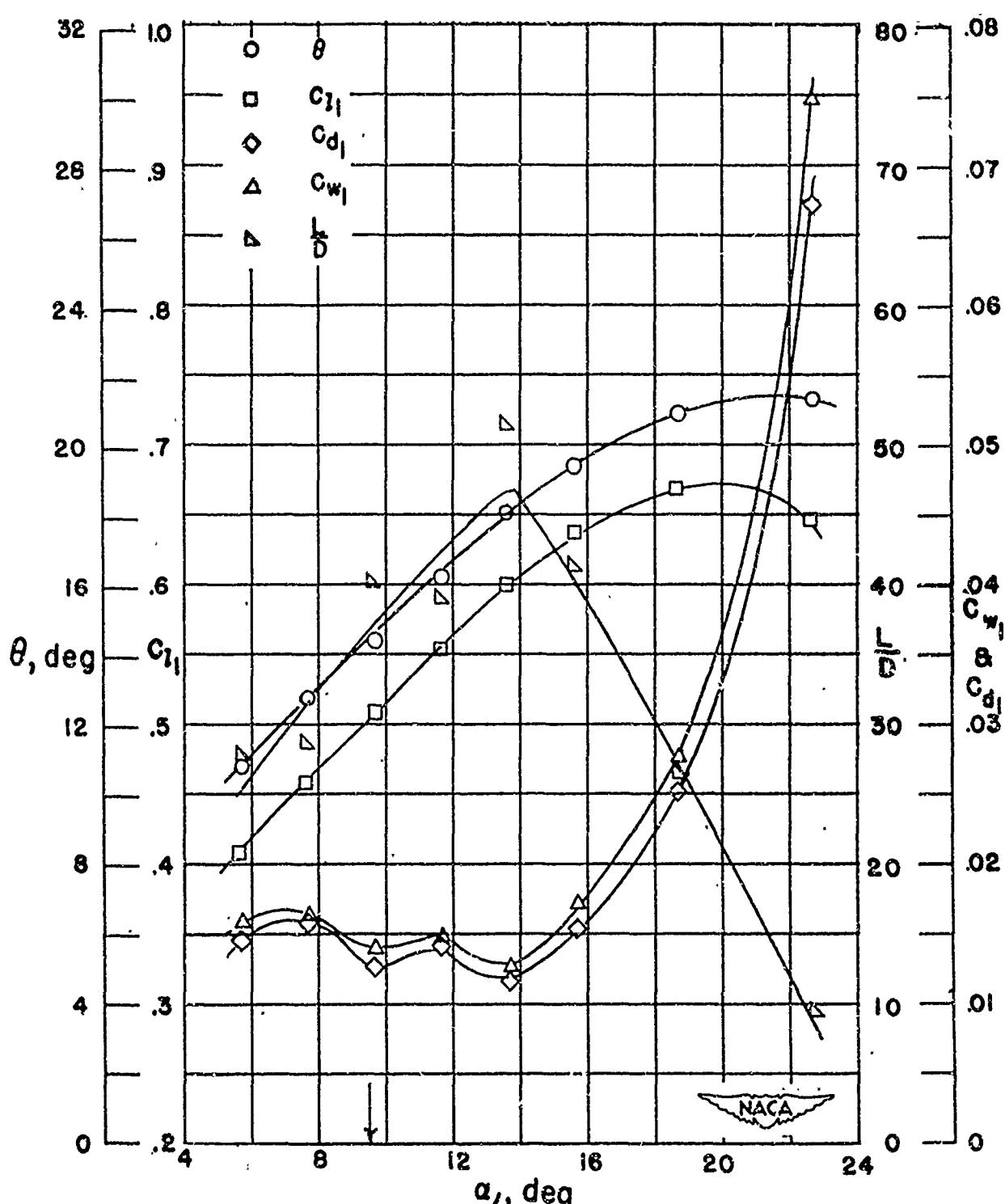
Figure 4-32
(Source: Ref. 4-4)



Section characteristics; arrow shows design angle of attack.

Cascade combination, $\beta_1 = 45^\circ$, $\sigma' = 1.00$
blade section, NACA 65-410

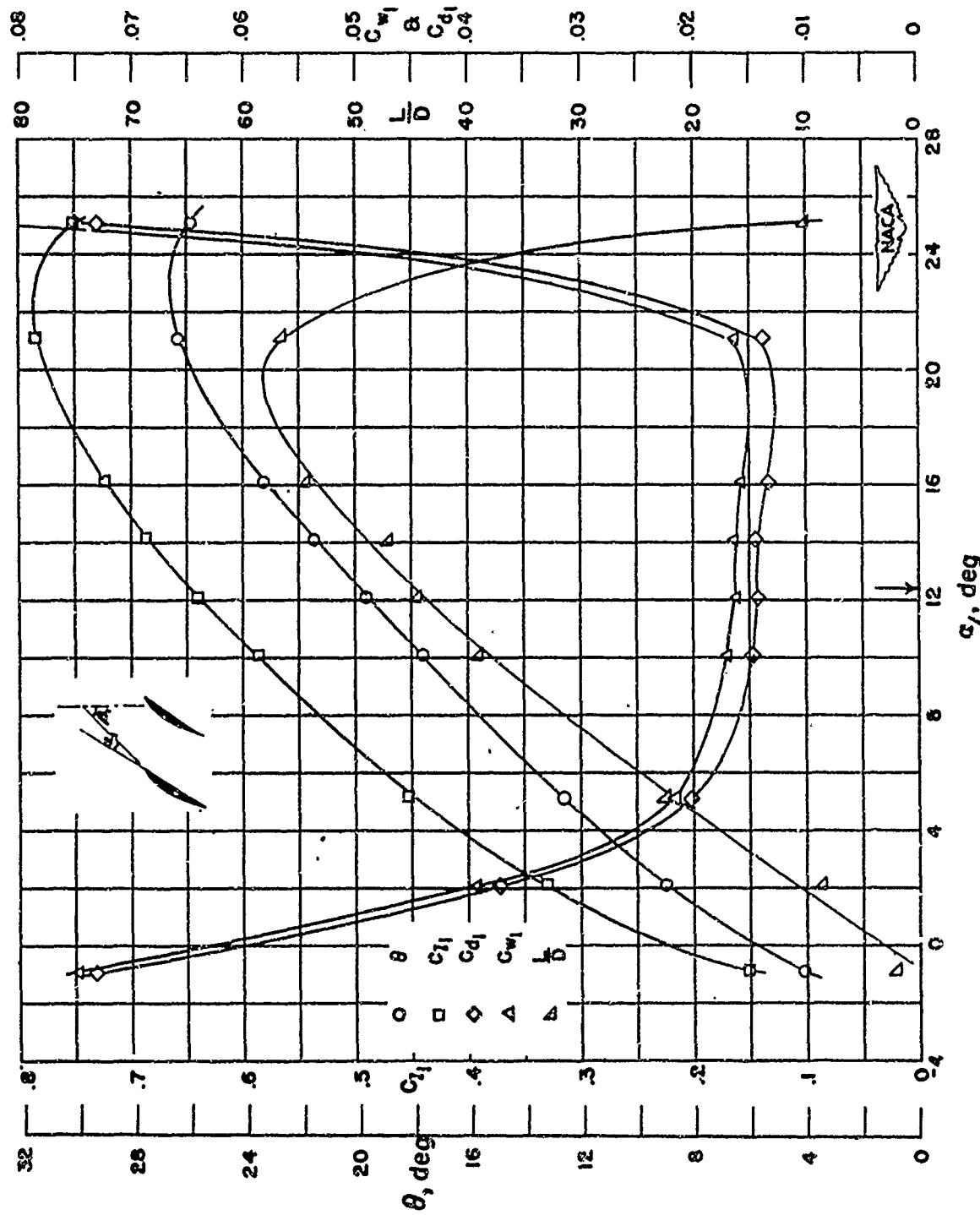
Figure 4-33
(Source: Ref. 4-4)



Section characteristics; arrow shows design angle of attack.

Cascade combination, $\beta_1 = 45^\circ$, $\sigma' = 1.00$
blade section, NACA 65-810

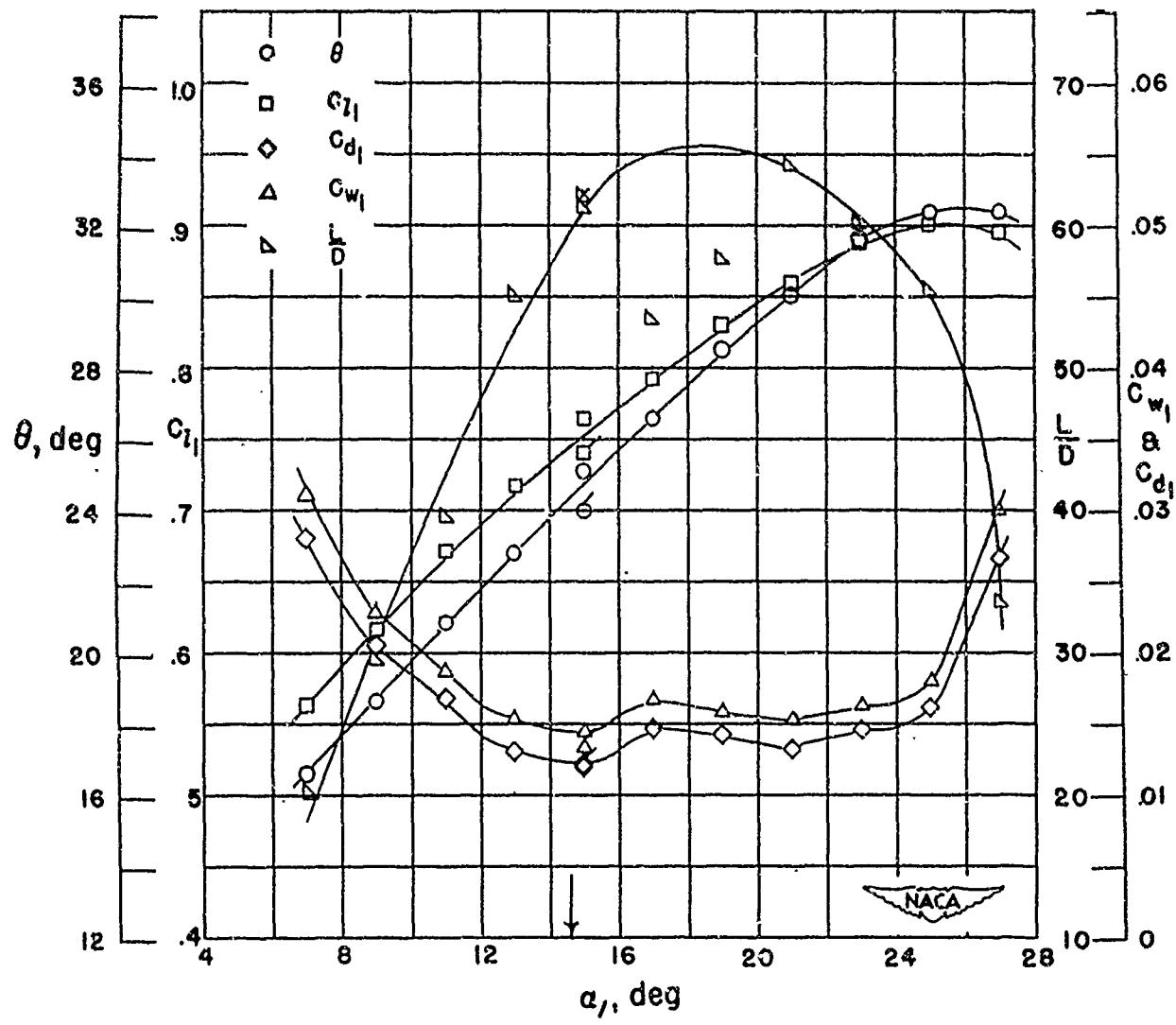
Figure 4-34
(Source: Ref. 4-4)



Section characteristics; arrow shows design angle of attack.

Cascade combination, $\beta_1 = 45^\circ$, $\sigma' = 1.00$
blade section, NACA 65-(12)10

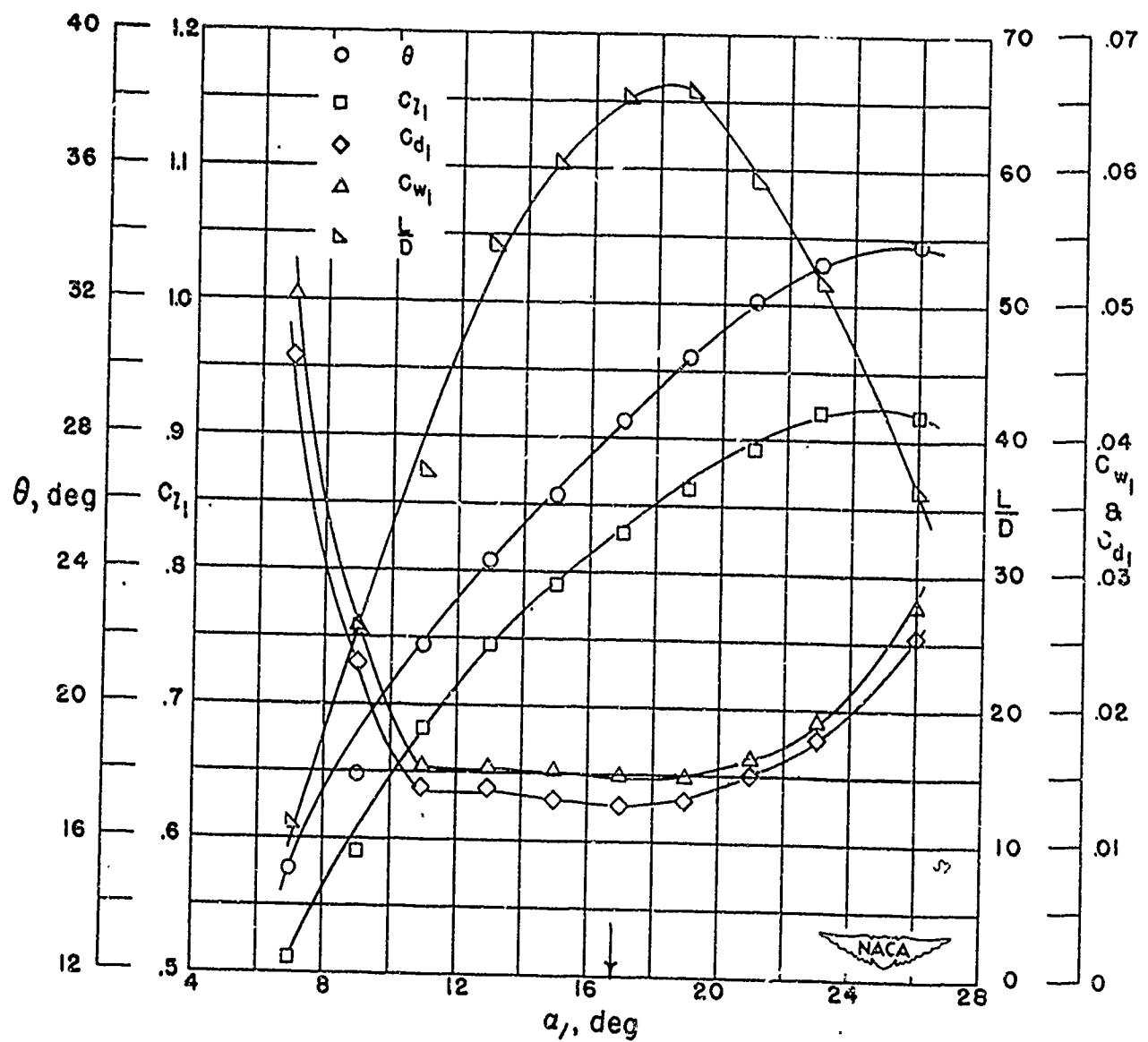
Figure 4-35
(Source: Ref. 4-4)



Section characteristics; arrow shows design angle of attack;
flagged symbol indicates leading-edge roughness.

Cascade combination, $\beta_1 = 45^\circ$, $\sigma' = 1.00$
blade section, NACA 65~(15)10

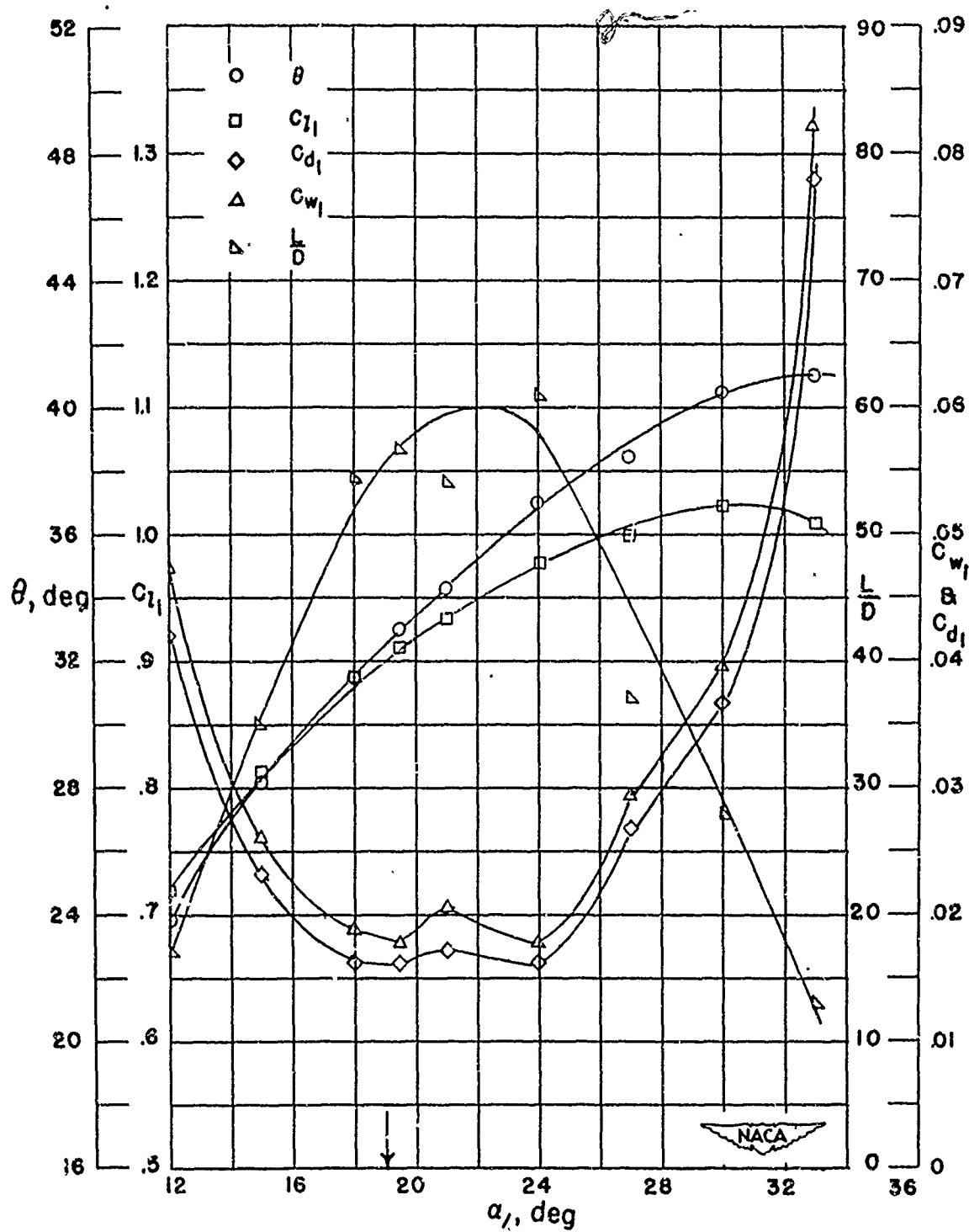
Figure 4-36
(Source: Ref. 4-4)



Section characteristics; arrow shows design angle of attack.

Cascade combination, $\beta_1 = 45^\circ$, $\sigma' = 1.00$
blade section, NACA 65-(18)10

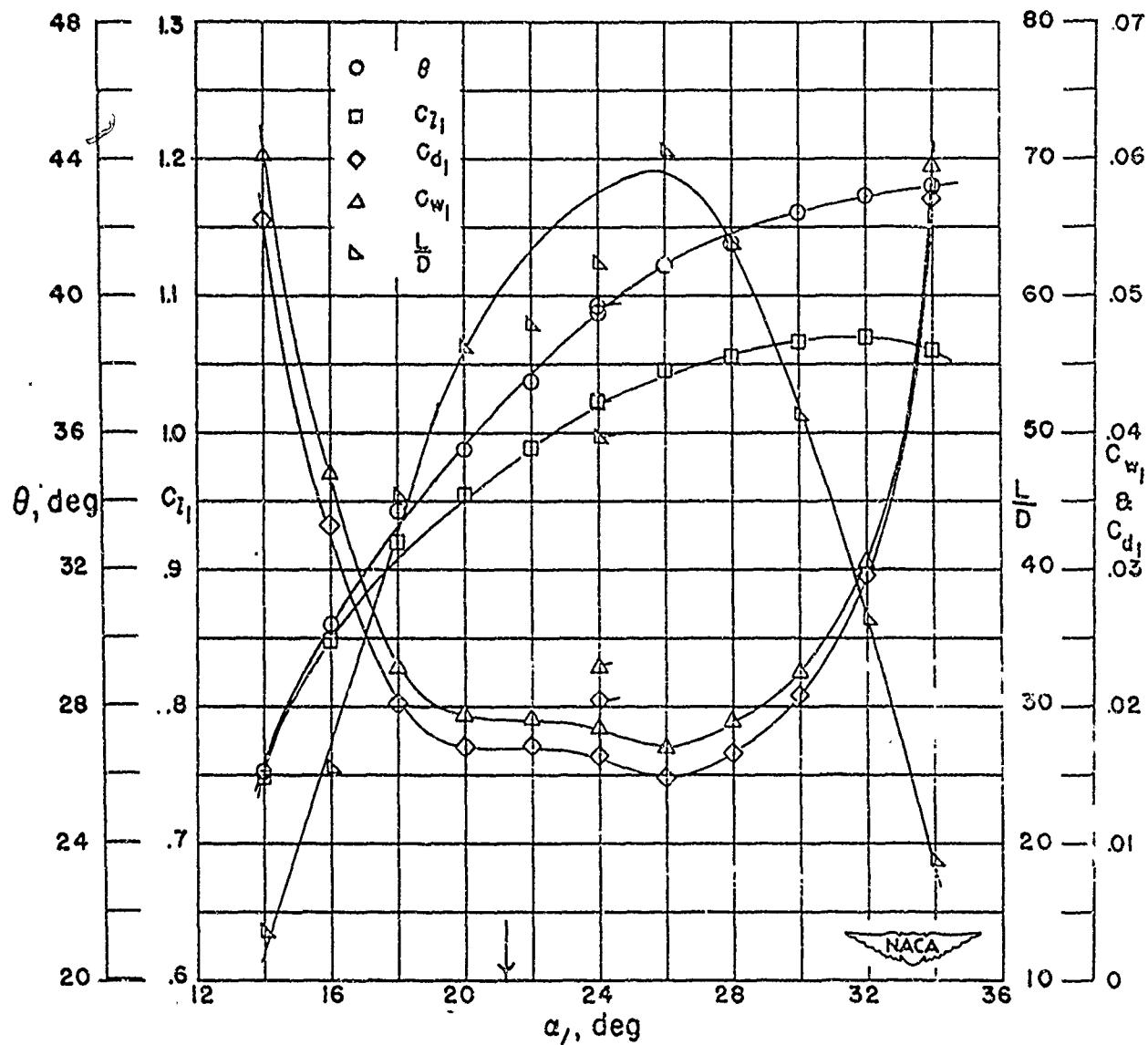
Figure 4-37
(Source: Ref. 4-4)



Section characteristics; arrow shows design angle of attack.

Cascade combination, $\beta_1 = 45^\circ$, $\sigma' = 1.00$
blade section, NACA 65-(21)10

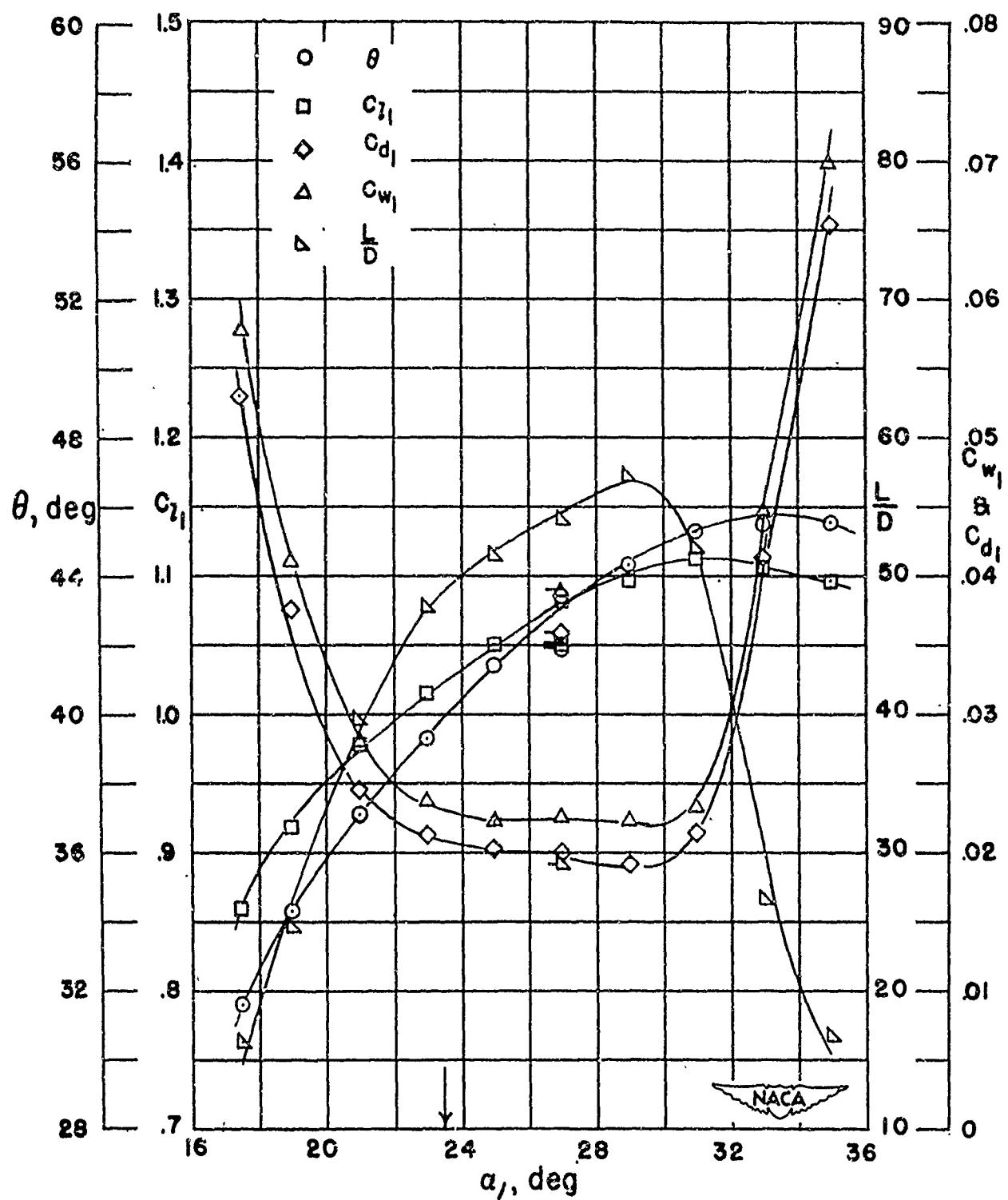
Figure 4-38
(Source: Ref. 4-4)



Section characteristics; arrow shows design angle of attack,
flagged symbol indicates leading-edge roughness.

Cascade combination, $\beta_1 = 45^\circ$, $\sigma' = 1.00$
blade section, NACA 65-(24)10

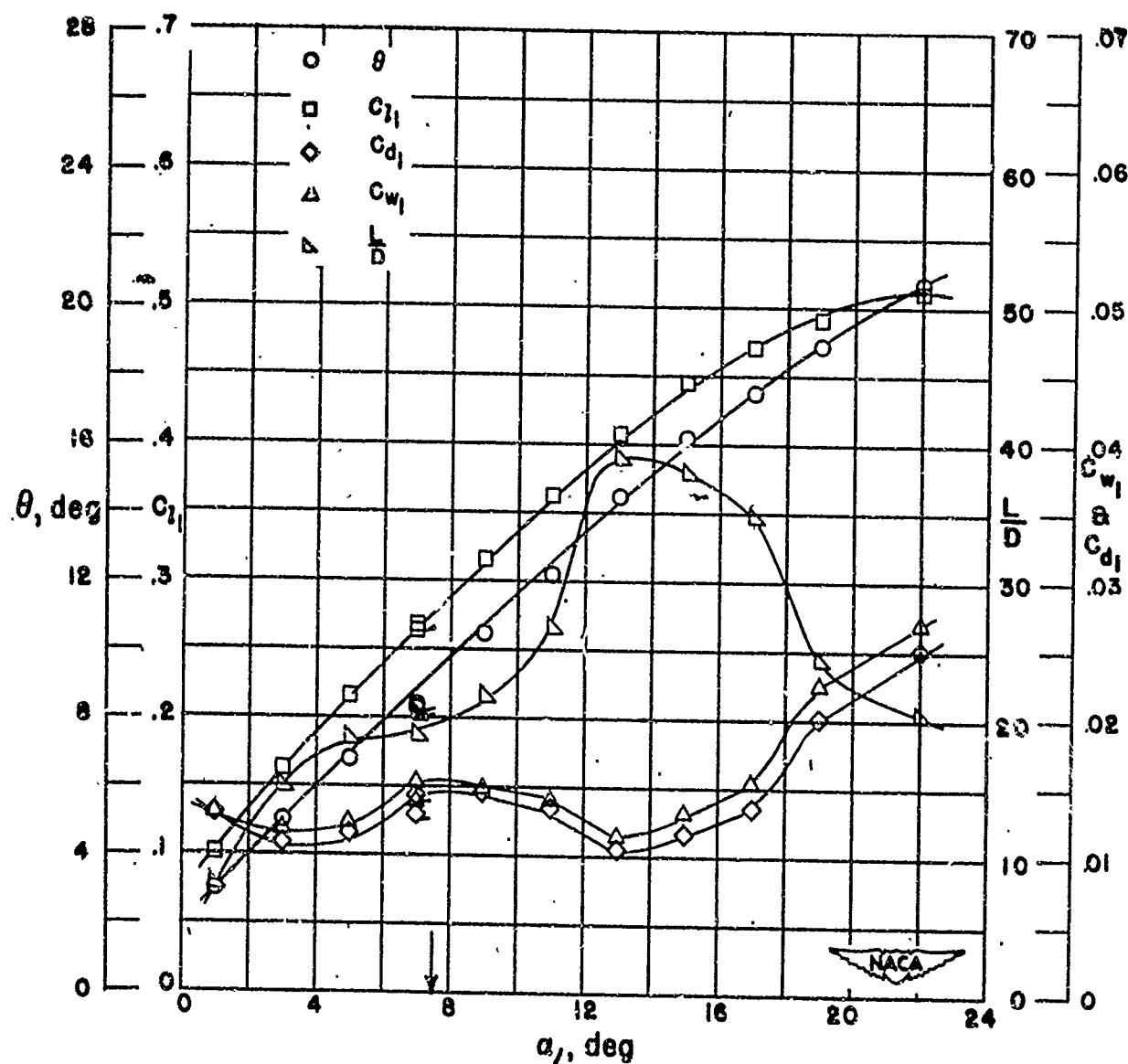
Figure 4-39
(Source: Ref. 4-4)



Section characteristics; arrow shows design angle of attack;
flagged symbol indicates leading-edge roughness

Cascade combination, $\beta_1 = 45^\circ$, $\sigma' = 1.00$
blade section, NACA 65-(27)10

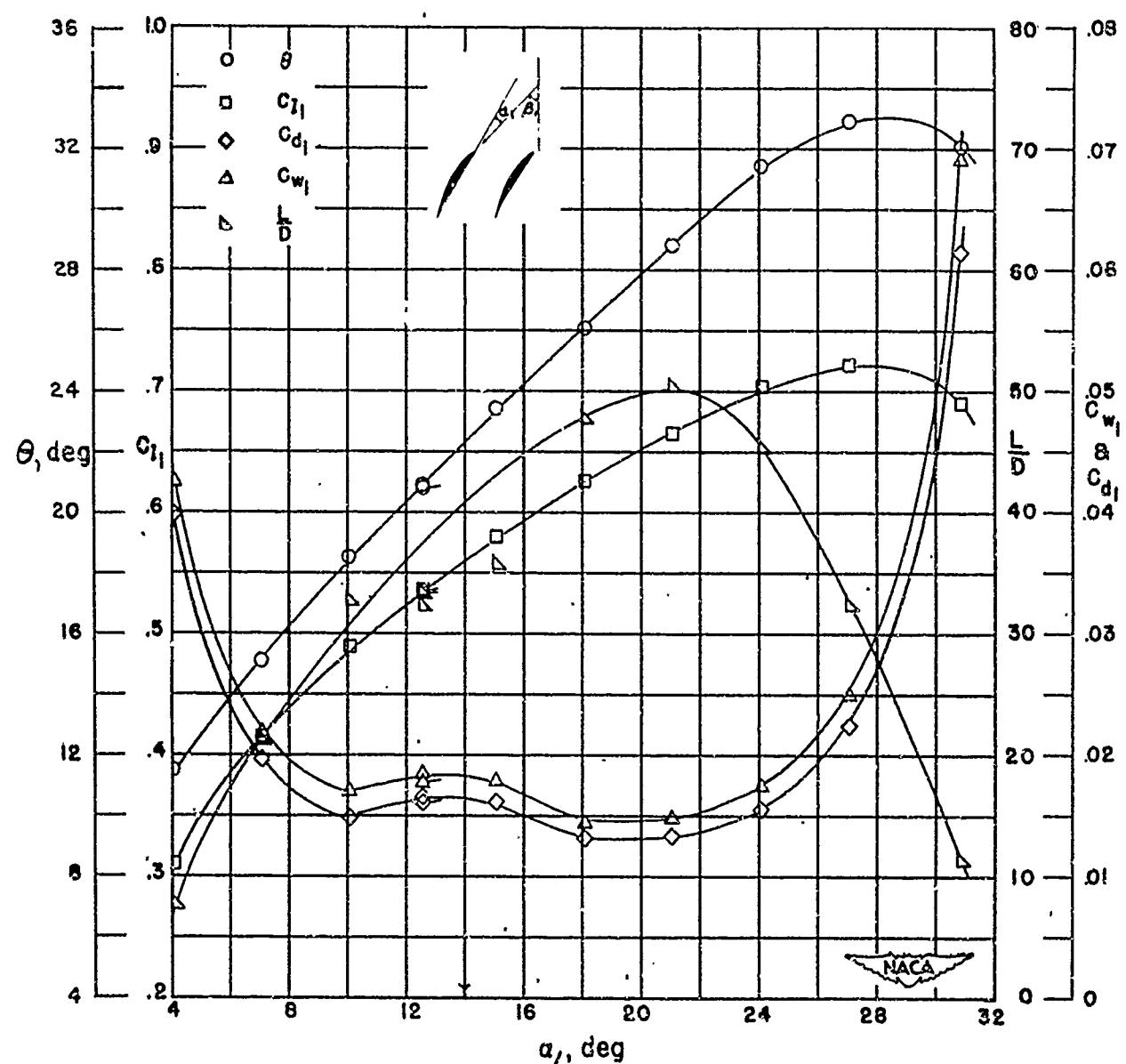
Figure 4-40
(Source: Ref. 4-4)



Section characteristics; arrow shows design angle of attack;
flagged symbol indicates leading-edge roughness.

Cascade combination, $\beta_1 \approx 45^\circ$, $\sigma' = 1.25$
blade section, NACA 65-410

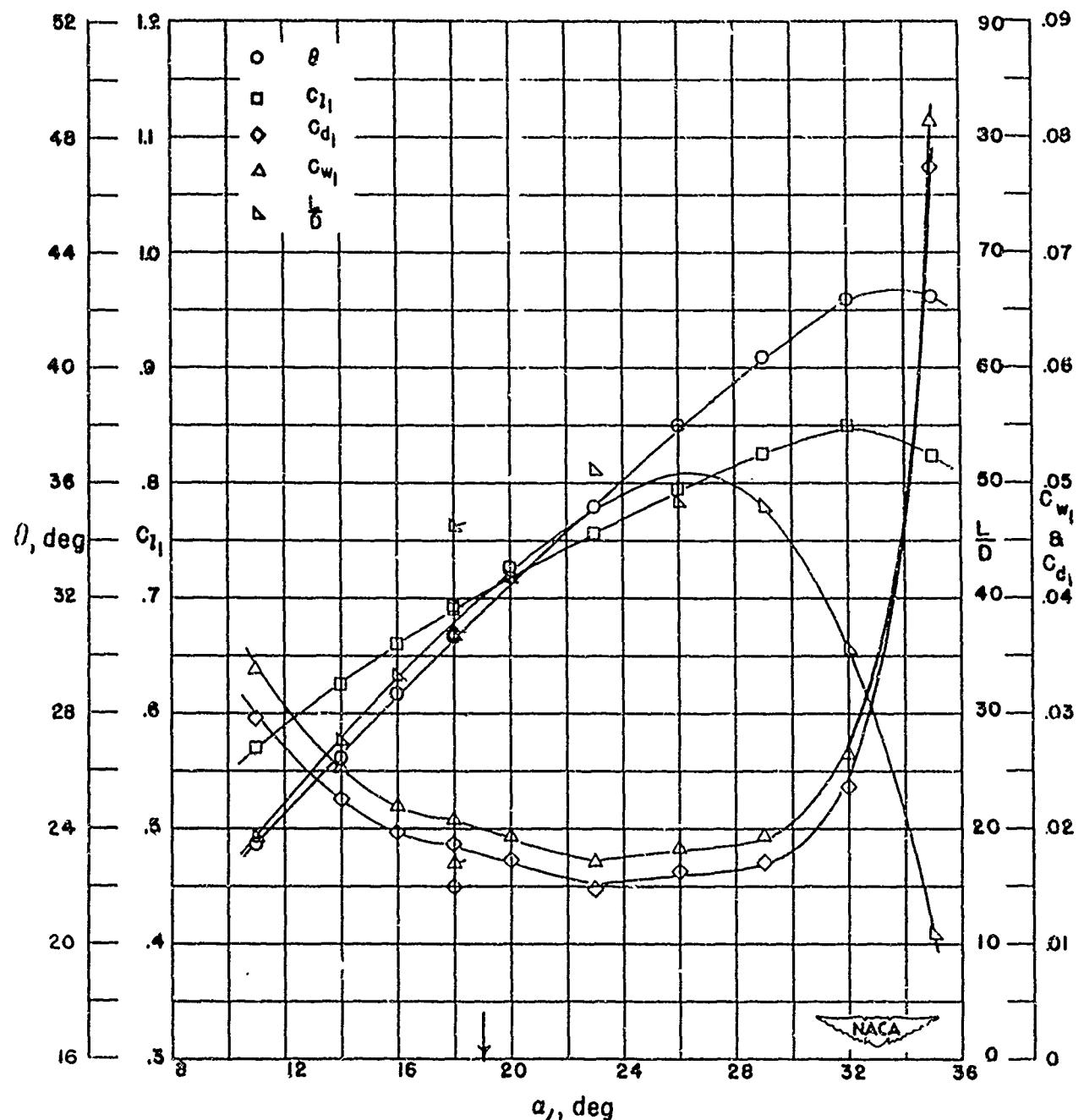
Figure 4-41
(Source: Ref. 4-4)



Section characteristics, arrow shows design angle of attack;
flagged symbol indicates leading-edge roughness.

Cascade combination, $\beta_1 = 45^\circ$, $\sigma' = 1.25$
blade section, NACA 65-(12)10

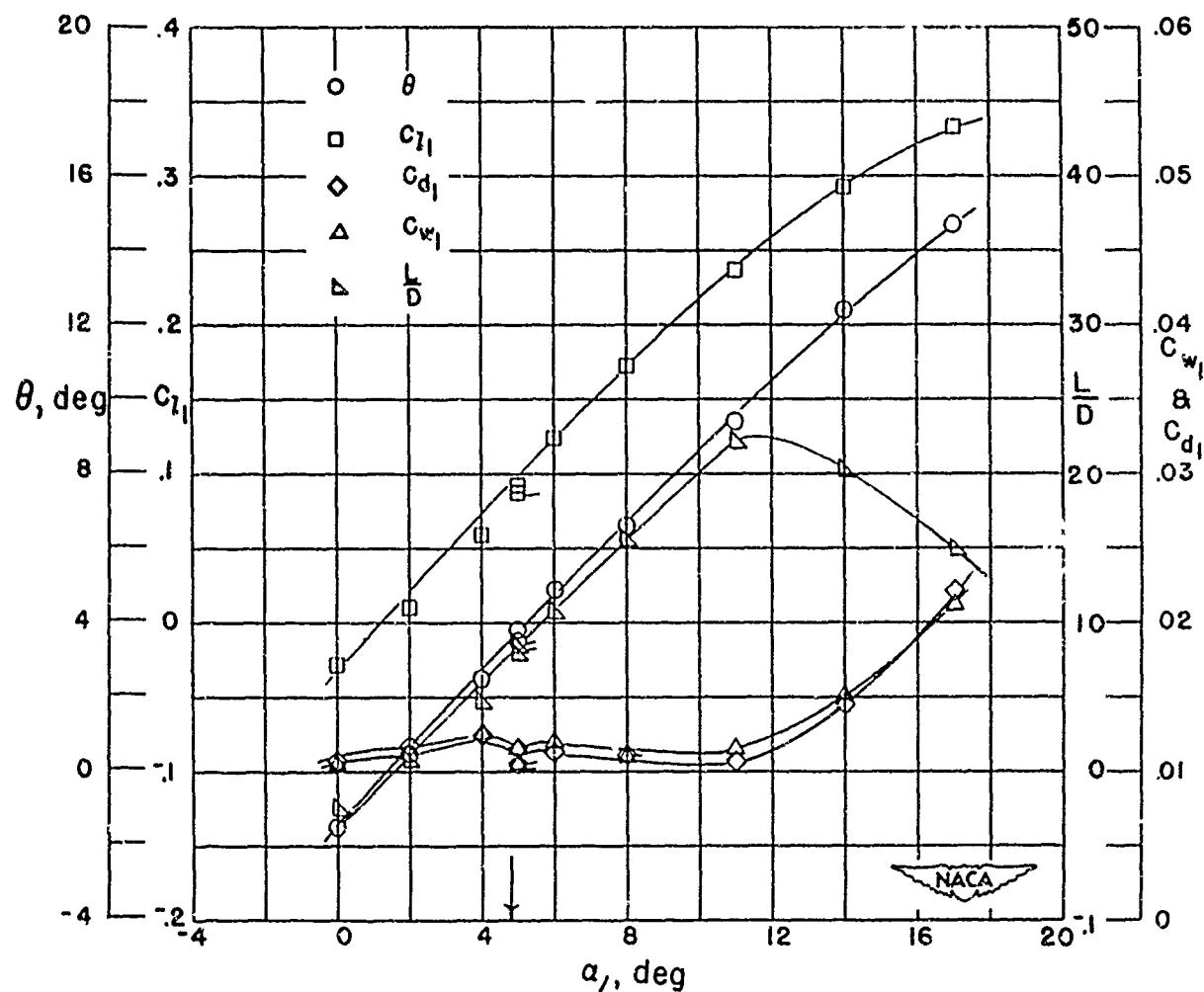
Figure 4-42
(Source: Ref. 4-4)



Section characteristics; arrow shows design angle of attack,
flagged symbol indicates leading-edge roughness.

Cascade combination, $\beta_1 = 45^\circ$, $\sigma' = 1.25$
blade section, NACA 65-(18)10

Figure 4-43
(Source: Ref. 4-4)



(g) Section characteristics; arrow shows design angle of attack;
flagged symbol indicates leading-edge roughness.

Cascade combination, $\beta_1 = 45^\circ$, $\sigma' = 1.50$
blade section, NACA 65-010

Figure 4-44
(Source: Ref 4-4)

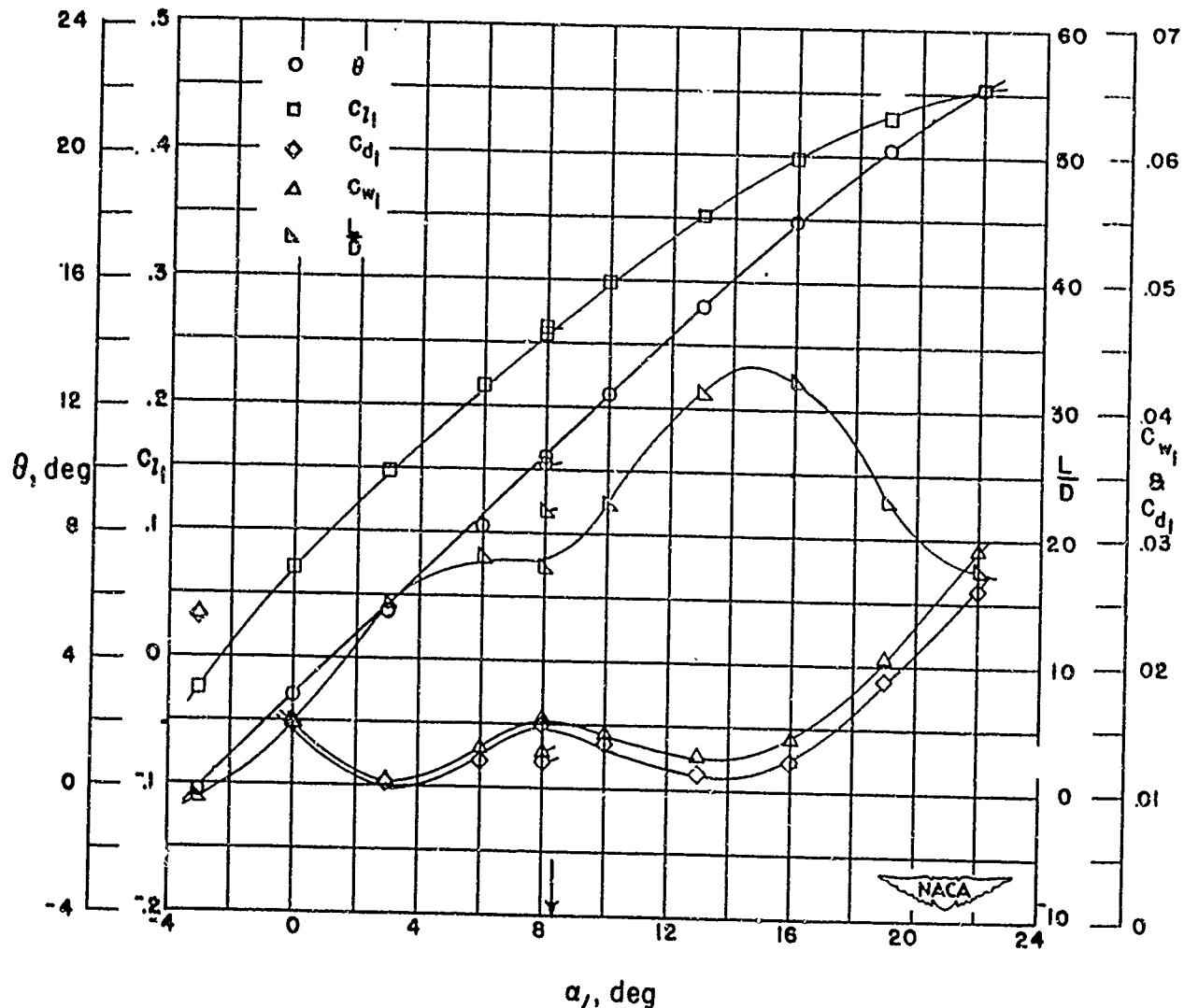
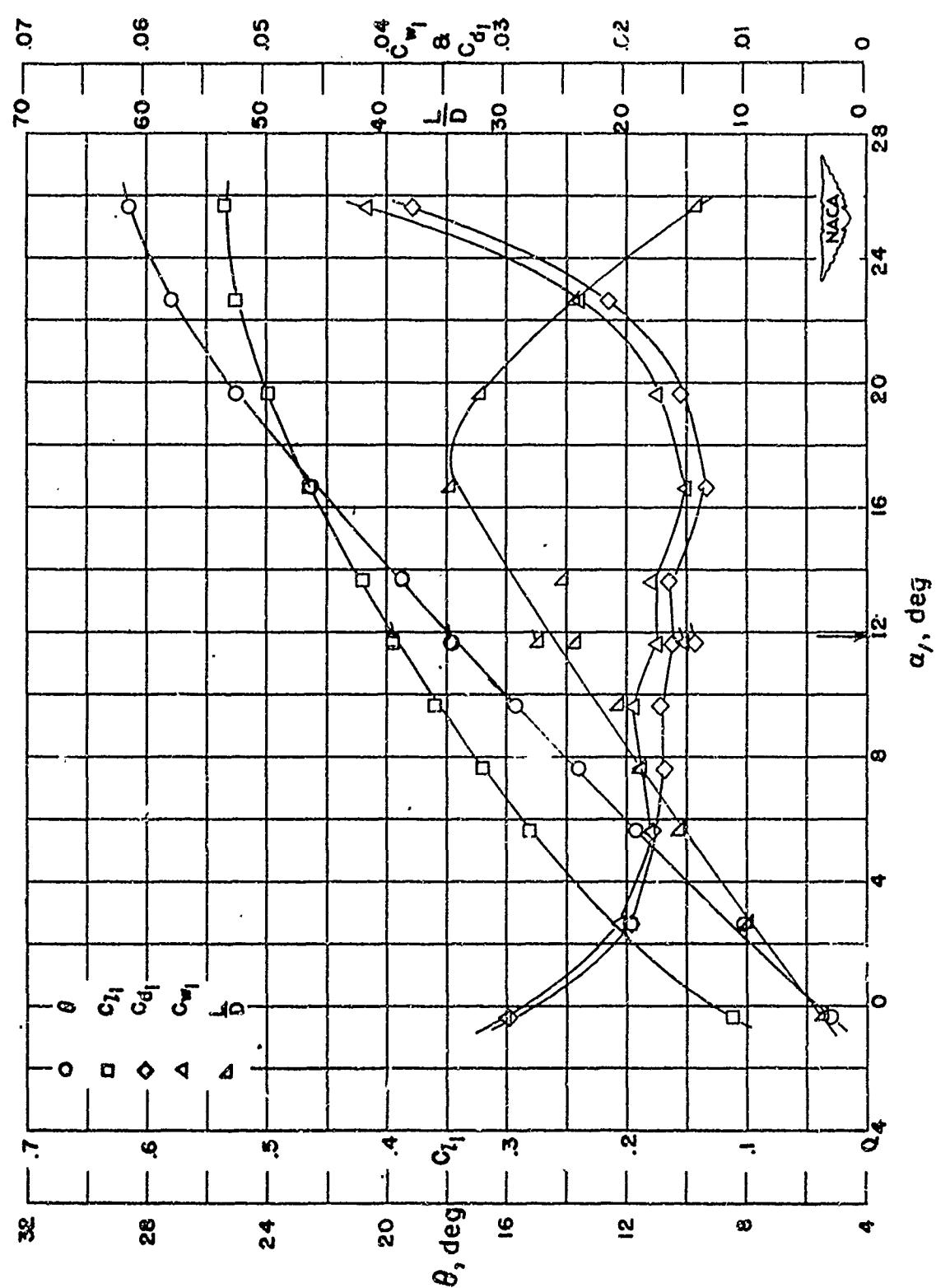


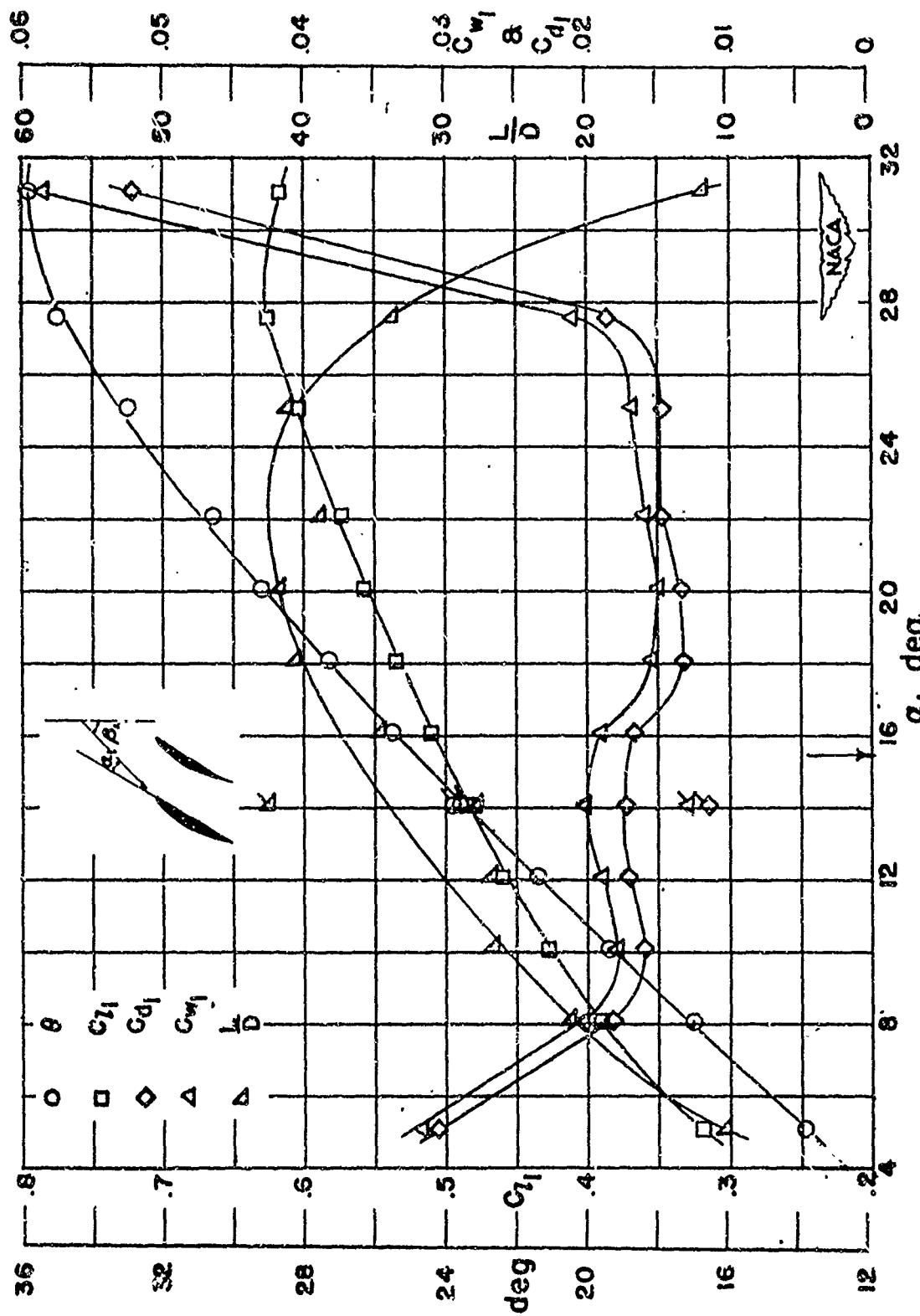
Figure 4-45
(Source: Ref. 4-4)



Section characteristics; arrow shows design angle of attack;
flagged symbol indicates leading-edge roughness.

Cascade combination, $\beta_1 = 45^\circ$, $\sigma' = 1.50$
blade section, NACA 65-810

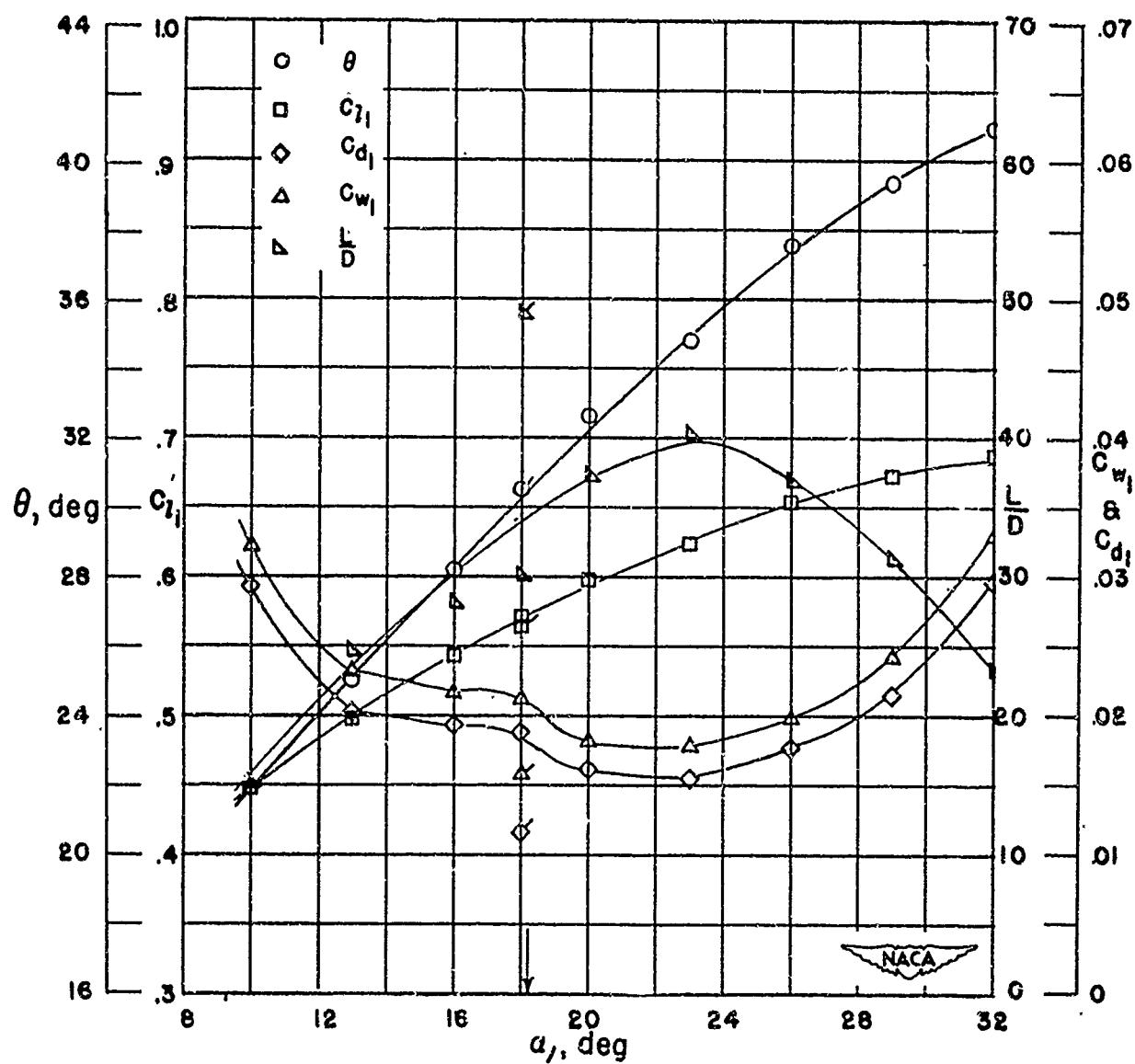
Figure 4-46
(Source: Ref. 4-4)



Section characteristics; arrow shows design angle of attack;
flagged symbol indicates leading-edge roughness

Cascade combination, $\beta_1 = 45^\circ$, $\sigma' = 1.50$
blade section, NACA 65-(12)10

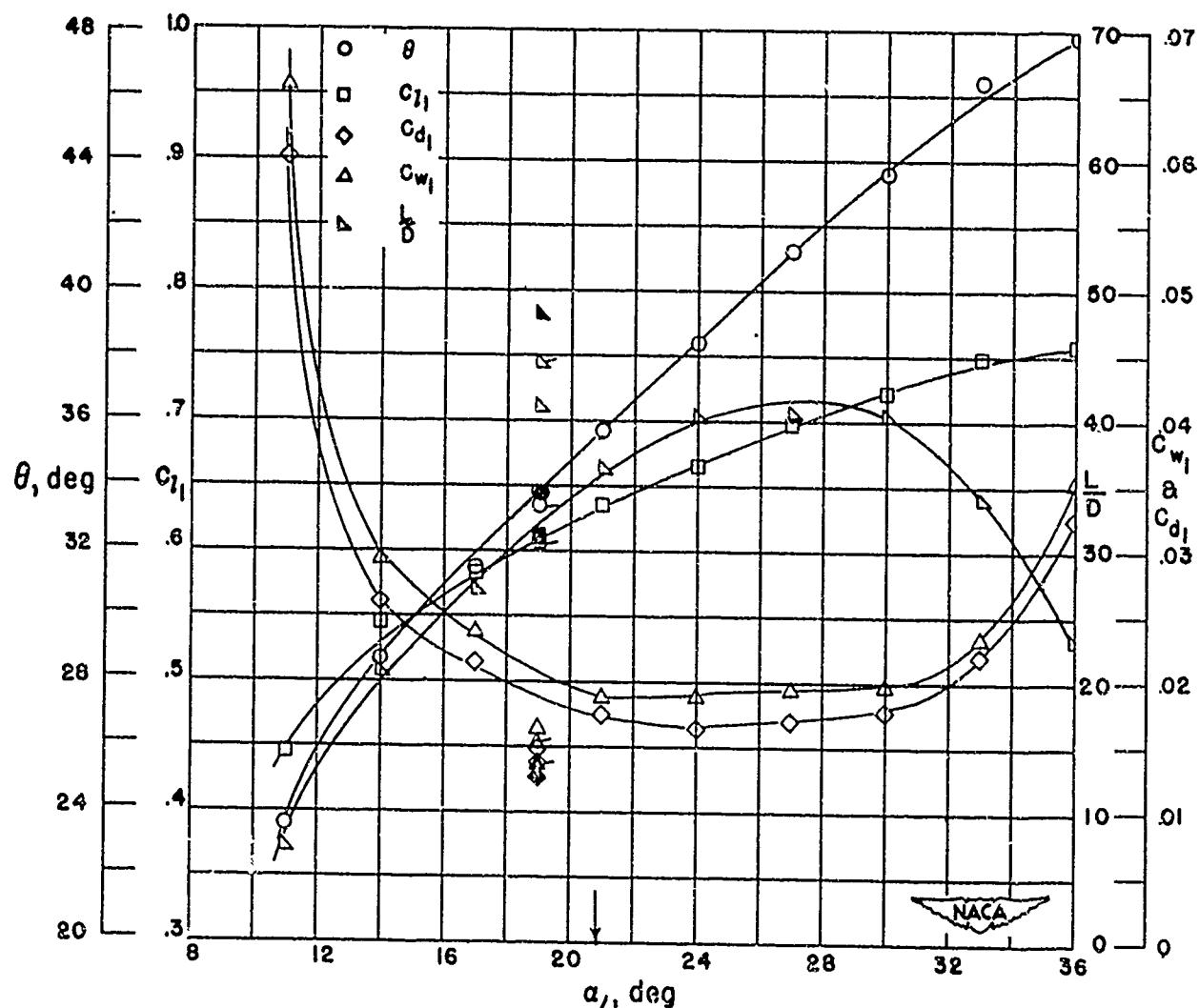
Figure 4-47
(Source: Ref. 4-4)



Section characteristics; arrow shows design angle of attack;
flagged symbol indicates leading-edge roughness.

Cascade combination, $\beta_1 = 45^\circ$, $\sigma' = 1.50$
blade section, NACA 65-(15)10

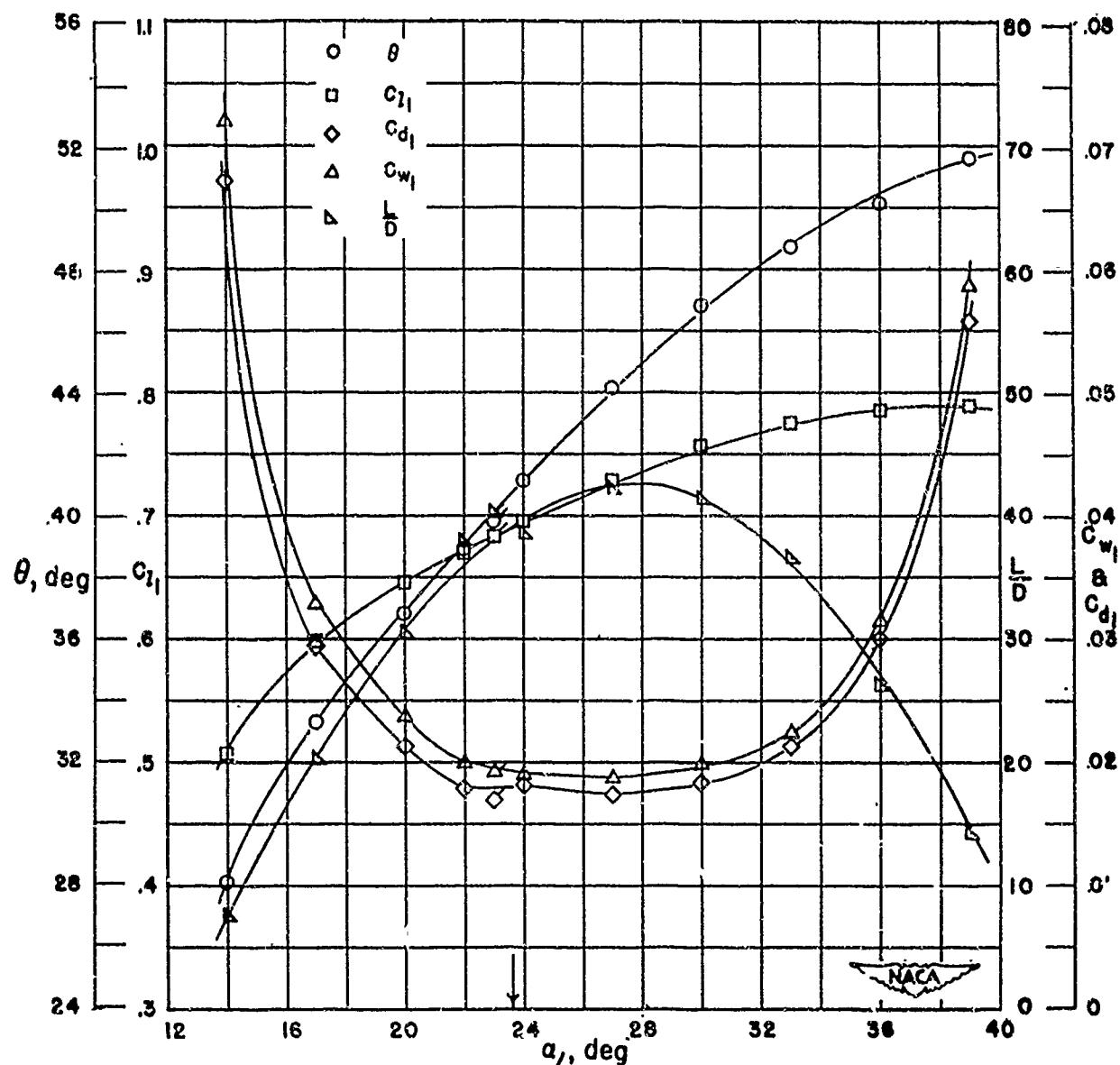
Figure 4-48
(Source: Ref. 4-4)



Section characteristics; arrow shows design angle of attack,
flagged symbol indicates leading-edge roughness; solid
symbol indicates high Reynolds number.

Cascade combination, $\beta_1 = 45^\circ$, $\sigma' = 1.50$
blade section, NACA 65-(18)10

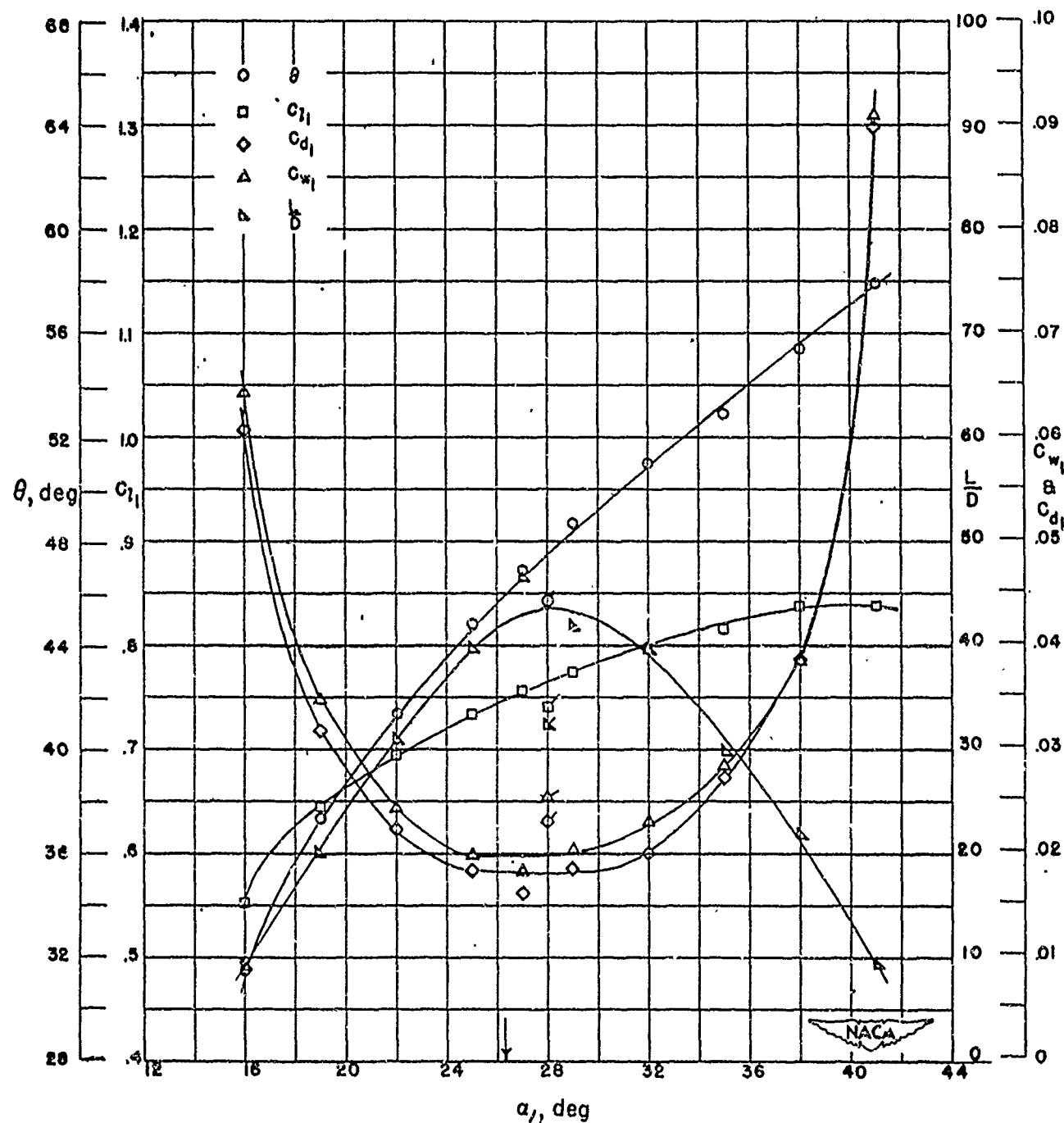
Figure 4-49
(Source: Ref. 4-4)



Section characteristics; arrow shows design angle of attack;
flagged symbol indicates leading-edge roughness.

Cascade combination, $\beta_1 = 45^\circ$, $\sigma' = 1.50$
blade section, NACA 65-(21)10

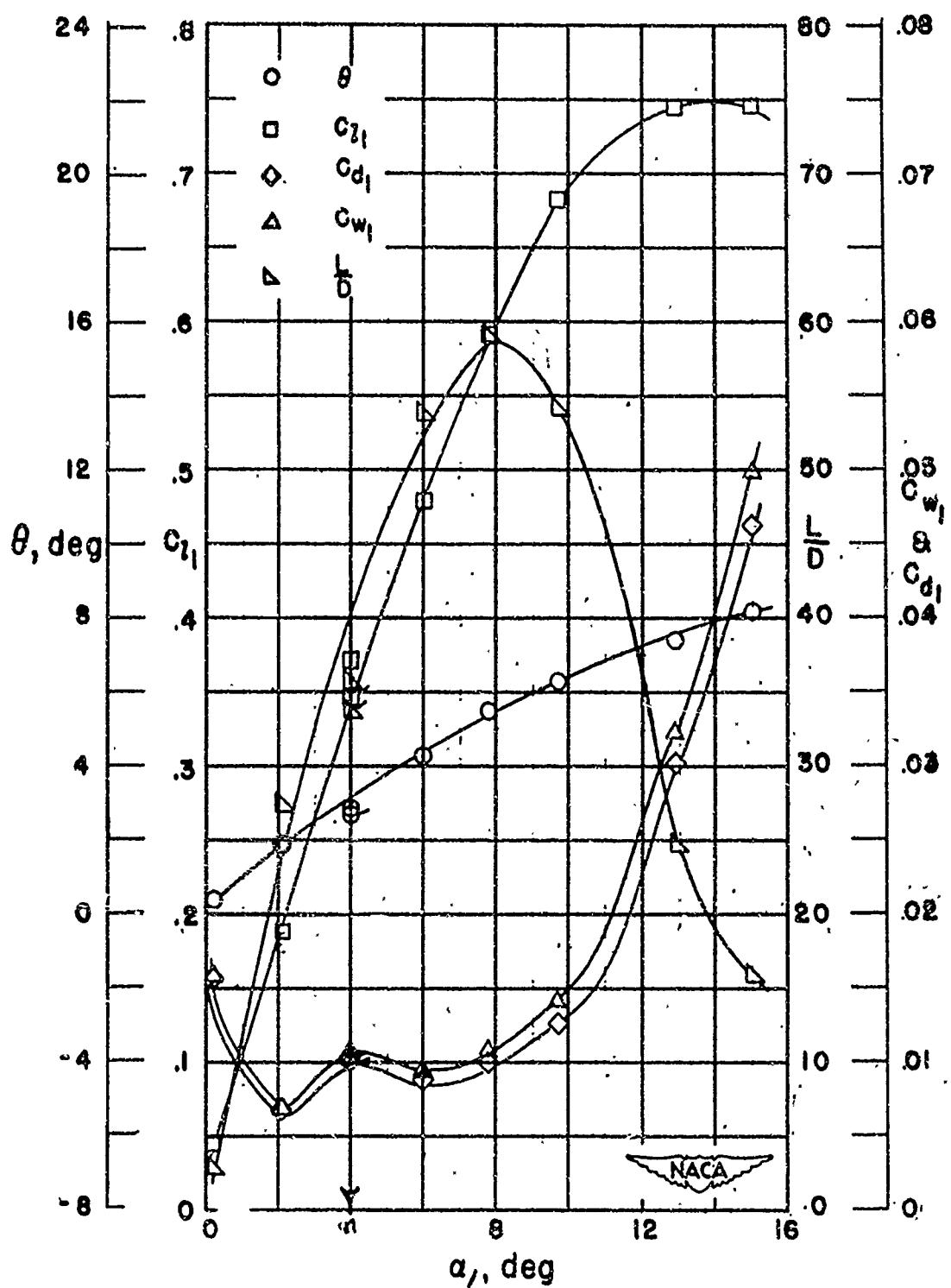
Figure 4-50
(Source: Ref. 4-4)



Section characteristics; arrow shows design angle of attack,
flagged symbol indicates leading-edge roughness.

Cascade combination, $\beta_1 = 45^\circ$, $\sigma' = 1.50$
blade section, NACA 65-(24)10

Figure 4-51
(Source: Ref. 4-4)



Section characteristics; arrow shows design angle of attack;
flagged symbol indicates leading-edge roughness

Cascade combination, $\beta_1 = 60^\circ$, $\sigma' = 0.50$
blade section, NACA 65-410

Figure 4-52
(Source: Ref. 4-4)

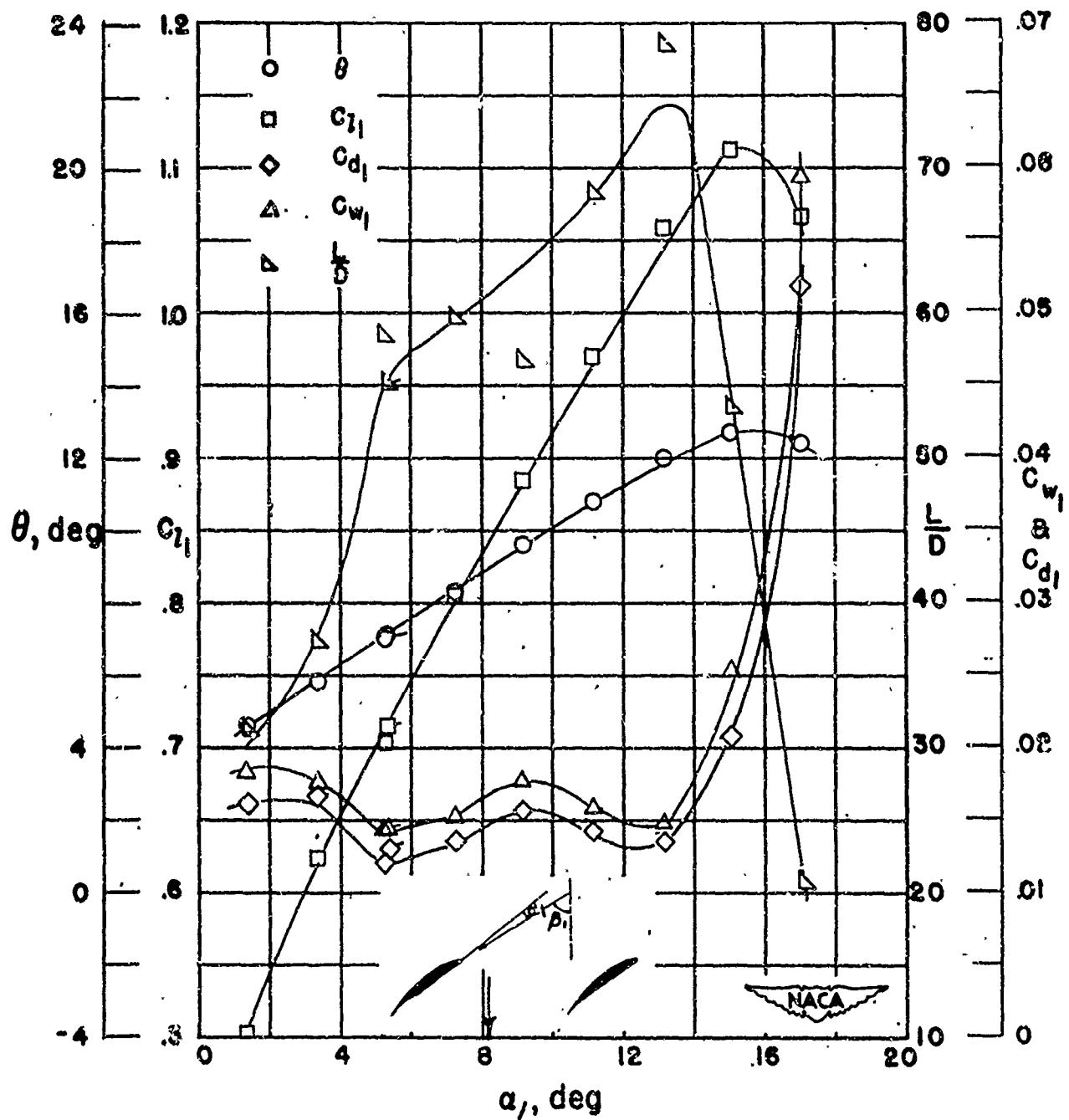
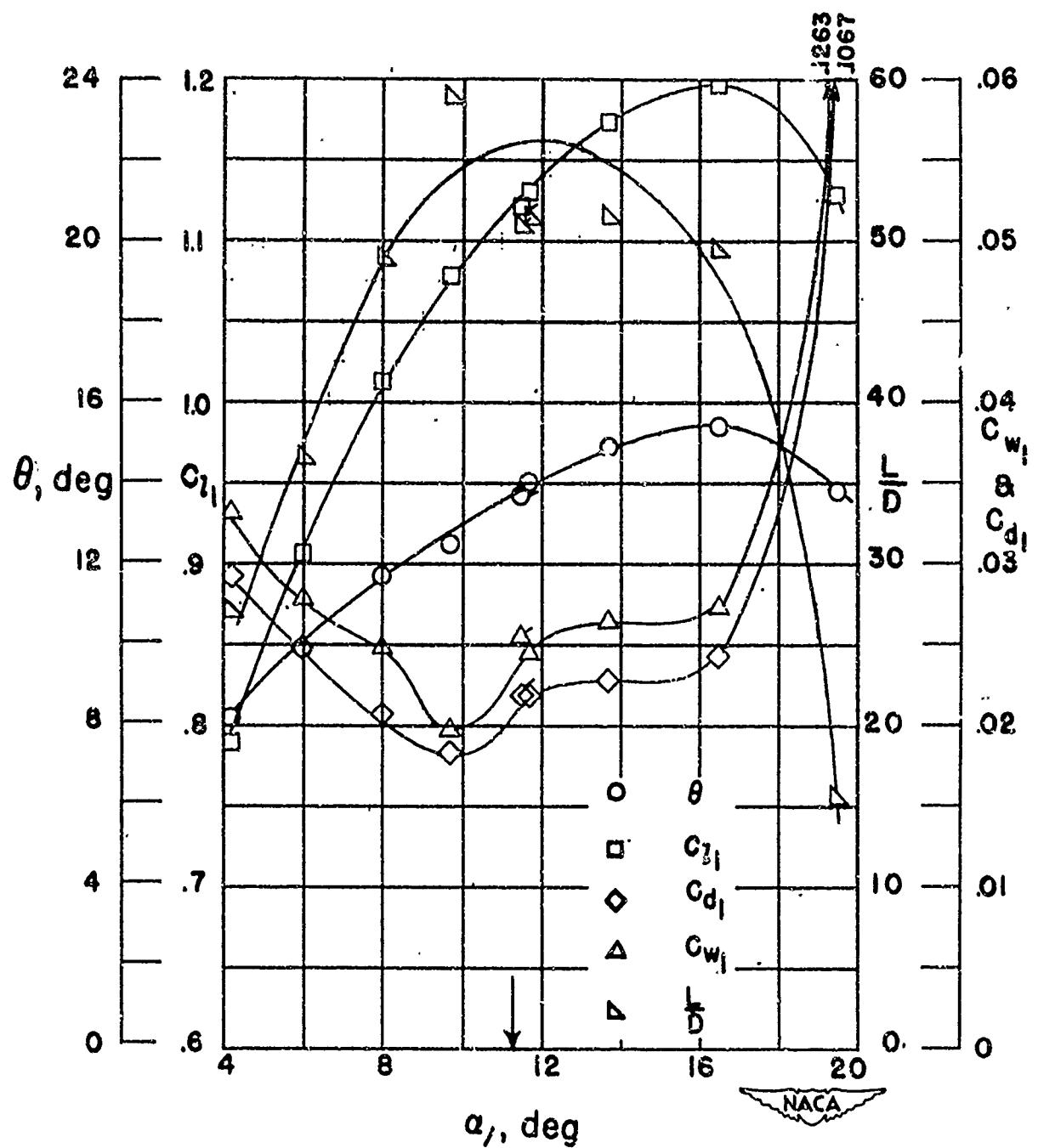


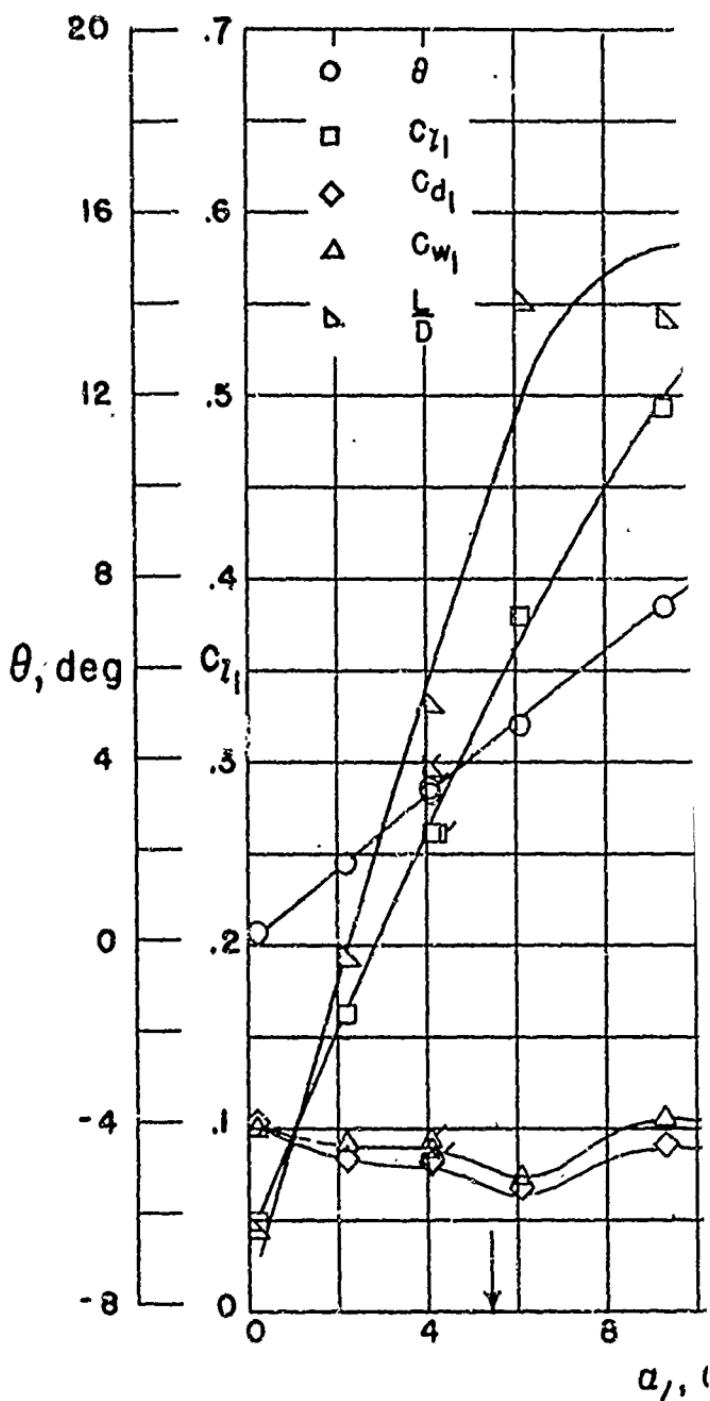
Figure 4-53
(Source: Ref. 4-4)



Section characteristics; arrow shows design angle of attack;
flagged symbol indicates leading-edge roughness.

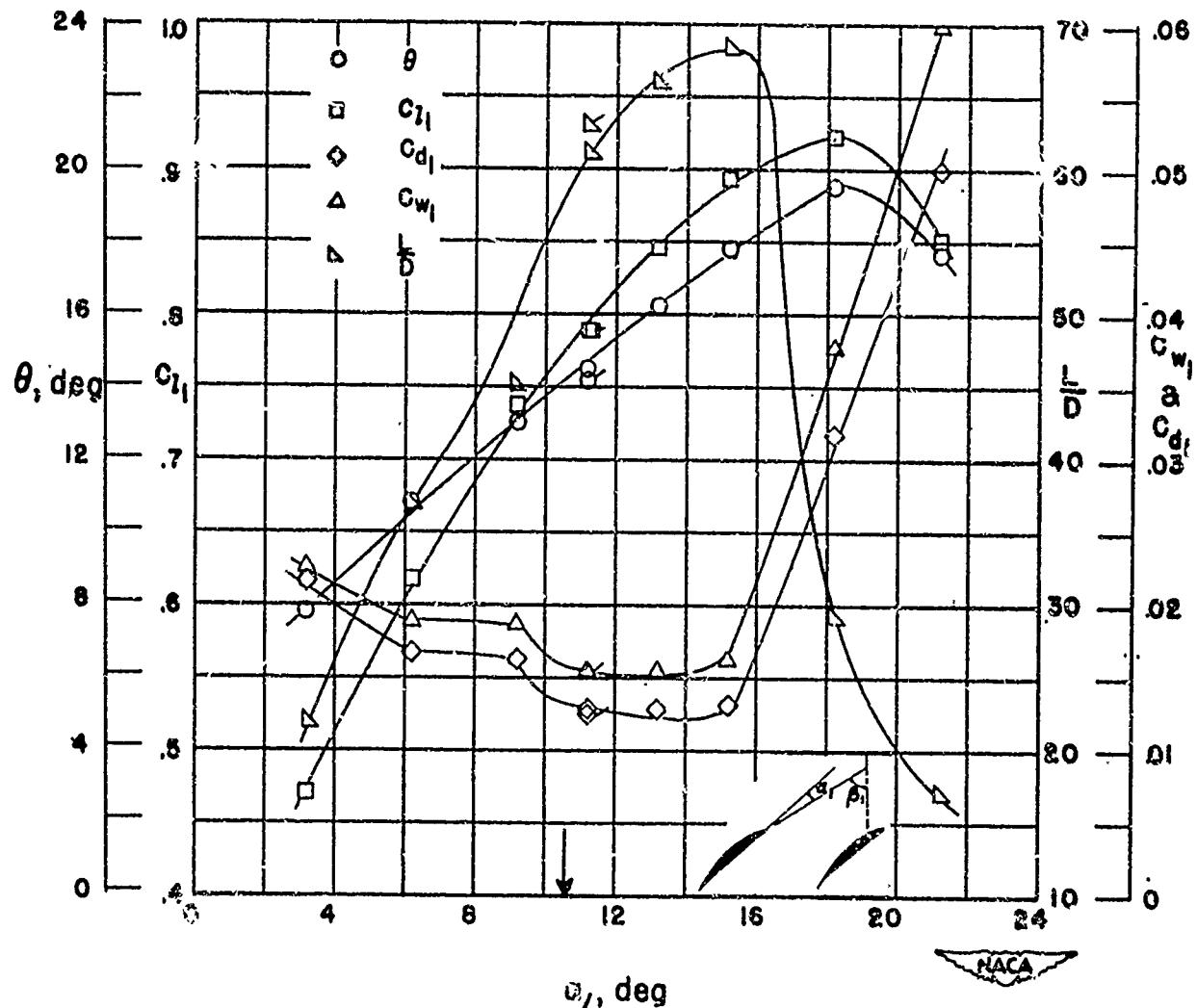
Cascade combination, $\beta_1 = 60^\circ$, $\sigma' = 0.50$
blade section, NACA 65-1810

Figure 4-54
(Source: Ref. 4-4)



Section characteristics; arrow flagged symbol indicates
cascade combination, blade section, NA

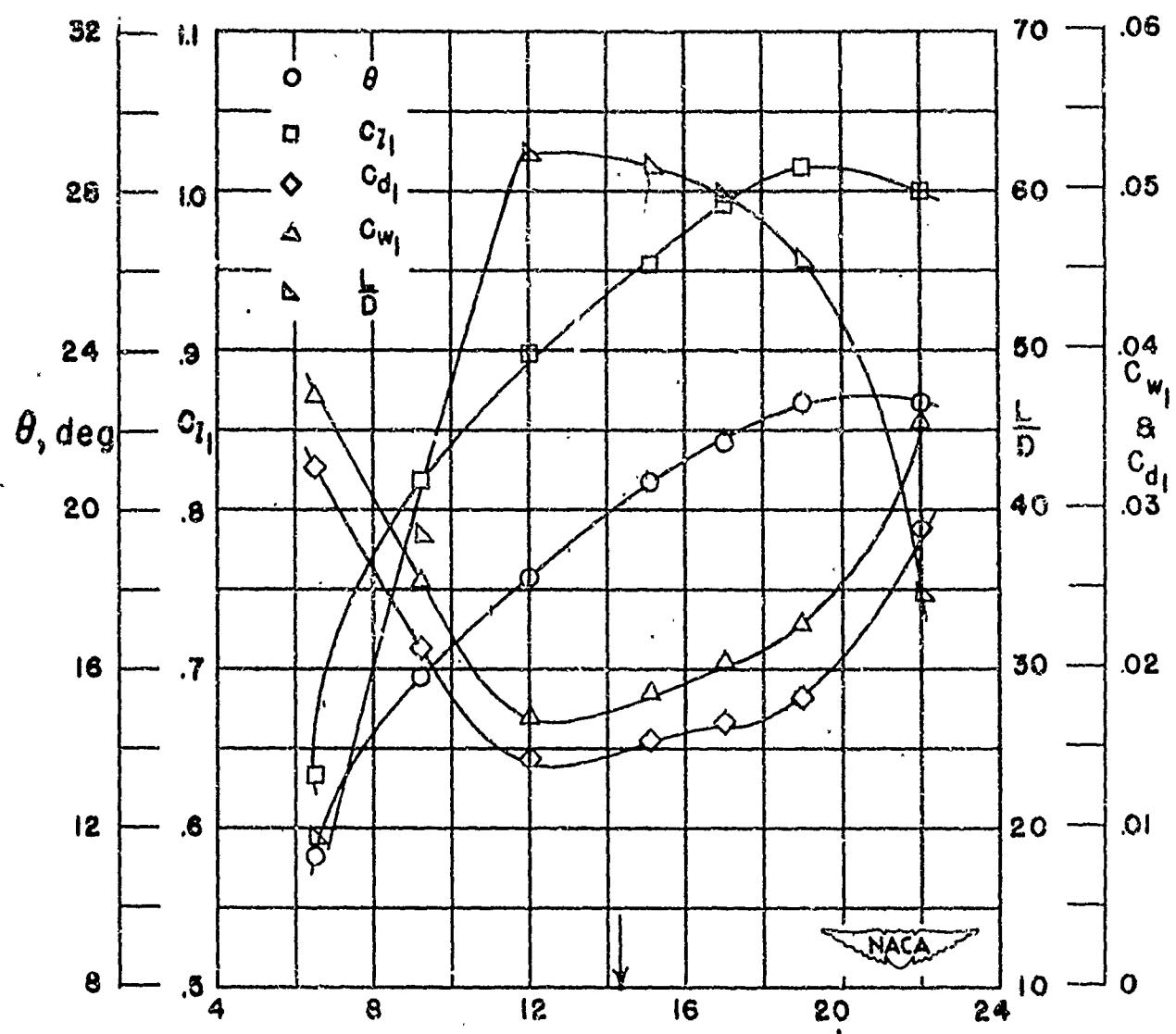
Fig
(Source)



Section characteristics; arrow shows design angle of attack;
flagged symbol indicates leading-edge roughness.

Cascade combination, $\beta_1 = 60^\circ$, $\sigma' = 0.75$
blade section, NACA 65-(12)10

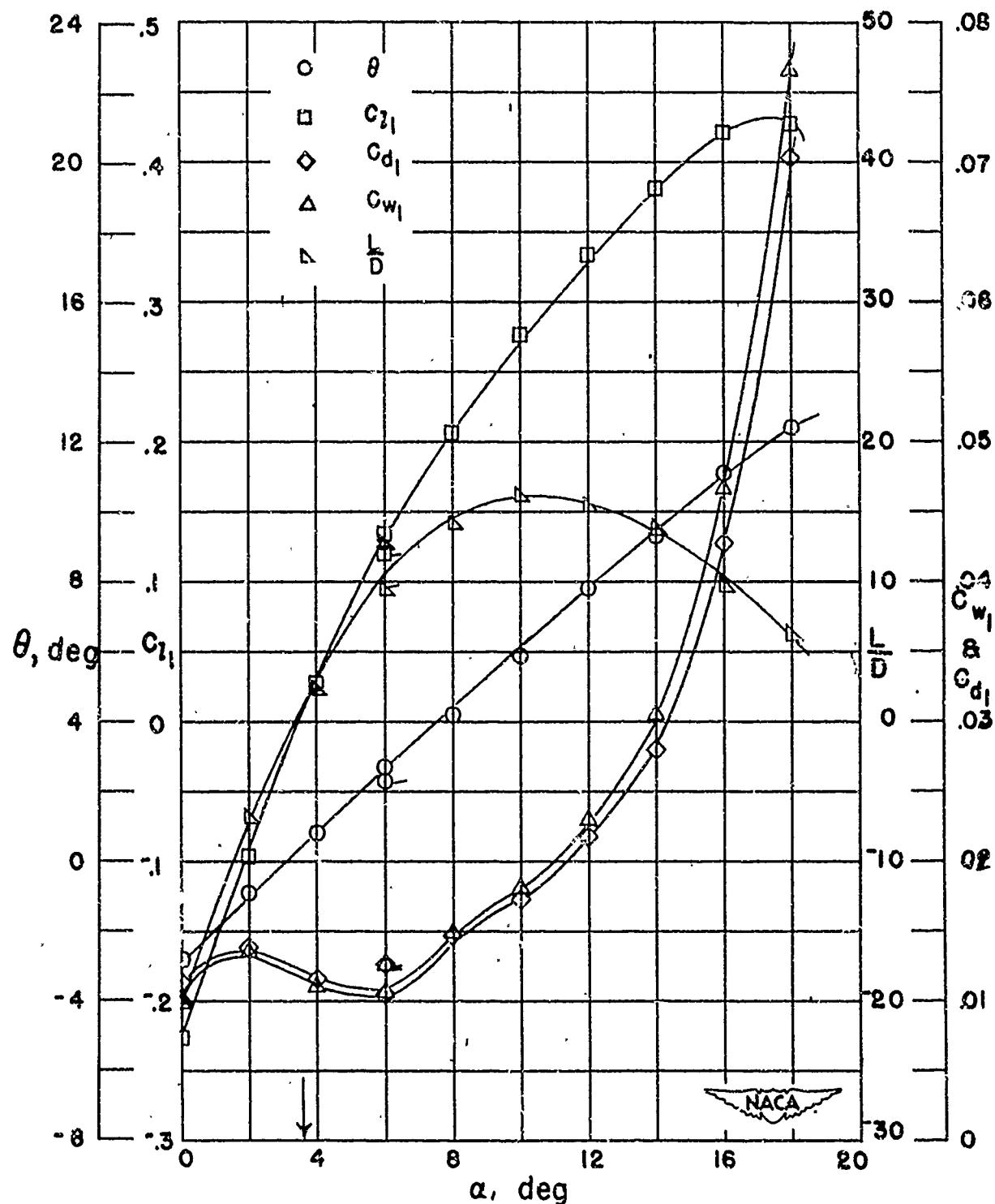
Figure 4-56
(Source: Ref. 4-4)



α_1 , deg
Section characteristics; arrow shows design angle of attack.

Cascade combination, $\beta_1 = 60^\circ$, $\sigma' = 0.75$
blade section, NACA 65-(18)30

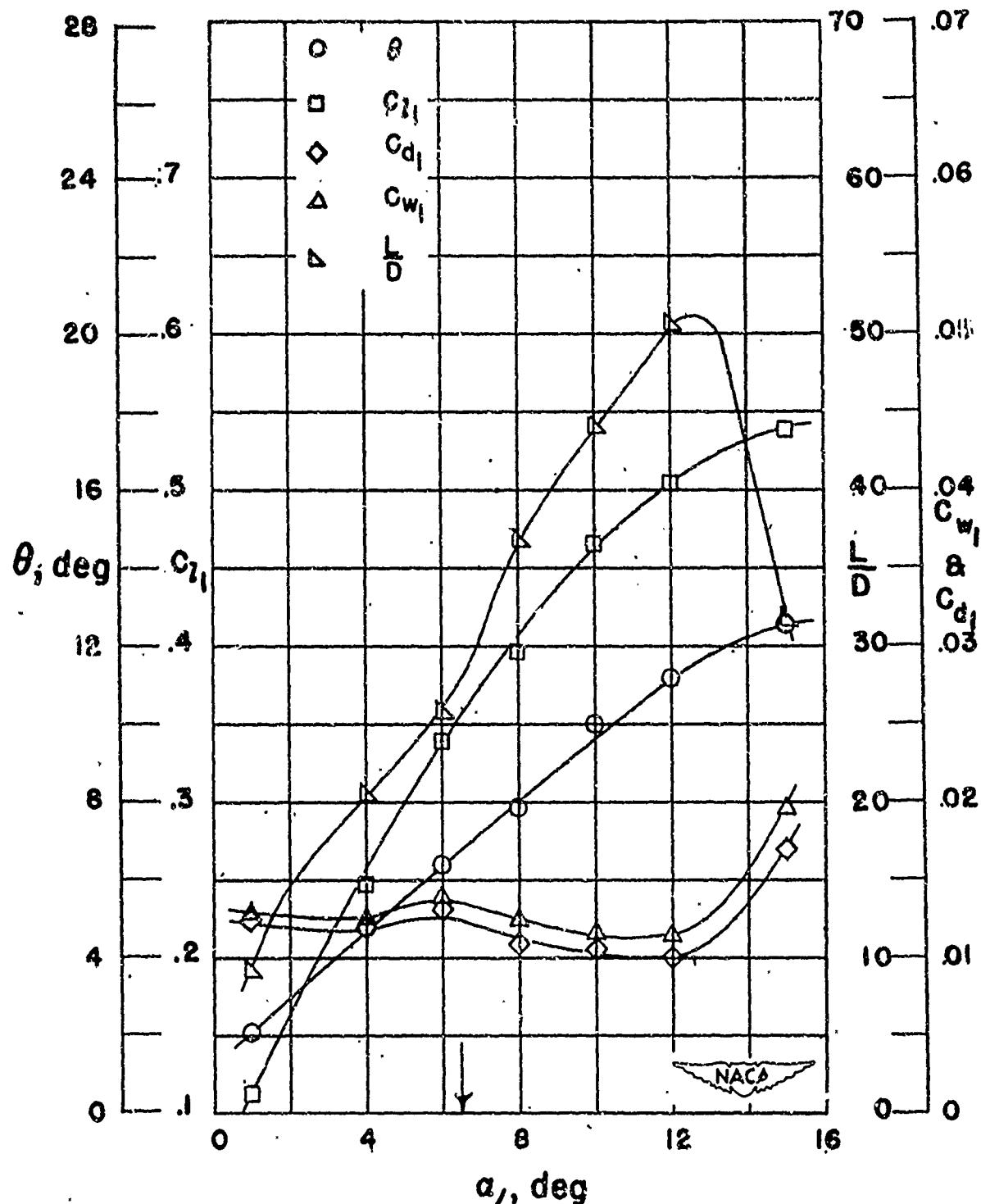
Figure 4-57
(Source: Ref. 4-4)



Section characteristics; arrow shows design angle of attack;
flagged symbol indicates leading-edge roughness.

Cascade combination, $\theta_1 = 60^\circ$, $\sigma' = 1.00$
blade section, NACA 65-010

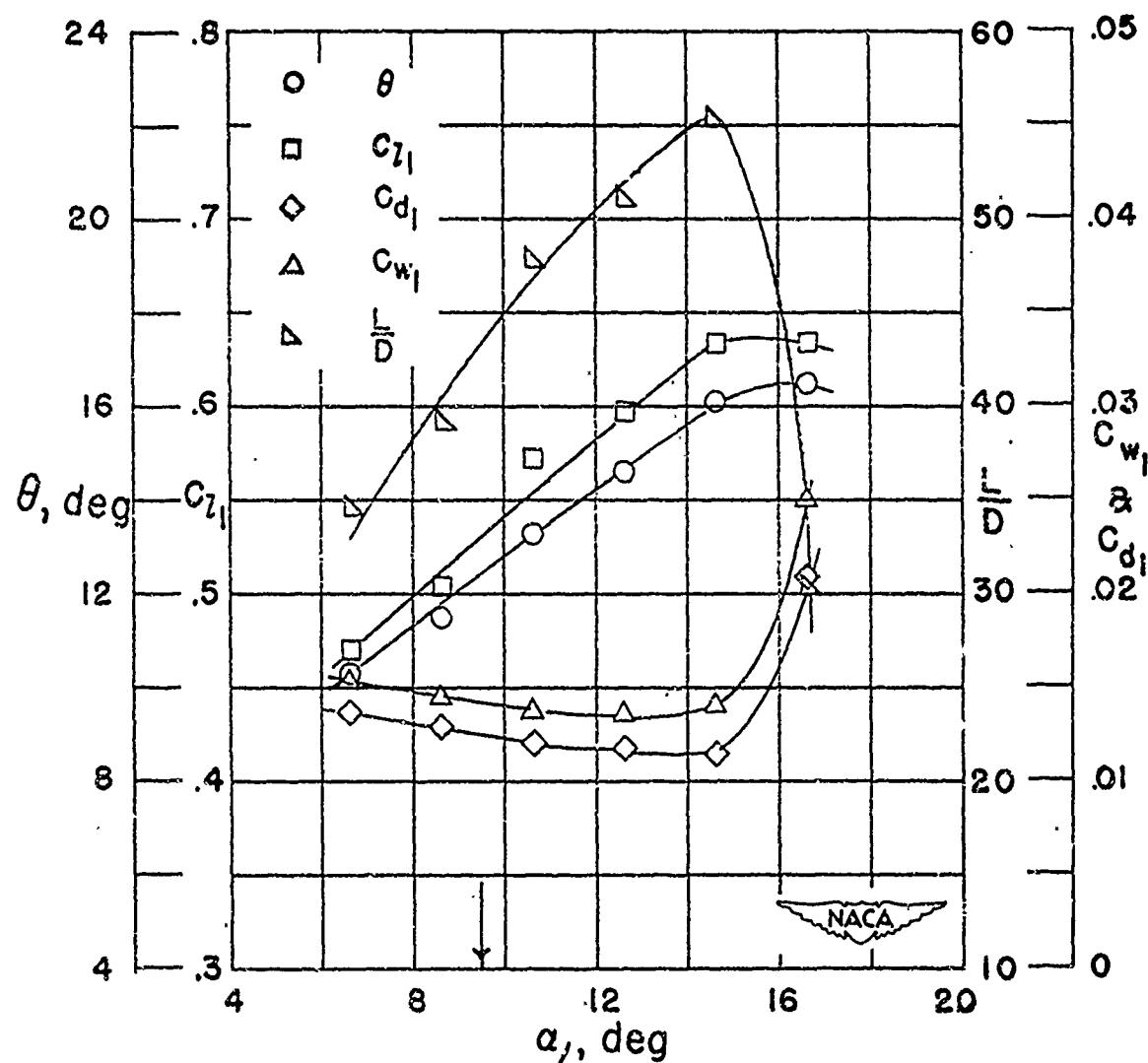
Figure 4-58
(Source: Ref. 4-4)



Section characteristics; arrow shows design angle of attack.

Cascade combination, $\beta_1 = 60^\circ$, $\sigma' = 1.00$
blade section, NACA 65-410

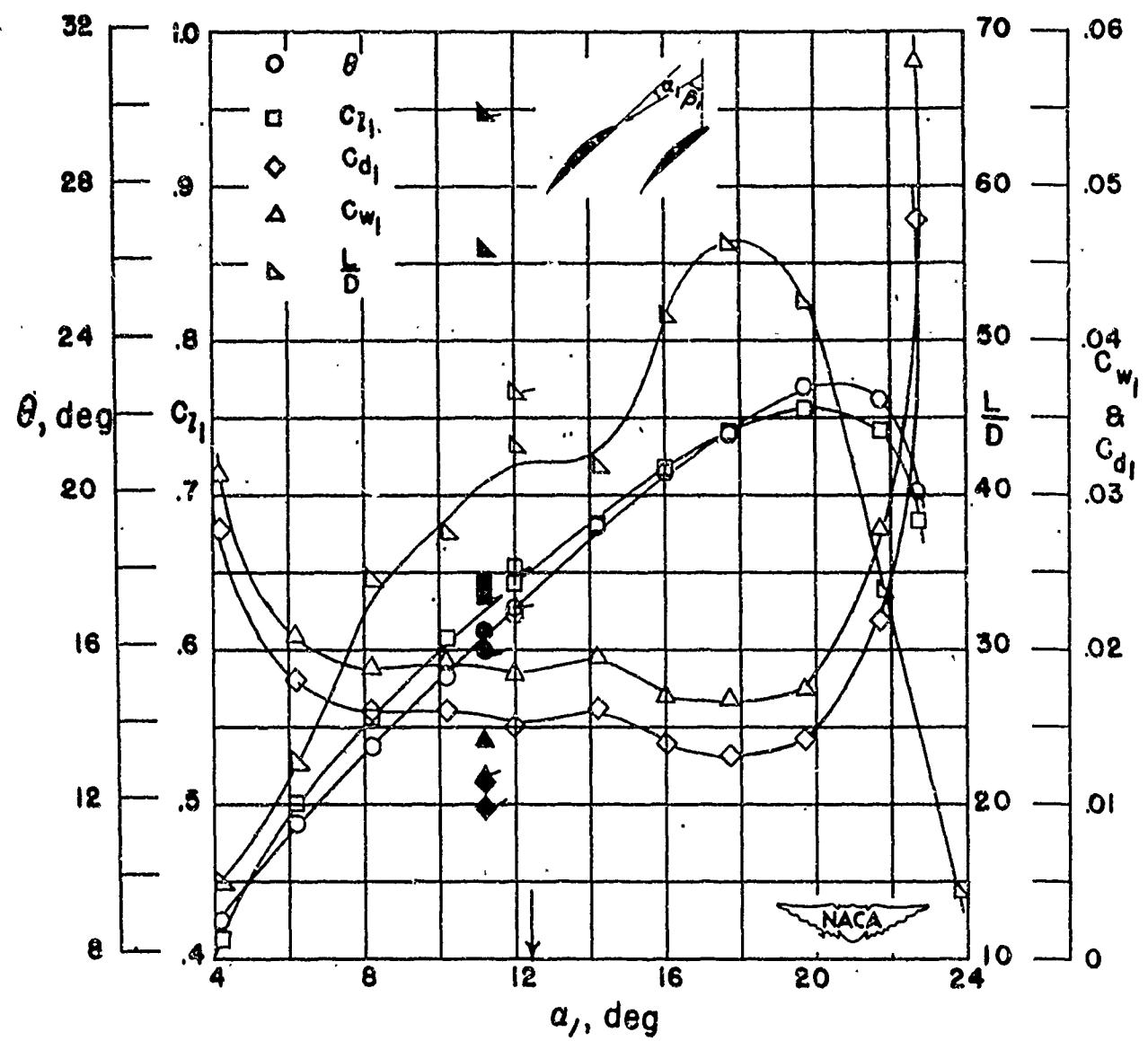
Figure 4-59
(Source: Ref. 4-4)



Section characteristics; arrow shows design angle of attack.

Cascade combination, $\beta_1 = 60^\circ$, $\sigma' = 1.00$
blade section, NACA 65-810

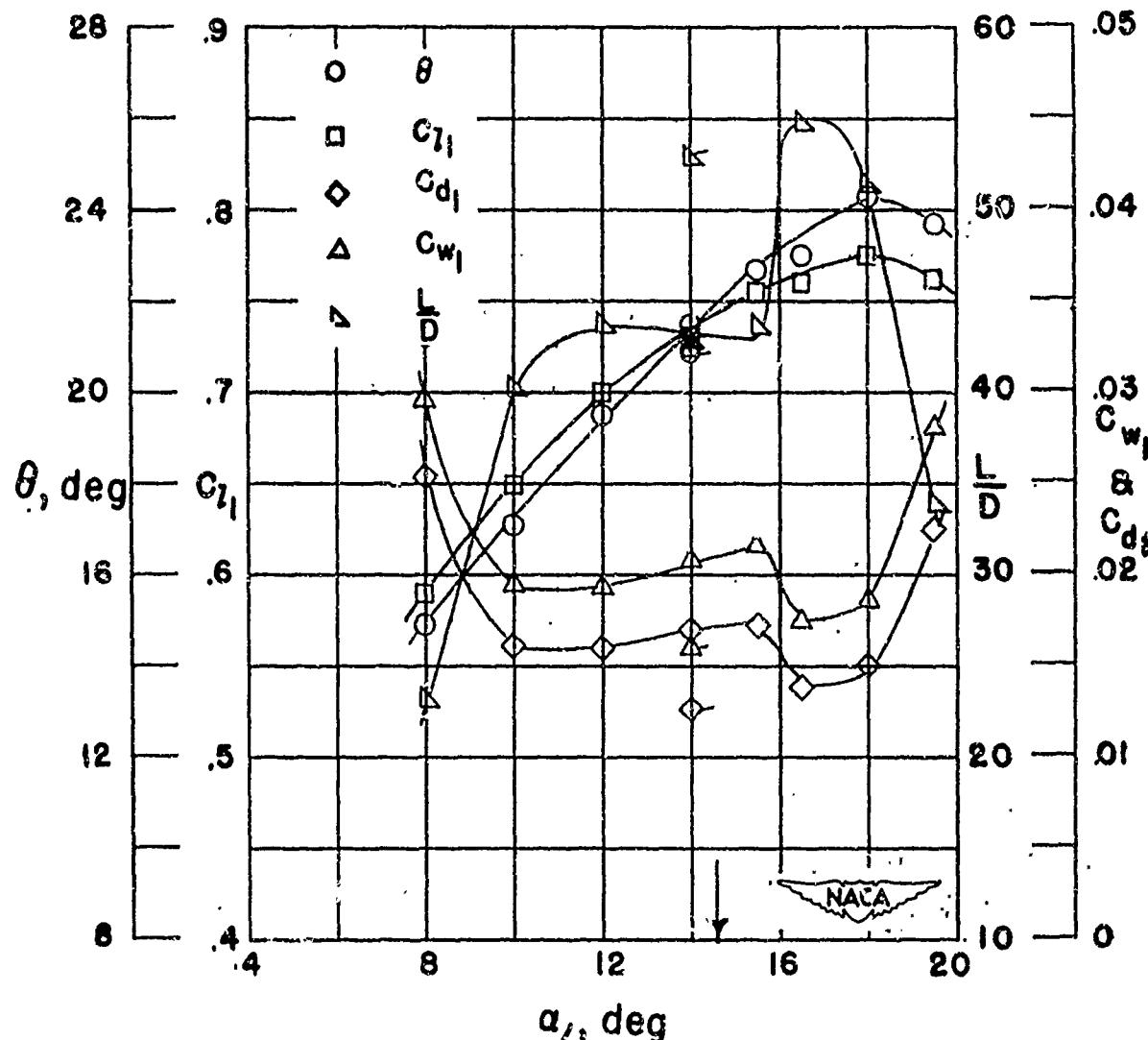
Figure 4-60
(Source: Ref. 4-4)



Section characteristics; arrow shows design angle of attack;
flagged symbol indicates leading-edge roughness; solid
symbol indicates high Reynolds number.

Cascade combination, $\beta_1 = 60^\circ$, $\sigma' = 1.00$
blade section, NACA 65-(12)10

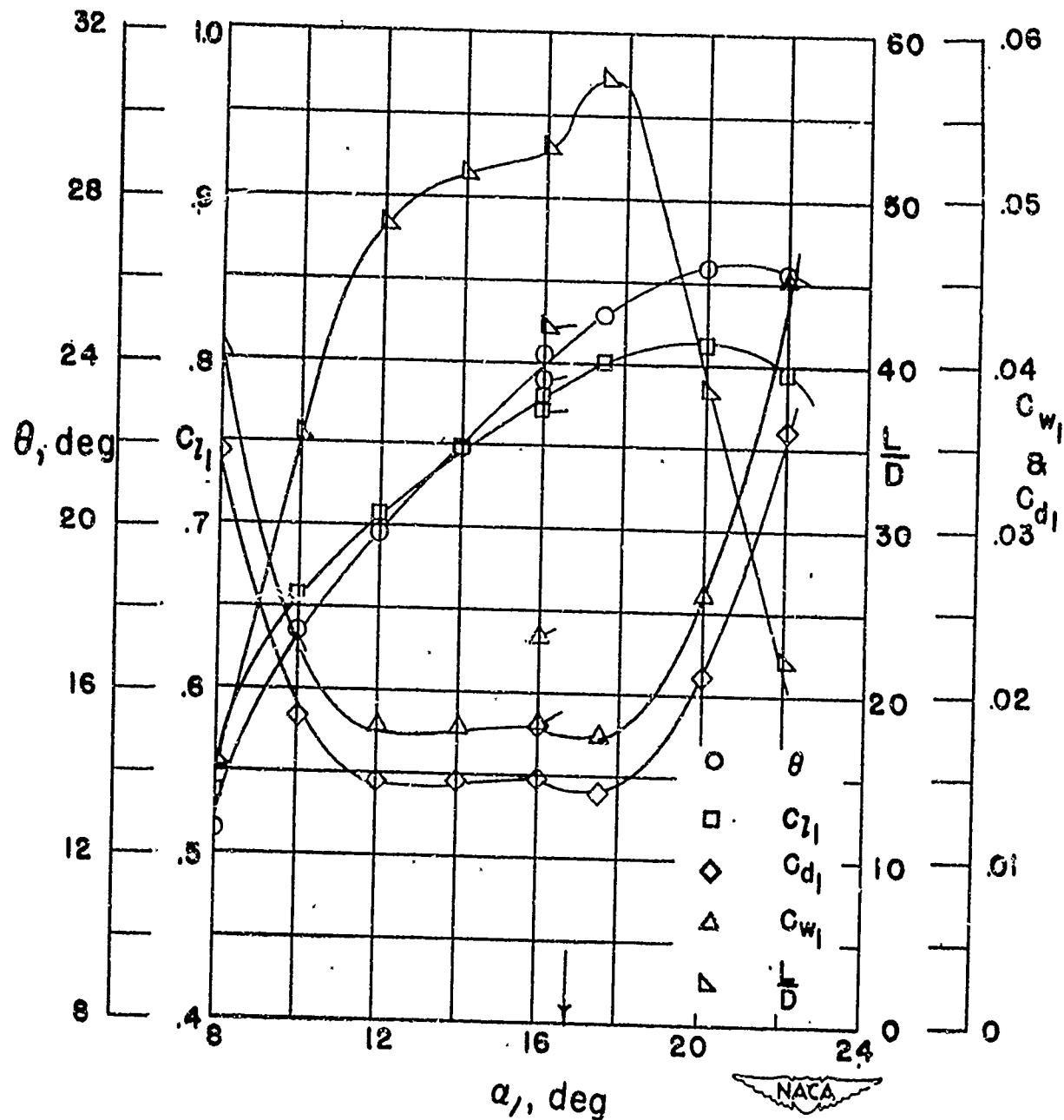
Figure 4-61
(Source: Ref. 4-4)



Section characteristics; arrow shows design angle of attack;
flagged symbol indicates leading-edge roughness.

Cascade combination, $\beta_1 = 60^\circ$, $\sigma' = 1.00$
blade section, NACA 65-(15)10

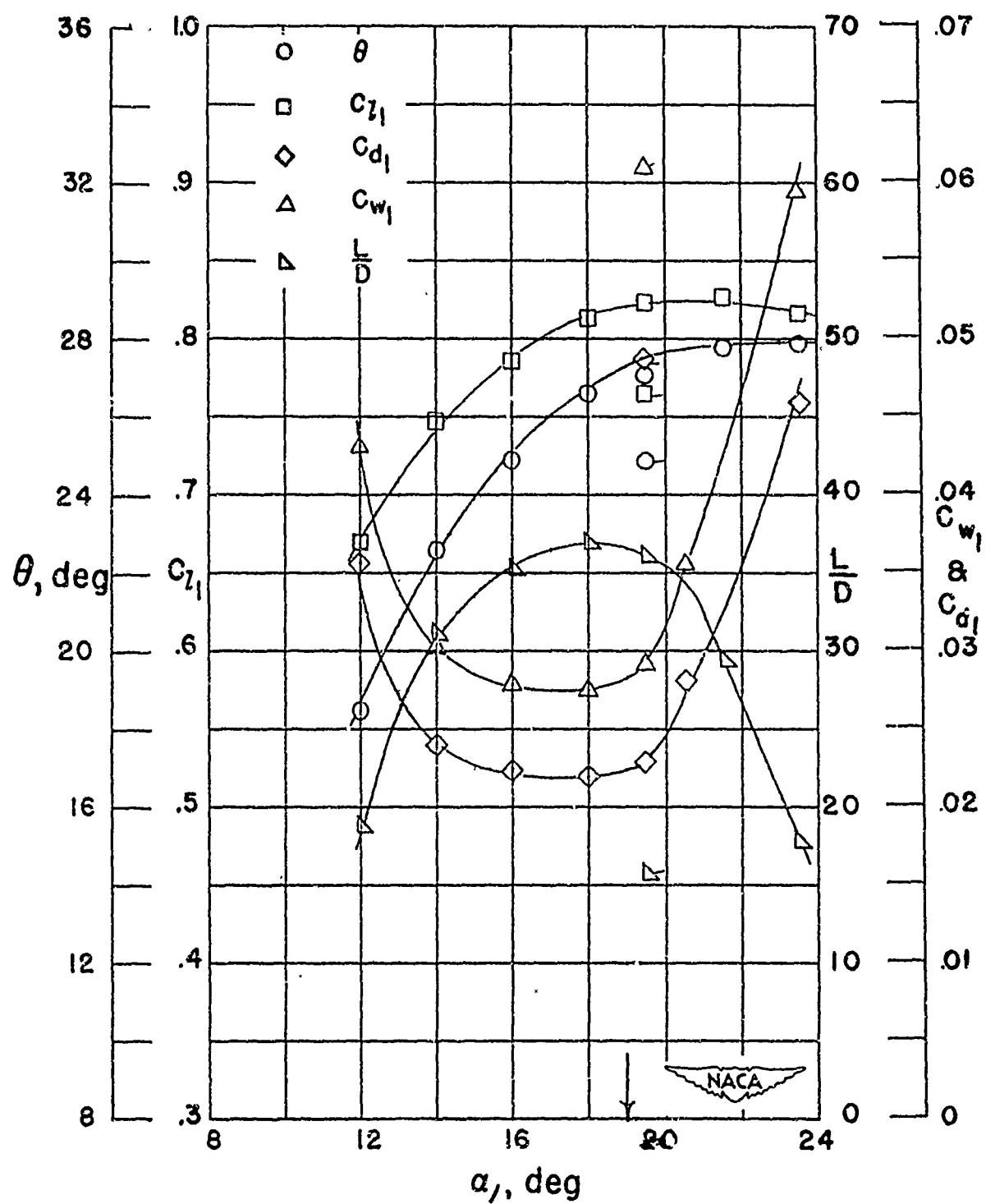
Figure 4-62
(Source: Ref. 4-4)



Section characteristics; arrow shows design angle of attack;
flagged symbol indicates leading-edge roughness.

Cascade combination, $\beta_1 = 60^\circ$, $\sigma' = 1.00$
blade section, NACA 65-(18)10

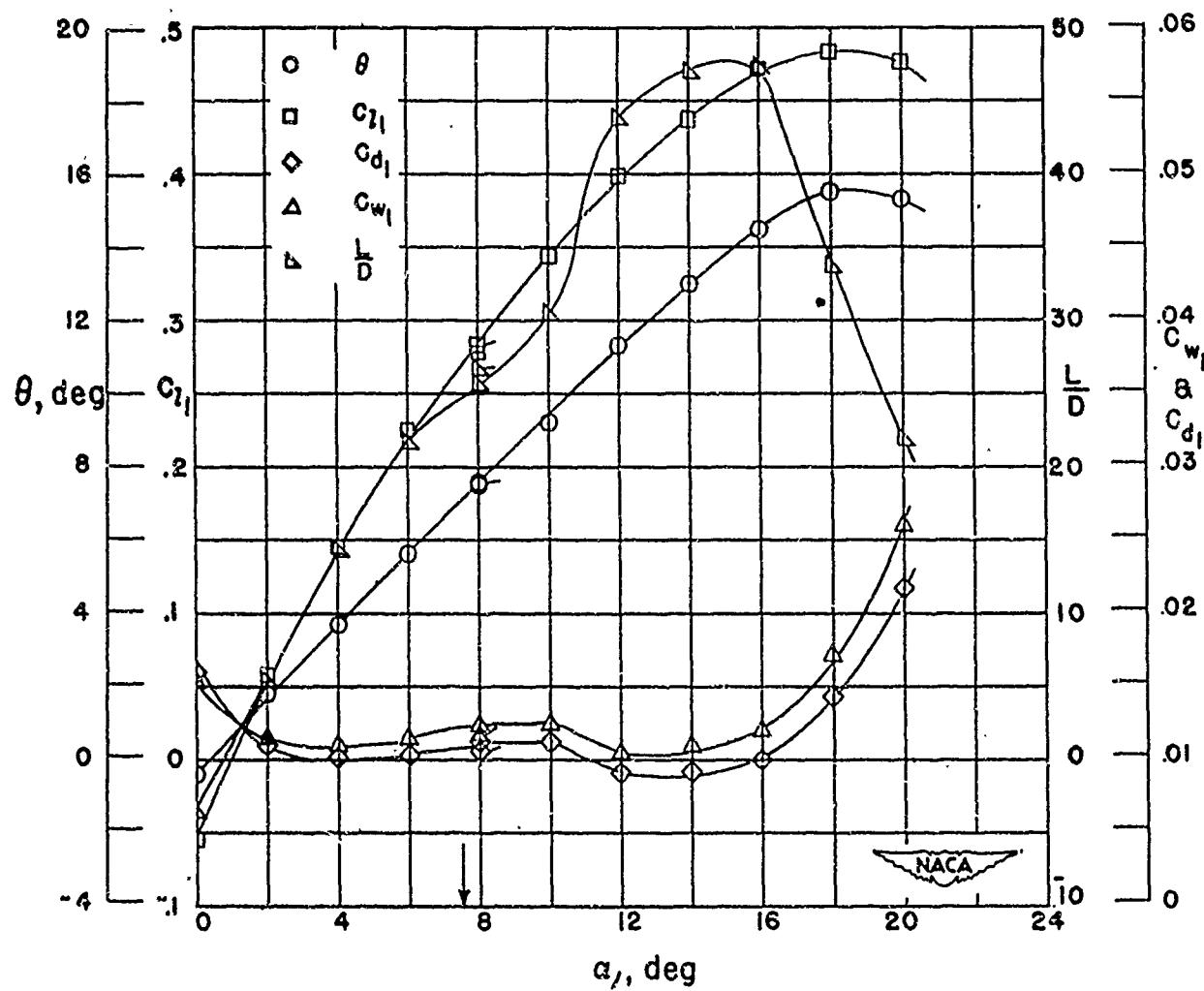
Figure 4-63
(Source: Ref. 4-4)



Section characteristics; arrow shows design angle of attack;
flagged symbol indicates leading-edge roughness.

Cascade combination, $\beta_1 = 60^\circ$, $\sigma' = 1.00$
blade section, NACA 65-(21)10

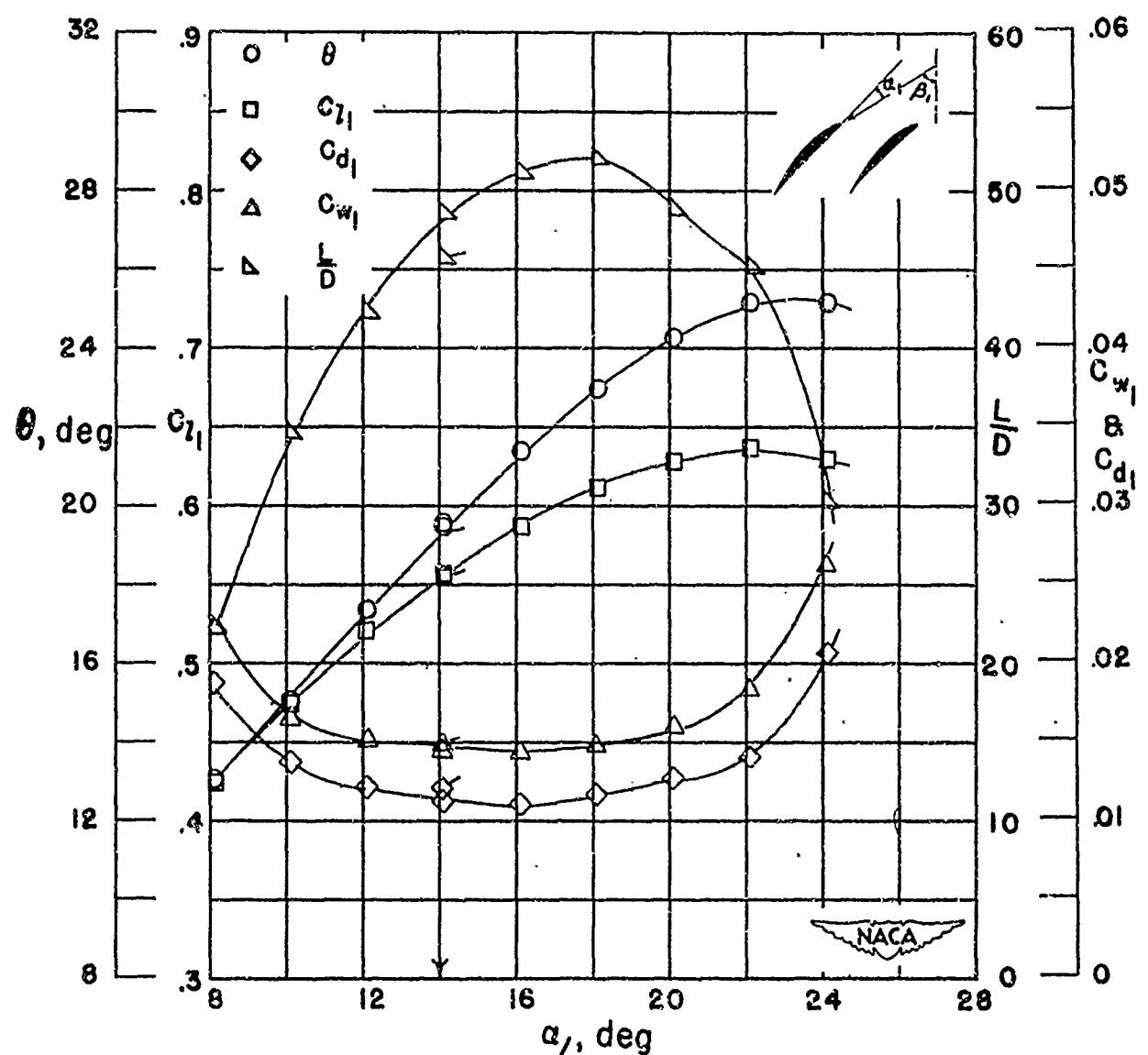
Figure 4-64
(Source: Ref. 4-4)



Section characteristics; arrow shows design angle of attack;
filled symbol indicates leading-edge roughness.

Cascade combination, $\beta_1 = 60^\circ$, $\sigma' = 1.25$
blade section, NACA 65-410

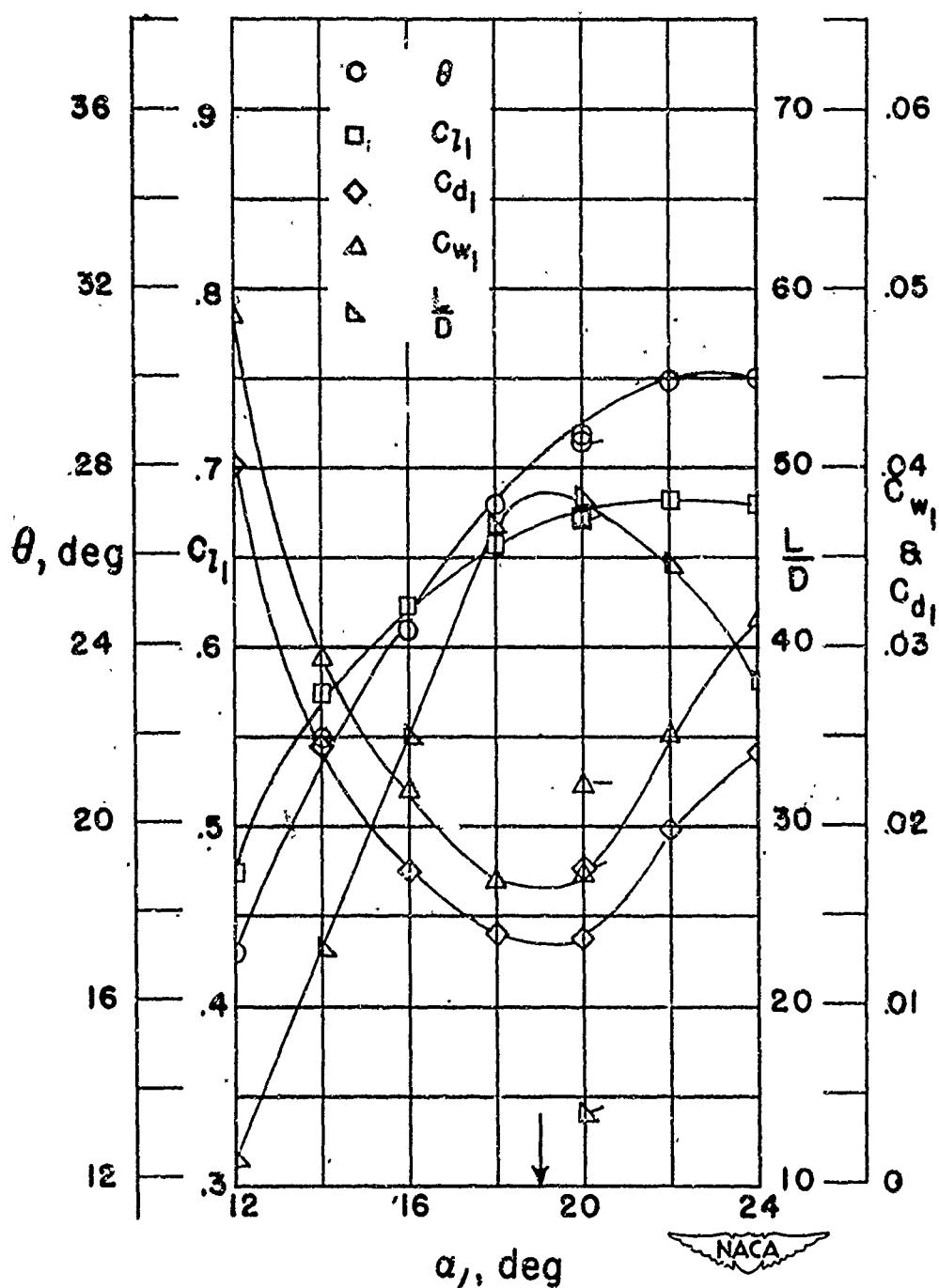
Figure 4-65
(Source: Ref. 4-4)



Section characteristics; arrow shows design angle of attack,
flagged symbol indicates leading-edge roughness

Cascade combination, $\beta_1 = 60^\circ$; $\sigma' = 1.25$
blade section, NACA 65-(12)10

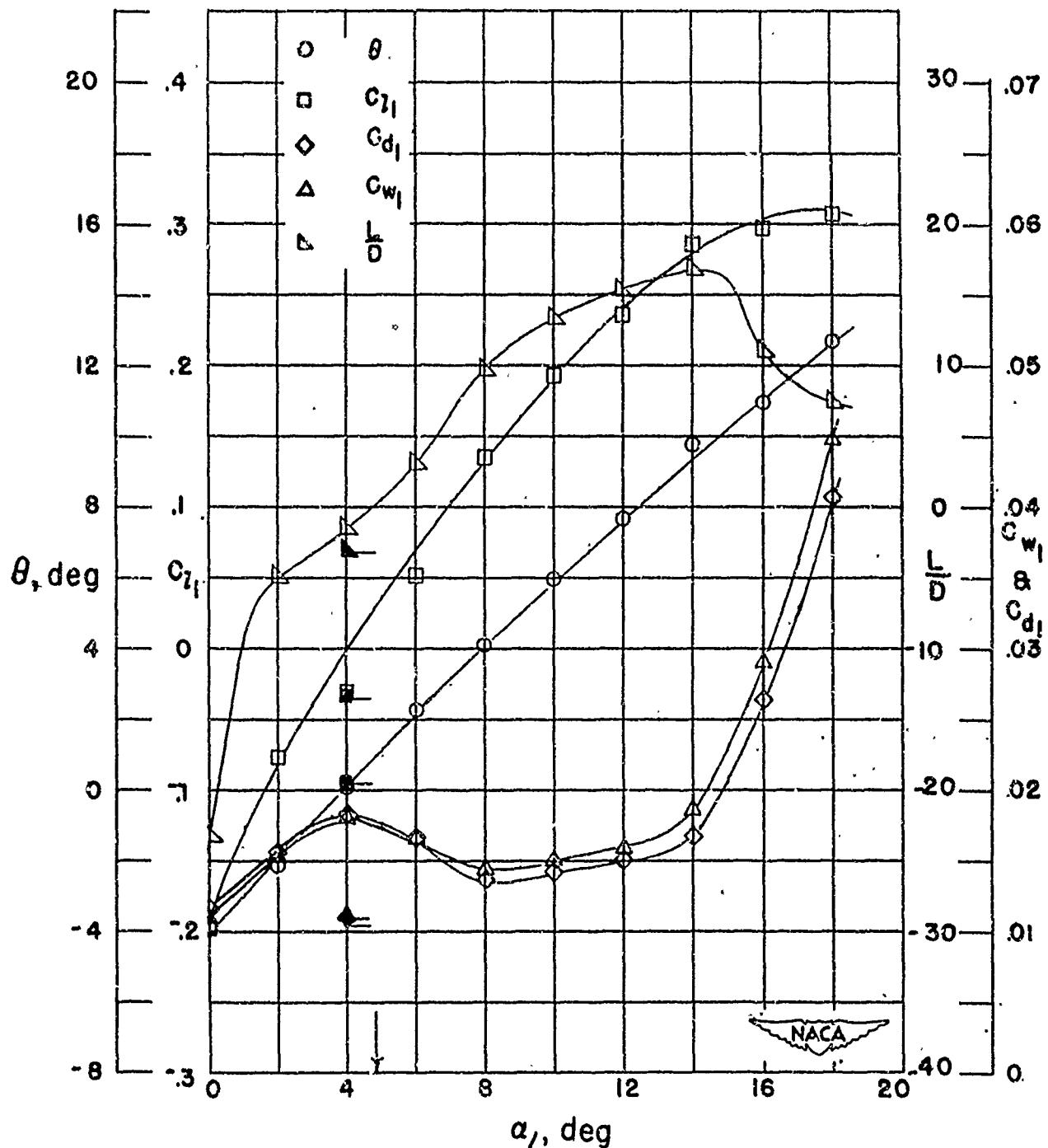
Figure 4-66
(Source: Ref. 4-4)



Section characteristics; arrow shows design angle of attack;
flagged symbol indicates leading-edge roughness.

Cascade combination, $\beta_1 = 60^\circ$, $\sigma^l = 1.25$
blade section, NACA 65-(18)10

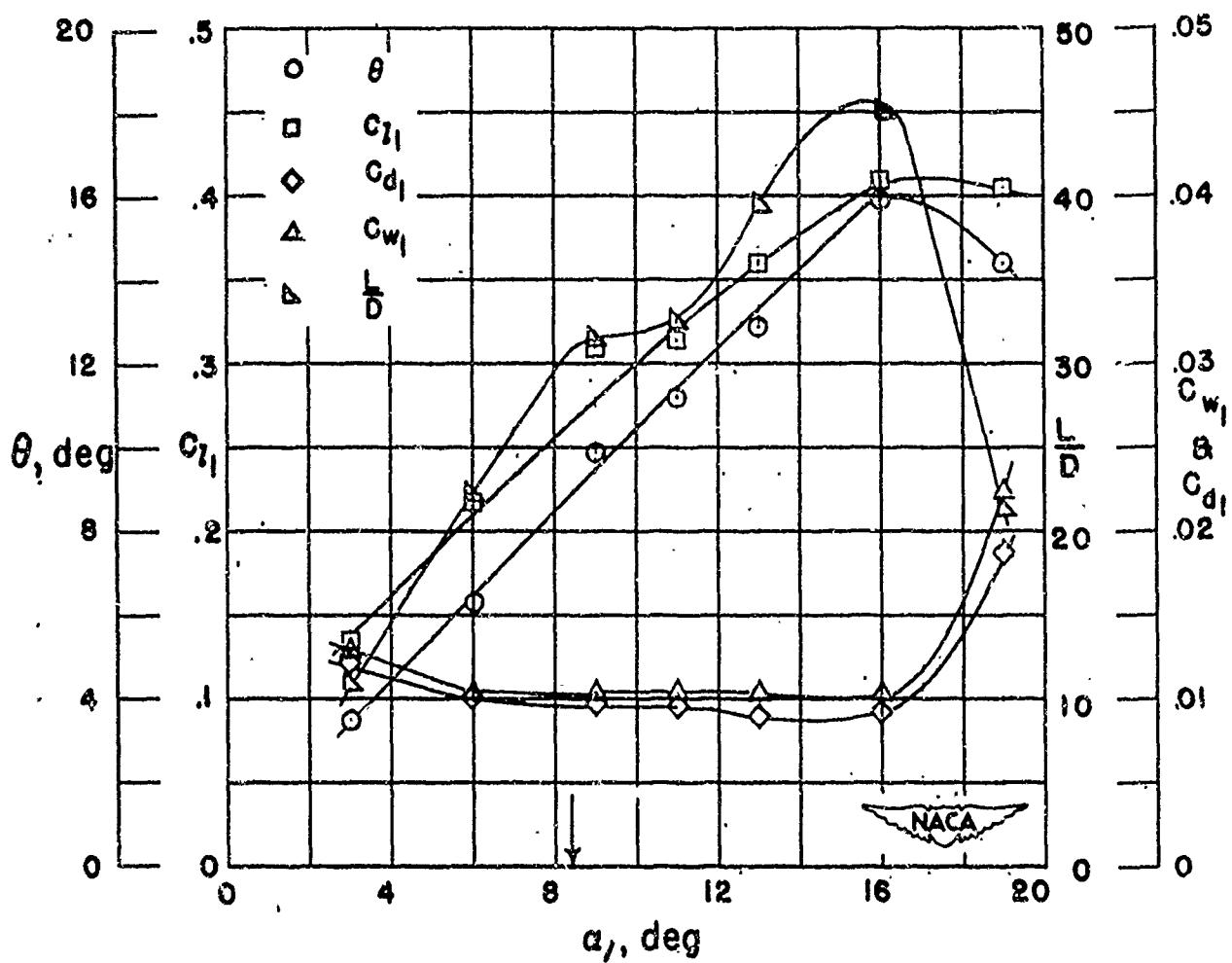
Figure 4-67
(Source: Ref. 4-4)



Section characteristics; arrow shows design angle of attack,
flagged symbol indicates leading-edge roughness, solid
symbol indicates high Reynolds number.

Cascade combination, $\beta_1 = 60^\circ$, $\sigma' = 1.50$
blade section, NACA 65-010

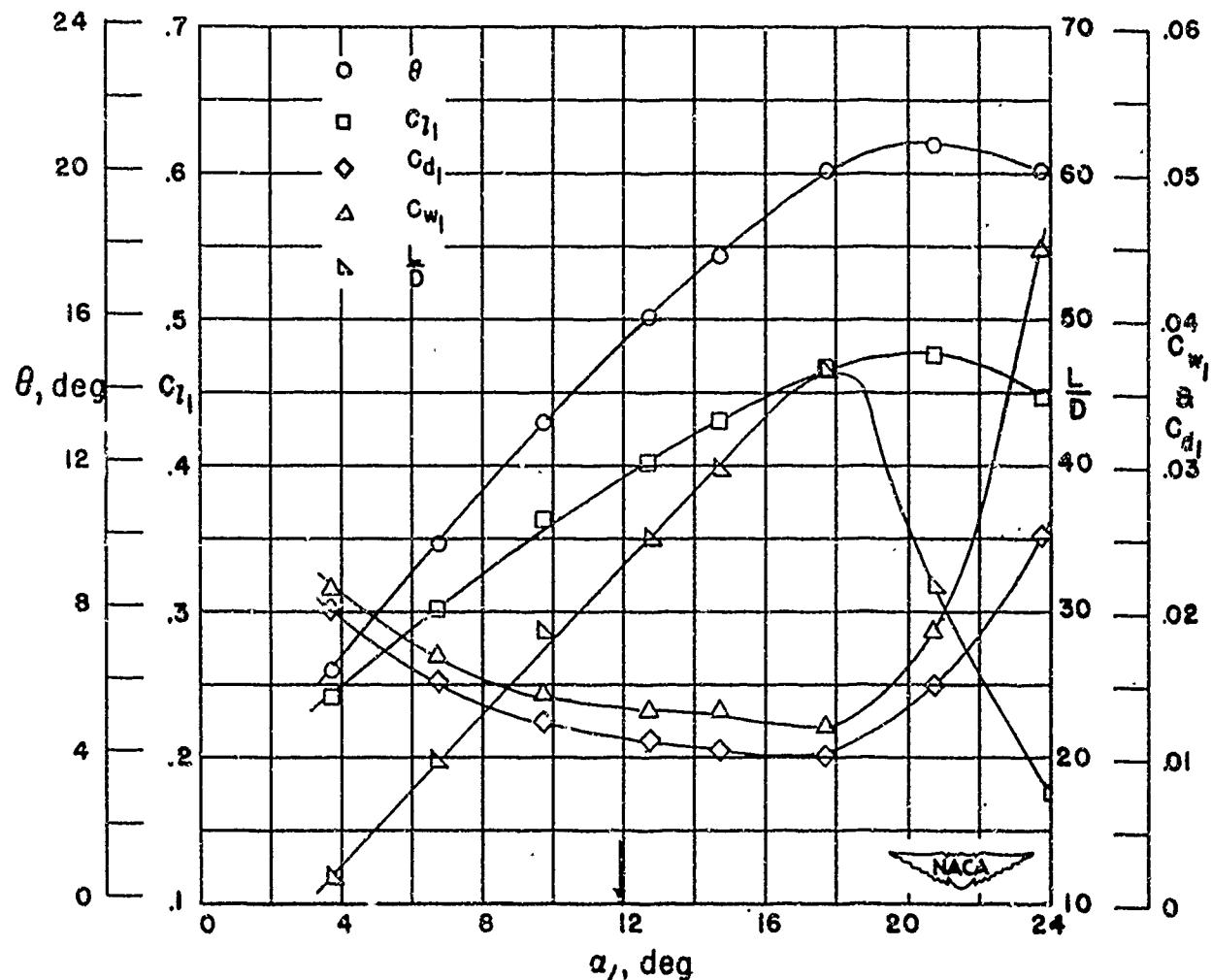
Figure 4-68
(Source: Ref. 4-4)



Section characteristics; arrow shows design angle of attack.

Cascade combination, $\beta_1 = 60^\circ$, $\sigma' = 1.50$
blade section, NACA 65-410

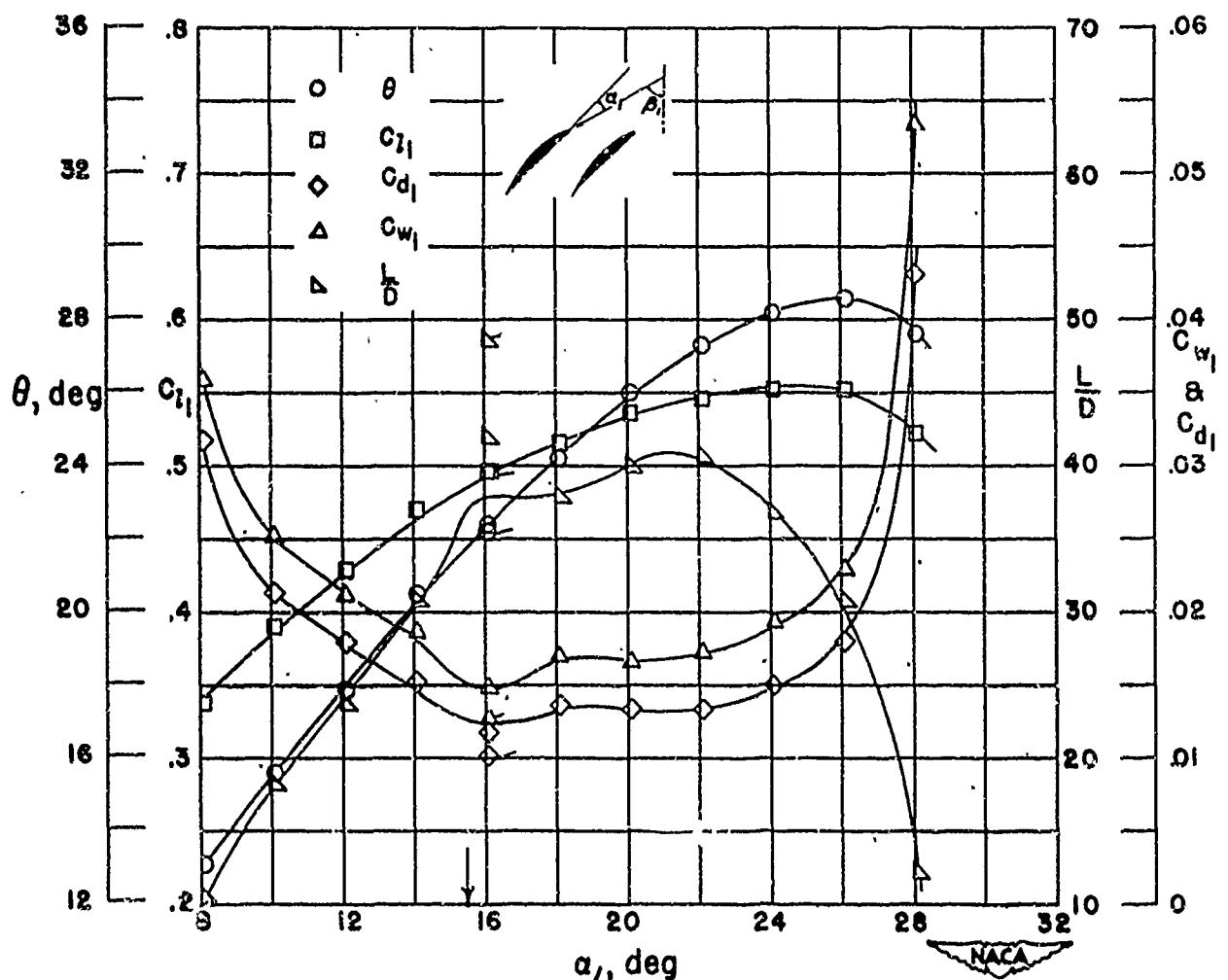
Figure 4-69
(Source: Ref. 4-4)



Section characteristics; arrow shows design angle of attack.

Cascade combination, $\beta_1 = 60^\circ$, $\sigma' = 1.50$
blade section, NACA 65-810

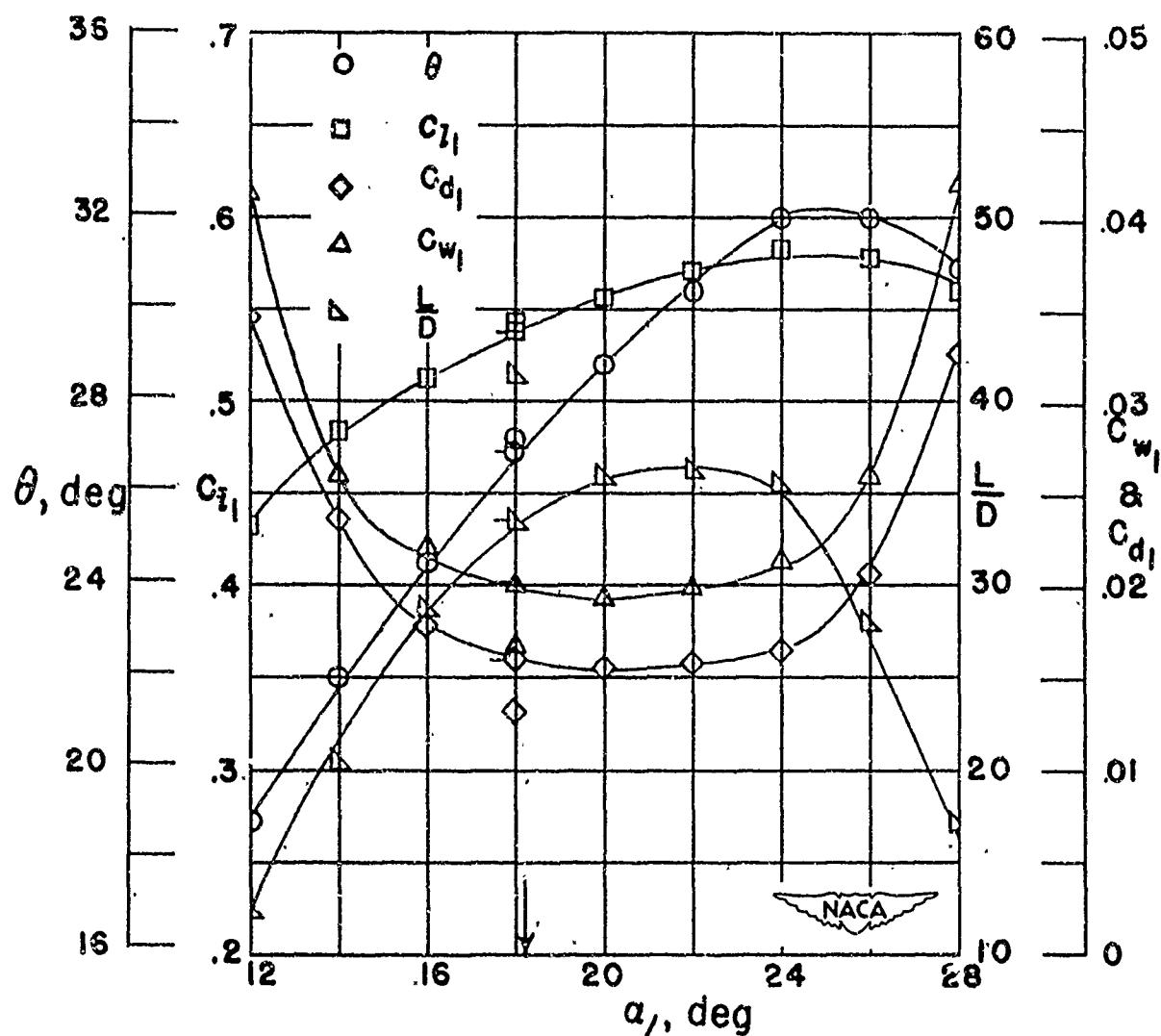
Figure 4-70
(Source: Ref. 4-4)



Section characteristics; arrow shows design angle of attack;
flagged symbol indicates leading-edge roughness.

Cascade combination, $\beta_1 = 60^\circ$, $\sigma' = 1.50$
blade section, NACA 65-(12)10

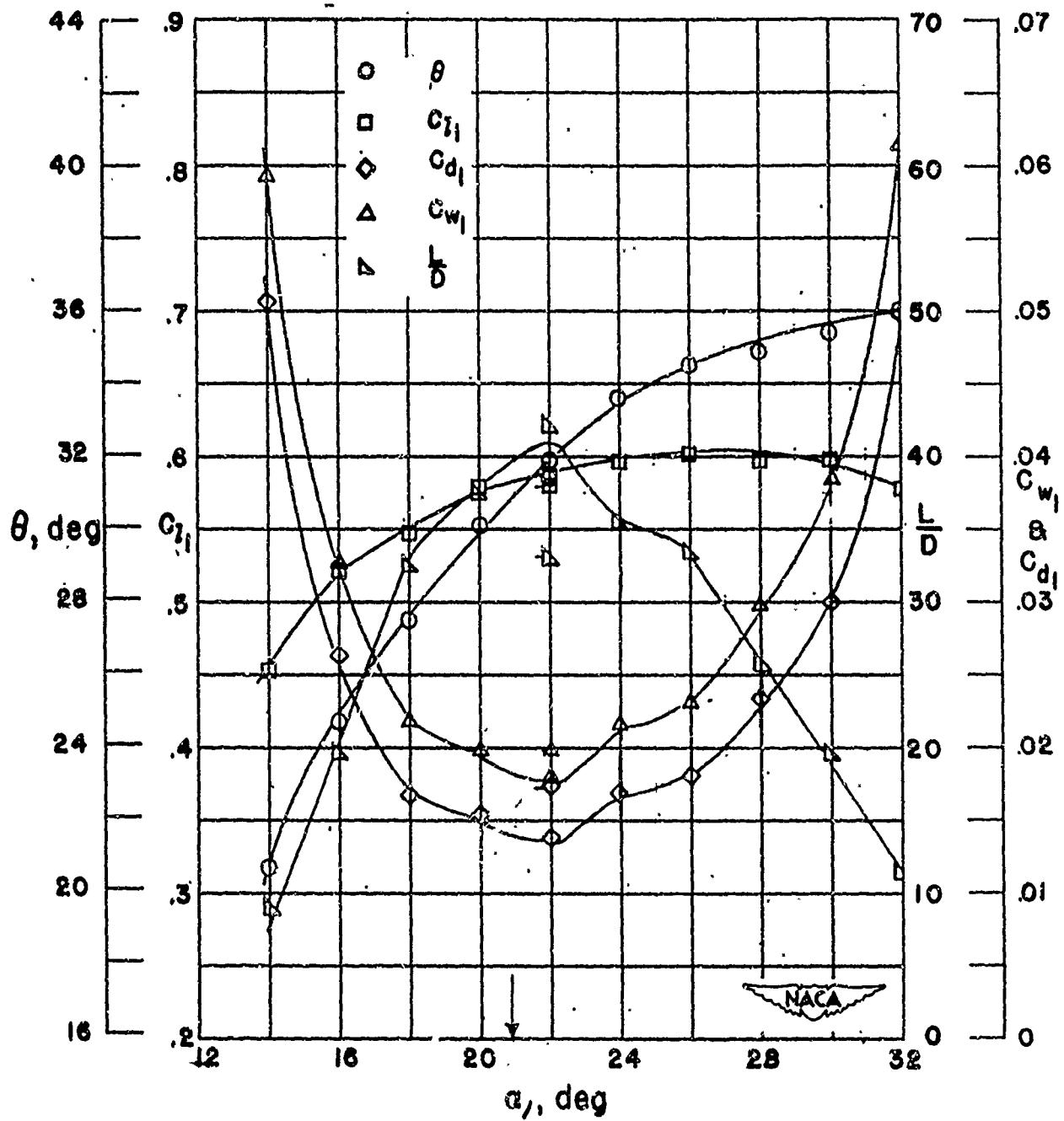
Figure 4-7
(Source: Ref. 4-4)



Section characteristics; arrow shows design angle of attack;
flagged symbol indicates leading-edge roughness.

Cascade combination, $\beta_1 = 60^\circ$, $\sigma' = 1.50$
blade section, NACA 65-(15)10

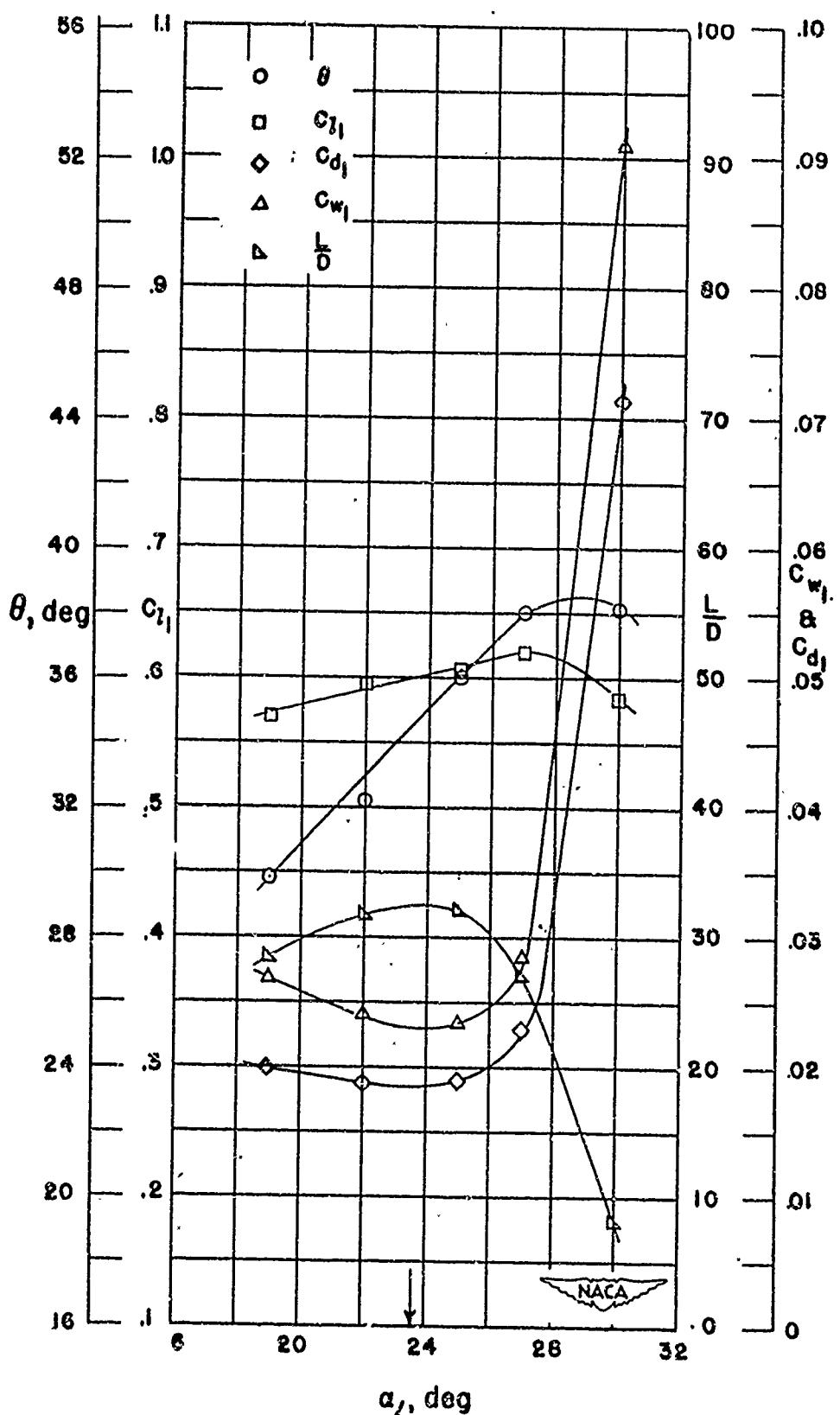
Figure 4-72
(Source: Ref. 4-4)



Section characteristics; arrow shows design angle of attack,
flagged symbol indicates leading-edge roughness

Cascade combination, $\beta_1 = 60^\circ$, $\sigma' = 1.50$
blade section, NACA 65-(18)10

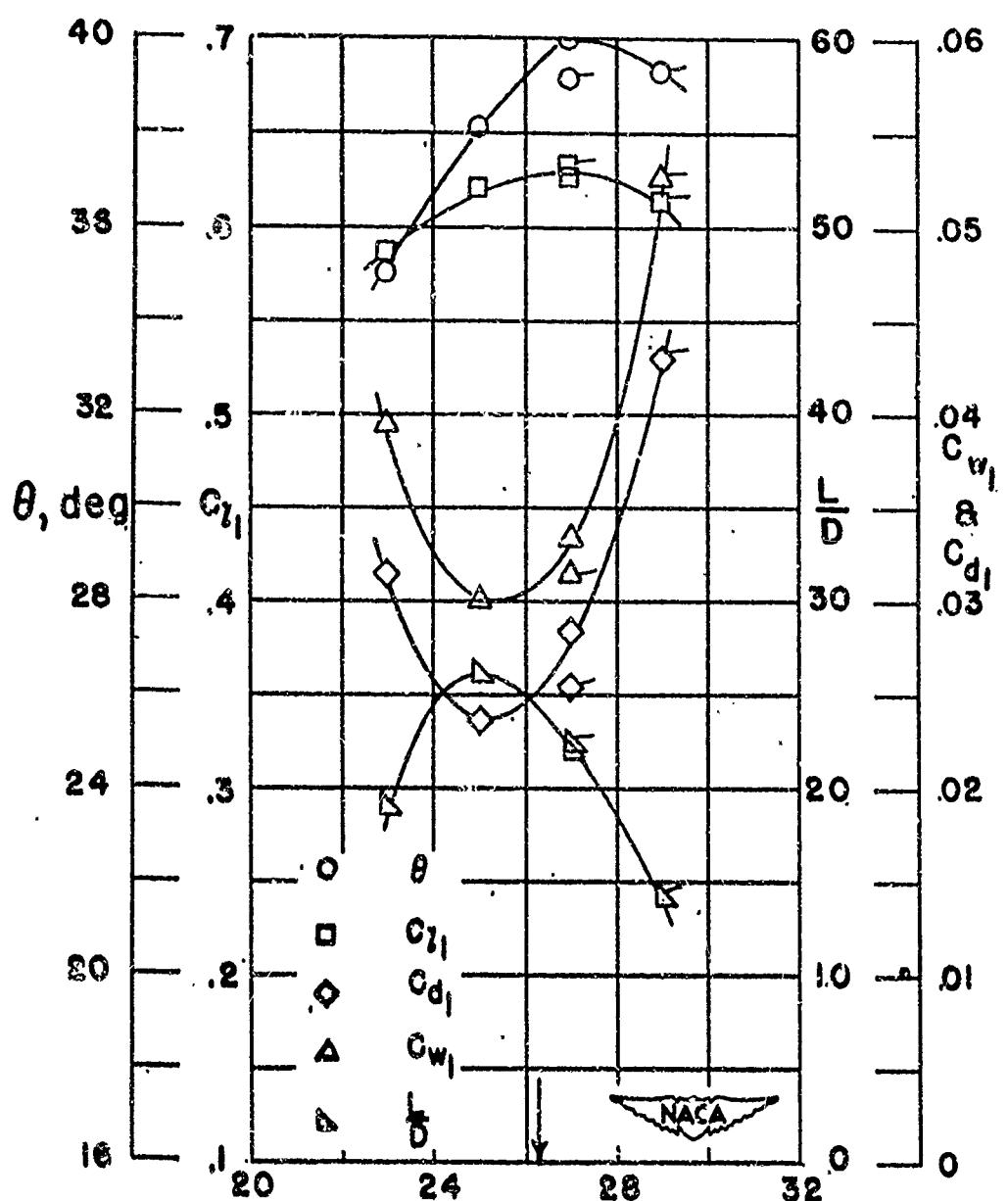
Figure 4-73
(Source: Ref. 4-4)



Section characteristics; arrow shows design angle of attack.

Cascade combination, $\beta_1 = 60^\circ$, $\sigma' = 1.50$
blade section, NACA 65-(21)10

Figure 4-74
(Source: Ref. 4-4)

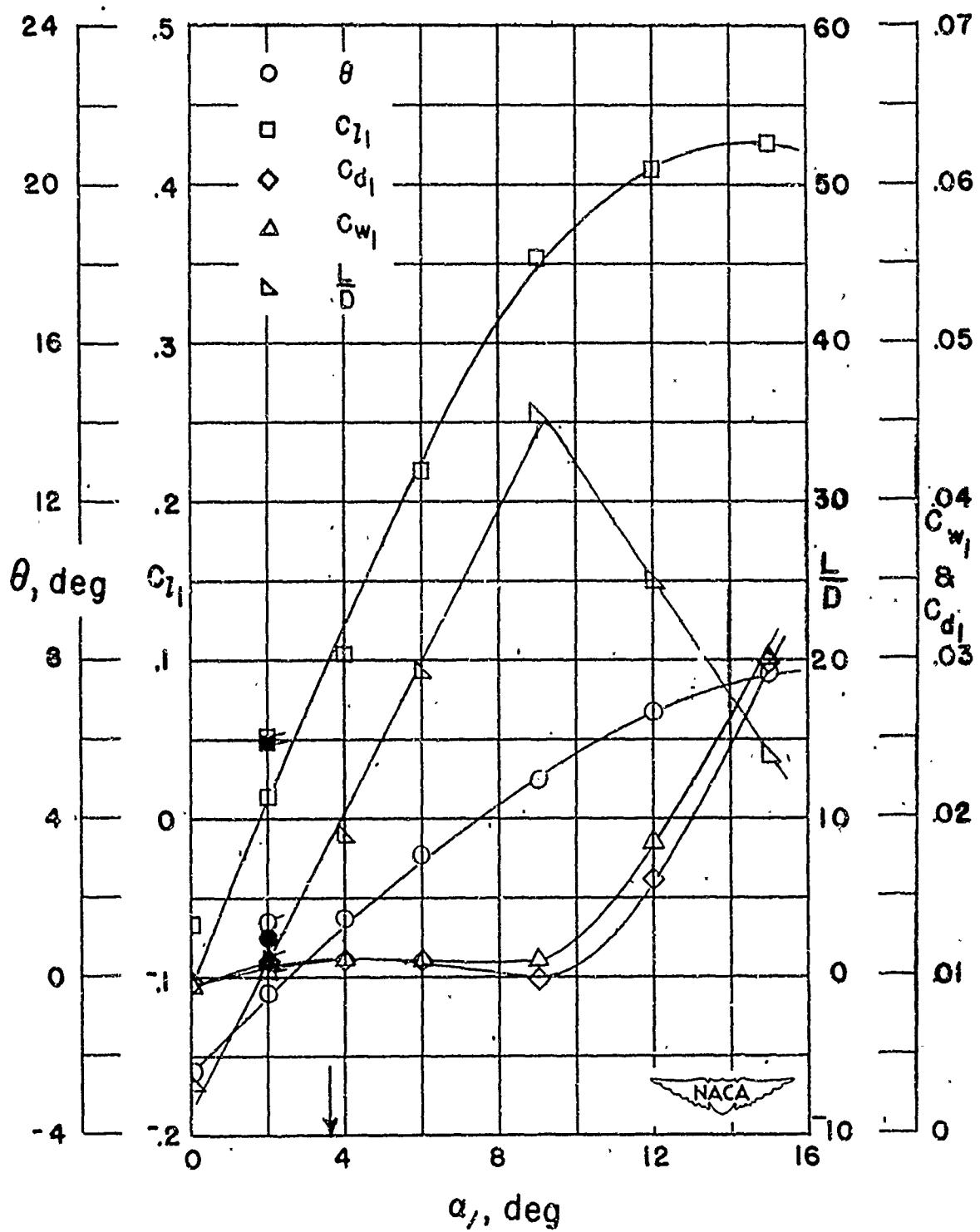


α_1 , deg

Section characteristics; arrow shows design angle of attack;
flagged symbol indicates leading-edge roughness.

Cascade combination, $\beta_1 = 60^\circ$, $\sigma' = 1.50$
blade section, NACA 65-(24)10

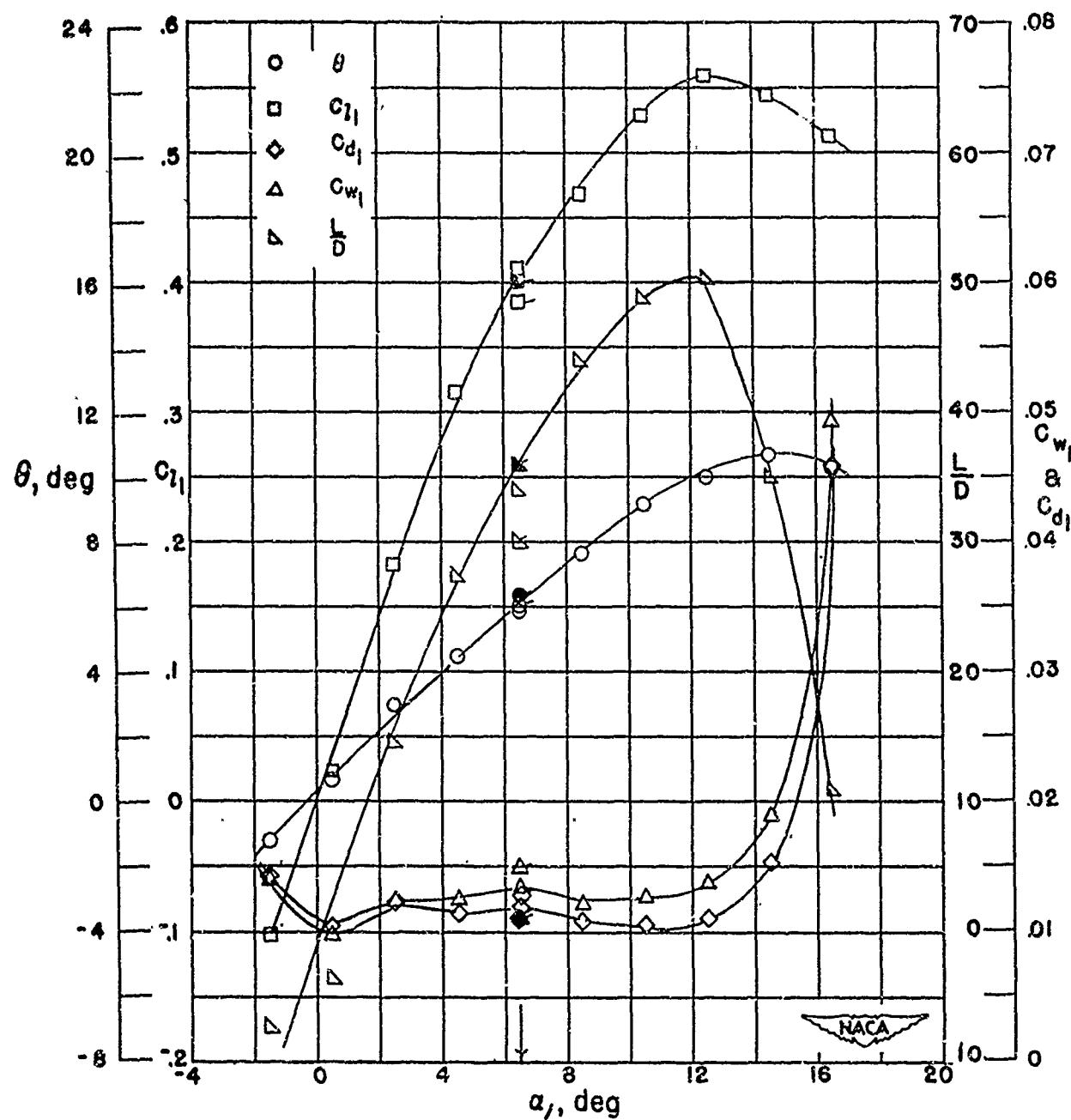
Figure 4-75
(Source: Ref. 4-4)



Section characteristics; arrow shows design angle of attack;
flagged symbol indicates leading-edge roughness; solid
symbol indicates high Reynolds number.

Cascade combination, $\beta_1 = 70^\circ$, $\sigma' = 1.00$
blade section, NACA 65-010

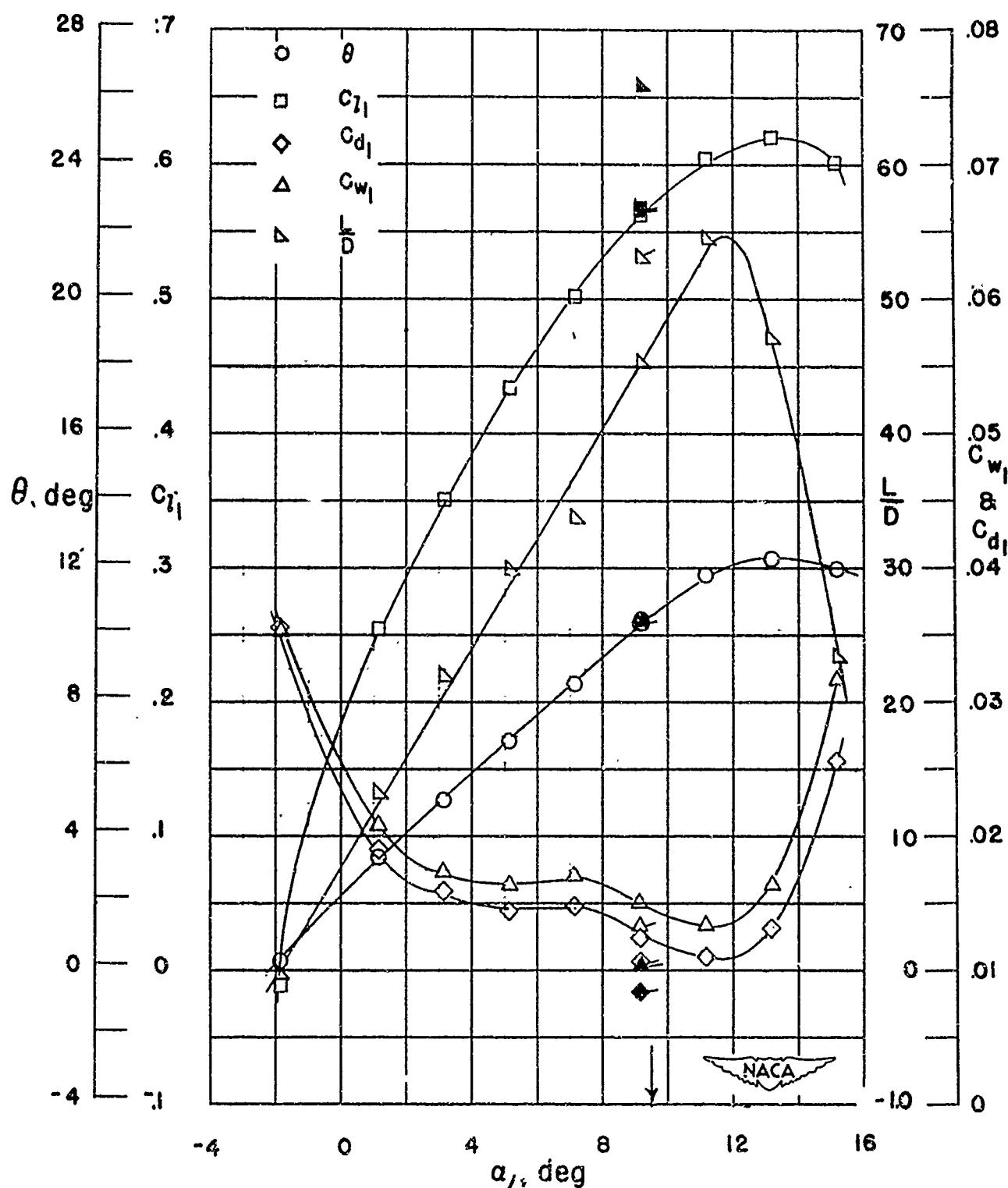
Figure 4-76
(Source: Ref. 4-4)



Section characteristics; arrow shows design angle of attack;
 flagged symbol indicates leading-edge roughness; solid
 symbol indicates high Reynolds number.

Cascade combination, $\beta_1 = 70^\circ$, $\sigma' = 1.00$
 blade section, NACA 65-410

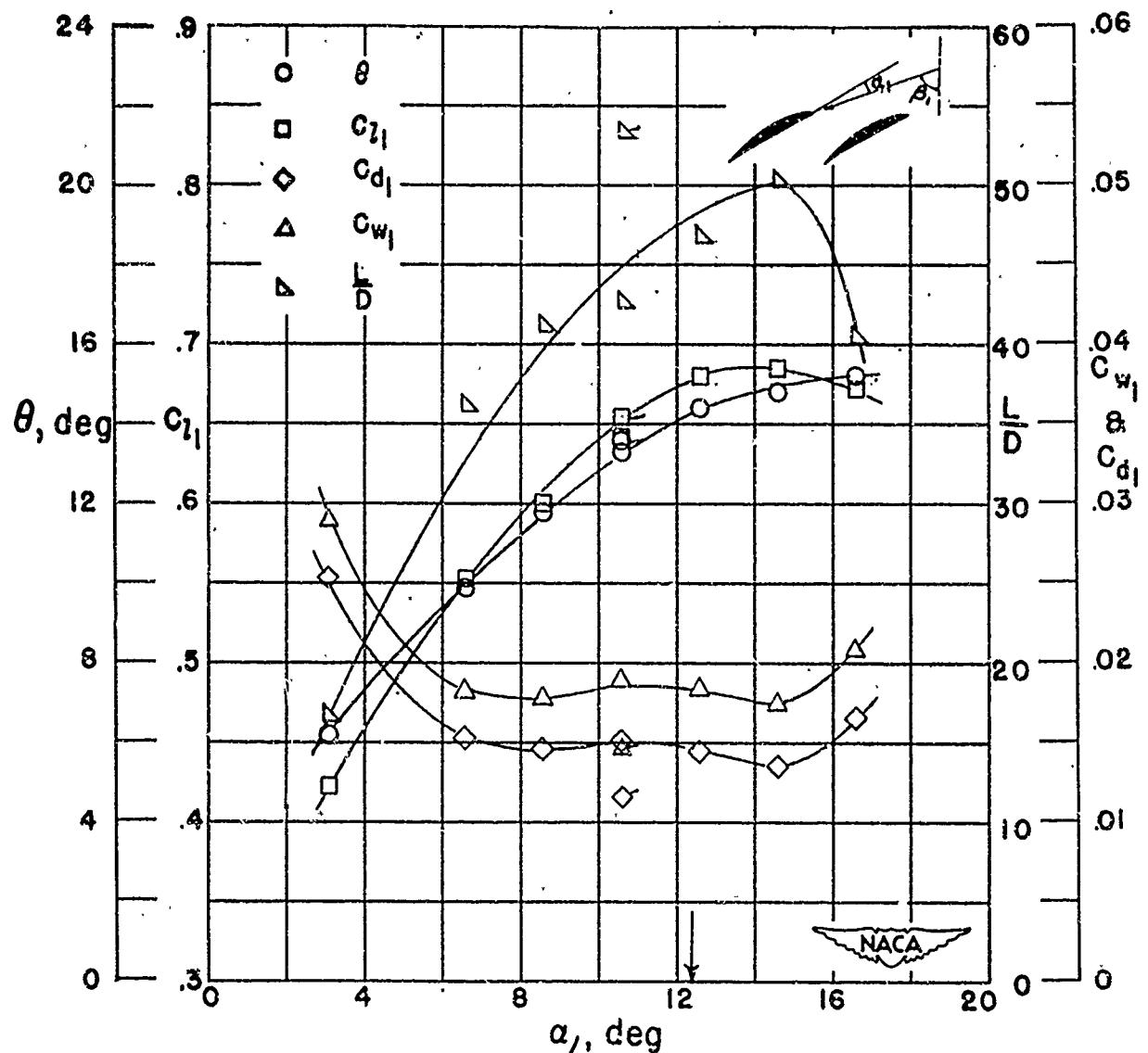
Figure 4-77
 (Source: Ref. 4-4)



Section characteristics; arrow shows design angle of attack,
flagged symbol indicates leading-edge roughness; solid
symbol indicates high Reynolds number.

Cascade combination, $\beta_1 = 70^\circ$, $\sigma' = 1.00$
blade section, NACA 65-810

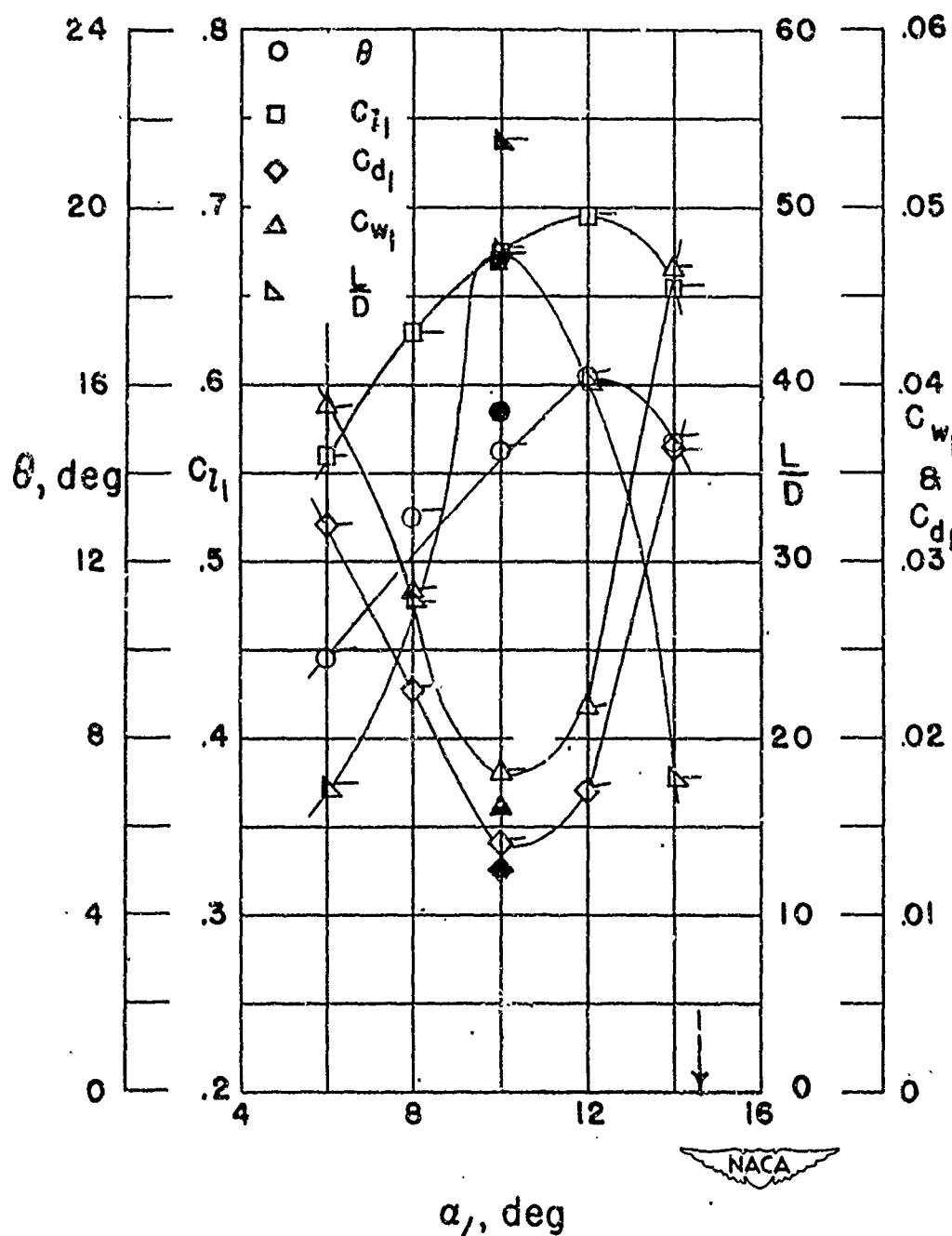
Figure 4-78
(Source: Ref. 4-4)



Section characteristics; arrow shows design angle of attack;
flagged symbol indicates leading-edge roughness.

Cascade combination, $\beta_1 = 70^\circ$, $\sigma' = 1.00$
blade section, NACA 65-(12)10

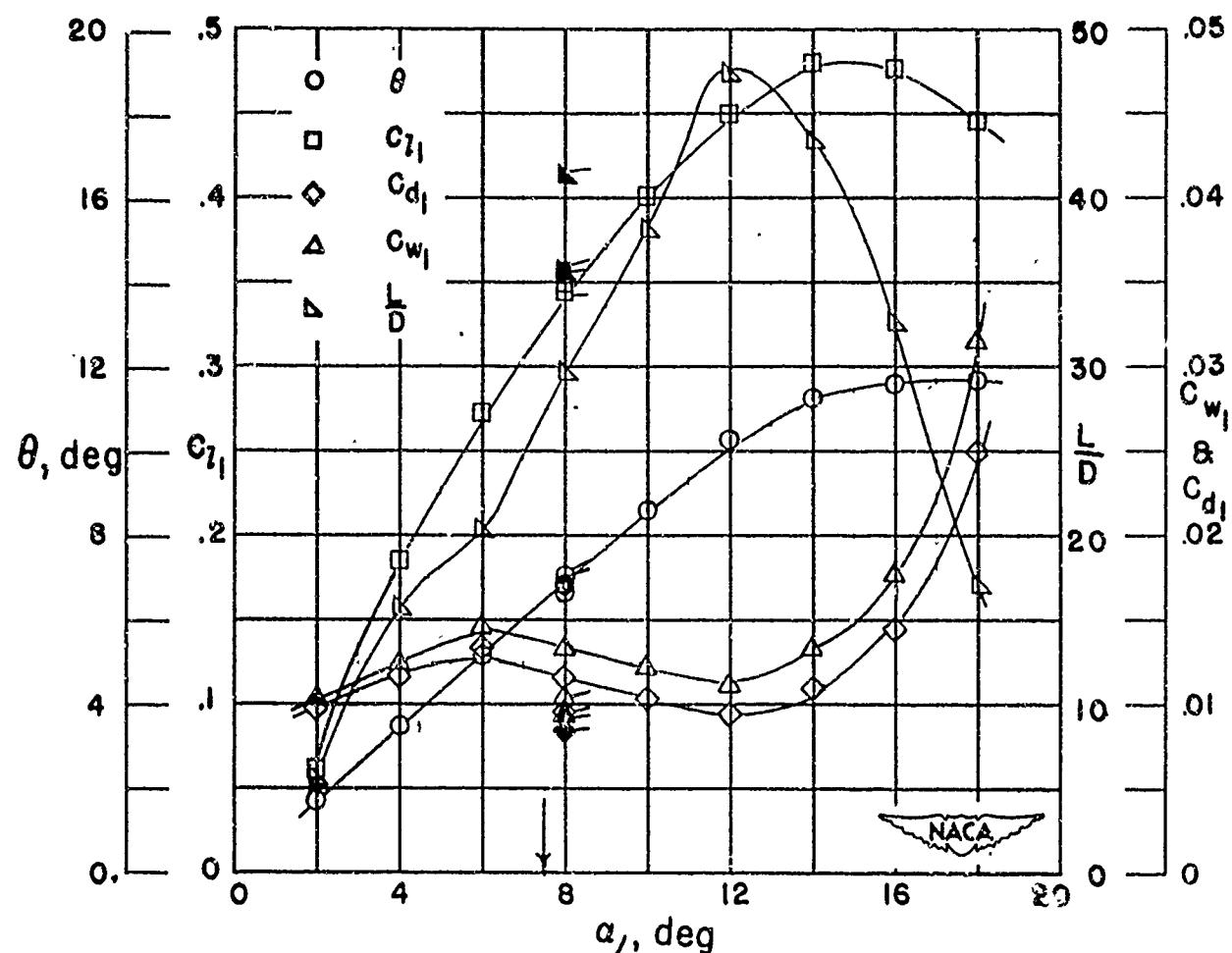
Figure 4-79
(Source: Ref. 4-4)



Section characteristics; no design point was obtained;
flagged symbol indicates leading-edge roughness; solid
symbol indicates high Reynolds number.

Cascade combination, $\beta_1 = 70^\circ$, $\sigma' = 1.00$
blade section, NACA 65-(15)10

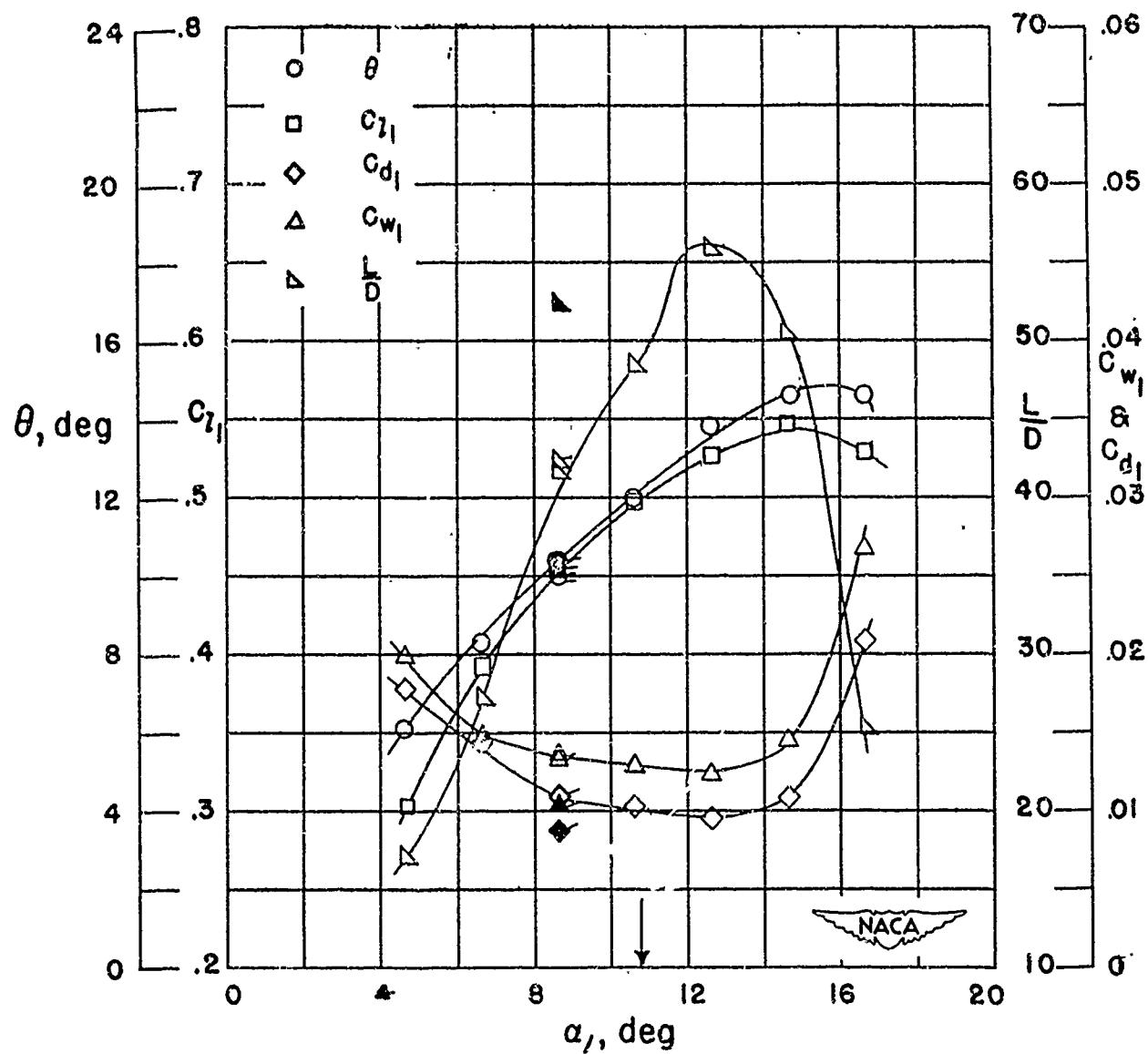
Figure 4-80
(Source: Ref. 4-4)



Section characteristics; arrow shows design angle of attack,
flagged symbol indicates leading-edge roughness; solid
symbol indicates high Reynolds number.

Cascade combination, $\beta_1 = 70^\circ$, $\sigma' = 1.25$
blade section, NACA 65-410

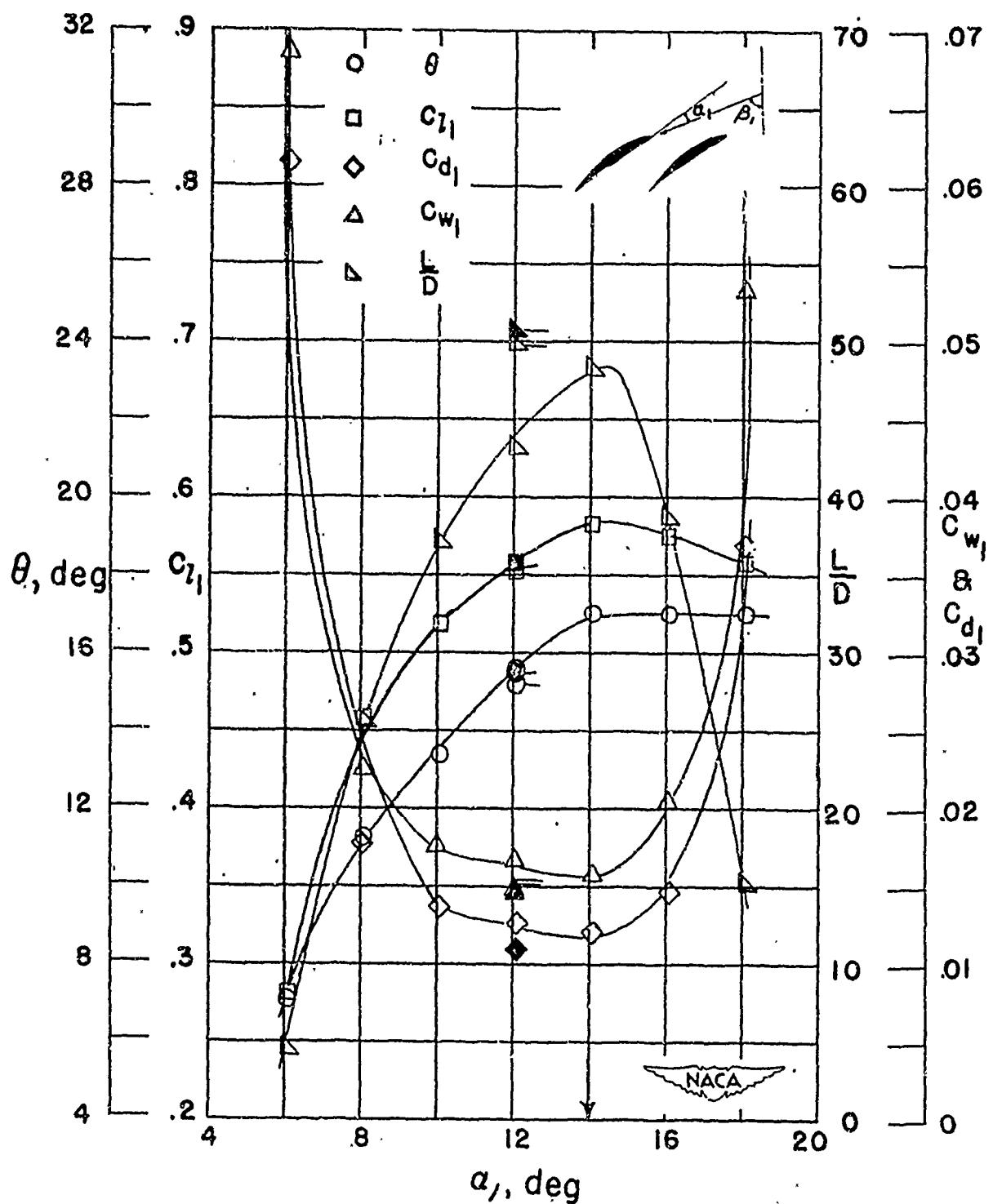
Figure 4-81
(Source: Ref. 4-4)



Section characteristics; arrow shows design angle of attack;
flagged symbol indicates leading-edge roughness; solid
symbol indicates high Reynolds number.

Cascade combination, $\beta_1 = 70^\circ$, $\sigma' = 1.25$
blade section, NACA 65-810

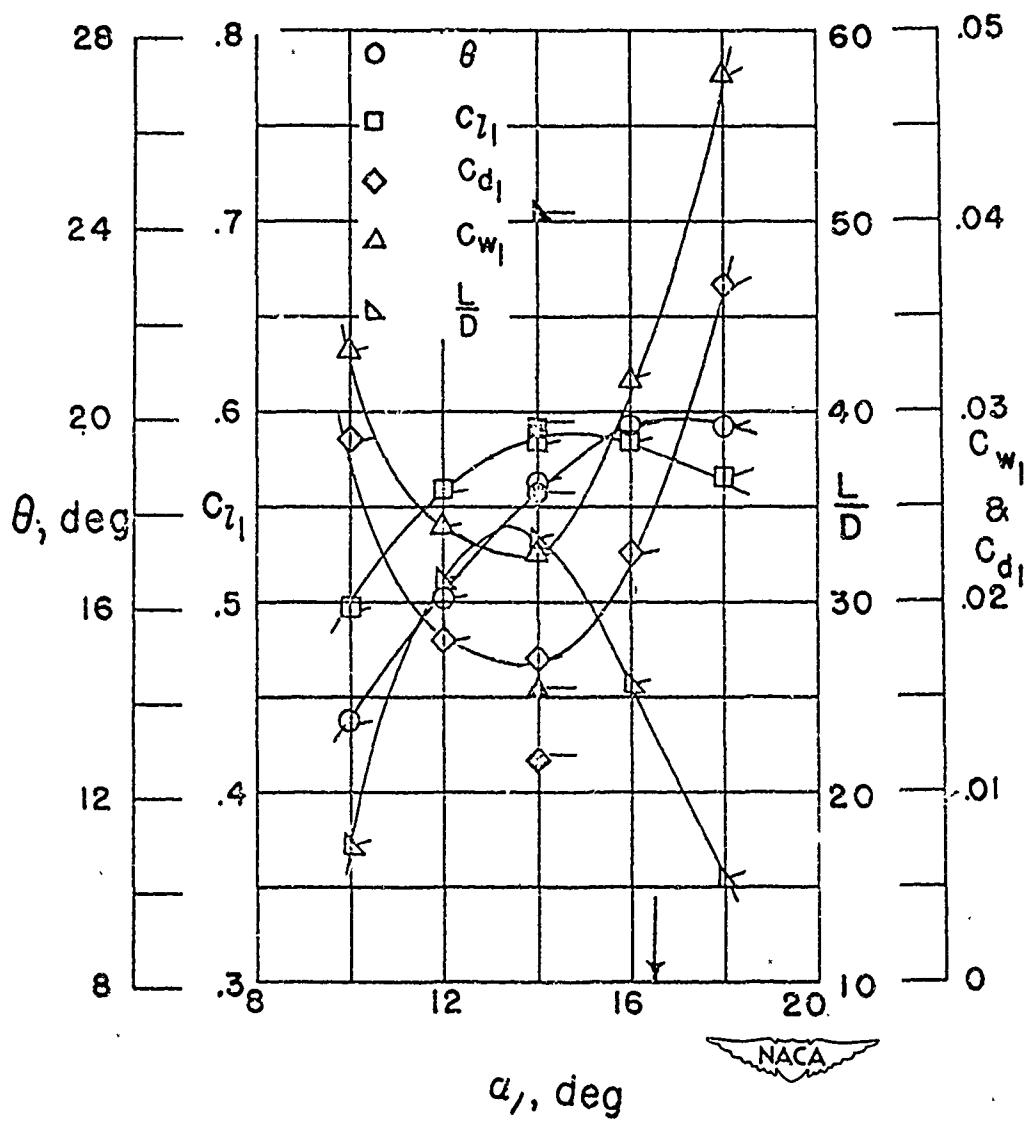
Figure 4-82
(Source: Ref. 4-4)



**Section characteristics; arrow shows design angle of attack;
flagged symbol indicates leading-edge roughness; solid
symbol indicates high Reynolds number**

Cascade combination, $\beta_1 = 70^\circ$, $\sigma' = 1.25$
blade section, NACA 65-(12)10

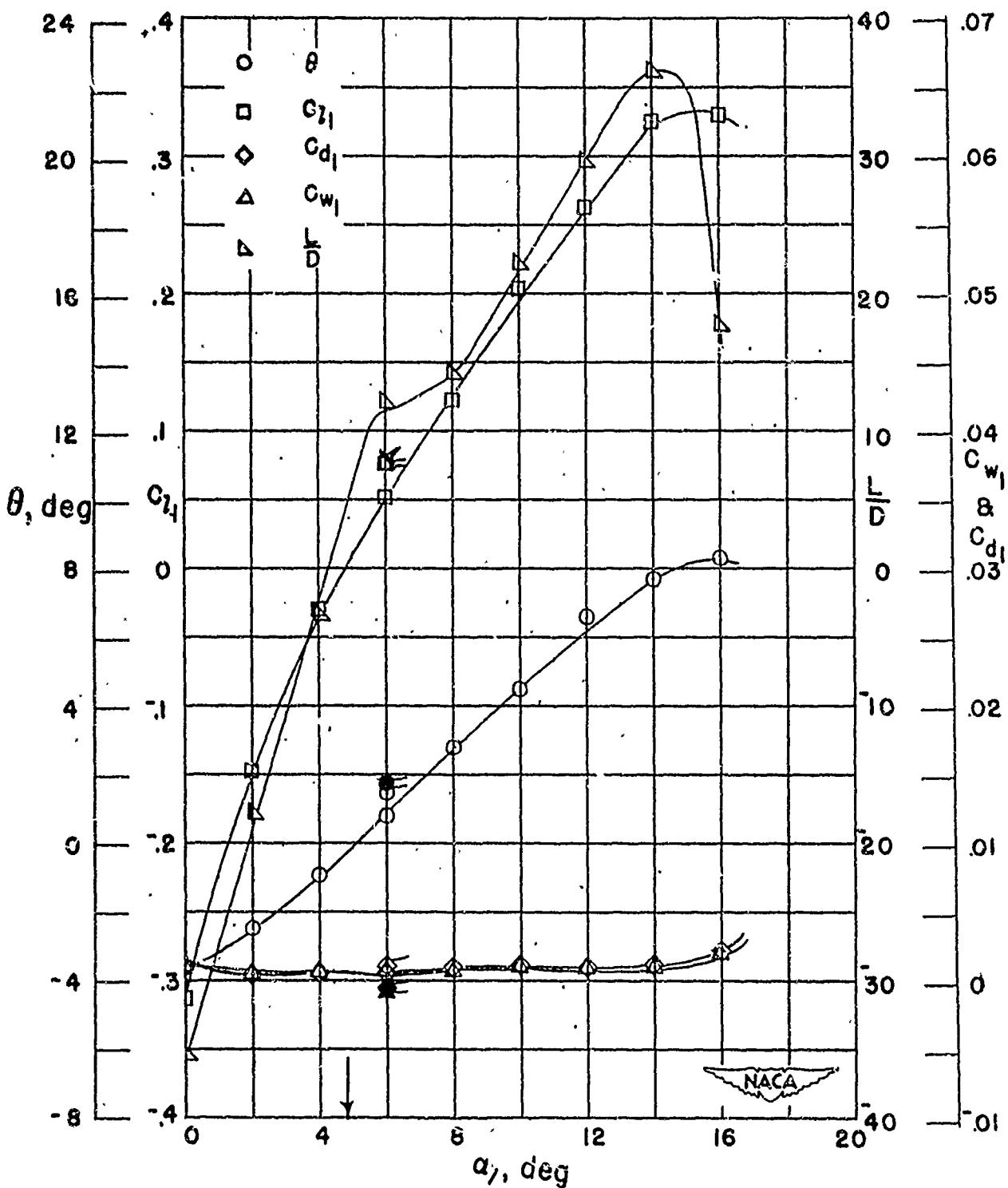
Figure 4-83
(Source: Ref. 4-4)



Section characteristics; arrow shows design angle of attack;
flagged symbol indicates leading-edge roughness; solid
symbol indicates high Reynolds number.

Cascade combination, $\beta_1 = 70^\circ$, $\sigma' = 1.25$
blade section, NACA 65-(15)10

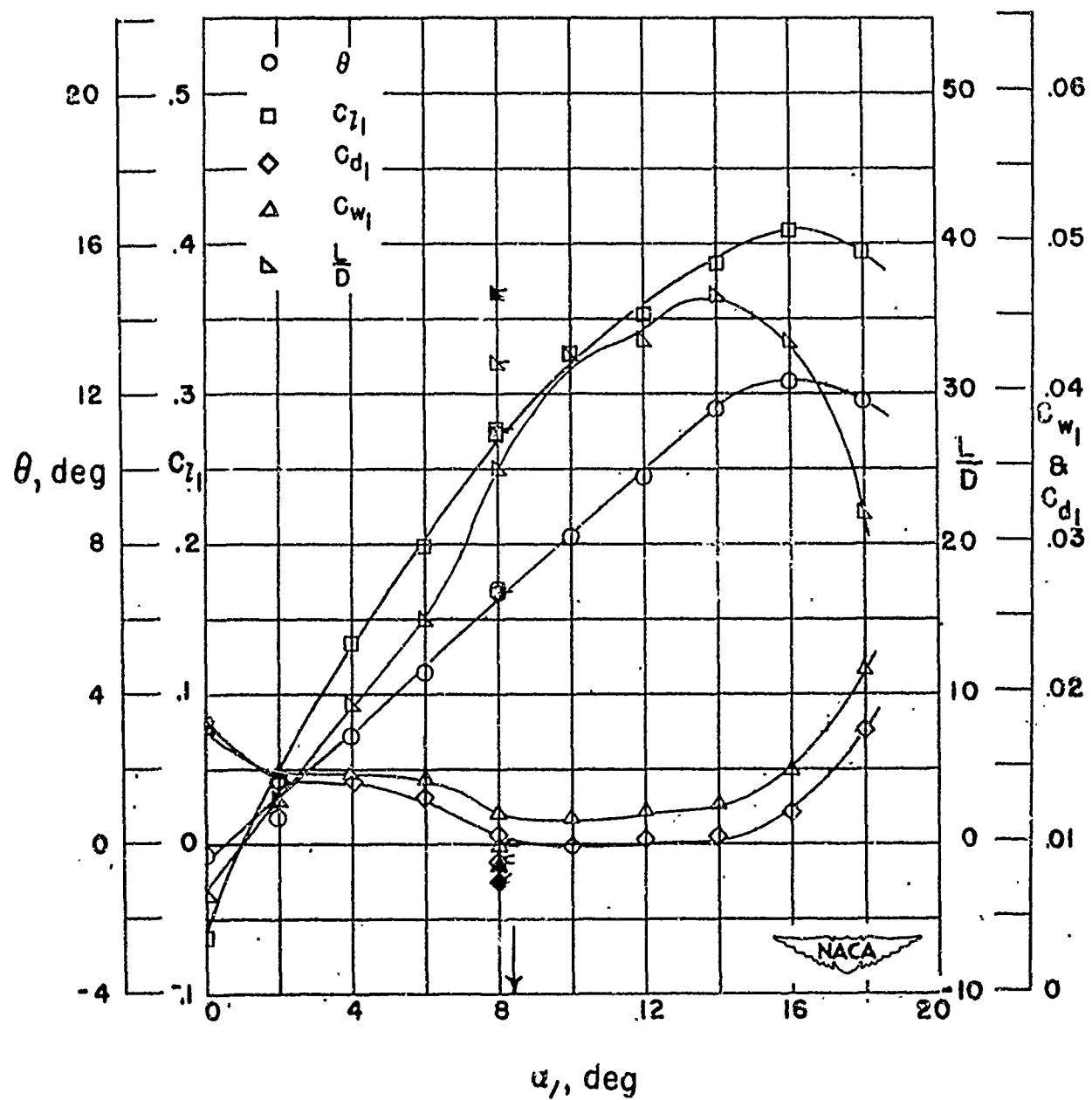
Figure 4-84
(Source: Ref. 4-4)



Section characteristics; arrow shows design angle of attack;
flagged symbol indicates leading-edge roughness; solid
symbol indicates high Reynolds number.

Cascade combination, $\beta_1 = 70^\circ$, $\sigma' = 1.50$
blade section, NACA 65-010

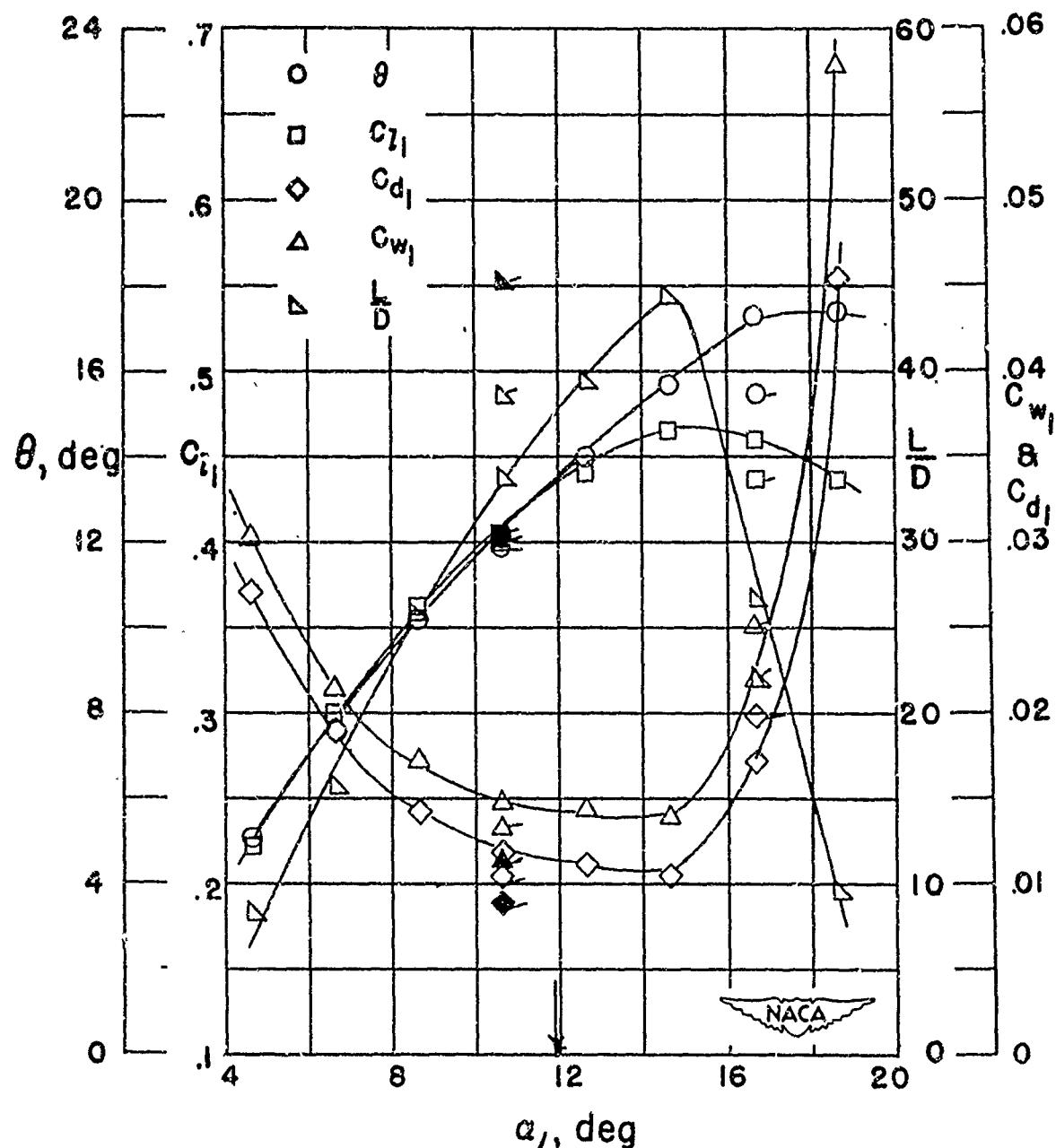
Figure 4-85
(Source: Ref. 4-4)



Section characteristics; arrow shows design angle of attack;
 flagged symbol indicates leading-edge roughness, solid
 symbol indicates high Reynolds number.

Cascade combination, $\beta_1 = 70^\circ$, $\sigma' = 1.50$
 blade section, NACA 65-410

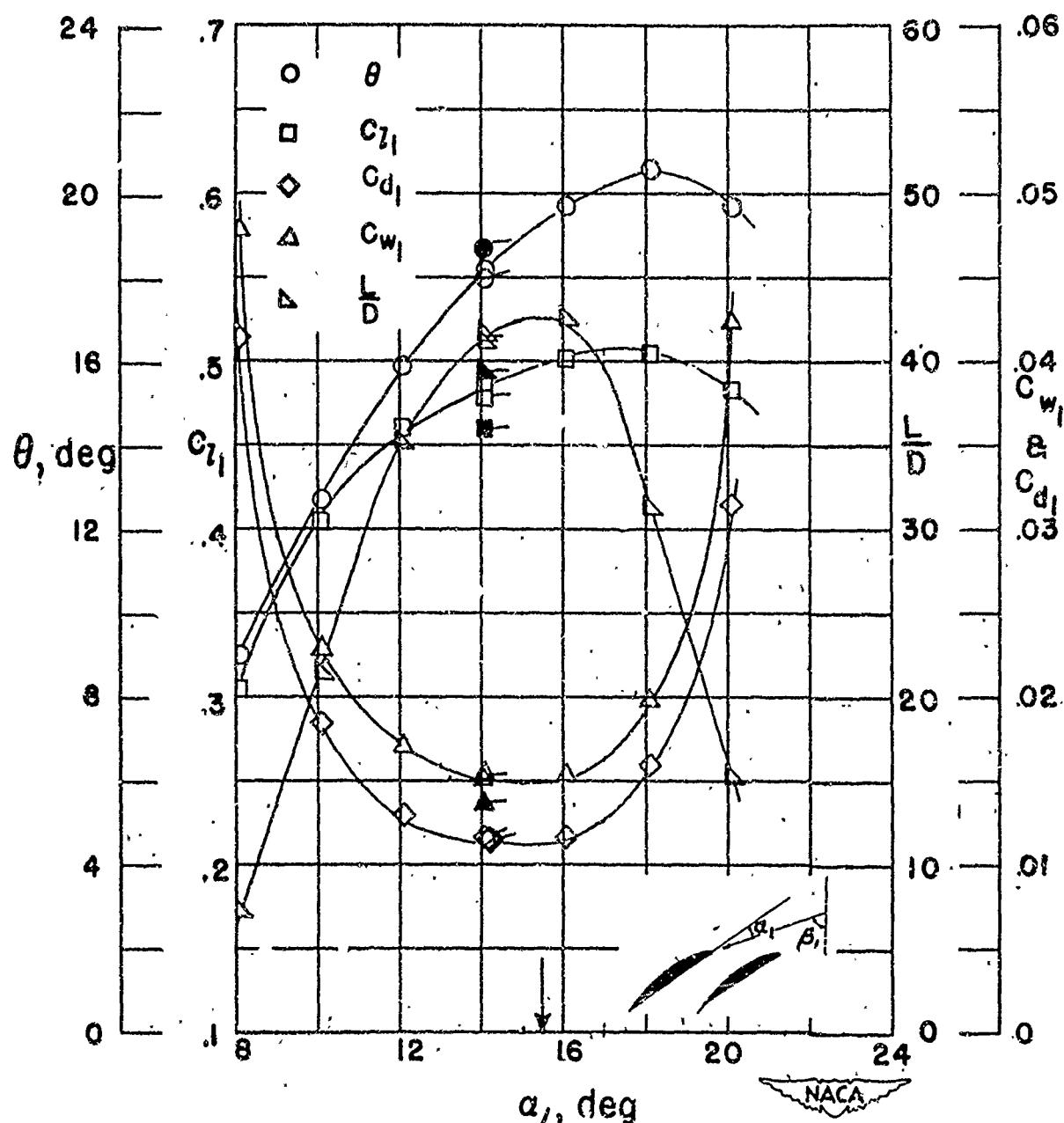
Figure 4-86
 (Source: Ref. 4-4)



Section characteristics; arrow shows design angle of attack;
 flagged symbol indicates leading-edge roughness; solid
 symbol indicates high Reynolds number.

Cascade combination, $\beta_1 = 70^\circ$, $\sigma' = 1.50$
 blade section, NACA 65-810

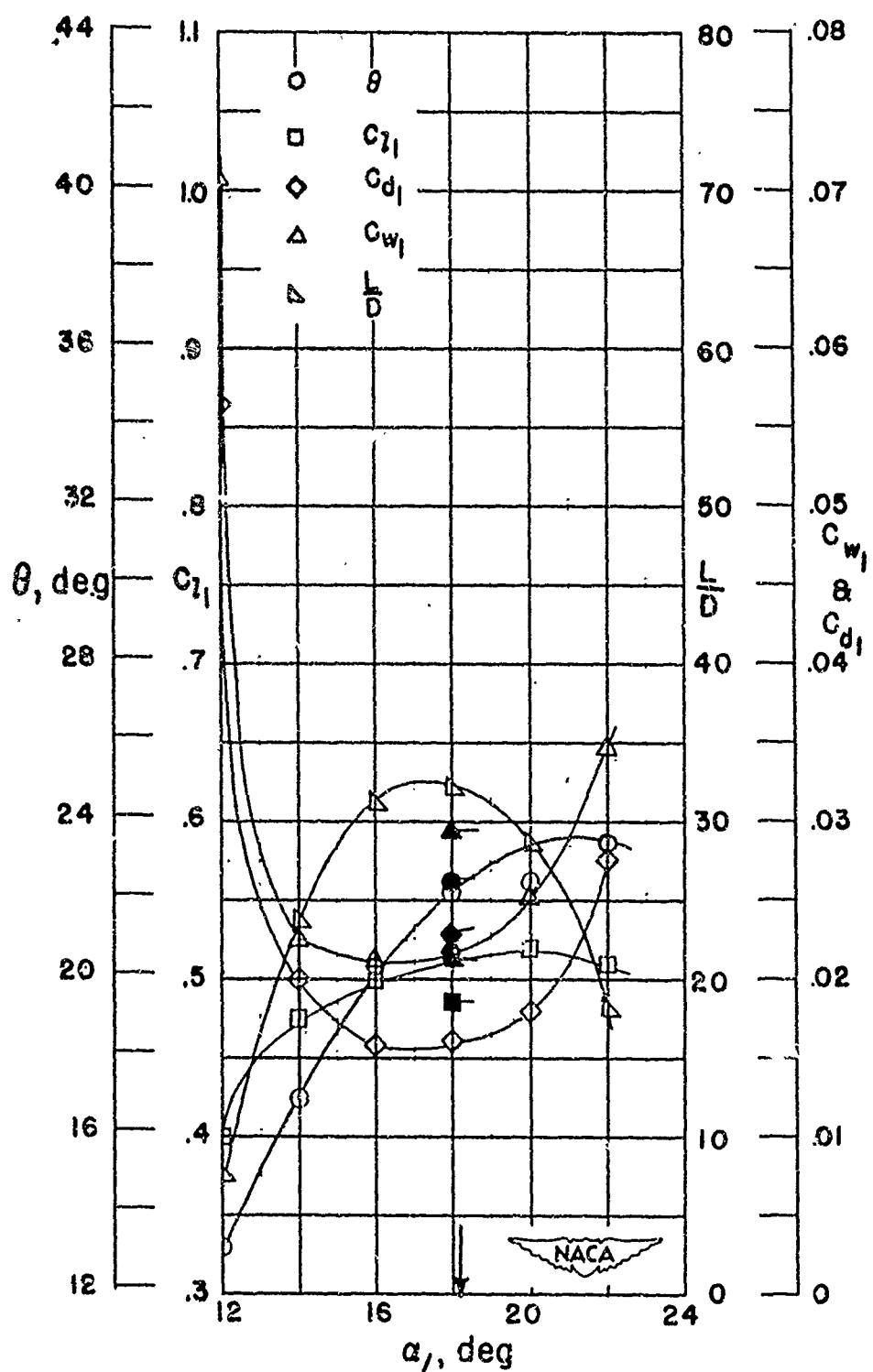
Figure 4-87
 (Source: Ref. 4-4)



Section characteristics; arrow shows design angle of attack;
flagged symbol indicates leading-edge roughness; solid
symbol indicates high Reynolds number.

Cascade combination, $\beta_1 = 70^\circ$, $\sigma' = 1.50$
blade section, NACA 65-(12)10

Figure 4-88
(Source: Ref. 4-4)



Section characteristics; arrow shows design angle of attack;
 flagged symbol indicates leading-edge roughness; solid
 symbol indicates high Reynolds number.

Cascade combination, $\beta_1 = 70^\circ$, $\sigma' = 1.50$
 blade section, NACA 65-(15)10

Figure 4-89
 (Source: Ref. 4-4)

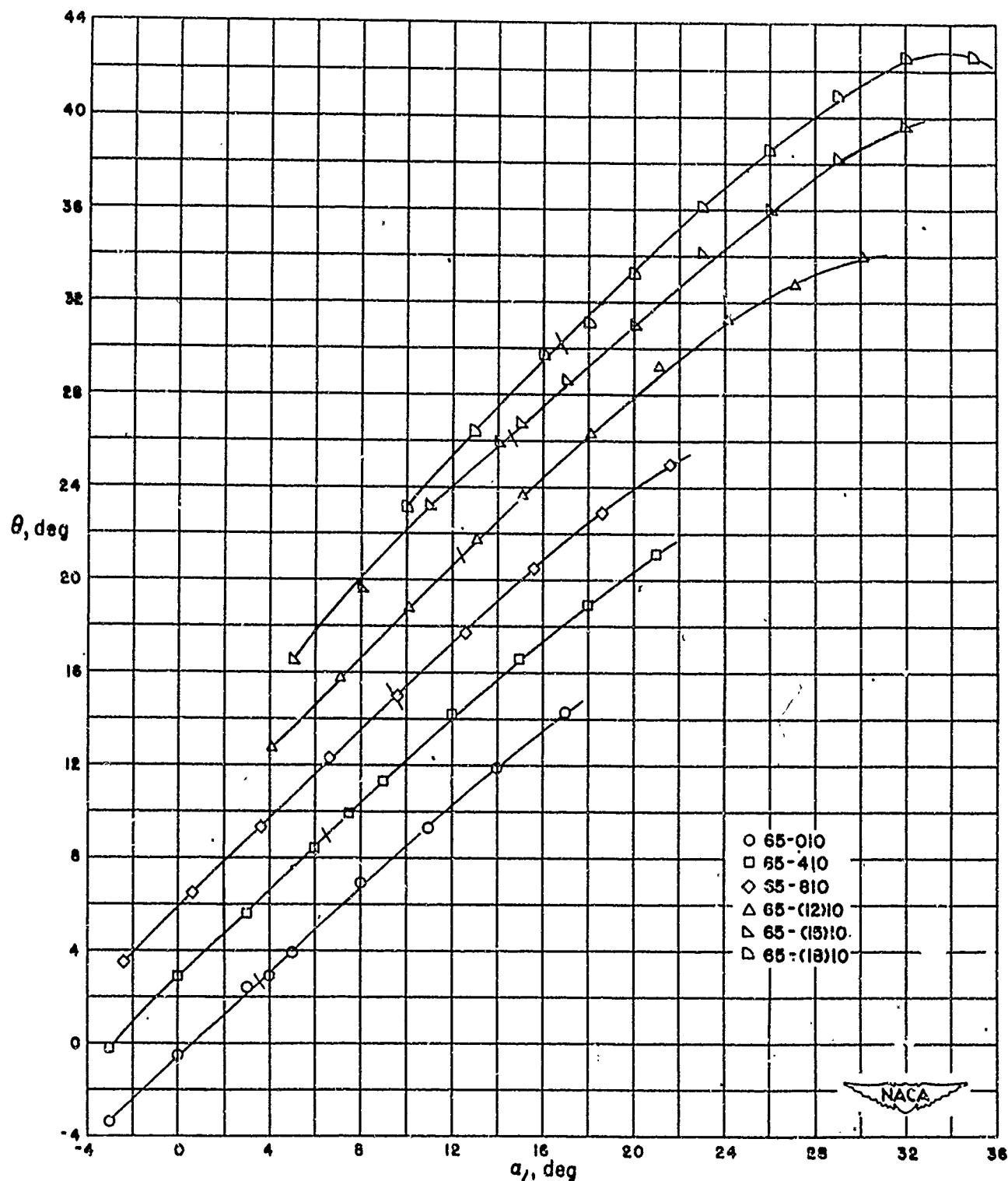


Figure 4-90 Summary of turning angle, θ , angle of attack, α , relationship for the blade sections tested at $\beta_1 = 30^\circ$, $\sigma' = 1.00$. Short bars across curves indicate design points. (Source: Ref. 4-4)

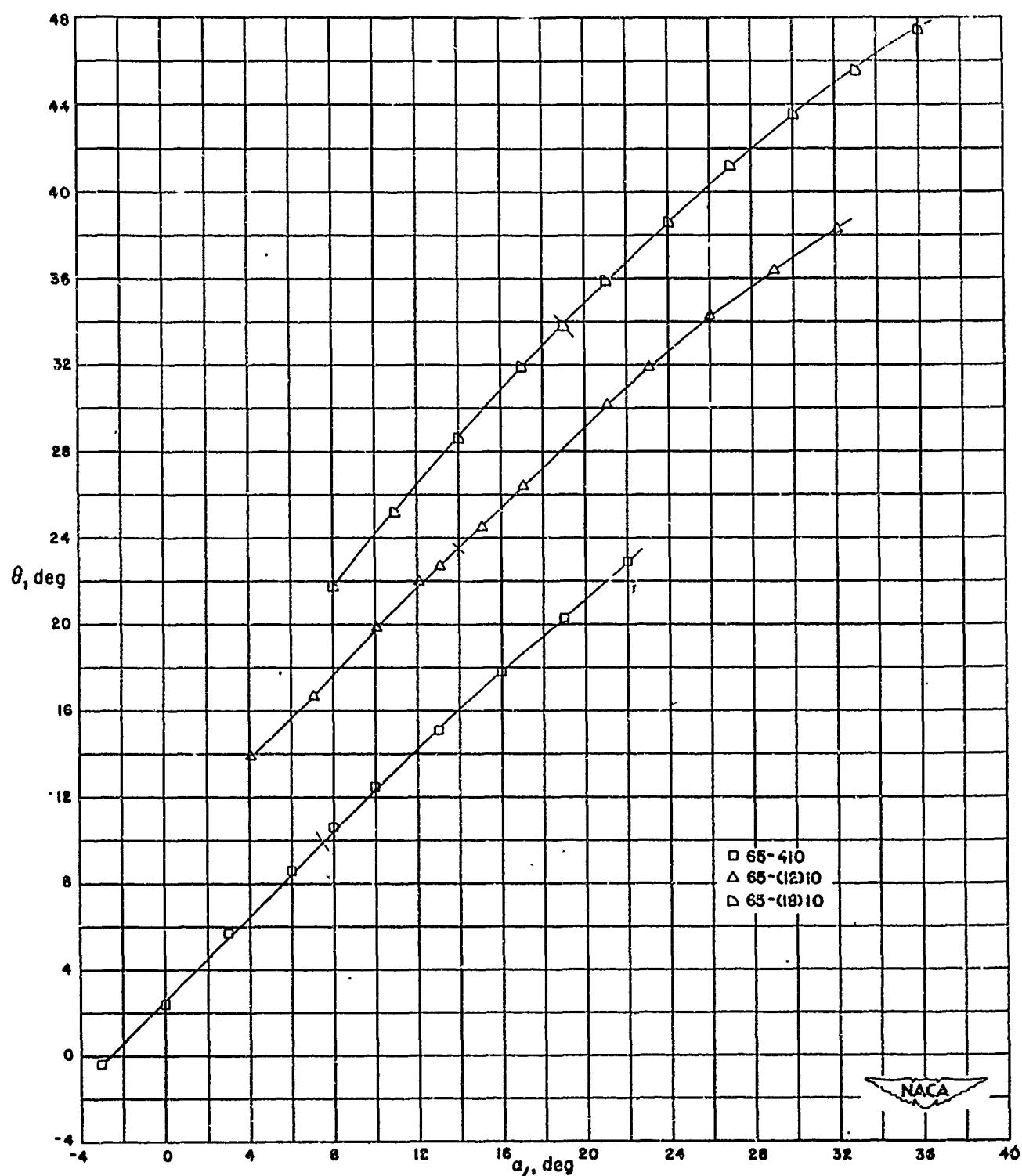


Figure 4-91 Summary of turning angle, θ , angle of attack, α , relationship for the blade sections tested at $\beta_1 = 30^\circ$, $\sigma' = 1.25$. Short bars across curves indicate design points. (Source: Ref. 4-4)

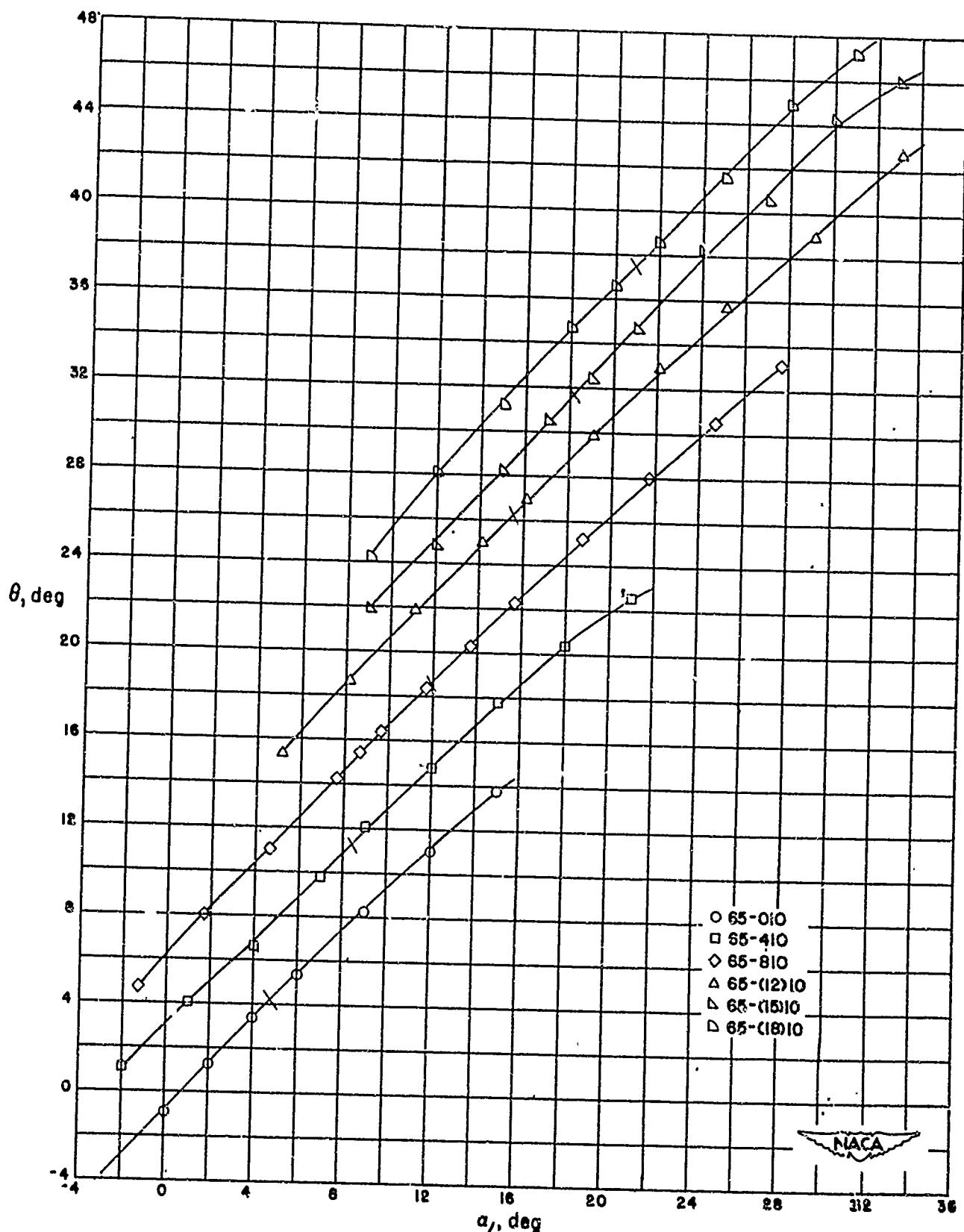


Figure 4-92 Summary of turning angle, θ , angle of attack, α , relationship for the blade sections tested at $\beta_1 = 30^\circ$, $\sigma = 1.50$. Short bars across curves indicate design points. (Source: Ref. 4-4)

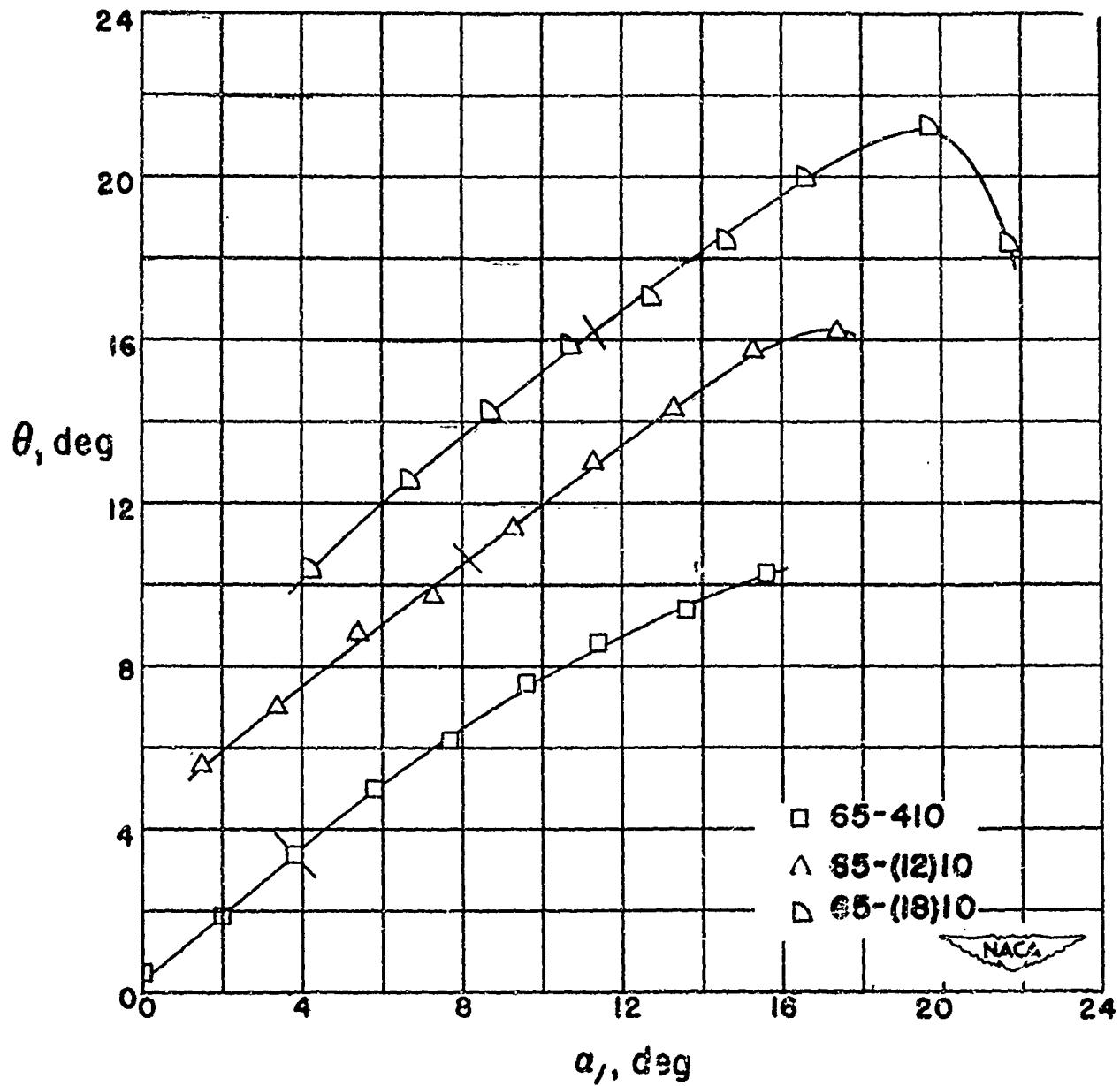


Figure 4-93 Summary of turning angle, θ , angle of attack, α , relationship for the blade sections tested at $\beta_1 = 45^\circ$, $\sigma = 0.50$. Short bars across curves indicate design points. (Source: Ref. 4-4)

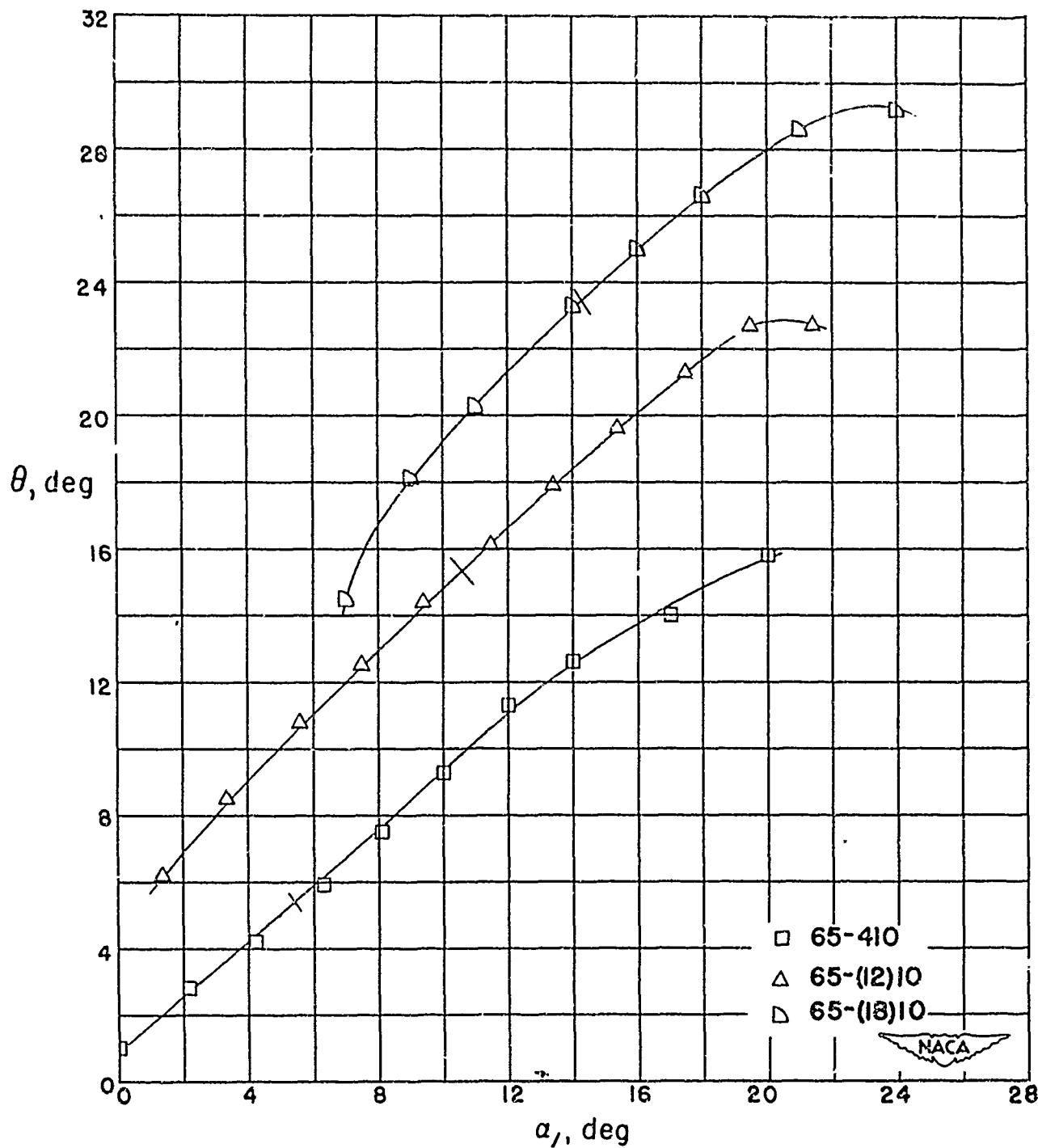


Figure 4-94 Summary of turning angle, θ , angle of attack, α , relationship for the blade sections tested at $\beta_1 = 45^\circ$, $\sigma' = 0.75$. Short bars across curves indicate design points. (source: Ref. 4-4)

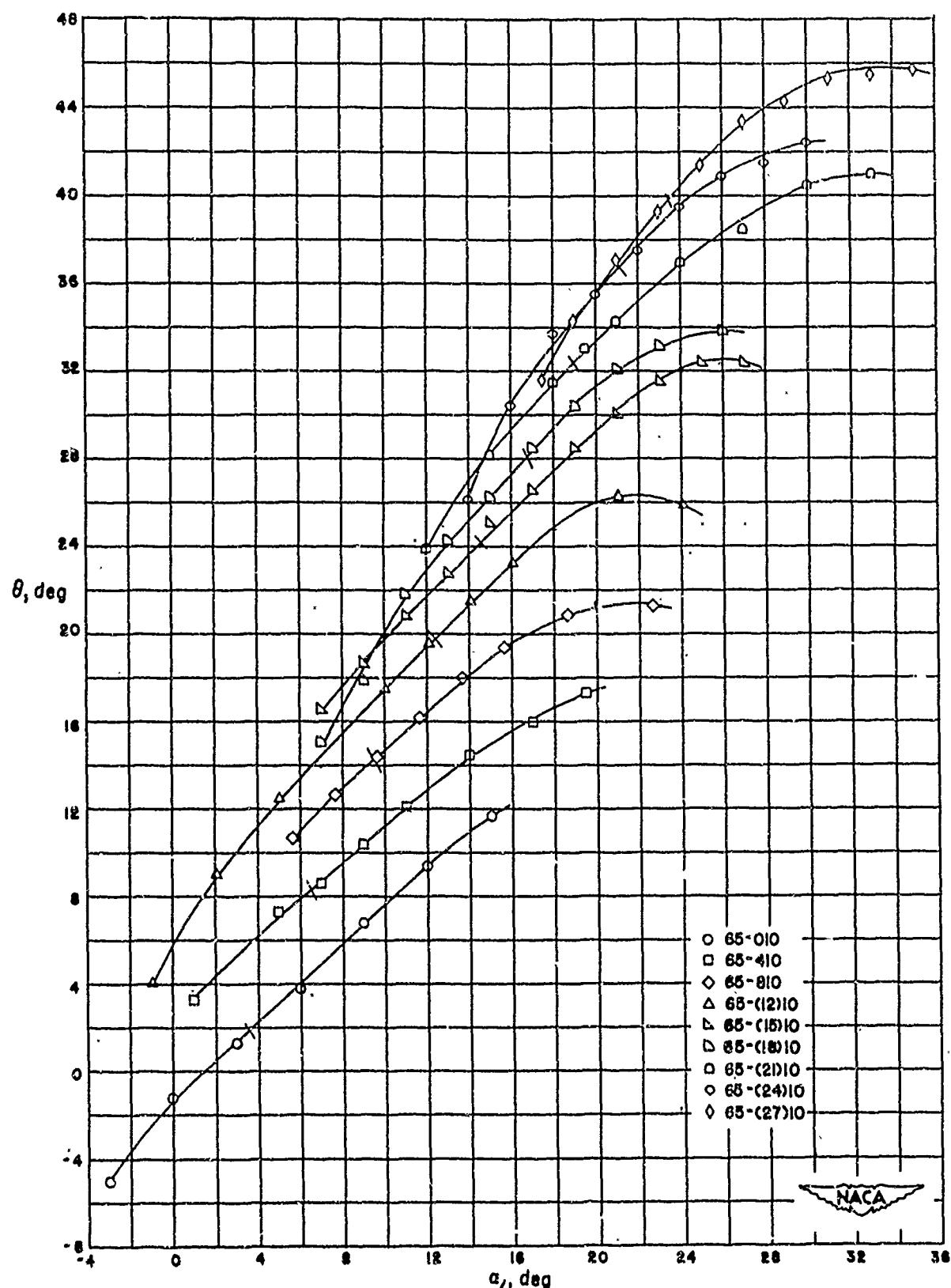


Figure 4-95 Summary of turning angle, θ , angle of attack, α , relationship for the blade sections tested at $\beta_1 = 45^\circ$, $\sigma' = 1.00$. Short bars across curves indicate design points. (Source: Ref. 4-4)

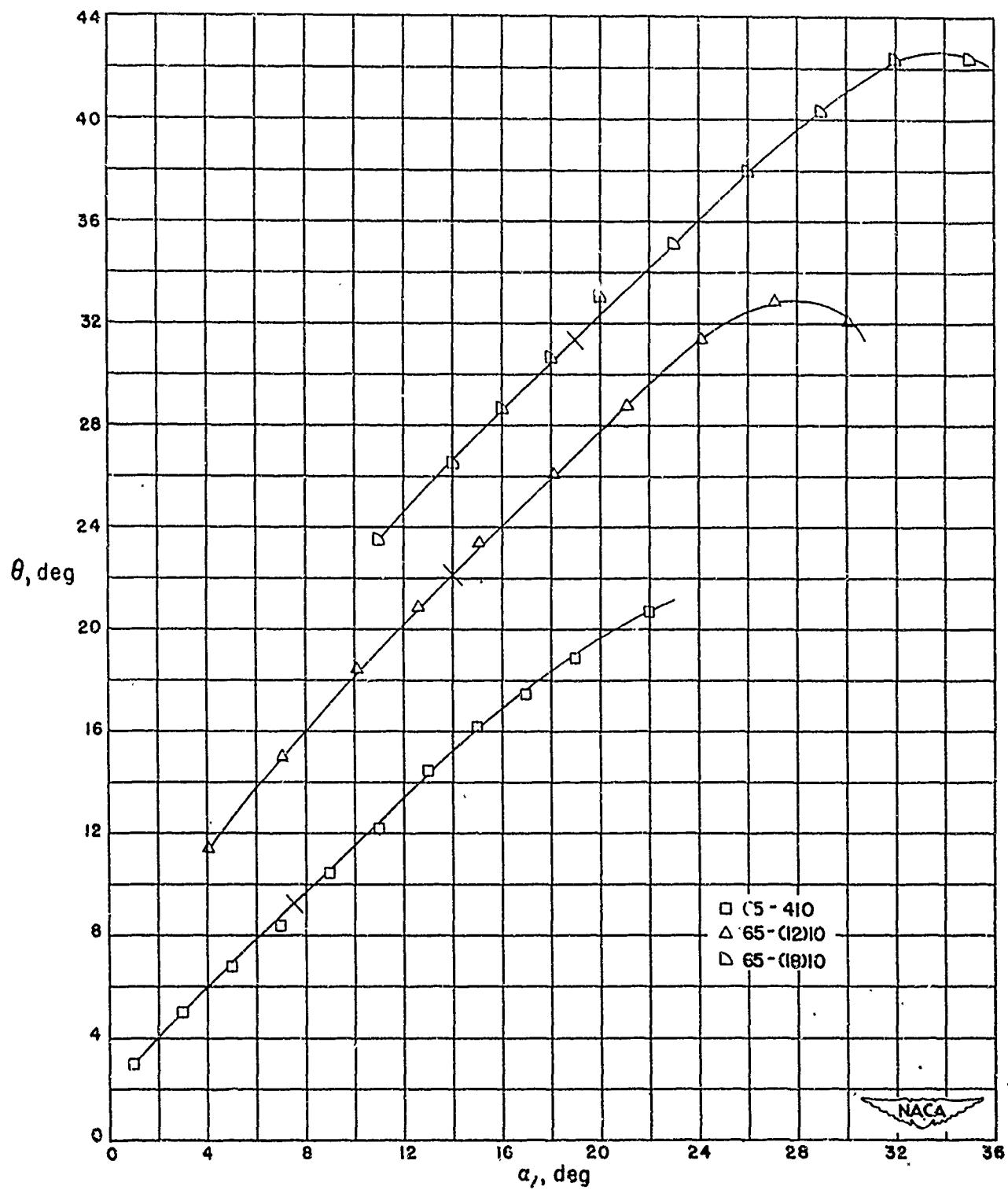


Figure 4-96 Summary of turning angle, θ , angle of attack, α , relationship for the blade sections tested at $\beta_1 = 45^\circ$, $\sigma' = 1.25$. Short bars across curves indicate design points. (Source: Ref. 4-4)

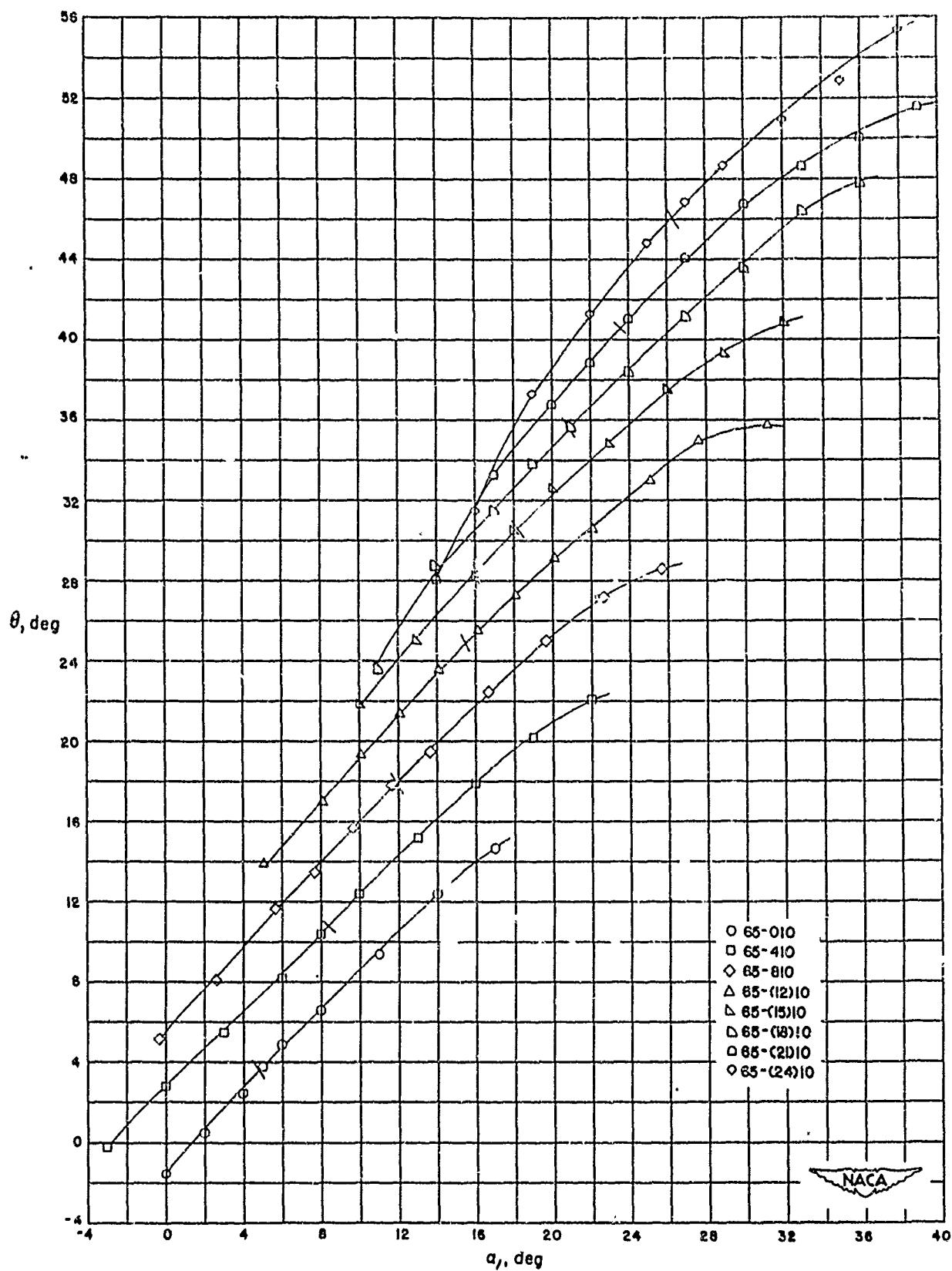


Figure 4-97 Summary of turning angle, θ , angle of attack, α , relationship for the blade sections tested at $\beta_1 = 45^\circ$, $\sigma' = 1.50$. Short bars across curves indicate design points. (Source: Ref. 4-4)

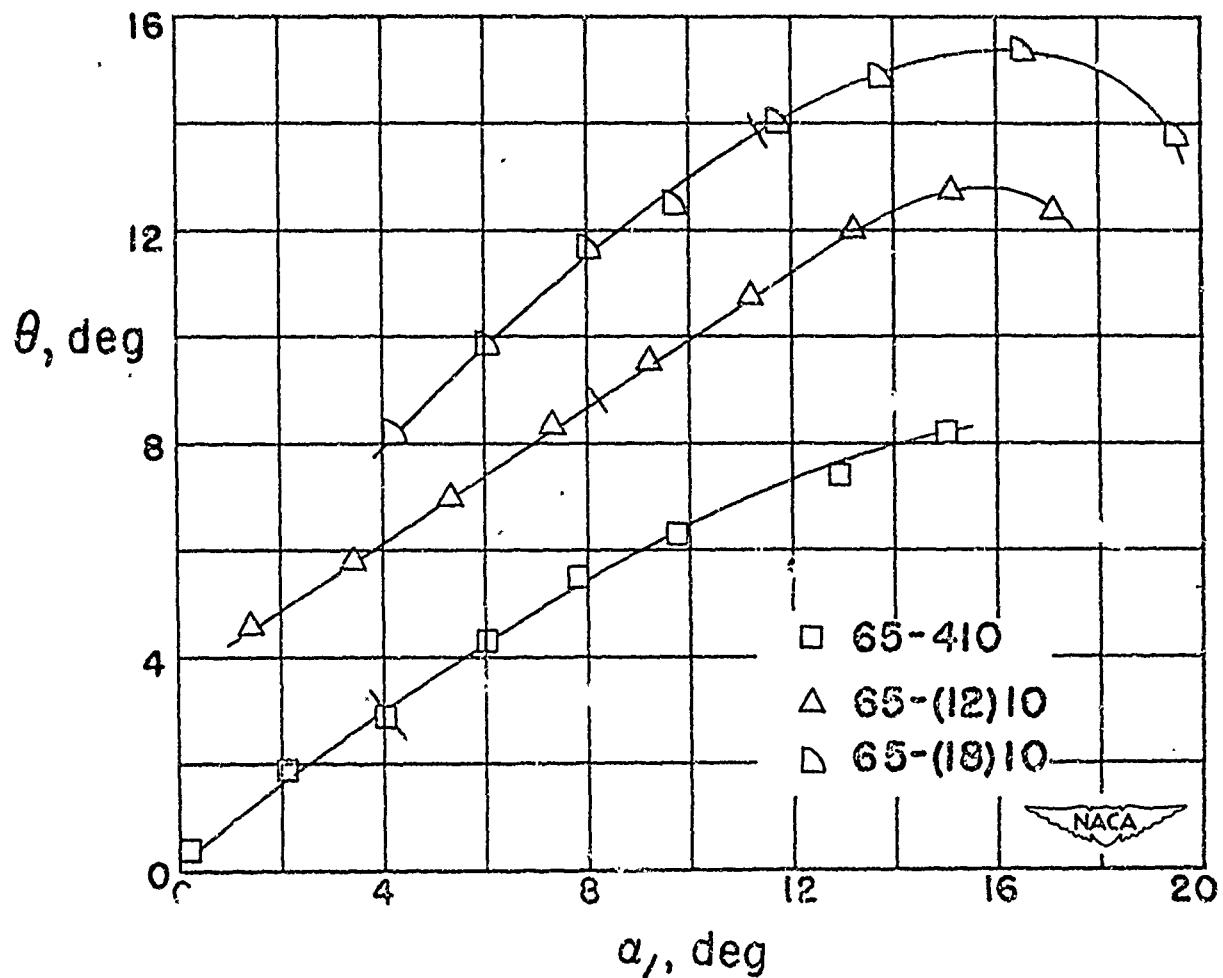


Figure 4-98 Summary of turning angle, θ , angle of attack, α , relationship for the blade sections tested at $\beta_1 = 60^\circ$, $\sigma' = 0.50$. Short bars across curves indicate design points. (Source: Ref. 4-4)

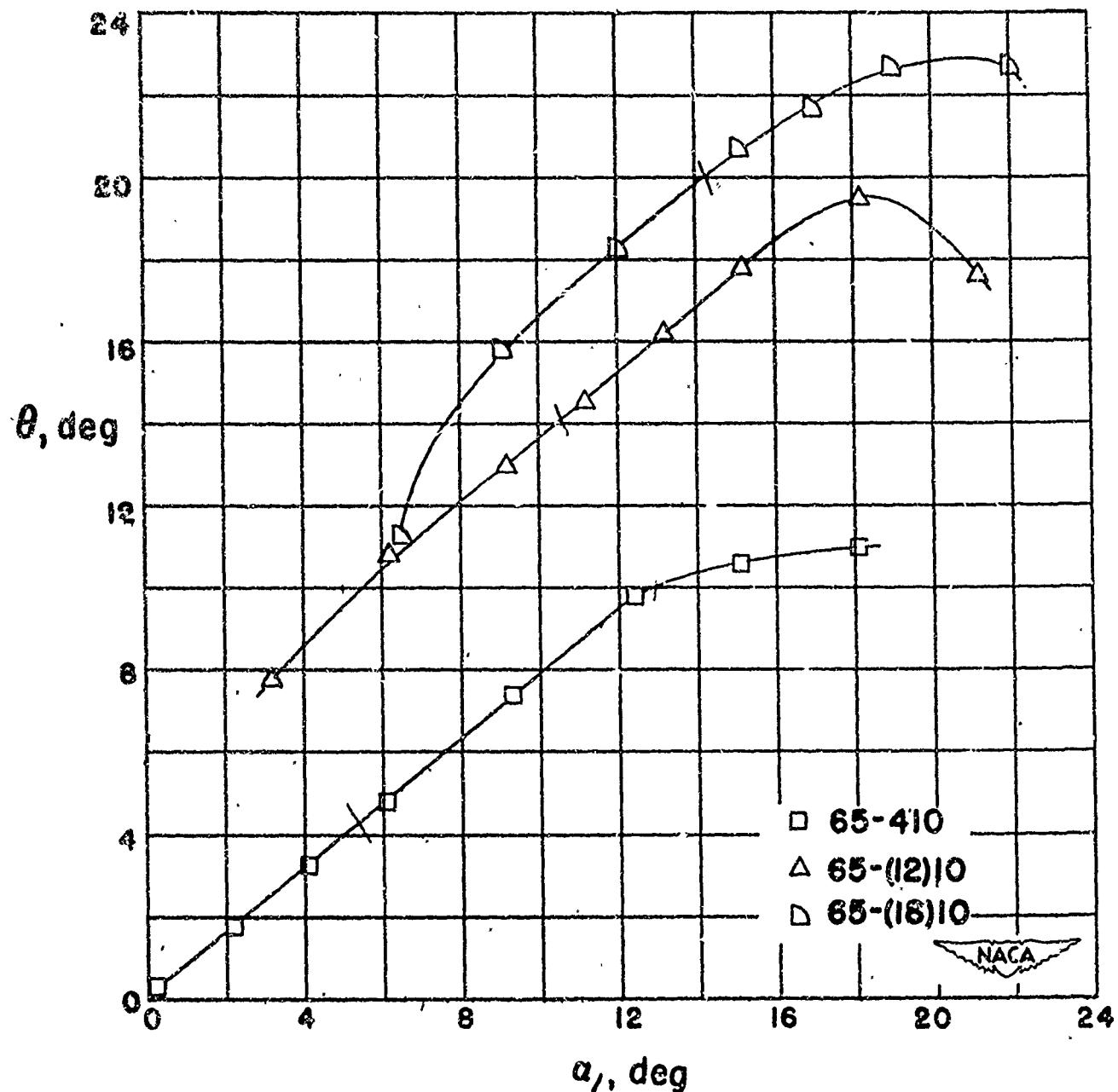


Figure 4-99 Summary of turning angle, θ , angle of attack, α , relationship for the blade sections tested at $\beta_1 = 60^\circ$ $a' = 0.75$. Short bars across curves indicate design points. (Source: Ref. 4-4)

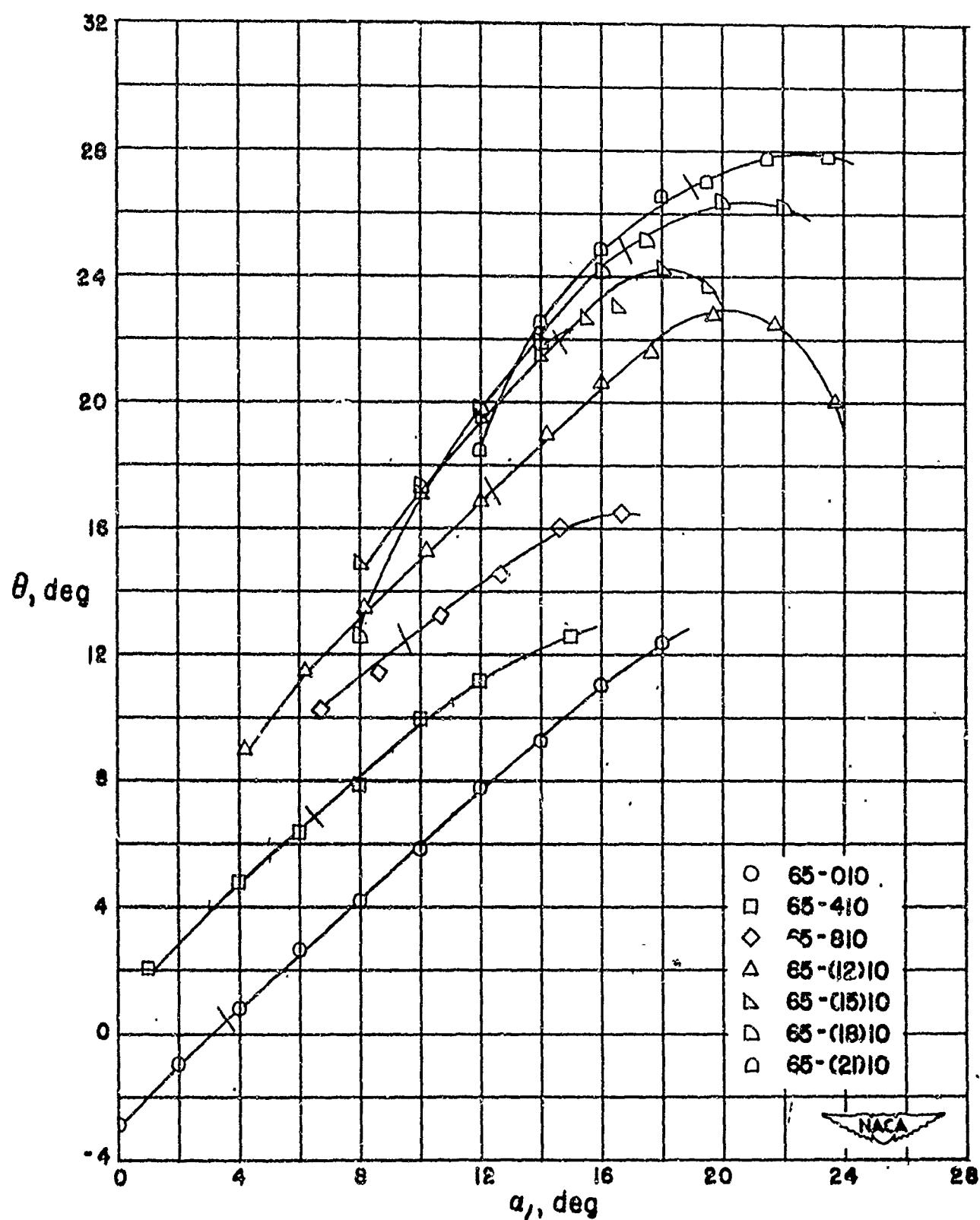


Figure 4-100 Summary of turning angle, θ , angle of attack, α , relationship for the blade sections tested at $\beta_1 = 60^\circ$, $\sigma' = 1.00$. Short bars across curves indicate design points. (Source: Ref. 4-4)

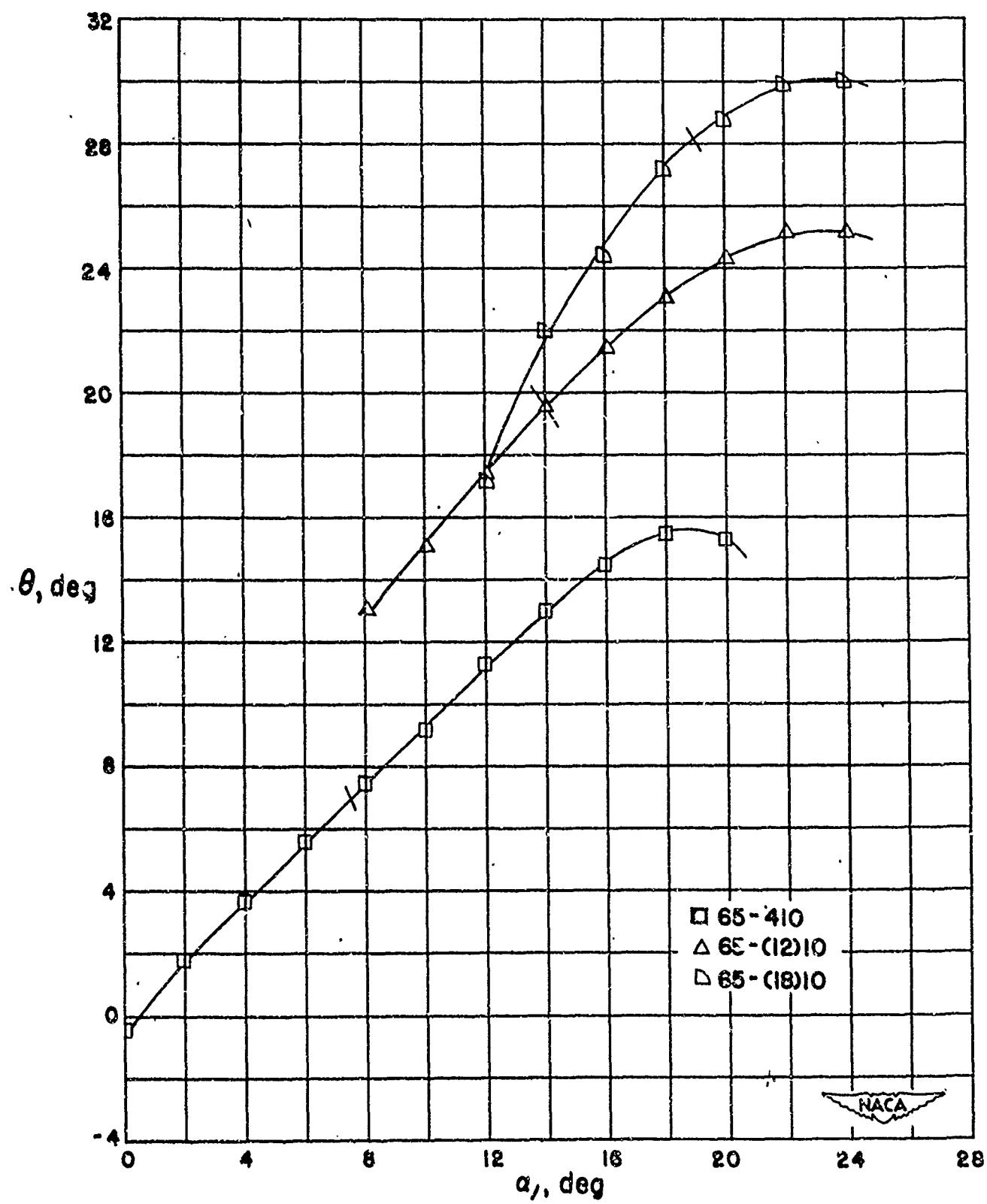


Figure 4-101 Summary of turning angle, θ , angle of attack, α , relationship for the blade sections tested at $\beta_1 = 60^\circ$, $\sigma' = 1.25$. Short bars across curves indicate design points. (Source: Ref. 4-4)

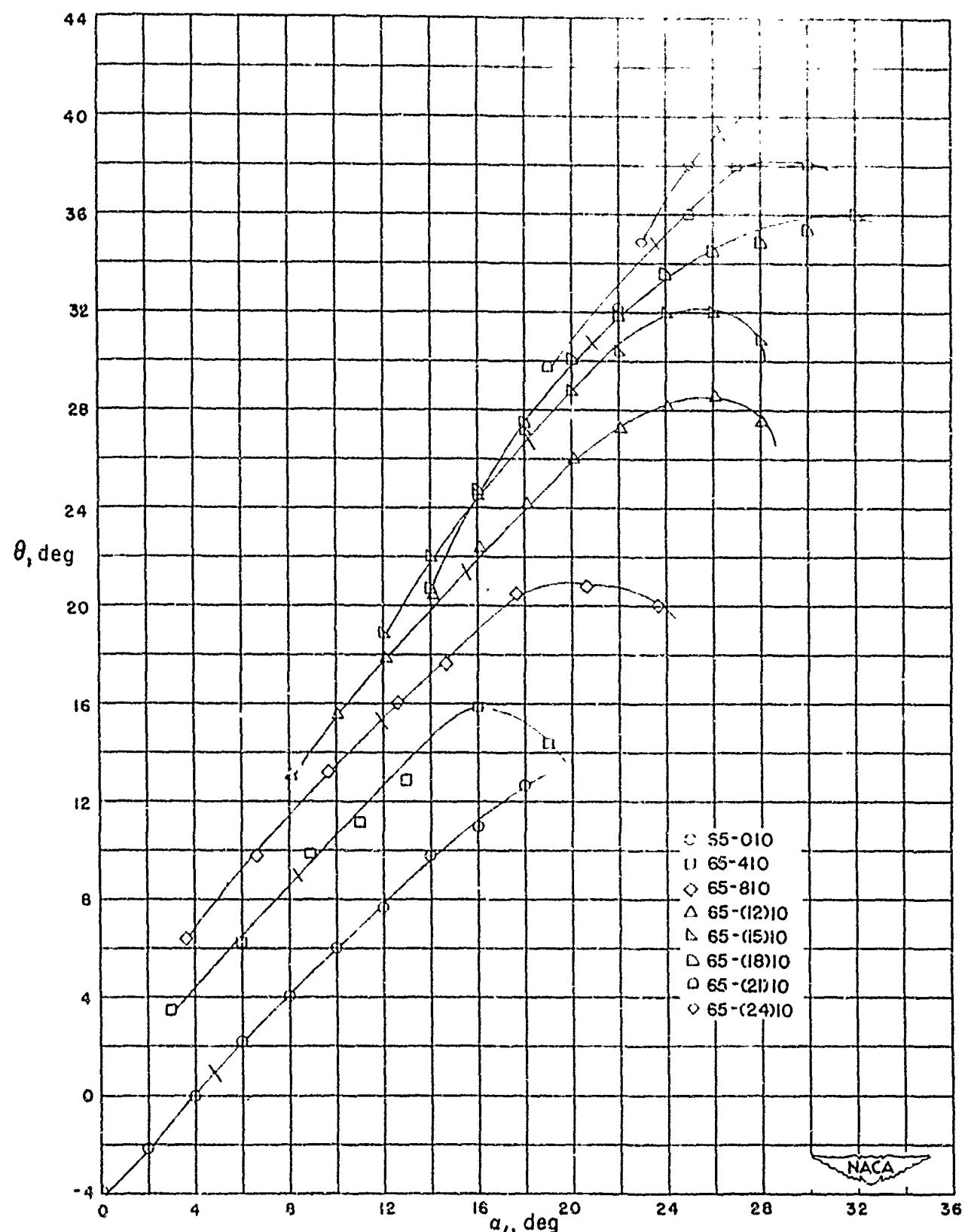


Figure 4-102 Summary of turning angle, θ , angle of attack, α , relationship for the blade sections tested at $\beta_1 = 60^\circ$. $\sigma' = 1.50$. Short bars across curves indicate design points. (Source: Ref. 4-4)

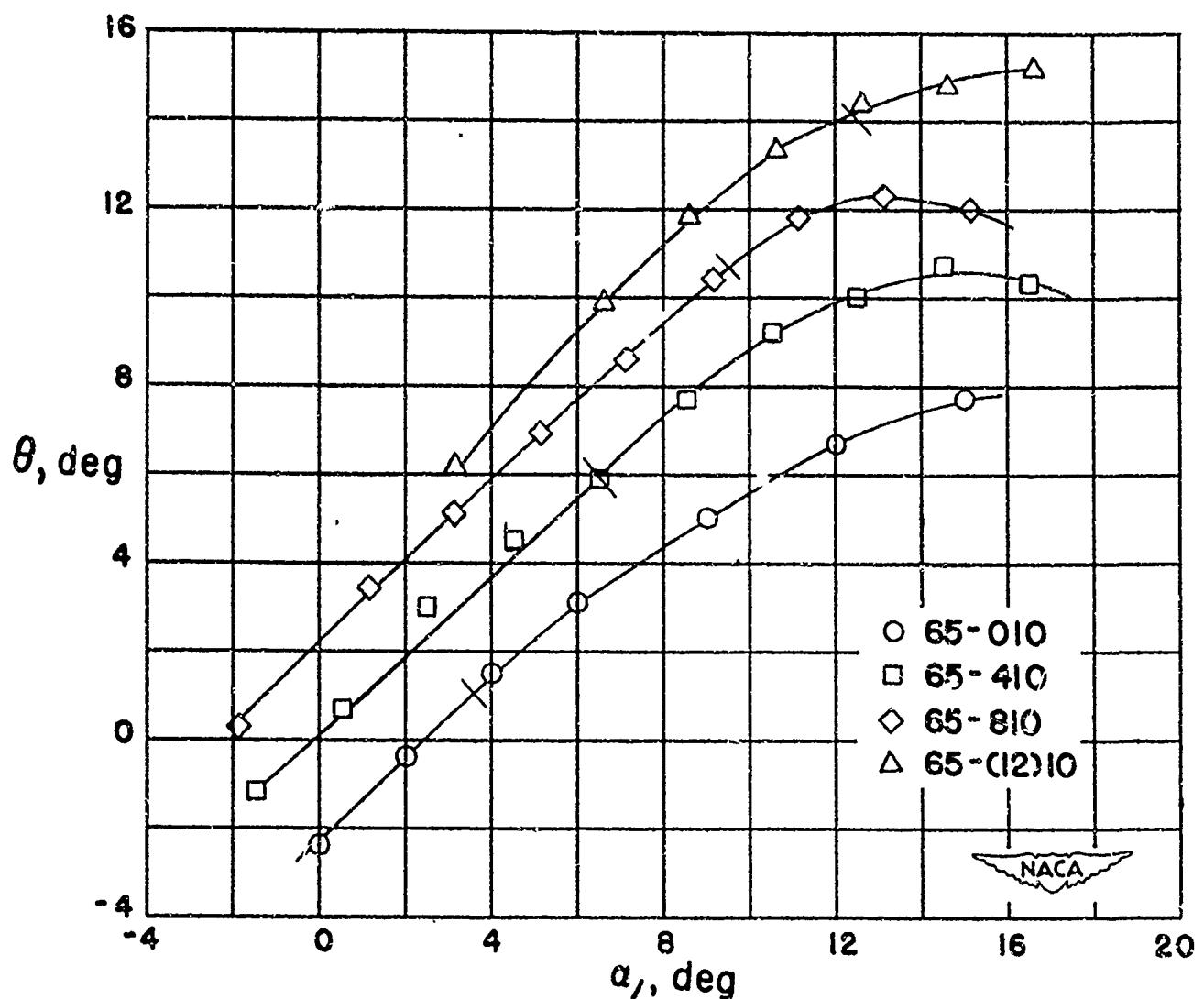


Figure 4-103 Summary of turning angle, θ , angle of attack, α , relationship for the blade sections tested at $\beta_1 = 70^\circ$, $\sigma' = 1.00$. Short bars across curves indicate design points. (Source: Ref. 4-4)

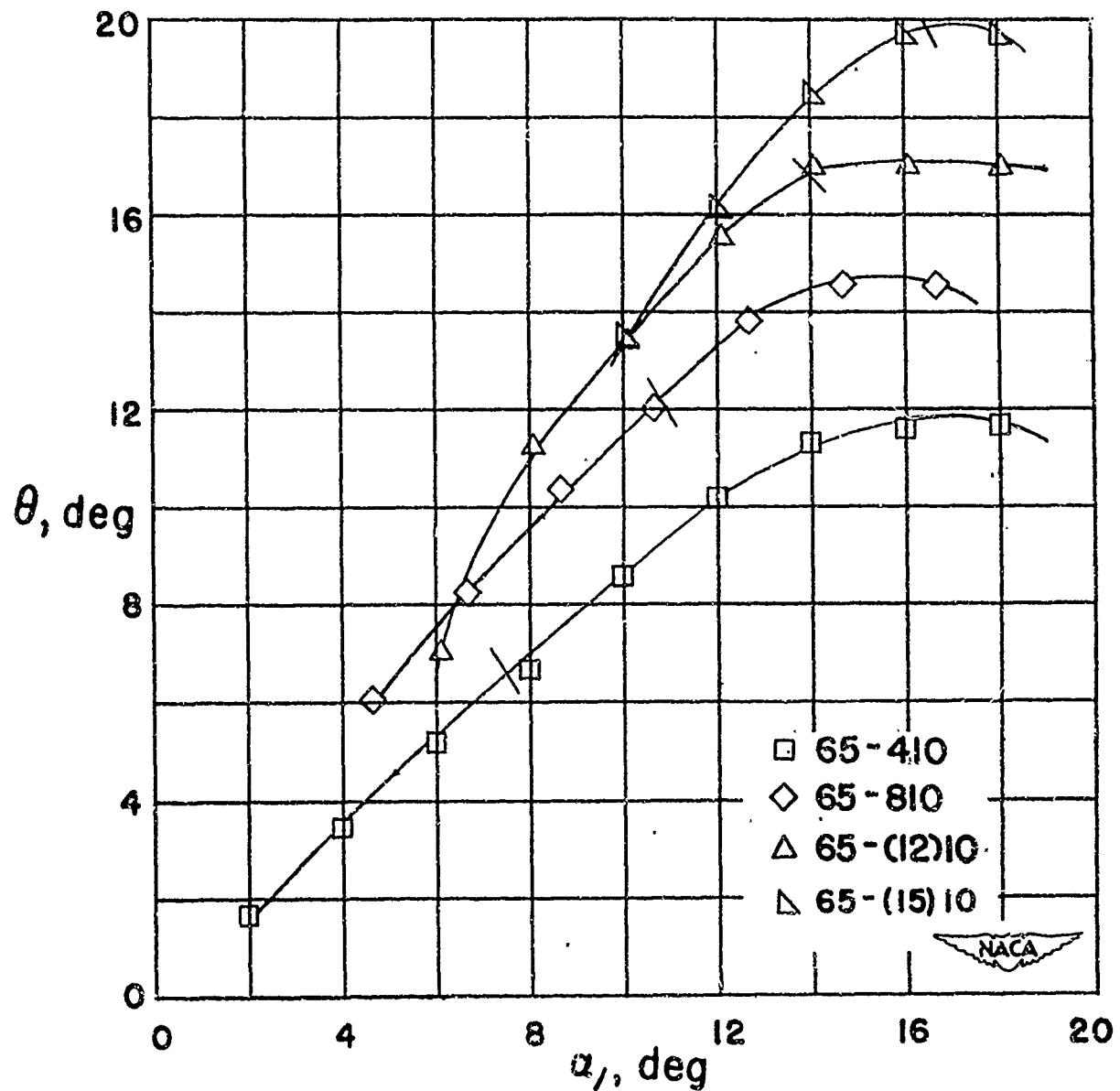


Figure 4-104 Summary of turning angle, θ , angle of attack, α , relationship for the blade sections tested at $\beta_1 = 70^\circ$, $\sigma' = 1.25$. Short bars across curves indicate design points. (Source: Ref. 4-4)

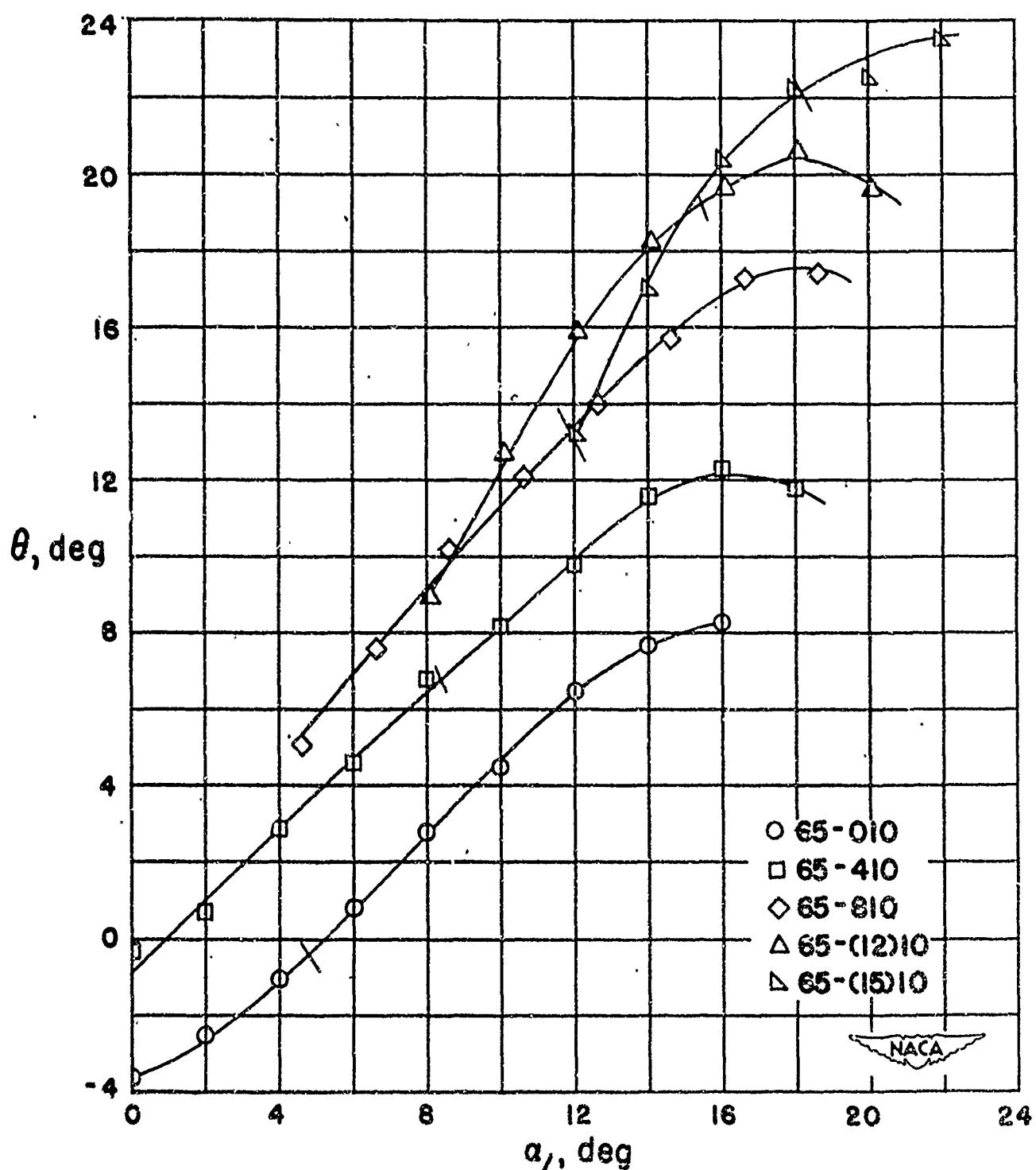
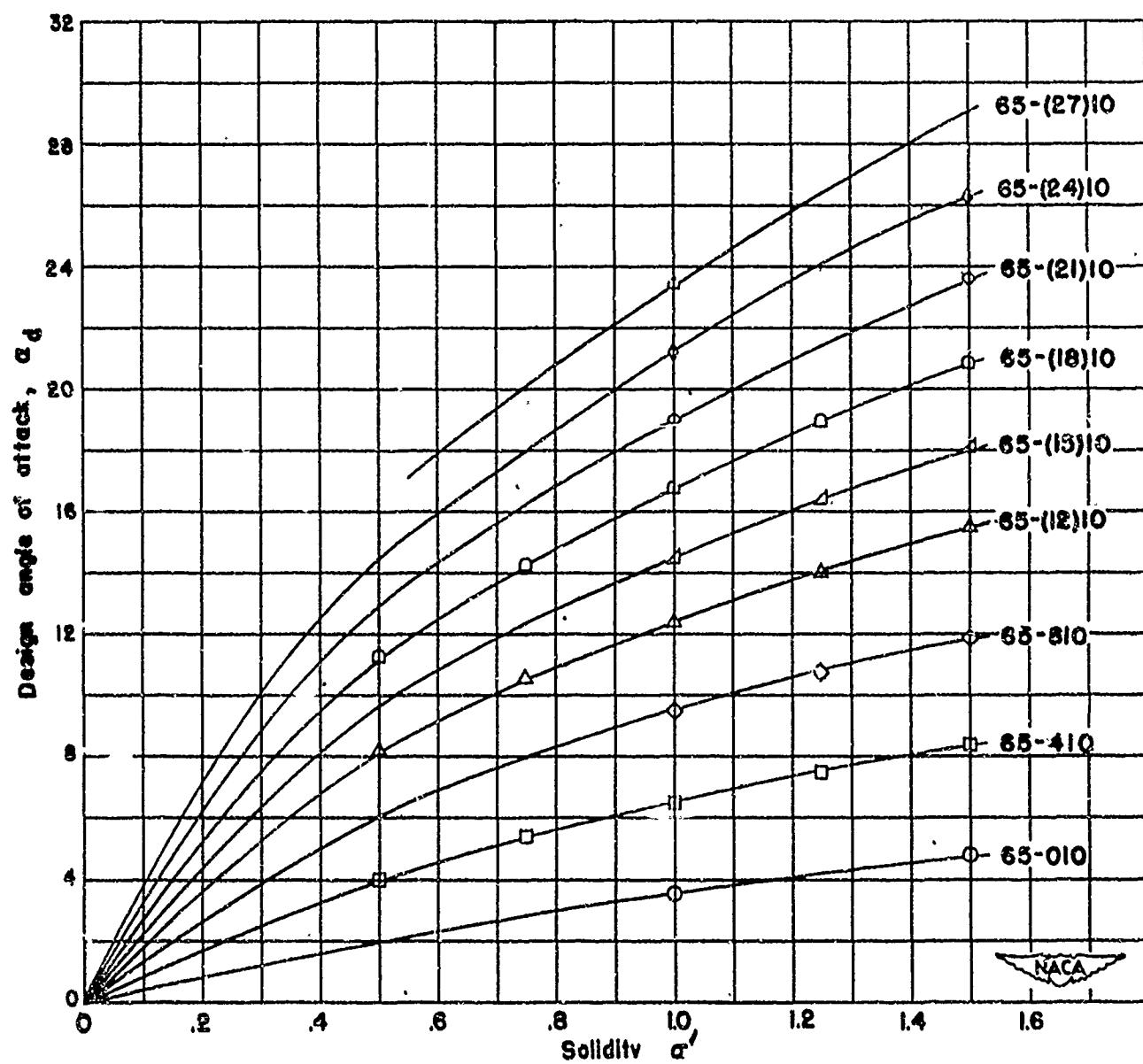
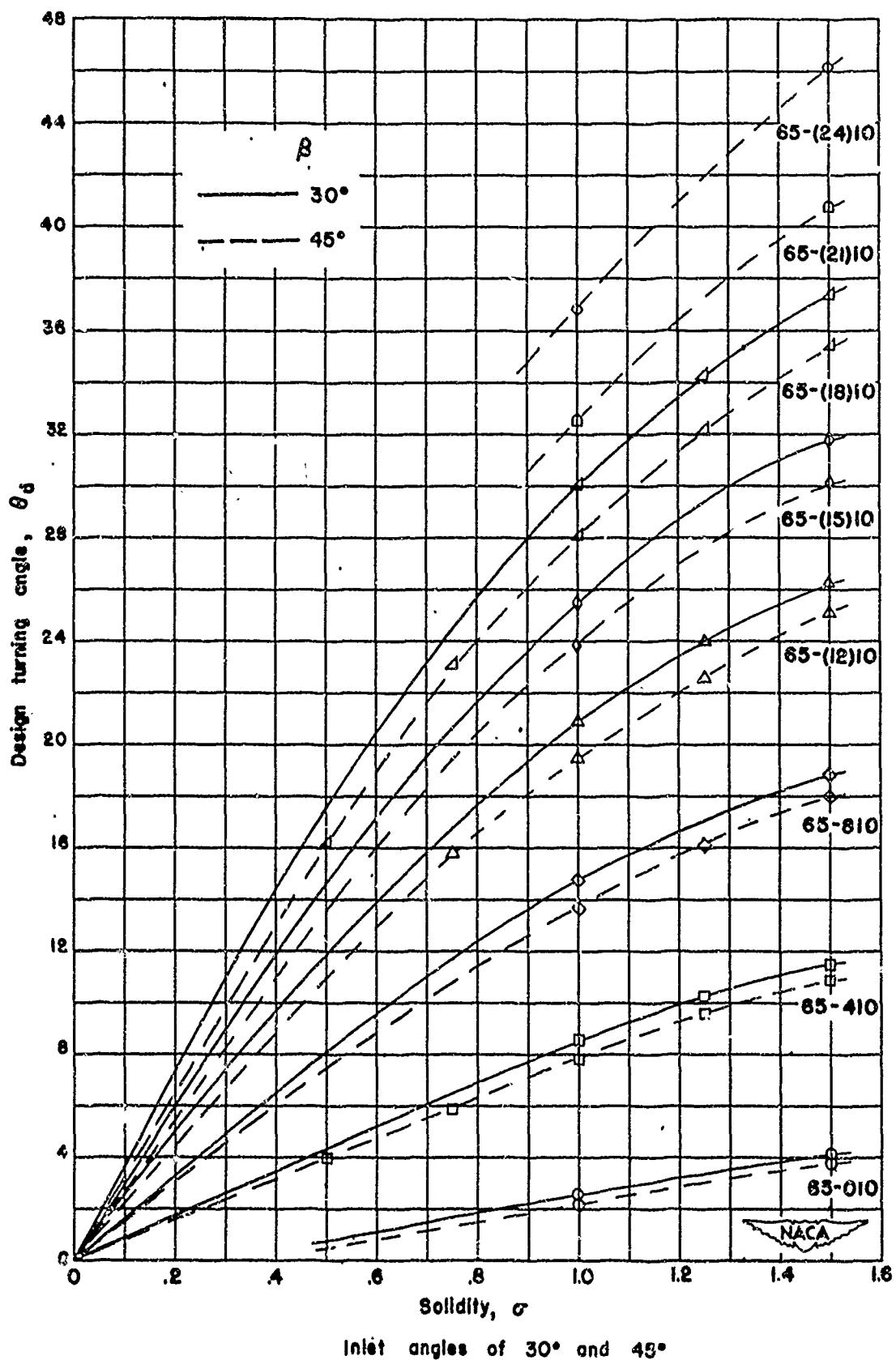


Figure 4-105 Summary of turning angle, θ , angle of attack, α , relationship for the blade sections tested at $\beta_1 = 70^\circ$, $\sigma = 1.50$. Short bars across curves indicate design points. (Source: Ref. 4-4)



Variation of design angle of attack with solidity for the sections tested.

Figure 4-106
(Source: Ref. 4-4)



Variation of design turning angle with solidity and inlet angle for the sections tested.

Figure 4-107 (a)
(Source: Ref. 4-4)

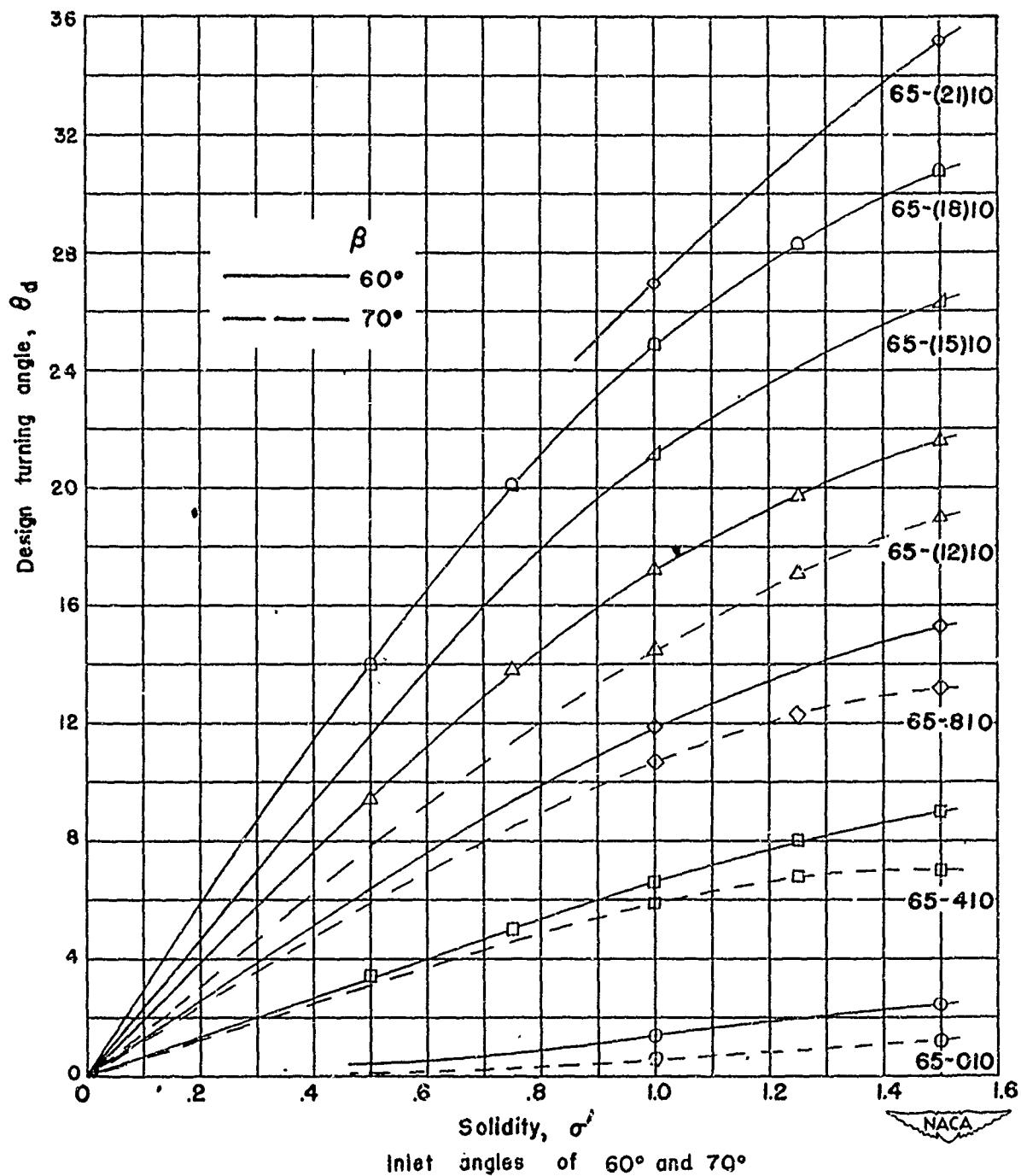


Figure 4-107 (b)
(Source Ref. 4-4)

FIGURE 4-108. Chart for Rap Determination of Fan Diamete

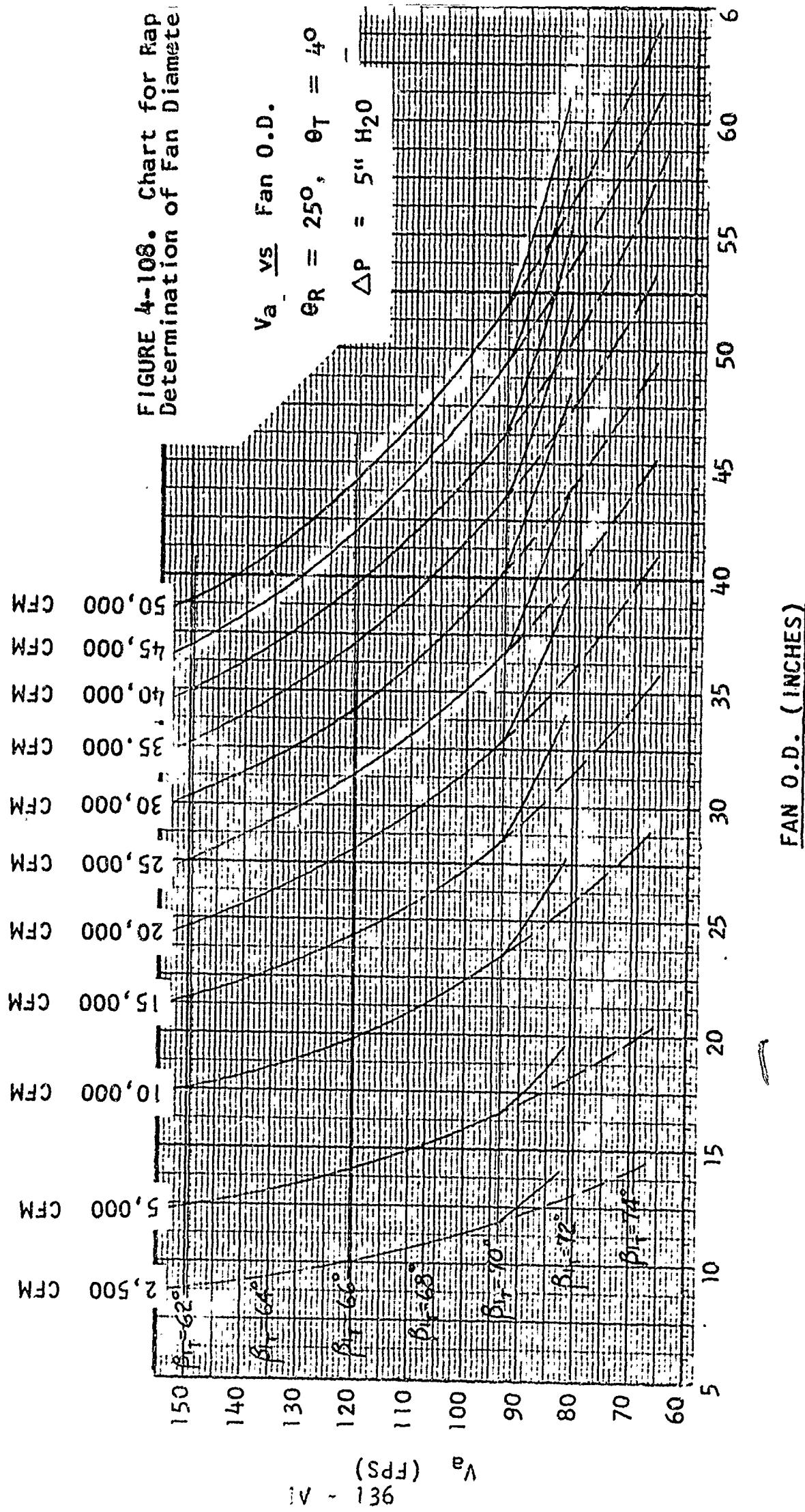


FIGURE 4-109. Chart for Rapid Determination of Fan Diameters

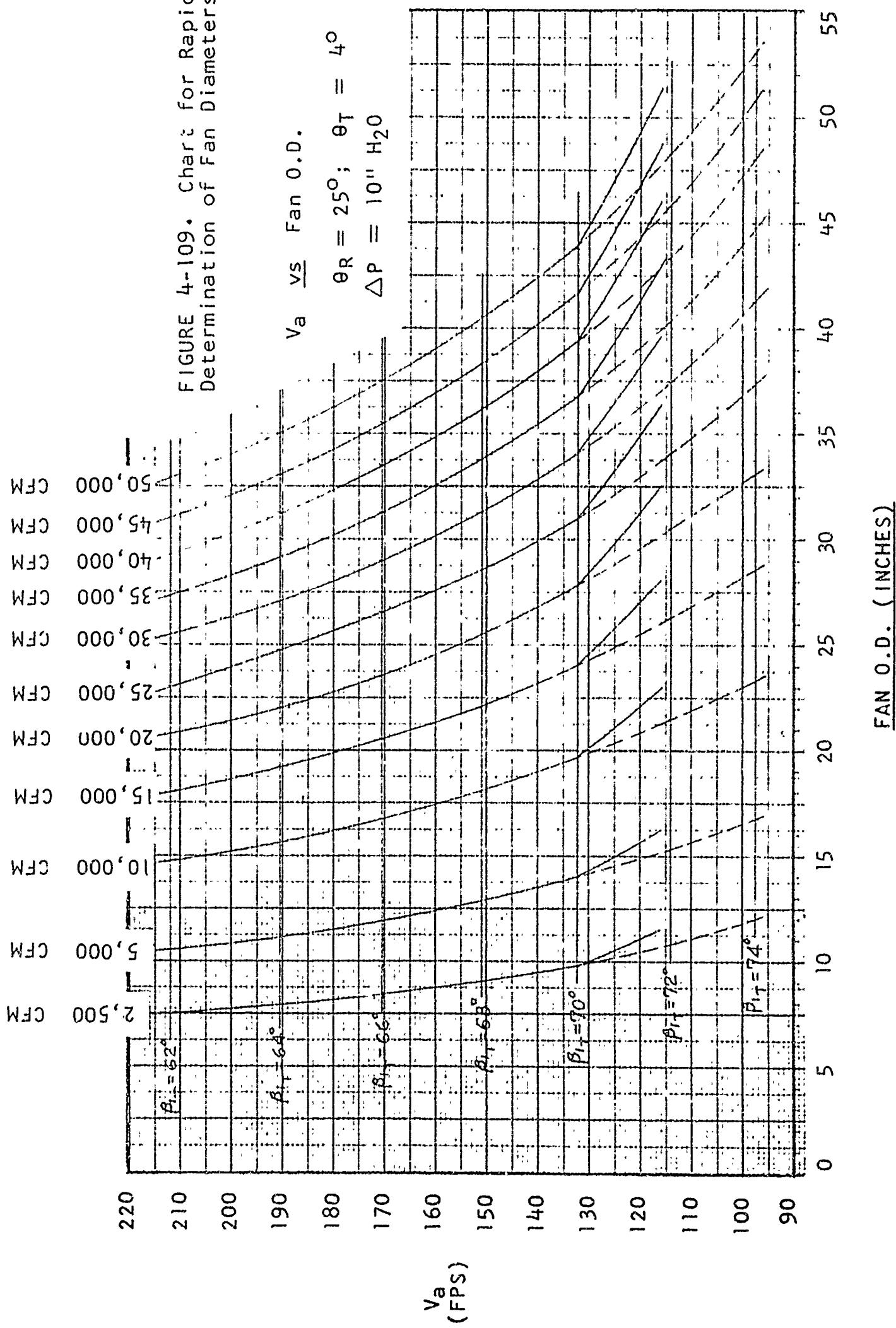


FIGURE 4-110. Chart for Radio Determination of Fan Diameters

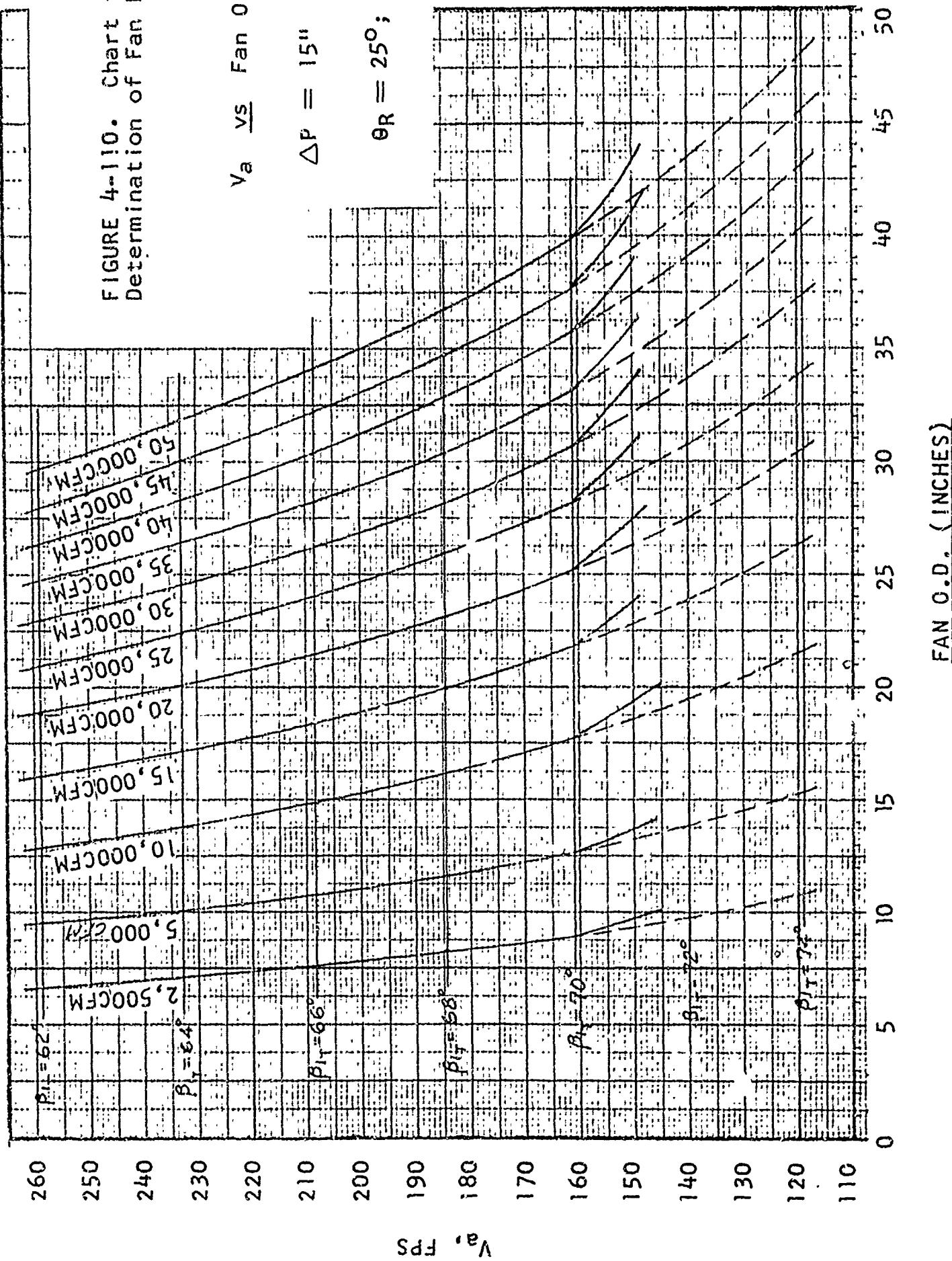
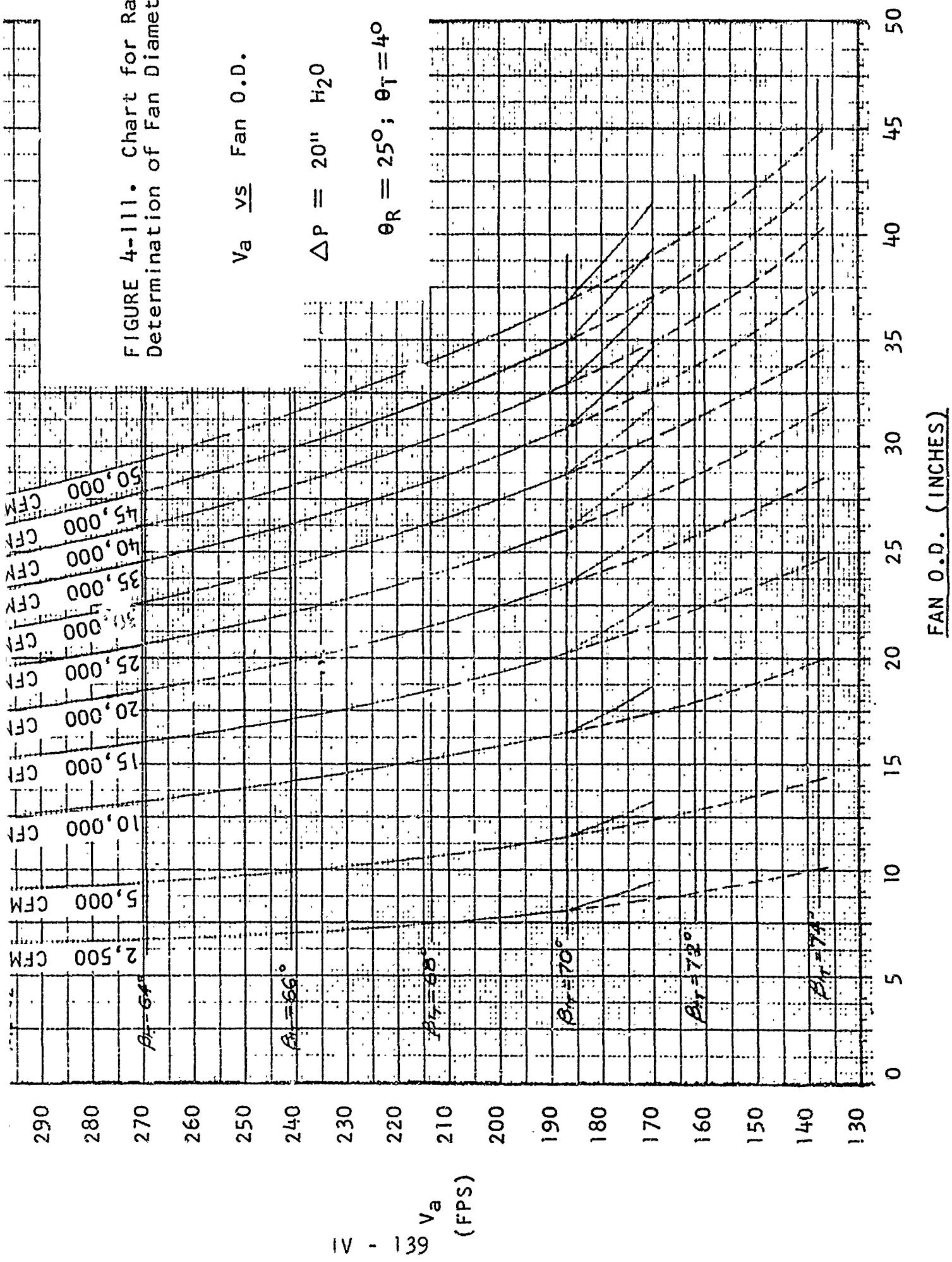
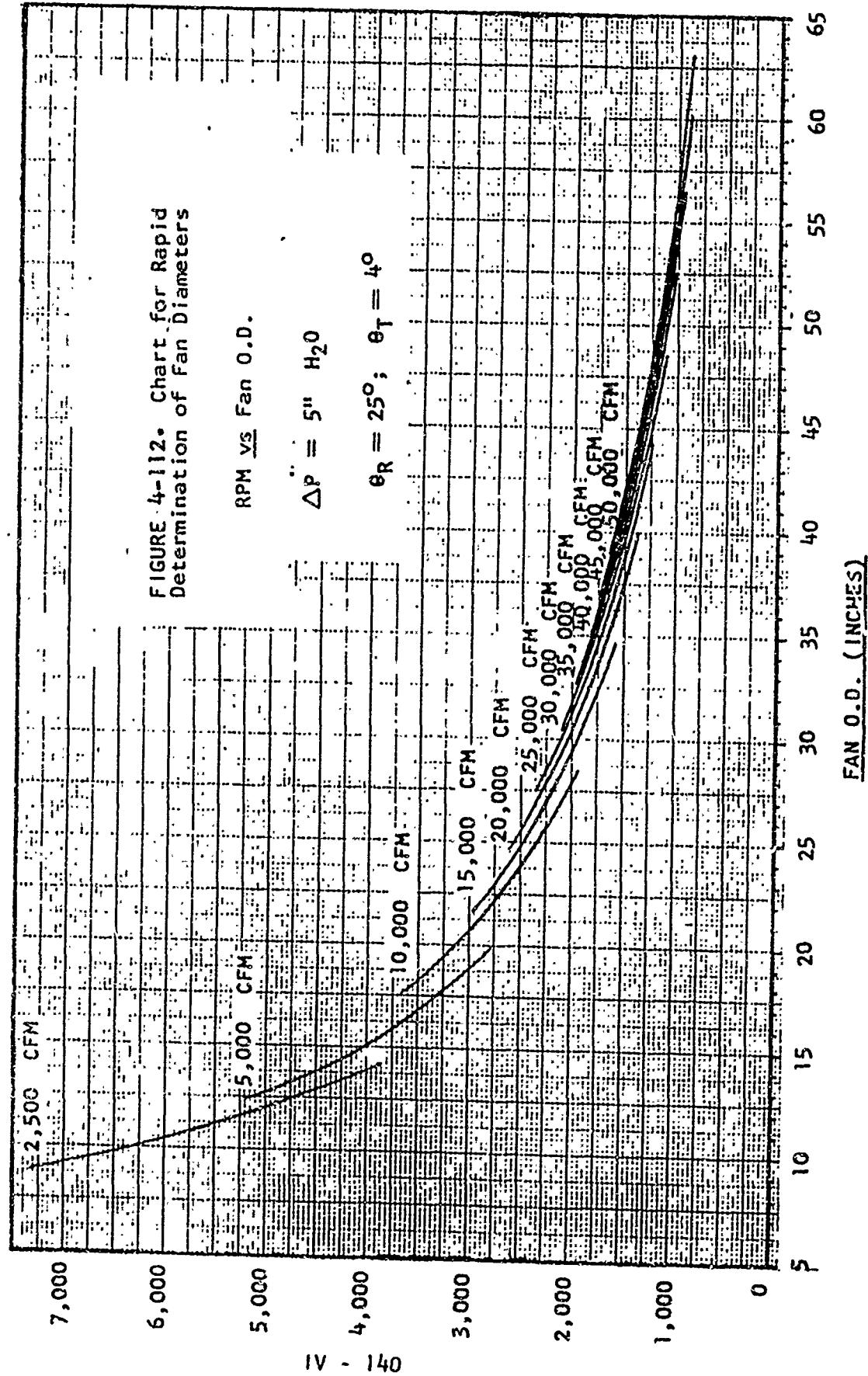
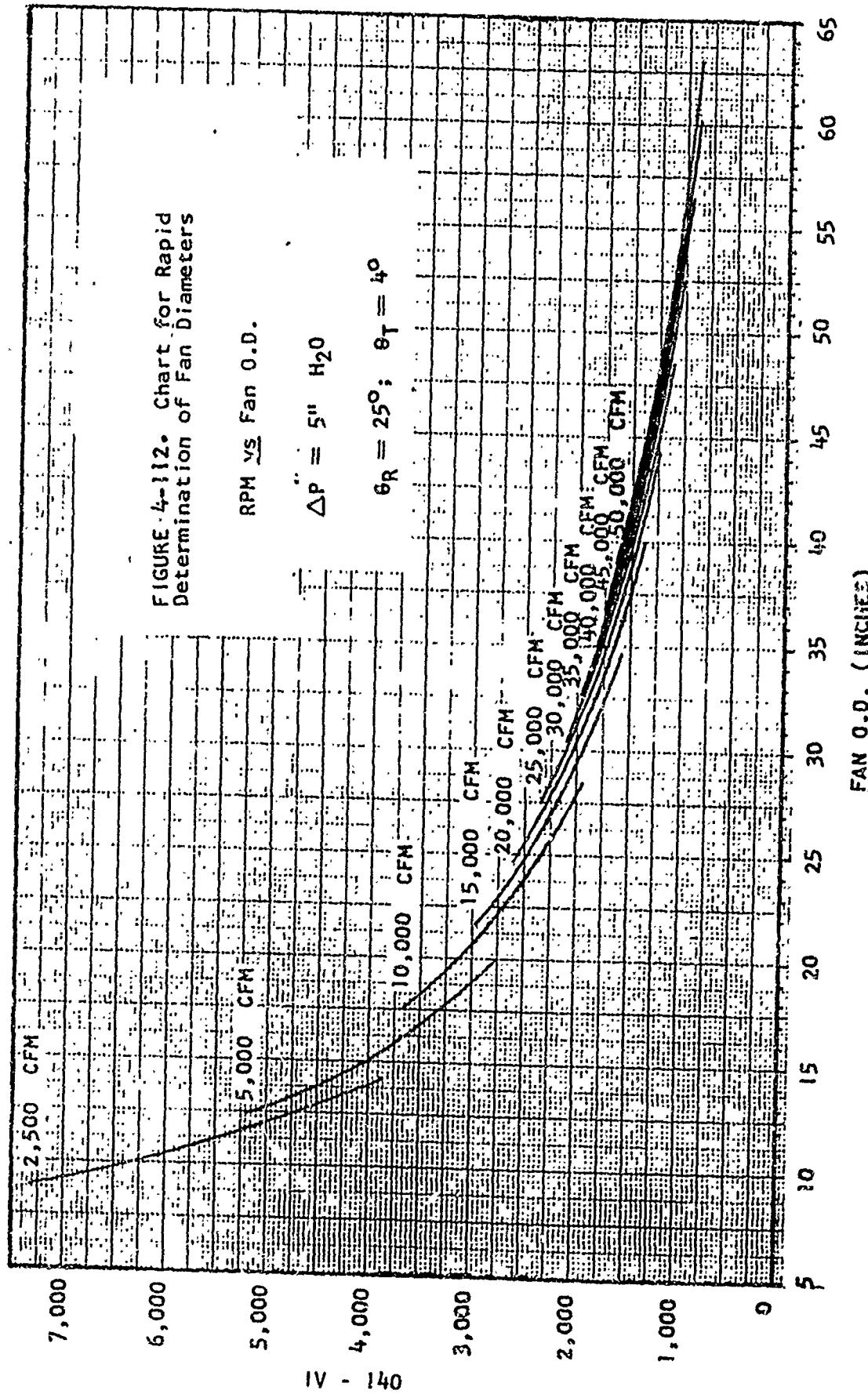


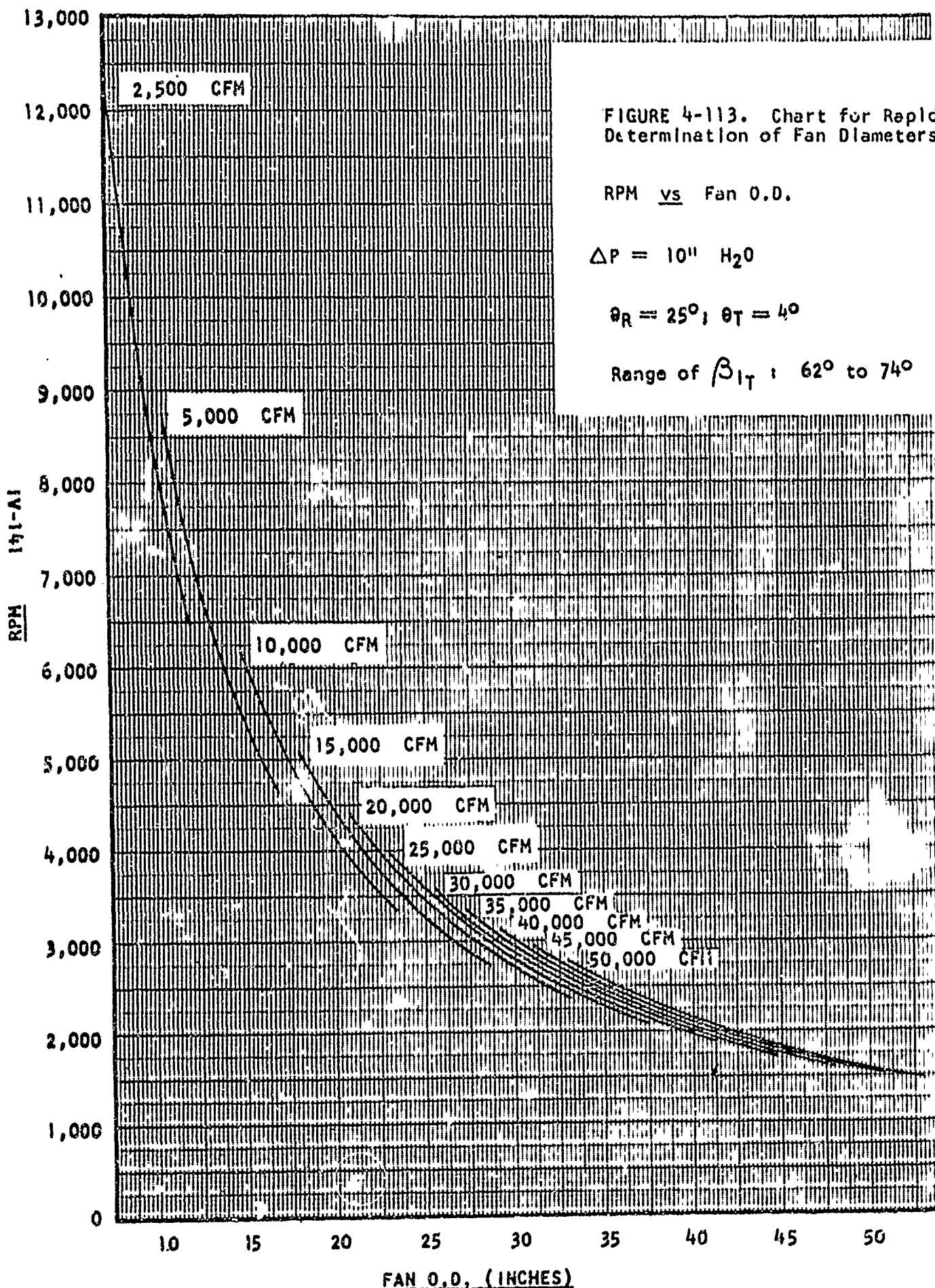
FIGURE 4-111. Chart for Rapid Determination of Fan Diameters



$\frac{\Delta P}{\text{in}}$







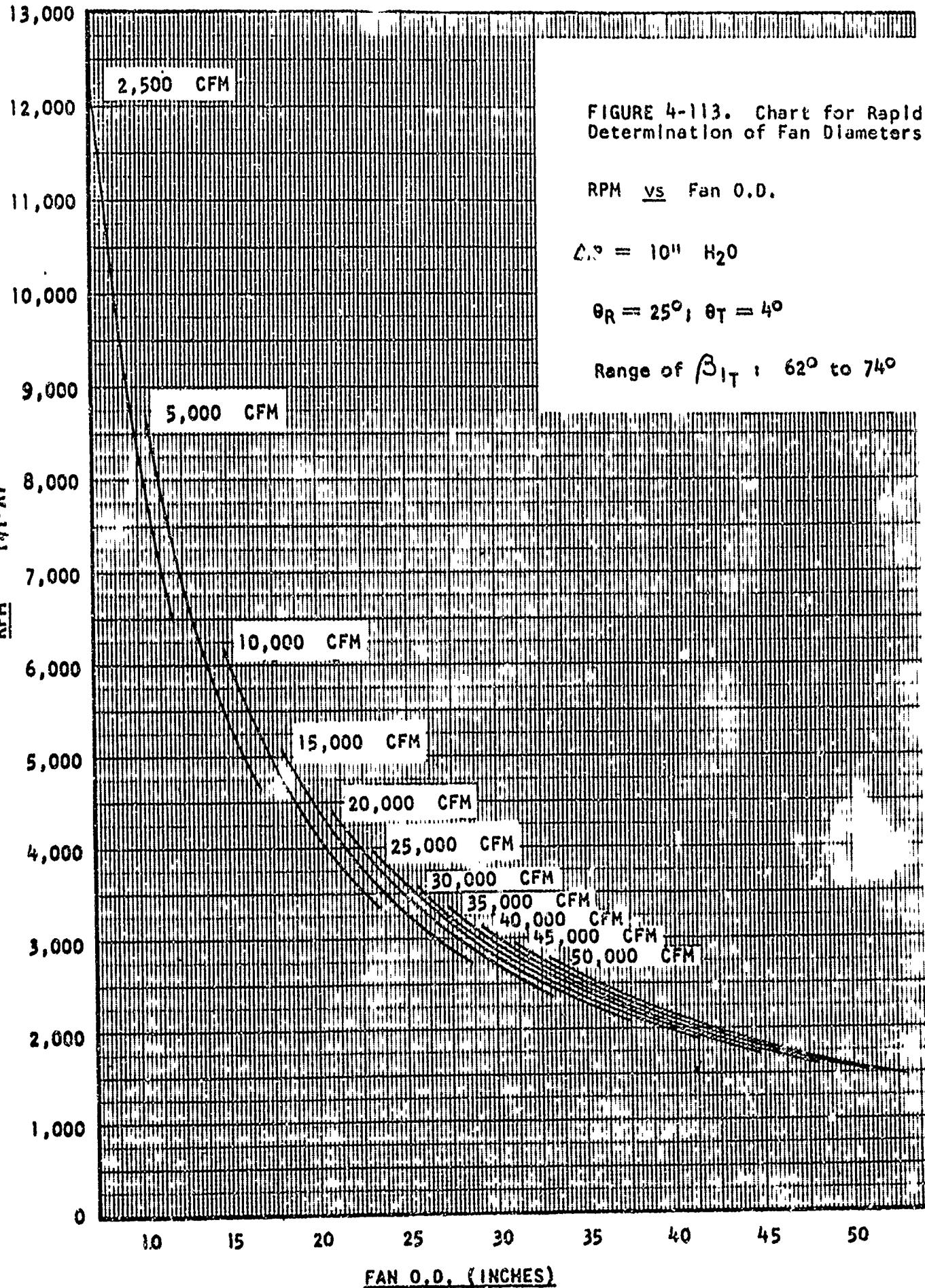


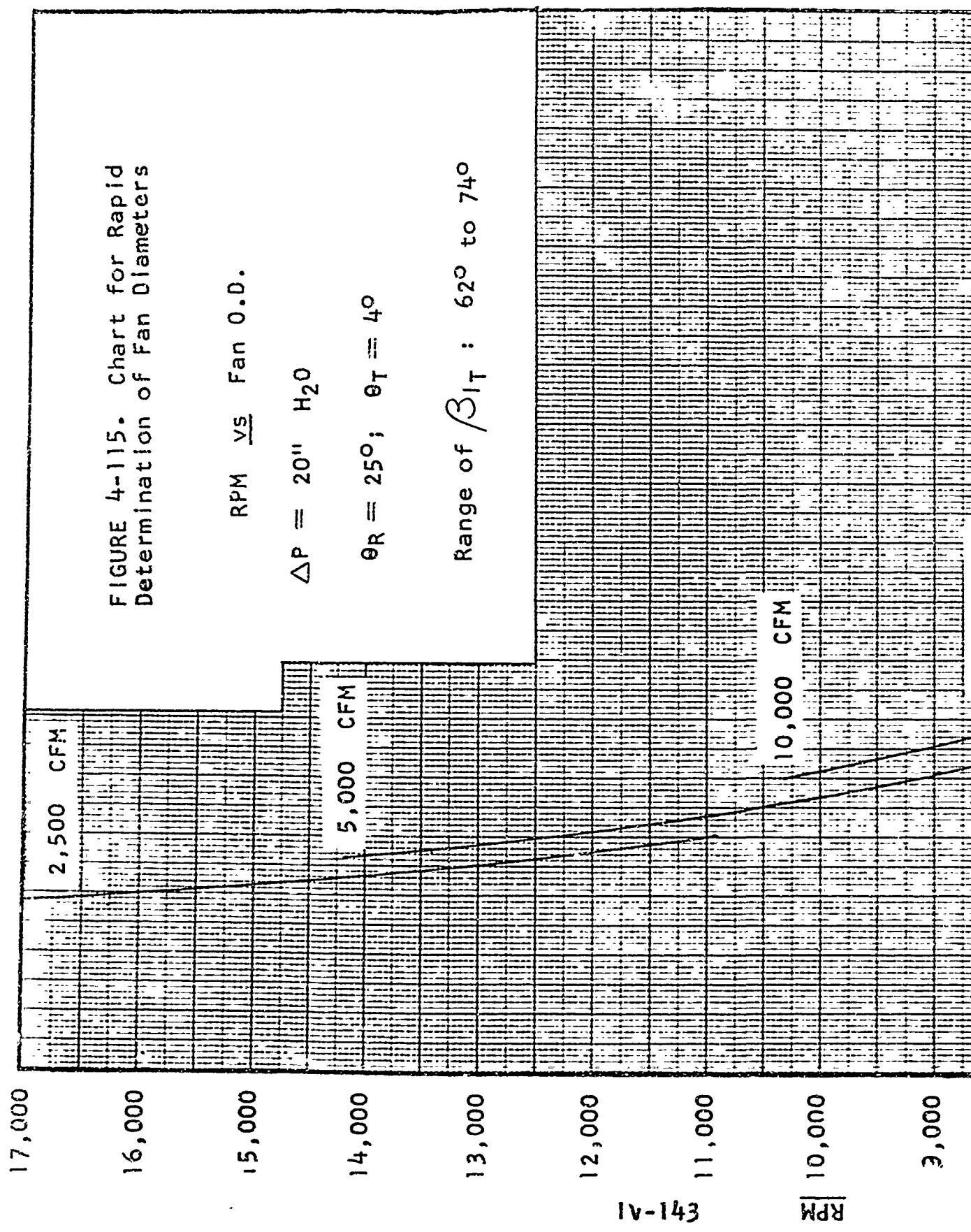
FIGURE 4-113. Chart for Rapid Determination of Fan Diameters

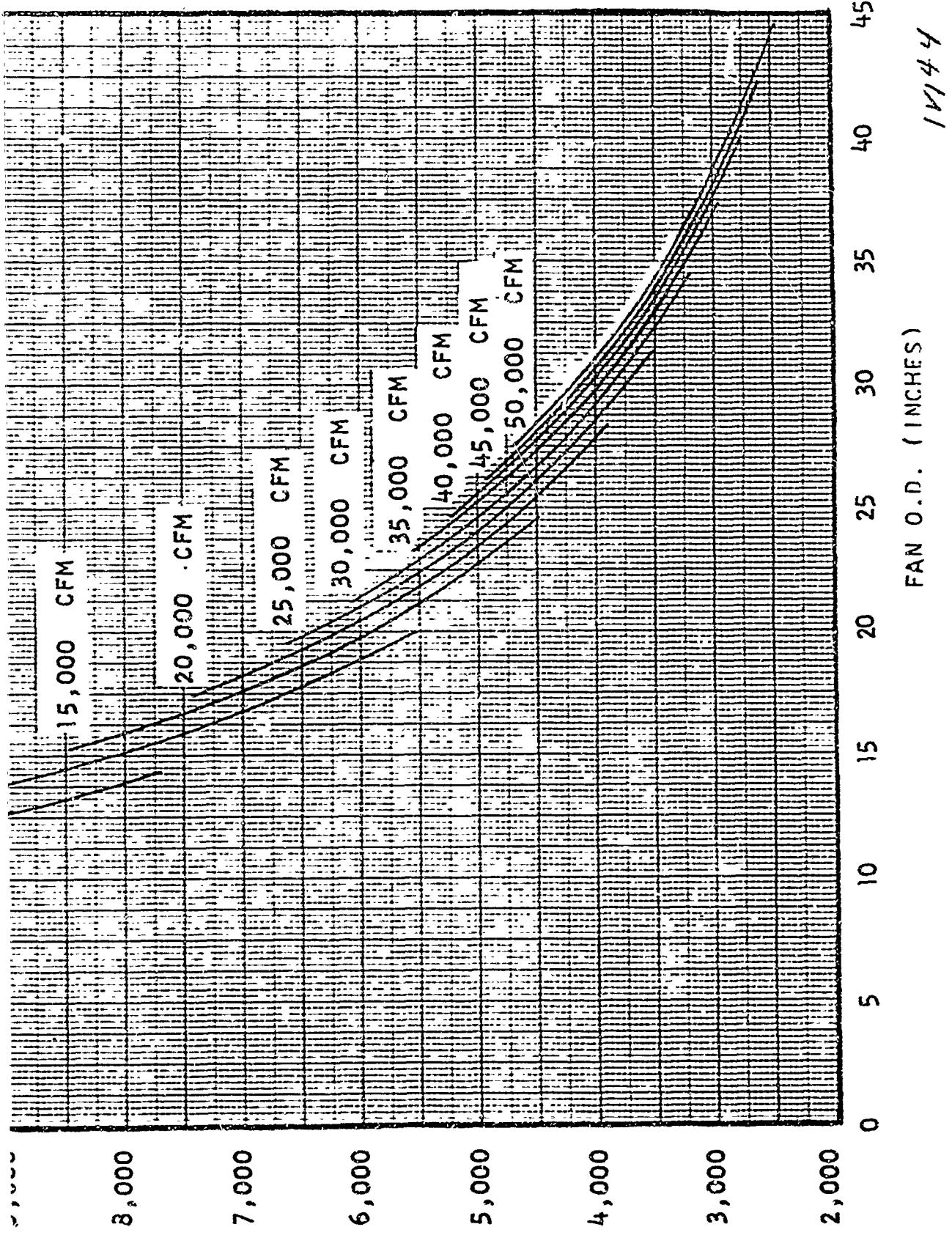
RPM vs. Fan O.D.

$$\Delta P = 10'' \text{ H}_2\text{O}$$

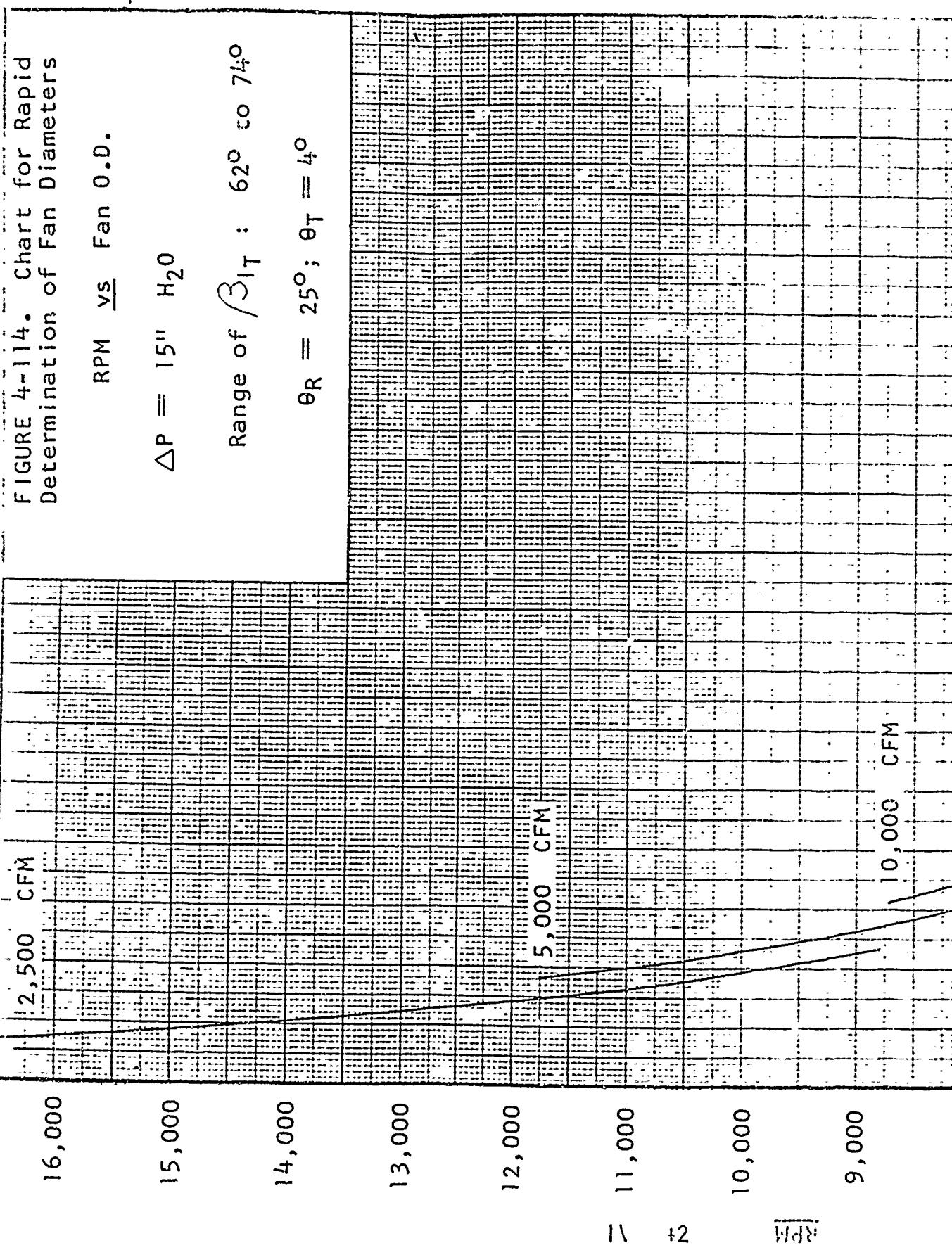
$$\theta_R = 25^\circ, \theta_T = 40^\circ$$

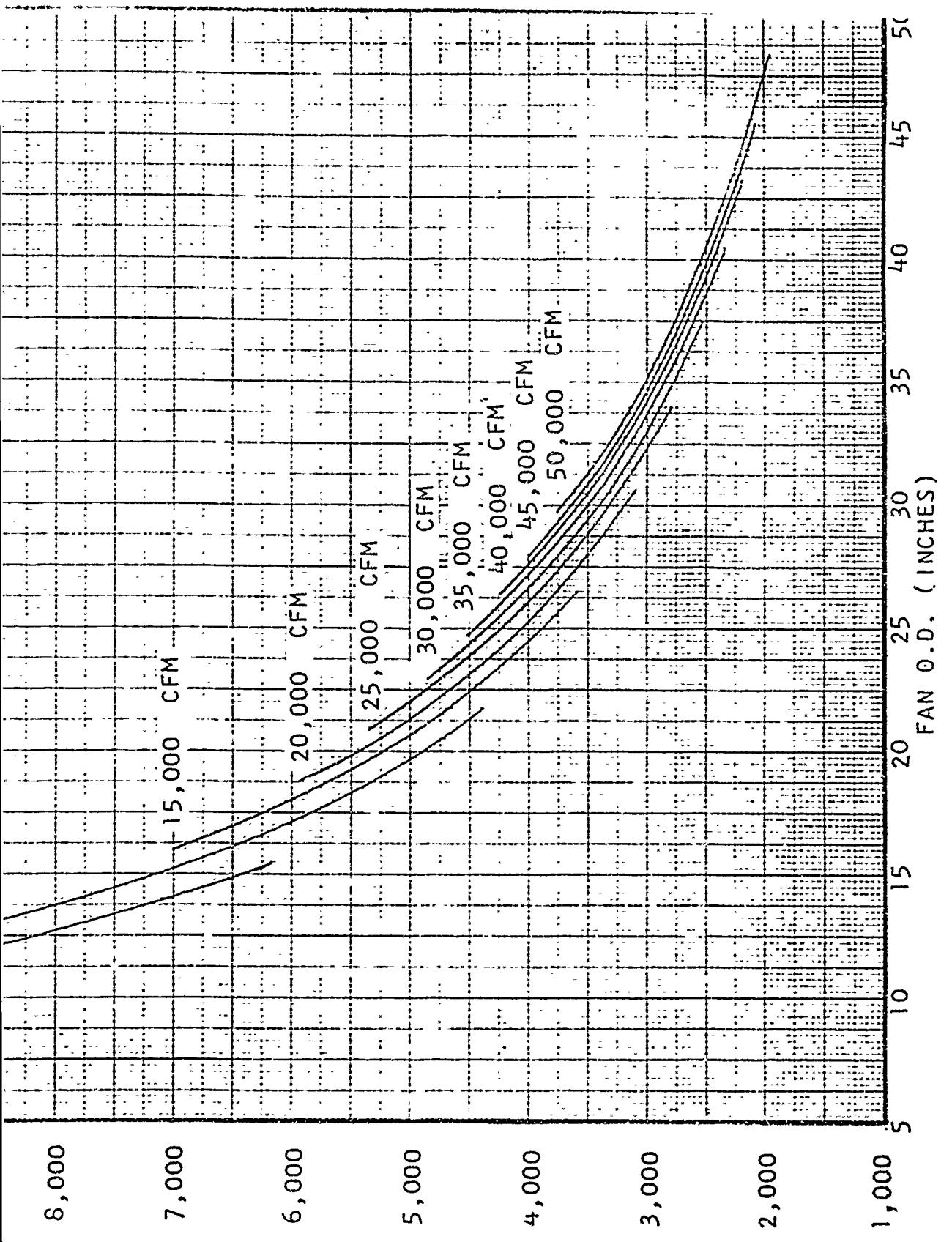
$$\text{Range of } \beta_{1T} : 62^\circ \text{ to } 74^\circ$$





1V144





1143

4-2.5.0 Physical Fan Design Considerations

This chapter, so far, has been devoted almost exclusively to the aerodynamic considerations of fan design. In this section the physical design and fabrication methods for various fan configurations will be discussed. The data and recommendations presented are based on the currently known state of the art and must, therefore, be tempered by continual cognizance of development progress.

4-2.5.1 General

A fan installation basically consists of a rotor assembly and a stator assembly together with their necessary mounting provisions. The design of this unit must always be a compromise to achieve the most advantageous combination of the following requirements:

- (a) Aerodynamic performance.
- (b) Minimum horse power absorption.
- (c) Adequate moment of inertia if rotor must contribute flywheel assistance.
- (d) Minimum weight.
- (e) Acceptable vibration and dynamic balance characteristics.
- (f) Adequate strength and service life.
- (g) Minimum cost.
- (h) Climatic and environmental suitability.
- (i) Ease of maintenance.
- (j) Fabrication methods compatible with available equipment and anticipated production quantities.
- (k) Customer installation and detail specifications.
- (l) Interchangeability of the installation, sub-assemblies and detail parts to the extent practicable.
- (m) Minimum dimensional envelope compatible with the overall arrangement.
- (n) Optimum material selection.

The fan installation and its components should function satisfactorily throughout the temperature range in which they may be required to operate. The effect of latent heat after shutdown and the customer's specified range for equipment of this type should be considered in establishing this temperature range.

The workmanship should be in accordance with high grade aircraft manufacturing practice for this type of equipment. The fan and its component parts should be designed for a minimum of 500 hours service tour, or an engine overhaul, whichever is greater.

4-2.5.1.1 Drawings and Procurement Specifications

The drawing, together with all procurement specifications, is very much a part of good fan design. The drawing should be so executed that the function and assembly of all components can be readily determined. The assembly and/or outline drawing should contain all reference data (functional, dimensional, weight) and loading conditions essential to its usage. The various loading conditions to which the fan assembly must be designed should be noted in the procurement specification or on the face of the assembly drawing. Following is an example of the loading conditions that should be applied to a typical fan design. The exact values for the various conditions depend on the particular fan under consideration and should be so noted on the drawing:

OPERATION	CONDITION	UNITS
Start-Stop	Angular Acceleration	Radians/Sec ²
Overspeed	Rotational Speed Brake Horsepower	RPM
Maneuver with fan at maximum operating speed	Pitch, Yaw or Roll Velocity Rotational Speed Brake Horsepower	Radians/Sec. RPM
Continuous	Rotational Speed Brake Horsepower	RPM

The following factors should be considered in establishing the loading conditions:

- (a) Aerodynamic loads should be used in conjunction with the above design conditions except "Start and Stop".
- (b) The fan should not yield under loads arising from any of the above operating conditions. For the purpose of stress analysis, the loads should be increased by a limit load factor of at least 1.25. Further, the fan should have an infinite operating life under the continuous operating condition.
- (c) Consideration should be given to the fan oscillation through pitch and yaw angles at a specified rotational speed (RPM).
- (d) The selection of the overspeed RPM should insure that the fan will not disintegrate if it is inadvertently operated over the maximum normal operating speed.
- (e) The ultimate loads should be one and one-half (1.5) times the limit load.

To assure interchangeability, the drawing should indicate the tolerances required between the component parts.

4-2.5.1.2 Materials and Processes

The material used for fan construction will depend largely on the method of fabrication and the use for which the fan is intended. However, under all circumstances the materials should be of aircraft quality and chemically analyzed and inspected to make certain that they conform to all applicable specifications. The material should have resistance to corrosion, fungi, moisture, operational temperature extremes, direct sunlight and other similar atmospheric phenomena such as ozone and dust without depending upon protective coatings. When protective coatings are specified they should conform to applicable specifications. Dissimilar metals in contact should be either passivated or mechanically insulated to avoid galvanic action. Care should be exercised in selecting the location for any permanent identification marking of dynamic parts.

Standard materials used in design of units other than fans can be used. Typical alloys for consideration are weldable 6061 aluminum alloy, castings of 356-T6 aluminum alloy and AZ91 or magnesium-rare earth alloy, magnesium alloy plate AZ31, 2014 or 7075 aluminum alloy forgings. Each of the materials varies in minimum properties, has limitations in fabrication, reproducibility of quality and may have a significant effect on the design. Several of these significant factors are (a) porosity of castings may lead to trouble in balancing of the fan, (b) alloy quality and surface finish obtainable by some of the fabrication techniques affect endurance limit and life of the component, (c) damping characteristics of alloys vary and may affect endurance life of the component. Good fatigue strength is desirable for fan blades.

As vibration may subject the unit to fretting, proper material selection or the appropriate processing, such as "hardcoating", chrome-plating, or local cold working may increase the endurance life of the unit.

4-2.5.2.0 Rotor Assembly (See Figures 4-116 and 4-117)

A rotor assembly basically consists of a wheel assembly and fan blades. Consideration may be given to casting or forging the rotor as a one piece unit with integral blades. This approach may, for some configurations, show advantages in weight, production cost, and vibration and balance control. However, the inherent disadvantages of one piece fabrication such as tooling costs, rejection costs, maintenance costs and inefficient flywheel characteristics may dictate a multi-detail assembly. The combination mold method of integral sand cast disc and plaster cast blades is limited to the following conditions:

- (a) Blade angle minimum tolerance $\pm 2^\circ$.
- (b) Finest surface finish - 150 RMS for plaster cast blades.
- (c) Present state of the art limits the rotor diameter to approximately twenty inches.
- (d) Casting material is limited to aluminum alloy where the plaster mold process is used in the area of the blades. Magnesium alloy does not cast satisfactorily in plaster molds unless the molds are especially prepared.
- (e) A single defective blade integrally cast to the disc and hub may cause rejection of the complete unit. Damage to a single blade in service may also cause rejection of the complete unit.

For certain applications such as the cooling fan for a reciprocating engine which does not directly drive a propeller, the rotor must also function as a flywheel. The moment of inertia which must be contributed by the rotor assembly is specified by the engine manufacturer. This obligation can be most efficiently satisfied in the early stages of the rotor design by the judicious distribution of its component mass. A separate inertia ring may be required.

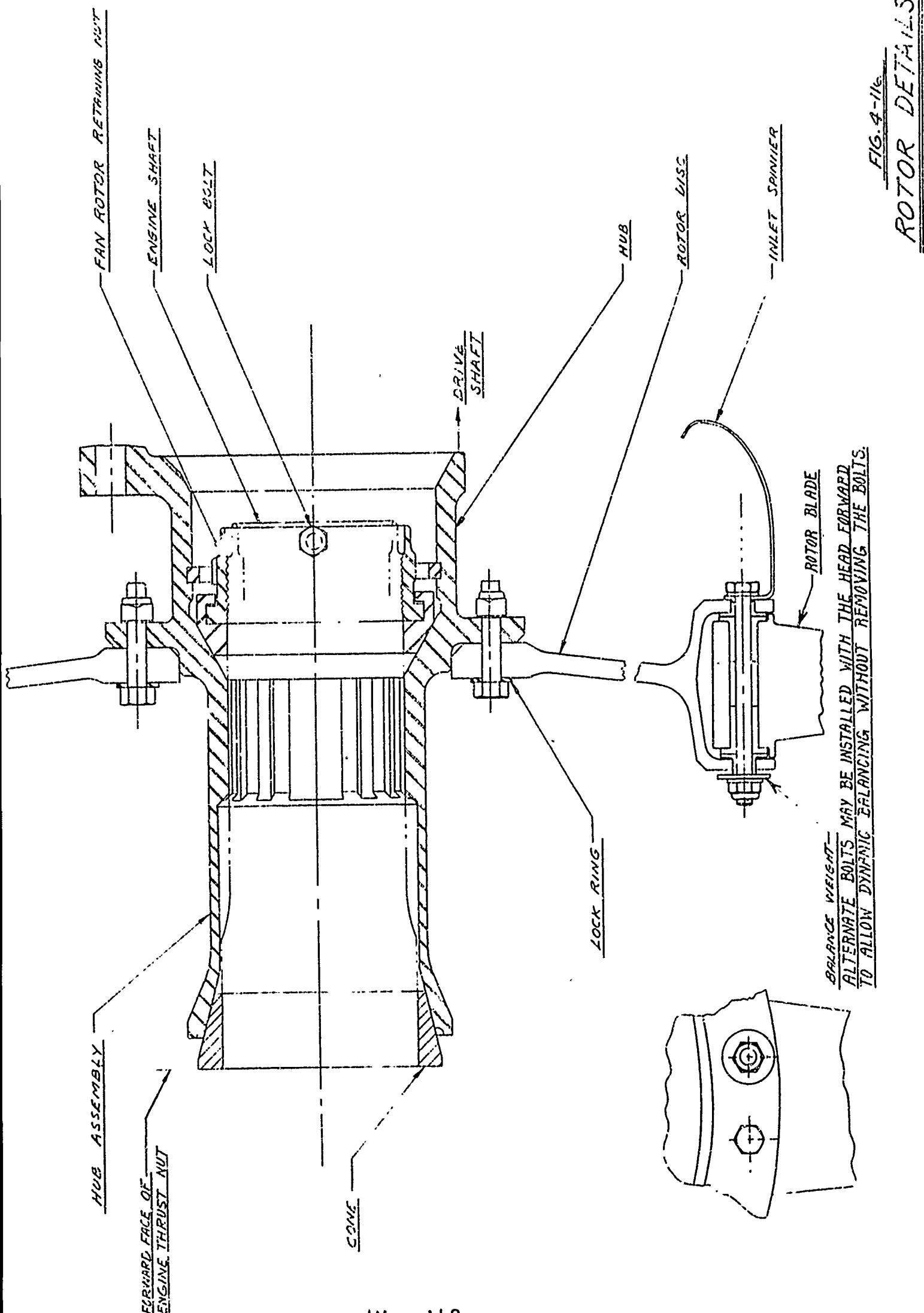
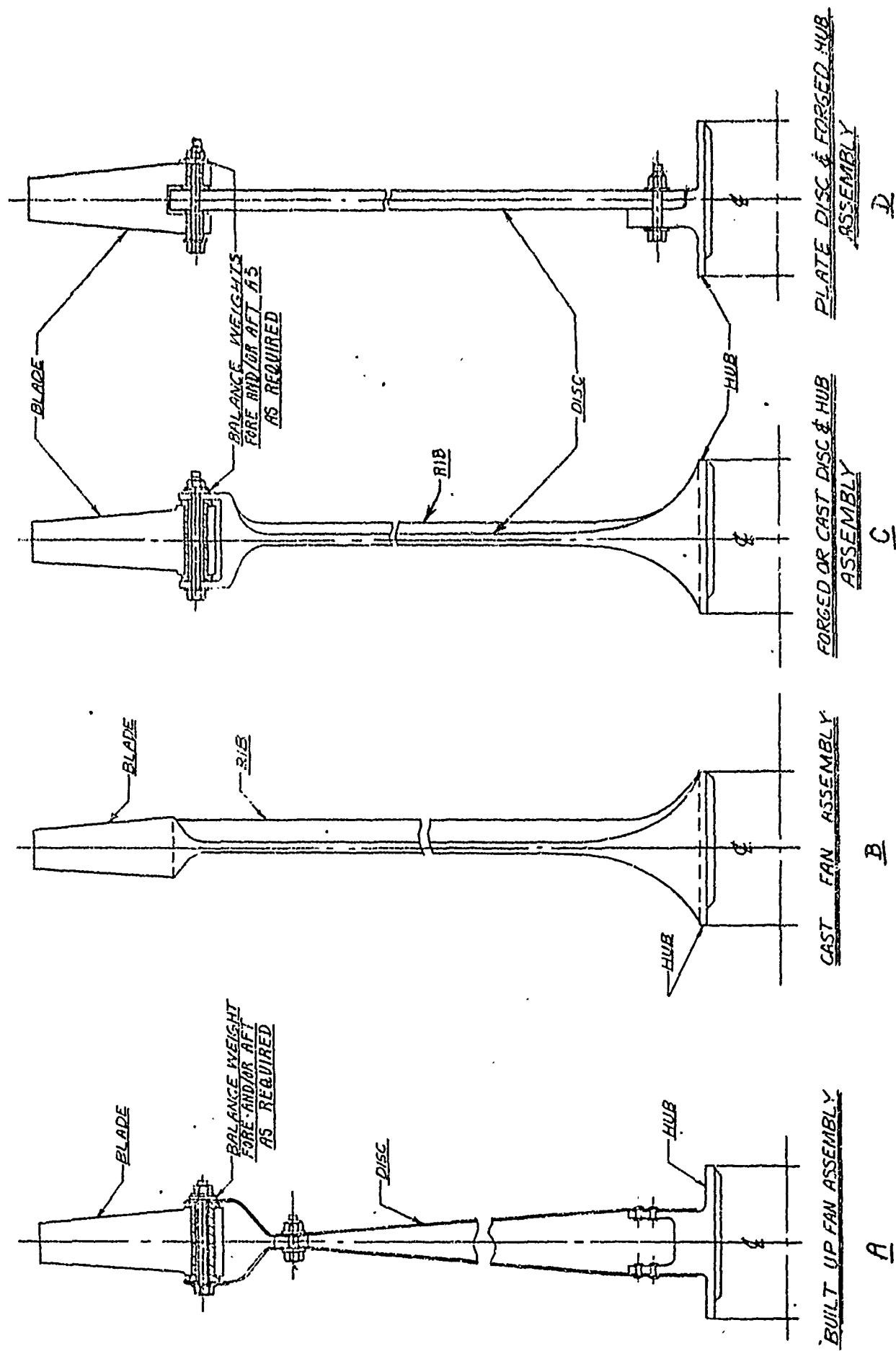


FIG. 4-117 TYPICAL FAN
ROTOR ASSEMBLIES



ROTOR ASSEMBLIES

Gaps in the blade root surface should be eliminated or reduced to a practical minimum to increase the available pressure rise and efficiency. Since the clearance between the blade tips and the rotor cowling should be maintained at a minimum to avoid undesirable flow behavior with resultant losses, the dimensional tolerance and the concentricity of the diameter over the blade tips should be closely controlled. In addition to manufacturing and assembly tolerances, the growth of components such as elastically mounted blades under centrifugal loading should be considered. Grinding the blades on the assembled rotor to the prescribed diameter may be considered.

After the wheel and blades are assembled and the blade tips ground, if necessary, the assembly should be tracked normal to the axis of rotation, checked for concentricity about the axis of rotation, and dynamically balanced.

4-2.5.2.1 Wheel Assembly

The wheel basically consists of a hub, web, peripheral means of adapting the blades and an inlet spinner. The inlet spinner should extend upstream from the blade root line and be contoured to provide an efficient entry for the fan. (See Figure 4-116).

The wheel can be an assembly with the individual components riveted or bolted together or the wheel can be forged or cast as a unit. Standard tolerances may preclude the use of both the forging and casting. Large working tolerances may involve too much dead weight or require excessive machining to remove the unwanted weight. In addition to the fabrication tolerances, the minimum thickness required of both the castings and forgings may add to the over-all weight.

A performance tested method, of attaching the disc to the hub, is provided by a series of bolts parallel to the axis of rotation, extending through the disc and a radial flange on the hub. These bolts, however, should not be the prime means of holding disc to hub concentricity. This concentricity should be provided for by means of a shoulder on the hub bearing against an accurately bored hole in the disc. (See Figure 4-117D) In the design shown in Figure 4-117A, a series of rivets is used to attach the double sheet metal disc to the hub. This method provides a positive mechanical joint as a result of the hole filling characteristics of the rivets.

Some other possible methods of fabrication which may be improved by development programs are:

- (a) Fusion welding
- (b) Spot welding
- (c) Bonding
- (d) Honeycomb construction
- (e) Dip brazing
- (f) Molding

These methods present many problems in control so that their use in high velocity fans should be considered with caution.

4-2.5.2.1.1 Hub

The hub may be splined, keyed or bolted to the driving shaft or bolted to a driving surface. As a rule, the shaft configuration determines the type of mounting. Splined hubs retained by friction cones should result in the lightest configuration as the ultimate load is distributed among many splines, thus requiring a minimum of hub material. A bolted connection of the hub to the shaft is not as satisfactory as a splined attachment retained by friction cones, particularly if significant vibratory loads are present.

4-2.5.2.1.2 Disc

The disc can be cast, forged, built-up or made of plate. Standard tolerances may well decide the methods of fabrication. As stated previously, the minimum thickness required for forgings and the variation of the over-all tolerance of the plate, forging or casting may lead to an excess of unwanted weight or to expensive machining to remove this dead weight. The built-up method utilizing sheet metal, with its inherent close tolerances, may prove the most feasible. However, quantity of production, as a rule, decides which method would be cheapest and easiest for fabrication. When large quantities are involved, machining and die costs diminish per unit, whereas the cost of assembly increases.

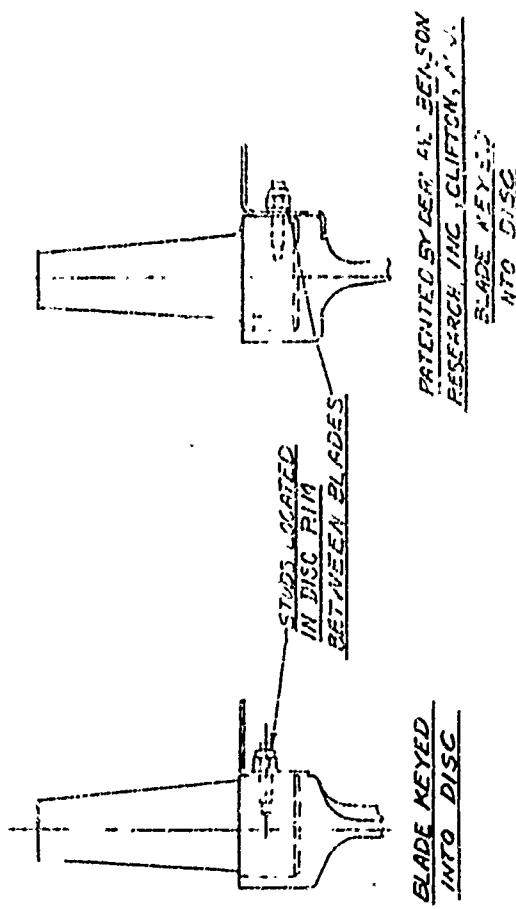
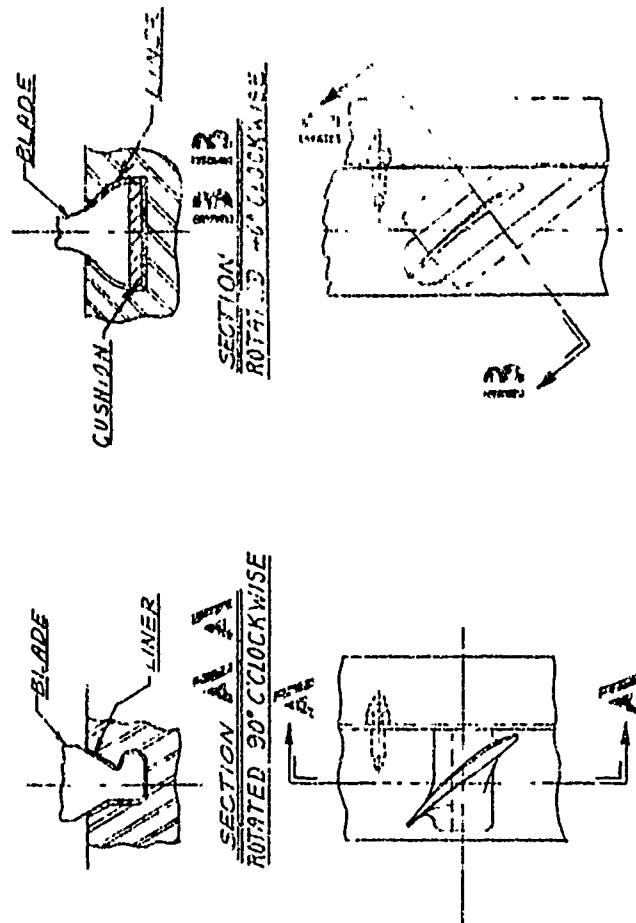
Obtaining the required disc stiffness with a light weight disc not only involves methods for eliminating the sources of blade vibration but also a thorough search for suitable high strength-weight materials. Eliminating the source of blade vibration should also help to keep the thickness and chord length of the blade to a minimum. The bulkhead or disc should have enough strength and stiffness to resist the stresses created by centrifugal force, vibration loads, and axial forces resulting from the pressure acting on the disc face, which increases with the diameter and fan pressure ratio. In addition, the disc should be stiff enough to be handled and manufactured readily without the danger of warping.

4-2.5.2.2 Blades

The blade consists of an airfoil and its mounting base. Due to the variation in configuration between individual designs, such as blade twist, taper, method of mounting, etc., the design itself can affect the method of fabrication as well as the material used.

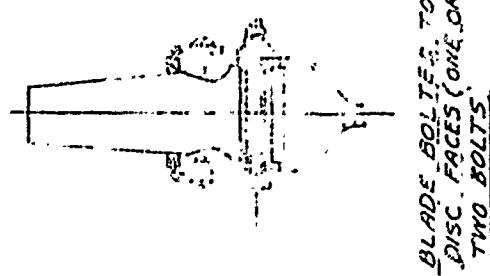
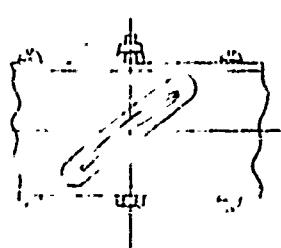
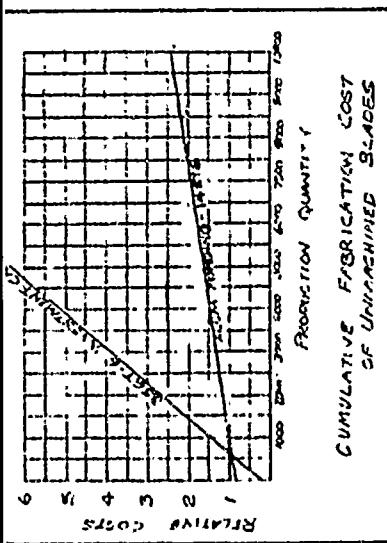
Investment precision casting is probably the cleanest method of blade fabrication, requiring a negligible amount of after-machining. Blade thickness tolerances of $\pm .005$ inches to the mean chord line and surface finishes of 80 R.M.S. may be attained by this process. 356 aluminum alloy with an obtainable U.T.S. of 30,000 P.S.I. is a very satisfactory casting material. The casting must conform to rigid specifications.

Forgings, as a rule, require some clean-up machining especially if the leading and trailing edge are along the parting plane. Irregularities of contour at the leading and trailing edges are particularly serious in their effect on aerodynamic performance. Die wear makes it difficult to hold consistently close contour or leading edge tolerances.



PATENTED BY LEATH & EYERSON
RESEARCH INC., CLIFTON, N.J.
FILED MAY 21, 1952
N.Y.O. DISC

THESE ARE FOUR TYPICAL
BLADE ATTACHMENTS



BLADE BOLTED TO
DISC. FACES ONE OR
TWO BOLTS.

BLADE WITH
CONE SEAT

Blade thickness tolerances of $\pm .012$ inches to the mean chord line and surface finishes of 80 R.M.S. may be attained by forging. 2014 aluminum alloy with an obtainable U.T.S. of 65,000 P.S.I. is very adaptable for blade forging. See Figure 4-118 for a comparison chart of fabrication costs.

Other types of blade fabrication, which are currently under development, may produce cheaper blades which meet the necessary functional requirements.

Minor deviations from the specified blade leading edge contour can affect appreciably the overall fan efficiency. Any clean-up operations required should be planned to preclude the possibility of affecting the designed leading edge contour.

Mechanical problems arising from aerodynamic sources, such as blade vibration, should be predicted in the early design stages and avoided. The judicious selection of blade material can affect potential blade failure. For example, blades fabricated from some forms of plastic materials have better damping qualities than those of aluminum.

Obviously, the damping properties of a blade may also be improved by changing the design of the blade. Such modifications as altering the thickness-chord ratio, the aspect ratio or fillet radius may substantially increase the stiffness and fatigue strength of the blades. In addition, the method of blade attachment or blade support is a design variable that can alter its damping characteristics. One method that should be considered is mounting the blade elastically by use of non-metallic pads or bushings. It may be worthwhile to run tests to predict stall frequencies for new designs and thus "tune" the blade out of the dangerous blade-vibration frequencies.

4-2.5.2.3 Assembly of Wheel and Blades (See Figure 4-118)

Good design practice provides a number of ways of attaching the blades to the wheel. An evaluation should be made to establish the most advantageous method for each rotor design. Two of the more common methods are keying and bolting.

Keying is an acceptable method, but the design should include means to prevent fretting corrosion, such as insulating the blade from the wheel with phenolic liners and non-metallic cushions. The design loads and required bearing area determine the size and shape of the key.

Bolting provides a simplified method of blade attachment. One or two bolts may be installed parallel to the axis of rotation to attach each blade base to the wheel. The blade should be insulated from the bolts by the use of bushings in the base of the blade. If single bolt retention is selected, the blades may be insulated from each other by non-metallic cushions attached to the blades or to the wheel. Judicious design of the non-metallic liners, cushions and bushings may also provide advantageous blade damping characteristics. For designs in which the base of the blade is nested between two flanges on the disc rim, it is advisable to use steel bushings through these flanges. One bushing should be shorter than the thickness of the flange in which it is installed and the bushing in the opposite flange should be longer than

the thickness of that flange. The flange strain, as a result of bolt tension, may be eliminated in this manner. This method also provides a simplified method of balancing the rotor by placing washers or balance weights under the head or nut of the bolt, as required. (See Figure 4-116) Photographs of keyed and bolted assemblies of wheels and blades are shown in Figures 4-119 to 4-122, inclusive.

Cover plates or seals may be necessary for any gaps in the blade root area to prevent leakage and resultant pressure losses.

4-2.5.2.4 Balancing

Each rotor assembly, when mounted on a shaft to simulate the physical installation in the aircraft, should be dynamically balanced about the axis of rotation to within specified limits. For example, one manufacturer has established a limit of ± 1 inch ounce for an engine cooling fan designed to operate at 2700 RPM and $\pm 1/2$ inch ounce for an oil cooling fan designed to operate at 6000 RPM. Unbalance in a rotor can result in a tendency toward translation of the axis of rotation, running out of track and vibration problems, which may result in the failure of the rotor or other aircraft parts.

Compensation for unbalance may be made by the addition or removal of weight in a single plane or in two planes perpendicular to the rotational axis of the assembly. Large cooling fans, as a rule, have sufficient axial length to require two plane correction to remove force and moment unbalance, since only force unbalance can be effected by single plane correction. The rotor assembly drawing should indicate the specific areas in which corrections for balance are to be applied and the method of correction, such as drilling, milling, grinding, washers, balance weights, etc. Limiting dimensions for material removal should be specified. Generally, the lightest assembly will be obtained by the method of adding balance weights rather than by removing material, since a ring of dead weight usually must be added to provide removal areas.

4-2.5.3 Stator and Rotor Cowling Assembly (See Figure 4-123)

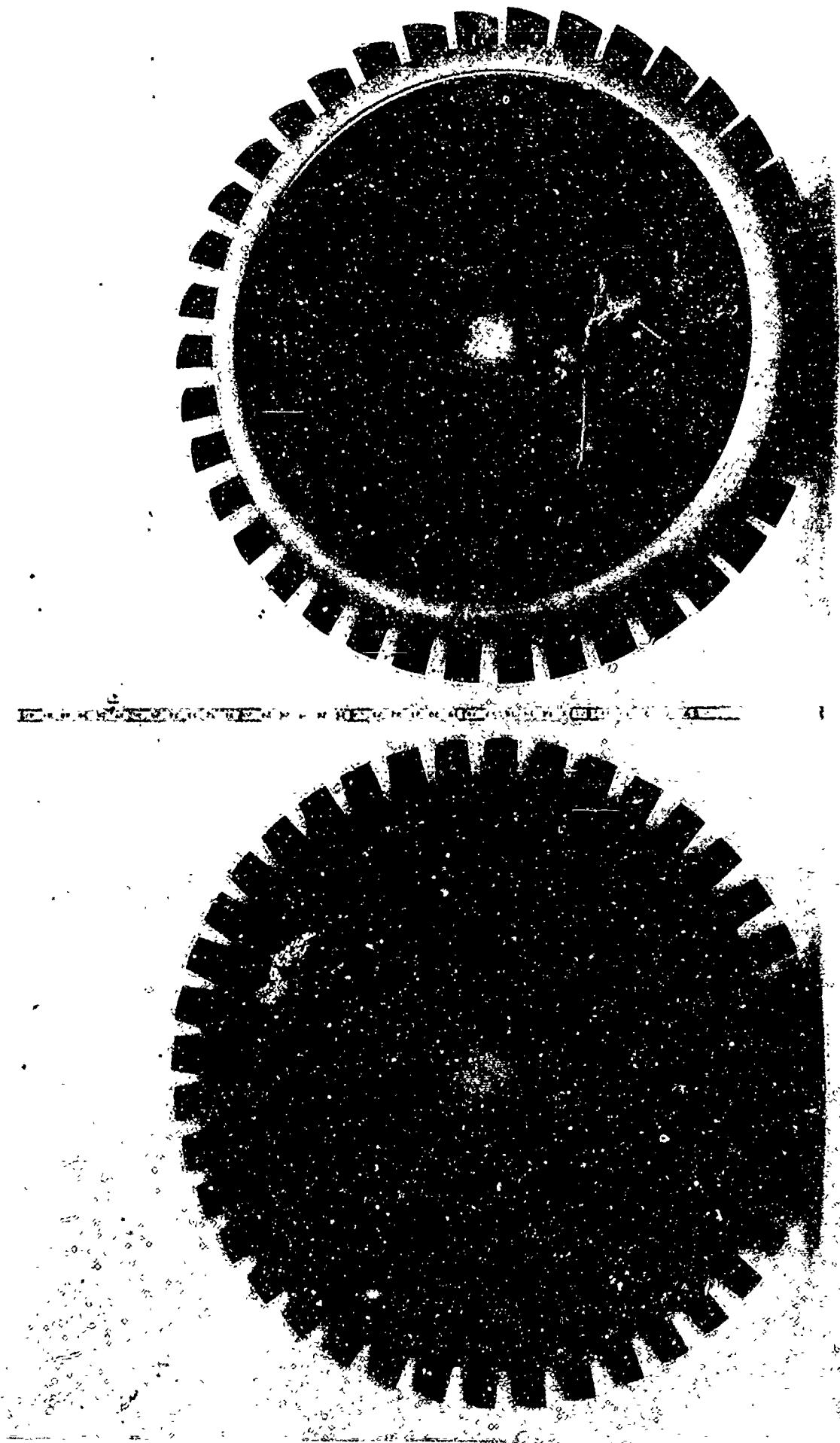
The stator assembly, as a rule, is made with the rotor cowling as an integral part; thus not only assuring good alignment, but also eliminating gaps. The cowling should be sufficiently rigid in the plane of the rotor to assure a constant minimum blade-tip clearance around the periphery and not be permitted to warp or deform during handling, installation or long hours of operation. Re-circulation through the stator should be prevented by either a sealed stator support disc or a minimum gap between the rotor section at the blade root area and the inner stator shell surface. For smooth air entrance to the fan, the inner face of the cowling should be smooth and free of any irregularities and should extend some distance upstream of the fan with the leading edge providing the required bellmouth entrance.

The cowling and stator assembly lends itself easily to many methods of fabrication with each method having its choice of material. The cowling and disc may be spun or rolled out of aluminum alloy with the stator blades, also made out of aluminum alloy, either spotwelded, dip brazed, or riveted, or the entire unit, i.e., cowling, stator blades and disc, may be cast out of aluminum alloy or magnesium alloy. Fiberglas lends

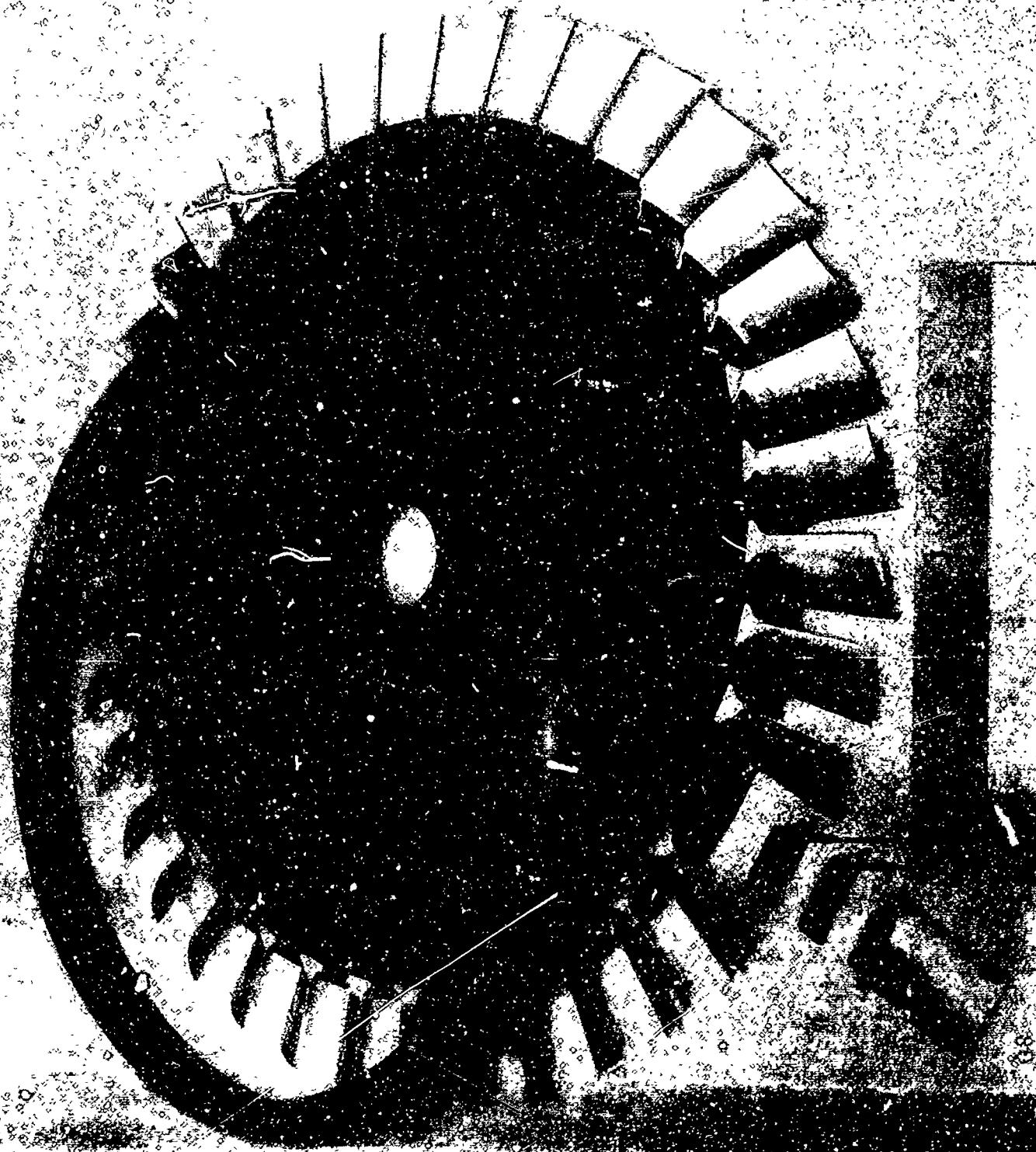
FIGURE 4-119. Exploded Photograph of an Axial Flow Fan Showing Single Bolt Blade Mounting Method

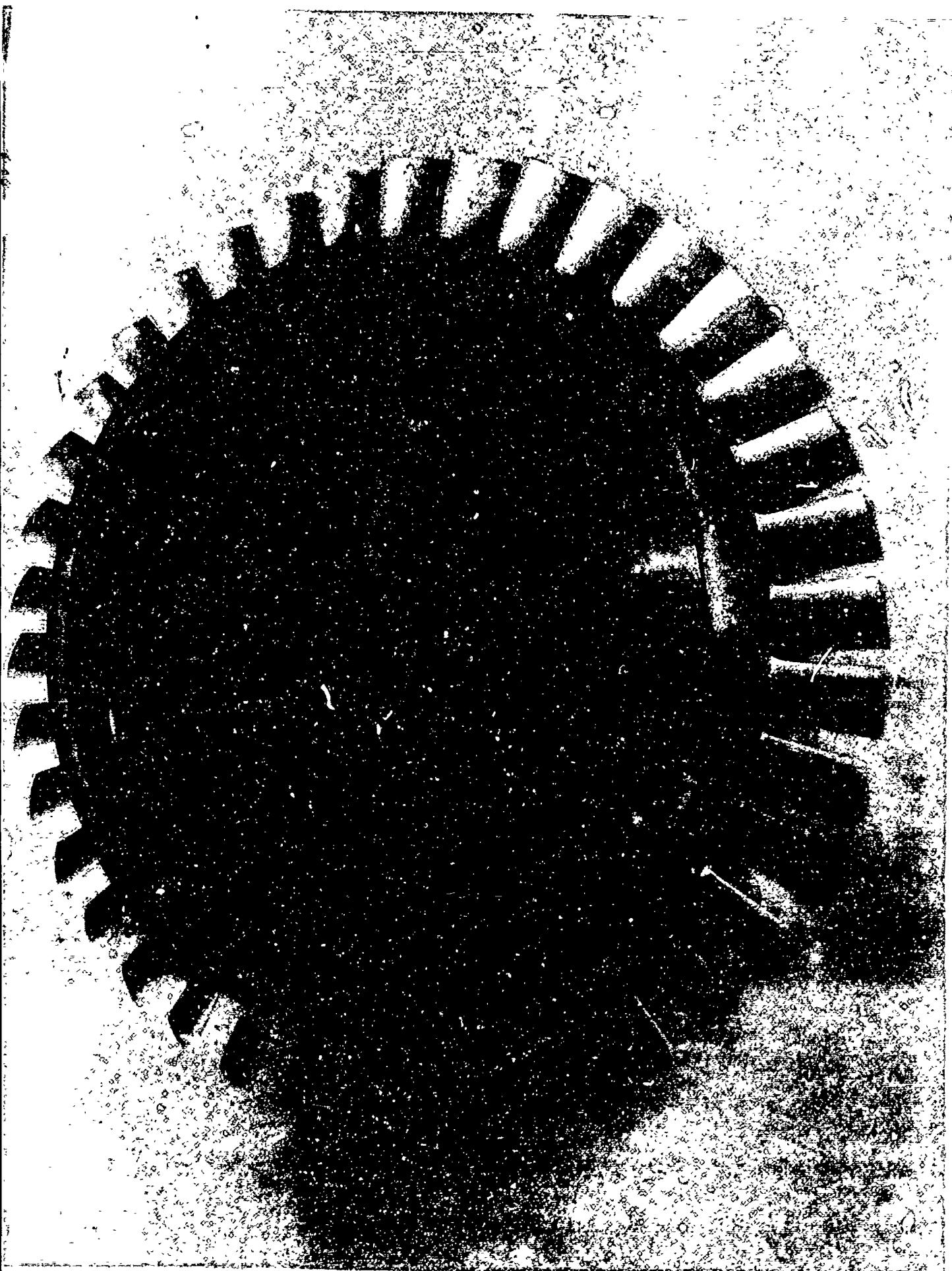


FIGURE 4-120. Photographs of Two
Types of Axial Flow Cooling Fans



FIG' RE 4-121. Exploded Photograph of an Axial Flow Fan Showing Keyed Blade Mounting Method





IV-158

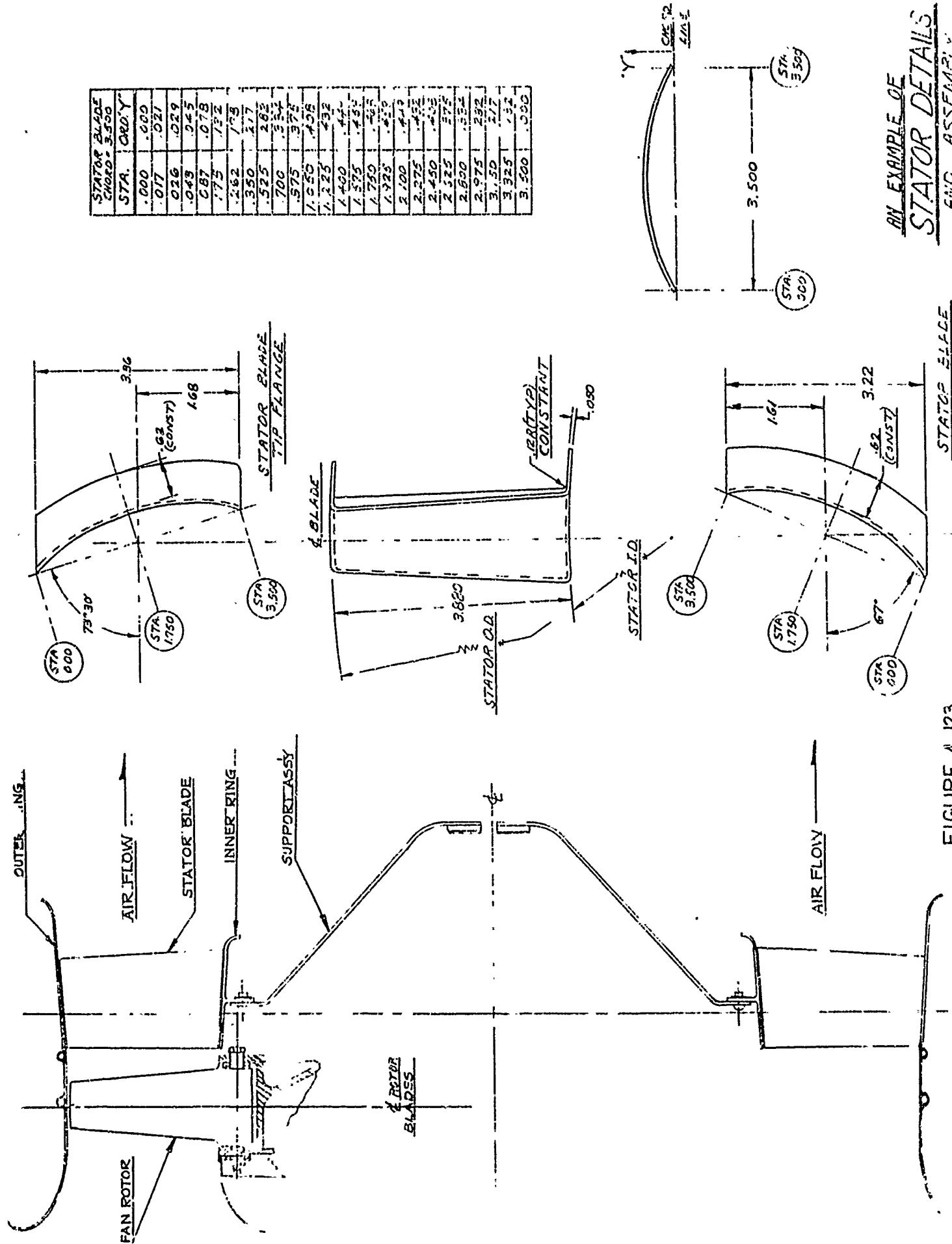


FIGURE 4-123

AN EXAMPLE OF
STATOR DETAILS
END ASSEMBLY

STATOR
ASSEMBLY

itself well to this type of fabrication where the entire unit can be molded out of fiberglas or just the cowling or cowling and blades can be made out of fiberglas with the other components being made out of aluminum alloy and the assembly riveted together. The disc should be protected against "oil canning" with built-in beaded reinforcement or built-up stiffeners, either spotwelded or riveted.

Maintaining blade contour is very important for the stator blade because, if air separation occurs, pressure recovery of the energy imparted to the air by the rotor will be poor. In addition, separation may give rise to vibration loads sufficiently high to create cracks in the stator blades.

4-2.6 Fan References

- 4-1 Mutterperl, William: High Altitude Cooling. VI Axial Flow Fans and Cooling Power, NACA WR L-776, 1944. (Formerly NACA APR L41 11e)
- 4-2 Ruden, P.: Investigation of Single Stage Axial Fans. NACA TM No. 1062, 1944.
- 4-3 Keller, Curt, and Marks,: The Theory and Performance of Axial Flow Fans. McGraw-Hill Book Company, Inc., 1937.
- 4-4 Herrig, L. Joseph; Emery, James C., and Erwin, John R.: Systematic Two - Dimensional Cascade Tests of NACA 65-Series Compressor Blades at Low Speeds. NACA RM L51G31, 1951.
- 4-5 Kantrowitz, Arthur, and Daum, Fred L.: Preliminary Experimental Investigation of Airfoils in Cascade. NACA CB, July, 1942.
- 4-6 Stepanoff, A. J.: Turbo-blowers - Theory, Design, and Application of Centrifugal and Axial Flow Compressors and Fans. John Wiley & Sons, Inc., N. Y., Library of Congress Catalogue Card Number: 55-6546. (Copyrighted)
- 4-7 Sorenson, Harry A.: Gas Turbines. The Ronald Press Company, N. Y., 1951 (Copyrighted)
- 4-8 Marble, Frank E.: Propagation of Stall in a Compressor Blade Row. A paper, Journal of the Aeronautical Sciences, Volume 22, August 1955, Number 8.
- 4-9 Abbott, Ira H., Von Doenhoff, Albert E., and Stivers, Louis S., Jr.: Summary of Airfoil Data. NACA Report 24, 1945. (Formerly NACA ACR L5C05)
- 4-10 Felix, A. Richard: Summary of 65-Series Compressor - Blade Low-Speed Cascade Data by Use of the Carpet-Plotting Technique. NACA RM L54H18a, November 2, 1954.
- 4-11 Greene, Richard S.: Aerodynamic Design of a Cooling Fan for the Piasecki XH-16 Helicopter. W.A.C. Serial Report Number 1470, Wright Aeronautical Corporation, Division of Curtiss-Wright Corporation, Wood-Ridge, N. J.
- 4-12 Author Unspecified: Performance Test of Piasecki XH-16 Helicopter Cooling Fan. Dean and Benson Research Report Number 102, Dean and Benson Research, Incorporated, Clifton, New Jersey.
- 4-13 Committee A-9, Aircraft Air Conditioning Equipment, Society of Automotive Engineers, New York: Airplane Heating and Ventilating Equipment Engineering Data, SAE Aeronautical Information Report No. 2, 1943.
- 4-14 Rogallo, F. M.: Internal Flow Systems for Aircraft. NACA Report No. 713, 1941.

- 4-15 Rogallo, F. M., Collection of Balanced-Aileron Test Data. NACA Report ACR 4AII (Wartime Report L-419)
- 4-16 Senger, W. I.: Static or Dynamic Balancing, Tool Engineer's Handbook, First Edition
- 4-17 Vertol Aircraft Corporation Specification PS-184: Procurement Specification for the YH-21 Cooling Fan.
- 4-18 ARDC Manual: Handbook of Instructions for Aircraft Designers. ARDCM 80-1. Headquarters, Air Research and Development Command.

4-3.0 Ejectors

4-3.1.0 General

4-3.1.1 Nomenclature

The symbols used in the section on ejectors are included in the list of symbols in Appendix IV. Diagrams of cylindrical and conical ejectors are presented in Figures 4-124 and 4-125, respectively, on which are shown symbols used in the ejector section. Several types of ejectors are shown in Figures 4-126, -127, and -128. Reference matter used in the preparation of Section 4-3.0 is listed in Section 4-3.7.

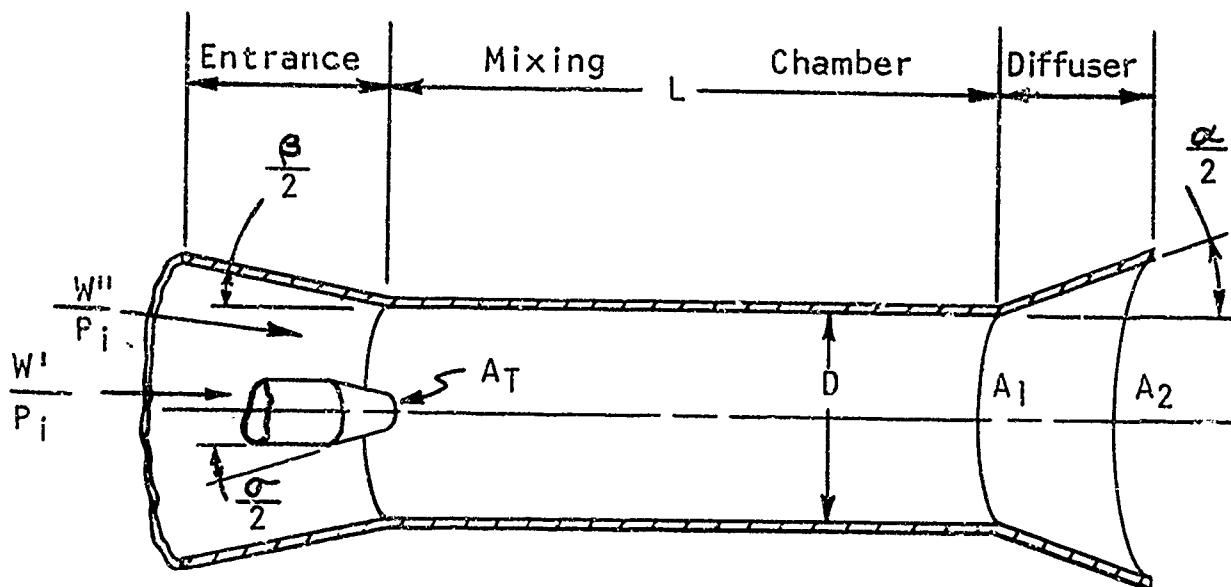


FIGURE 4-124
Cylindrical Ejector

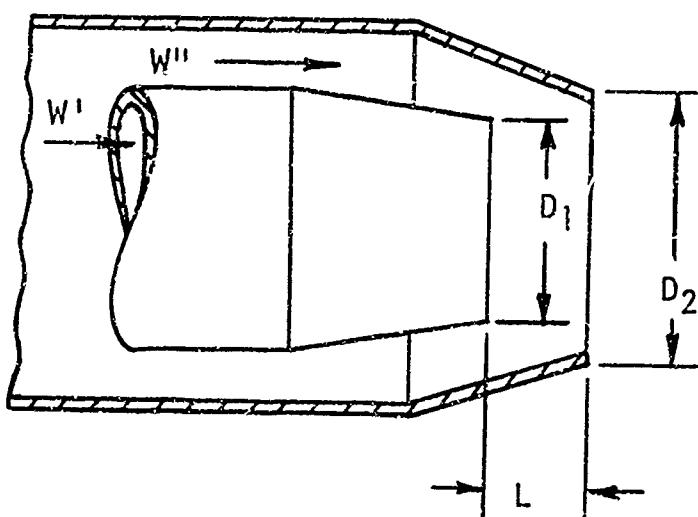


FIGURE 4-125
Conical Ejector

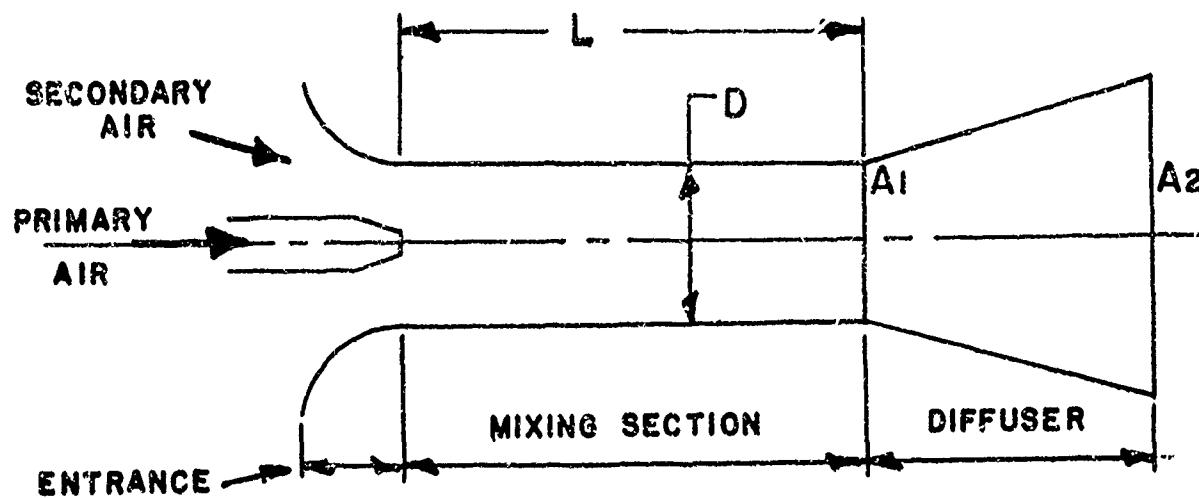


FIG.4-126 TYPICAL SINGLE STAGE CYLINDRICAL EJECTOR

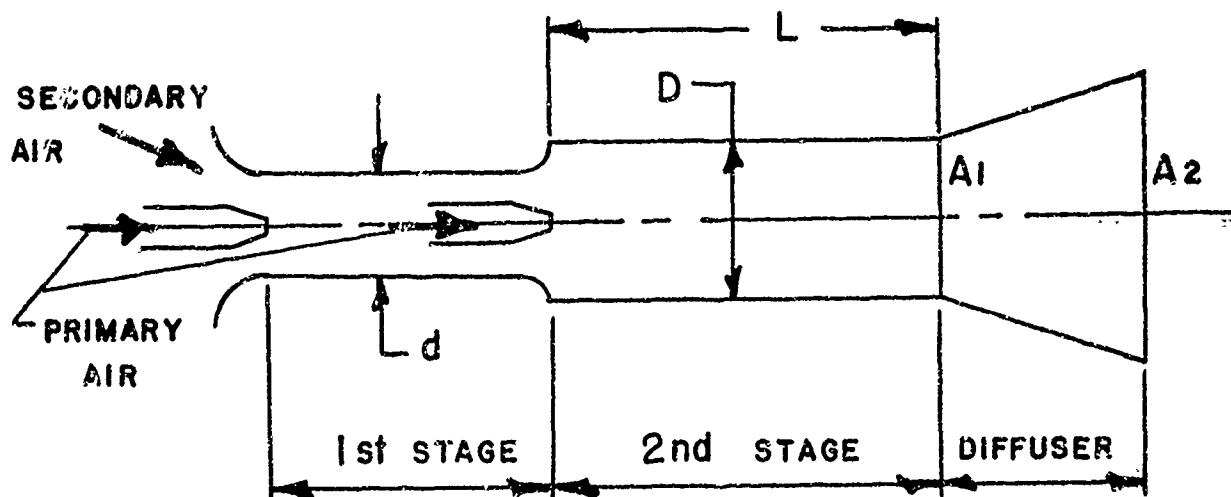


FIG.4-127 TYPICAL TWO STAGE CYLINDRICAL EJECTOR

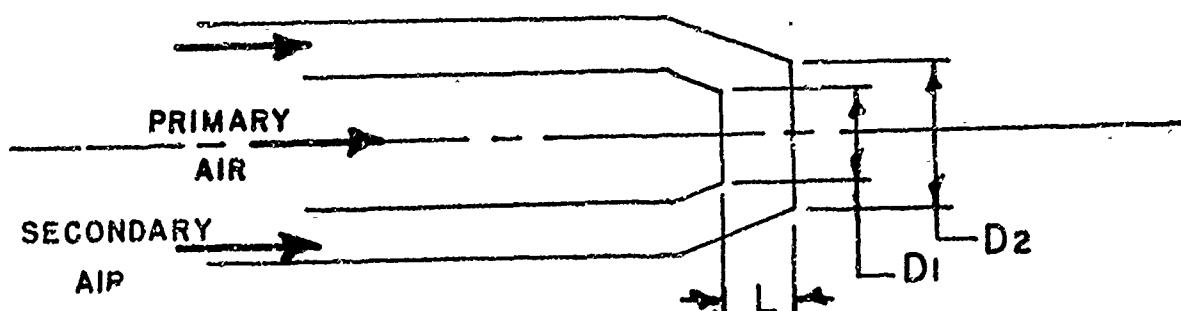


FIG.4-128 TYPICAL CONICAL EJECTOR

4-3.1.2 Definition

An ejector is a device in which the kinetic energy of one fluid (the primary fluid) is used to move another fluid (the secondary fluid). When the action occurs through a positive pressure differential (increase in secondary fluid pressure) the ejector functions as a pump. When the pressure differential is zero (no secondary fluid pressure rise) the ejector functions as a blower. The usual application of an ejector is as a pump to induce atmospheric air through a constriction (with a loss in total pressure) and to discharge this air back into the atmosphere.

Ejectors can operate with any fluid as the primary or secondary fluid. However, only air-to-air and engine exhaust gas-to-air ejectors are considered herein.

4-3.1.3 Types of Ejectors

Figures 4-126, -127 and -128 are schematics of several types of ejector configuration. Ejectors can be divided into two basic groups: cylindrical (Figure 4-124) and conical (Figure 4-125). In each group there are sub-classifications and combinations of the two groups. For example, there is a single stage cylindrical ejector (figure 4-126) and a two-stage cylindrical ejector (Figure 4-127). There is a constant pressure mixing cylindrical ejector and a constant area mixing cylindrical ejector (figure 4-126). There is a conical ejector (Figure 4-128) and a conical ejector with a cylindrical extension or shroud.

Conical ejectors are used when a weight flow ratio less than one is required, as in gas-turbine exhaust ejectors (see Section 4-3.4). They are used to pump across a relatively small secondary pressure rise and do not perform efficiently at off-design conditions. See Section 4-3.4 for a more detailed discussion of conical ejectors and their design.

To accomplish mixing at constant pressure in a cylindrical ejector the entrance and mixing chamber profile must be of a unique mathematical shape for a particular operating condition. This requires care in both ejector design and fabrication. Since the profile is designed for a particular operating condition, the constant pressure mixing ejector does not perform efficiently at off-design conditions and it will not pump across a positive pressure differential without a diffuser.

A constant area mixing cylindrical ejector (Figure 4-126) is the most universal type of ejector, producing a high weight flow ratio across a positive pressure differential, performing with acceptable efficiency at off-design conditions and is easy to fabricate. As it is the most versatile, the constant area cylindrical ejector is the type of ejector analyzed in detail in Section 4-3.2.0. Included is a design chart for establishing the optimum configuration for various flow requirements and predicting the effects of a number of variables, singularly or in combination.

The design chart can be used only for constant area cylindrical ejectors with a primary pressure ratio greater than $\frac{1}{2}$ critical pressure ratio for the primary fluid used. Conical ejectors and cylindrical ejectors with a primary pressure ratio less than critical cannot be sensibly analyzed mathematically and must be designed by trial and error.

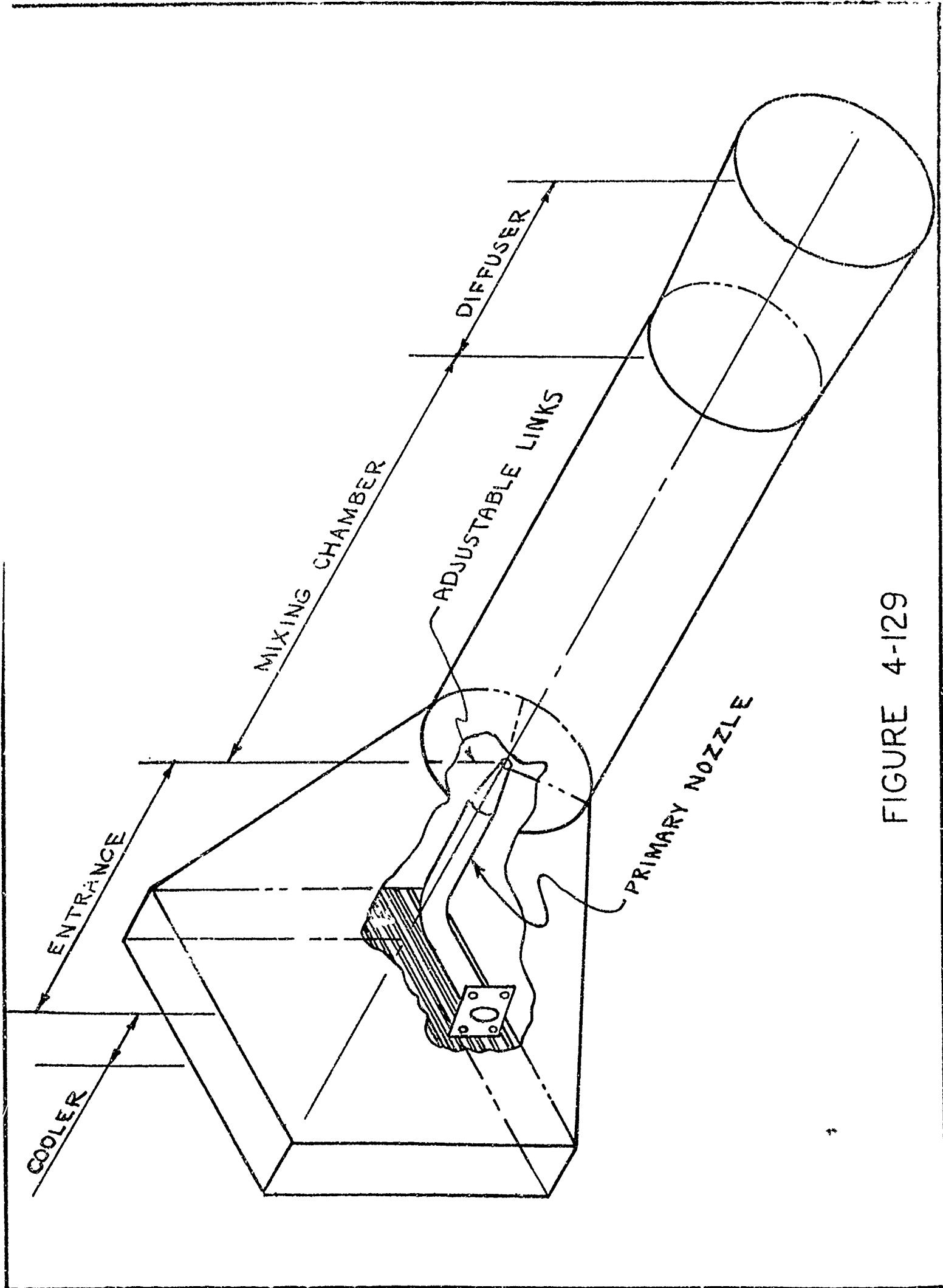


FIGURE 4-129

4-3.1.4 Method of Establishing Secondary Flow Requirements

The amount of cooling (secondary) air flow required is determined in the manner described in Chapters I and II. For any particular application the amount of cooling air required will establish the pressure rise required across the pumping device, in this instance, the ejector. The actual air flow required must be corrected to an equivalent value at standard temperature by

$$W_C'' = W'' \text{ actual} \sqrt{\frac{T_1}{518.4}}$$

Similarly, the pressure rise must be corrected to an equivalent value at standard pressure by

$$\Delta P_C = \frac{\Delta P \text{ actual}}{P_0/14.7}$$

(See the design chart, Figures 4-130 and 4-131, for the use of these corrected values).

4-3.1.5 Method of Determining Primary Flow Requirements

If the ejector uses the engine exhaust as the pumping (primary) fluid the amount and characteristics of the primary flow are fixed within certain limits. The quantity of flow is the engine air flow plus the engine fuel flow. The total pressure and temperature of the exhaust gas are functions of the engine design and operating condition and the values can be obtained from the engine specifications, operating curves, or the engine manufacturer. See Section 4-3.3 for a method of modifying the exhaust gas characteristics of reciprocating engines.

If gas-turbine compressor bleed is used as the primary fluid the engine specification indicates a limit to the amount of air which can be bled and the specification includes charts for determining the total pressure and temperature of the bleed air under all conditions.

As is done with the secondary air, the primary air flow must be corrected to an equivalent value at standard temperature by

$$W' = W' \text{ actual} \sqrt{\frac{T_1}{518.4}}$$

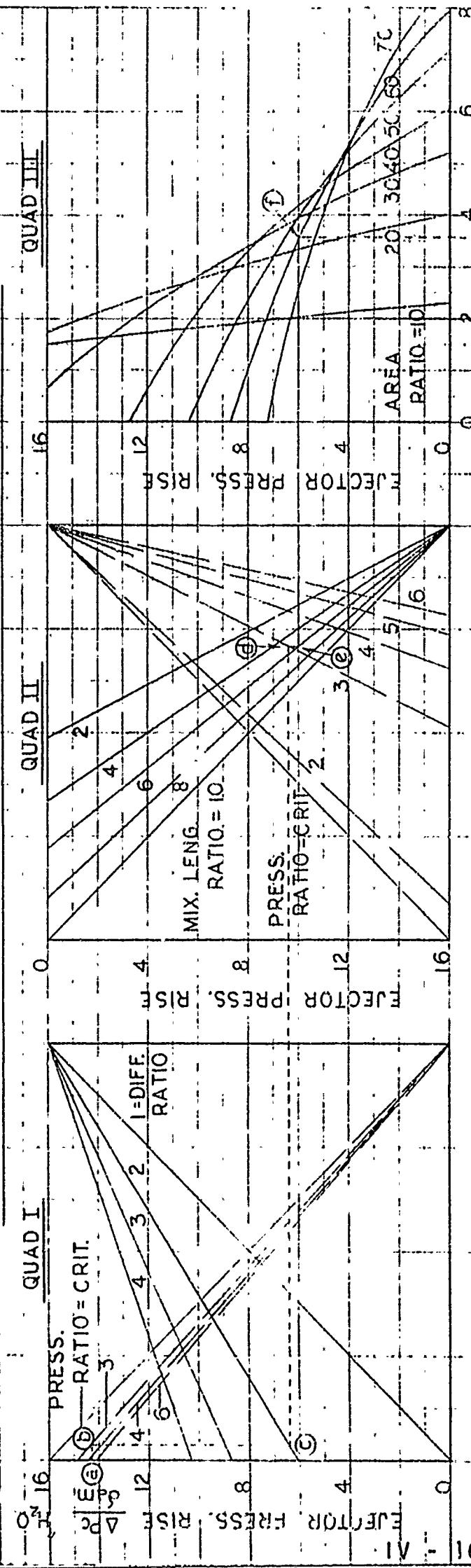
4-3.2.0 Theory of Constant Area Cylindrical Ejectors

4-3.2.1 Design Parameters

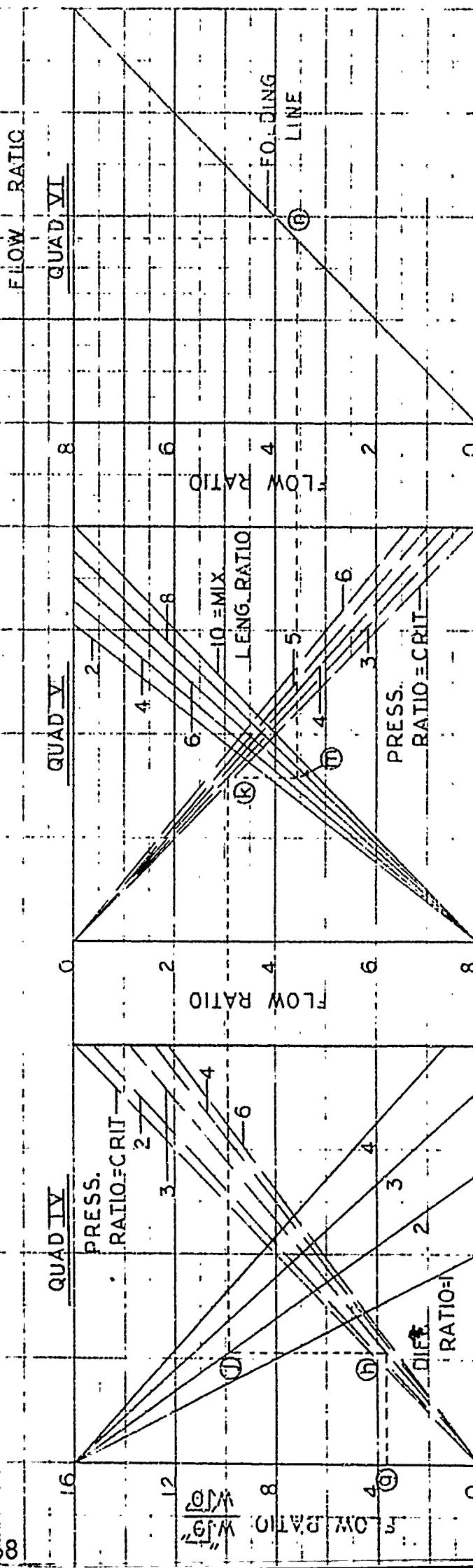
The performance of constant area cylindrical ejectors, as illustrated in Figure 4-129, is dependent upon many variables. Listed below are the more common ones, both geometrical and functional.

FIGURE 4-1130
CONNECTA NIT

DESIGN - CHART - CONSTANT AREA CYL. EJECTOR



QUAD III



<u>Geometrical</u>	<u>Functional</u>
1. Area ratio, A_1/A_t	1. Primary air quantity, W'
2. Mixer length ratio, L/D	2. Primary air total pressure, P_t
3. Diffuser ratio, A_2/A_1	3. Primary air total temperature, T_t
4. Diffuser angle, α	4. Primary air composition
5. Primary nozzle angle, σ	5. Secondary air quantity, W''
6. Primary nozzle position	6. Secondary air total pressure, P_t
7. Primary nozzle number	7. Secondary air total temperature, T_t
8. Mixer entrance angle, β	8. Secondary air composition
	9. Ejector pressure rise, ΔP

4-3.2.2.0 Discussion

A qualitative discussion of the factors affecting the performance of a constant area cylindrical ejector follows, and the relative importance of the variables is established. A design chart is presented which illustrates numerically the influence of the most important variables.

The design chart is good only for constant area cylindrical ejectors with a primary pressure ratio greater than the critical pressure ratio for the primary fluid used.

4-3.2.2.1 Area Ratio

Ratio of the mixing chamber area to the primary nozzle throat area. Given a particular primary flow (primary nozzle throat area) the selection of an area ratio will determine the quantity of secondary flow and the pressure rise through which it can be pumped. (See Quad. III, Figure 4-130). There is an optimum area ratio for a given pressure rise and/or flow ratio. Any deviation from the optimum area ratio will result in a decrease in either flow ratio or pressure rise.

4-3.2.2.2 Mixer Length Ratio

Ratio of the length of the mixing chamber to the diameter of the mixing chamber. When referring to a perfectly mixed state of the primary and secondary flow (the ideal end condition) the existence of a uniform transverse velocity distribution is implied. Theoretically, to obtain such a condition, an infinitely long mixing chamber is required. However, the effect of turbulent shearing forces results in a reasonably uniform transverse velocity distribution within a finite distance. The location of the effective uniform transverse velocity distribution coincides with the location of the maximum average static pressure across the mixing chamber. This location determines the optimum length of mixing chamber. Increasing the length beyond this optimum length increases the friction loss resulting in reduced overall performance.

4-3.2.2.3 Diffuser Ratio

Ratio of the exit area of the diffuser to the area of the mixing chamber. For a given constriction at the entrance to the ejector the secondary flow increases as the pressure rise across the ejector increases (entrance pressure, P_t , is lowered). Adding a diffuser lowers the static pressure in the mixing chamber which, in turn, increases the secondary flow. A conical diffuser with an included angle, α , of 8 to 10 degrees is optimum. A diffuser angle greater than 10 degrees will result in flow separation from the side of the diffuser with an accompanying loss in performance.

4-3.2.2.4 Primary Nozzle

Usually a cylindrical ejector operates with a primary pressure greater than critical, and theoretically a convergent-divergent nozzle is indicated for the primary flow. However, since most ejectors are required to operate at off-design conditions (including the primary pressure) and under-expanding convergent nozzle is the best and the performance loss due to the under-expansion is small. The primary nozzle is usually a conical convergent nozzle with an included convergent angle, σ' , of 20 to 30 degrees. The throat, or exit area A_T can be computed by

$$A_T = \frac{W'}{C_1 P_i \sqrt{\frac{2g}{T_i R} \frac{n}{n-1}}} \quad (\text{For } P_i \text{ greater than critical})$$

The velocity issuing from the primary jet nozzle is

$$v = C_2 \sqrt{T_i 2g \frac{n}{n-1}} \sqrt{1 - \left(\frac{P_i}{P_o}\right)^{\frac{n-1}{n}}}$$

To obtain the optimum performance the axis of the primary nozzle must be coincident with the axis of the mixing chamber. This is an extremely critical requirement. To accomplish this with a minimum of difficulty the exit of the primary nozzle can be located flush with the entrance to the mixing chamber. This location also eliminates much of the effect of entrance configuration and is relatively insensitive to the entrance angle θ . A rounded entrance can be used having a radius as small as one-sixth the diameter of the mixing chamber.

4-3.2.2.5 Temperature Ratio

The performance of an ejector is directly related to the temperature ratio of the two fluids. The weight flow ratio tends to increase proportionately as the square root of the temperature ratio

$$\frac{W''}{W'} = K \left(\frac{T_i}{T_1} \right)^{1/2}$$

For the above reason, the actual weight flows are corrected for temperature as explained in Sections 4-3.1.4 and 4-3.1.5 for use in the design chart, Figure 4-130.

4-3.2.2.6 Molecular Weight Ratio

In general the weight flow ratio decreases as the density ratio increases above unity. This text, dealing with air-to-air and exhaust-gas-to-air ejectors, considers the applicable molecular weight variable negligible.

4-3.2.3.0 Ejector Design Chart

4-3.2.3.1 General

As previously discussed, in any specific aircraft installation, some of the parameters associated with ejector design can be determined by the installation itself. The primary and secondary flows are determined in the manner discussed in Sections 4-3.1.4 and 4-3.1.5; also the pressure and temperature characteristics of the two streams. The permissible overall length is usually limited by the space available in the aircraft. The design chart, Figure 4-130, can be used to predict the various geometric combinations of mixer length ratio, diffuser ratio and area ratio that will produce the predetermined flow ratio and pressure rise. The design chart is a graphical trial and error procedure that can be repeated if the selected geometric combination is not suitable for the particular installation. The design chart is based upon a constant area cylindrical ejector with a critical primary pressure ratio; a diffuser ratio of 1 (no diffuser), and a mixing chamber length ratio of 10. The ambient temperature and pressure are assumed to be standard (518.4° R and 14.7 PSIA respectively).

The design chart, Figure 4-131, is reproduced as an insert at the back of the book. Figure 4-130 is a reduced version of the chart and is included for illustrative purposes.

4-3.2.3.2 Procedure

- a) With the corrected weight flow ratio and ejector pressure rise arbitrarily select a mixer length ratio and a diffuser ratio.
- b) Enter Quad. I and IV with the corrected flow ratio and pressure rise (a and g).
- c) Proceed horizontally to the primary pressure ratio (b and h).
- d) Go vertically to preselected diffuser ratio (c and i).
- e) Proceed horizontally to Quads. II and V and the corresponding primary pressure ratio (d and k).
- f) Go vertically to preselected mixer length ratio (e and m).
- g) From point e continue horizontally to Quad. III.
- h) From point m proceed horizontally to the folding line in Quad. VI (n) and then vertically to Quad. III.
- i) The intersection (f) of the two lines in Quad. III indicates an area ratio necessary to obtain the required flow ratio and pressure rise with the selected mixer length ratio and diffuser ratio.

Note: If the area ratio lies to the right of the area ratio envelope in Quad. III, or if the area is impractical, the entire procedure can be repeated for new values of mixer length ratio and diffuser ratio.

4-3.3 Reciprocating Engine Exhaust Ejectors

Ejectors can be installed around the exhaust tubes of reciprocating engines to induce cooling air flow through the engine, oil coolers or accessories. Such ejectors are usually bulky with complex inter-

connected exhaust tubes. However, by considering certain design criteria reasonable exhaust ejectors can be designed to give adequate performance.

As the exhaust gas pressure ratio to ambient is much less than critical an exhaust ejector cannot be calculated but must be designed by trial and error. There are too many independent variables involved in less-than-critical primary flow to allow rigorous analysis. The design chart (Figure 4-130) included in this Section is not applicable to low primary pressure ratio design. The following information, while not leading to analytical design, can be used as a guide.

Most exhaust tubes for reciprocating engines are designed to approximate the following:

$$A = 0.04 \times I.H.P. \times \frac{n}{N}$$

where A = Tube area, sq. in.

I.H.P. = Total Indicated Horse Power

n = Number of cylinders discharging into the tube

N = Total number of cylinders.

The resulting velocity of the exhaust gas issuing from the tube may not be sufficient to pump the required secondary flow. Constrictive nozzles can be added at the open end of the exhaust tube to increase the velocity of the exhaust gas or primary air. The constrictive nozzles will increase the back pressure on the engine, which, in turn, will reduce the engine output. Another method which can be used to increase the pumping is to combine into one ejector the exhaust from two or more cylinders. Any proposed combination of exhausts must be studied in detail to assure that the desired effect will be realized without an accompanying power penalty.

Pressure waves of very high amplitudes exist in the exhaust tubes and the proper relation of portions of these waves with the valve timing of the engine is the controlling factor which influences the power output and the exhaust gas thrust produced by the engine. Control of the exhaust gas frequency and proper phasing of the exhaust gas pulses in the exhaust system provides a means for reducing power losses. However, the pipe lengths necessary to obtain optimum results may be too long to conveniently fit into an aircraft installation.

It has been found that interference will occur between exhaust gas pulses in a manifold common to two or more cylinders unless certain design parameters are considered. The exhausts of no more than two cylinders firing in 360° intervals, or no more than three cylinders firing in 240° intervals should be fed into a common section of the exhaust manifold.

A reduction, or elimination, of the loss in power output due to the exhaust pipes is possible if the amplitude of the wave in the exhaust pipe and its phase relationship to the engine valve timing are controlled. The peak of the first negative half cycle after the exhaust valve opening should be coincident with the midpoint of the intake and

exhaust valve overlap. The velocity vector of the wave should be at a maximum, in the direction of the exhaust tube outlet, when the exhaust valve is starting to open. These parameters can be determined, experimentally, by observation of the instantaneous pressures in the exhaust system of the operating engine.

Constrictive nozzles attached to the exhaust pipe reduce the power output of the engine, and, except with extremely short exhaust pipes, also reduces the mean effective exhaust gas thrust. The addition of nozzles to an exhaust system increases the mean effective exhaust gas thrust when relatively short length exhaust systems are employed (42" or less in length). When relatively long lengths (60" or more in length) are employed, the mean effective exhaust gas thrust is reduced by the addition of nozzles.

Usually the length of an ejector mixing chamber is 8 to 10 times the mixing chamber diameter. The area of the mixing chamber can be approximated by

$$A = (0.2 \text{ to } 0.3) \text{ I.H.P.} \times \frac{n}{N}$$

where A = Area of mixing chamber, sq. in.

I.H.P. = Total Indicated Horse Power

n = Number of cylinders discharging into the ejector

N = Total number of cylinders.

This area, compared with the exhaust tube area, will give an area ratio of about 6 to 1. Any diffuser installed should have an included angle of 8 to 10 degrees.

Any increase in back pressure due to the installation of an ejector will affect the power output of the engine. The power loss resulting from an increase in back pressure is between 1/4% to 1% of the engine power for each inch of mercury increase in back pressure. Aspiration and gear supercharged engines are in the lower part of this range, whereas turbo-supercharged and turbo-compound engines are more affected by increased back pressure.

Although experimental engine installations have been cooled without power loss by the action of exhaust ejectors, the required "tuned" exhaust stacks and large diffusing ejectors are usually considered too large for production aircraft application. For a specific engine and operating condition the effect of exhaust back pressure can be approximated from the power charts by determining the change in power for a lower altitude (increased back pressure) at constant MAP and R.P.M. with the CAT at the lower altitude corrected to give the density of the higher altitude. The difference in the back pressure is the difference in ambient pressure at the two altitudes considered. Any effect of ejectors on the engine must be coordinated with the engine manufacturer.

Reciprocating engine exhaust ejectors will have to be estimated, tested and modified as necessary.

4-3.4 Turbine Exhaust Ejectors

Frequently a cooling and fire containing "can" is installed around the "hot" end of a gas turbine engine. To induce cooling and ventilating air flow through the space between the engine and the can a conical ejector is included around the exhaust nozzle of the engine. A conical ejector is used since the flow ratio required is considerably less than unity and the conical ejector requires little additional space.

The design of conical ejectors, especially for application with turbo-prop engines with a low exhaust pressure, does not lend itself to mathematical analysis. As such, design must be on a trial and error basis.

The operation of the ejector varies with the primary fluid pressure ratio, the secondary pressure ratio, and the ejector geometry which is described by the area ratio, A_2/A_1 , and the spacing ratio, L/D. The weight flow ratio for this type installation will vary from about 0.02 to 0.10, increasing slightly with altitude. Cooling air flow must be maintained with a primary pressure ratio of about 1.05 to 1.2 for turbo-props and 1.7 to 4.0 for turbo jets. With a variable area exhaust nozzle flow must be maintained with changes in area ratio and spacing ratio. Ejector design must consider all these factors in conjunction with the possible thrust loss and weight penalty.

Optimum pumping characteristics may be approximated over a wide range of operating conditions with an ejector having a fixed spacing ratio. The maximum weight flow ratios generally occur at larger spacing ratios for ejectors having large diameter ratios; for example, at a spacing ratio of about 1.3 to 1.5 for a diameter ratio of 1.2 and at a spacing ratio of approximately 1.0 for a 1.1 diameter ratio.

The ejector spacing required to pump the maximum weight flow is independent of the primary and secondary pressure ratios for the larger diameter ratios. The spacing for 1.0 diameter ratio ejector varies considerably with primary pressure ratio and to a lesser extent with secondary pressure ratio. The range of spacings giving measurable secondary weight flow decreases rapidly with decrease in diameter ratio to an extremely narrow useful spacing range at a diameter ratio of 1.0. The narrow range of useful spacings and the variation of ejector effectiveness with changes in primary and secondary pressure ratios indicates that operation of a 1.0 diameter ratio ejector is very critical and the use of ejectors with this low a diameter ratio should be avoided. The larger the diameter ratio, the less sensitive is the ejector to operational and constructional variables.

Ejectors which provide high pumping pressure ratios generally produce high thrust losses. Furthermore, any attempt to control the cooling air flow by throttling upstream of the ejector can lead, in some configurations, to thrust losses approaching 35% of the convergent nozzle thrust. It is evident that ejectors should be designed with spacing ratios smaller than that which will produce the maximum secondary pressure ratio for any one diameter ratio. This type configuration will give sufficient secondary flow with a minimum of thrust loss.

The turbo-prop engine loses power at the rate of approximately 3% to 6% per inch of mercury increase in back pressure, in the range of powers from military to 60% normal rated power. The power loss rate increases with decreasing power.

For a given engine, the power loss can be determined from the engine performance curves provided in the engine specifications. Effect of engine exhaust pressure changes are usually included in all performance data.

4-3.5 Turbine Compressor Bleed Air Ejectors

High performance ejectors (those with flow ratios over unity) require a primary pressure well over the critical pressure ratio for the primary fluid used. Such high primary pressures are available only from the compressor of a gas-turbine engine. This type of ejector, constant-area cylindrical ejector, is the subject of Section 4-3.2.0 of this chapter and reference may be made to that section for a complete discussion of ejector design.

For bleed air, the rate of power loss of a turbo-prop engine is from 2% to 5% for each per cent engine air bleed between military and 50% normal rated power. The rate of power loss increases with decreasing power. Power loss, as a result of compressor air bleed, can be obtained from the engine specification.

4-3.6.0 Ejector Design Considerations

4-3.6.1 General

An ejector, being a static device containing no moving parts, is basically simple to design and fabricate and, excepting possible corrosion or cracking due to vibration, has an infinite service life. The only part of an ejector which need be other than of circular section is the entrance which may be an adapter from a non-circular shape to a circle at its junction with the mixing section.

The primary air system consists of the ducting for the primary air to the primary nozzle at the entrance to the mixing chamber. In reciprocating engine exhaust ejectors the exhaust stacks of the engine are the primary flow ducting. In compressor air bleed ejectors flexible ducting is required to carry the high pressure compressed air from the engine to the ejector. In gas turbine exhaust ejectors the engine itself is the primary fluid ducting.

The secondary fluid system is, in all cases, the outer shell. The secondary system may require ducting from an engine accessory or may have a bell mouth entrance to take air from a general area.

4-3.6.2.0 Support

The ejector must be treated as a complete unit, the primary and secondary systems assembled as a unit and supported in such a manner as to maintain the relative alignment in assembly. The position of the primary nozzle with respect to the mixing chamber is extremely critical. The axis of the primary nozzle must be coincident with the axis of the mixing chamber. Any misalignment of the primary nozzle will result in a finite reduction in ejector performance.

4-3.6.2.1 Reciprocating Engine Exhaust Ejectors

The ejector can be supported from the engine in such a manner as to maintain alignment of the primary and secondary systems. In the event that the secondary system is built into the fuselage structure some

provision must be made to prevent engine motion, and thus exhaust stack motion, from disturbing the ejector alignment. This can be accomplished by supporting the primary nozzles from the ejector shell and providing flexible ducting from the engine to the ejector.

4-3.6.2.2 Gas Turbine Exhaust Ejectors

The usual installation, consisting of a "can" shroud around the engine, can be installed on and supported from the engine. This type installation inherently maintains the alignment of the ejector.

4-3.6.2.3 Compressor Air Bleed Ejectors

The long ejector assembly is usually supported by the fuselage structure, and it is necessary to provide flexible ducting for the primary air from the engine to the fuselage mounted ejector assembly. The primary nozzle should be supported at the side of the entrance adapter and by adjustable links at the nozzle exit (See Figure 4-129).

4-3.6.3 Materials

Ordinarily, for parts not subjected to high pressures or temperatures aluminum or fiberglass can be used for ejector fabrication. The primary flow ducting for reciprocating engine exhaust ejectors and for compressor air bleed ejectors is subject to high temperature and/or high pressure operation. As such the ducting is usually of corrosion resistant steel of sufficient gauge to withstand the temperature and bursting pressure. The shells of reciprocating engine exhaust ejectors and compressor air bleed ejectors are not subject to high temperature and can usually be made of aluminum or fiberglass. The shell, or shroud, of a gas turbine exhaust ejector, being a fire container, must be made of stainless steel.

Consideration must be given to the possibility of vibration effects and suitable thickness provided to prevent cracking of any component.

4-3.6.4 Service

The only service required is inspection for cracks or alignment. Consideration must be given to accessibility for inspection of the primary duct system and the ejector shell and for adjustment of the ejector alignment.

4-3.6.5 Miscellaneous

Upstream of the mixing chamber entrance leakage of air from the outside must be held to a minimum. Any air leakage will of course affect the performance or effectiveness of the ejector. Downstream of the mixing chamber entrance leakage should be kept to a minimum but it is not too important.

Ejectors, especially the high pressure compressor air bleed ejectors, can be very noisy in operation. The ejector installation should be such as to point the ejector discharge away from occupied areas in the aircraft.

4-3.7 Ejector References

4-19 Contributions to Jet Pump Theory

I. Comparison of Ideal Mixing Process, by H. B. Helmbold, Engineering Study No. 105, June 1953, University of Wichita, School of Engineering, Wichita, Kansas

4-20 Contributions to Jet Pump Theory

II. Integral Relations on Mixing Processes, by H. B. Helmbold, Engineering Study No. 106, June 1953, University of Wichita, School of Engineering, Wichita, Kansas

4-21 Contributions to Jet Pump Theory

III. Simplified Theory of Mixing - Zone Spreading, by H. B. Helmbold, Engineering Study No. 107, July 1953, University of Wichita, School of Engineering, Wichita, Kansas

4-22 Contributions to Jet Pump Theory

IV. Approximate Theory of Jet Diffusion in a Constant Pressure Mixing Tube, by H. B. Helmbold, Engineering Study No. 118, November 1953, University of Wichita, School of Engineering, Wichita, Kansas

4-23 Contributions to Jet Pump Theory

V. A Simplified Theory of the Plane Jet in a Parallel Stream under Constant Pressure, by H. B. Helmbold, Engineering Study No. 137, May 1954, University of Wichita, School of Engineering, Wichita, Kansas

4-24 Review of a Systematic Theoretical Investigation of Jet Pumps, by H. B. Helmbold, Engineering Study No. 122, November 1953, University of Wichita, School of Engineering, Wichita, Kansas

4-25 Energy Transfer by Turbulent Mixing under a Longitudinal Pressure Gradient, by H. B. Helmbold, Engineering Study No. 182, August 1955, University of Wichita, School of Engineering, Wichita, Kansas

4-26 Gas Jets, by S. Chaplygin, Scientific Memoirs, Moscow University, 1902, (Available as N.A.C.A. TM 1063, August 1944)

4-27 The Diffusion of a Hot Air Jet in Air in Motion, by W. Szablewski, (Available as N.A.C.A. TM 1288, December 1950)

4-28 Airflow and Thrust Characteristics of Several Cylindrical Cooling - Air Ejectors with a Primary to Secondary Temperature Ratio of 1., by W. K. Greathouse and D. P. Hollister, N.A.C.A. RM E52L24, March 6, 1953, Confidential

4-29 The Design of Jet Pumps, by Gustav Flugel, (Available as N.A.C.A. TM 982, July 1941)

- 4-30 Performance Characteristics of Aircraft Cooling Ejectors having Short Cylindrical Shrouds, by Fred D. Kochendorfer and Morris D. Rousso, N.A.C.A. RM E51E01, May 1951, Confidential
- 4-31 Preliminary Investigation of Cooling - Air Ejector Performance at Pressure Ratios from 1 to 10, by C. W. Ellis, D. P. Hollister and A. F. Sargent, Jr., N.A.C.A. RM E51H21, October 17, 1951, Confidential
- 4-32 Analysis of Ejector Thrust by Integration of Calculated Surface Pressures, by John C. Sanders and Virginia L. Brightwell, N.A.C.A. TN 1958, October 1949
- 4-33 An Investigation of the Pumping and Thrust Characteristics of a Jet Ejector Operating at High Temperature and Pressure, by F.E. Mickey, Douglas Aircraft Company, Inc., El Segundo Plant, California, June 24, 1949, AT: 115547
- 4-34 Oil Cooler Airbleed Ejector Test, YH16-A, Power Plant, by A. W. Gabriel, Report No. 45-T-06, July 22, 1955, Vertol Aircraft Corp., Morton, Pa.
- 4-35 Aircraft Ejector Performance, by Frank A. McClintock and J. Hall Hood, Institute of Aeronautical Sciences, March 21, 1946
- 4-36 Effect of Temperature on Performance of Several Ejector Configurations, by H. D. Wilsted, S. C. Huddleston and C. W. Ellis, N.A.C.A. RM E9E16, June 13, 1949
- 4-37 Ejector Experiments, by W. G. Lewis and J. S. Drabble, Report R151, February 1954, National Gas Turbine Establishment, Pyestock, Hants-Whetstone, Leics, England
- 4-38 Investigation of Mixing of Confined Streams, by E. E. Weynand, Doctor of Science Thesis, Department of Mechanical Engineering, M.I.T., Cambridge, Mass., 1953
- 4-39 Fluid Dynamics of Jets, by Shin-i Pai, D. Van Nostrand Company, Inc., New York, N. Y., 1954
- 4-40 Aerodynamics of Propulsion, by Dietrich Kuchemann and Johanna Weber, McGraw-Hill Book Company, Inc., New York, N. Y., 1953
- 4-41 The Theory of Ejectors, by H. G. Elrod, Jr., Journal of Applied Mechanics, Volume 12, No. 3 pp A170-A174, Discussion Volume 13, No. 2 pp A162-A165
- 4-42 Effect of Molecular Weight of Entrained Fluid on the Performance of Stream - Jet Ejectors, by W. C. Holton, Transactions of the A.S.M.E., Volume 73, No. 7, pp 905-910, October 1951
- 4-43 Effect of Temperature of Entrained Fluid on the Performance of Steam - Jet Ejectors, by W. C. Holton and E. J. Schulz, Transactions of the A.S.M.E., Volume 73, No. 7, pp 911-913, October 1951

- 4-44 Momentum and Mass Transfer in Coaxial Gas Jets, by Walton Forstall, Jr. and Ascher H. Shapiro, Journal of Applied Mechanics, Volume No. 17, No. 4, pp 399-408, December 1950
- 4-45 The Turbulent Mixing of Coaxial Gas Jets, by Fred Landis and Ascher Shapiro, Heat Transfer and Fluid Mechanics Institute, 1951
- 4-46 A Simple Air Ejector, by Joseph H. Keenan and E. P. Neumann, Journal of Applied Mechanics, June 1942, pp A75-A81
- 4-47 An Investigation of Ejector Design by Analysis and Experiment, by J. H. Keenan, E. P. Neumann, and F. Lustwerk, Journal of Applied Mechanics, September 1950, pp 299-309
- 4-48 Mixing of Compressible Fluid Streams, by K. K. Klingensmith, Report R-12006-02, February 17, 1948, United Aircraft Corporation, Research Department, East Hartford, Conn., (ASTI AD-81223)
- 4-49 Further Experiments on the Flow and Heat Transfer in a Heated Turbulent Air Jet, by Stanley Corrsin and Mahinder S. Uberol, N.A.C.A. TN 1865, April 1949
- 4-50 Theory of the Jet Syphon, by B. Szczeniowski, N.A.C.A. TN 3385, May 1955
- 4-51 Investigation of Free Turbulent Mixing, by Hans Wolfgang Liepmann and John Laufer, N.A.C.A. TN 1257, August 1947
- 4-52 Calculation of Turbulent Expansion Processes, by Walter Tollmien, N.A.C.A. TM 1085, September 1945
- 4-53 Jet Diffusion in Proximity of a Wall, by D. Kuchemann, N.A.C.A. TM 1214, May 1949
- 4-54 An Investigation of the Round Jet in a Moving Air Stream, by Lt. Comdr. J. B. Deodati, U.S.N. and Lt. Comdr. E. B. Monteath, U.S.N., Jet Propulsion Laboratory, California Institute of Technology, Pasadena, Calif., Memorandum No. 3-8, ATI-12038
- 4-55 The Effect of Molecular Weight Ratio on the Mixing Length of an Ejector, by Charles H. Lee, Jr., Bachelor of Science Thesis, Department of Mechanical Engineering, M.I.T., Cambridge, Mass., 1950
- 4-56 Characteristics of an Ejector Mixing Tube of Constant Area, by Anthony J. Szynkiewicz and William D. Tierney, Bachelor of Science Thesis, Department of Mechanical Engineering, M. I. T., Cambridge, Mass., 1944
- 4-57 A Theoretical Consideration of the Performance of Air Ejectors, by Harold G. Elrod, Jr., Bachelor of Science Thesis, Department of General Engineering, M.I.T., Cambridge, Mass., 1942
- 4-58 The Mixing Tube Length of Constant Area Ejectors, by Angus B. Bower, Master of Science Thesis, Department of Aeronautical Engineering, M.I.T., Cambridge, Mass., 1951

- 4-59 Performance and Operating Characteristics of a Steam Ejector, by T. H. Anderson and J. M. Graham, Master of Science Thesis, Department of Chemical Engineering, M.I.T., Cambridge, Mass., 1933
- 4-60 Effects of Velocity Ratio and Initial Turbulence on the Mixing of Coaxial Gas Streams, by Robert S. Crosby, Master of Science Thesis, Department of Mechanical Engineering, M.I.T., Cambridge, Mass., 1949
- 4-61 A Study of the Air Ejector with Diffuser, by Gardner Mason Ketchum, Master of Science Thesis, Department of Mechanical Engineering, M.I.T., Cambridge, Mass., 1944
- 4-62 The Complete Air Ejector, by Edwin George Kispert, Master of Science Thesis, Department of Mechanical Engineering, M.I.T., Cambridge, Mass., 1943
- 4-63 Mixing of Gas Streams in Coaxial Circular Jets and Parallel Flat Jets, by Dale U. Von Rosenberg, Doctor of Science Thesis, Department of Chemical Engineering, M.I.T., Cambridge, Mass., 1953
- 4-64 Material and Momentum Transfer in Coaxial Gas Streams, by Walton Forstall, Jr., Doctor of Science Thesis, Department of Mechanical Engineering, M.I.T., Cambridge, Mass., 1949
- 4-65 Turbulent Mixing of Coaxial Gas Jets, by Fred Landis, Doctor of Science Thesis, Department of Mechanical Engineering, M.I.T., Cambridge, Mass., 1949
- 4-66 XR-10 Engine Cooling Survey, by W. E. Cobey, Kellett Report No. 1260.3, July 1946, Kellett Aircraft Corporation, Philadelphia, Penna.
- 4-67 Advances in Thrust Augmentation for Radial Engine Installations, by William A. Clegern, S.A.E. Quarterly Transactions, Volume 2, No. 1, pp 60-71, January 1948
- 4-68 Preliminary Air-Flow and Thrust Calibrations of Several Conical Cooling-Air Ejectors with a Primary to Secondary Temperature Ratio of I. I. Diameter Ratios of 1.21 and 1.10, by W. K. Greathouse and D.P. Hollister, N.A.C.A. RM E52E21, July 22, 1952, Confidential
- 4-69 Preliminary Air-Flow and Thrust Calibrations of Several Conical Cooling-Air Ejectors with a Primary to Secondary Temperature Ratio of I. II. Diameter Ratios of 1.06 and 1.40, by W. K. Greathouse and D. P. Hollister, N.A.C.A. RM E52F26, August 12, 1952, Confidential
- 4-70 Performance of Several Air Ejectors with Conical Mixing Sections and Small Secondary Flow Rates, by S. C. Huddleston, H. D. Wilsted and C. W. Ellis, N.A.C.A. RM E8D23, July 19, 1948, Restricted
- 4-71 An Investigation of the Performance and Design of the Air Ejector Employing Low Pressure Air as the Driving Fluid, by Prof. L. J. Kastner and J. R. Spooner, Proceedings of the Institute of Mechanical Engineers, Volume 162, Jan.-Dec. 1950, pp 149-166

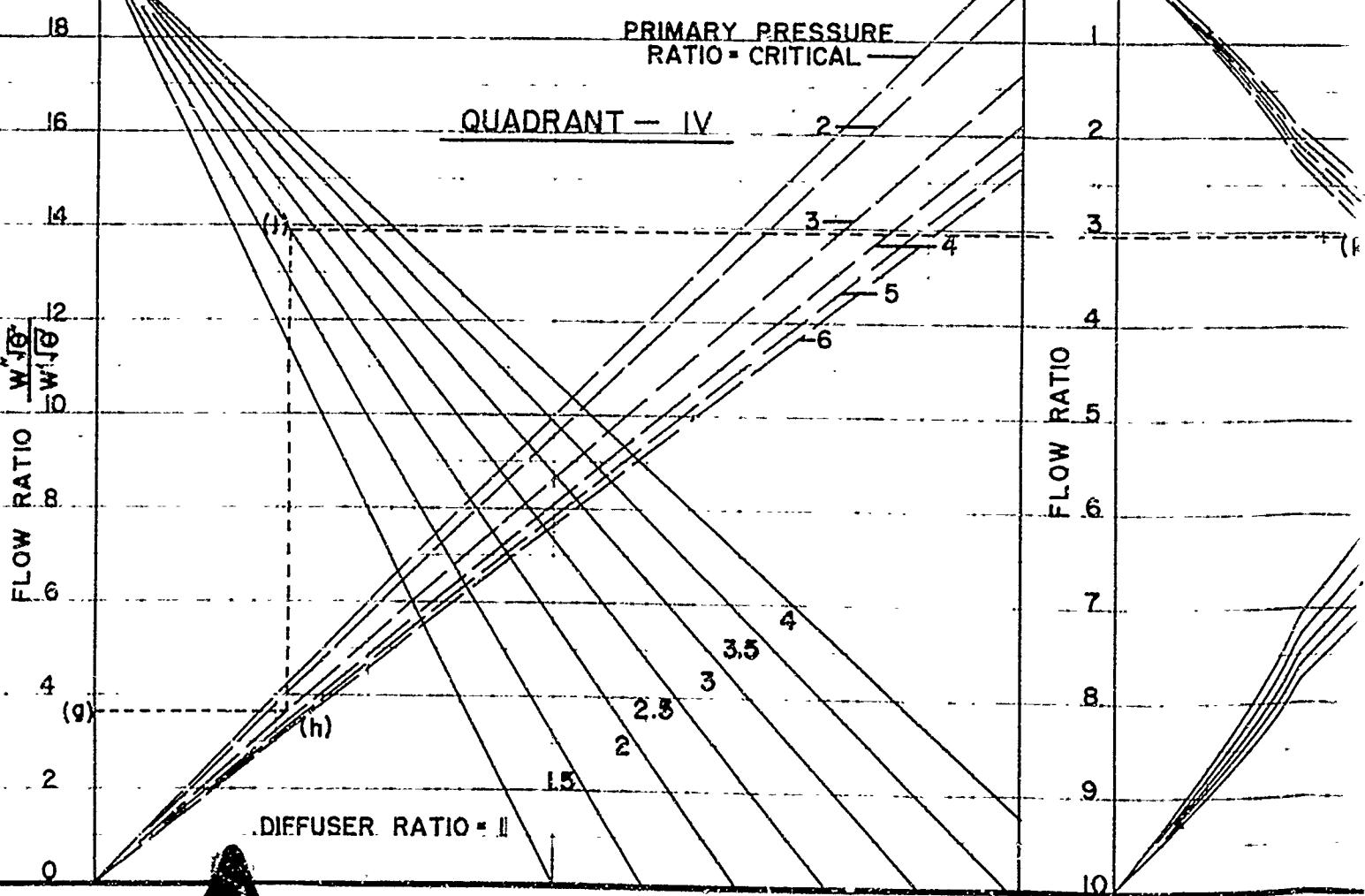
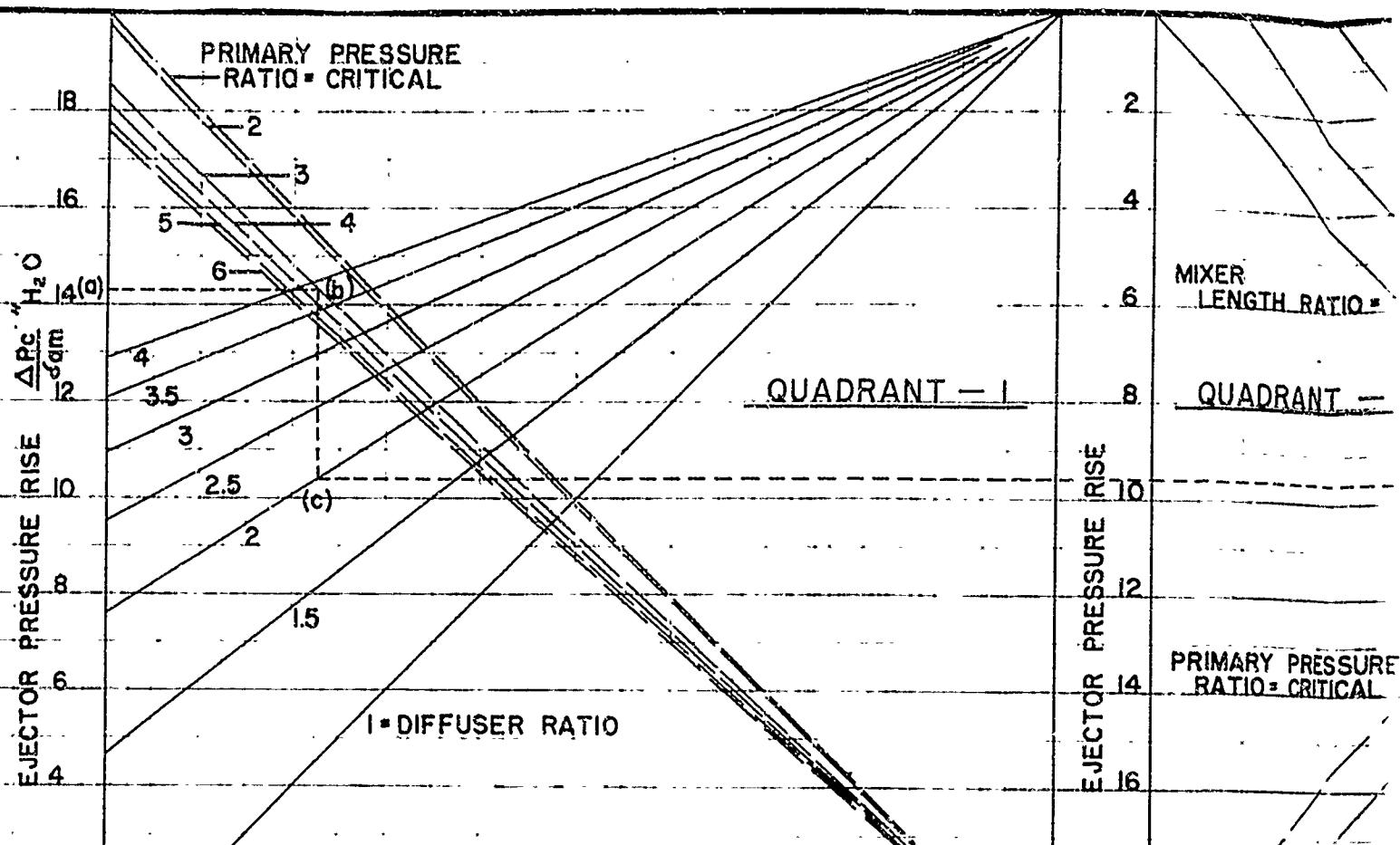
- 4-72 Pumping Characteristics for Several Simulated Variable-Geometry Ejectors with Hot and Cold Primary Flow, by John L. Allen, N.A.C.A. RM E54G15, September 8, 1954, Confidential
- 4-73 Pumping and Thrust Characteristics of Several Divergent Cooling-Air Ejectors and Comparison of Performance with Conical and Cylindrical Ejectors, by S. C. Huntley and Herbert Yanowitz, N.A.C.A. RM E53J13, January 20, 1954, Confidential
- 4-74 Installation Handbook for Turbo-Jet Engines, General Electric Company, Aircraft Gas Turbine Division, Evendale, Ohio
- 4-75 The Correction of Engine Output to Standard Conditions, by Donald S. Hersey, United Aircraft Corp., Journal of the Aeronautical Sciences, Volume 9, No. 10, pp 355 to 371, August 1942
- 4-76 Final Report on Exhaust Ejector Cooling Research, Contract No. Nonr 1437(00), Office of Naval Research, Lycoming Division, Report No. 1703, AVCO Manufacturing Corp., August 19, 1955
- 4-77 Installation Handbook, Pratt and Whitney Aircraft, East Hartford, Conn., 1943

4-4 List of Symbols

<u>Symbols</u>		<u>Subscripts</u>
σ'	Ejector Primary Nozzle Included Angle, Degrees Air Density Relative to Standard Sea Level Conditions = ρ/ρ_0	a Axial
ΔP	Differential Pressure at Existing Air Density	T Tangential Tip Throat
V	Velocity, Feet Per Second	R Root
ω	Rotational Velocity, Radius	l Entering
r	Radius, Feet	2 Leaving
α	Diffuser Included Angle, Degrees Angle of Attack, Degrees	FAN Fan
Q	Volume Flow Rate, Cubic Feet Per Second (or Minute)	m Mean
D	Diameter, Feet	d Drag
β	Inlet Angle, Degrees	l Lift
W	Resultant Fan Inlet Velocity Vector Relative to Blades, Feet Per Second	i Ideal Induced Inner
q	Dynamic Pressure (Velocity Head), Pounds Per Square Foot	o Outer, Zero
ρ	Air Density, Slugs Per Cubic Foot	f Fan
θ	Turning Angle, Degrees	i_r Ideal Rotor
C	Coefficient Chord	γ_R Rotor Entrance
A	Area	u In Plane of Rotation
f	Fan Function of Roughness Factor	2_r Rotor Exit
σ'	Stage Solidity	i_s Stator Entrance
S	Tangential Spacing or Gap Between Adjacent Blades	2_s Stator Exit
ΔW	Difference Between Resultant Velocity Vectors	i_s Ideal Stator
		i_{fan} Ideal Fan
		ACTUAL Actual
		IDEAL Ideal
		PRO Profile
		FAN Fan

4-4 List of Symbols (Continued)

<u>Symbols</u>	<u>Subscripts</u>
b Number of Blades	PROR Profile, Rotor
c Blade Chord, Feet	PROS Profile, Stator
ϕ Incidence Angle, Degrees	OUTPUT Output
HP Horsepower	T.C. Tip Clearance
γ Efficiency	REQ Required
W' Primary Air Flow Rate	ELEMENT Blade Element
W'' Secondary Air Flow Rate	TIP Tip
n Number of Engine Cylinders Discharging Into Exhaust Ejector	des Design
N Total Number of Engine Cylinders	
IHP Ideal Horsepower	



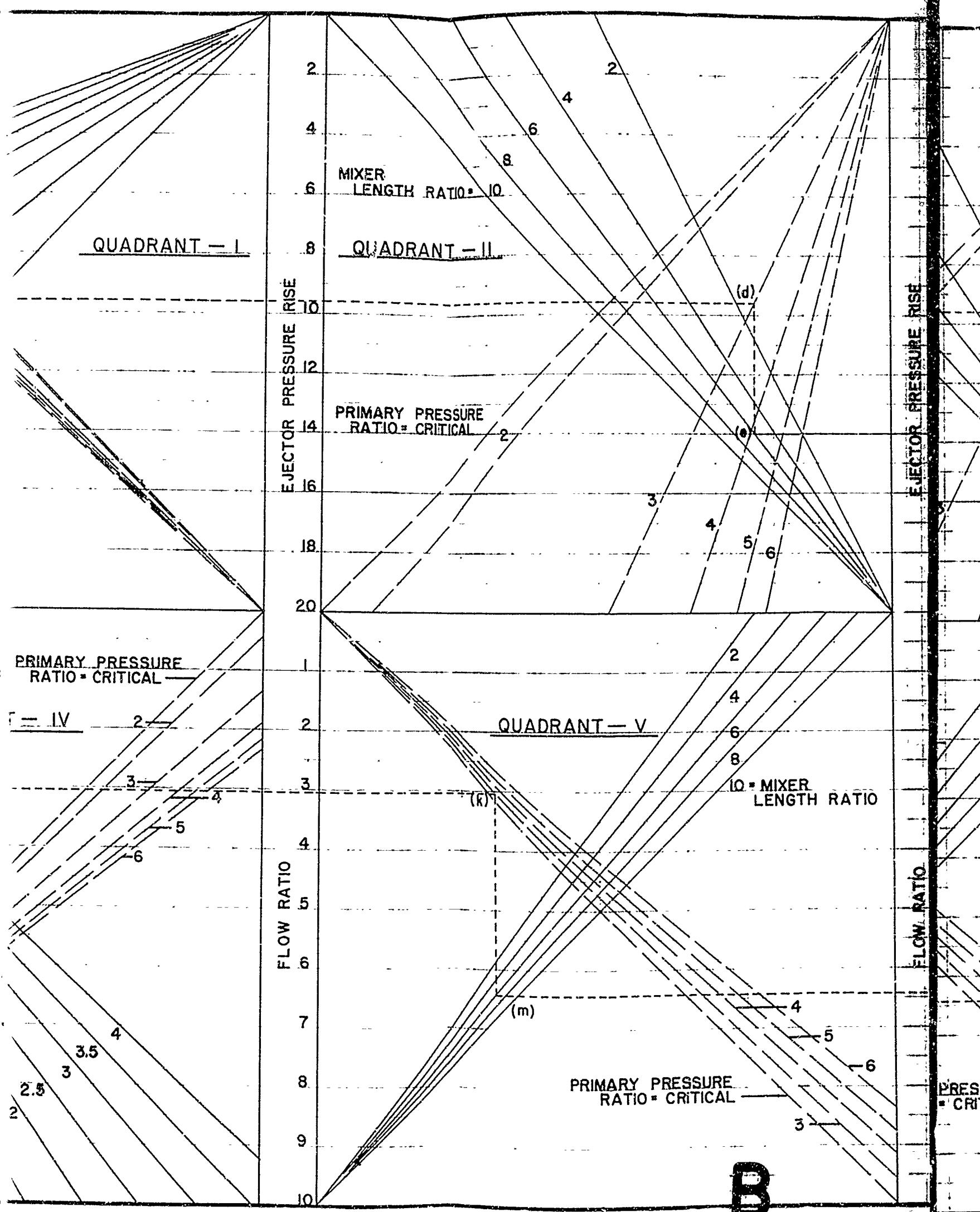
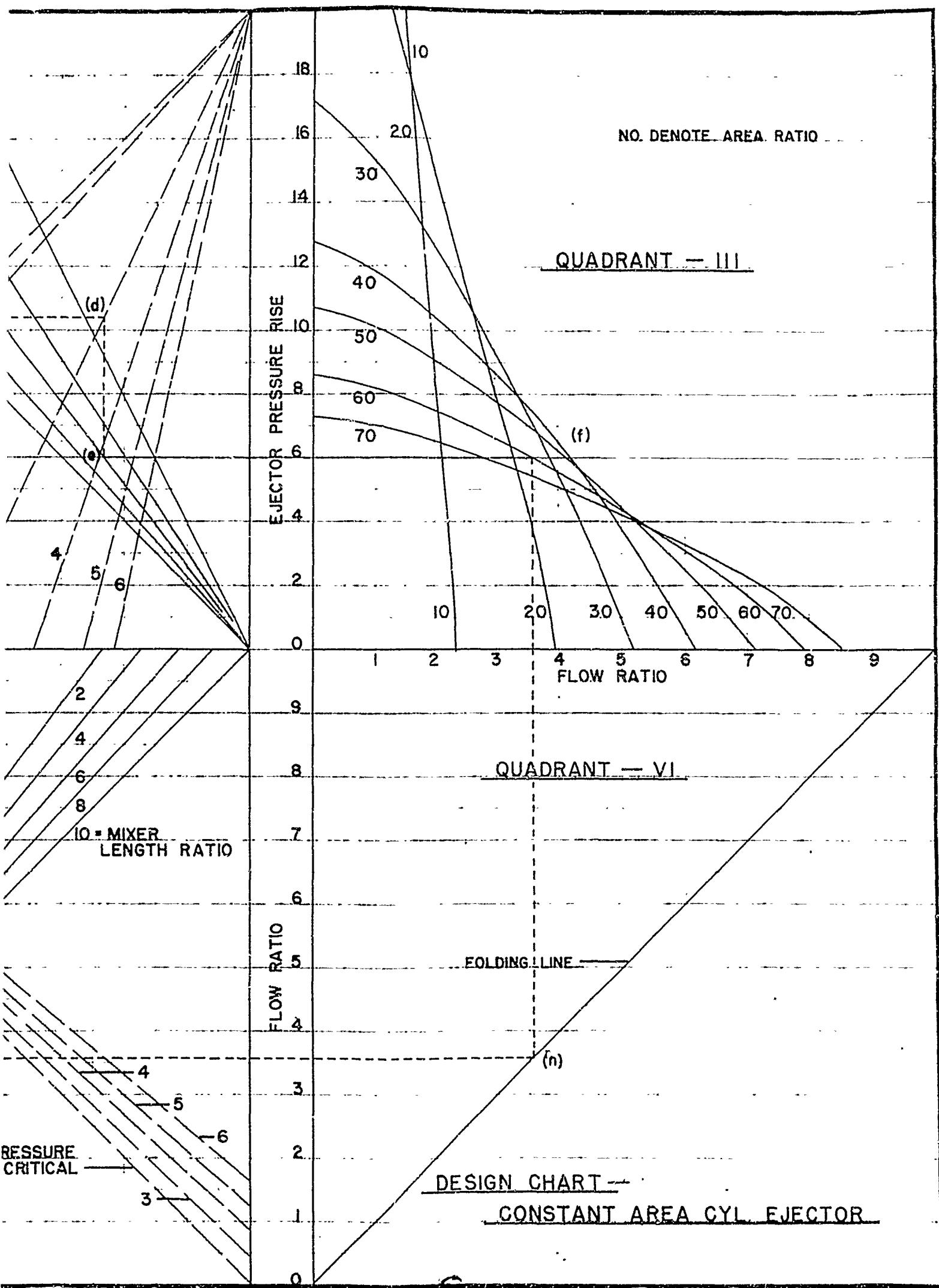


FIGURE 4-131



CHAPTER V

OIL COOLERS*

Table of Contents

Section	Title	Page
5-1	Oil Cooler Parameters	V - 3
5-2	Determination of Optimum Core Size	V - 5
5-3	References	V - 8

* The entire contents of this chapter, courtesy of Harrison Radiator Division, General Motors Corporation.

CHAPTER V

OIL COOLERS

List of Illustrations

Figure	Title	Page
5-1	Oil Side Heat Transfer and Pressure Loss Characteristics	V - 7

CHAPTER V

OIL COOLERS

5-1. Aircraft oil coolers for helicopters are generally procured to the requirements of Reference 5-2. The helicopter manufacturer's design specification will, in addition, establish the individual and detailed requirements for a given oil cooler installation.

In order to determine the oil cooler core size required, the following information should be given to the oil cooler manufacturer:

- a. Oil grade; e.g., MIL-L-6082 Grade 1100 or MIL-L-7808.
- b. Oil flow rate, pounds per minute.
- c. Heat rejection rate, Btu per minute.
- d. Oil temperature in degrees Fahrenheit, either into the oil cooler, or out of the oil cooler, but preferably both.
- e. Temperature of the air being supplied to the oil cooler.
- f. Maximum air-flow rate if known, pounds per minute, that will be provided for cooling.
- g. Air pressure loss allowable in the oil cooler (not including external ducting), usually expressed as static pressure in minus static pressure out, multiplied by the density of the air at the core face, divided by standard air density, .07651 pounds per cubic foot (see Reference 5-2, Paragraph 4.2.9.). Sometimes it may be found more reasonable to state the allowable air pressure loss in terms of total pressure in minus static pressure out. In any case, it should be made clear which method is used.
- h. Oil pressure loss allowable, p.s.i. (if different from Reference 5-2).
- i. The general configuration of oil cooler desired should also be stated if this is known in the early design stages; if not, the cooler manufacturer can, on the basis of past experience, readily suggest an arbitrary size and shape for initial consideration. If, however, there is some preliminary idea of the configuration desired, the following points might be mentioned:
 1. Maximum dimension in the direction of air flow.
 2. The general shape of the cooler face: whether rectangular (and if so, approximate ratio of height to width), curved (mean radius and height), round, etc. In general, core configurations other than rectangular tend to be more costly to build.

3. The approximate relation of oil in and out connections to the intended configuration.

Items c through g above should be evaluated at the "critical design condition", which might be explained as being that steady state operation which will require the largest oil cooler. There may be some brief transient states during which it may be considered reasonable to allow the oil temperature to exceed the usual maximum. The critical design condition will usually involve:

- a. The maximum required heat rejection.
- b. The maximum ambient air temperature (plus any additional allowance for heat pick-up before the cooler).
- c. The minimum air flow rate and pressure loss.
- d. The maximum oil temperature level to be maintained under these circumstances, at some definite point (into the oil cooler, into the engine, etc.).

For a given installation, these factors may not reach a minimum or maximum value all at the same operating condition, and it may be reasonable to select some intermediate point, or furnish an operating range, for the oil cooler specification. As an example, it sometimes happens that maximum heat rejection coincides with maximum air flow availability, and the "critical" point may actually be at a lower heat rejection figure, when there is a minimum of air available. This situation might, perhaps, be rather unusual on a helicopter. If, after a preliminary size estimate it seems that the cooler will be too large for the installation, it may be well for the helicopter designer to reconsider the values of heat rejection and oil temperature specified. Sometimes these are estimated with rather liberal "safety factor" allowances, and a reduction in the heat transfer requirement or an increase in the allowable oil temperature level can effect substantial savings in cooler size and weight. It has been difficult to establish any relation between cooling air horsepower and cooler weight. However, it should be pointed out that limiting cooling air availability to anything approaching the thermodynamic minimum, or specifying an air pressure loss of only one or two inches of water, is bound to result in very large and heavy oil cooler installations.

No mention was made here of the influence of oil flow rate on the critical design point, since normally this has very little effect on the cooler size. Increasing or decreasing the oil flow rate (everything else being held constant) does not change appreciably the temperature of the oil out of the cooler, but it will affect the inlet oil temperature considerably. In the past, it appears, aircraft power-plant designers have determined oil flows so that, for a given heat rejection, the oil temperature rise through the system will be of the order of 40°F., usually not exceeding 60°F.

After a cooler core size has been determined, and before the final specification is established, the oil cooler manufacturer should be supplied the following additional information:

- a. Exact location, size and type of oil connections.

- b. Whether or not a warm-up by-pass is required.
- c. Method of mounting the cooler to the air frame.
- d. Method of attaching the air ducts, if any.
- e. Location and type of drain, if any.
- f. Whether or not a temperature control valve will be required, and if so what minimum oil outlet temperature is desired, below which the valve will begin to open to allow oil to by-pass the cooler, and above which the valve will be closed forcing all of the oil flow through the cooler core. This temperature should be at least 10° below the maximum allowable oil out temperature mentioned above and should be given with a tolerance of $\pm 5^{\circ}\text{F}$. The two valve operating temperatures most commonly in use at the present time are $185^{\circ} \pm 5^{\circ}$, and $160^{\circ} \pm 5^{\circ}\text{F}$., although some others are also in use. Normally, a pressure relief spring is incorporated in the thermostatic control valve, to assist in decongealing the cooler core, and is usually set to relieve at a pressure differential between the cooler inlet and outlet of 40 p.s.i. If any other pressure relief setting is desired, it should be remembered that the greater the force required for pressure relief the more easily and quickly will decongealing be accomplished. If the requirements of MIL-C-7488 are adhered to, it is not necessary to provide for any additional pressure relief, or any surge protection mechanism. From its function, it will be noted that the valve is located adjacent to the oil outlet port, at the outlet end of the warm-up by-pass.
- g. The required hydrostatic test pressure, if less than the 400 p.s.i. requirement of Reference 5-2.
- h. Any special qualification test requirements, although it is expected that qualification tests will very rarely be different from the requirements of Reference 5-2.

5-2. In determining the optimum core size to meet the heat transfer requirements, the oil cooler designer can vary the core components as well as the core dimensions:

- a. Core depth, the dimension in direction of air flow.
- b. Plate length (= oil flow length).
- c. Core height, or the "no-flow" dimension.
- d. Height of air side fins and number of fins per inch.
- e. Surface characteristics of air side fin: whether plain, louvered, or one of several other fin shapes (see Reference 5 - 1); if louvered, what louver form and spacing, etc.
- f. Oil side fin characteristics: several different types are available, some tending to have high, and some low pressure loss characteristics.

As a practical matter, the designer, in varying these factors, will usually attempt to use dimensions and materials compatible with available tooling in order to keep cost and delivery time within reason. It will be appreciated, therefore, that for this reason the tentative oil cooler configuration set up by the aircraft manufacturer should not be too rigid but rather flexible enough to allow for the maximum use of available tooling.

Because of the wide variation possible in the factors noted above and since no single combination represents an optimum for all the various operating requirements in the aircraft field, it is considered impractical to attempt to set up any rule-of-thumb method for establishing preliminary cooler sizes. If the oil cooler manufacturer is consulted as early in the development as possible, even with only preliminary data available, an approximate size determination can be made very quickly. Since the design variables are so numerous, experience in their application is almost essential for the selection of a reasonably compact, light-weight unit. The speed with which this can be done is greatly enhanced by the use of electronic computers.

However, using published data, it is possible to select a core geometry and size arbitrarily and calculate the performance - heat transfer and pressure losses - over a wide range of flows and temperatures. A very good source for such data, and also for the methods of analysis, correlation and application, is Reference 5-1. Not all the variations possible are covered in the data presented, but a sufficiently wide choice is available to get an approximation of a reasonable size. Unfortunately, this reference does not cover the types of fin material usually found on the oil side of aircraft oil coolers, which makes it difficult to estimate a reasonable oil side conductance. The magnitude of its value, however, is usually much greater than that of the air side conductance which for this type of heat transfer unit is the controlling factor. To illustrate, the equation relating overall conductance to oil side and air side conductance (neglecting wall resistance, which is very small) is

$$\frac{1}{\text{Overall Conductance}} = \frac{1}{\text{Air Side Conductance}} + \frac{1}{\text{Oil Side Conductance}}$$

If, for example, the air side conductance had a value of 1 and the oil side 10, then the overall conductance would be 0.909. It can be seen that increasing the oil side conductance by, say, 20% would increase the overall by only 1.5%, with a negligible effect on the actual heat transfer rate; but increasing the air side by 20% would increase the overall by nearly 18% and give a substantial increase in the heat transfer rate.

In order to provide some method of evaluating the oil side conductance and to get a fair approximation of oil side pressure loss, the chart, Figure 5-1, gives a correlation of heat transfer and pressure loss characteristics for two such fin geometries, using the same methods and definitions as Reference 5-1. These values are merely typical and representative and do not necessarily reflect the best possible selection for any given oil cooler problem.

The analytical treatment of oil cooling is included in Sections A-2.2 and A-2.3 of the illustrative problem in Appendix 1.

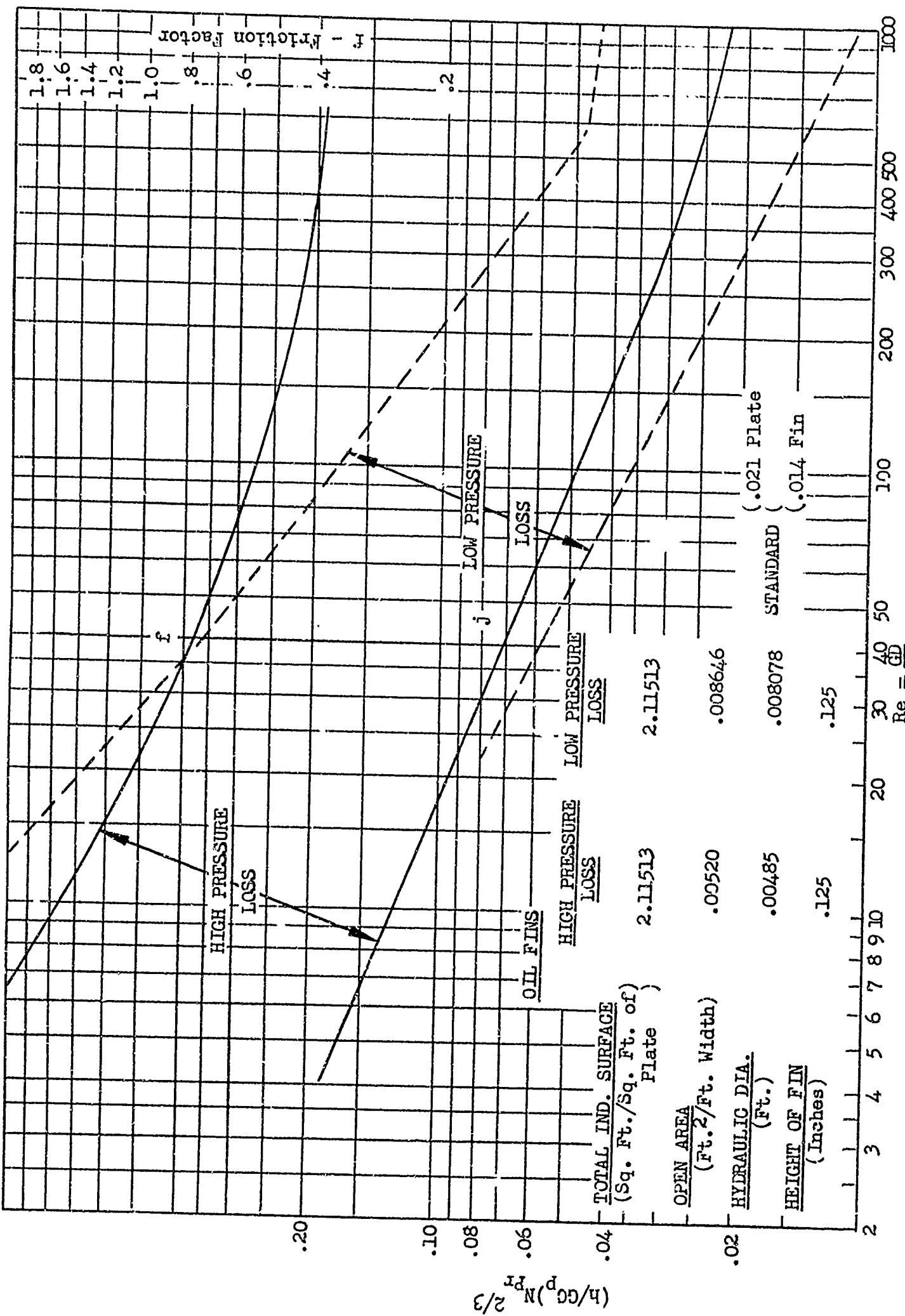


FIGURE 5-1. OIL SIDE HEAT TRANSFER AND PRESSURE LOSS CHARACTERISTICS

SECTION 5-3

REFERENCES

- 5-1. W. M. Kays and A. L. London: Compact Heat Exchangers. National Press, Palo Alto, California
- 5-2. Military Specification MIL-C-7488, Coolers, Oil, Plate, Aircraft
- 5-3. E. F. Busch: Method of Analysis Extended Surface Oil Coolers. AiResearch Manufacturing Company Report No L-5175-R, Revision 1, February 8, 1955.

CHAPTER VI

TESTING METHODS

TABLE OF CONTENTS

<u>Section</u>	<u>Title</u>	<u>Page</u>
6-1	Introduction	VI-3
6-2.0	Component Testing	5
6-2.1	Fan Tests	5
6-2.1.1	Static and Dynamic Testing	5
6-2.1.2	Natural Frequency Testing	7
6-2.1.3	Aerodynamic Performance Testing	8
6-2.1.4.0	Structural Tests	36
6-2.1.4.1	Overspeed Proof Testing	36
6-2.1.4.2	Acceleration - Deceleration Testing	37
6-2.1.4.3	Fan Endurance Testing	37
6-2.1.5	Inertia Testing	39
6-2.1.6	Sound Testing	42
6-2.2.0	Duct Tests	45
6-2.2.1	Model Testing	46
6-2.2.2	Aerodynamic Performance Testing	47
6-2.2.3.0	Structural Tests	50
6-2.2.3.1	Duct Endurance Testing	50
6-2.2.3.2	Backfire Pressure Testing	50
6-2.3.0	Ejector Testing	50
6-3	Ground and Flight Testing	55
6-4	References	62
6-5	List of Symbols	70

CHAPTER VI

TESTING METHODS

LIST OF FIGURES

<u>Figure</u>	<u>Title</u>	<u>Page</u>
6-1	Set Up #1	VI-10
6-2	Set Up #2	10
6-3	Set Up #3	11
6-4	Set Up #4	12
6-5	Set Up #5	11
6-6	Straightener	15
6-7	Pitot Tube	15
6-8	Marked Pitot Tube	17
6-9	Performance Curve	20
6-10	Fan Deflection Inspection	28
6-11	Centrifugal Fan-Sound Set Up	44
6-12	Axial Fan with Ducts - Sound Set Up	44
6-13	Axial Fan without Ducts - Sound Set Up	44
6-14	Turbine Compressor Air Bleed Ejector	51
6-15	Static Flow Test Set Up, Compressor Air Bleed Ejector	54
6-16	Turbine Exhaust Ejector Instrumentation	55
6-17	ANA Standard Hot & Cold Days	60

LIST OF TABLES

<u>Table</u>	<u>Title</u>	<u>Page</u>
6-1	Calculation Guide	28, 29
6-2	Fan Performance Calculation Outline	31
6-3	Log Sheet - Traverse Readings	32
6-4	Log Sheet - Summary	33
6-5	Report Outline	34-36 Incl.

CHAPTER VI

TESTING METHODS

6-1 INTRODUCTION

Elsewhere in this handbook, information has been provided to permit the design of a fan, duct and ejector cooling system in compliance with specific requirements. These requirements considered such criteria as size, weight, cost, drag, pressure, volume, power absorption and temperature as well as numerous layout design problems.

This Chapter is devoted to the purpose of defining the test methods used to determine the degree of success to which the above requirements have been met.

To accomplish this objective, certain testing is required to either a greater or lesser extent, depending upon the nature of the design, specification requirements and desires of the Contractor and Customer.

Essentially such tests consist of methods to permit proper evaluation of the performance of the fan, duct and/or ejector system as installed in the aircraft. Tests which may be performed in their approximate chronological order are as follows:

A. Component Tests

1. Fan Tests

- a. Static and Dynamic Balance Tests
- b. Natural Frequency Tests
- c. Aerodynamic Performance Tests
- d. Structural Tests (overspeed, acceleration-deceleration, and endurance)
- e. Inertia Tests
- f. Sound Tests

2. Duct Tests

- a. Model Tests (static tests for internal studies, wind tunnel tests for external studies)
- b. Aerodynamic Performance Tests
- c. Structural Tests (endurance, backfire pressure)

3. Ejector Aerodynamic Performance Tests

B. Flight Tests

- 1. Cooling Tests
- 2. Duct System Tests
- 3. Ejector System Tests

In accordance with the Contract under which this handbook was prepared, the procedures outlined herein are applicable for testing of fans, ducts, and ejectors for airflow at speeds from 0 to Mach No. = 0.5, at pressure altitudes from sea level to 35,000 feet and over the range of air temperatures encompassed by the curves of Figure 1 of ANA Bulletin No. 421 (Figure 6-17) Reference 6-44. Also, cooling fans with the following parameters can be evaluated:

- | | |
|---|----------------------------|
| a. 20" to 45" diameter | e. 2" to 8" blade span |
| b. 5 HP to 150 HP absorption | f. 300 to 600 ft./sec. tip |
| c. 5" to 20" H ₂ O total pressure rise | speed |
| d. 4 to 30 blades | g. 5,000 to 50,000 cfm. |

For testing of cooling fan, duct and ejector systems, the criteria may be obtained from one or more of the below listed sources.

A. For Navy Contracts

1. The Basic Contract
2. MIL-C-8678 (Aer) Reference 6-61
3. SD-24 Reference 6-42
4. MIL-D-17984A (ASG) Reference 6-66

B. For Air Force Contracts

1. The Basic Contract
2. MIL-C-7220 (USAF) Reference 6-56
3. AN-T-62 Reference 6-45
4. WCNEI-525-460 (USAF) Reference 6-46
5. H.I.A.D. Reference 6-30

Additional information may be obtained in the following:

1. List of Military Specifications and Standards used by the Bureau of Aeronautics.
2. List of Military Specifications and Standards used by the U.S. Air Force.
3. AGARD Flight Test Manual, Reference 6-29.
4. AF Technical Report 6273 (Flight Test Engineering Manual) Reference 6-28.

The review of the above sources will result in numerous detail requirements, some of which may be superfluous or impractical. In such cases, the Contractor should resolve with the Customer, all requirements which are not desired. Neither party wishes to expend test funds or time to obtain unnecessary data; therefore, such preliminary action is the moral responsibility of the Contractor.

As in all test work, reliable data can be obtained at reasonable cost and in reasonable time only by a properly planned and coordinated program. An example of a Ground and Flight Test Program is presented in Appendix VI.

6-2.0 COMPONENT TESTING

Component tests are conducted to obtain individual evaluation of a specific system prior to flight testing. In this manner, early evaluation and economical improvements can be made.

Such tests are customarily programmed in chronological sequence to assure safe operation as well as for obtaining correlated data.

Components are considered as the entire fan assembly and its installation, the entire individual duct system and its installation, the entire ejector system and its installation or perhaps any portion of a system.

The test methods employed for evaluation and/or qualification of the component tests are as follows:

6-2.1.0 Fan Tests

Fan evaluations and/or qualifications may be accomplished through the use of several or all of the following test methods:

- a. Static and Dynamic Balance Tests
- b. Natural Frequency Tests
- c. Aerodynamic Performance Tests
- d. Structural Tests
 - 1. Overspeed Proof
 - 2. Acceleration-Deceleration
 - 3. Endurance
- e. Inertia Tests
- f. Sound Tests

6-2.1.1.0 Static and Dynamic Balance Testing

Prior to any whirl testing, it is necessary that the fan be tested to insure that it is statically and dynamically balanced. Although balance testing is essentially an inspection test on each fan manufactured, it is included herein as a means of evaluating the effect of shop tolerances permitted in the design. After several fans are thus tested, corrections may be required or means of changing weights provided.

Unbalance will produce vibration and stresses which may result in premature failure and serious damage to test equipment and personnel. It may be the result of numerous conditions including one or more of the following: (These conditions can occur on every fan even though fabricated to one design.)

- a. The introduction of manufacturing tolerances on the detail fabrication and the assembly.
- b. Use of standard repairs to correct errors or deficiencies.
- c. Non-homogeneity of the material, caused by blow hole, slag inclusions, etc.

- d. Irregularities in mass distribution such as surface condition of forgings and castings.
- e. Unsymmetrical distortion of individual parts on the body while rotating, such as elongation of material, slippage in holes, diaphragm action of webs, etc.

Balancing of the fan is accomplished by placing or removing weight on the fan at some specific location thereby providing static and dynamic balance. Additional information may be obtained in References 6-1, 6-7, 6-8, and 6-9.

6-2.1.1.1 Static Balance

Static unbalance exists if the fan is not in static equilibrium when the two ends of the fan shaft are placed on parallel horizontal rails, i.e., the fan tends to rotate. In the event that dynamic balancing will be performed, static balance may be omitted since, in dynamic balance, static balance is also obtained.

Static unbalance may be determined and measured by the use of a pair of knife edged absolutely-horizontal parallel rails. The ends of the fan shaft are placed on the rail, and if the fan center of gravity is not coincident with the axis of rotation, the fan will rotate until the heaviest portion of the fan is in the lowest position. The magnitude and location of corrective measures to place the fan in static equilibrium can thus be determined. A number of commercially produced balancing machines are also available for balancing purposes.

In the event that the fan is unbalanced, then mass should be added (lengths of solder strip material of required cross section and length, washers, cast weights, etc.) until the fan becomes statically balanced about the rotational axis. In the event that it is determined that mass must be removed, then the required amount of weight should be removed by milling, grinding, drilling, shaping, etc., as required. All mass changes should be made as near to the center of the plane of the fan as possible.

6-2.1.1.2 Dynamic Balance

Dynamic unbalance exists if the fan, upon rapid rotation, reveals a disturbing couple of centrifugal forces acting on the shaft. Such unbalance can be observed visually or by various indicating equipment.

For both static and dynamic balancing, a dynamic balancing machine may be used. Such a machine will indicate the magnitude and angular location of unbalance, and will enable corrective measures to be applied and checked. In dynamic testing, the fan shaft is suspended on flexible supports, the unbalanced fan is rotated, and the deflections at the supports are measured by mechanical or electrical means. The amplitude of deflection at the support is an indication of the unbalance in the fan. Calibrations may be made to obtain precise relations between an unbalance and the resulting measured amplitudes to facilitate balancing other specimens of the same fan.

More advanced machines are also available which determine both the axial and angular unbalance locations, and indicate the correction required.

In using the balancing machine, the machine should be run at the normal fan operating speed if possible. This is especially true for fans with elastically mounted blades, where blade motion may affect results. Corrections made at lower speeds can result in some unbalance under normal speed due to slight changes in structural deflection. Where possible, mass corrections should be made in the plane of the unbalancing forces in order to eliminate moments on the fan shaft. It should be noted that in dynamic testing the unbalance force precedes the displacement by an amount which can vary dependent upon the rotational speed. This condition is known as angle of lag and its value is normally between 5° to 15° , but increases to 90° at the critical speed and 180° as the speed is increased above the first critical speed.

Upon determination of the corrective measures required, the mass change may be made as in Static Balancing.

(Detail schematics of various types of testers may be observed in Section 89 of Tool Engineers Handbook, Reference 6-9.)

6-2.1.2.0 Natural Frequency Testing

Resonance of a fan exists when the natural frequency of the fan or fan blades is exactly equal to the exciting frequency introduced into the fan by some exciter. Such excitors may be propellers, rotors, engines, gears, starters, generators, motors, etc. The amount of their influence upon the fan is a function of distance, speed, and method of transmission. Since the fan, including its blades, have been designed to consider these conditions, the purpose of a fan resonance test is to determine the fan natural frequencies and its acceptability.

Two methods may be employed to obtain the natural frequencies: bang test or shaker test. The method employed is at the discretion of the Contractor. The bang test is the fastest, most economical, and the results generally satisfactory, but usually only provides the fundamental natural frequency. The shake test permits evaluation at all ranges of the exciting frequencies and can furnish the values of the higher natural frequencies and also provide mode shapes.

6-2.1.2.1 Bang Tests

Bang testing consists of striking a properly mounted fan with a rubber mallet and recording the frequency response. Repeating this action several times at several points near the circumference of the fan will result in an average value for the fan body. Similarly by striking several fan blades, the local fundamental frequency of the blade may be established.

Upon acceptance of the results, the arithmetic average frequency of the blades and the fan may be determined. These results should compare with those calculated during the fan design. In the event that a change in natural frequency is necessary, the changes in stiffness, moment of inertia, section modulus, or mass distribution must be made.

6-2.1.2.2 Shaker Test

Shaker tests consist of exciting a properly mounted fan with a vibrator at various rates and observing and/or recording the frequency response. The response is measured at several places on the fan in order to observe the modal shapes and the number of pickups required can range

from two for natural frequency to ten or more for accurate definition of modal shapes. The response can be measured through the use of acceleration, amplitude or velocity pick-ups for the fan frequencies and strain gages for the blade frequencies. The strain gages on the blades, if required, should be located between anticipated nodes. Additional data on instrumentation is available from References 6-4, 6-6, and 6-29.

The full range of frequencies normally encountered in operation should be reproduced with the shaker. This range should include all the running speeds and the respective multiples of the various excitors, i.e., engine, propellers, rotors, gears, starters, generators, motors, the product of the number of fan blades and the stator blades, etc.

The output arm of the shaker should be applied at the anti-node and in an area where the specimen mass is large in order to prevent the mass of the shaker arm from influencing the result by becoming an effective specimen. For frequency determination of cantilevered blades and for most fan bodies the anti-node will be at the outer periphery.

6-2.1.3.0 Aerodynamic Performance Testing (Test Block)

The purpose of the aerodynamic testing of a fan is to verify the air delivery against a given resistance pressure and usually to measure the horsepower to perform this work. Either one or more points of operation are required, depending upon the nature of the test. In an installation test, the system with which the fan is connected generally offers a fixed resistance and so a single point (or at most 2 to 3 such points) of operation need be tested. In most cases it is difficult to make accurate tests of an installed fan owing to the proximity of the fan to duct elbows or transformations which leave no length of straight duct in which to take accurate readings. In such cases, approximate results only may be expected from the test. When a fan can be subjected to a fan tunnel test, the complete range of fan performance from free delivery to no delivery may be obtained. This type of testing is usually necessary for a full performance evaluation of the fan or for research and development work.

By employing fan tunnel testing, control over specified test conditions, i.e., straightness of air flow, flow uniformity, density, velocity, etc., can be exercised to provide the desired data. By strict adherence to specified test conditions of fan speed and air density, consistent results of the following may be obtained.

- a. The pressure rise produced
- b. The quantity of air or gas delivered
- c. The power supplied to the fan shaft
- d. The efficiency of the fan

Axial and centrifugal flow machines, in which the fluid undergoes a density change exceeding 7%, Reference 6-14, must be tested as compressors. Machines in which this change does not exceed 7%, Reference 6-15, should be tested as fans. This handbook will deal with fans. This entire Section 6-2.1.3 to Section 6-2.1.3.4, inclusive, is from Reference 6-15, except as noted.

Essentially the basic objective in axial and centrifugal fan aerodynamic testing is to determine the flow rate, pressure, and horsepower. In order to properly interpret the resulting data, it is necessary to obtain other readings, such as temperature, humidity, barometric pressure, fan speed, etc. for the proper correction of these values.

Fan tunnel tests should be performed on all new fan designs as required by SD-24 or H.I.A.D. References 6-42 and 6-30.

Additional data on fan and compressor testing may be obtained from References 6-1, 6-3, 6-14, 6-15, 6-34, 6-35, and 6-36.

In the event that the airflow through the fan is desired under flight conditions, it is advantageous to calibrate permanent instrumentation with fan airflow. This can be accomplished during these performance tests. One method of providing such a calibration consists of permanently installing several radially located pitot static tubes, to record total and static pressure, in a stator parallel to the stator blades. Thus, while the performance tests are being conducted, the pressures are correlated with the precisely established flow to result in a flow vs. pressure calibration curve. This calibration can later be used to determine the flow equilibrium point actually established in the aircraft.

In order to establish an envelope of data, testing should be accomplished through the entire operating range of RPM and airflow.

6-2.1.3.1.0 Set-Up and Components

Facilities for the aerodynamic performance testing of fans consist of tunnel sections, plenum chamber, flow straighteners, throttling device, measurement equipment and drive system. Important factors affecting fan performance are density of the air, resistance of the external system and the speed of the fan. Care must be exercised to assure constancy of these factors during each run.

In order to establish a standard of understanding, the description and definition of terms as recommended by the ASME are provided in Appendix V.

As noted in Paragraph 6-2.1.3.0, a test set-up must be determined in the initial phases of the test program. There are five basic set-ups established by the ASME Power Test Codes for Fans, Reference 6-15, and they are as follows: (Supplementary information on wind tunnel design may be obtained in References 6-12, 6-13, and 6-26.)

6-2.1.3.1.1. Set-Up No. 1 - With Discharge Duct Only

Figure 6-1 is used for fans intended for installation with discharge duct, but no inlet ducts or inlet boxes. The discharge Set-up of No. 1 should have an area equal to that of the fan outlet within plus or minus 5 per cent. The tunnel must be straight, of uniform circular cross-section, and not less than 10 diameters in length. Openings for insertion of pitot tubes are to be so located that the impact ends of the tubes must be not less than 7.5 tunnel diameters from the fan end of the tunnel. The straightener should be located not less than 6 tunnel diameters from the fan end of the tunnel. The distance between the pitot tube traverse plane and the straightener must be not less than 1 1/2 tunnel diameters.

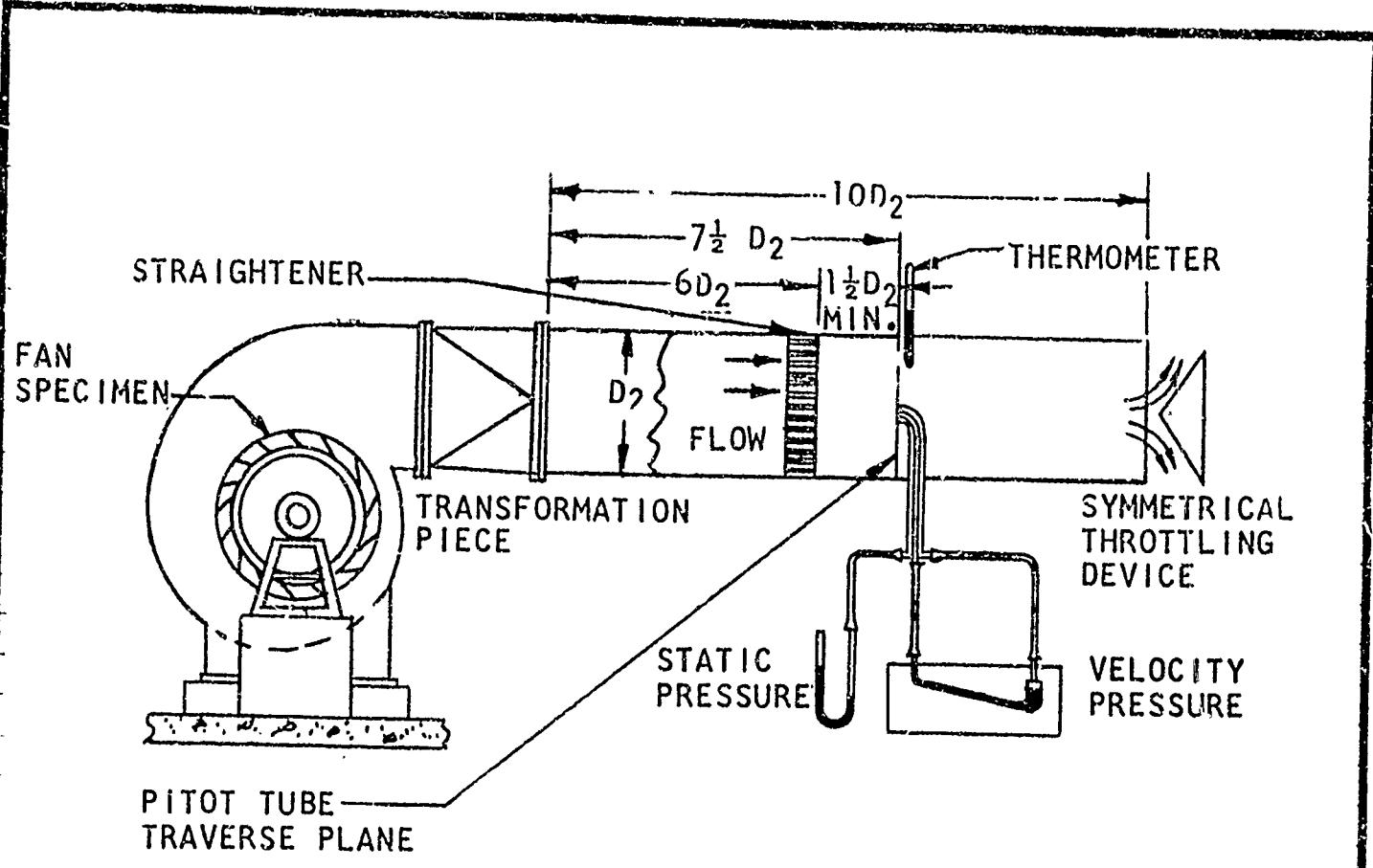


FIGURE 6-1. Test Set-Up No. 1 with Discharge Duct Only

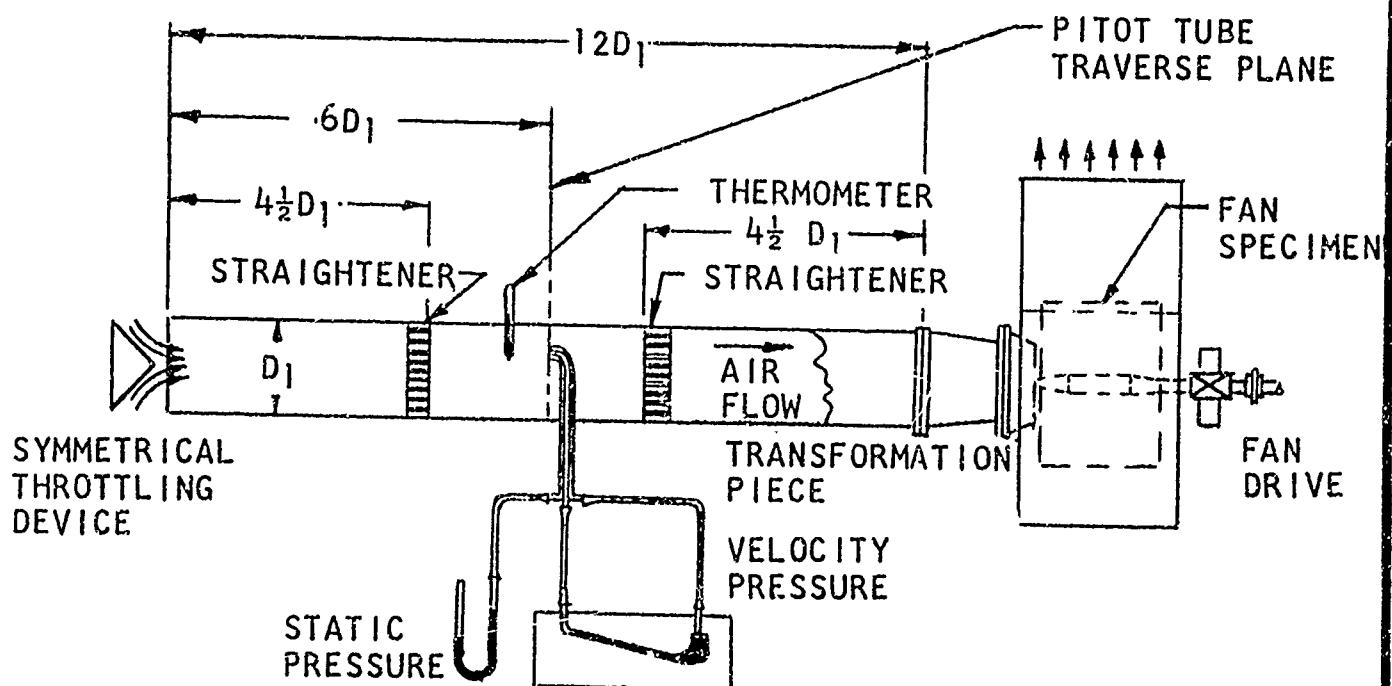


FIGURE 6-2. Test Set-Up No. 2 with Inlet Duct Only

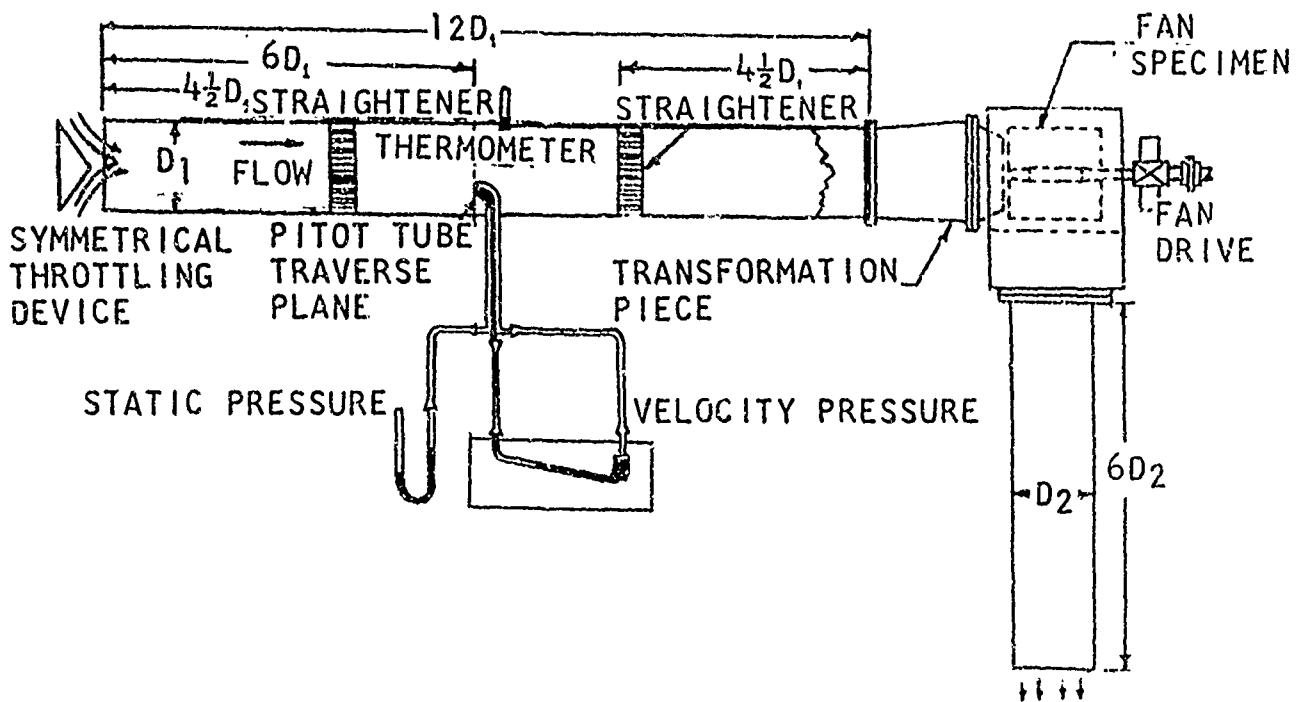


FIGURE 6-3. Test Set-Up No. 3 with Inlet and Discharge Ducts

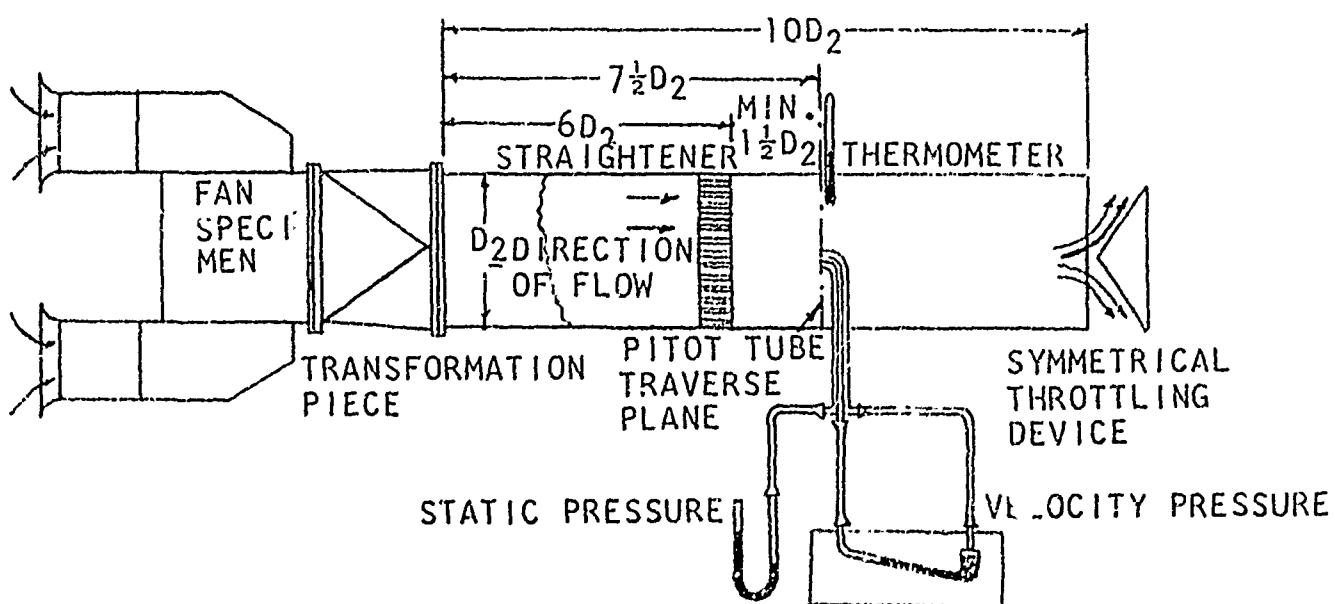


FIGURE 6-5. Test Set-Up No. 5 with Double Inlet Boxes & Discharge Duct

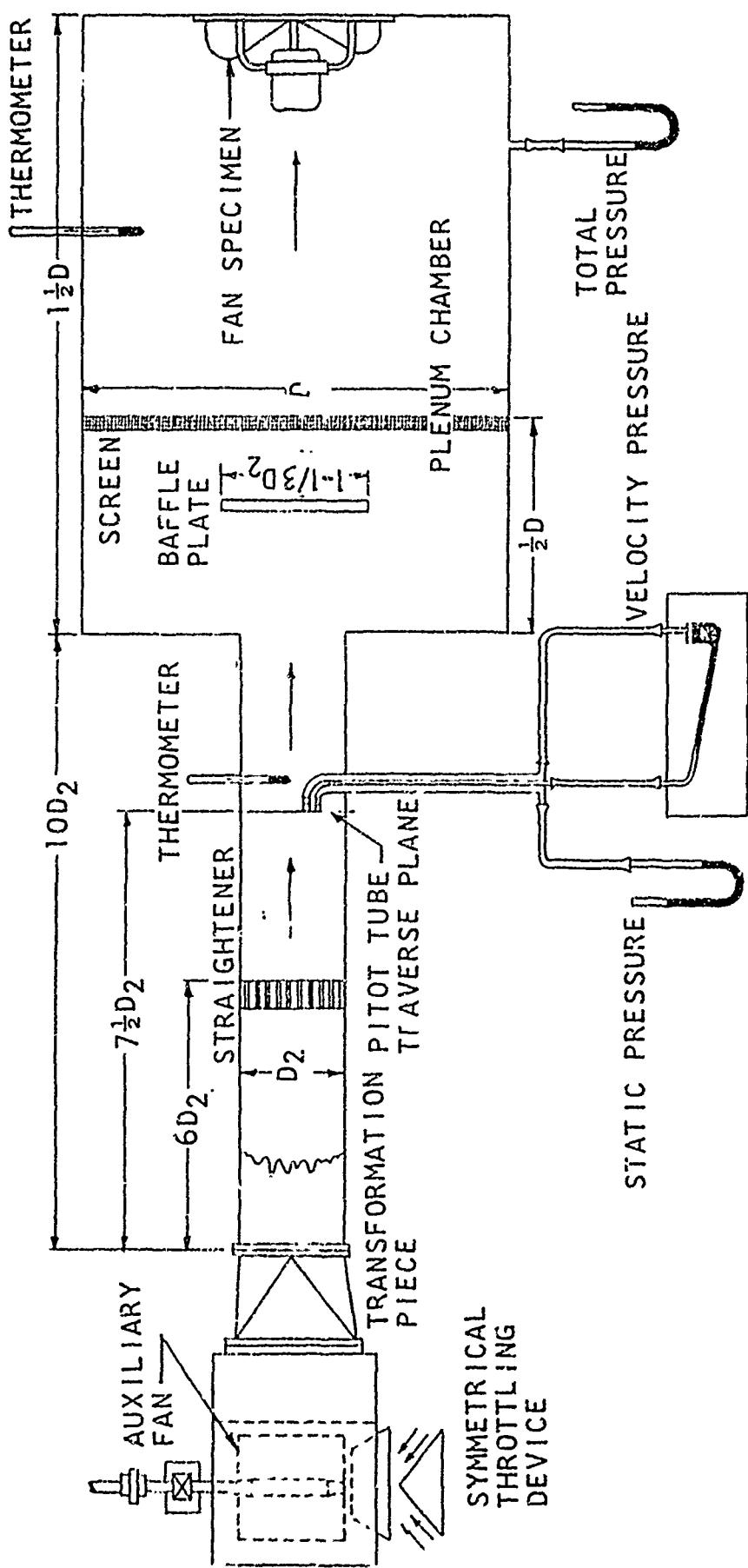


FIGURE 6-4. Test Set-Up No. 4 with Fan In Wall of Plenum Chamber

6-2.1.3.1.2 Set-Up No. 2 - With Inlet Duct Only

Figure 6-2 is used for fans intended for installation with inlet duct but with no discharge duct. The tunnel inlet of Set-up No. 2 should have an area equal to that of the fan inlet within plus or minus five per cent. The tunnel must be straight, of uniform circular cross-section, and not less than 12 diameters in length. Openings for insertion of pitot tubes are to be so located that the impact ends of the tubes must not be less than 6 tunnel diameters from the inlet end of the tunnel. Straighteners should be located as shown on Figures 6-2 and 6-3.

6-2.1.3.1.3 Set-Up No. 3 - With Inlet and Discharge Ducts

Figure 6-3 is used for fans intended for installation with both inlet and discharge ducts. The tunnel inlet of Set-up No. 3 should have an area equal to that of the fan inlet within plus or minus 5 per cent. The tunnel must be straight, of uniform circular cross-section, and not less than 12 diameters in length. Openings for insertion of pitot tubes are to be so located that the impact ends of the tubes must not be less than 6 tunnel diameters from the inlet end of the tunnel. Straighteners should be located as shown in Figures 6-2 and 6-3.

The discharge end of the tunnel of Set-up No. 3 must be straight, of the same section as the fan outlet, and not less than 6 or more than 8 tunnel diameters in length. No measurements are made in this section of the tunnel. Its sole purpose is to provide an outlet simulating the conditions of installation.

6-2.1.3.1.4 Set-Up No. 4 - With Fan in Wall of Plenum Chamber

Set-up No. 4 with no inlet section and no discharge section is shown in Figure 6-4 and is used for fans intended for installation with neither inlet nor discharge ducts. The plenum chamber of Set-up No. 4 should be round or rectangular and substantially airtight. The cross-sectional area in the direction of airflow must be sufficient to assure a calculated average velocity at the specified fan rating less than 400 fpm. The length in the direction of airflow should be at least one and a half times the diameter if round, and twice the longest dimension if rectangular. The chamber is to be fitted with a solid baffle plate and screen as shown in Figure 6-4.

The air measuring tunnel section of this set-up leading from auxiliary fan to plenum chamber, should be of a diameter such that the range of air velocities in the tunnel shall be between 1200 and 16000 fpm.

The auxiliary fan shown may be of any convenient size, provided only that it have sufficient capacity to produce, when desired, atmospheric pressure in the plenum chamber, and the rate of airflow required.

6-2.1.3.1.5 Set-Up No. 5 - With Double Inlet Boxes and Discharge Duct

Figure 6-5 is used for fans intended for installation with inlet box or boxes and discharge ducts. The discharge section of the tunnel of Set-up No. 5 should have an area equal to that of the fan outlet within plus or minus 5 per cent. This section must be straight, of uniform

circular cross-section, and not less than 10 diameters in length. Openings for insertion of pitot tubes are to be so located that the impact ends of the tubes must not be less than 7.5 tunnel diameters from the fan end of the tunnel. The straightener is to be located not less than 6 tunnel diameters from the fan end of the tunnel. The distance between the pitot tube traverse plane and the straightener must not be less than 1 1/2 tunnel diameters.

6-2.1.3.1.6 Transformation Section

A transformation is used where it is desirable to change the shape of the tunnel section without changing the area and velocity of flow. It is so constructed that the angle between any longitudinal element and the tunnel axis will not exceed 7 degrees.

6-2.1.3.1.7 Air Straighteners

Air straighteners are used to remove the rotation from the fan slip-stream. Frequently spiral flow exists in test tunnels. The ASME Fan Test Code requires that the straightener should be in accordance with Figure 6-6 and suggests that material be of No. 22(031) U. S. gage sheet metal.

6-2.1.3.1.8 Throttling Device

The primary device used in establishing test condition is the throttling device to regulate the airflow.

Various throttling devices which may be employed are as follows: one of a group of orifices of various sizes, a conical throttle forming a large needle valve, a frame holding slats like a picket fence (slats being added symmetrically to restrict the flow) perforated plate, flat plate or nozzles.

Additional information on orifices and nozzles may be obtained from References 6-1, 6-3, 6-5, and 6-7.

6-2.1.3.1.9 Instrumentation and Measuring Technique

Equipment must be provided for measuring the values of static pressure, velocity pressure, total pressure, barometric pressure, dry and wet bulb temperatures, time, power input, and fan speed.

Initial calibration of instruments involved shall be available prior to the test.

Whenever possible, a camera should be used to permanently record all measurements for future reference. Data on calibration may be obtained from the Engineering Measurement Section of Reference 6-7, and from References 6-1, 6-2, 6-16, and 6-29.

6-2.1.3.1.10 Pitot Tube

Air pressure may be measured with a conventional pitot tube. The ASME Test Code for Fans Reference 6-15 specifies the configuration shown in Figure 6-7, however, similar types may be employed provided they have the same basic features. The static openings should not be less than

$$S = 7\frac{1}{2}\% \text{ to } 15\% \text{ of } D$$

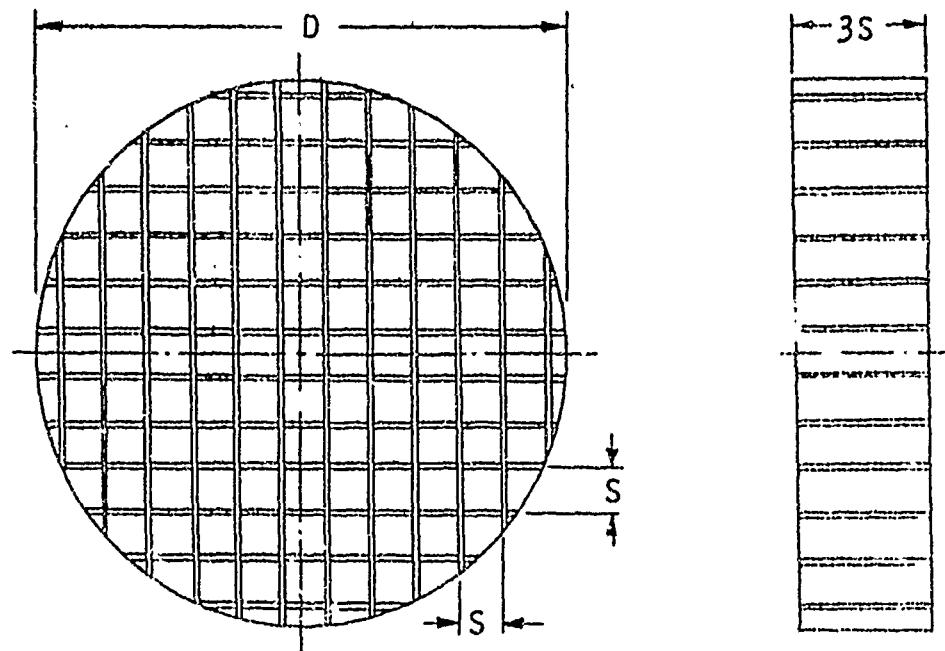


FIGURE 6-6. Air Straightener

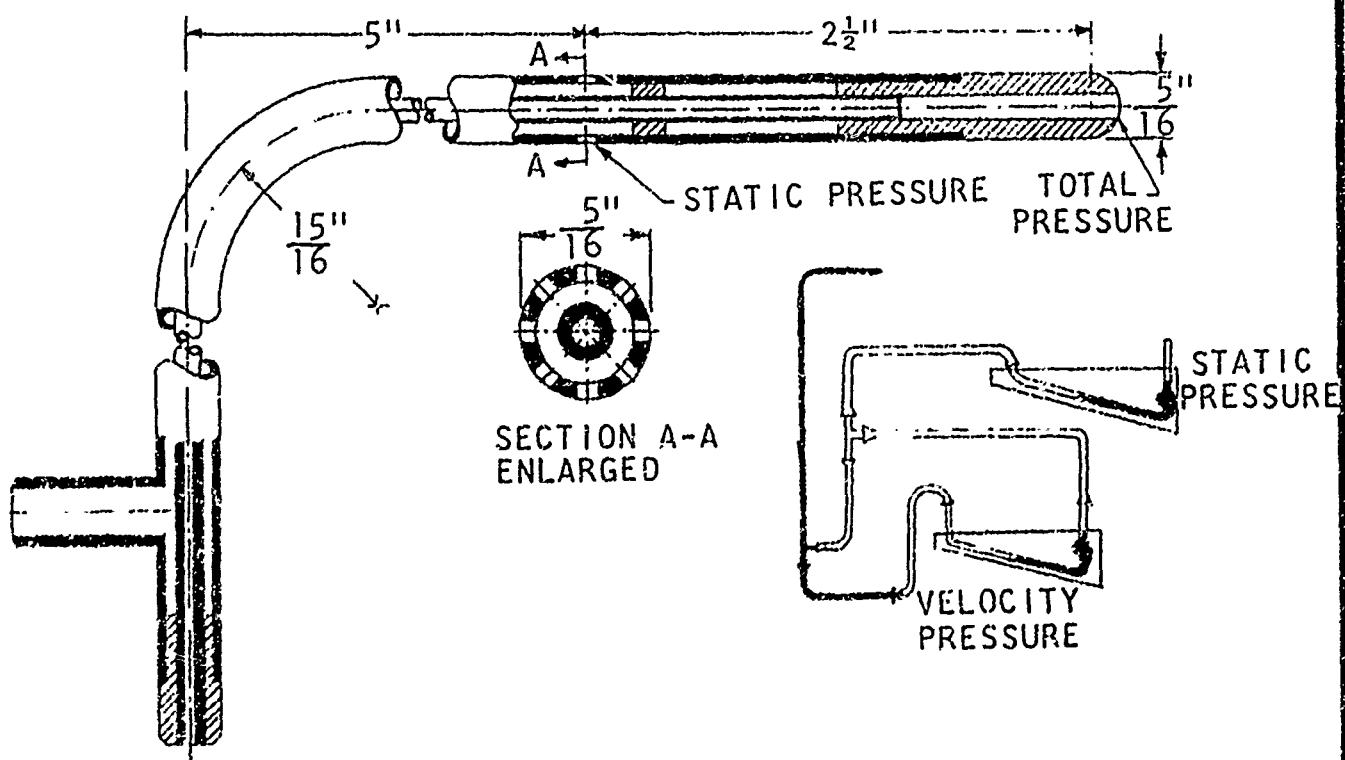


FIGURE 6-7. Pitot Tube

0.02 in diameter. The open end of the tube is always pointed upstream in a direction parallel with the axis of the tunnel. In order to prevent error in readings due to swirl such pitot readings should be taken downstream from the straighteners. Where orifices or nozzles exist immediately forward of the pitot tube the measurements should be at the point of greatest flow contraction. If the discharge has no contraction, then the point can be held at the plane of the orifice. Pressure readings in round tunnels are taken at the locations specified in Figure 6-8. Twenty locations represent two traverses along axes normal to each other. When tunnels are of rectangular cross-section, the procedure is to divide the total area into a large number of small equal areas and to take a reading of velocity and static pressure in the center of each small area. Although the number of readings are generally more by this method than that of the round tunnel traverse, it gives a better distributed sampling in irregular flow. The number of areas and readings are not less than 16 and need not be more than 64. Where less than 64 are taken, the number of equal spaces is such that the centers of the areas are not more than 6 inches apart. The readings thus taken in a rectangular tunnel are averaged in the same manner as for a round tunnel. Additional data are available in References 6-1, 6-5, 6-7, 6-12, 6-17, 6-18, 6-19, and 6-20.

6-2.1.3.1.11 Manometer

The familiar U tube manometer is most commonly used to measure the velocity, static and total pressures obtained through the pitot tube. This liquid filled tube which indicates pressure differences, may be vertical, or for more accurate readings inclined not more than 84 degrees from the vertical-(slope 10:1). The bore of the manometer glass must not be less than 1/4 inch, nor more than 3/8 inch. All manometers, other than vertical-leg tubes filled with distilled water, should be calibrated in position, with all tubing in place, by a water filled hook gage or micromanometer before and after test.

The atmospheric opening of the static pressure manometer is so located that readings will not be affected by local air velocity.

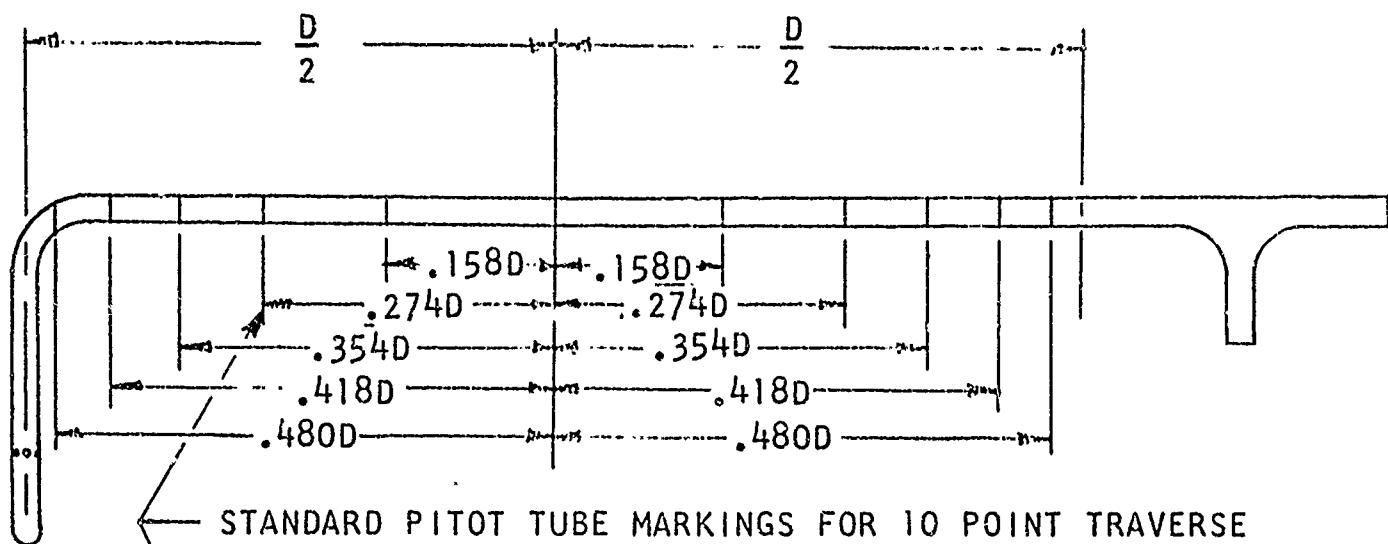
All readings should be taken at the level of the middle of the meniscus, i.e.: the bottom of the curve for water and the top for mercury. These positions are away from the maximum effects of capillary attraction and are nearest to the proper level. Additional data is available in References 6-5, 6-7, 6-17, 6-18, 6-19, and 6-20.

6-2.1.3.1.12 Power Input

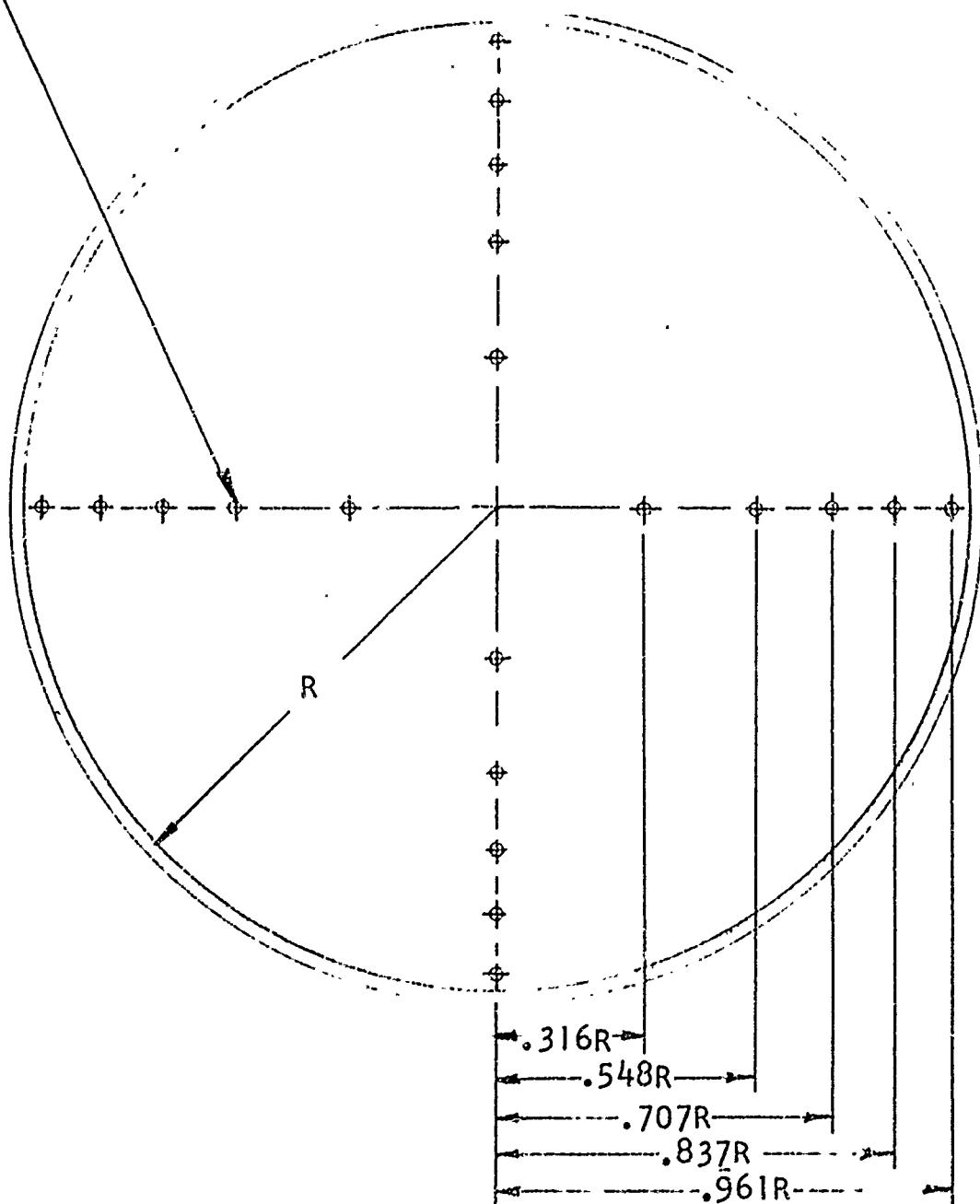
Although several methods of power input measurement are available, the simplest and most reliable method for determining the power input necessary to drive the fan is by means of the electric cradle dynamometer. With such a device a correction for the efficiency of the driving unit is thus eliminated and the power input to the fan is directly given in the foot pounds per minute units.

Where the power is of such a magnitude that a cradle dynamometer cannot be employed, then a calibrated test motor may be used. The brake horsepower will then be as follows:

FIGURE 6-8. Standard Pitot Tube
Markings for 10 Point Traverse



STANDARD PITOT TUBE MARKINGS FOR 10 POINT TRAVERSE



Horsepower = watts x motor efficiency

746

In installation tests, the power input is read by a wattmeter and the horsepower input to the fan is determined by the efficiency curve of the motor. This can usually be obtained from the motor manufacturer's test on a similar type motor. Where three phase current is used a single wattmeter will not indicate true power and the usual two-wattmeter method of determining power in two of the three phases is recommended to eliminate the power factor. The brake horsepower of the fan will then be as indicated above. Additional data on power input measuring devices may be obtained in References 6-1, 6-7, 6-14, and 6-15.

6-2.1.3.1.13 Fan Speed

Rotational speeds may be measured by a counter, tachometer, or a stroboscope. The instrument employed is at the discretion of the testing agency. Hand tachometers are useful for noting speed but revolution counters should always be used for accurate work. The References 6-14 and 6-15 ASME Test Codes recommend a minimum of three speed measurements to be taken spaced throughout the period of the test run and not more than 5 minutes apart. Speed is maintained as nearly constant as possible throughout each traverse and test run.

Additional data on rotational speed measuring devices may be obtained from References 6-1, 6-7, 6-24, and 6-29.

6-2.1.3.1.14 Barometric Pressure

The preferred method of measuring barometric pressure is by means of a mercury column with a brass scale. The ASME Power Test Codes require that for accurate work all barometer readings should be corrected for temperature, gravity elevation and instrument calibration.

Barometric pressure may be read once every two hours during testing. Assurance must be had that the barometric pressure recorded is that actually prevailing at the manometers. Additional data on barometers may be obtained in References 6-7 and 6-17.

6-2.1.3.1.15 Humidity and Temperature

The most popular method of measuring the humidity of the air is by use of the sling psychrometer. Psychrometric measurements in the free atmosphere in the path of inflowing air are taken at the start and completion of each test run with an interval not exceeding one hour between readings. When using the sling psychrometer the instrument is whirled at a rate where the velocity of air past the wet bulb is between 800 to 900 fpm average and the whirling is continued until no further drop in wet-bulb reading is noted. A psychrometric chart is presented in Appendix III.

Dry-bulb temperature readings should be obtained in the fan inlet and in the discharge section of the tunnel at the point of air traverse. When recording dry-bulb temperatures at the points of a pressure traverse, care must be exercised such as not to interfere with the pitot tube readings.

Additional data on temperature measuring devices are available in References 6-3, 6-5, 6-7, 6-12, 6-21, 6-22, and 6-23.

6-2.1.3.2 Test Procedure

Prior to the start of actual testing, preliminary tests may be run (a) to determine whether the fan is in suitable condition for an acceptance or performance test, (b) to check and calibrate instruments, or (c) for personnel familiarization tests.

Steady state conditions should prevail while readings are being recorded. The duration of any one test should be sufficient to assure that the readings will demonstrate uniformity of conditions during test runs.

Generally 8 to 10 throttle settings are adequate to obtain sufficient data to permit construction of a complete set of performance curves from practically free delivery to no delivery. Approximately equal increments of flow should be selected. Figure 6-9 illustrates the results obtained from such data.

The following general procedure is normally followed in fan testing.

- a. The test is started with no obstruction at the throttling section. The only resistance will be the duct friction. At this setting, the fan is said to be wide open. A large quantity flows. The static pressure developed is small (static pressure must be zero for free discharge) but the velocity pressure has its maximum value, and hence total pressure cannot be zero. The shaft power is high. With this throttling (free delivery) setting, an RPM sweep is accomplished and the data recorded following stabilization at each point.
- b. Next, the throttling setting is advanced from free delivery to its next position. The flow, Q (cfm), is reduced, the pressure rise, H (inches of water, static or total), is increased, and the shaft power, P (horsepower), may be less, or more, in a restricted range for some fans. At this setting another RPM sweep is accomplished and the data recorded following stabilization at each point.
- c. Repeat "b" at each of the throttling and speed settings until the duct is restricted with the maximum throttling.

6-2.1.3.3.0 Data Reduction

Once the data have been corrected for instrument calibration, reviewed and accepted, calculation of the results may be started, although data reduction may have started concurrent with testing. Caution must be exercised to keep the algebraic signs of quantities correct at all times.

6-2.1.3.3.1 Density of Atmospheric Air

Density of atmospheric air is determined from observed barometric pressure and the dry-and-wet-bulb-temperature of the atmospheric air in the vicinity of the fan inlet:

PERFORMANCE CHARACTERISTICS OF FAN

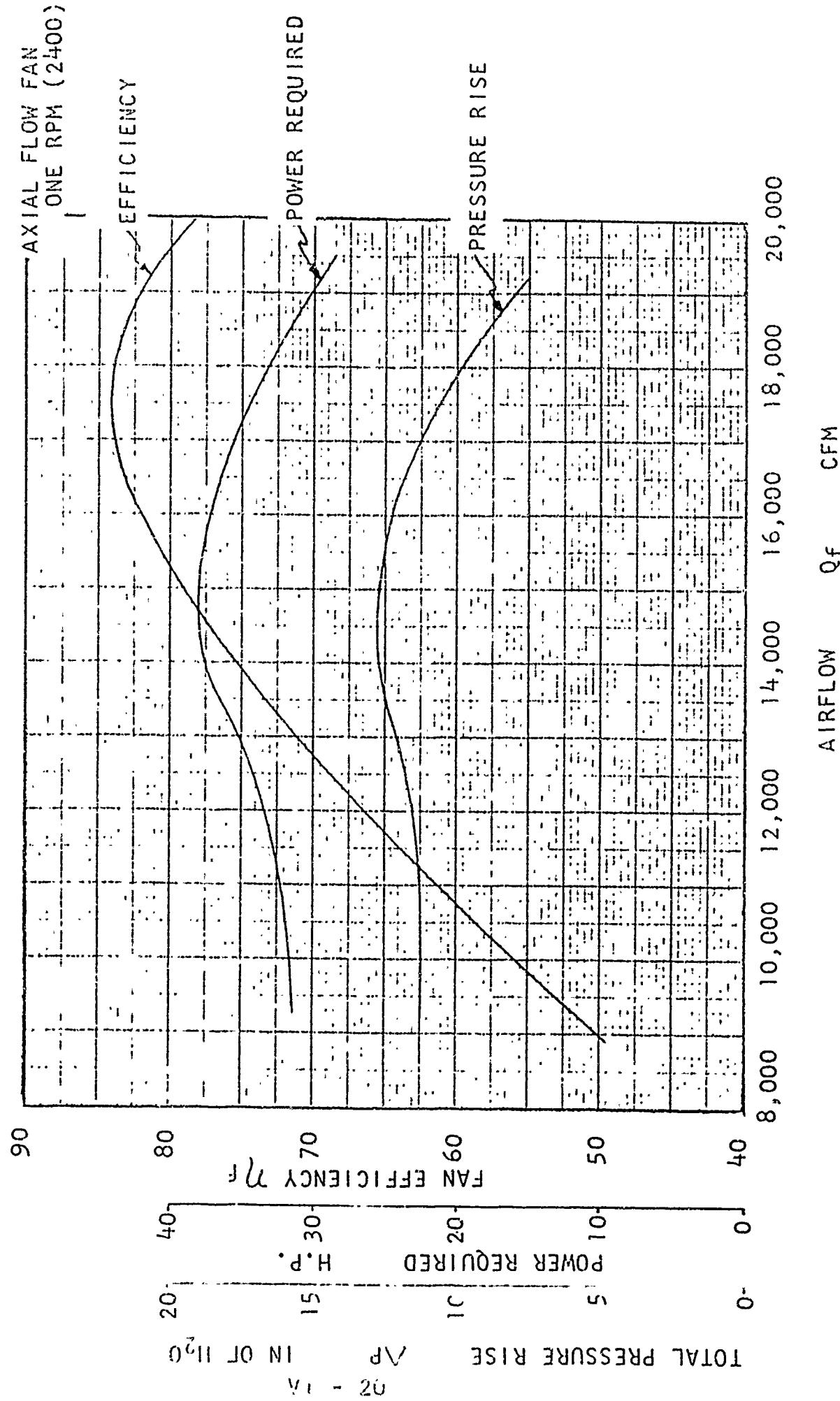


FIGURE 6-9

$$w_a = \frac{p_a - 0.38 p_p}{0.754 T_a}$$

Where: w_a = Density of atmospheric air, lb. per cu. ft.
 T_a = Absolute temperature of atmospheric air, $^{\circ}\text{F}$ + 460°
 p_a = Barometric pressure, inches of Hg at 32°F
 p_p = Partial vapor pressure in atmosphere, inches of Hg and is determined as follows:

$$p_p = p_g - \frac{p_a (t_a - t_w)}{2700}$$

Where: p_g = Saturated vapor pressure at wet-bulb temperature. Inches of Hg (from steam tables, Reference 6-11, corresponding to t_w)
 t_a = Dry-bulb temperature, $^{\circ}\text{F}$
 t_w = Wet-bulb temperature, $^{\circ}\text{F}$

Example: Given 95°F dry bulb, 78°F wet-bulb, 29.52 inches of Hg barometric pressure

$$p_g = 0.9666 \text{ inches Hg from steam tables (Reference 6-11)}$$

$$p_p = 0.9666 - \frac{29.52 (95-78)}{2700} = 0.9666 - 0.186$$

$$p_p = 0.7806 \text{ inches Hg}$$

$$w_a = \frac{29.52 - 0.38(0.7806)}{0.754(460 + 95)} = \frac{29.52 - 0.295}{419}$$

$$w_a = 0.0696 \text{ lb. per cu. ft.}$$

Air density may be selected from recognized tables or charts of properties of moist air.

6-2.1.3.3.2 Tunnel Air Density

Since it is not practically possible to measure humidity in a tunnel by direct means, the air density in a tunnel is determined as follows:

- Obtain density of atmospheric air w_a outside the tunnel per Paragraph 6-2.1.3.3.1.
- Compute density in tunnel by correcting w_a (Paragraph a) for tunnel pressure and temperature.

$$w_t = w_a \frac{p_a + (p_s / 13.6)}{p_a} \frac{(T_a)}{(T_t)}$$

Where: w_a = Density of atmospheric air, lb. per cu. ft. - see Paragraph 6-2.1.3.3.1.

w_t = Air density in tunnel at plane of traverse, lb. per cu. ft.

p_s' = Measured static pressure at plane of velocity traverse, in. water from Paragraph 6-2.1.3.3.3.

T_t = Absolute temperature of air in tunnel at plane of traverse, deg F + 460°

T_a = Absolute temperature of atmospheric air, deg F + 460°

p_a = Barometer pressure, inches of Hg.

Example: Given: 20 inches of water static pressure in tunnel; temperature in tunnel 105° F; other conditions in Paragraph 6-2.1.3.3.1

$$w_t = 0.0696 \times \frac{29.52 + 20/13.6}{29.52} \times \frac{95 + 460}{105 + 460}$$

$$w_t = 0.0718 \text{ lb. per cu. ft.}$$

6-2.1.3.3.3 Static Pressure

A traverse may result in twenty readings, one for each traverse point shown in Figure 6-11. An arithmetic average of these readings corrected for manometer calibration yields a static pressure at the plane of traverse.

6-2.1.3.3.4 Velocity Pressure

The traverse may result in twenty readings of velocity pressure, one for each traverse point shown in Figure 6-8. The square root of each corrected reading is then taken and the average calculated. This average squared yields true average velocity pressure. Since the velocity varies as the square root of the pressure, then:

$$p_v' = \frac{(\sqrt{a} + \sqrt{b} + \sqrt{c} + \sqrt{d} \dots \text{etc.})^2}{n}$$

Where: p_v' = Velocity pressure corresponding to average velocity
 $a, b, c, d, \text{ etc.}$ = Velocity pressures at each point of traverse
 n = Number of pitot tube recordings in each traverse

Each velocity pressure should be corrected by the gauge calibration curve before averaging as above.

6-2.1.3.3.5 Velocity at Plane of Traverse

The average velocity can be determined from the average velocity pressure obtained in Paragraph 6-2.1.3.3.4.

$$V = 1096.2 \sqrt{(p'_{v}) (w_t)}$$

Where: V = Average velocity in tunnel at plane of traverse, fpm.

p'_{v} = Average velocity pressure at plane of traverse in water- Paragraph 6-2.1.3.3.4.

w_t = Density of air at plane of traverse lb. per cu. ft. - Paragraph 6-2.1.3.3.2.

Example: Given $p'_{v} = 1.0$ inches of water and 0.0718 for w_t

$$V = 1096.2 \sqrt{1.00/0.0718}$$

$$V = 4090 \text{ fpm}$$

6-2.1.3.3.6 Volume Rate of Flow at Plane of Traverse

$$Q_t = AV$$

Where: Q_t = Volume rate of airflow at plane of traverse, cfm

V = Average velocity at plane of traverse, fpm, Paragraph 6-2.1.3.3.5

A = Area of tunnel at plane of traverse, sq. ft.

Example: Given: $A = 2.41$ sq. ft.
 $V = 4090$ FPM

$$Q_d = 2.41 (4090)$$

$$Q_d = 9860 \text{ CFM}$$

6-2.1.3.3.7 Volume Rate of Flow Corrected to Fan Inlet (Set-Ups #1 & 5)

$$Q_a = \left(\frac{w_t}{w_a} \right) \times Q_t$$

Where:

Q_a = Volume rate of airflow at fan inlet, cfm

Q_t = Volume rate of airflow at plane of traverse, cfm, Paragraph 6-2.1.3.3.6

w_t = Air density in tunnel at plane of traverse, lb. per cu. ft. Paragraph 6-2.1.3.3.2

w_a = Density of atmospheric air, lb. per cu. ft. Paragraph 6-2.1.3.3.1

This correction is required only in test Set-ups Nos. 1 and 5. For test Set-ups Nos. 2, 3, and 4, the volume rate of flow at inlet is considered to be the same as the volume rate of flow measured in the tunnel because of the relatively small pressure change from plane of measurement to fan inlet.

6-2.1.3.3.8 Tunnel Friction

The tunnel total pressure shall be corrected for tunnel friction pressure loss to give conditions at the fan by adding the loss of pressure due to friction of the tunnel between the fan and the pitot tube. For a round tunnel, the following formula shall be used.

$$p_f = \frac{0.02 L p'_v}{D}$$

Where:

p_f = Pressure loss inches of water

p'_v = Average tunnel velocity pressure inches of water - Paragraph 6-2.1.3.3.4

L = Distance from fan to the pitot tube location, ft.

D = Diameter of tunnel, ft.

Loss in a transformation piece is computed as part of the total length L and as if it were a round tunnel of diameter D. Loss in a possible rectangular discharge tunnel (Test Set-up No. 3) is computed on the basis of the loss in a round tunnel of the same hydraulic radius. Methods of determining various losses are discussed in detail in Chapter III.

6-2.1.3.3.9 Straightener Loss

The loss of pressure due to friction of the straightener shall be considered as equivalent to the loss in a length equal to four diameters of the tunnel as calculated by the above formula.

6-2.1.3.3.10 Discharge Velocity Pressure

The discharge velocity pressure measured in the tunnel shall be corrected to obtain discharge velocity pressure as follows:

$$p_v = p'_v \left(\frac{A}{A_o} \right)^2 \times \left(\frac{w_o}{w_t} \right)$$

Where:

p_v = Discharge velocity pressure, inches of water

A_o = Fan outlet area sq. ft.

A = Area of tunnel at plane of traverse, sq. ft.

p'_{v} = Velocity pressure at plane of traverse, inches of water

w_o = Density of air at fan outlet

w_t = Density of air at plane of traverse

When the velocity is measured at the tunnel discharge, the ratio $\frac{w_o}{w_t} = 1$.

6-2.1.3.3.11 Total Pressure at a Tunnel Traverse Plane

Total pressure at a tunnel traverse plane is the algebraic sum of the velocity pressure and the static pressure in the tunnel. The velocity pressure is a positive quantity in both discharge and inlet section. The static pressure is usually positive in a discharge section and negative in an inlet section.

Examples

Discharge Section -

Velocity pressure from traverse = ± 1.00 inches of water

Static pressure from traverse = ± 2.00 inches of water

Total pressure = ± 3.00 inches of water

Inlet Section -

Velocity pressure from traverse = ± 1.00 inches of water

Static pressure from traverse = $- 2.00$ inches of water

Total pressure = $- 1.00$ inches of water

The total pressure in the inlet section is usually negative because of the loss at the tunnel entrance and the loss due to inlet friction.

6-2.1.3.3.12 Fan Total Pressure (Set-Ups No.s 1 & 5)

Fan total pressure is the total pressure at the plane of traverse plus the straightener loss plus the friction loss in the discharge section between the fan outlet and the traverse plane. The fan static pressure, is the fan total pressure minus the discharge velocity pressure.

6-2.1.3.3.13 Fan Total Pressure (Set-Up No. 2)

Fan total pressure is the discharge velocity plus one straightener loss plus the friction loss in the inlet between the plane of traverse and the fan minus the inlet total pressure at the plane of traverse. The fan static pressure is the fan total pressure minus the discharge velocity pressure.

Example:

Fan total pressure = $0.5 + 0.1 + 0.2 - (-1.0) = 1.8$ inches of water

Fan static pressure = $1.8 - 0.5 = 1.3$ inches of water

6-2.1.3.3.14 Fan Total Pressure (Set-Up No. 3)

Fan total pressure is the discharge velocity pressure plus the friction loss for both inlet and outlet sections plus one straightener loss minus the inlet total pressure. The fan static pressure is the fan total pressure minus the discharge velocity pressure.

6-2.1.3.3.15 Fan Total Pressure (Set-Up No. 4)

Fan total pressure is the discharge velocity pressure minus the total pressure in the plenum chamber. The discharge static pressure is assumed to be zero. The fan static pressure is the fan total pressure minus the discharge velocity pressure, or alternately, is numerically equal to the total pressure in the plenum chamber, but of opposite sign. If the plenum total pressure is positive, the fan static pressure becomes negative, and the characteristic curve extends below the zero pressure axis. It is noted that the plenum chamber static and total pressures are essentially equal because of negligible velocity pressure in plenum chamber.

6-2.1.3.3.16 Volume Rate of Flow-Correction to Specified Fan RPM

Volume rate of flow-correction to specified fan RPM depends upon the fact that for a given setting of the throttling device, the volume rate of flow at a given plane varies directly as the rotational speed and does not vary at all with density at that plane.

$$\text{Volume rate of flow correction factor} = \frac{n_s}{n_x}$$

Where n_s = specified RPM
 n_x = test RPM in any consistent units

The volume rate of flow at fan inlet thus corrected to specified RPM is termed: the capacity of the fan for the given setting of the throttling device.

6-2.1.3.3.17 Pressure Correction to Specified Fan RPM and Air Density

Pressure correction to specified fan RPM and air density depends upon the fact that for a given setting of the throttling device, pressure at a point varies as the square of RPM and directly as the density at that point.

$$\text{Pressure Correction Factor} = \left(\frac{n_s}{n_x} \right)^2 \frac{w_s}{w_x}$$

Where:

w_s = Specified density, ordinarily standard sea level density

w_x = Air density at fan inlet during test

n_x = Test RPM

n_s = Specified RPM

6-2.1.3.3.18 Power Input

Power input as delivered to the fan coupling shall be computed by any appropriate method. For example, if a dynamometer is used:

$$P = \frac{2 \pi WLn}{33000}$$

Where:

P = Power input, hp

L = Length of arm from shaft center to knife edge, ft.

W = Force measured at distance L from shaft center, lb.

n = Rotational speed, RPM

If no dynamometer is available, the power input may be calculated from the measured input to an alternating-current or direct reading current motor multiplied by the motor efficiency as determined by test by the motor manufacturer.

6-2.1.3.3.19 Power Input Correction to Specified RPM and Density

Power input correction to specified RPM and density depends upon the fact that power input varies as the cube of the RPM and directly as the density:

$$\text{Power input correction factor} = \left(\frac{n_s}{n_x} \right)^3 \frac{w_s}{w_x}$$

Where the same terms as listed in Paragraph 6-2.1.3.3.17 apply.

6-2.1.3.3.20 Total Efficiency is calculated as follows:

$$\text{Total Efficiency} = \frac{Q_a (P_t)}{6356(P)}$$

Where: Q_a = Capacity; cfm

P_t = Fan total pressure, inches of water (at standard air density)

P = Power input, hp

The quantities Q_a, P_t, and P are all as corrected to specified speed and density.

6-2.1.3.3.21 Static Efficiency is calculated as follows:

$$\text{Static Efficiency} = \frac{Q_a (P_s)}{6356(P)}$$

CALCULATION GUIDE

TABLE 6-1

No.	Item	Test Set-UP No.			
		1 and 5	2	3	4
1.	Density of atmospheric air	6-2.1.3.3.1			
2.	Static pressure in discharge section	6-2.1.3.3.3			
3.	Static pressure in inlet section		6-2.1.3.3.3		
4.	Static pressure in measuring section			6-2.1.3.3.3	
5.	Static pressure in plenum chamber	6-2.1.3.3.2			
6.	Air density in discharge section		6-2.1.3.3.2		
7.	Air density in inlet section			6-2.1.3.3.2	
8.	Air density in measuring section				6-2.1.3.3.2
9.	Air density in plenum chamber	6-2.1.3.3.4			
10.	Velocity pressure in discharge section		6-2.1.3.3.4		
11.	Velocity pressure in inlet section			6-2.1.3.3.4	
12.	Velocity pressure in measuring section				6-2.1.3.3.4
13.	Velocity pressure in plenum chamber	6-2.1.3.3.5			
14.	Velocity in discharge section		6-2.1.3.3.5		
15.	Velocity in inlet section			6-2.1.3.3.5	
16.	Velocity in measuring section	6-2.1.3.3.6			
17.	Volume rate of flow in discharge section		6-2.1.3.3.6		
18.	Volume rate of flow in inlet section			6-2.1.3.3.6	
19.	Volume rate of flow in measuring section				6-2.1.3.3.6
20.	Volume rate of flow at fan inlet	6-2.1.3.3.11			
21.	Total pressure at traverse plane in discharge section		6-2.1.3.3.7		
22.	Total pressure at traverse plane in inlet			6-2.1.3.3.11	

TABLE 6-1

CALCULATION GUIDE (CONTINUED)

No.	Item	Test Set-Up No.			
		1 and 5	2	3	4
23.	Total pressure in plenum chamber	6-2.1.3.3.8			6-2.1.3.3.15
24.	Pressure loss in discharge section		6-2.1.3.3.8		
25.	Pressure loss in inlet section		6-2.1.3.3.9		
26.	Pressure loss at straightener		6-2.1.3.3.9		
27.	Discharge velocity pressure		6-2.1.3.3.10		
28.	Fan total pressure	6-2.1.3.3.12	6-2.1.3.3.13	6-2.1.3.3.14	6-2.1.3.3.15
29.	Fan static pressure	6-2.1.3.3.12	6-2.1.3.3.13	6-2.1.3.3.14	6-2.1.3.3.15
30.	Power input		6-2.1.3.3.18		
31.	Capacity (Volume rate of flow at fan inlet corrected to specified speed)		6-2.1.3.3.16		
32.	Fan total pressure corrected to specified speed and inlet air density		6-2.1.3.3.17		
33.	Fan static pressure corrected to specified speed and inlet air density		6-2.1.3.3.17		
34.	Power input corrected to specified speed and inlet air density		6-2.1.3.3.19		
35.	Total efficiency		6-2.1.3.3.20		
36.	Static efficiency		6-2.1.3.3.21		

Where:

Q_a = Capacity, cfm

P_s = Fan static pressure, inches of water (at standard air density)

P = Power input, hp

The quantities Q_a , P_s , and P are all as corrected to specified RPM and density.

Efficiencies calculated under test conditions are identical with efficiencies calculated for specified conditions.

6-2.1.3.3.22 Calculation Guide

The basis of fan performance consists of the capacity, pressure, horsepower, fan size and speed. The performance results are usually presented as plotted data with pressures and horsepower as ordinates and capacity as abscissae for a given fan size at constant speed as in Figure 6-9. Because of variations of fan test speeds and air density, corrections to standard conditions must be made for these items.

A calculation guide is presented as Table 6-1, in which the applicable paragraph is noted for the calculation items for the various setups.

The computation procedure is shown on Table 6-2. In this typical calculation sheet, the items are computed as follows:

For each air delivery rate, the dynamometer speed and force are entered in Columns A and B. The no load or tare force C is that with the dynamometer running at the average test speed with the fan coupling disconnected. The difference between the total and no-load forces is the net force D. The product of the dynamometer constant, the net dynamometer force and the dynamometer speed is the actual horsepower E at test speed A. If the speed is expressed in RPM and the force in pounds, the dynamometer constant equals $2 \times 3.1416 \times$ the dynamometer arm length in feet divided by 33,000. The horsepower corrected for speed, Column F, is computed by multiplying the values E by the cube of the ratio of curve fan speed to test fan speed, H. To correct the horsepower for air density, the values F are multiplied by the air ratio constant to obtain the values in Column G. The air ratio is defined under Test Constants in Table 6-2. For a belt driven fan test, Column F should also be multiplied by one (1) belt loss. In this case, both dynamometer and fan speeds are recorded (Columns A and H), the former being used only for horsepower determination and the latter for speed correction.

The average static and velocity pressures are entered in Columns I and J, determined as explained in Paragraphs 6-2.1.3.3.3 and 6-2.1.3.3.4. Columns I and J, corrected from the test speed to curve speed give Columns K and L, respectively. Column M is obtained by adding to the static pressure K the tunnel frictional loss from the point of traverse to the fan outlet. The pressures, Columns M and L, are multiplied by the air ratio constant to obtain Columns N and O, respectively, corrected to standard air density. The velocity, Column P, is obtained

TABLE 6-2

FAN PERFORMANCE CALCULATION OUTLINE

TEST OF _____ FAN AT _____ R.P.M.
DATE _____ TEST NO. _____ TESTED BY _____
DUCT SIZE _____ AREA, SQ. FT. _____
DISTANCE FROM FAN OUTLET TO PLANE OF TRAVERSE, FT. _____
EQUIVALENT TO _____ DUCT DIA. _____ DUCT FRICTION CONSTANT _____
DRY BULB TEMP., °F _____ WET BULB TEMP., °F _____ BAR. PRESS., IN. HG. _____
TEST AIR WEIGHT, LB./CU. FT. _____ AIR RATIO = WT. OF STD. AIR =
WT. OF TEST AIR
DYNAMOMETER CONSTANT _____
REMARKS _____

* CORRECT FOR TRANSMISSION LOSSES WHEN DYNAMOMETER IS OTHER THAN DIRECT OR BELT CONNECTED

FAH CAPACITY CFM	STATIC PRESSURE IN. H ₂ O	VELOCITY PRESSURE IN. H ₂ O	TOTAL PRESSURE IN. H ₂ O	HORSEPOWER	STATIC EFFICIENCY PERCENT	TOTAL EFFICIENCY PERCENT
R	S	T	U	V	W	X
READ FROM CURVE	S.P. CORRESPONDING TO VALUES OF R	$\left(\frac{1}{4005} \times \frac{R}{DUCT\ AREA} \right)^2$	$S^{\frac{1}{2}} T$ (PLOT AGAINST R)	HORSEPOWER CORRESPONDING TO VALUES OF R	$.000157 \frac{X}{V} R X S$ (PLOT AGAINST R)	$.000157 \frac{X}{V} R X U$ (PLOT AGAINST R)

CITY MIN.		FAN CAPACITY CFM
DUCT AREA X	$\frac{P_{\text{DISCHARGE}}}{P_{\text{INLET}}} \times P$	0

TABLE 6-3
(Source: Reference 6-25)
LOG SHEET - TRAVERSE READINGS

SIZE & TYPE OF FAN DRAWING NO. OBSERVERS - MAN'T'R	TEST PLATE NO.	ASSIGNMENT						DETERMINATION NO.	DATE	
		RPM	CALC. BY BEAM			BEAM				
TRAVERSE READING	1	P_t^2	P_t^3	P_v	P_v^*	6	7	8	9	10
INLET		OUTLET	READING	R	CORR.	VEL	REVS.	TIME	BEAM READING	WATTS
1										
2										
3										
4										
5										
6										
7										
8										
9										
10										
11										
12										
13										
14										
15										
16										
17										
18										
19										
20										
21										
22										
23										
24										
25										
26										
AVERAGE CORRECTIONS										
MAN. SLOPE										
MAN. CALIB.										
$P_v = \frac{P_t}{R.P.M.}$										
FOR K ₁										
$P_t^2 + P_t^3 + P_v^2$										
FOR K ₂										
$P_t^2 + P_t^3 + P_v^2$										
FOR K ₃										
$P_t^2 + P_t^3 + P_v^2$										
FOR K ₄										
$P_t^2 + P_t^3 + P_v^2$										
FINAL VALUES	P_s	P_t	P_v	V	$C.F.M.$	$h.p.t.$	RPM	$S.h.p.$	e_t	e_s
* COL. 5 IS P_v OF COL. 4 (AS READ) CORRECTED FOR MANOMETER SLOPE AND CALIBRATION										
** R.P.M. X = SPEED AS READ COL. 8 AND R.P.M. = STD. SPEED										
+ LENGTH OF DUCT (L) INCLUDES INLET DUCT AND TRANSFORMATION PIECES.										

LOG SHEETSUMMARY

NAME OF COMPANY	SIZE & TYPE OF FAN	DRAWG. NO.	ASSIGNMENT NO.	SUMMARY SHEET NO. _____												
				CALC. BY	CHECKED BY	DATE	DETERMINATION									
REMARKS	FINAL VALUES	1	2	3	4	5	6	7	8	9	10	11	12	13	14	15
	P _S															
	P _t															
	P _v															
	C.F.M.															
	V															
	R.P.M.															
	S.h.p.															
	H.p.t.															
	M.E. (e _t)															
	S.E. (e _s)															

TABLE 6-4

(Source: Reference 6-25)

by multiplying the square root of the velocity pressure in Column 0 by 4005. The tunnel area times the velocity P is the fan capacity, Q. When there is appreciable compression, Q is the area times P times Y, where Y is the ratio of the discharge to the inlet air density. Final static pressure and horsepower curves are plotted as smooth curves drawn through the test points, with capacity, Q, as the abscissa and static pressure, N, and horsepower, G, as ordinates.

Arbitrary values of capacity, Q, are then placed in Column R. Corresponding values of static pressure and horsepower read from the curves are recorded in Columns S and V, respectively. The velocity pressures for these arbitrary capacities are then calculated as indicated in Column T. The static pressures, S, and velocity pressures, T, are added and entered in U as total pressures. These total pressures are plotted against the corresponding capacities, R. Static and total efficiencies are calculated as indicated in Columns W and X, respectively, and entered there. These efficiencies, W and X, are also plotted against R, giving the static and total (or mechanical) efficiency curves.

6-2.1.3.3.23 Records and Test Reports

Only such observations and measurements need be made as apply and are necessary to attain the object of the test. Instrument indications, or readings, shall be recorded as observed. Corrections and corrected values shall be entered separately in the test record. Samples of log sheets extracted from NAFM-ASHVE Fan Test Code, Reference 6-25, are shown in Tables 6-3 and 6-4.

6-2.1.3.4 Test Report

The amount and type of data to be reported is dependent upon the specification requirements. Table 6-5 and Figure 6-9 present a general outline of presentation format as recommended by the ASME Test Code on Fans, Reference 6-15.

Table 6-5

Report Outline

General Information

1. Date of Test
2. Location
3. Owner
4. Manufacturer
5. Object of Test
6. Test Conducted by
7. Owner Represented by
8. Manufacturer Represented by

Fan and Test Installation

9. Type of Fan (Centrifugal, Axial-Flow, etc.)	
10. Brief Statement of Basic Feature of Fan Design	
(Blades, Intake, Bearings, etc.)	
11. Name Plate Data	
12. Outside Diameter of Fan Rotor	in.
13. Inside Diameter of Fan Rotor	in.
14. Dimensions of Fan Inlet	in.
15. Dimensions of Fan Outlet	in.
16. Test Set-Up Used	
17. Dimensioned Sketch of Test Set-Up	
18. Description of Pitot Tube Used	
19. Description of Manometers Used	
20. Description of Thermometers Used	
21. Description of Speed Measuring Instruments Used	
22. Method of Determining Shaft Horsepower Input	
23. Description of Throttling Device	
24. Additional Instruments or Methods Used	
25. Description of Driving Unit	
26. Name-Plate of Driving Unit	
27. Additional Data on Driving Unit	

Mean Observations and Calculated Results, Under Test Conditions

28. Time of Starting and Stopping of Test	
29. Barometric Pressure at Manometer	in Hg
30. Temperature of Atmospheric Air	OF
31. Wet-Bulb Temperature of Atmospheric Air	OF
32. Density of Atmospheric Air	lb. per cu. ft.

Items 33 to 46 are to be tabulated for each setting of the throttling device.

33. Speed of Fan	RPM
34. Static Pressure at Plane of Traverse	in. water
35. Velocity Pressure at Plane of Traverse	in. water
36. Total Pressure at Plane of Traverse	in. water
37. Total Pressure in Plenum Chamber	in. water
38. Temperature at Plane of Traverse	OF
39. Density of Air in Tunnel	lb. per cu. ft.
40. Velocity at Plane of Traverse	fpm
41. Volume Rate of Flow at Plane of Traverse	cfm
42. Volume Rate of Flow at Fan Inlet	cfm
43. Discharge Velocity Pressure	in. water
44. Fan Total Pressure	in. water
45. Fan Static Pressure	in. water
46. Power Input	hp
47. Speed	RPM
48. Fan Total Pressure	in. water
49. Fan Static Pressure	in. water
50. Capacity	cfm

Mean Observations and Calculated Results, Under Test Conditions (Contd.)

51. Inlet Air Density	lb. per cu. ft.
52. Power Input	hp
53. Total Efficiency	per cent
54. Static Efficiency	per cent
55. Range of Capacities and Pressures Within Specified Efficiencies and Speeds	

Calculated Results Corrected to Specified Speed and Density

Items 56 to 61 are to be tabulated for each setting of the throttling device.

56. Capacity	cfm
57. Fan Total Pressure	in. water
58. Fan Static Pressure	in. water
59. Power Input	hp
60. Total Efficiency	per cent
61. Static Efficiency	per cent

Items 62 to 66 are to be obtained from the performance curves

62. Fan Total Pressure at Specified Capacity	in. water
63. Fan Static Pressure at Specified Capacity	in. water
64. Power Input at Specified Capacity	hp
65. Total Efficiency at Specified Capacity	per cent
66. Static Efficiency at Specified Capacity	per cent

Include any photographs of the test set-up or of any detail conditions which may be of value.

6-2.1.4.0 Structural Tests

Requirements for structural testing is dependent upon customer specification requirements, i.e., SD-24 and H.I.A.D., References 6-42 and 6-30, as well as the Contract.

Structural testing (with a balanced fan), consists of the following test methods:

- a. Overspeed Proof Testing
- b. Acceleration-Deceleration Testing
- c. Endurance Testing

6-2.1.4.1 Overspeed Proof Testing

The object of the overspeed test is to determine if the fan will withstand inadvertent overspeed conditions. Since the result of this test is a function of high centrifugal force, rather than endurance, it is only necessary that this test be of short (minutes) duration. The Contractor should program this test for all new designs.

The fan should be tested up to design limit R.P.M.

Overspeed testing facilities consist of a spin pit, adequate safety precautions, a drive system, and speed measuring devices (see References 6-1, 6-7, 6-24, and 6-29 for information on speed measuring devices).

During overspeed testing, the fan must repeatedly be inspected visually and a record of the dimensional inspections should be maintained. Any indications or evidence of failures should result in zyglo, dy-check, and magnaflux inspections as required. During this test, a deflection test may be performed if desired - see sample set-up illustrated in Figure 6-10.

6-2.1.4.2 Acceleration-Deceleration Testing

The object of the acceleration test is to determine if the fan will withstand the high acceleration experienced with inadvertent overspeed conditions. Acceleration and deceleration should be evaluated between 50% and 140% of the maximum possible operating speed. Test time is arbitrary; however, normally approximately 30 complete cycles is deemed adequate. The rate of acceleration and deceleration must be determined and for some fans have been established as 15% less than the design limit value.

The same facilities employed in the overspeed proof test are used for this test. The method of control and measurement of acceleration is at the option of the Contractor.

During testing, the fan should repeatedly be inspected for evidences of failures as was done during the overspeed proof testing.

6-2.1.4.3 Fan Endurance Testing

Endurance testing is the first opportunity for the test agency to evaluate the fan in an actual installation under simulated flight conditions. An endurance test of the fan is necessary when the fan is used in propulsion or transmission system or for equipment cooling. Such tests are performed in compliance with the cooling specification requirements.

The longer a fan remains installed in operation the more completely will the endurance capabilities of the fan be observed. These capabilities may continue to be further explored by the continuous satisfactory accumulation of installation test time. This may be accomplished by the continued use of the same fan in various installations, i.e., fan tunnel tests, tie-down tests, ground tests, flight tests, etc. By endurance testing the fatigue characteristics of the fan are automatically explored without actually performing a special fatigue test. (Fatigue testing of a fan is too costly a venture, as such a program would require sufficient tests to permit preparation of a stress-cycle diagram (S-N). Such tests are not conducted unless the Contractor has specific requirements, i.e., (contractual) for such a program. This test will not be outlined herein since it is rarely performed on fans. Fatigue testing of the individual fan blades although not normally required may be accomplished in the conventional manner by employing strain gages and vibrator equipment.)

(In the event that the fan structure does not lend itself to theoretical analysis, or if service experience is not available or if a radically new fan is being developed, the Contractor may decide to conduct a fan stress survey during endurance testing. Such a program is not normally required; therefore, this test will not be outlined herein.)

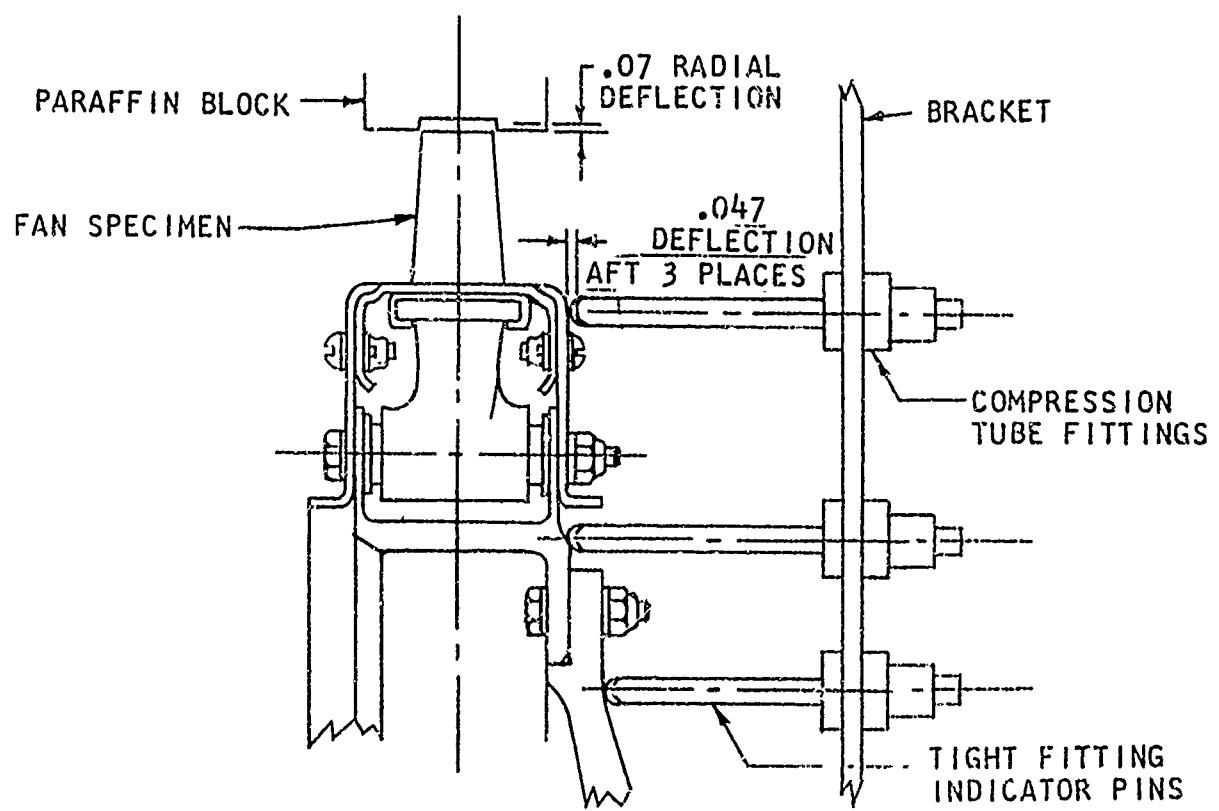


FIGURE 6-10. Deflection Inspection

See References 6-4, 6-6, 6-7, and 6-8 for additional information.

Aircraft tie-down tests are essentially endurance tests used to evaluate and qualify components including fans, systems, and systems in combination. The tie-down tests are designed to simulate flight conditions, and permit structural and performance evaluation and qualification of the fan. Tie-down tests can range from 20 hours through 50,150, 250 and 500 hours depending upon the nature of the contractual requirements. Instrumentation to record cooling data can be installed at this time and is identical to that provided for flight testing Paragraph 6-3.0. Pressure pick-ups radially located on either side of the fan as well as in the stator - see Paragraph 6-2.1.3.0 - will permit determination of the operating pressure and flow. Such endurance tests are in compliance with the requirements SD24 and H.I.A.D. References 6-42 and 6-30, and comply with such specifications as follows:

- Ref. 6-52, MIL-R-6754 - Rotor, Main, Rotary Wing Aircraft, Type Test of
- Ref. 6-53, MIL-R-6755 - Rotor, Auxiliary, Rotary Wing Aircraft, Type Test of
- Ref. 6-51, MIL-G-6641A(ASG) - Gearbox, Aircraft Accessory Drive, General Specification for
- Ref. 6-57, MIL-E-7470(USAF) - Shaft, Power Transmission, Aircraft, Accessory, General Specification for
- Ref. 6-62, MIL-C-8679 - Test Requirements, Ground Helicopter

Endurance test results are obtained at the power and speed settings employed for the other tests being conducted as required in the basic Contract and SD-24 or H.I.A.D., References 6-42 and 6-30.

The fan should be inspected for evidences of cracks, prior to start, at completion of, and during the running of the program. Such inspections may be visual, dimensional and/or penetrant.

6-2.1.5 Inertia Testing

In the design section of this handbook one of the parameters for fan designs was compliance with moment of inertia requirements (required to provide engine fly wheel effect) as established by the engine manufacturer. Moment of inertia values which fall outside these limits may result in faulty engine operation. Although the moment of inertia may be calculated, occasions may arise when it may be advisable to test the fan to verify the calculated results as well as to include changes due to fan balancing corrections. Such tests are at the discretion of the Contractor. In the event that such a test is desired, the torsional vibration (Trifiler) method for solid (no cushioning of blades, etc.) fans may be employed. In the Trifiler method, the platform is rotated several degrees and released. The platform will then rotate clockwise and counter-clockwise in diminishing amounts and the number of cycles for a given time are recorded and the data substituted in a formula to provide the required moment of inertia.

Where blades are elastically mounted, consideration must be given to the amount of their effectiveness to the instantaneous moment of inertia of the fan.

During this test, the following conditions must be maintained:

- a. The platform should be rotated and released without lateral sway and without imparting rotational motion.
- b. The center of gravity of the fan must be equal distance from all supporting cables, i.e., directly in the center of the platform.
- c. There should be no external disturbance, i.e., wind, vibration, etc.

The platform (wood or metal) should be hung from the ceiling by three long thin cables such that the cables are parallel to each other, form an equilateral triangle, and are of equal length. These cables should be extremely long, such that the ratio of the radius (to the center of the equilateral triangle formed by the wires on the base) to length is approximately 1/8 to 1/9. The platform must be level and may be just large enough to accomodate the fan.

To determine the moment of inertia of the fan, it is necessary to obtain the moment of inertia of the platform, then of the platform and fan combined and the difference between the two is the required moment of inertia.

Example:

To determine the moment of inertia of the fan, obtain the average (time and number of complete cycles) as outlined above and obtain the time per cycle:

Ex. #1 Platform (40.92 seconds for 20 cycles)

$$\text{Seconds/cycle} = \frac{40.92}{20} = 2.05$$

#2 Platform and fan (45.6 seconds for 20 cycles)

$$\text{Seconds/cycle} = \frac{45.6}{20} = 2.28$$

With the time per cycle and the weight available for both the platform and the fan, the following formula can be used to determine the moment of inertia:

$$I_F = I_{p+F} - I_p$$

I_F = Fan moment of inertia (lb. in. sec.²)

I_p = Platform moment of inertia (lb. in. sec.²)

I_{p+F} = Platform & fan moment of inertia (lb. in. sec.²)

During this test, the following conditions must be maintained:

- a. The platform should be rotated and released without lateral sway and without imparting rotational motion.
- b. The center of gravity of the fan must be equal distance from all supporting cables, i.e., directly in the center of the platform.
- c. There should be no external disturbance, i.e., wind, vibration, etc.

The platform (wood or metal) should be hung from the ceiling by three long thin cables such that the cables are parallel to each other, form an equilateral triangle, and are of equal length. These cables should be extremely long, such that the ratio of the radius (to the center of the equilateral triangle formed by the wires on the base) to length is approximately 1/8 to 1/9. The platform must be level and may be just large enough to accomodate the fan.

To determine the moment of inertia of the fan, it is necessary to obtain the moment of inertia of the platform, then of the platform and fan combined and the difference between the two is the required moment of inertia.

Example:

To determine the moment of inertia of the fan, obtain the average (time and number of complete cycles) as outlined above and obtain the time per cycle:

Ex. #1 Platform (40.92 seconds for 20 cycles)

$$\text{Seconds/cycle} = \frac{40.92}{20} = 2.05$$

#2 Platform and fan (45.6 seconds for 20 cycles)

$$\text{Seconds/cycle} = \frac{45.6}{20} = 2.28$$

With the time per cycle and the weight available for both the platform and the fan, the following formula can be used to determine the moment of inertia:

$$I_F = I_{p+F} - I_p$$

I_F = Fan moment of inertia (lb. in.sec.²)

I_p = Platform moment of inertia (lb. in.sec.²)

I_{p+F} = Platform & fan moment of inertia (lb. in.sec.²)

The individual moments of inertia are as follows:

$$I_{p+F} = \frac{W_{(p+F)} r^2 [t_{(p+F)}]^2}{4 \pi^2 l}$$

$$I_p = \frac{W_p r^2 t_p^2}{4 \pi^2 l}$$

W_{p+F} = Weight of platform and fan (lbs.)

W_p = Weight of platform (lbs.)

r = Distance from center of equilateral triangle to one of its support wires (inches)

t_p = Period of oscillation of platform (sec.)

l = Length of the suspension wires (inches)

$t_{(p+F)}$ = Period of oscillation of platform and fan (sec.)

- Ex. #3 For a platform 7.56 lbs, with a radius of 18.44" and cable length of 120.9" find the moment of inertia if the time per cycle is 2.05 seconds

$$I_p = \frac{W_p r^2 t_p^2}{4 \pi^2 l} = \frac{7.56 \times 18.44^2 \times 2.05^2}{4 \times (3.1416)^2 \times 120.9}$$

$$I_p = 2.14 \text{ lb. in.sec.}^2$$

- Ex. #4 For a platform and fan whose combined weight is 58.75 with a platform radius of 18.44 and cable length of 120.9" find the moment of inertia if the time per cycle is 2.28 seconds.

$$I_{(p+F)} = \frac{W_{(p+F)} r^2 t^2 (p+F)}{4 \pi^2 l} = \frac{58.75 \times 18.44^2 \times 2.28^2}{4 \times 3.1416^2 \times 120.9}$$

$$I_{(p+F)} = 20.7 \text{ lb. in.sec.}^2$$

- Ex. #5 Find the moment of inertia of a fan in Examples 3 and 4.

$$I_F = I_{(p+F)} - I_p = 20.7 - 2.14$$

$$I_F = 18.56 \text{ lb. in. sec.}^2$$

6-2.1.6.0 Sound Testing

Sound (or noise) is produced by air particles set in motion by a vibrating component. The frequency with which the source vibrates determines the pitch of the sound and the amplitude or displacement of the wave determines the intensity and loudness level.

In Section 3-19 of SD-24, Reference 6-42, the Navy requires that aircraft should be tested for noise level values per MIL-A-18150(Aer), "formerly SR-181", Reference 6-67. Similar requirements for sound testing exist for the USAF in Section A5 of H.I.A.D., Reference 6-30.

Since under certain conditions fans can contribute to an increase in the noise level readings, consideration should be given to determination of the fan noise level. If the fan is located a remote distance away from the aircraft occupants, the fan noise may be far below the predominant noises such as to be entirely negligible. When such a condition is found to exist, sound tests are not required. However, if fan noises can be easily transmitted to the occupants, then it may be necessary to evaluate the noise level of the fan. Such occasions may arise when the fan and its drive system are submerged in the proximity of the occupants (as in airships, large helicopters, etc.).

To determine the noise level of the fan and to assist in the evaluation of certain designs or modifications, the sound measurement test code listed below for centrifugal and axial fans by the National Association of Fan Manufacturers may be used. These measurements are made in the vicinity of the fan and permit comparison between fans. The usual procedure is to seek out the vibrating surfaces responsible for producing the noise and take the necessary corrective measures which will reduce the vibration or which will prevent the effective radiation of noise from the vibrating surfaces.

6-2.1.6.1 N.A.F.M. Test Code - General (Reference 6-25) *

All definitions, standards and specifications used in this Code are based on the American Standards Acoustical Terminology, Bulletin Z 24.1 - 1942; the American Standard for Noise Measurement, Bulletin Z 24.2 - 1942; and the American Tentative Standard Specification Sound Level Meters for the Measurement of Noise and Other Sounds, Bulletin Z 24.3 - 1936, published by the American Standards Association.

The reference pressure shall be 0.0002 dynes per square centimeter. (Editor's Note: When compliance with MIL-A-18150, Reference 6-67, is contractually required, the values specified in Paragraph 4 shall be used.) Sound pressure levels may be expressed in decibels.

Sound level readings shall be overall sound as measured by flat response without network. Response with either 40 or 70 decibel network is not a quantity covered by this Code. It may be taken if desired, but shall be clearly designated as network response and shall not be reported unless accompanied by flat response values.

Instrument calibration and test tolerances shall be in accordance with A.S.A. standards.

* Reference 6-25 is currently being revised.

The sound that is emitted at the fan outlet and carried through the duct system is not determined under this Code since there is no known means at present for measuring the sound level in an air stream. In general, a fan with a higher ambient sound level will have a greater sound level in the air stream, but its exact amount is not measurable under the present state of the art.

Correction for variations of fan speed not exceeding plus or minus 10% may be made in accordance with the following formulae, for flat response observations:

$$\text{Db change} = 50 \log_{10} \frac{\text{RPM}_2}{\text{RPM}_1}$$

$$L_2 = L_1 + 50 \log_{10} \frac{\text{RPM}_2}{\text{RPM}_1}$$

where L_2 and L_1 are sound levels in decibels for speeds RPM_2 and RPM_1 respectively.

6-2.1.6.2 N.A.F.M. Test Code - Room Effects (Reference 6-25)*

No standard room sizes are required under this Code. It is desirable that the room sound level at remote points, when the apparatus is in operation, be 10 db below the sound produced by the apparatus, although lower values are permissible. Treatment of the test room with sound absorbent materials is also permissible.

6-2.1.6.3 N.A.F.M. Test Code - Centrifugal Fan Sound Tests (Reference 6-25)*

The fan shall be rigidly attached to a foundation or may be mounted on a substructure of wooden beams not greater than 4" x 4", but in no case shall sound absorption material be used between the fan and the foundation or the substructure.

The fan shall be equipped with an outlet duct having an area equal to the fan outlet with a tolerance not to exceed plus or minus 5%. The duct shall be straight, of uniform circular cross-section and not less than ten diameters in length. A symmetrical throttling device shall be placed at the discharge end of test duct. The use of a canvas connection between the fan outlet and the duct is recommended.

Determinations of sound measurements shall be made with the fan having all structural features and appurtenances in place. A standardized assembled factory fan unit shall be tested with its own drive and motor at rated speed.

Sound readings shall be taken at seven stations at a distance equivalent to one wheel diameter from edge of fan housing, but not less than 5'-0". (See Figure 6-11)

The position of the microphone at each station shall be in a plane parallel to the floor and coinciding with the horizontal center line of the fan.

* Reference 6-25 is currently being revised.

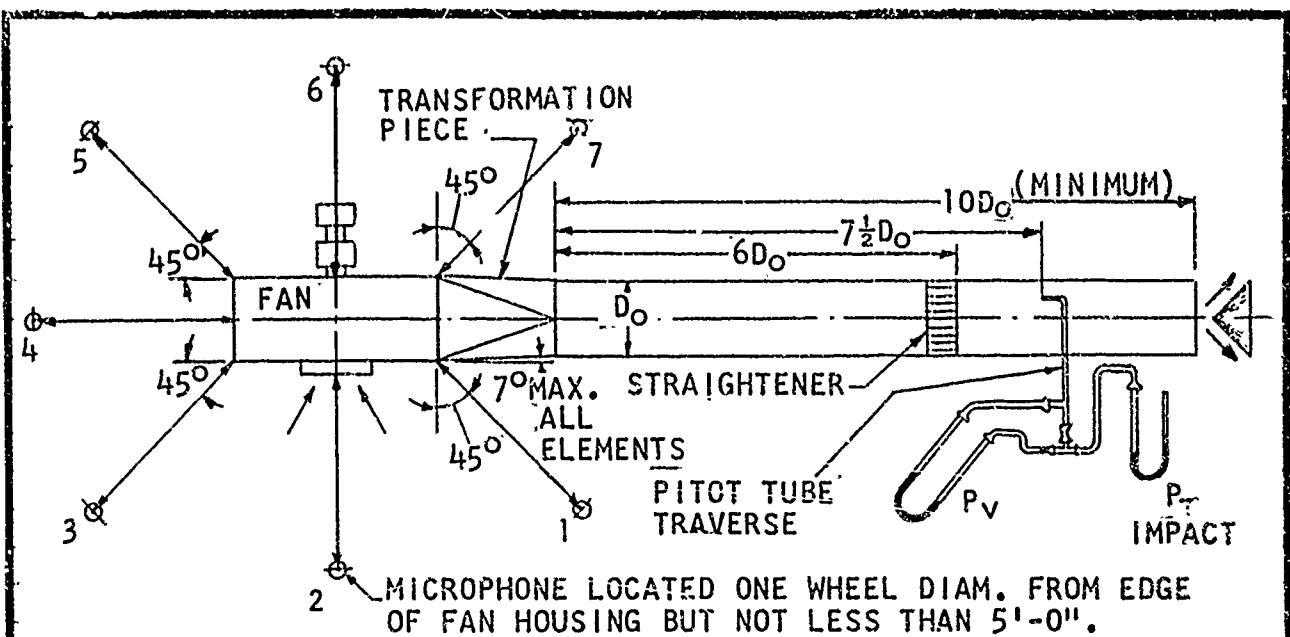


FIGURE 6-11. Centrifugal Fans - Single or Double Inlet
(Source: Ref. 6-25, which is currently being revised)

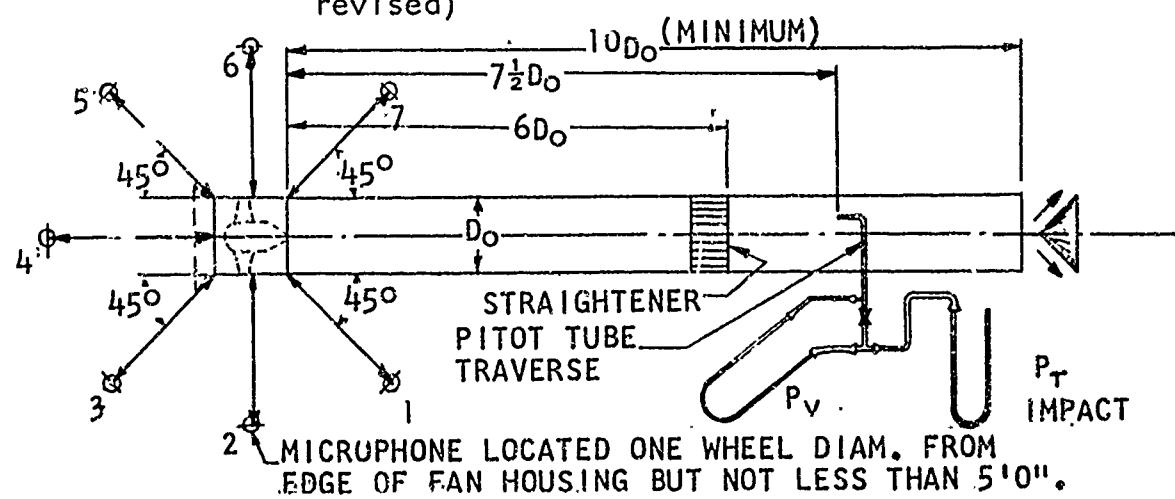


FIGURE 6-12. Axial Fans with Ducts
(Source: Ref. 6-25, which is currently being revised)

MICROPHONE LOCATED ONE WHEEL DIAM. FROM EDGE OF FAN HOUSING, BUT NOT LESS THAN 5'-0".

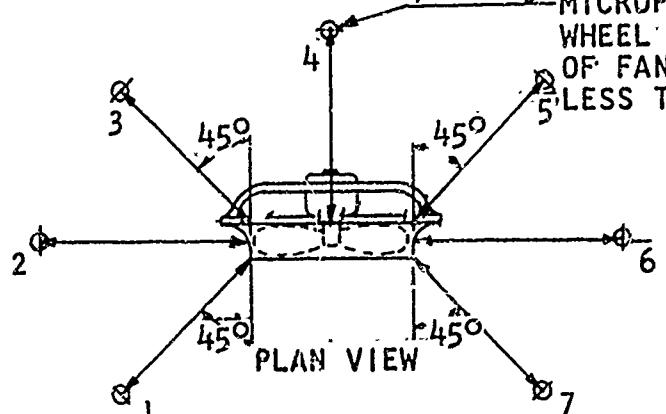


FIGURE 6-13. Axial Fans without Ducts Noise Level Tests
(Source: Ref. 6-25, which is currently being revised)

The arithmetic average of the sound readings obtained shall be used. (Authorities agree that where the variation of the readings is 12 db or less, the arithmetic average is a sufficiently close approximation. For larger variations, the properly weighted logarithmic average should be used.)

6-2.1.6.4 N.A.F.M. Test Code - Axial Fan Sound Tests (Reference 6-25)*

Case I - Where axial type fans are to be operated for general application with ducts attached, the method of test shall be that outlined under Paragraph 6-2.1.5.3 for the centrifugal type fan. (See Figure 6-12 for set-up)

Case II - Where axial type fans are to be operated for general application with neither inlet nor outlet ducts attached, the fan shall be supported by flexible means.

The fan, in both cases, shall be tested with its own motor and drive in place at rated speed.

Sound readings shall be taken from seven stations at a distance equivalent to one wheel diameter from edge of fan housing but not less than 5'-0". (See Figures 6-12 and 6-13)

The position of the microphone at each station shall be in a plane parallel to the floor and coinciding with the horizontal center line of the fan.

The arithmetic average of the sound readings obtained shall be used. (Authorities agree that where the variation of the readings is 12 db or less, the arithmetic average is a sufficiently close approximation. For larger variations, the properly weighted logarithmic average should be used.)

6-2.1.6.5 Test Results

Upon completion of the requirements of the Test Code above, the results of each fan can be evaluated with those contractually required and in the event several fans are being tested, with each other. Such comparisons can result in an optimum fan from the standpoint of noise.

Additional data on sound testing may be obtained from References 6-1, 6-5, 6-7, 6-10, 6-36, and 6-40.

6-2.2.0 Duct Tests

A satisfactory duct system is that system which can transport the airflow from the duct origin to the objective in the most efficient manner. Since efficiency is a function of pressure loss through the duct system, it is necessary to direct the airflow with a minimum of drop in pressure across the individual elements of the system, e.g., entry, diffuser, turns, vanes, across cooler, fan, engine section, nozzles, and exit.

In the design section of this handbook, effort is directed toward designing an efficient duct system. During the design, numerous concepts were ordinarily analyzed until that configuration which satisfied both the physical and flow requirements was determined.

* Reference 6-25 is currently being revised.

Duct systems considered in this handbook are those employed for cooling and induction purposes. In testing such systems, the objective is: (a) the determination of pressure loss and the flow distribution at the carburetor, the fan entry, or the compressor inlet in the case of the turbine engine and (b) the evaluation of the structural capabilities of the system through endurance and backfire pressure testing.

In helicopter and airship duct systems the flow is usually in the Reynolds number range where fully developed turbulent flow is expected, and as was explained in the design section of this handbook, duct losses will be closely a function of velocity squared.

Local disturbances in a duct system can provide uneven pressure losses and, therefore, uneven pressure distributions across some specific cross sections. In the case of a turbine inlet duct, such uneven distributions are critical and must be within the limits established by the engine manufacturer (for example, 5% of the mean weighted value of total head at the compressor housing).

Although individual sections of duct for the most common applications (i.e. elbows, transitions, straight sections, etc.) have been tested and the data applied to theoretical analysis it must be realized that such data is not entirely accurate nor directly applicable because the design being developed is rarely a duplication of the above tested components. For this reason, as well as for reasons of the requirement of composite system evaluation, it is necessary to conduct tests of a duct system to substantiate the theoretically computed performance.

In addition, when numerous efficiency reducing components exist, i.e.: duct restrictions, interruptions, interferences, sharp bends, changes in shapes, etc., it then becomes desirable to perform flow tests in order to evaluate the performance of the duct system. During such tests, flow through branches of a duct system may be balanced to assure that each branch receives the required quantity of air. In such a test program, the Contractor can evaluate and/or improve his preliminary design prior to release for flight evaluation and production.

Duct evaluation and/or qualification may be accomplished through the use of the following test methods:

- a. Model tests (flow and wind tunnel)
- b. Aerodynamic performance tests
- c. Structural tests (endurance and backfire proof tests)

6-2.2.1 Model Testing

Model testing can be used for evaluating or developing the inlets, exits or any intermediate sections of the duct system. Model testing is extremely profitable when the duct design is restricted to size, shape and routing, thereby requiring such testing in order to obtain the optimum configuration.

For testing inlets, entries and exits, the use of scale models can be employed. The model is submerged in a conventional wind tunnel similar to those outlined in the ASME setup of Paragraph 6-2.1.3.1 and the pressure, drag and airflow patterns are obtained. During these tests

it is necessary to assure that the airflow at the entry is a true replica of actual operating conditions. This is especially necessary in regard to angle of attack and type of flow (turbulent or laminar) condition. Special entries may be required to provide such a condition, i.e. bellmouth, length of leading edge of aircraft surface, etc. The exit of the duct may also require similar consideration and treatment

By analysis of these data, the critical areas can be estimated and by temporary (i.e. use of clay and wire mesh buildup) alterations and retests, they can be repeatedly improved.

For testing the interior duct system, the model is connected to a source of air supply, i.e. blower, propeller, etc., and the pressure and flow can be determined. Again the critical areas can be estimated and by temporary alterations and retests these areas can be improved. Whenever possible, it is advisable to provide an inspection window in the duct in order to observe smoke and tuft action. Where reasonable dimensional symmetry exist, it is desirable to "split" the duct into a "half shell" with a flat plexiglas panel replacing the streamline plane of symmetry. This permits observations of the entire duct length.

6-2.2.2 Duct Aerodynamic Performance (or Wind Tunnel) Tests

Duct wind tunnel tests are performed for the purpose of determining pressure losses, airflow and leakage. The test configuration should be as nearly as possible a replica of the installation. A continuous source of airflow is required. This airflow must be of uniform pressure and velocity and of controlled rate of flow in order to provide reliable comparative data. Care should be exercised to provide adequate airflow past the entry to insure that the boundary layer is not too shallow and that it be as nearly as possible representative of operating conditions. Relative flow volume (of wind tunnel flow to duct flow) should be at least 10 to 1 to prevent excessive tunnel interferences.

Measuring equipment consists of the properly calibrated pitot static tubes, manometer, indicator, barometer and sling psychrometer as described in Section 6-2.1.3.1 as well as drag measuring equipment when required.

The locations of pressure (static and total) and temperature pickups in the duct system are determined by the realization that complete visualization of the air characteristics throughout the duct may be the ultimate goal and this requires a study of flow patterns, temperature variations, pressure variations and velocity. To achieve this goal, each section must be reviewed and measurement points established. Such points or planes may be in the areas where hot spots may occur due to proximity of engines, coolers, etc., or where local protuberances introduce flow disturbances, or downstream of sharp bends where vanes may be required, or at junctions where splitters may be employed, etc.

Although an infinite number of traverses for all conditions would result in the most complete survey, this is not practical, and experience has proven that 3 to 5 planes are adequate for the majority of installations.

As in the case of model testing, consideration and proper treatment must be given to the entry and exit condition in order to assure that the flow is a true replica of the actual operating conditions. This should include a visual analysis of the boundary layer and flow characteristics upstream of the entry. In some conditions, this may require sufficient structure to reproduce the required flow condition. In like manner the exit also must be considered and treated. Unless such conditions are realistically reproduced the results of the tests may be both inaccurate and misleading.

Provisions may be furnished to permit local substitution of alternate type configurations to permit evaluation of several designs to result in an optimum design. In the event flow visualization studies are planned, scanning windows should be provided (and with the necessary access holes to permit tuft or pressure pickups traverses when desired).

The visualization of flow may be accomplished by a number of means and is discussed in References 6-12 and 6-13. The two most popular and simple methods are smoke and tuft techniques. Others include hot wire, spark, gas filament, china-clay, and liquid film techniques.

Flow visualization, as applied to duct performance tests, may be used to minimize duct losses. The technique is to determine the location of turbulent (high loss) regions by flow visualization means. The turbulence is then reduced or, if possible, eliminated by altering duct shapes to improve the flow pattern. This technique is extremely useful during developmental model tests in the design stage.

Tufts are very useful for flow visualization studies in ducts because they permit the determination of flow characteristics close to solid surfaces. They are usually made of fine silk or of yarn such as "baby wool". If they are to be attached to a surface they are usually about three-quarters of an inch long. They may be attached with Scotch tape, glue or some other adhesive. The downstream end of a silk tuft is ordinarily frayed. The upstream end is attached so that the tuft lies flat against the test surface. The general direction of the local velocity may be observed from the actions of the tufts. In a laminar flow region they remain relatively smooth and undisturbed. In a region of turbulence they move violently. If in a separated turbulent region their movements are violent and, in addition, random with respect to the surface to which they are attached. An easily made arrangement for flow visualization along a surface approximately normal to the flow direction is achieved by attaching a number of tufts to a strip of Scotch tape and then taping the arrangement to the surfaces. The use of parallel rows of such multiple tuft assemblies, placed normal to the flow direction, permits the visualization of flow over the surface in the direction of flow. Care must be exercised that the tuft installation does not have any appreciable effect on the aerodynamic characteristics of the flow.

Often, the use of a single streamer attached to the end of a piece of wire will better serve the purpose than will the installation of a number of surface tufts. The wire is ordinarily hand held and placed at the various locations, both at surfaces and in the stream; under investigation. The streamer length should be such that it will assume the shape of the flow (i.e., straight or properly curved) path. This length

will vary with the tuft material and is usually two to five inches. Baby wool or light cotton are good materials. Extreme caution must be exercised so that the wire and streamer are not introducing disturbances which affect the flow. Tufts may be used to determine the flow pattern outside of the entry or exit to a duct system by attaching them to a wire grid mounted on the aircraft exterior.

Smoke is useful for flow visualization but its use in duct tests presents the problem of providing sufficient smoke to be visible. In velocities above approximately 100 feet per second or in systems of large cross-sectional area, smoke generators should be used. Below this velocity or in small ducts, a hand held smoke generator proves very useful. One such device is the hand held ventilation smoke tube assembly which is supplied commercially by the Mine Safety Appliances Company, Pittsburgh 8, Pennsylvania as Catalogue Number BH-5607.

Characteristics of smoke required for satisfactory testing are that the smoke:

- a. Shall not form deposits which either alter the airflow over the test item or which block the smoke supply system,
- b. Shall be "light" and of low inertia so that it reflects, within satisfactory limits, the motions of the flow it is intended to portray. Any appreciably different effect on the smoke filament from the air stream filament by gravitational, centrifugal or other forces will cause non-representative flow visualization.
- c. Should be generally satisfactory regarding visibility, non-corrosiveness and non-toxicity.
- d. Should be easily produced and controlled and of reasonable cost.

For some tests, a single smoke filament will suffice, and the emitting device may be stationary or movable. In some tests, a number of filaments are required, in which case a group of smoke tubes may be placed upstream of the model. Smoke filaments must, of course, be released into the air flow upstream of the test model in the same sense in which the air is moving.

Some criteria for the choice of tufts or smoke are:

- a. Tufts are cheaply and quickly made and installed and are readily visible,
- b. Hand held smoke devices are inexpensive and simple in operation. However, a smoke filament from such a device is very short in the direction of flow so that visualization of the flow is difficult, especially at high velocities,
- c. Smoke generators can be used to provide one or more continuous smoke filaments which permit excellent flow visualization. Relative cost and complexity must be considered.
- d. For the ordinary duct within the scope of the parameters considered in this handbook, tufts or hand held smoke devices suffice.

Several other flow visualization methods are used. These include the hot spark, liquid film and other techniques. If the hot spark technique is to be used, the flow studies are best performed at the end of runs so that any slight atmospheric changes do not affect flow measurements. The liquid film method produces pattern impressions on a surface. It is, therefore, useful for boundary layer studies.

Most aircraft flow conditions occur above the critical Reynold's number. Therefore, caution must be exercised that scale-model flow visualization studies are conducted at realistic (full-scale) Reynold's numbers, rather than at sub-critical Reynold's numbers, at which flow separations occur, whereas they do not at full-scale Reynold's numbers. This requires an increase in duct velocities above values representative of the full scale flow rates.

Additional information on flow visualization studies is presented in References 6-12, 6-13, 6-26, 6-31, and 6-41.

6-2.2.3.0 Structural Tests

Requirements for structural test of duct systems is dependent upon customer specification requirements, i.e., SD-24 and H.I.A.D. references 6-42 and 6-30, as well as the contract.

Structural testing consists of the following test methods:

- a. Endurance Testing
- b. Backfire Pressure Testing (reciprocating engines)

6-2.2.3.1 Duct Endurance Testing

Endurance testing of duct systems consists of evaluation of the duct during an aircraft tie down test and ground and flight testing.

The conditions outlined in fan endurance testing Paragraph 6-2.1.4.3 are also applicable to duct testing.

During these tests, pressure pickups may be installed throughout the duct for the purposes of determining the pressure distribution and drop between the inlet and outlet.

6-2.2.3.2 Backfire Pressure Testing

SD-24 and H.I.A.D. References 6-42 and 6-30, require assurance that the air induction system on reciprocating engines be capable of withstanding engine backfire and its accompanying pressures. Part D of H.I.A.D. (Section 2-8.3.1) stipulates that the system should be capable of withstanding 25 psig internal pressure when blocked off.

During this test, distortion should be observed and the amount recorded and reviewed for its affect on the installation.

6-2.3.0 Ejector Aerodynamic Performance Tests

The purpose of the ejector in an aircraft internal flow system is to cause an airflow quantity, the secondary airflow, to move through some resistance. To induce this secondary airflow, the fluid entrainment

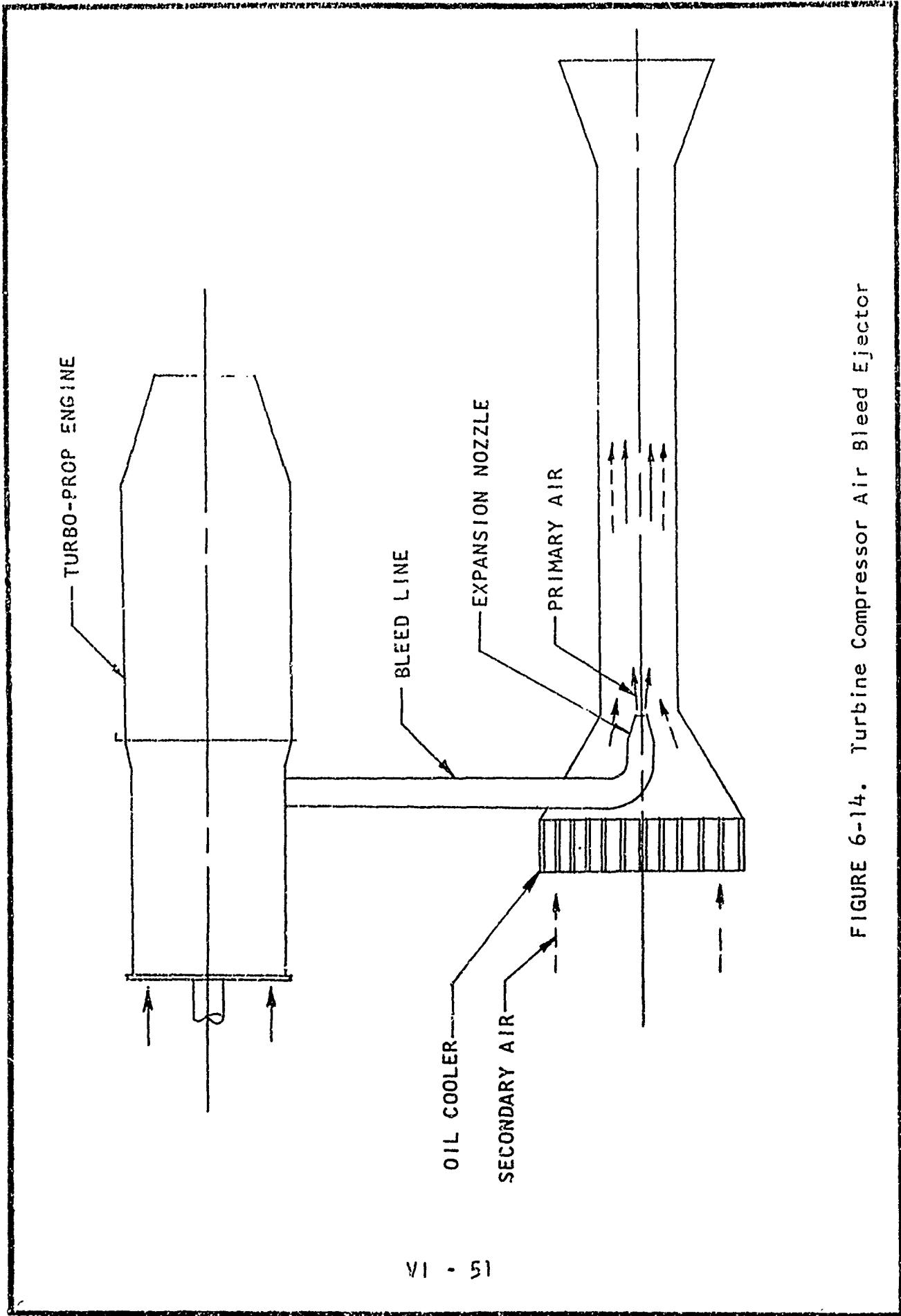


FIGURE 6-14. Turbine Compressor Air Bleed Ejector

action of a primary flow is utilized. The primary air source may be the engine exhaust (turbine or reciprocating) or some other source, such as turbine compressor air bleed. A turbine compressor air bleed ejector is illustrated in Figure 6-14.

Through the use of aerodynamic testing, the performance of the ejector may be determined. With fans, it may be recalled, the input and output were as follows:

- a. Input - shaft power.
- b. Output - pressure increase (ΔP) and airflow (Q).

For ejectors -

- a. Input - primary flow pressure ratio, airflow (Q), temperature (T), and the effect of the primary flow on the providing source, such as the loss in engine power due to increased exhaust back pressure.
- b. Output - secondary air flow pressure rise ($\Delta P_{sec.}$) and air flow ($Q_{sec.}$).

The output of an ejector may be measured in a manner similar to that for any air pump. The instrumentation may be arranged to measure the secondary flow quantity through various resistances or through the given resistance of the aircraft installation. The technique of secondary flow measurements may be exactly the same as discussed in the section on fan testing, Paragraph 6-2.1.3.

The method of measuring the state of the primary flow input to an ejector is also relatively standard. Instrumentation may be provided to measure the air pressure, quantity, and temperature. The primary flow conditions of the actual aircraft installation must be duplicated in a bench test in order to correctly evaluate ejector performance.

The most common ejectors in use are those which use as their primary flow one of the following:

1. Reciprocating engine exhaust.
2. Turbine engine exhaust.
3. Turbine compressor air bleed.

This discussion will be limited to the consideration of these three types.

Aerodynamic performance testing of ejectors may be accomplished during flight. However, as in the case of the testing of fans, Paragraph 6-2.1.3, it is desirable to accomplish tests as far in advance of production and flight testing as possible.

It is, therefore, suggested that bench (static flow) tests or installation (stand tests or aircraft tie-down) tests be performed.

6-2.3.1 Bench Testing

A sample bench static flow test set-up is shown in Figure 6-15. The following test conditions must be carefully controlled during ejector bench testing:

1. Primary air flow quantity, pressure, and temperature, equal to that anticipated in the final aircraft installation, must be provided. Ordinarily, a number of test runs are made to vary these parameters to include the expected installation values.
2. In order to measure the secondary flow, the ejector must be connected to a test tunnel (See Figure 6-1 through 6-5 and 6-15) equipped with a variable resistance. The ejector is instrumented to measure its output, i.e., secondary flow (Q_{sec}) and pressure differential (ΔP_{sec}).
3. Ambient conditions of secondary air must be controlled. Altitude simulation may be effected by using an altitude chamber.
4. Sufficient test variables should be provided to permit evaluation of several alternate configurations in order to arrive at the optimum installation. These variables may include the following:
 - a. Adjustable mixer length.
 - b. Adjustable diffuser ratio.
 - c. Adjustable primary air supply pressure and flow rate.
 - d. Adjustable mixer diameter.
 - e. Adjustable diffuser angle.
 - f. Adjustable cooler block configuration (including inlet duct).
 - g. Adjustable primary air nozzle geometry and location.

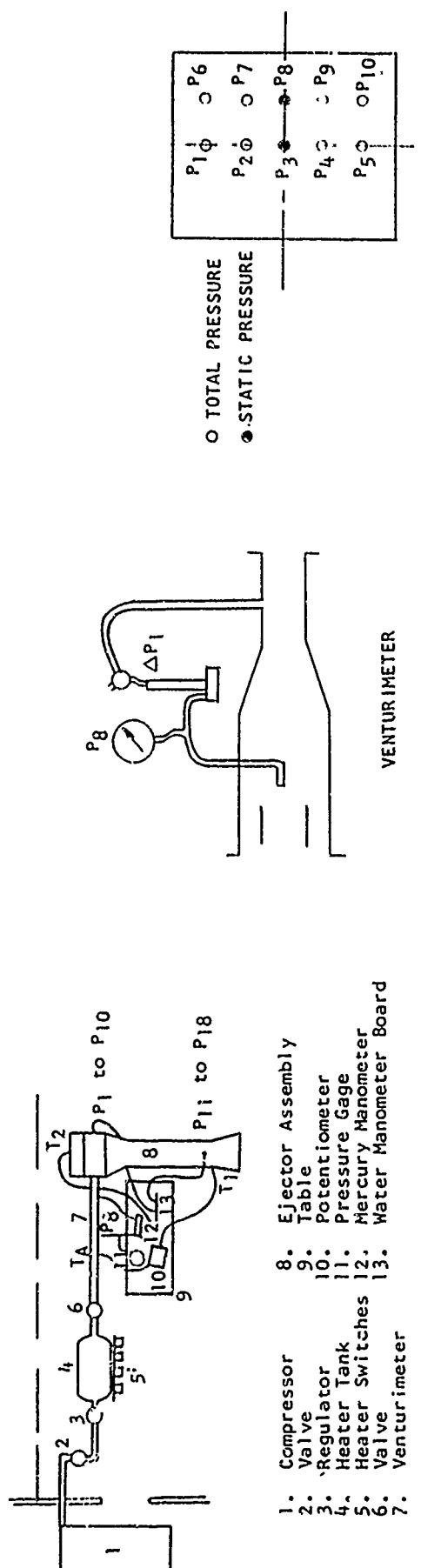
6-2.3.2 Installation Stand Testing

Installation stand tests consist of measuring the aerodynamic performance of the ejector under normal aircraft operating conditions. Such tests may be performed in the aircraft tie-down (concurrent with endurance testing of the entire propulsion system) but preferably in an engine test stand which can be erected to perform this test.

Although the installation stand may not maintain all the carefully controlled conditions outlined in Paragraph 6-2.3.1, it employs the actual source supplying the primary flow, thereby eliminating many problems inherent with the simulated primary flow required in bench testing. Unless an altitude chamber is available, such tests are conducted at the pressure altitude of the test stand.

In the installation stand testing, the following conditions must be maintained:

TEST APPARATUS

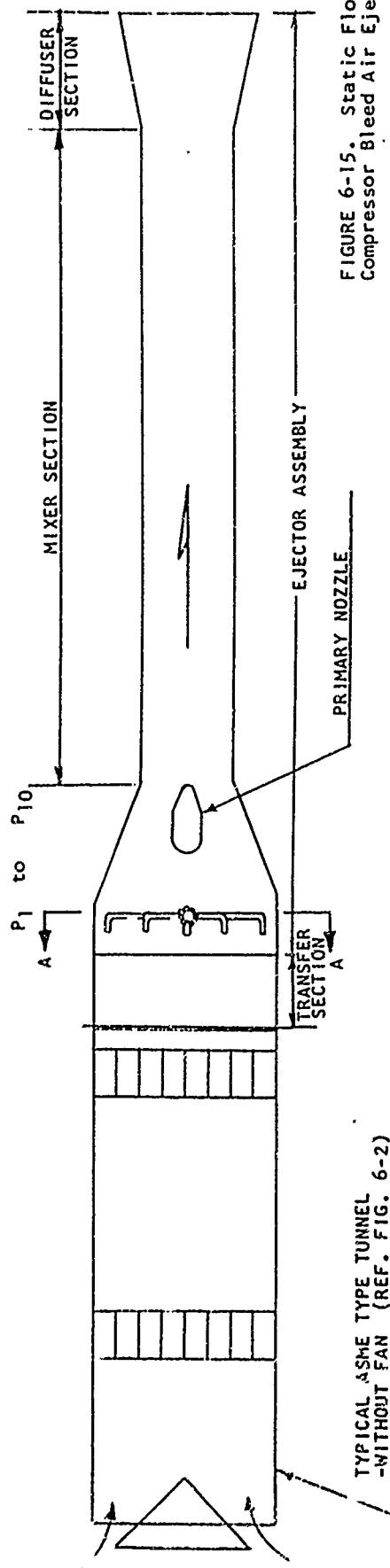


O TOTAL PRESSURE
● STATIC PRESSURE

P_1	Φ	P_6
P_2	Φ	P_7
— P ₃ —		— P ₈ —

P_4	Φ	P_9
P_5	Φ	P_{10}

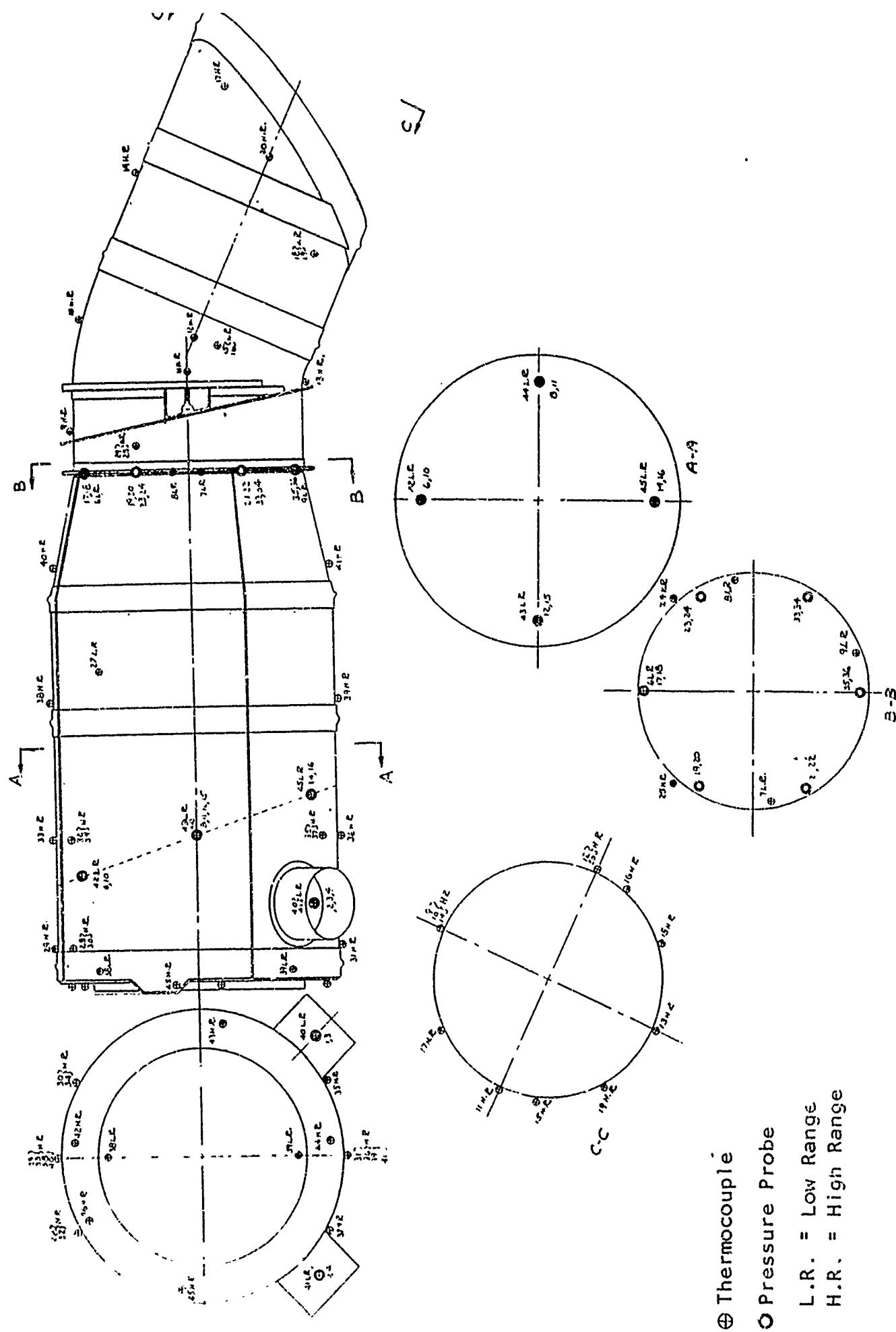
A-A



TYPICAL ASME TYPE TUNNEL
WITHOUT FAN (REF. FIG. 6-2)

FIGURE 6-15. Static Flow Test Set-Up.
Compressor Bleed Air Ejector.

FIGURE 6-16. Sample Turbine Exhaust
Ejector Installation



1. A torquemeter must be employed to measure engine power.
2. As many of the variables of Paragraph 6-2.3.2.4 must be evaluated as the stand will permit.
3. The actual secondary flow resistances or variable resistances may be employed.
4. The primary and secondary flow must be measured as outlined in bench tests, Paragraph 6-2.3.1. A sample instrumented turbine exhaust ejector is illustrated in Figure 6-16.
5. For reciprocating engine exhaust ejectors, the exhaust and nozzle must be "tuned" (as limited by space availability) to the exhaust system in order to maintain the proper mean effective gas thrust pressure. Tuning tests consist of measuring the pressures of the exhaust gases and properly phasing the results (as outlined in Paragraph 4-3.3 of Chapter IV) with the valve timing concurrent with development of exhaust length and nozzle shape. These pressures are measured immediately downstream (approx. 6") of the exhaust valves and immediately downstream (approx. 2") of the exhaust exit.
6. When a turbine compressor air bleed is used, the bleed flow and temperature must be determined and the results compared with acceptable values determined in design analysis, Paragraph 4-3.0 of Chapter IV.

6-3.0 GROUND AND FLIGHT TESTING (FAN, DUCT, AND/OR EJECTOR)

The final evaluation and qualification of the fan, duct and/or ejector is conducted during the ground and flight test program (See Appendix VI for a sample duct and fan program).

These flight tests are divided into three categories, (a) the engine cooling tests, (b) the equipment tests, and (c) the ejector tests.

6-3.1 Engine Cooling Tests

A newly designed engine cooling fan and/or duct system requires an engine cooling qualification test in compliance with SD-24 and H.I.A.D. References 6-42 and 6-30 which include the following specifications:

- Ref. 6-61, Mil-C-8678 (Aer) - (Formerly E-59d). Cooling Requirements of Power Plant Installation.
- Ref. 6-66, MIL-D-17984 ASG - (Formerly MIL-R-17984 (Aer)). Data Presentation Requirements, Installed Engine Performance and Air Induction Systems.

The basic objectives and their purposes in this test are as follows:

- a. Obtain the temperature measurements of the engine and its accessories as well as the required pressure measurements to confirm that the installation is functionally sound and complies with Specification requirements.

- b. Measure the power and fuel metering characteristics of the engine to establish the engine condition at which the cooling capabilities exist.
- c. Measure ambient conditions to permit correction of the data to standard conditions.

6-3.2 Fuel Air Ratio or BSFC

In reciprocating engine testing, a prime requirement is the determination of the fuel-air ratio or brake specific fuel consumption (BSFC). This is necessary since the cooling system is designed to fulfill the heat dissipation requirements established by the engine manufacturer. Improper fuel metering results in engine conditions different than those specified as follows:

- a. An over-rich fuel-air mixture provides extra cooling and reduces the heat rejected to the cooling system. Similarly an over-lean mixture causes extra heat rejection.
- b. Poor flow distribution at the carburetor deck may cause faulty metering by the carburetor, resulting in poor mixture control.

These conditions can be evaluated through use of the BSFC data. The BSFC may be determined in two manners: (a) by measuring power and fuel flow, and (b) by measuring power and the metering suction differential pressure (MSDP) in the carburetor. In both cases, the measuring equipment, as well as the carburetor, must be calibrated.

In (a), the fuel flow rate and the power required are measured at various RPM's and BHP's. The BSFC, in pounds of fuel flow per brake horsepower hour, is then compared to the carburetor's design and calibration BSFC data over the BHP range.

In (b), the MSDP and the power required are measured at various RPM's and BHP's. The BSFC corresponding to each MSDP data point is then determined from the carburetor fuel flow calibration data and, again, the BSFC-BHP performance is compared to the design data.

Since the BSF is influenced by pressure distribution at the carburetor deck, it is necessary to assure that the airflow distribution and, therefore, MSDP is in accordance with the carburetor requirements. This airflow pressure distribution is determined through air box testing of the induction system. As in the case of the model and duct tunnel tests of Paragraph 6-2.2.1 and 6-2.2.2, consideration and proper treatment of the duct entry must be provided to insure proper airflow and distribution.

The facilities required for the engine cooling tests for fans and/or duct systems consist of the test aircraft in flight status, recording equipment, instrumentation and the test specimen.

The fan and/or duct specimen to be tested must be as nearly as possible a replica of the final design. Workmanship must be typical, in order that friction losses will be identical with that of the production version. The specimen instrumentation installation must be carefully controlled to prevent obstructions upstream of the specimen from disturbing the flow and affecting the performance.

The type and amount of instrumentation employed is determined by the applicable specification, as well as by the requirements of the contractor. The following outline is suggested for a reciprocating engine fan and duct cooling test:

1. Temperature

- a. Flexible Engine Mount Rubber
- b. Magneto Coil
- c. Generator
- d. Fuel
- e. Oil Cooler Air
- f. Engine Compartment
- g. Carburetor Air
- h. Cylinder Heads
- i. Cylinder Bases
- j. Exhaust Shroud
- k. Spark Plug Elbows
- l. Each Oil Cooler, Oil In and Out
- m. Outside Air Temperature
- n. Upstream of Fan 3 Places 120° Apart
- o. Downstream of Fan 3 Places 120° Apart

2. Pressures

- a. Cylinder Baffle Pressure Drop
- b. Pressure Drop Across Heat Exchangers
- c. Pressure Change Across Fan Section
- d. Pressure At All Intake Ports
- e. Pressure At All Air Exits
- f. Generator Pressure Differential
- g. Carburetor Deck

3. General Data

- a. Airspeed
- b. Altimeter
- c. Run Counter
- d. Attitude Gyro
- e. Wet Bulb Temperature
- f. Ice Bath
- g. M.A.P. Gage
- h. Tachometer (Sensitive)
- i. Yaw and/or Pitch Angle Indicator (If Either Angle is Pertinent)
- j. Intervalometer

6-3.3 Equipment Tests

A newly designed equipment cooling fan and duct requires qualification tests in compliance with SD-24 and H.I.A.D., References 6-42 and 6-30 which include the following specifications:

Ref. 6-49, MIL-G-6099 - (Formerly 17G15) Generator and Regulator; Aircraft, Alternating Current, General Specifications for

Ref. 6-50, MIL-G-6162 - Generator, 30 Volt, Direct Current, Aircraft Engine Driven, General Specification for

Ref. 6-55, MIL-E-7080A- Electric Equipment, Piloted Aircraft Installation and Selection of, General Specification for

The basic objectives and the purposes of this test are as follows:

- a. Obtain temperature measurements of the equipment as well as the required pressure measurements to confirm that the installation is functionally sound and complies with Specification requirements.
- b. Measure ambient conditions to permit correction of data to standard condition.
- c. Obtain other data measurement as required by the specification to establish the conditions at which the cooling capabilities exist.

The instrumentation required to evaluate such equipment will be dictated largely by the installation and should include the following instrumentation:

- a. Those units mentioned earlier in Paragraph 6-3.0 and considered pertinent to this evaluation.
- b. Those units specified in the applicable specification.
- c. Any additional instrumentation desired by the contractor.

6-3.4 Ejector Cooling Tests

The use of ejectors to cool aircraft equipment such as engines, oil coolers, etc. must be substantiated by adequate tests. These cooling tests consist of component aerodynamic tests, as described in Paragraph 6-2.3.0 for the initial development and evaluation test, and the following flight qualification tests.

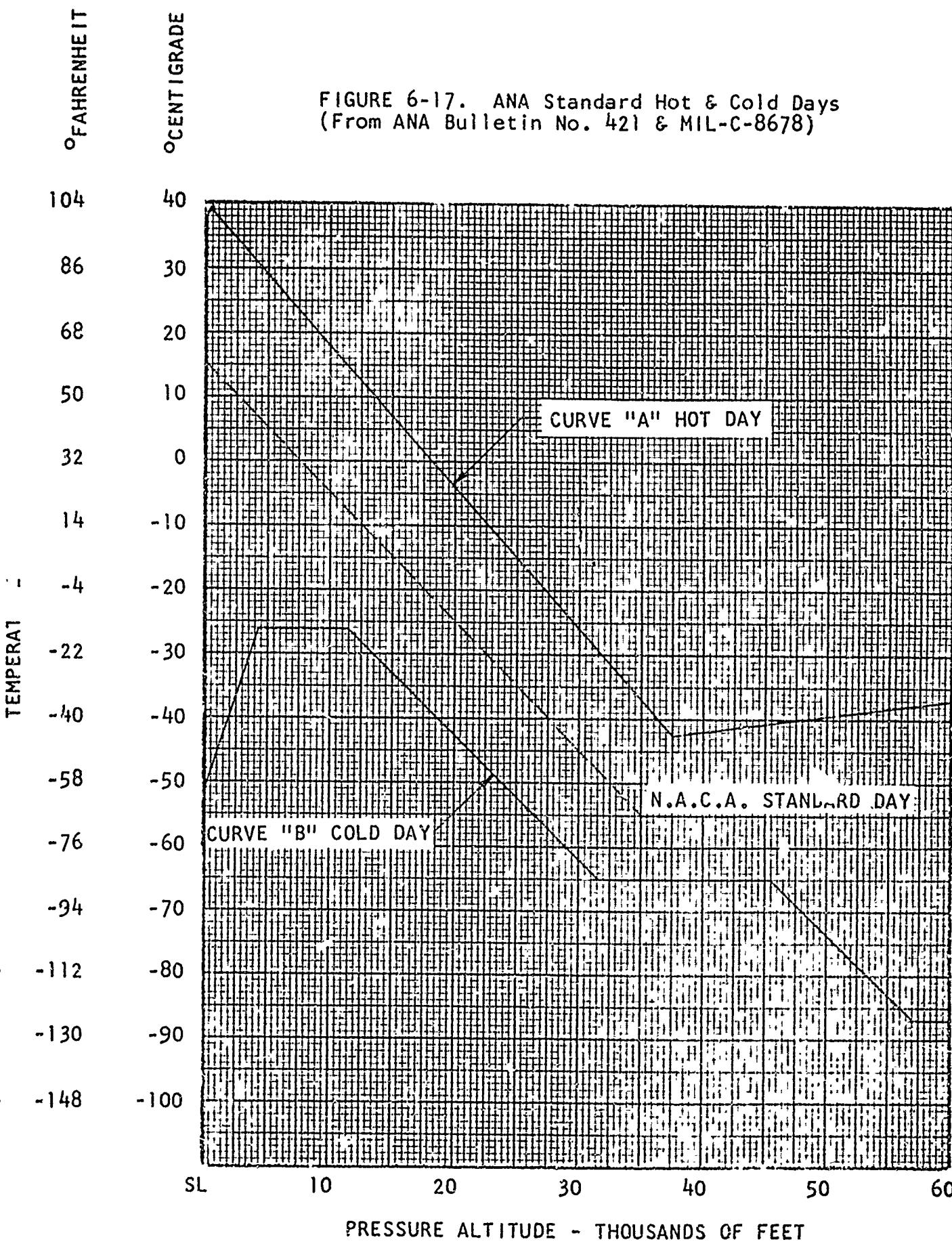
When ejectors are used to cool reciprocating and turbine engines, a complete engine cooling test must be performed in compliance with SD-24 and H.I.A.D. References 6-42 and 6-30 which include the following specifications:

- a. For reciprocating engines -

MIL-C-8678 (Aer) Reference 6-61
MIL-D-17984 (ASG) Reference 6-66
AN-T-62 Reference 6-62 (Cancelled)

- b. For turbine engines -

MIL-C-8678 (Aer) Reference 6-61
MIL-C-7220 (USAF) Reference 6-56
NCNEI-525-460 (USAF) Reference 6-46



To summarize the items to be investigated during an actual cooling performance test of an ejector installation, instrumentation must be provided to measure:

1. Secondary flow quantity and pressure drop and the temperature of the components being cooled.
2. Primary flow state and the effect of the ejector on the source of the primary flow.
 - a. Reciprocating engine exhaust-engine power output (by torque-meter) and flow state (temperature and pressure instrumentation in the exhaust flow).
 - b. Turbine engine exhaust-engine power output (by torque-meter), and flow state.
 - c. Compressor bleed - engine power output (torque-meter), flow quantity, and state.

6-3.5 Results

During ground tests, wind velocity, ambient temperature, relative humidity and barometric pressure measurements are required. The wind velocity should be measured and recorded at 10 minute intervals and the barometer may be read twice daily.

The data obtained should be corrected for instrument error and reduced to standard summer day conditions (See Figure 6-17). When reducing data, usually one or more of the test variables (i.e., pressure altitude, density altitude or true airspeed) is reduced to standard and the reduction process then revolves around these standards. Information on data correction and reduction, in addition to that furnished in Section 6-2.1.3, can be obtained from the following sources:

- a. ASME Test Codes - General Considerations, Reference 6-16.
- b. ASME Test Codes - Pressure Measurements, References 6-17 and 6-20.
- c. ASME Test Codes - Temperature Measurements, References 6-22 and 6-23.
- d. Flight Testing, Reference 6-2.
- e. USAF Flight Test Manual, Reference 6-28.

Additional information on flight test equipment is available in Reference 6-29 and additional information on test conditions is available in the applicable Specifications, e.g., References 6-45 through 6-50, 6-55, 6-56, 6-61, and 6-66.

6-4.0 REFERENCES

The following references have been among those utilized in the preparation of Chapter VI:

(Books)

- 6-1 Fan Engineering
By R. D. Madison

Organization: Buffalo Forge Co.
Buffalo, N. Y.

- 6-2 Flight Testing
By Benson Hamlin

Organization: The MacMillan Company
New York, N. Y.

- 6-3 Flow and Fan
By C. Harold Berry

Organization: The Industrial Press
148 Lafayette St.
New York 13, N. Y.

- 6-4 The Strain Gage Primer
By C. C. Perry
H. R. Lissner

Organization: McGraw Hill Book Co., Inc.
New York

- 6-5 Heating, Ventilating, Air Conditioning Guide 1956
By American Society of Heating & Air-Conditioning Engineers,
Inc.,
New York 13, N. Y.

- 6-6 Introduction to the Study of Aircraft Vibration and Flutter
By Robert H. Scanlon - Robert Rosenbaum

Organization: The MacMillan Company
New York, N. Y.

- 6-7 Mechanical Engineer's Handbook
By Lionel S. Marks & Gordon McKay

Organization: McGraw Hill Book Company, Inc.
New York, N. Y.

- 6-8 Mechanical Vibrations (1947)
By J. P. Den Hartog

Organization: McGraw Hill Book Company, Inc.
New York, N. Y.

- 6-9 Tool Engineer's Handbook
Organization: American Society of Tool Engineers
- 6-10 Theory of Sound (1945)
By J. W. Strutt & Barm Rayleigh
Organization: Dover Publications
New York, N. Y.
- 6-11 Thermodynamic Properties of Steam (1936)
By Keevan & Keyes
Organization: John Wiley & Sons, Inc.
New York
- 6-12 Wind Tunnel Technique
By R. C. Pankhurst & D. W. Holder
Organization: Sir Isaac Pitman & Sons, Ltd.
London
- 6-13 Wind Tunnel Testing, First Edition 1950, Second Edition 1954
By Alan Pope
Organization: John Wiley & Sons, Inc.
New York

(Test Codes)

- 6-14 ASME Power Test Code PTC 10-1949
"Centrifugal Mixed Flow and Axial Flow Compressors & Exhausters"
By ASME Power Test Codes Committee
Organization: The American Society of Mechanical Engineers
29 West 39th St.
New York 18, N. Y.
- 6-15 ASME Power Test Code PTC 11-1946
"Test Code for Fans"
By ASME Power Test Codes Committee
Organization: The American Society of Mechanical Engineers
29 West 39th St.
New York 18, N. Y.
- 6-16 ASME Power Test Codes
"Instruments and Apparatus" - Part I - General Considerations
By ASME Power Test Codes Committee
Organization: The American Society of Mechanical Engineers
29 West 39th St.
New York 18, N. Y.

- 6-17 ASME Power Test Codes PTC 19.2.1.6 - 1941
"Information on Instruments and Apparatus", Part 2 - Pressure Measurement, Chapter 1 - Barometers, Chapter 6 Tables, Multiplier and Standards for Barometer, Mercury & Water Columns, and Pressure Measurement.
By ASME Power Test Codes Committee
- Organization: The American Society of Mechanical Engineers
29 West 39th St.
New York 18, N. Y.
- 6-18 ASME Power Test Codes PTC 19.2.2.3 - 1949
"Supplement on Instruments and Apparatus", Part 2 - Pressure Measurement, Chapter 2 - Static & Total Pressure, Static Holes and Tubes & Support Tubes, Chapter 3 - Pipes for Pressure Measurement.
By ASME Power Test Codes Committee
- Organization: The American Society of Mechanical Engineers
29 West 39th St.
New York 18, N. Y.
- 6-19 ASME Power Test Codes
"Instruments and Apparatus", Part 2 - Pressure Measurement, Chapter 4 - Bowdon, Bellows, Diaphragm and Deadweight Gages.
By ASME Power Test Codes Committee
- Organization: The American Society of Mechanical Engineers
29 West 39th St.
New York 18, N. Y.
- 6-20 ASME Power Test Codes
"Supplement on Instruments and Apparatus", Part 2 - Pressure Measurement, Chapter 5 - Liquid Column Gages
By ASME Power Test Codes Committee
- Organization: The American Society of Mechanical Engineers
29 West 39th St.
New York 18, N. Y.
- 6-21 ASME Power Test Code PTC 19.3.2 - 1936
"Supplement to Power Test Codes" - Part 3 Instruments & Apparatus Temperature Measurement, Chapter 2 - Radiation Pyrometers
By ASME Power Test Codes Committee
- Organization: The American Society of Mechanical Engineers
29 West 39th St.
New York 18, N. Y.
- 6-22 ASME Power Test Codes PTC 19.3.3 - 1940
"Information in Instruments & Apparatus" - Part 3 Temperature Measurement, Chapter 3 - Thermocouple Thermometers or Pyrometers
By ASME Power Test Codes Committee
- Organization: The American Society of Mechanical Engineers
29 West 39th St.
New York 18, N. Y.

6-23 ASME Power Test Code PTC 19.3.4 - 1945
"Supplement on Instruments and Apparatus", Part 3 - Temperature Measurement, includes Chapter 4 - Resistance Thermometers
By ASME Power Test Codes Committee

Organization: The American Society of Mechanical Engineers
29 West 39th St.
New York 18, N. Y.

6-24 ASME Power Test Code PTC 19.13 - 1939
"Information on Instruments and Apparatus", Part 13 - Speed Measurements
By ASME Power Test Codes Committee

Organization: The American Society of Mechanical Engineers
29 West 39th St.
New York 18, N. Y.

6-25 NAFM Test Code
"Standard Code for the Testing of Centrifugal and Axial Fans"
By The National Association of Fan Manufacturers, Inc.
Detroit, Michigan

(U. S. Navy Publications)

6-26 AD-53052-C-1
"Smoke Flow Studies Conducted at Princeton University",
Contract N6onr27016, Report No. 290
By D. C. Hazen and R. F. Lehnert

6-27 Massachusetts Institute of Technology (1949)
Report on Excitation of Pure Natural Modes of Complex Structure, Phase A.
By Robert C. Lewis & Donald L. Wrisley

Organization: Contract #N1 56a-25797
Naval Air Material Center

(USAF Publications)

References

6-28 AF Technical Report 6273 (1953)
Flight Test Engineering Manual
By Russel M. Herrington & Paul Schoemacher

Organization: USAF Air Research and Development Command
Edwards Air Force Base
Edwards, California

6-29 Flight Test Manual
Advisory Group for Aeronautical Research & Development
By Courtland D. Perkins & Daniel O'Donnard

Organization: U.S. Air Force Contract 18(600)-1323
Administered by the Air Force Office of Scientific Research of the Air Research and Development Command

- 6-30 ARDC Manual (H.i.A.D.)
Handbook of Instructions for Aircraft Designs ARDCM 80-1
Headquarters
Air Research and Development Command
- 6-31 ATI 50706 (British Report 10,296 F.M. 1058 dated 22 Jan. 1947)
Central Air Documents Office, Navy Air Force
Wright Patterson Air Force Base
- 6-32 Policies and Procedures Governing Approval of Air Force Equipment (1952)
Organization: Headquarters Air Research and Development
Command
Baltimore, Maryland

(NACA Publications)

- 6-33 NACA Report #218
Standard Atmosphere Tables and Data
- 6-34 NACA Report #729 (1942)
Test of a Single-Stage Axial-Flow Fan
By E. Barton Bell
Organization: National Advisory Committee for Aeronautics
Washington, D. C.
- 6-35 NACA Report #842 (1946)
Sonic Effects of Compressibility on the Flow Through Fans and
Turbines
By W. Pell and H. T. Epstein
Organization: National Advisory Committee for Aeronautics
Washington, D. C.

(Miscellaneous Publications)

- 6-36 Preliminary Copy of Final Technical Report TECRDCMP 400.1
(8.50-02-001) DA 44-009 eng. 1355
"Research on Air Flow Engine Cooling Fan Drives, Contract DA
44.009 eng. 1355, Project 8-50-02-001.
By J. H. Gary, Research Associate, Engineering Experiment
Station, University of Virginia
Organization: Engineering Research & Development Laboratories
United States Army
Fort Belvoir, Virginia
- 6-37 SAE Aeronautical Information Report #2
"Airplane Heating and Ventilating Equipment Engineering Data"
By Committee A-9, Aircraft Air Conditioning Equipment
Organization: Society of Automotive Engineers, Inc.
29 West 39th St.
New York, N. Y.

- 6-38 SAE Aeronautical Information Report #23
"Airplane Heating and Ventilating Equipment Engineering Data Fluid Dynamics"
By Committee A-9, Aircraft Air Conditioning Equipment
- Organization: Society of Automotive Engineers, Inc.
29 West 39th St.
New York, N. Y.
- 6-39 SAE Aeronautical Information Report #25
"Airplane Air Conditioning Engineering Data - Part 4 Thermodynamics"
By Committee A-9, Aircraft Air Conditioning Equipment
- Organization: Society of Automotive Engineers, Inc.
29 West 39th St.
New York, N. Y.
- 6-40 OSRD #1543 (1944);
Principles of Sound Control in Airplanes
By L. L. Beranels, R. H. Nichols, H. W. Rudnose, H.P. Sleeper, R.L. Wallace and H. L. Ericson, Research on Sound Control by Cruft Laboratory, Howard University
- Organization: Office of Scientific Research & Development
National Defense Research Committee
- 6-41 R&M. 2023 (1943) (English Report)
"An Improved Smoke Generation for Use in the Visualization of Airflow Particularly Boundary-Layer Flow at High Reynolds Number"
By J. H. Preston and N. E. Sweeting

(Specifications)

- 6-42 SD-24
General Specification for the Design and Construction of Airplanes for the United States Navy
- 6-43 ANA Bulletin 143
Air Force - Navy Aeronautical Bulletin Specifications and Standards, Use of
- 6-44 ANA 421
Air Force-Navy Aeronautical Bulletin Atmospheric Properties - Extreme Cold and Hot; Standard for Aeronautical Design
- 6-45 AN-T-62 (Cancelled)
Air Force- Navy Aeronautical Specification Test Procedure for Aircraft Power Plant Installation
- 6-46 WCNE1-525-460 (USAF)
USAF Memorandum Report
Test Procedure for Turbo Prop and Turbo Jet Aircraft Power Plant Installation

- 6-47 MIL-I-5072
Military Specification
Instrument Systems Pitot-Static Tube Operated, Installation of
- 6-48 MIL-T-5522B
Military Specification
Test Procedure for Aircraft Hydraulic and Pneumatic System, General
- 6-49 MIL-G-6099 (Formerly 17G15)
Military Specification
Generator and Regulation; Aircraft Alternating Current, General Specifications for

References

- 6-50 MIL-G-6162
Military Specification
Generator, 30 Volt, Direct Current, Aircraft Engine Driven
General Specification for
- 6-51 MIL-G-6641A (ASG)
Military Specifications
Gearbox, Aircraft Accessory Drive, General Specification for
- 6-52 MIL-R-6754
Military Specification
Rotor, Main, Rotary Wing Aircraft, Type Test of
- 6-53 MIL-R-6755
Military Specification
Rotor, Auxiliary, Rotary Wing Aircraft, Type Test of
- 6-54 MIL-T-68166
Military Specification
Test Procedure for Aircraft Carbon Monoxide Detection and Control
- 6-55 MIL-E-7080A
Military Specification
Electric Equipment Piloted Aircraft Installation and Selection
of, General Specification of
- 6-56 MIL-C-7220 (USAF)
Military Specification
Cooling Installation, Aircraft Gas Turbine Engine
- 6-57 MIL-E-7470 (USAF)
Military Specification
Shaft, Power Transmission, Aircraft Accessory, General Specification for
- 6-58 MIL-G-7940
Military Specification
Gages, Fuel Quantity, Capacitor Type, Installation and Calibration of

- 6-59 MIL-H-8501 (Formerly Part of SR 189)
Military Specification
Helicopter Flying Qualities, Requirements for
- 6-60 MIL-A-8629 (Aer)
Military Specification
Airplane Strength and Rigidity
- 6-61 MIL-C-8678 (Aer) (Formerly E-5Sd)
Military Specification
Cooling Requirements of Power Plant Installation
- 6-62 MIL-C-8679
Military Specification
Test Requirements, Ground Helicopter
- 6-63 MIL-S-8698 (ASG) (Formerly Part of SR 189)
Military Specification
Structural Design Requirements, Helicopter
- 6-64 MIL-F-8785 (ASG) (Formerly SR119B)
Military Specification
Flying Qualities of Piloted Aircraft
- 6-65 MIL-F-17874 (Aer) (Formerly SR73D)
Military Specification
Fuel Systems; Aircraft, Installation and Test of
- 6-66 MIL-D-17984A (ASG) (Formerly MIL-R-17984 Aer)
Military Specification
Data Presentation Requirements, Installed Engine Performance and Air Induction Systems
- 6-67 MIL-A-18150 (Aer) (Formerly SR-181)
Military Specification
Acoustical Noise Level in Naval Aircraft, General Specification for
- 6-68 MIL-F-18372 (Aer)
Military Specification
Flight Control System, Design Installation and Test of; Aircraft (General Specification for)

6-5 List of Symbols

No list of symbols is presented in this chapter because each symbol is defined where it appears in the subject matter.

APPENDIX I

ILLUSTRATIVE PROBLEM
HELICOPTER SUBMERGED COOLING INSTALLATION
RECIPROCATING ENGINE WITH COOLING FAN

A
A

COOLING REQUIREMENTS
DESIGN OF AXIAL-FLOW FAN
FAN PERFORMANCE TEST

A

A

A
A

APPENDIX I

ILLUSTRATIVE PROBLEM

Table of Contents

	Page
A-1.0 Introduction	A-1-6
A-2.0 Cooling Requirements	8
A-2.1 Engine Cylinder Cooling Air Requirements	8
A-2.2 Engine Oil Cooling Requirements	13
A-2.3 Transmission Oil Cooling Requirements	15
A-2.4 Accessories Cooling Requirements	19
A-2.5 Summation of the Cooling Requirements	19
A-3.0 Fan Design	20
A-3.1 Statement of Defining Parameters	20
A-3.2.0 Design of Blade Sections	21
A-3.2.1 Rotor Blade Root Airfoil Section Design	21
A-3.2.2 Stator Blade Root Constant Thickness Section Design	22
A-3.2.3 Rotor Blade Tip Airfoil Section Design	23
A-3.2.4 Stator Blade Tip Constant Thickness Section Design	24
A-3.2.5 Summary of Cooling Fan Design Parameters	25
A-3.3 Actual Fan Pressure Rise	26
A-3.4 Calculations for Fan Efficiency and Power Required	27
A-3.5 Calculation of Ordinates for a Typical Airfoil Section	29
A-4.0 Fan Performance Test	34
A-4.1 Discussion	34
A-4.2 Test Procedure	34
A-4.3 Data Analysis	36
A-4.4 Results and Conclusions	37
A-5.0 References	66
A-6.0 List of Symbols	67

APPENDIX I

ILLUSTRATIVE PROBLEM

List of Figures

Figure No.	Description	Page
A-1	Engine Baffle Pressure Drop Determination	A-1-7
A-2	Engine Baffle Cooling Airflow Determination	9
A-3	Engine Oil Heat Rejection Determination	12
A-4	Engine Oil Cooler Performance Characteristics	14
A-5	Forward Transmission Oil Cooler Performance Characteristics	16
A-6	Aft Transmission Oil Cooler Performance Characteristics	17
A-7	Velocity Vector Diagram, Rotor Blade Root	21
A-8	Velocity Vector Diagram, Stator Blade Root	22
A-9	Velocity Vector Diagram, Rotor Blade Tip	23
A-10	Velocity Vector Diagram, Stator Blade Tip	24
A-11	Pictorial Definition of Fan Blade Design Parameters	25
A-12	Diagram of Fan Pressure Drop versus Airflow	36
A-13	Diagram of Fan Configurations Tested	39
A-14	Diagram of Fan Test General Arrangement	40
A-15	Determination of Fan Inlet Loss Coefficient	41
A-16	Determination of Test Fan Expansion Loss	42
A-17	Phase 1 Configuration Performance Chart, Pressure Rise versus Airflow	50
A-18	Phase 1 Configuration Performance Chart, Power Required versus Airflow	51
A-19	Phase 1 Configuration Performance Chart, Fan Efficiency versus Airflow	52
A-20	Phase 1 Configuration Performance Chart, Fan Efficiency versus Flow Parameter, \emptyset	53
A-21	Phase 1 Configuration Performance Chart, Pressure Parameter, γ , versus Flow Parameter, \emptyset	54
A-22	Phase 2 Configuration Performance Chart, Pressure Rise versus Airflow	55
A-23	Phase 2 Configuration Performance Chart, Power Required versus Airflow	56
A-24	Phase 2 Configuration Performance Chart, Fan Efficiency versus Airflow	57
A-25	Phase 2 Configuration Performance Chart, Fan Efficiency versus Flow Parameter, \emptyset	58
A-26	Phase 2 Configuration Performance Chart, Pressure Parameter, γ , versus Flow Parameter, \emptyset	59
A-27	Phase 3 Configuration Performance Chart, Pressure Rise versus Airflow	60
A-28	Phase 3 Configuration Performance Chart, Power Required versus Airflow	61

Figure No.	Description	Page
A-29	Phase 3 Configuration Performance Chart, Fan Efficiency versus Airflow	62
A-30	Phase 3 Configuration Performance Chart, Fan Efficiency versus Flow Parameter, \emptyset	63
A-31	Phase 3 Configuration Performance Chart, Pressure Parameter, Ψ , versus Flow Parameter	64

APPENDIX I

ILLUSTRATIVE PROBLEM

List of Tables

Table No.	Description	Page
A-1	Engine Cooling Air Requirements	A-1-11
A-2	Engine Oil Cooling Requirements	11
A-3	Transmission Oil Cooling Requirements	18
A-4	Cooling Fan Design Parameters	26
A-5	Ordinates for NACA 65-010 Basic Thickness Forms	30
A-6	Ordinates for the NACA $a = 1.0$ Mean Line	31
A-7	Tabulation of Blade Surface Ordinates in Percent of Chord Length	32
A-8	Tabulation of Blade Surface Ordinates in Inches	33
A-9	Tabulation of Fan Configurations Tested	37
A-10	Determination of Fan Inlet Loss	43
A-11	Phase 1 Configuration Data Analysis Sheet	44
A-12	Phase 1 Configuration Data Analysis Sheet	45
A-13	Phase 2 Configuration Data Analysis Sheet	46
A-14	Phase 2 Configuration Data Analysis Sheet	47
A-15	Phase 3 Configuration Data Analysis Sheet	48
A-16	Phase 3 Configuration Data Analysis Sheet	49
A-17	Measured Blade Angles for Fan Tests, Phase 3	65

APPENDIX I

ILLUSTRATIVE PROBLEM

A-1.0 INTRODUCTION

An illustrative problem is presented in this Appendix, consisting of the treatment of the following phases of design and testing of a cooling system for a helicopter submerged reciprocating engine, engine accessories and transmissions:

- a. Determination of cooling requirements.
- b. Design of an axial-flow cooling fan.
- c. Airflow test of the axial-flow cooling fan.

This illustrative problem is composed of selected portions of the actual analytical design and testing work that was done for a cooling system for a submerged engine installation and submerged transmissions in a United States Navy helicopter. It may be noted that the system provided ample cooling of the engine, engine oil, engine accessories and transmissions in engine cooling tests performed in accordance with reference A-1.

It is to be assumed that the following information, which defines the limits of some cooling system parameters, is known:

- a. An engine has been chosen to provide the required power.
- b. The envelope of flight operating regimes has been defined to accomplish the required missions.
- c. An axial-flow fan shall move the cooling air.
- d. Approximate space limitations have been established.

The cooling requirements of flow and pressure must be determined for the following items:

- a. Engine
- b. Engine Oil
- c. Transmission Oil
- d. Engine Accessories

The following flight conditions have been chosen for this illustrative problem to require investigation to determine the critical cooling condition:

HELICOPTER INSTALLATION
ESTIMATED COOLING REQUIREMENTS
CONSTANT ENGINE RPM
NORMAL MIXTURES
 (1). BPD IS THE MINIMUM AT ANY
 POINT AROUND THE ENGINE.

EXAMPLE: 480 BHP, 2200 RPM
 NORMAL MIXTURE E
 15,000 FT. ALT.
 35° F. OAT
 BPD = 3.20"

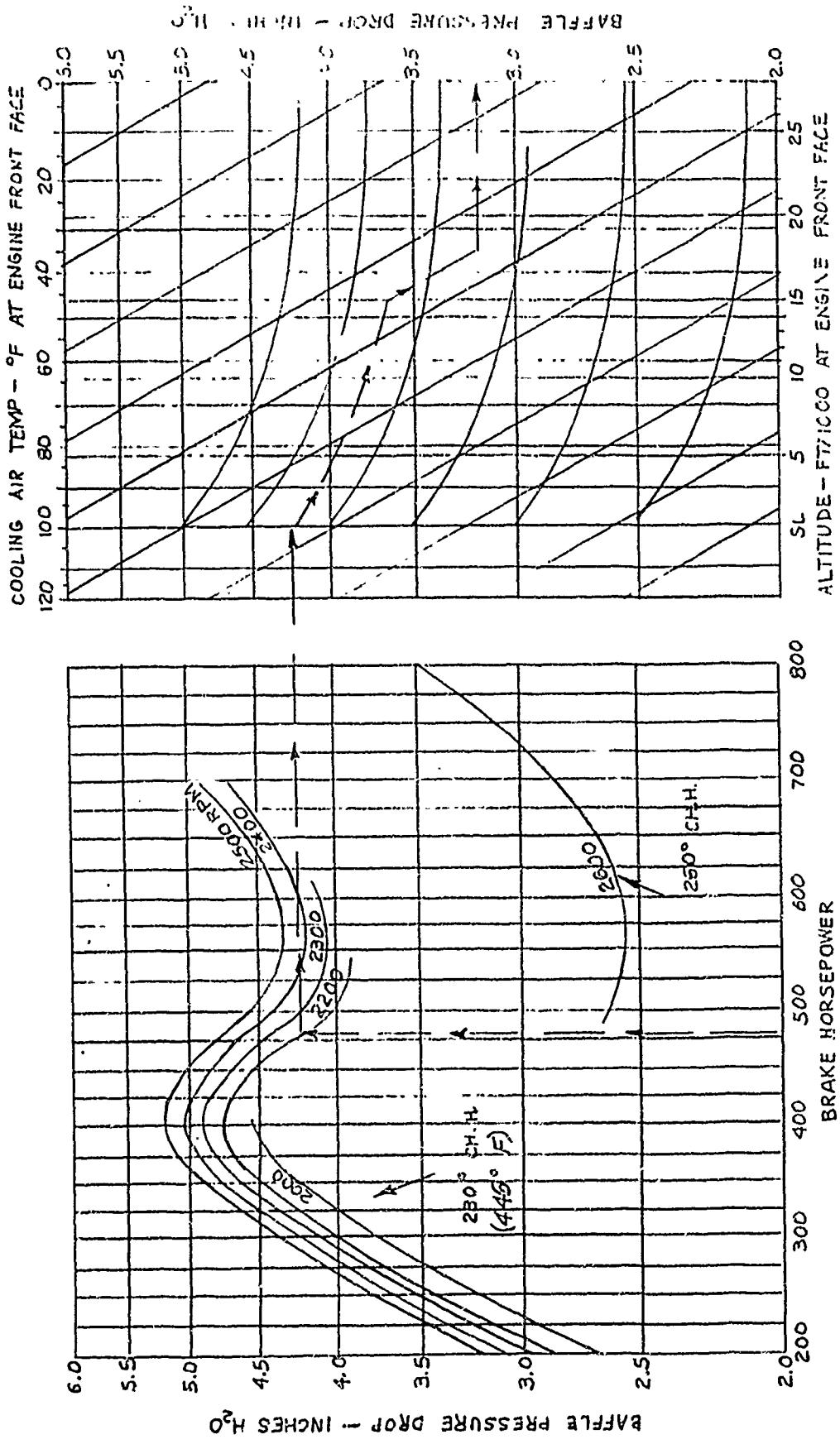


FIGURE A-1

A - 1 - 7

1. Hover at sea level, normal rated RPM, ANA hot day.
2. Hover at 5000 feet, normal rated RPM, ANA hot day.
3. Cruise at 5000 feet, cruise RPM, ANA hot day.
4. Cruise at 7500 feet, cruise RPM, ANA hot day.
5. Cruise at 10,000 feet, cruise RPM, ANA hot day.

A-2.0 COOLING REQUIREMENTS

A-2.1.0 Engine Cylinder Cooling Air Requirements

Using the first condition (hover at sea level, NRS, OAT = 103°F), the procedure for determining the cooling air requirements is as follows:

a. Determine the Inlet Air Temperature Rise

This can be done by estimating the heat transfer due to the surroundings and the expected fan compression. A value of 10°F temperature rise is typical for a helicopter cooling system and will be used here. The cooling air temperature then is $103 + 10 = 113^{\circ}\text{F}$.

b. Determine the BHP Required

This is specified by the aircraft manufacturer's estimated performance calculations for the given flight regime. For condition 1, BHP = 700.

c. Determine the Engine RPM

This too is governed by the specific flight regime, and for condition 1, RPM = 2400.

d. Determine the Mixture

Although a rich mixture will provide better cooling, a normal mixture is ordinarily specified for nearly all operating regimes by the engine manufacturer for lower brake specific fuel consumption.

e. Determine the Maximum Allowable Head Temperature - °F.

This is specified by the engine manufacturer and for the engine used in this illustrative problem is 450°F.

f. Determine Baffle Pressure Drop - ΔP

Using the foregoing parameters and the applicable manufacturer's engine cooling requirements chart, Figure A-1, proceed as follows:

- i. Enter the chart vertically at 700 HP and proceed to the 2400 RPM curve.

COOLING AIRFLOW (ESTIMATED)

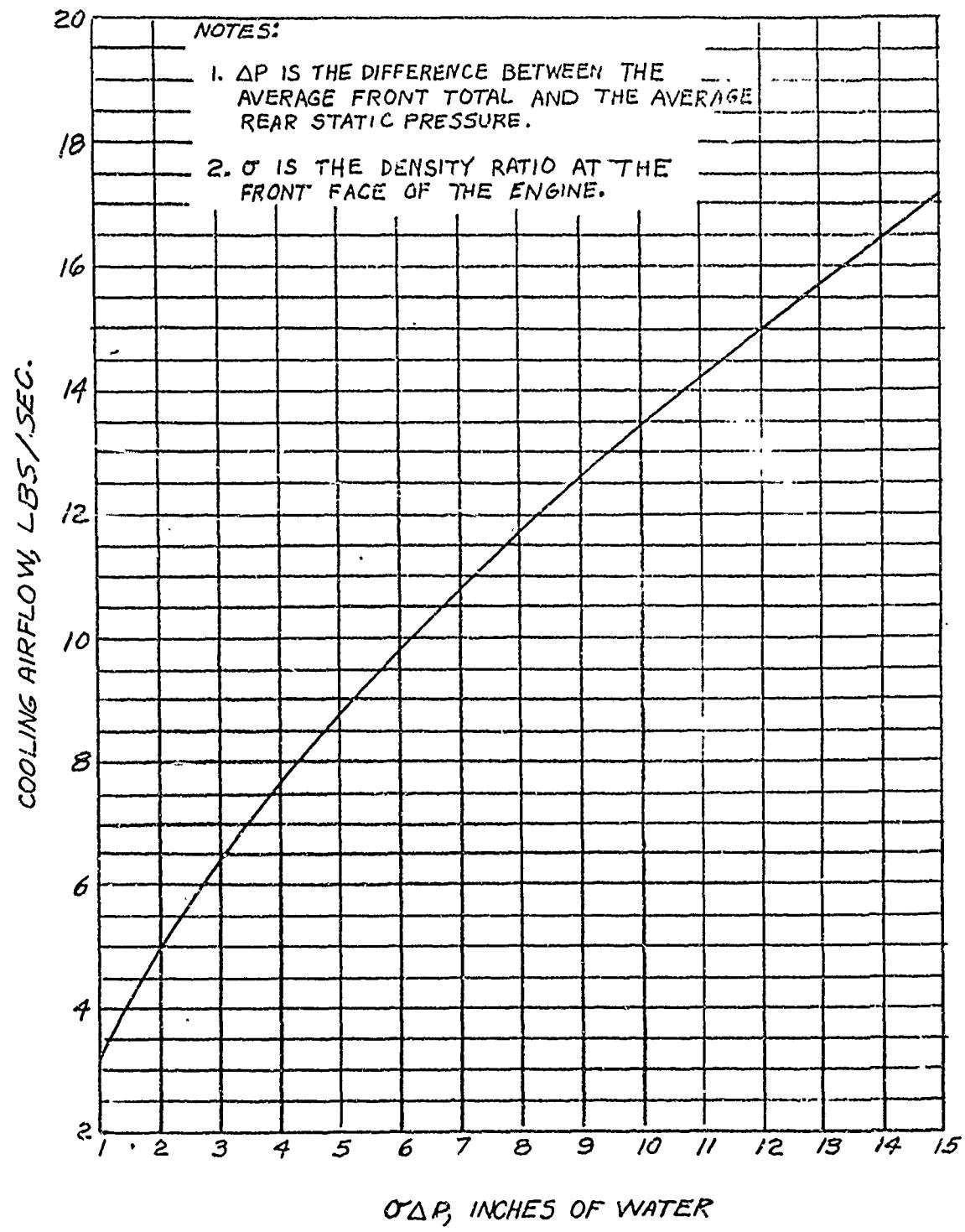


FIGURE A-2

A - 1 - 9

2. Go to the right to sea level and then follow the curvature of the chart until the required altitude is reached, which in this case is sea level.
3. Follow the slant of the chart to the cooling air temperature ($113^{\circ}\text{F}.$), and read the baffle pressure drop of $5.4'' \text{ H}_2\text{O}$.
- g. Determining the density ratio, σ , which is the ratio of the air density at the flight regime to that at sea level standard day. (At sea level standard day, $\sigma = 1.0$) Since the density is inversely proportional to the absolute temperature, and directly proportional to the absolute pressure,

$$\sigma = \frac{T_{sl}}{T} \times \frac{P}{P_{sl}}$$

$$\sigma_{\text{condition 1}} = 1 \times \frac{519}{103 \times 460} = 0.92$$

h. Determine $\sigma \Delta P$

Using f and g,

$$\sigma \Delta P = 5.0'' \text{ H}_2\text{O}$$

i. Determine Airflow - W, #/Sec.

Using the engine manufacturer's cooling airflow chart, Figure A-2,

$$W = 8.7 \text{ #/sec.}$$

j. Determine Airflow - Q - cfs

$$Q = \frac{W}{\sigma w} \quad \text{Where } w = \text{specific weight at sea level standard day conditions}$$

$$= \frac{8.7}{0.92(0.0765)}$$

$$= 124 \text{ cfs}$$

The engine air cooling requirements for the 5 conditions are presented on Table A-1.

TABLE A-1
ENGINE COOLING AIR REQUIREMENTS

ITEM	CONDITION	Altitude Based on C_L Limit			CONDITION	CONDITION			1	2	3	4	5
		1	2	3		4	5						
Engine Rating	NRP	NRP	Cruise	Cruise	Cruise	Cruise	Cruise	Heat Rejection Req'd, H_0	2300	2300	1970	2080	2210
Flight Condition	Hover	Hover	Cruise	Cruise	Cruise	Cruise	Cruise	Oil Flow, W_O lb/min	80	80	80	80	80
Type of Day	S.L.	5000'	5000'	7500'	10,000'			P (estimated) " H_0	.92	.79	.73	.68	
Pressure Altitude	103	85	85	76	67			H BTU/HIN/1250 ITD	4.0	3.4	3.4	3.2	2.9
OAT - OF	.92	.79	.79	.73	.676			t Air into Cooler F	2280	2200	2200	2150	2100
c								t Oil into Engine F	113	95	95	86	77
Inlet Air Temp. Rise					10°F			T _{0:L} thru engine	185	185	185	185	185
BHP	700	700	400	400	400			t QIL Out of Engine F	58	58	49	52	55
rpm	2400	2400	2200	2300	2400			ITD = (10) - (7)	243	243	234	237	240
Mixture				Normal				H [*] REL = $\frac{ITD}{125}$	2370	2590	2450	2690	2740
Max. Alt w. Head Temp. - Of				450				WAIR, lb/min **	250	225	225	214	205
Cooling Air Temp. OF	113	95	95	86	77			Q = WAIR/.0765	3560	3730	3730	3820	3970
*Surface Pressure Drop - P	5.4	5.0	5.1	5.2	5.3								
P @ S.L.	5.9	6.3	6.5	7.1	7.8								
P	5.0	4.0	4.0	3.8	3.6								
**Airflow - W - lb sec.	8.7	7.6	7.7	7.45	7.1								
Airflow - Q - CFS	124	125	127	132	137								

* Must be equal to or greater than H_0 for adequate cooling.

**Oil cooler manufacturer's chart, Figure A-4.

* Ref.: Figure A-1
**Ref.: Figure A-2

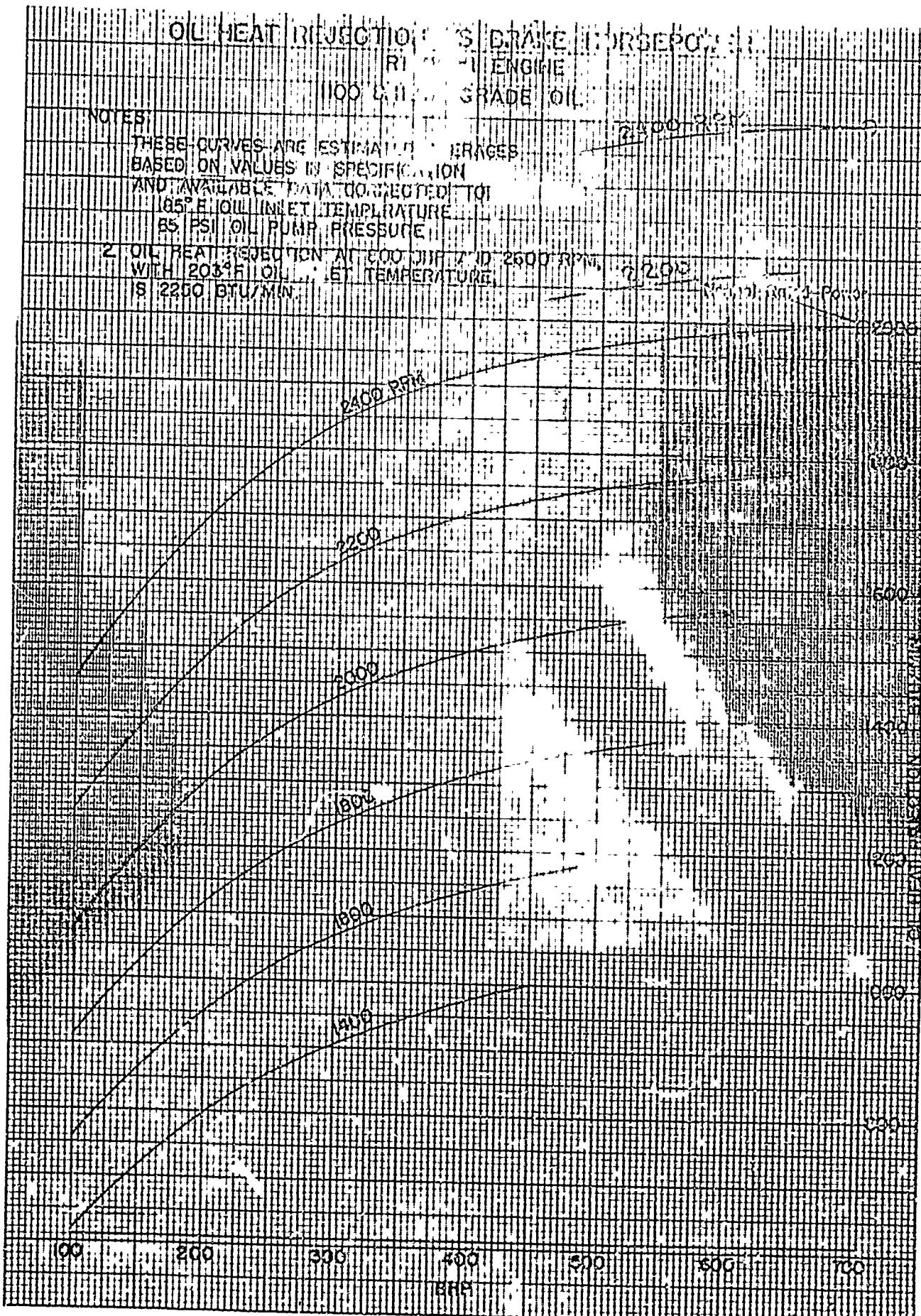


Figure A-3

A-2.2 Engine Oil Cooling Requirements

a. Determine the Heat Rejection Required H_o

Using the engine manufacturer's estimated oil heat rejection versus brake horsepower chart, Figure A-3, at the BHP & RPM as determined from condition 1, read the required heat rejection, $H_o = 2000 \text{ Btu/min}$. However, the engine manufacturer's test results for this particular engine showed the H_o to be 2300 Btu/min. Therefore the curves were shifted, keeping the same slopes, as shown by the dashed lines on the chart, Figure A-3, and readings were taken from these.

b. Determine the Oil Flow, W_o

Ordinarily, the engine manufacturer's oil flow versus crankshaft RPM chart is used to determine the oil flow rate. However, the oil pump for this particular engine was equipped with a pressure relief valve which restricted the flow rate to 80#/minute at all engine RPM's above 1480.

c. Determine the Engine Oil Cooler Air Total Pressure Drop, $\sigma' \Delta P$

Since the required engine baffle pressure drop is 5.4" water, this value is taken as the available pressure at the oil cooler air duct entrance. The assumption is made that no net flow pressure losses occur downstream of the cooler. Cooler duct losses, including entry losses, must be computed and subtracted from the 5.4" H₂O in order to determine the available air total pressure at the engine oil cooler upstream face. Multiplying the available cooler pressure by the density ratio,

$$\sigma' \Delta P = (5.4 - 1.0 \text{ cooler duct loss}) (.92) \approx 4.0" \text{ H}_2\text{O}$$

for condition (1)

Duct loss estimates should be made to provide a conservative available pressure drop across the cooler. However, it should be remembered that cooler weight increases with decreasing oil cooler air pressure drop.

d. Determine Heat Transfer, H

Supply the oil cooler manufacturer with the above data. Using the oil cooler manufacturer's chart, Figure A-4, enter the chart with the available $\sigma' \Delta P$ of 4" H₂O and proceed horizontally to the left to the pressure drop curve. Then proceed vertically upward to the oil flow curve of 80#/minute. Read the heat transfer horizontally to the left as 2280 Btu/Min/125°F ITD (see g below).

e. Determine the Change in Oil Temperature Thru Engine

The oil heat rejection of an engine is a function of the mass of oil flowing thru the engine, the specific heat of the oil, and the difference in temperature of the oil between the inlet and the exit of the engine. This relationship may be expressed as follows:

ALUMINUM OIL COOLER
 AIR CENTER : 1000 LBS.
 OIL CENTER : 7 CONN.
 OIL INLET TEMP: 60°
 AIR INLET P.D.: 10°
 TYPE OIL: SAE 50 GRADE 1100
 CALCULATED CHART

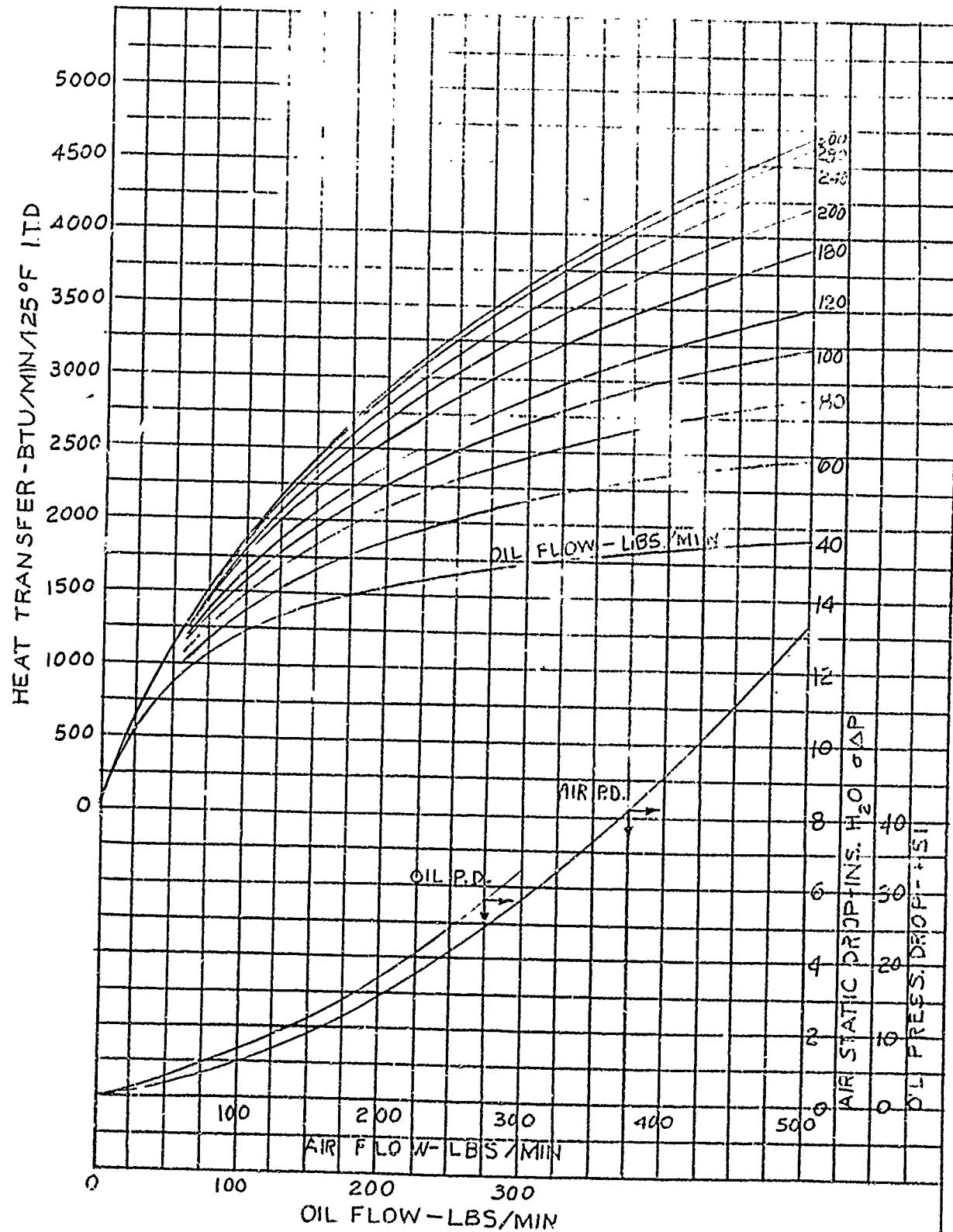


FIGURE A-4

$$H_o = W_o c_p \Delta T_{oil}$$

$$\text{For condition (1)} \quad 2300 = 80(0.5) \Delta T_{oil}$$

$$\Delta T_{oil} = 58^{\circ}\text{F.}$$

f. Determine the Temperature of the Oil out of the Engine

The allowable temperature of the oil into the engine is given by the engine manufacturer as 185°F . $T_{oil \text{ into cooler}} = T_{oil \text{ into engine}} + \Delta T_{oil} = 185 + 58 = 243^{\circ}\text{F}$.

g. Determine the ITD of the Cooler

The ITD is the temperature difference between the air into the cooler and the oil out of the engine, essentially into the cooler. For condition 1 the ITD = $243 - 113 = 130^{\circ}\text{F}$.

h. Determine the Actual Heat Transfer, H_{rel}

$$H_{rel} = H \left(\frac{ITD}{125}\right)$$

$$\text{For condition 1} \quad H_{rel} = 2280 \left(\frac{130}{125}\right) = 2370 \text{ Btu/min.}$$

The actual heat transfer must be equal to or greater than the required heat rejection for adequate cooling.

i. Determine the Airflow, W

Using the oil cooler manufacturer's chart, Figure A-4, enter the chart with the available $\sigma' \Delta P = 4'' \text{ H}_2\text{O}$ and go horizontally to the left to the air pressure drop curve. Read airflow vertically downward as approximately 250#/minute.

j. Determine Airflow, Q

$$Q = \frac{W}{\sigma' w}$$

$$Q = \frac{250}{0.92(0.0765)} = 3560 \text{ cfm}$$

The engine oil cooling requirements for the 5 flight regimes of Section A-1.0 are presented in Table A-2.

A-2.3 Transmission Oil Cooling Requirements

An oil cooler must be provided for each transmission in the helicopter. In this illustrative problem, a forward and aft transmission are to be cooled.

ALUMINUM OIL COOLER
14 PLATES 825 LONG
SURFACE 31SS2

OIL SAE 30
INLET TEMP. OIL 200° F.
AIR 100° F.

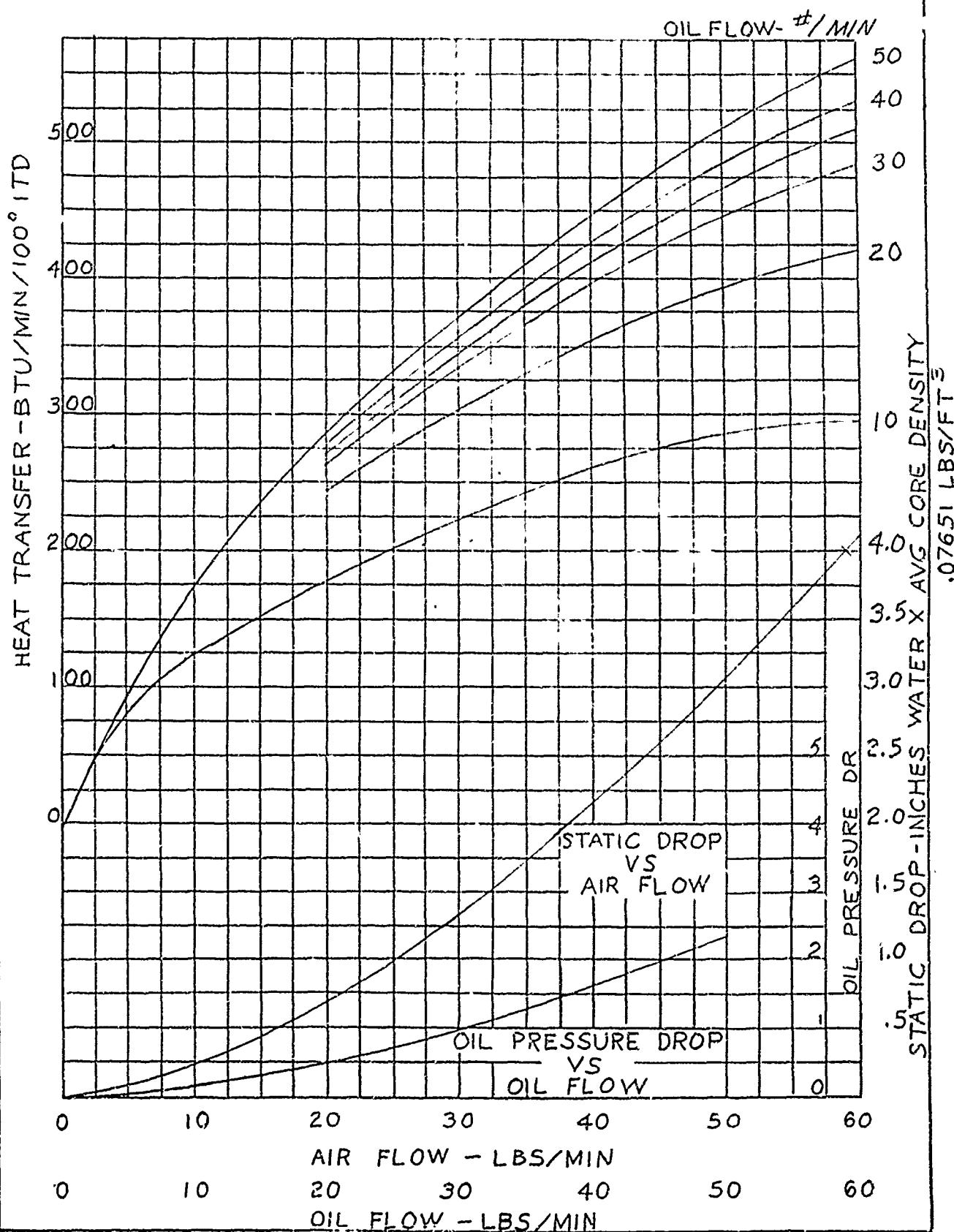


FIGURE A-5

ALUMINUM OIL COOLER
9 PLATES 825 LONG
SURFACE 81552

OIL - SAE 30
INLET TEMP OIL 200° F
AIR 100° F

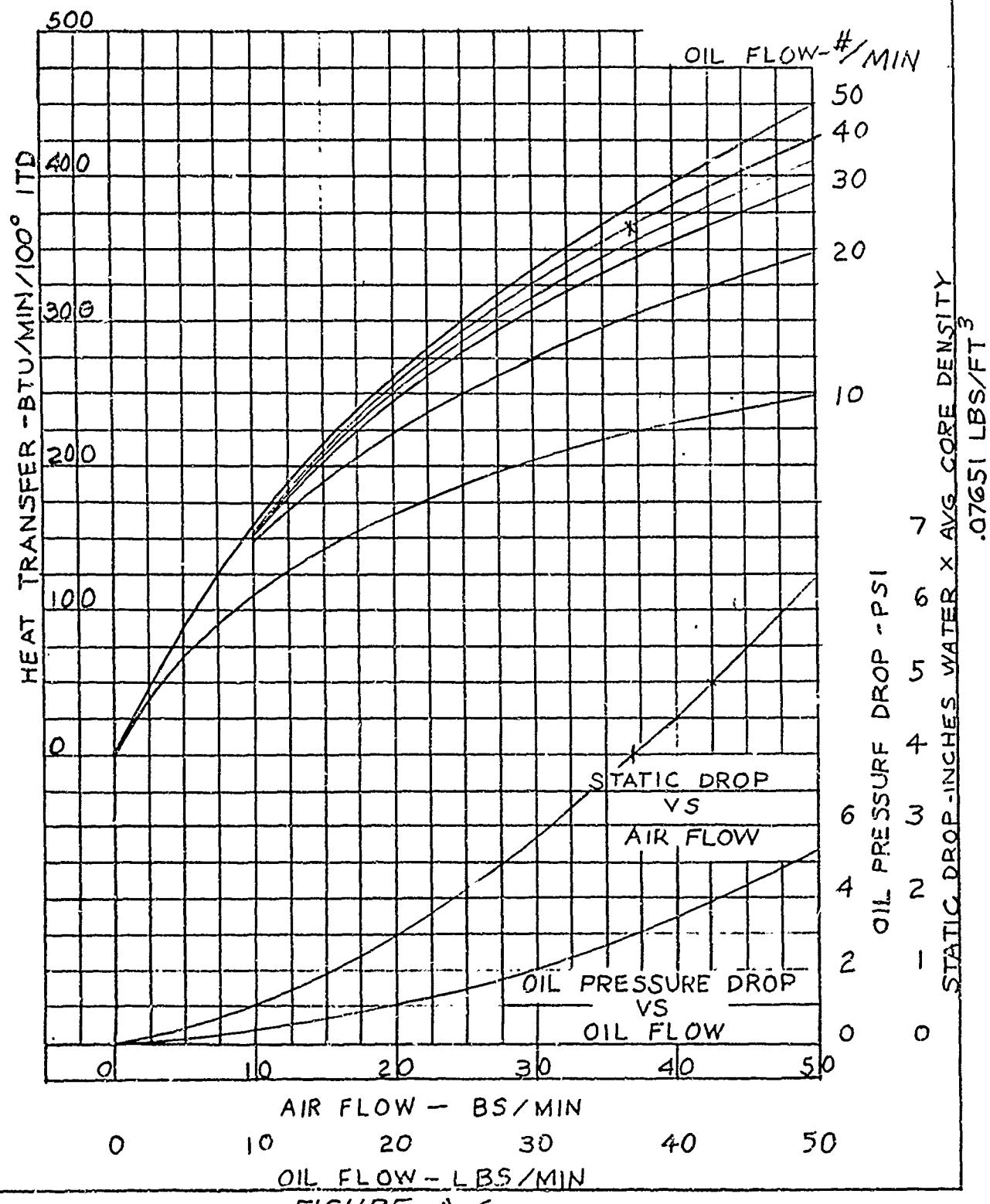


FIGURE A-6

A - I - 17

TABLE A-3

TRANSMISSION OIL COOLING REQUIREMENTS

CONDITION	FORWARD TRANSMISSION COOLER					REAR TRANSMISSION COOLER				
	1	2	3	4	5	1	2	3	4	5
BHP Transmitted (60% of BHPENG)	420	420	240	240	240	420	420	240	240	240
Meshes	2	2	2	2	2	3	3	3	3	3
BHP Loss at 0.65% per Mesh *	5.5	5.5	3.1	3.1	3.1	8.2	6.2	4.7	4.7	4.7
Heat Loss - BTU/MIN	235	235	135	135	135	350	350	200	200	200
Oil Flow - lbs/min	35	35	35	35	35	35	35	35	35	35
Oil into Cooler - °F	185	185	185	185	185	185	185	185	185	185
Air into Cooler - °F	113	95	95	86	77	113	95	95	86	77
o - Air Density Ratio	.92	.79	.79	.73	.68	.92	.79	.79	.73	.68
o P (estimated)	4.0	3.4	3.4	3.2	2.9	4.0	3.4	3.4	3.2	2.9
Air Flow - lbs/min	37	33.5	33.5	32	30.5	59	53	53	51	48
Air Flow - CFM	526	555	555	575	590	840	880	880	910	930

Oil cooler performance based on Performance Charts, Figure A-5 and A-6.

* Transmission Test Evaluation.

a. Determine BHP Transmitted

The BHP transmitted through a rotor transmission of the sample tandem rotor helicopter is based on the maximum horsepower one rotor will absorb under certain flight maneuvers. This is considered to be sixty percent of the engine horsepower. Therefore, the BHP transmitted for condition 1 is $(0.60) \times (700) = 420$, in either the forward or aft rotor transmission.

b. Determine Number of Meshes

The number of gear meshes in a transmission is dependent upon the speed and direction changes of the power to be transmitted. In this sample problem, there are 2 meshes in the forward transmission and 3 in the aft.

c. Determine BHP Loss per Mesh

Based on bench tests on helicopter transmissions at normal rated power, the BHP loss per mesh = 0.65 percent in References A-2 and A-3. Therefore, for condition 1, the BHP loss = 5.5 in the forward transmission and 8.2 in the aft. This calculation is conservative for lower powers.

d. Determine Heat Loss

The heat loss is simply the BHP loss \times 42.4, which is the conversion factor from BHP to Btu/minute. Therefore the heat loss = $(42.4) (5.5) = 235$ Btu/minute for the forward transmission and $(42.4) (8.2) = 350$ Btu/minute for the aft transmission.

e. Determine Oil Flow Rate

The oil flow rate is dependent upon the heat rejection required, the oil temperature into (or out of) the cooler and the cooling air temperature. The transmission design determines the oil flow rate and in this problem established a value of 35 #/minute.

The remainder of the transmission oil cooler requirement calculations is computed in the same manner as for the engine oil cooler and is presented in Table A-3, using Figures A-5 and A-6 for the forward and aft transmission coolers, respectively.

A-2.4 Accessories Cooling Requirements

The cooling requirements of the various accessories must be investigated. For this illustrative problem they are assumed to be negligible. A discussion of this item is included in Chapter II of this Handbook.

A-2.5 Summation of the Cooling Requirements for the Critical Condition (Cruise at 10,000' Hot Day)

In a reciprocating engine installation, the most critical single cooling air item is the engine cylinder cooling air, and this is the criterion for selecting the most critical cooling condition. Therefore, condition 5 is chosen as the most critical, since the available ΔP , referred to sea level for comparison, is the highest. A summation of the pressure rise for condition 5 follows:

Pressure (to be supplied by the fan at $\sigma' = 0.676$)

ΔP Engine	5.3
ΔP System	1.7
ΔP Velocity Pressure	1.6

Total 8.6" H₂O

A summation of the cooling airflow requirements for condition 5, including a leakage allowance, follows:

Airflow (to be accomplished by the fan)

Engine	8230 cfm
Engine Oil	3970 cfm
<u>Transmission Oil</u>	<u>1520 cfm</u>

13720 cfm

Plus Ten Percent 1370 cfm

Total 15090 cfm

The critical cooling requirement for the fan is therefore approximately 15000 cfm at 8.6" H₂O at a density ratio of 0.676 or 15000 cfm at 12.7" H₂O at sea level standard air density.

A-3.0 FAN DESIGN

A-3.1 Statement of Defining Parameters

A 34" fan diameter was chosen on the basis of the maximum possible extrapolation of rotor tip [3] from NACA cascade data of Reference A-4. This was necessary to provide the desired axial velocity of 100 fps with a specified fan RPM. The critical cooling condition was cruise at 10,000' hot day, where the RPM = 2400, airflow = 15,000 CFM, and the pressure rise = 8.6" H₂O when $\sigma' = 0.676$.

The design axial velocity is chosen as 100 feet per second.

Therefore the design conditions are as follows:

Cruise at 10,000 Ft.

$$RPM = 2400 \omega = \frac{2\pi}{60} (2400) = 251 \text{ radians/second}$$

$$V_{ax} = 100 \text{ feet/second}$$

$$\Delta P_i \text{ for Rotor} = 8" H_2O \text{ (assumed)}$$

$$\Delta P_i \text{ stator: to be determined}$$

$$Q = 15,000 \text{ CFM} = 250 \text{ CFS}$$

$$\sigma = 0.676 \text{ (density ratio)}$$

$$A_{\text{fan}} = Q/v = 250/100 = 2.5 \text{ square feet}$$

$$D_o = 34" \text{ (chosen)}$$

$$D_i = 26.4" \text{ from } A_F = (\pi/4) (D_o^2 - D_i^2)$$

The fan is now to be designed from these criteria.

A-3.2.0 Design of Blade Sections

A-3.2.1 Rotor Blade Root Airfoil Section Design

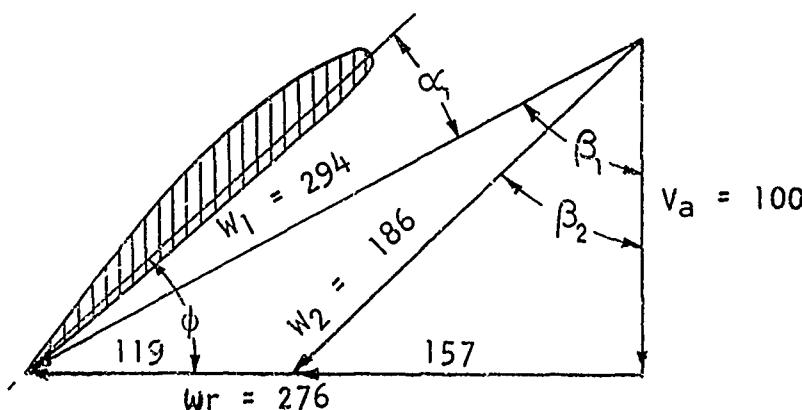


FIGURE A-7

$$\beta_1 = \tan^{-1} \frac{276}{100} = 70.08^\circ$$

$$\Delta P_i = 8" H_2O (5.2) = 1/2 \rho (w_1^2 - w_2^2)$$

$$41.6 = 1/2 (.001608) (86,200 - w_2^2)$$

$$w_2^2 = 34,500$$

$$w_2 = 186 \text{ fps}$$

$$\beta_2 = \cos^{-1} \frac{100}{186} = \cos^{-1} .539 = 57^\circ 23' = 57.38^\circ$$

$$\text{Turning angle, } \theta = \beta_1 - \beta_2 = 70.08 - 57.38$$

$$\theta = 12.70^\circ$$

$\sigma' c = 1.34$ (Fig. 4-107 (b)) Section chosen using θ & β_1
 65 - 810 section to give a $\sigma' \geq 1$ since
 design data is only available for $\sigma' > 1$

$\alpha_{i\text{design}} = 11.2^\circ$ (Fig. 4-106) Using σ' & airfoil section

$c_d = .011$ (Fig. 4-82 and Fig. 4-87) Using α_i

$$\phi_{\text{FAN ROOT}} = 90 - \beta_1 + \alpha_1 = 90 - 70.08 + 11.2 = 31.12^\circ$$

$$\sigma' c = \frac{Bc}{2\pi r}; \quad c_{\text{FAN ROOT}} = \frac{1.34(2)\pi(13.2)}{32} = 3.47"$$

The number of blades (B) is chosen by the approximate chord length desired ($B = \frac{2\pi r \sigma'}{c}$) and then rounded off to the nearest whole blade. Then the actual chord is determined as above.

A-3.2.2 Stator Blade Root Constant Thickness Section Design

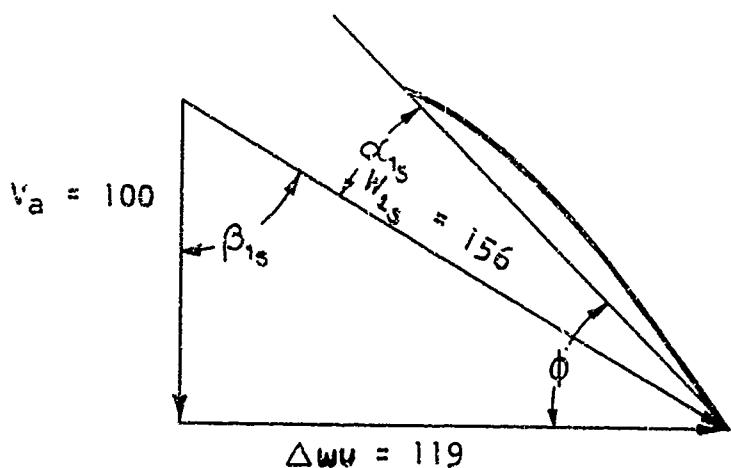


FIGURE A-8

$$w_{1s}^2 = (100)^2 + (119)^2 = 10,000 + 14,170 = 24,170$$

$$w_{1s} = 156 \text{ fps}$$

$$\beta_{1s} = \tan^{-1} \frac{119}{100} = 49.058^\circ = 49.96^\circ \approx 50^\circ$$

$$\Delta P_{\text{STATOR}} = 1/2 \rho (w_{1s}^2 - w_{ax}^2) = 1/2 (.001608) (24,170 - 10,000)$$

$$= 11.4 \text{ psf} \approx 2.19" \text{ H}_2\text{O}$$

$$\theta_s = \beta_{1s} = 50^\circ$$

$\theta = 48^\circ$ is obtained with the following:

$$\sigma' c = 1.6 \quad (\text{Fig. 4-107 (a)})$$

65 - (24)10 airfoil (Fig. 4-107 (a))

$$\alpha_{1s} \approx 27^\circ \quad (\text{Fig. 4-106})$$

$$c_d = .02 \quad (\text{Fig. 4-51})$$

$$\phi_{\text{STATOR ROOT}} = 90 - 50 + 27 = 67^\circ$$

$$c_{\text{STATOR ROOT}} = \frac{1.6(2)\pi(13.2)}{36} = 3.69"$$

A-3.2.3 Rotor Blade Tip Airfoil Section Design

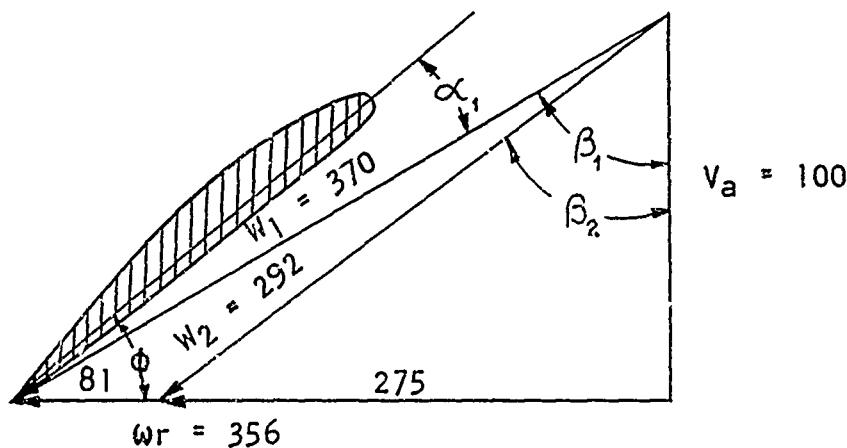


FIGURE A-9

$$\beta_1 = \tan^{-1} \frac{356}{100} = 74.3^\circ$$

$$\Delta P_i = 8" H_2O (5.2) = 1/2 \rho (w_1^2 - w_2^2)$$

$$41.6 = 1/2 (.001608) (137,000 - w_2^2)$$

$$w_2^2 = 85,000$$

$$w_2 = 292 \text{ fps}$$

$$\beta_2 = \cos^{-1} \frac{100}{292} = \cos^{-1} .343 = 69^{\circ}56' = 69.93^{\circ}$$

$$\theta = \beta_1 - \beta_2 = 74.3 - 69.9 = 5.0^{\circ}$$

$$\sigma_c = .8 \quad (\text{Fig. 4-107 (b)})$$

65 - 410 airfoil

$$\alpha_{1\text{ design}} = 5.5^{\circ} \quad (\text{Fig. 4-106})$$

$$c_d = .01 \quad (\text{Fig. 4-77})$$

$$\phi_{\text{FAN TIP}} = 90 - \beta_1 + \alpha_1 = 90 - 74.3 + 5.5 = 21.2^{\circ}$$

$$c_{\text{FAN TIP}} = \frac{(.8)2\pi(17)}{32} = 2.66"$$

A-3.2.4 Stator Blade Tip Constant Thickness Section Design

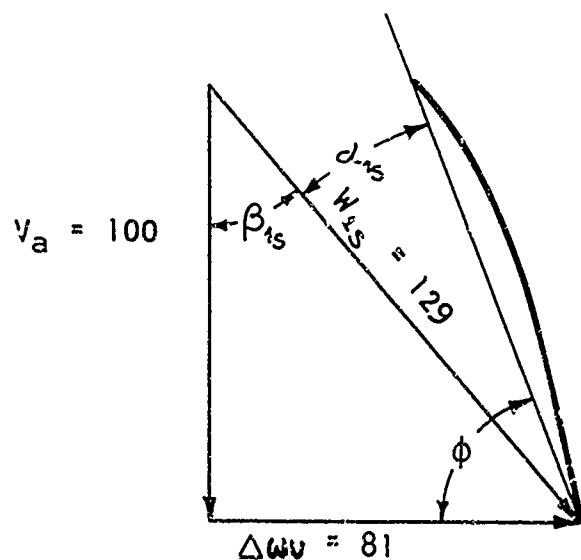


FIGURE A-10

$$\beta_{1s} = \tan^{-1} \frac{81}{100} = 39^{\circ}0' = 39^{\circ}$$

$$W_{1s}^2 = (100)^2 + (81)^2 = 10,000 + 6,560 = 16,560$$

$$W_{1s} = 129 \text{ fps}$$

$$\Delta P_{\text{STATOR}} = 1/2 \rho (W_{1S}^2 - W_{ax}^2) = 1/2 \rho (16,560 - 10,000)$$

$$= 5.34 \text{ psf} = 1.03" \text{ H}_2\text{O}$$

$$\theta_S = \beta_{1S} = 39^\circ$$

$$\sigma' c = 1.1 \quad (\text{Fig. 4-107 (a)})$$

$$65 - (24)10 \quad (\text{Fig. 4-107 (a)})$$

$$\alpha_{1S} = 22.5^\circ \quad (\text{Fig. 4-106})$$

$$C_d = .015 \quad (\text{Fig. 4-26})$$

$$\phi_{\text{STATOR TIP}} = 90 - 39 + 22.5 = 73.5^\circ$$

$$c_{\text{STATOR TIP}} = \frac{(1.1)2\pi(17)}{36} = 3.26"$$

A-3.2.5 Summary of Cooling Fan Design Parameters

The cooling fan design parameters which have been determined in Sections A-3.2.1 through A-3.2.4, inclusive, are presented in Table A-4. These parameters are presented pictorially in Figure A-11, which adjoins Table A-4.

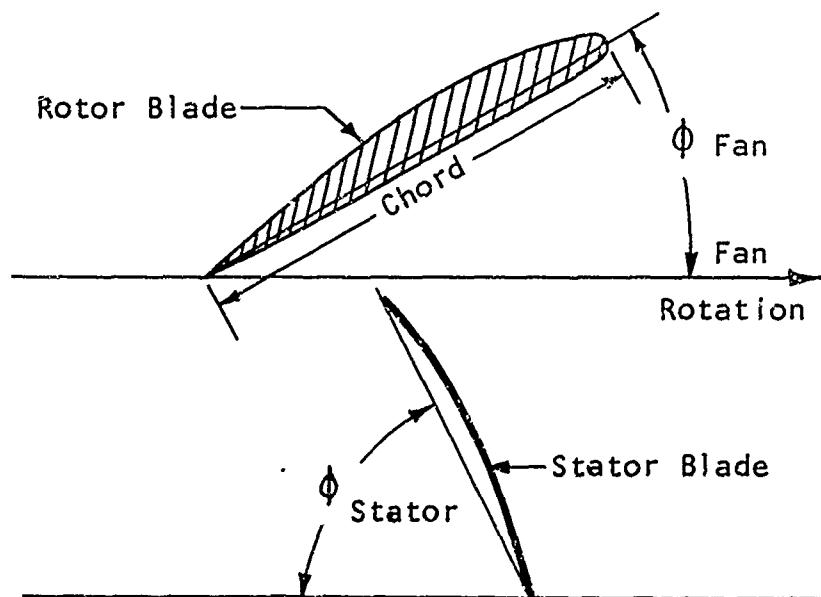


FIGURE A-11
Cooling Fan Design Parameters

	AIRFOIL SECTION	(DEGREES)	CHORD (INCHES)
Fan Blade Tip	65-410	21.20	2.66
Fan Blade Root	65-810	31.1	3.47
Stator Blade Tip	65-(24)10	73.5	3.26
Stator Blade Root	65-(24)10	67.0	3.69

Radius to Blade Tip = 17"
 Radius to Blade Root = 13.2"

TABLE A-4

A-3.3 Actual Fan Pressure Rise

Neglecting tip clearance effects, the pressure rise for a given section may be defined as

$$\Delta P_i = \Delta P_{pro} \text{ where}$$

$$\Delta P_i = \frac{1}{2} \rho (w_1^2 - w_2^2)$$

$$\Delta P_{pro} = C_d (1.5) * \sigma' \frac{w_1}{V_a} q$$

*Assumed 50% increase in C_d to allow for blade surface roughness as discussed in Chapter IV.

The actual pressure rise may be estimated by evaluating the tip clearance losses from Figure 4-3, Chapter IV, where

$$\text{Design Tip Clearance} = 3.25\% \text{ Span} \quad (\text{The tip clearance was chosen as } 0.125" \text{ for this problem})$$

$$\text{Tip Loss} = 11\%$$

$$\text{Then the pressure rise} = (1.00 - 0.11) (\Delta P_i) - \Delta P_{pro}$$

The actual pressure rise for the rotor, stator, and complete fan assembly may be estimated as follows for the design condition:

Rotor Root

$$\Delta P_i = 0.89(8) = 7.12" H_2O$$

$$\Delta P_{pro} = (0.011) (1.5) (1.34) \frac{294}{100} \times \frac{(8.04)}{5.2} = 0.10" H_2O$$

Rotor Tip

$$\Delta P_i = 0.89(8) = 7.12" H_2O$$

$$\Delta P_{pro} = (0.01)(1.5)(0.8) \frac{270}{100} \times \frac{8.04}{5.2} = 0.07" H_2O$$

Σ Rotor

$$\Delta P = \frac{7.12 + 7.12}{2} - \frac{0.10 + 0.07}{2} = 7.04" H_2O$$

Stator Root

$$\Delta P_i = 0.89(2.19) = 1.95" H_2O$$

$$\Delta P_{pro} = 0.02(1.5)(1.1) \frac{156}{100} \times \frac{8.04}{5.2} = 0.12" H_2O$$

Stator Tip

$$\Delta P_i = 0.89(1.03) = 0.92" H_2O$$

$$\Delta P_{pro} = 0.015(1.5)(1.1) \frac{129}{100} \times \frac{8.04}{5.2} = 0.04" H_2O$$

Σ Stator

$$\Delta P = \frac{1.95 + 0.92}{2} - \frac{0.12 + 0.04}{2} = 1.41" H_2O$$

$$\Delta P_{Fan} = 7.04 + 1.41 = 8.45" H_2O \text{ at } \sigma = 0.676$$

Although the required ΔP is 8.60" H_2O and the fan design will provide 8.45" H_2O , the deficiency is less than two percent, which is within the tolerance of the design calculation. It is, therefore, assumed to be sufficient.

A-3.4 Calculations for Fan Efficiency & Power Required

Now that the cooling fan has been designed, the fan efficiency and power required can be computed.

The only parameter that has not been evaluated is the mean flow velocity relative to the blades (w_m) which may be calculated as follows:

$$w_m = \sqrt{v_a^2 + \left[\omega r - \frac{\Delta w_u}{2} \right]^2}$$

With all of the fan parameters known, the fan efficiency and power required may now be determined.

CALCULATIONS FOR FAN EFFICIENCY AND POWER REQUIRED

$$\eta_{ELEMENT} = \frac{\eta_{T.C.}}{1 + C_{dR} \sigma' R \frac{W_m}{4V_a} \left(\frac{2\omega_r}{\Delta W_u} - 1 \right) \left[\frac{C_{dS} \sigma'_s \sqrt{V_a^2 + \left(\frac{\Delta W_u}{2} \right)^2} + C_{dR} \sigma' R W_m}{2\Delta W_u + (C_{dR} \sigma' R W_m) \left(\frac{\omega_r - \frac{\Delta W_u}{2}}{V_a} \right)} \right]}$$

Substituting the following in the above equation:

	TIP	ROOT
$\eta_{T.C.}$.89	.89
* C_{dR}	.015	.016
$\sigma' R$.80	1.34
W_m	331	238.5
V_a	100	100
ω_r	356	276
ΔW_u	81	119
* C_{dS}	.022	.030
σ'_s	1.1	1.6

and solving gives

$$\eta_{FAN TIP} = 81.5 \text{ percent}$$

$$\eta_{FAN ROOT} = 80.7 \text{ percent}$$

$$\eta_{FAN} = \frac{81.5 + 80.7}{2} = 81 \text{ percent}$$

*Increased 50% to allow for roughness

$$\begin{aligned}
 HP_{\text{Req.}} &= \frac{\Delta P_{\text{FAN}} \times Q}{33,000} \div \eta_{\text{FAN}} \\
 &= \frac{(12.7 \times 5.2) \quad 15000}{33,000} \div .81 \\
 &= 37 \text{ HP at } \frac{P}{P_0} = 1.0
 \end{aligned}$$

A-3-5 Calculation of Ordinates for a Typical Airfoil Section

The shape of the rotor and stator airfoil sections is defined by ordinates.

Surface ordinates for NACA 65-010 basic thickness forms are presented in Table A-5 from Reference A-4.

Ordinates for the NACA $a = 1.0$ mean line are presented in Table A-6 from Reference A-4.

The surface ordinates, expressed as plus or minus increments to be constructed perpendicularly to the mean line at the specified percent chord, define the blade surface contour for the NACA 65-010 basic thickness forms. These ordinates are obtained in inches by multiplying each of them by the blade chord length in inches.

The right-hand column of ordinates in Table A-5 is for the NACA 65-010 airfoil which had been derived analytically for optimum performance and which therefore had no trailing edge thickness. The left-hand column is for the NACA 65(216)-010 airfoil which was modified to provide trailing edge thickness 0.0015 of the chord length. This latter airfoil section was used for the cascade tests of Reference A-4. These two sets of ordinates are considered to be interchangeable within the accuracy of the results of the Reference A-4 cascade tests. In this illustrative problem, the right-hand (derived) ordinates will be used.

In order to ease blade fabrication tolerance criteria and to prevent blade damage during handling, increased trailing edge thicknesses are customarily provided. In this problem, the trailing edge is to be made .060 inch thick with a trailing edge radius of .030 inch. To accomplish this without materially affecting the performance of the airfoil, it is necessary to gradually increase the thickness of the blade above the basic thickness from the chordwise station of maximum thickness to the trailing edge. That is, the incremental added thickness varies from zero at forty percent chord to .060 inch at the trailing edge. Depending on the trailing edge thickness chosen, the maximum thickness chord section may be moved slightly aft.

In this problem, the rotor blades are of cast aluminum alloy and the stator blades are of constant thickness aluminum alloy sheet. Therefore, the above procedure will be used to define the mean line and surface contours of the rotor blades, with ordinate tolerances specified to 0.001 inch, which is the accuracy of the chosen casting process. The stator blades are to be formed to the mean line so that only a definition of the airfoil mean line need be provided.

STATION, x	ORDINATES, $\frac{t}{c}$ y	
	65(216)-010 AIRFOIL COMBINED WITH $y = 0.0015x$	DERIVED 65-010 AIRFOIL
0.	0.	0.
.5	.752	.772
.75	.890	.932
1.25	1.124	1.169
2.5	1.571	1.574
5.0	2.222	2.177
7.5	2.709	2.647
10	3.111	3.040
15	3.746	3.666
20	4.218	4.143
25	4.570	4.503
30	4.824	4.760
35	4.982	4.924
40	5.057	4.996
45	5.029	4.963
50	4.870	4.812
55	4.570	4.530
60	4.151	4.146
65	3.627	3.682
70	3.038	3.156
75	2.451	2.584
80	1.847	1.987
85	1.251	1.385
90	.749	.810
95	.354	.306
100	.150	0
L.E. radius	.666	.687

Stations and Ordinates in Percent of Chord

TABLE A-5
Ordinates for NACA 65-010 Basic Thickness Forms

(Source: Reference A-4)

$C_{l_0} = 1.0$		
STATION, x	ORDINATE, y	SLOPE, dy/dx
0	0	-----
.5	.250	0.42120
.75	.350	.38875
1.25	.535	.34770
2.5	.930	.29155
5.0	1.580	.23430
7.5	2.120	.19995
10	2.585	.17485
15	3.365	.13805
20	3.980	.11030
25	4.475	.08745
30	4.860	.06745
35	5.150	.04925
40	5.355	.03225
45	5.475	.01595
50	5.515	0
55	5.475	-.01595
60	5.355	-.03225
65	5.150	-.04925
70	4.860	-.06745
75	4.475	-.08745
80	3.980	-.11030
85	3.365	-.13805
90	2.585	-.17485
95	1.580	-.23430
100	0	-----

Stations and Ordinates in Percent of Chord

TABLE A-6
Ordinates for the NACA $a = 1.0$ Mean Line

(Source: Reference A-4)

x _m	65 - (10)10							y _m	Tan ['] _m	Sin _m	Cos _m	y'	% Addition in y'	y _{sin_m}	y _{Cos_m}	Upper Surface				Lower Surface			
	y _m	Tan ['] _m	0.8 x ②	0.8 x ③	Table A-5	⑧ x ⑨	⑩ x ⑥	⑩ x ⑦	① - ⑪	y _f ⑫	x	y	x	y	⑪ - ⑫	④ - ⑬							
0	0	0	0	0	0	0	0	0	0	0	0	0	0	0	0	0	0	0	0	0			
0.5	0.250	0.42120	0.200	0.33696	-31932	-94765	0	0.772	0.247	0.732	0.253	0.732	0.753	0	0	0	0	0	0	0			
0.75	0.350	0.38775	0.280	0.31100	-29696	-95489	0.932	0.277	0.890	0.473	1.170	1.170	1.170	1.170	0	0	0	0	0	0	0		
1.25	0.535	0.570	0.428	0.29155	-27816	-96342	1.169	0.313	1.126	0.933	1.554	1.554	1.554	1.554	0	0	0	0	0	0	0		
2.50	0.930	0.29155	0.744	0.23324	-22714	-97386	1.578	0.358	1.533	2.142	2.277	2.277	2.277	2.277	0	0	0	0	0	0	0		
5.0	1.580	0.23430	1.264	1.18744	-18423	-98288	2.177	0.401	2.140	4.593	3.404	3.404	3.404	3.404	0	0	0	0	0	0	0		
7.5	2.120	0.19995	1.696	1.59996	-1.5725	-98745	2.647	0.418	2.614	5.401	4.310	4.310	4.310	4.310	0	0	0	0	0	0	0		
10	2.585	0.17985	2.068	1.39988	-1.38553	-99036	3.040	0.421	3.011	7.082	7.918	7.918	7.918	7.918	0	0	0	0	0	0	0		
15	3.365	0.13805	2.692	1.1044	-1.0977	-99396	3.566	0.402	3.644	14.579	10.421	10.421	10.421	10.421	0	0	0	0	0	0	0		
20	4.980	0.10300	3.184	0.8824	-0.8888	-99604	4.143	0.368	4.127	19.732	19.732	19.732	19.732	19.732	0	0	0	0	0	0	0		
25	4.475	0.98745	3.580	0.6779	-0.6779	-99756	4.503	0.314	4.492	24.686	24.686	24.686	24.686	24.686	0	0	0	0	0	0	0		
30	4.860	0.6745	4.120	3.888	-0.5388	-99855	4.760	0.256	4.753	29.744	29.744	29.744	29.744	29.744	0	0	0	0	0	0	0		
35	5.150	0.6925	4.120	0.3940	-0.3940	-99923	4.924	0.194	4.886	34.806	34.806	34.806	34.806	34.806	0	0	0	0	0	0	0		
40	4.284	0.02525	4.284	0.2580	-0.2580	-99966	4.996	0.129	4.954	39.871	39.871	39.871	39.871	39.871	0	0	0	0	0	0	0		
45	5.475	0.01595	4.380	0.01276	-0.01276	-99992	4.963	0.072	5.035	44.976	44.976	44.976	44.976	44.976	0	0	0	0	0	0	0		
50	5.515	0	4.412	0	0	1.00000	4.812	0.144	4.956	50.000	50.000	50.000	50.000	50.000	0	0	0	0	0	0	0		
55	5.475	-0.01598	4.380	-0.01276	-0.01276	-99992	4.510	0.216	4.746	-0.061	9.126	9.126	9.126	9.126	9.126	0	0	0	0	0	0	0	
60	5.355	-0.03225	4.284	-0.02580	-0.02580	-99966	4.116	0.283	4.434	-1.114	6.014	6.014	6.014	6.014	6.014	0	0	0	0	0	0	0	
65	5.150	-0.04925	4.120	-0.03940	-0.03940	-99923	3.662	0.360	4.042	-1.59	4.039	65.159	65.159	65.159	65.159	65.159	0	0	0	0	0	0	0
70	4.860	-0.06745	3.888	-0.05396	-0.05396	-99855	3.156	0.432	3.588	-1.93	3.563	70.193	70.193	70.193	70.193	70.193	0	0	0	0	0	0	0
75	4.475	-0.08745	3.580	-0.06596	-0.06596	-99756	2.564	0.504	3.083	-2.16	3.083	75.216	75.216	75.216	75.216	75.216	0	0	0	0	0	0	0
80	3.980	-0.11030	3.184	-0.08824	-0.08824	-99604	1.987	0.576	2.563	-2.28	2.553	88.228	88.228	88.228	88.228	88.228	0	0	0	0	0	0	0
85	3.365	-0.13805	2.692	-0.1044	-0.1044	-99396	1.385	0.648	2.033	-2.23	2.021	85.223	85.223	85.223	85.223	85.223	0	0	0	0	0	0	0
90	2.585	-0.17485	2.068	-0.13988	-0.13988	-99036	0.810	0.729	1.515	-2.12	1.515	89.777	89.777	89.777	89.777	89.777	0	0	0	0	0	0	0
95	1.580	-0.23430	1.264	-0.18744	-0.18744	-98288	0.306	0.792	1.098	-2.02	1.098	94.798	94.798	94.798	94.798	94.798	0	0	0	0	0	0	0
100	0	0	0	0	0	0	0	0	0	0	0	0	0	0	0	0	0	0	0	0	0	0	

Chord = 3.470"
L.E. Radius = 0.024"
T.E. Radius = 0.030"

TABLE A-7

MEAN LINE		UPPER SURFACE		LOWER SURFACE	
X	Y	X	Y	X	Y
0	0	0	0	0	0
.017	.007	.009	.032	.026	-.018
.026	.010	.016	.041	.036	-.021
.043	.015	.033	.054	.054	-.024
.087	.026	.074	.079	.099	-.027
.074	.044	.160	.118	.187	-.030
.260	.059	.246	.150	.275	-.032
.347	.072	.332	.176	.362	-.033
.521	.093	.507	.220	.534	-.033
.694	.110	.685	.254	.707	-.033
.868	.124	.857	.280	.878	-.032
1.041	.135	1.032	.300	1.050	-.030
1.215	.143	1.208	.313	1.221	-.027
1.388	.149	1.384	.322	1.392	-.025
1.562	.152	1.561	.327	1.564	-.023
1.735	.153	1.735	.325	1.735	-.019
1.909	.152	1.911	.317	1.906	-.013
2.082	.149	2.086	.302	2.078	-.005
2.256	.143	2.261	.283	2.250	.003
2.429	.135	2.436	.259	2.422	.011
2.603	.124	2.610	.231	2.595	.017
2.776	.110	2.784	.199	2.768	.022
2.950	.093	2.957	.164	2.942	.023
3.123	.072	3.130	.124	3.116	.019
3.297	.044	3.304	.081	3.289	.006
3.470	0	-----	-----	-----	-----

Chord = 3.470"
 L.E. Radius = 0.024"
 T.E. Radius = 0.030"

TABLE A-8
 Sample Problem
 Distance from Chord Line for NACA 65-810
 Rotor Root Section in Inches

Ordinates for the airfoil mean line and surfaces should be drawn over-scale, approximately ten times size for the ordinary helicopter or airship cooling fan blade. Contoured curves are then drawn through the ordinates defining the surfaces.

The airfoil is defined as a 65-8-10 section with a chord of 3.470".

In the sample calculation in Table A-7, it should be noted that:

1. Columns (4) and (5) are 0.8 times (2) and (3), since the sample airfoil is a 65-810 section and the ordinates in (2) and (3) are for a 65-(10)10 airfoil. There is a direct relationship of camber $\frac{8}{10} = 0.8$.
2. Column (8) is the right-hand column from Table A-5.
3. Column (9) shows the tapered thickening of the airfoil section in order to have a trailing edge radius of 0.030". This is done by dividing the 0.030" into 12 equal parts and tapering the increment from a maximum of 0.030 at 100 percent chord to zero at 40 percent chord. These values are expressed in percent of chord.
4. Table A-8 shows the ordinates converted from percent to inches.

A-4.0 FAN PERFORMANCE TESTING

This section is presented in the past tense because it is essentially a fan test report.

A-4.1 Discussion

Fan testing was run in three phases. The first phase tests utilized the first fan constructed and incorporated both performance and structural tests. This fan had damaged tip trailing edges on many of the blades and also had an improper fan blade-stator ring clearance. For the second phase tests the above deficiencies were corrected by straightening the blade trailing edges and extending the stator inlet ring. For the third phase tests the fan blade incidence angles were increased by 3° in order to provide a spread of data by which to finally determine the required blade incidence angle setting.

A-4.2 Test Procedure

The full scale test fan was mounted in the fan tunnel, which consisted of an entrance blower, a plenum chamber, a venturi, duct work and variable exit dampers. A variable speed electric motor was used to drive the fan rotor. The general arrangement of the test facility is illustrated in Figure A-14.

Instrumentation consisted of: a venturi draft gage for measuring flow, a Baldwin SR-4 Shaft Torquemeter for measuring torque, a tachometer for measuring fan speed, a barometer and thermometers for measuring atmospheric pressure and wet and dry bulb temperatures, and the following pressure pickups for measuring the pressure rise across the fan. This test arrangement was a variation of the fan test tunnel installations described in Chapter VI.

Static pressure immediately before and after the fan;
total pressures immediately after the fan;
total and static pressures 3 feet downstream of fan;
total and static pressures 5 feet downstream of fan;
total and static pressures 4 feet upstream of fan.

Prior to fan performance tests, the venturi draft gage was calibrated by making a velocity traverse in the venturi at various flows.

The entrance blower was used to overcome the upstream pressure losses of the system, i.e., system entrance loss, duct losses, and loss across the venturi. Prior to each test run, the total pressure pickup (4 feet upstream of fan) was balanced against atmospheric pressure by adjusting the speed of the entrance blower. In this way, air at atmospheric pressure was assured at the entrance to the test fan.

The test procedure for a typical run was as follows:

1. Position exit dampers to the approximate setting for the desired flow.
2. Start test fan driving motor and adjust speed to the required RPM.
3. Adjust speed of the entrance blower to balance the upstream total pressure pickup against atmospheric pressure.
4. Reset test fan RPM.
5. Take all readings, checking test fan RPM and upstream total pressure for possible variation.

During the first phase tests, successive runs were conducted at various exit damper positions for a given fan speed. Then the procedure was repeated for the other fan speeds desired. For the second and third phase tests, the exit damper was locked at the lowest flow position while successive runs were conducted at the three desired fan speeds. Then the damper opening was increased and again runs were conducted for the three fan speeds. This procedure was repeated until the damper was completely open, giving the maximum flow. This second method resulted in quicker run times; therefore, more test points were obtained. The fact that test points were made at a constant flow restriction for three fan speeds was also advantageous in plotting performance curves because any error would be obvious.

As initially fabricated, the fan had exceptionally large blade root gaps. For each of the three test phases, performance tests were conducted at 2200, 2400, 2600 RPM with the gaps open. The fan was then removed from the tunnel to facilitate sealing the gaps with transparent tape. After taping the gaps, the fan was remounted in the tunnel and the performance tests were then repeated. During phase one testing, runs with the gaps sealed were conducted only at 2400 RPM. For the second and third phase tests, runs were performed at 2200, 2400 and 2600 RPM in which the gaps were sealed.

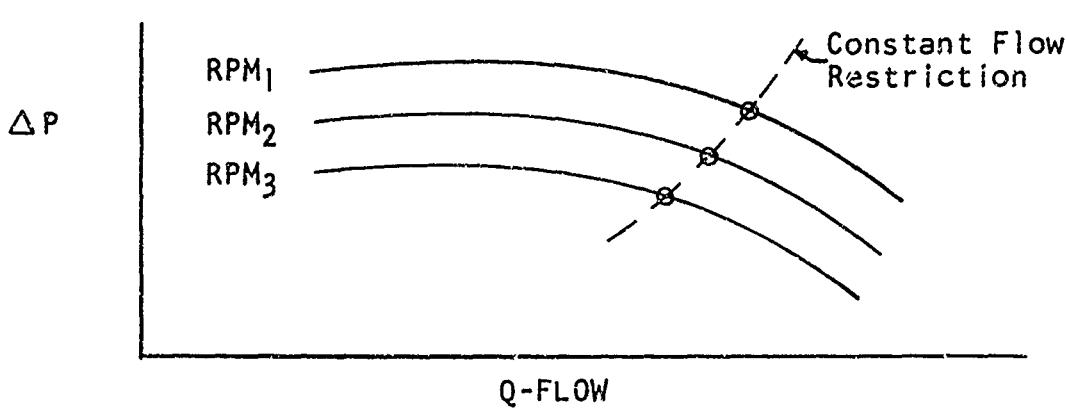


FIGURE A-12

While the fan blade root gaps were being sealed (and therefore the fan removed from the tunnel), the fan driving motor was started and torque readings were recorded at speeds of 2200, 2400 and 2600 RPM. These static torque readings (due to bearing friction of the shaft) were subsequently subtracted from the torque measurements recorded during the test runs, thereby obtaining the true torque required by the fan.

A-4.3 Data Analysis

The fan pressure rise was determined by the difference between the total pressures 4 feet upstream and 5 feet downstream of the fan, with a correction for the fan inlet loss and the fan exit diffusion loss. Since the total pressure pickup upstream of the fan was balanced against atmospheric pressure (by use of the tunnel entrance blower), the pressure rise across the fan was the summation of (1) the total gage pressure downstream, (2) the fan entry loss and (3) the fan diffusion loss.

The fan entry loss was the total pressure loss at the fan entrance. The entry loss could therefore be determined by the algebraic sum of the static pressure and the velocity pressure at the fan entrance. The static pressures at this location were recorded and the velocity pressure was calculated by $1/2 \rho V^2$, where V is the fan axial velocity or Q/A_{fan} . However, since the static pressure measurements were especially erratic at the lower flows, the entry loss was calculated as described above for the medium and higher flows, then plotted against the velocity pressure. The resulting ΔP vs. q graph should plot as a straight line passing through the origin. The slope of the resulting line ($\Delta P/q$), found to be .15, when multiplied by the velocity pressure gives the fan entry loss. Inlet loss calculations and resulting ΔP vs q plot are presented on Table A-10 and Figure A-15.

The fan exit diffusion loss was determined by the method presented on page 10 of Reference A-5 for losses due to an abrupt expansion. The exit loss coefficient, as determined on page 45 of this Reference was 0.58 (the exit loss, therefore, was .58 multiplied by the velocity pressure). The summation of the fan entry and exit losses (for the test

configuration) was $.15 q_f + .58 q_f = .73 q_f$. For all calculations in this section, the fan losses were described by $.73 \times$ fan axial velocity pressure and the fan total pressure rise was therefore determined by the downstream $P_{TOTAL} - (.73 \times$ velocity pressure). Test performance calculations are presented on Tables A-11 to A-16 inclusive and the fan performance curves are included in Figures A-17 to A-31, inclusive.

A-4.4 Results and Conclusions

As was previously noted, the fan performance tests were conducted in three phases, each phase representing slight variations of the basic fan. The variations were as follows:

TEST		CONFIGURATION			
Phase	Part	Incidence Angle	Fan Inlet Ring	Blade Trailing Edges	Blade Root Gaps
1	A	Design	Original	Damaged	Open
1	B	Design	Original	Damaged	Sealed
2	A	Design	Extended	Straightened	Open
2	B	Design	Extended	Straightened	Sealed
3	A	Design + 3°	Extended	Straightened	Open
3	B	Design + 3°	Extended	Straightened	Sealed

TABLE A-9

Tests were performed during each phase with the fan blade root gaps open and with the gaps sealed. The tests indicated, without exception, that higher pressure rises and slightly higher efficiencies were attained by sealing the gaps.

The fan tested during Phase 2, part B, represented the fan as designed in Section A-3.0 of this report. This fan delivered 15,000 CFM at a ΔP of 12.6" H₂O and required 38 HP at an efficiency of 79 percent. Use of this fan in the helicopter would insure adequate cooling at all flight conditions.

As would be expected, the fan efficiency was slightly decreased when the fan blade incidence angle was changed (as for the Phase 3 tests). The pressure rise, however, was increased by increasing the blade incidence angle. Measured rotor blade incidence angles are presented on Table A-17. It is not recommended that the increased blade angle (Phase 3) fan be used for the following reasons:

- A. At design flow the Phase 3 fan with gaps open provided a lower pressure rise but required more power than the Phase 2 fan with gaps sealed.
- B. The Phase 3 fan with gaps sealed operated in an unstable condition at an airflow very close to the design flow. (This unstable condition was also present in the Phase 2 fan with gaps sealed, but to a lesser degree and at a much lower airflow than

design flow. The condition was therefore not considered objectionable in the Phase 2 fan.) See plots on Figures A-22, -23, -27 and -28.

The total pressure rise, power required, and efficiency are tabulated below for the design airflow:

SEA LEVEL, STANDARD DAY
FLOW = 15,000 CFM

FAN	ΔP ("H ₂ O)	HP	EFF.
Gaps Open			
Phase 1	10.2	33	74
Phase 2	10.9	34	77
Phase 3	11.7	39	72
Gaps Sealed			
Phase 1	11.4	35	77
* Phase 2	12.6	38	79
Phase 3	13.6	43	74

* Represents the fan as designed; design estimation 12.7" H₂O at 81 percent efficiency.

ENGINE COOLING FAN TEST

FIGURE SHOWING ORIGINAL AND EXTENDED

FAN INLET RING

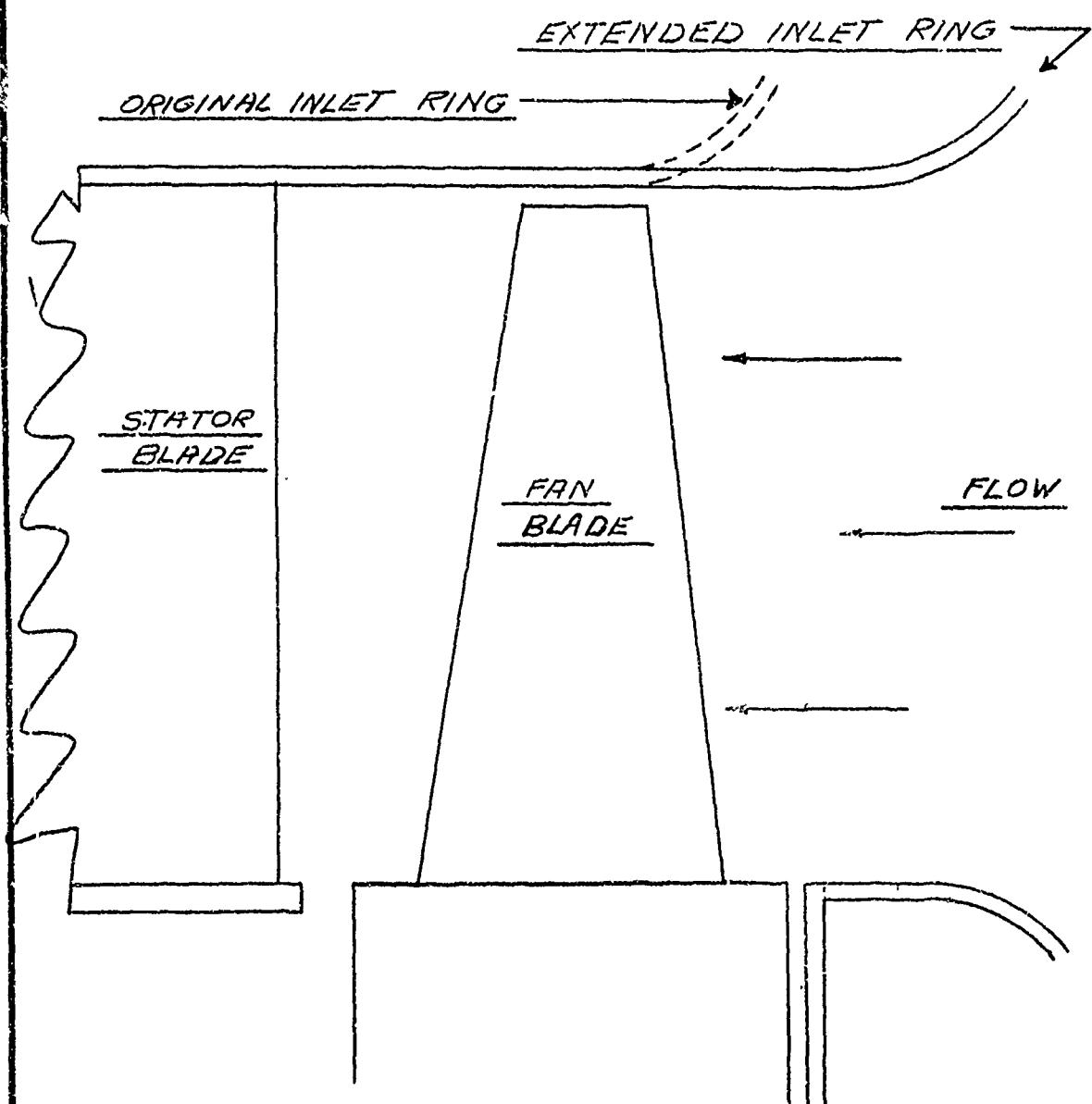
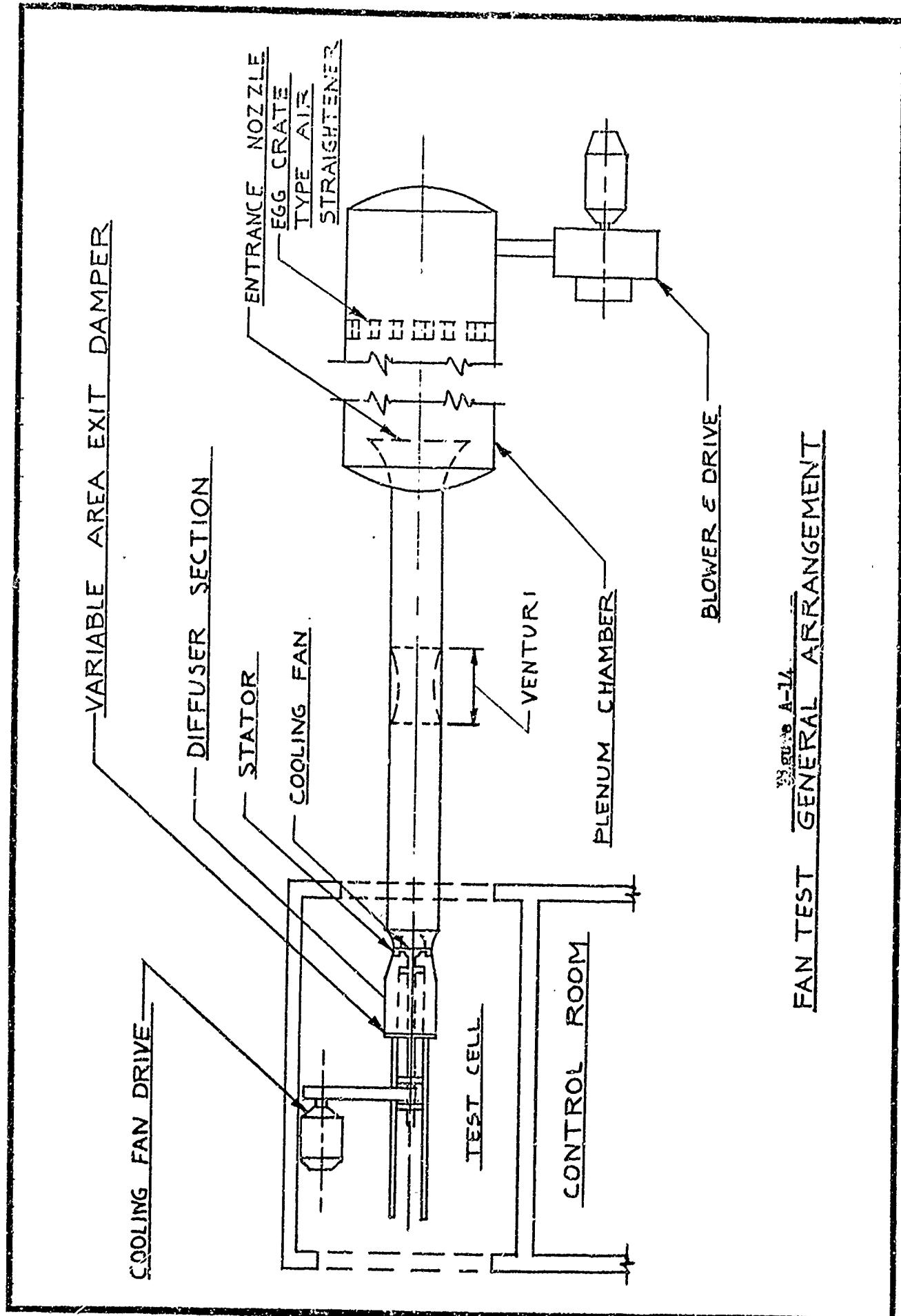


FIGURE A-13



DETERMINATION OF INLET LOSS COEFFICIENT

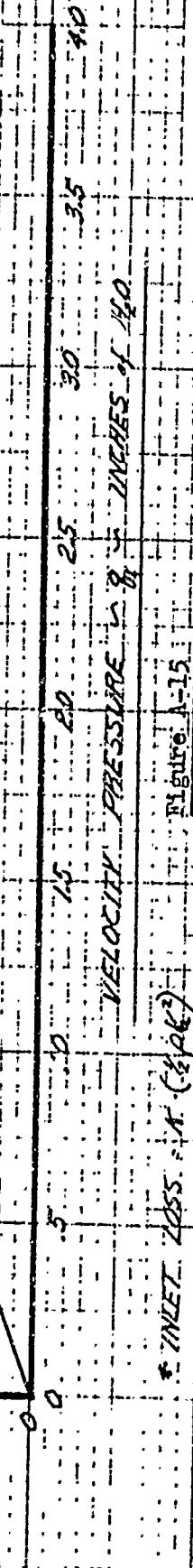
A_{loss} = 8.20

LEGEND

Δ 2200 rpm
 \circ 2400 rpm
 \square 2600 rpm

CUBIC INLET LOSS - INCHES of H₂O

A - 1 - 41



* INLET LOSS = $K \cdot (V^2)^{1/3}$

Figure 115

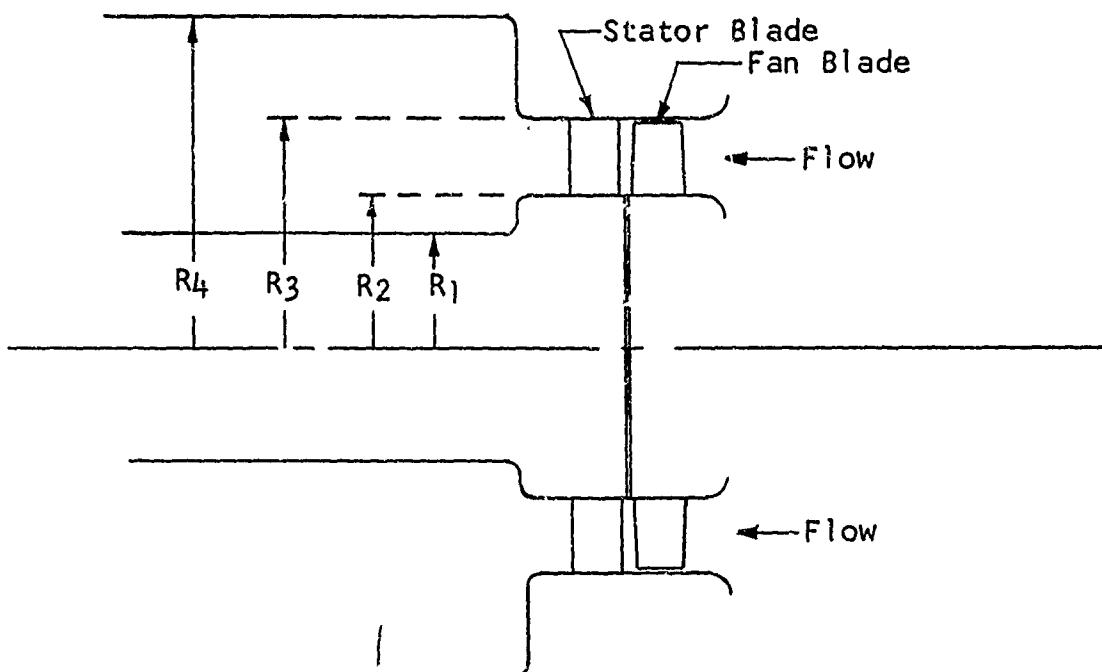


FIGURE A-16

Reciprocating Engine Cooling Fan Test
Determination of Test Fan Expansion Loss

$$R_1 = 10.63"$$

$$R_2 = 13.20"$$

$$R_3 = 17.00"$$

$$R_4 = 24.00"$$

$$A_1 = (R_3^2 - R_2^2)$$

$$= 360 \text{ in}^2$$

$$A_2 = (R_4^2 - R_1^2)$$

$$= 1460 \text{ in}^2$$

$$A_1/A_2 = .245$$

$$* \text{ Expansion Loss} = K \cdot 1/2 \cdot v^2$$

$$\text{where } K = (1 - A_1/A_2)^2 = (.76)^2$$

$$= .58$$

$$\text{Expansion Loss} = .58 \times \text{Velocity Pressure}$$

* Reference A-5

1	2	3	4	5	6	7	8	9
Fan Speed	Volume Flow q_f	Fan Axial Velocity V_a	Fan Velocity Pressure $\frac{1}{2} \rho V^2 / 5.2$	Manometer Number	Aver. P_{sfwd}	- P_T GAGE ④ / ⑧	Fan Inlet Loss	
RPM	CFM	FPS	In. of H_2O	Inches of H_2O			In. of H_2O	
2200	12520	83.5	1.54	-1.6	-1.7	-1.9	-1.73	.19
2200	13650	91.0	1.83	-2.2	-2.0	-2.3	-2.03	.20
2200	14750	98.4	2.14	-2.5	-2.2	-2.4	-2.37	.23
2200	15650	104.4	2.41	-3.1	-2.6	-2.8	-2.83	.42
2200	17710	118.1	3.08	-3.9	-3.2	-3.4	-3.63	.55
2400	11300	75.4	1.26	-1.4	-1.4	-1.4	-1.40	.14
2400	13620	90.7	1.82	-1.9	-2.0	-2.1	-2.00	.18
2400	14800	98.7	2.16	-2.4	-2.3	-2.6	-2.43	.27
2400	16000	106.6	2.52	-3.0	-2.6	-2.9	-2.83	.31
2400	17250	115.0	2.93	-3.7	-3.1	-3.2	-3.33	.40
2400	19220	128.0	3.62	-4.6	-3.8	-4.0	-4.13	.51
2600	14800	98.7	2.15	-2.4	-2.4	-2.5	-2.43	.25
2600	16250	108.3	2.60	-2.9	-2.7	-3.1	-2.90	.30
2600	17300	115.2	2.94	-2.7	-3.2	-3.5	-3.47	.47
2600	18600	124.0	3.40	-4.3	-3.5	-3.7	-3.83	.43
2600	20870	139.2	4.29	-5.6	-4.6	-4.8	-5.00	.71

TABLE A-10

Reciprocating Engine Cooling Fan Test
Determination of Fan Inlet Loss
(Based on Tests with Root Gaps Open)

Date of Test

Page 8

Noted = 2.5 Sq. Ft.

All Pressures in inches of Water unless Otherwise Indicated
 * Summation of Fan Entry and Diffusion Losses

TABLE A-11

Fan Spec	RPM	Volume Flow	Fan Axial Velocity			Total Pressure Downstream			Losses			Fan Total Pressure Rise			Air-HP Corr.			Fan Power Required			Efficiency			ψ						
			Draft Gage	F _{lcm} (CFM)	V _a Q/A _f	Velocity Pressure	Hannometer No.	Average P _T Down- stream	0.73 × ⑦	①	ΔP _{corr.} ③ + ④	②	ΔP _{corr.} ③ + ④	①	②	③	④	⑤	⑥	⑦	⑧	⑨	⑩	⑪	⑫	⑬	⑭	⑮	⑯	⑰
2000	2000	1.68	8800	58.6	1.75	7.9	8.0	7.93	.55	8.48	8.82	12.2	6.45	6.45	22.5	23.4	52.1%	36.4	180	1.24	1.24	1.24	1.24	1.24	1.24	1.24	1.24	1.24		
2200	2200	1.34	12150	81.0	1.44	7.6	7.6	7.60	1.05	8.65	8.21	17.2	7.45	7.45	24.2	24.2	68.2	37.0	180	1.28	1.28	1.28	1.28	1.28	1.28	1.28	1.28	1.28		
2200	2200	1.72	13700	91.4	1.83	6.9	6.8	6.87	1.34	8.21	8.54	18.4	7.00	7.00	24.4	25.4	72.4	35.2	180	1.32	1.32	1.32	1.32	1.32	1.32	1.32	1.32	1.32		
2200	2200	2.05	15000	100.0	1.99	5.6	5.6	5.67	1.60	7.27	7.56	17.9	7.10	7.10	25.0	23.9	74.9	31.2	180	1.36	1.36	1.36	1.36	1.36	1.36	1.36	1.36	1.36		
2200	2200	2.41	16300	108.7	2.57	4.6	4.6	4.70	1.83	6.58	6.84	17.6	6.85	6.85	22.2	23.1	76.2	28.2	180	1.40	1.40	1.40	1.40	1.40	1.40	1.40	1.40	1.40		
2200	2200	2.81	17600	117.3	3.10	2.6	2.6	2.63	2.26	4.89	5.09	14.1	6.00	6.00	19.2	20.0	70.5	21.0	180	1.44	1.44	1.44	1.44	1.44	1.44	1.44	1.44	1.44		
2400	2400	1.81	9600	64.0	4.67	.90	10.9	11.0	10.97	.66	1.63	12.10	18.3	9.25	9.25	37.5	37.5	48.8%	35.6	180	1.20	1.20	1.20	1.20	1.20	1.20	1.20	1.20	1.20	
2600	2600	1.22	11600	77.4	6.82	1.31	10.6	10.7	10.7	10.67	1.63	12.10	22.1	9.60	9.60	37.5	37.5	56.7	35.6	180	1.29	1.29	1.29	1.29	1.29	1.29	1.29	1.29	1.29	
2600	2600	1.30	14400	96.0	10.52	2.02	10.3	10.2	10.3	10.27	1.47	1.74	12.21	27.7	10.10	9.60	39.6	41.2	180	36.0	180	1.30	1.30	1.30	1.30	1.30	1.30	1.30	1.30	1.30
2600	2600	2.28	15800	105.7	12.73	2.45	9.8	9.6	9.67	1.79	1.46	11.92	29.8	10.15	9.65	39.8	41.4	180	72.0	180	1.34	1.34	1.34	1.34	1.34	1.34	1.34	1.34	1.34	
2600	2600	2.82	17600	117.5	15.73	3.03	8.4	8.5	8.40	2.21	10.61	11.93	30.6	9.85	9.85	38.6	40.1	180	76.3	180	1.38	1.38	1.38	1.38	1.38	1.38	1.38	1.38	1.38	
2600	2600	3.09	18450	123.0	17.25	3.32	7.2	7.2	7.20	2.42	9.62	10.90	29.1	9.60	9.60	37.5	39.0	180	74.6	180	1.42	1.42	1.42	1.42	1.42	1.42	1.42	1.42	1.42	
2600	2600	3.91	20750	138.2	21.80	4.19	3.5	3.8	3.5	3.60	6.66	6.93	22.7	6.25	6.25	32.0	33.3	180	68.2	180	1.46	1.46	1.46	1.46	1.46	1.46	1.46	1.46	1.46	

Date of Test
 $\rho = .002285$
 $C = .961$
 $A_F = 2.5 \text{ sq. ft.}$
 Gaps Open

All Pressures in Inches of Water unless Otherwise Indicated
 * Summation of Fan Entry and Diffusion Losses

Fan Speed	Volume Flow	Fan Axial Velocity			Total Pressure Downstream			Losses			Fan Total Pressure Rise			Air HP Corr.			Fan Power Required			Ψ			ϕ				
		Draft Gage	Flow (CFM)	$v_a = Q/A_f$	Velocity Pressure	Manometer No.	Average $P_{T_{down-stream}}$	0.73 x ⑦	$\Delta P_f = \textcircled{1}$	$\Delta P_{\textcircled{3} \frac{\text{in.}}{\text{ft}^2}}$	$\textcircled{1} \textcircled{12} \frac{5.2}{33,000}$	$\Delta P_{\textcircled{3} \frac{\text{in.}}{\text{ft}^2}}$	$\textcircled{1} \textcircled{12} \frac{5.2}{33,000}$	Torque in. # $\times 10^{-2}$	HP	Total	Corr. for Test Rate	Corr. for Standard Condition	⑯ / ⑯	$\Delta P_{\text{Fan}} \frac{\text{in.}}{\text{ft}^2}$	v_a/v_t	$\textcircled{15} / \textcircled{15}$	$\Delta P_{\text{Fan}} \frac{\text{in.}}{\text{ft}^2}$	v_a/v_t	$\textcircled{15} / \textcircled{15}$		
2200	1.0 ^a	6.0	3800	56.7	3.97	1.16	7.9	7.9	.55	8.45	8.75	12.1	6.80	6.10	22.3	23.1	52.5%	180	.360	.180	.222	.399	.63.2	.222			
2200	1.43	1.08	10850	72.4	3.05	1.54	8.1	8.5	.85	9.38	9.71	16.6	7.65	7.25	25.3	26.0	72.6	75.1	.392	.392	.256	.392	.75.1	.256			
2200	1.70	1.25	12520	83.5	8.02	1.52	7.5	7.5	1.10	9.22	9.54	18.8	7.60	7.20	25.1	25.3	75.1	75.1	.376	.376	.276	.376	.75.1	.276			
2200	1.98	1.36	13650	91.0	9.52	1.83	7.5	7.5	1.34	8.84	9.15	19.7	7.65	7.20	25.3	25.7	80.6	80.6	.366	.366	.302	.366	.80.6	.302			
2200	2.23	1.47	14750	98.4	11.15	2.14	7.0	7.0	1.03	8.59	8.89	20.7	7.50	7.10	24.8	25.7	80.8	80.8	.326	.326	.320	.326	.80.8	.320			
2200	2.85	1.56	15610	104.4	12.55	2.41	5.8	6.0	1.56	7.66	7.93	19.6	7.19	6.70	23.4	24.2	77.0	77.0	.246	.246	.232	.246	.77.0	.232			
2200	1.18	1.77	17710	118.1	16.55	3.08	3.5	3.5	3.53	5.78	5.98	16.7	6.40	6.00	26.9	27.3											
2400	1.73	9.00	60.6	6.23	.81	9.1	9.1	9.10	.59	9.69	10.03	14.4	7.90	7.50	28.6	29.5	48.8%	170	.346	.346	.212	.384	61.1	.212			
2400	1.14	1.12	11210	75.4	6.54	1.26	9.8	9.8	9.83	9.92	10.75	19.8	8.65	8.25	31.4	32.4	71.3	71.3	.393	.393	.254	.393	71.3	.254			
2400	1.70	1.36	13620	90.7	9.46	1.82	9.6	9.6	9.60	1.3	10.99	11.37	24.4	9.10	8.70	33.1	34.2	75.3	75.3	.371	.371	.277	.371	75.3	.277		
2400	2.33	1.48	14800	93.7	11.20	2.16	8.8	8.8	8.80	1.38	10.38	10.74	25.0	8.85	8.45	32.2	33.2	80.2	80.2	.360	.360	.293	.360	80.2	.293		
2400	2.69	1.60	16000	106.6	13.19	2.52	8.2	8.2	8.23	1.84	10.97	10.42	26.3	8.75	8.35	31.6	32.3	81.9	81.9	.328	.328	.323	.328	81.9	.323		
2400	3.25	1.75	17520	115.0	15.20	2.93	6.9	7.2	7.0	1.03	2.4	9.49	25.3	8.40	8.00	30.5	31.5	78.4	78.4	.360	.360						
2600	1.73	9.90	128.0	13.85	3.62	4.1	4.4	4.0	4.17	2.64	6.81	7.65	21.4	7.35	6.95	26.5	27.3										
2600	1.42	1.0150	67.7	5.26	1.01	10.7	10.7	10.7	.74	11.48	11.88	19.0	9.30	8.90	36.7	38.0	49.9%	175	.348	.348	.215	.392	61.9	.215			
2600	2.00	1.2500	83.4	8.00	1.54	1.8	1.8	1.8	1.8	1.2	1.2	1.2	12.92	13.37	26.3	30.8	42.6	42.6	.388	.388	.255	.388	70.8	.255			
2600	2.39	1.4000	98.7	11.20	2.15	1.2	1.2	1.2	1.2	1.7	1.7	1.7	12.70	12.63	32.3	32.3	42.1	42.1	.370	.370	.281	.370	75.7	.281			
2600	2.71	1.6250	115.2	13.50	2.60	10.3	10.3	10.3	1.03	1.90	1.90	1.90	12.63	12.53	32.3	32.3	42.6	42.6	.370	.370	.281	.370	75.7	.281			
2600	3.16	17200	115.30	2.94	2.94	2.94	2.94	2.94	2.94	2.15	2.15	2.15	11.78	12.19	33.2	33.2	42.6	42.6	.358	.358	.323	.358	75.7	.323			
2600	3.97	18600	124.0	17.70	3.40	4.8	4.8	4.8	4.87	2.48	2.48	2.48	10.65	11.02	32.3	32.3	42.6	42.6	.343	.343	.323	.343	76.4	.323			
		20870	139.2	22.34	4.29	4.29	4.29	4.29	4.87	3.13	4.87	4.87	8.00	8.28	27.2	27.2	38.8	38.8	.354	.354							

All Pressures in Inches of Water unless otherwise indicated
* Summation of Fan Entry and Diffusion Losses

TABLE A-13

Date of Test

2 = .002297
J = .966
A_F = 2.5 Sq. Ft.

Gaps Open

Fan Speed RPM	Volume Flow Corrected Indicated	Fan Axial Velocity						Total Pressure Downstream	Losses *	Fan Total Pressure Rise	Air HP Corr.	Fan Power Required			Efficiency η	
		Draft Gage Flow (CFH)	V _a Q/A _F	Velocity Pressure	Manometer No.	Average P _T in. Hg. in. H ₂ O	10 20 22 -5					ρ = .002349	σ = .936	ΔP_f x 7 ①	$\Delta P_{corr.}$ ③ x 6	
		Psi	In. H ₂ O	20	22					Total	Corr. for Tare	Corr. for Standard Condition				
2200	.81	.32	9700	64.7	4.91	.94	9.0	9.0	.69	.981	10.01	16.3	.60	7.20	25.4	.404
2200	1.19	1.20	11600	77.3	7.02	1.35	8.9	8.9	.69	10.01	16.3	7.50	7.50	26.2	.198	
2200	1.55	1.57	13100	87.3	8.95	1.72	9.3	9.2	.93	10.69	22.1	8.05	8.05	28.1	.412	
2200	1.75	1.77	13900	92.7	10.1	1.94	9.1	9.1	.92	10.55	23.3	8.15	8.15	28.4	.269	
2200	2.70	2.73	17350	115.7	15.7	3.02	5.3	5.3	.60	7.70	21.0	7.45	7.45	24.9	.355	
A																
22	1.3	.86	9250	66.3	5.31	1.02	8.5	8.9	.74	9.47	14.8	7.50	7.10	24.4	.390	
2200	1.39	1.27	11850	79.0	7.56	1.35	9.2	9.2	.96	10.08	18.8	8.05	7.65	26.2	.263	
2200	1.37	1.33	14500	96.7	11.30	2.17	9.7	9.5	.58	10.00	22.8	8.70	8.20	28.5	.411	
2200	1.31	2.27	15300	105.3	13.45	2.58	7.6	7.6	.88	9.55	23.4	8.50	8.10	28.3	.386	
2400	1.84	.85	9850	65.7	5.07	.97	10.2	10.3	.71	10.94	11.07	8.55	8.15	31.4	.382	
2400	1.86	1.86	12250	81.7	7.84	1.86	10.6	10.2	.73	11.10	11.47	22.1	9.55	33.7	.184	
2400	1.84	2.09	14250	95.0	10.6	2.04	10.1	10.2	.70	11.10	12.59	28.6	10.25	38.5	.229	
2400	2.07	2.26	15150	101.0	12.0	1.0	0.7	0.8	.73	10.73	12.60	30.1	10.10	37.0	.440	
2400	2.26	2.66	15900	106.0	13.12	2.54	10.1	10.2	.73	10.13	11.98	32.4	9.70	37.4	.267	
2400	2.63	3.27	17100	114.0	15.3	2.94	8.7	8.9	.85	10.95	11.08	29.9	9.65	36.8	.284	
2400	3.03		18400	122.7	17.7	3.40	6.1	6.1	.20	2.48	8.68	8.78	25.5	8.15	35.2	.298
2400	1.07	1.05	10900	72.7	6.40	1.23	10.7	10.7	.70	10.70	11.50	1.018	$\sigma = .002421$	24.4	.390	
2400	1.47	1.44	12650	84.0	8.54	1.54	10.8	10.7	.73	11.20	11.93	11.72	23.3	9.50	32.2	.204
2600	1.08	1.09	11100	74.0	6.43	1.24	12.5	12.4	.40	12.40	12.46	13.30	10.35	9.95	41.5	.395
2600	1.65	2.28	12500	90.7	9.52	1.83	12.4	12.4	.37	12.37	12.34	13.71	23.5	11.00	44.2	.192
2600	2.25	2.40	15850	105.7	13.1	2.52	12.7	12.9	.83	12.83	14.67	14.85	32.7	11.50	47.4	.233
2600	2.47	2.64	16100	108.7	13.9	2.67	12.1	12.1	.10	12.10	12.95	14.05	36.5	11.40	48.0	.274
2600	2.60	3.07	17150	114.3	15.3	2.95	11.7	11.8	.73	11.73	12.51	14.05	38.0	11.45	45.5	.282
2600	3.64	3.68	18500	123.3	17.3	3.44	9.2	9.4	.10	2.51	12.74	12.89	37.6	11.15	44.3	.376
2600	1.27	1.27	11800	78.7	1.44	1.44	12.6	12.6	1.60	1.05	13.65	13.40	1.018	$\sigma = .002421$	24.4	.393
2600	1.81	1.78	13950	93.0	10.7	2.06	12.8	12.6	1.67	1.50	14.17	13.91	1.018	$\sigma = .002421$	44.2	.204

Date of Test
 ρ = Nuted
 A_F = 2.5 Sq. Ft.
 Gaps Sealed

All Pressures in Inches of Water unless Otherwise Indicated
 * Summation of Fan Entry and Diffusion Losses

1	2	3	4	5	6	7	8	9	10	11	12	13	14	15	16	17	18	19	20	21	22							
Fan Speed	Volume Flow	Fan Axial Velocity									Total Pressure Downstream			Losses			Fan Total Pressure Rise			Air HP Corr.			Fan Power Required			Efficiency	Ψ	Q
27% Craft Gage	Flow (CFM)	V_a^2 Q/A_f	Velocity Pressure			Manometer No. P Down-stream			0.73 x ①			$\Delta P_{corr} = \frac{①}{③}$			④ ⑨ 5.2 33,000			In. # x 10^-2			HP							
Indicated Corrected			PSF	In. H ₂ O	20	22	25									Total	Corr. for Tare	Test	Corr. for Standard Condition									
2200	6.5	.65	8600	57	3.9	1.75	8.3	8.3	8.3	8.3	8.3	.55	8.85	8.8	11.9	7.65	7.25	25.3	25.2	47.0%	.363	.175						
2200	9.7	.97	10500	70	5.9	1.13	8.3	8.3	8.3	8.3	8.3	.82	9.12	9.1	15.1	7.35	7.55	26.2	26.2	57.4	.374	.215						
2200	1.43	1.49	12800	85	8.6	1.65	8.6	8.7	8.7	8.7	8.7	.20	9.87	9.9	19.9	8.80	8.40	29.3	29.3	67.9	.405	.261						
2200	1.69	1.70	13600	91	9.9	1.90	8.4	8.4	8.4	8.4	8.4	.39	9.92	9.9	21.3	8.90	8.50	29.7	29.6	71.7	.407	.279						
2200	1.92	1.93	14500	97	12.9	2.15	8.1	8.1	8.1	8.1	8.1	.57	9.57	9.5	22.9	8.90	8.40	29.0	29.2	75.8	.397	.239						
2200	2.33	2.49	15700	104	12.9	2.48	7.4	7.4	7.4	7.4	7.4	.81	9.28	9.3	22.9	8.90	8.30	29.0	28.9	79.0	.381	.235						
2200	2.43	2.49	16600	110	14.5	2.78	6.9	6.9	6.9	6.9	6.9	.03	9.03	9.0	23.8	8.80	8.40	29.3	29.2	81.2	.371	.233						
2200	3.18	3.19	18700	125	18.6	3.58	3.7	4.2	3.8	3.90	3.90	.61	6.51	6.5	19.2	7.60	7.20	25.1	25.0	76.4	.267	.383						
2400	1.76	1.76	9300	62	4.6	.88	9.5	9.6	9.6	9.57	9.6	.64	10.2	10.2	15.0	8.95	8.55	32.6	32.5	46.0%	.352	.174						
2400	1.81	1.82	11400	94	6.9	1.32	9.0	9.0	9.0	9.0	9.0	.97	10.9	10.9	19.6	9.55	9.15	34.8	34.7	56.4	.376	.213						
2400	1.98	1.99	14700	98	11.4	2.00	10.5	10.5	10.5	10.43	10.43	.46	11.9	11.9	26.4	10.55	10.15	38.6	38.6	68.3	.410	.263						
2400	2.30	2.30	15900	106	13.4	2.20	10.7	10.7	10.7	10.7	10.7	.61	11.7	11.7	27.1	10.45	10.05	38.3	38.3	70.8	.403	.260						
2400	2.66	2.67	17000	114	15.6	3.05	8.8	8.8	8.8	8.73	8.73	.88	11.6	11.6	29.9	10.55	10.15	38.7	38.6	75.1	.400	.298						
2400	2.92	2.93	18000	120	17.1	3.28	8.0	8.0	8.0	8.1	8.1	.40	10.5	10.5	30.0	10.55	10.15	38.7	38.6	77.5	.383	.321						
2400	3.70	3.71	20200	135	21.7	4.17	4.4	4.4	4.5	4.63	4.63	.05	7.7	7.7	24.4	9.05	8.65	33.0	32.9	74.0	.265	.379						
2600	1.76	1.76	9300	62	4.6	.88	9.5	9.6	9.6	9.57	9.6	.64	10.2	10.2	15.0	8.95	8.55	32.6	32.5	46.0%	.352	.174						
2600	1.81	1.82	11400	94	6.9	1.32	9.0	9.0	9.0	9.0	9.0	.97	10.9	10.9	19.6	9.55	9.15	34.8	34.7	56.4	.376	.213						
2600	1.98	1.99	14700	98	11.4	2.00	10.5	10.5	10.5	10.43	10.43	.46	11.9	11.9	26.4	10.55	10.15	38.6	38.6	68.3	.410	.263						
2600	2.30	2.30	15900	106	13.4	2.20	10.7	10.7	10.7	10.7	10.7	.61	11.7	11.7	27.1	10.55	10.15	38.6	38.6	70.8	.403	.260						
2600	2.66	2.67	17000	114	15.6	3.05	8.8	8.8	8.8	8.73	8.73	.88	11.6	11.6	29.9	10.55	10.15	38.7	38.6	75.1	.400	.298						
2600	2.92	2.93	18000	120	17.1	3.28	8.0	8.0	8.0	8.1	8.1	.40	10.5	10.5	30.0	10.55	10.15	38.7	38.6	77.5	.383	.321						
2600	3.70	3.71	20200	135	21.7	4.17	4.4	4.4	4.5	4.63	4.63	.05	7.7	7.7	24.4	9.05	8.65	33.0	32.9	74.0	.265	.379						
2600	1.92	1.92	10300	68	5.5	1.06	11.2	11.2	11.2	11.2	11.2	.20	11.97	12.0	12.0	11.50	11.10	45.8	45.7	52.5	.351	.176						
2600	1.36	1.37	12300	82	8.0	1.54	11.5	11.5	11.5	11.5	11.5	.53	12.5	12.5	12.5	11.75	11.35	49.0	48.9	67.4	.262	.212						
2600	2.10	2.11	13200	101	12.2	2.34	12.0	12.0	12.0	12.0	12.0	.03	12.03	12.0	12.0	12.0	11.85	50.0	49.9	72.0	.403	.281						
2600	2.40	2.41	16300	103	14.2	2.73	12.3	12.3	12.3	12.3	12.3	.53	12.59	12.59	12.59	12.59	12.50	50.0	49.9	75.1	.395	.298						
2600	2.70	2.71	17300	115	15.8	3.03	12.1	12.1	12.1	12.1	12.1	.27	12.51	12.51	12.51	12.51	12.45	50.0	49.9	77.5	.392	.321						
2600	3.15	3.16	18700	124	18.4	3.53	12.3	12.3	12.3	12.3	12.3	.04	12.58	12.58	12.58	12.58	12.50	50.0	49.9	80.0	.360	.329						
2600	3.29	3.30	19100	127	19.5	3.69	12.5	12.5	12.5	12.5	12.5	.52	12.69	12.69	12.69	12.69	12.60	50.0	49.9	82.5	.360	.329						
2600	4.43	4.43	22000	146	25.4	4.88	5.2	5.2	5.2	5.2	5.2	.56	12.54	12.54	12.54	12.54	12.50	50.0	49.9	85.0	.265	.379						

Date of Test

All trademarks are the property of their respective owners.

2.5 Sq. Ft.

TABLE A-15

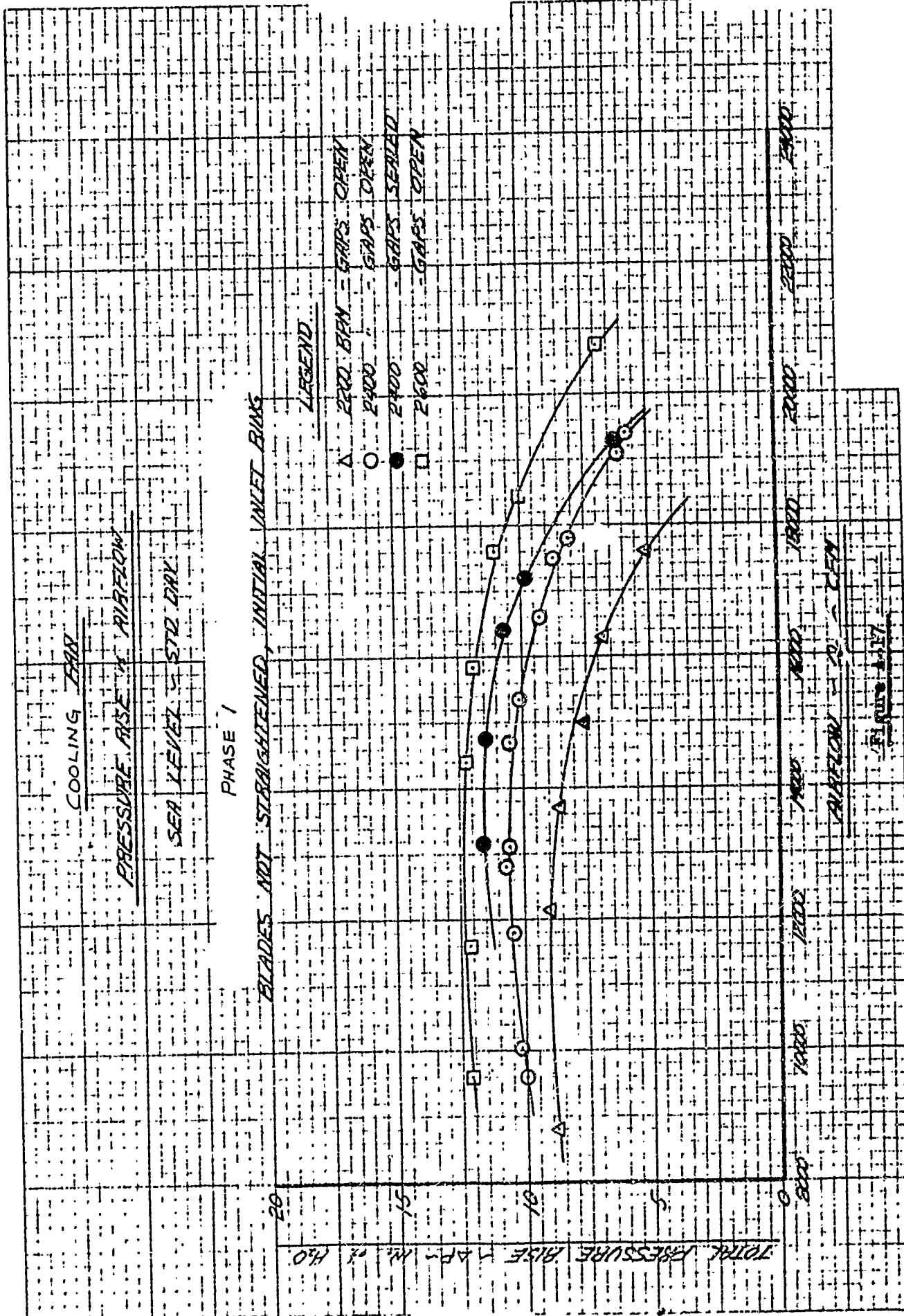
1	2	3	4	5	6	7	8	9	10	11	12	13	14	15	16	17	18	19	20	21	22					
Fan Speed	Fan Axial Velocity				Total Pressure Downstream				Fan Total Pressure Rise				Air HP Corr.				Fan Power Required				Efficiency		Ψ	ϕ		
RPH	Volume Flow		Flow (CFH)		Velocity Pressure		Manometer No.		Aero. P _t Down-stream		Losses *		$0.73 \times \text{⑦}$		$\Delta P_f^2 / \text{⑫}$		$\frac{\text{⑪} \text{⑬}}{33,000} \text{ s}^2$		In. #: 10-2		HP		$\text{⑯} / \text{⑯}$		$\Delta P_{\text{Fan}} / \frac{1}{2} \rho v_t^2$	v_a/v_t
	Draft Gage Indicated	Corrected			PSF	In. H ₂ O	20	22	25																	
2200	70	.70	8900	.59	4.2	.81	9.0	9.1	9.0	9.03	.59	.62	.62	13.6	8.75	8.35	29.1	46.7%	.395	.181						
2200	98	.98	10600	.70	5.9	1.13	9.2	9.3	9.4	9.23	.82	.05	10.4	16.7	8.10	8.10	28.3	59.0	.413	.215						
2200	1.32	1.32	12100	.80	7.0	1.14	9.3	9.3	9.3	9.33	.82	.05	10.4	19.8	9.10	8.70	30.4	65.0	.428	.245						
2200	1.57	1.57	13000	.87	9.1	1.75	9.3	9.3	9.3	9.30	1.28	.05	10.6	21.9	9.15	8.85	30.9	70.9	.434	.267						
2200	1.79	1.79	14000	.93	10.4	2.00	9.8	10.1	10.1	9.97	1.46	1.14	1.14	25.3	10.00	9.55	9.55	33.5	75.5	.469	.285					
2200	2.11	2.11	15200	1.01	12.2	2.34	9.5	9.4	9.4	9.43	1.71	1.43	1.43	22.9	8.85	8.45	8.45	29.5	77.6	.457	.310					
2200	2.73	2.73	17000	1.17	16.4	3.15	5.9	6.2	5.8	5.97	2.30	1.76	1.76	20.6	8.25	7.85	7.85	27.4	75.3	.340	.359					
2200	3.29	3.29	19100	1.27	19.2	3.69	4.0	4.1	4.17	6.87	2.70	2.70	2.70	20.6	8.25	7.85	7.85	27.4	75.3	.282	.390					
2400	.74	.74	9200	61	4.5	.86	10.3	10.3	10.3	10.30	.63	1.93	1.93	15.8	15.8	9.25	9.25	33.8	46.7%	.377	.172					
2400	.83	.83	9800	65	5.5	.97	10.6	10.6	10.6	10.63	.70	1.32	1.32	17.4	17.4	9.60	9.60	35.0	49.7	.391	.183					
2400	1.14	1.14	11300	.75	6.8	1.30	0.8	0.8	0.8	10.7	.77	.95	.95	20.9	20.9	10.95	10.95	35.8	55.7	.404	.240					
2400	1.53	1.53	13000	.86	8.9	1.71	0.8	0.8	0.8	10.9	.73	1.25	1.25	24.7	12.1	10.35	10.35	36.7	63.8	.417	.243					
2400	1.83	1.83	14200	.94	10.6	2.04	1.0	0.8	0.8	10.83	1.49	1.22	1.22	27.5	12.3	10.5	10.5	37.4	69.9	.425	.265					
2400	2.16	2.16	15400	1.03	12.6	2.42	1.8	1.8	1.8	12.0	1.87	1.76	1.76	33.6	13.6	11.80	11.80	43.4	76.0	.470	.285					
2400	2.47	2.47	16500	1.10	14.4	2.77	1.0	1.0	1.0	11.0	2.02	1.92	1.92	33.8	13.0	11.60	11.60	42.7	79.0	.449	.309					
2400	2.53	2.53	18000	1.32	19.8	3.92	6.9	6.9	6.9	7.00	2.91	2.91	2.91	30.8	8.9	8.9	8.9	36.5	60.0	.348	.390					
2400	3.94	3.94	20800	1.39	23.0	4.42	4.7	4.7	4.7	4.93	3.23	8.16	8.16	26.7	9.55	9.15	9.15	34.8	66.9	.281	.390					
2600	1.00	1.00	10700	71	6.0	1.15	12.6	12.6	12.5	12.57	.84	13.41	13.41	22.5	11.50	11.10	11.10	45.8	45.8	.393	.184					
2600	1.36	1.36	12200	81	7.0	1.20	12.7	12.8	12.8	12.7	1.11	1.34	1.34	22.5	11.55	12.15	12.15	47.7	55.6	.406	.210					
2600	1.84	1.84	14200	95	10.3	2.07	1.27	1.27	1.27	12.8	1.51	1.38	1.38	32.0	12.5	12.5	12.5	50.2	63.6	.419	.246					
2600	2.19	2.19	15500	103	12.7	2.44	12.8	12.8	12.8	12.8	1.78	1.98	1.98	35.6	14.6	12.35	12.35	51.0	69.8	.428	.267					
2600	2.54	2.54	16800	112	15.1	1.51	1.51	1.51	1.51	13.8	1.52	1.72	1.72	42.3	13.65	13.25	13.25	51.7	77.3	.468	.290					
2600	2.90	2.90	17900	119	17.0	3.26	12.9	12.9	12.9	12.93	2.38	1.53	1.53	43.2	15.3	13.5	13.5	52.3	80.0	.447	.303					
2600	4.18	4.18	21400	143	24.3	4.68	8.0	8.0	8.0	8.07	3.42	1.59	1.59	39.0	12.0	11.80	11.80	48.7	80.2	.340	.370					
2600	4.53	4.53	22200	148	26.1	5.02	6.0	6.0	5.4	5.57	3.66	9.23	9.23	32.3	10.75	10.35	10.35	42.7	75.6	.271	.383					

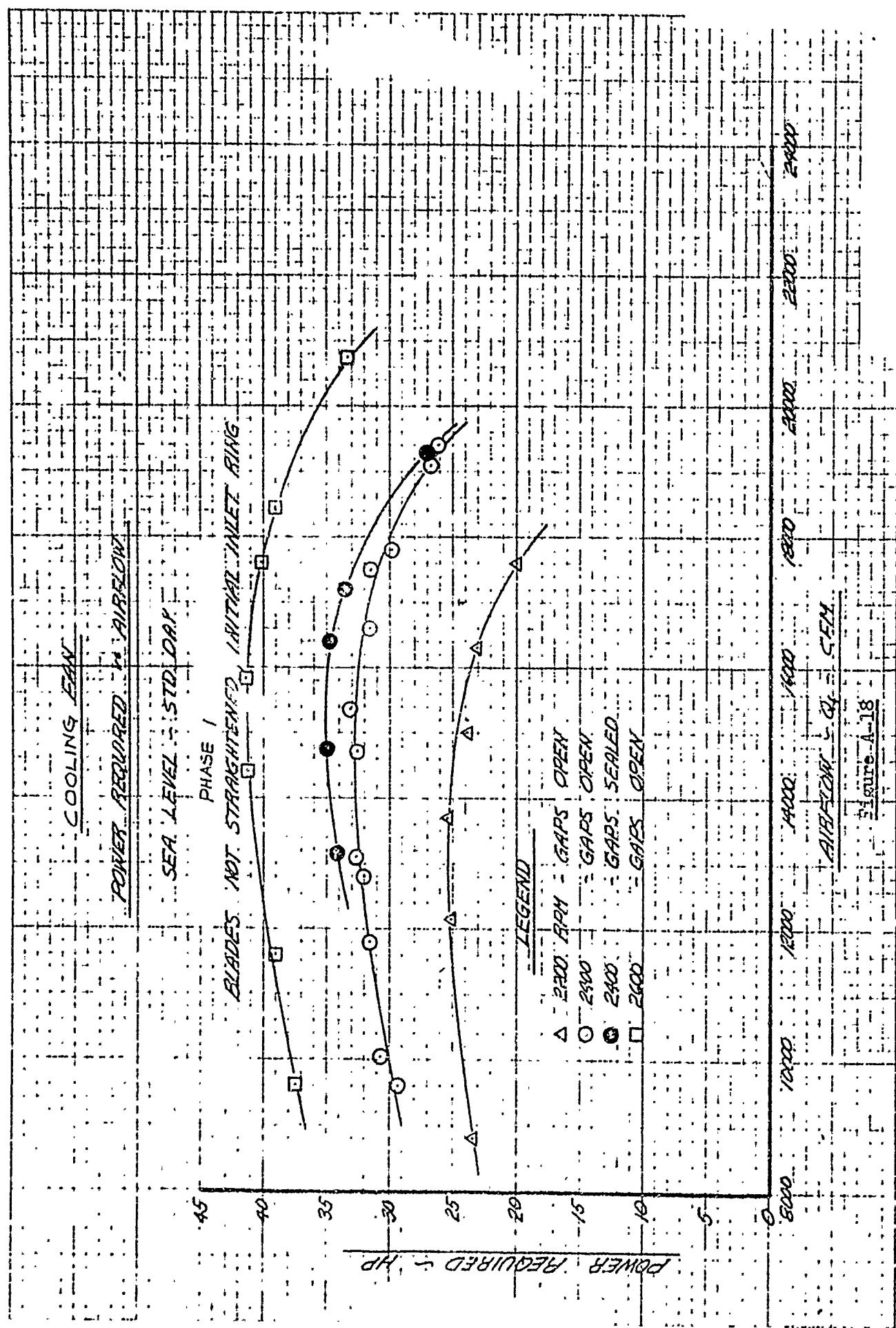
A - 1 - 49

Date of Test
 $\rho = 0.03380$
 $A_t = 1.00$
 $A_t = 2.5 \text{ Sq. Ft.}$
 Gaps Sealed

All Pressures in Inches of Water unless Otherwise Indicated
 * Summation of Fan Entry and Diffusion Losses

TABLE A-16





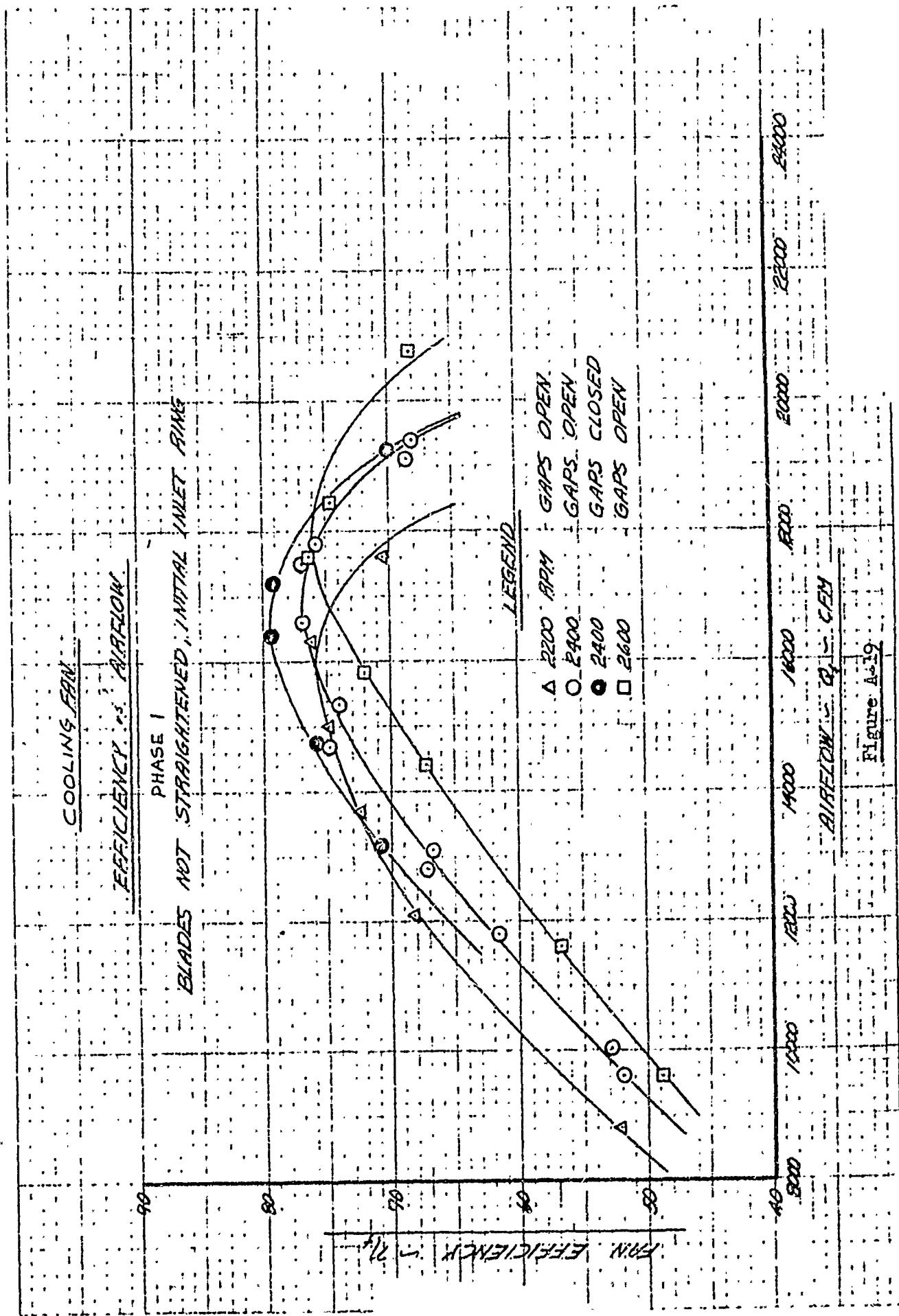
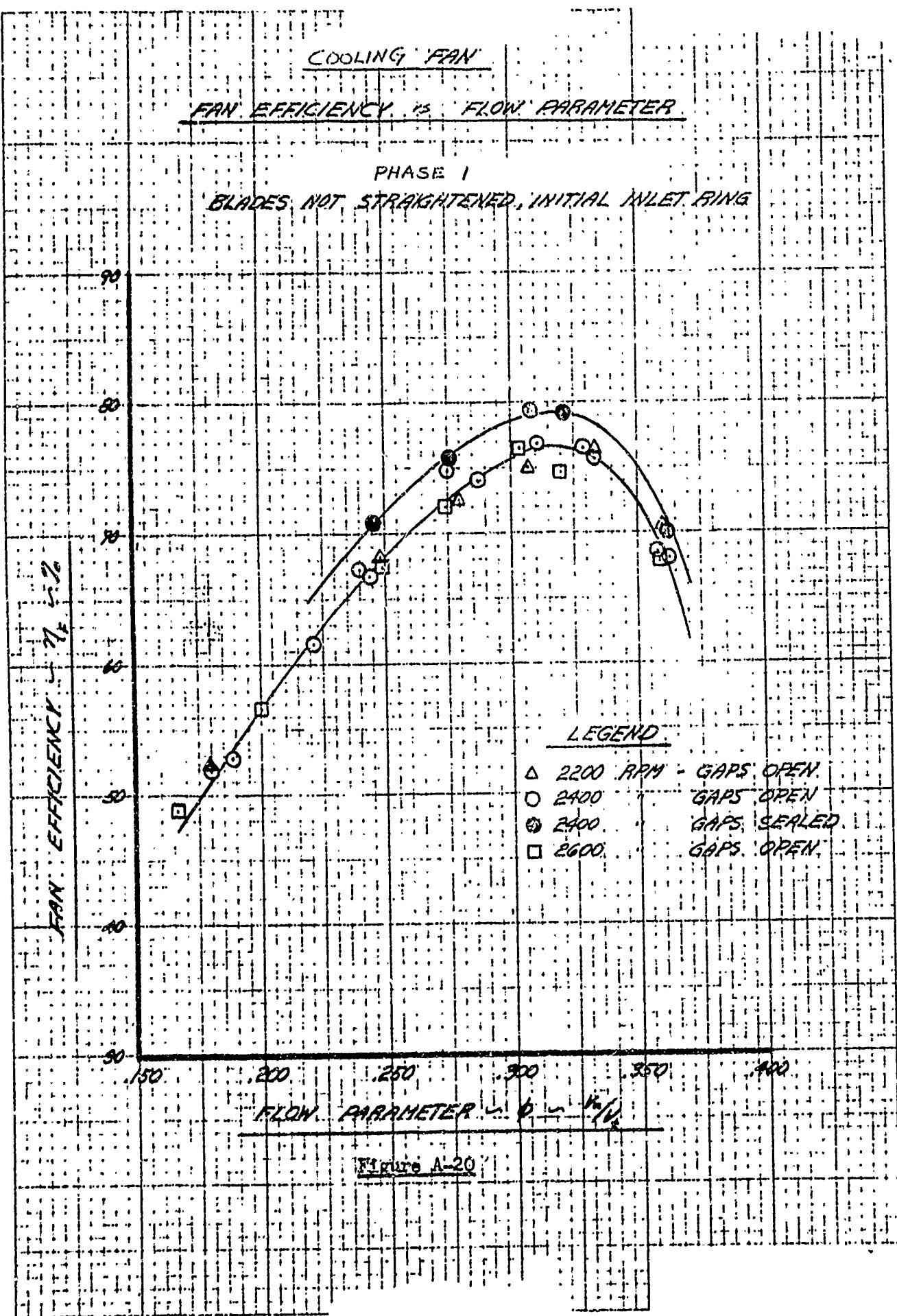
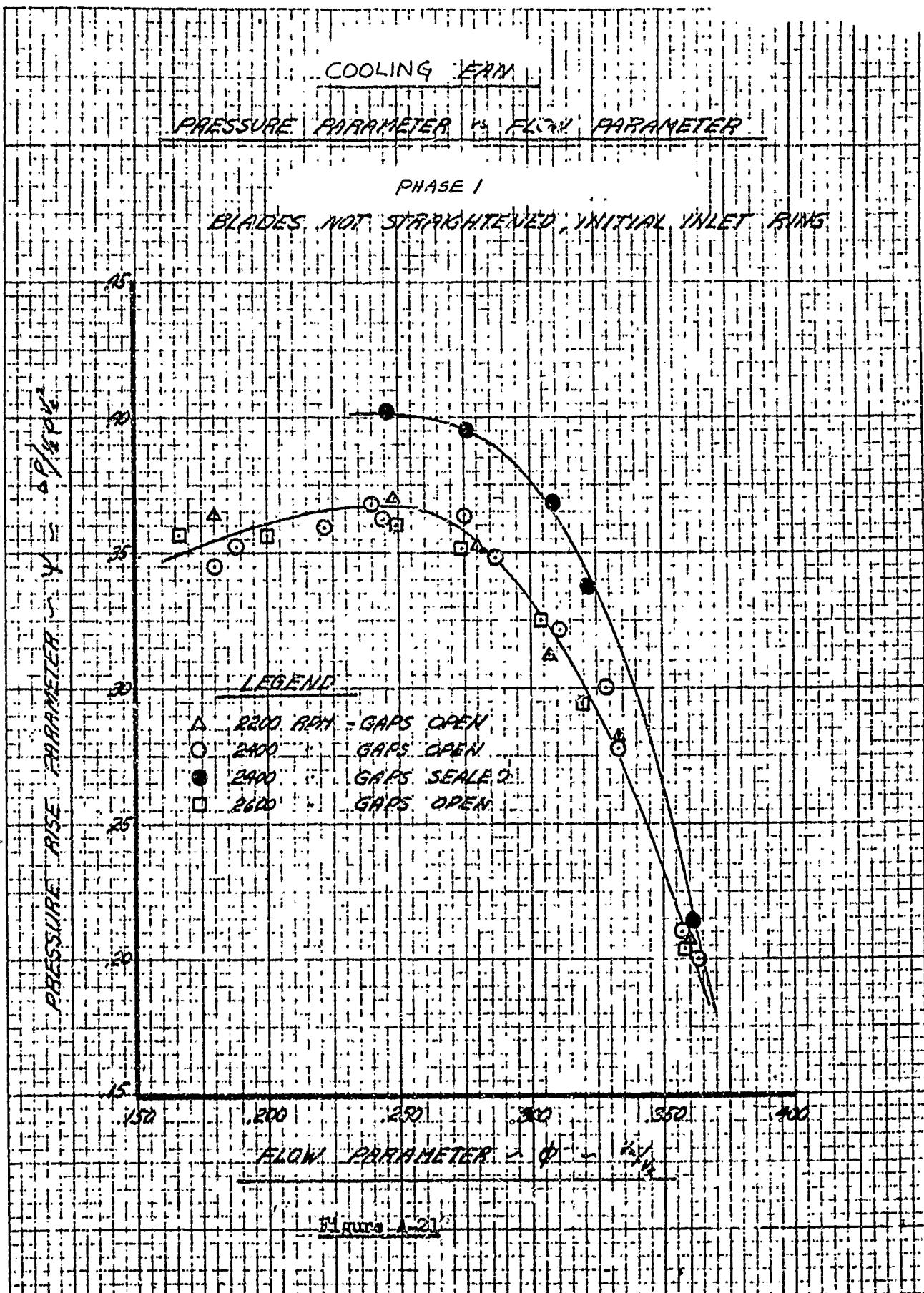
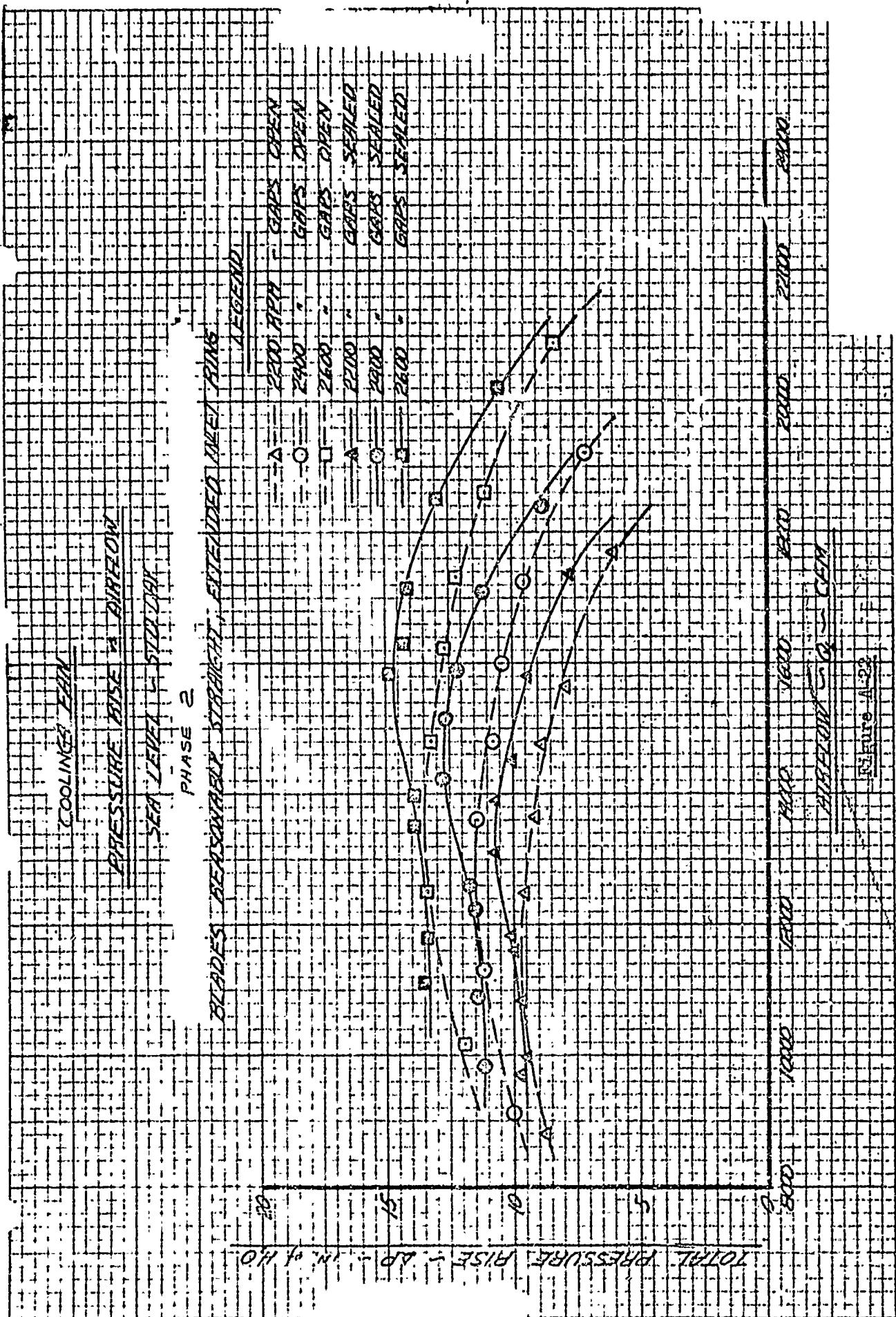
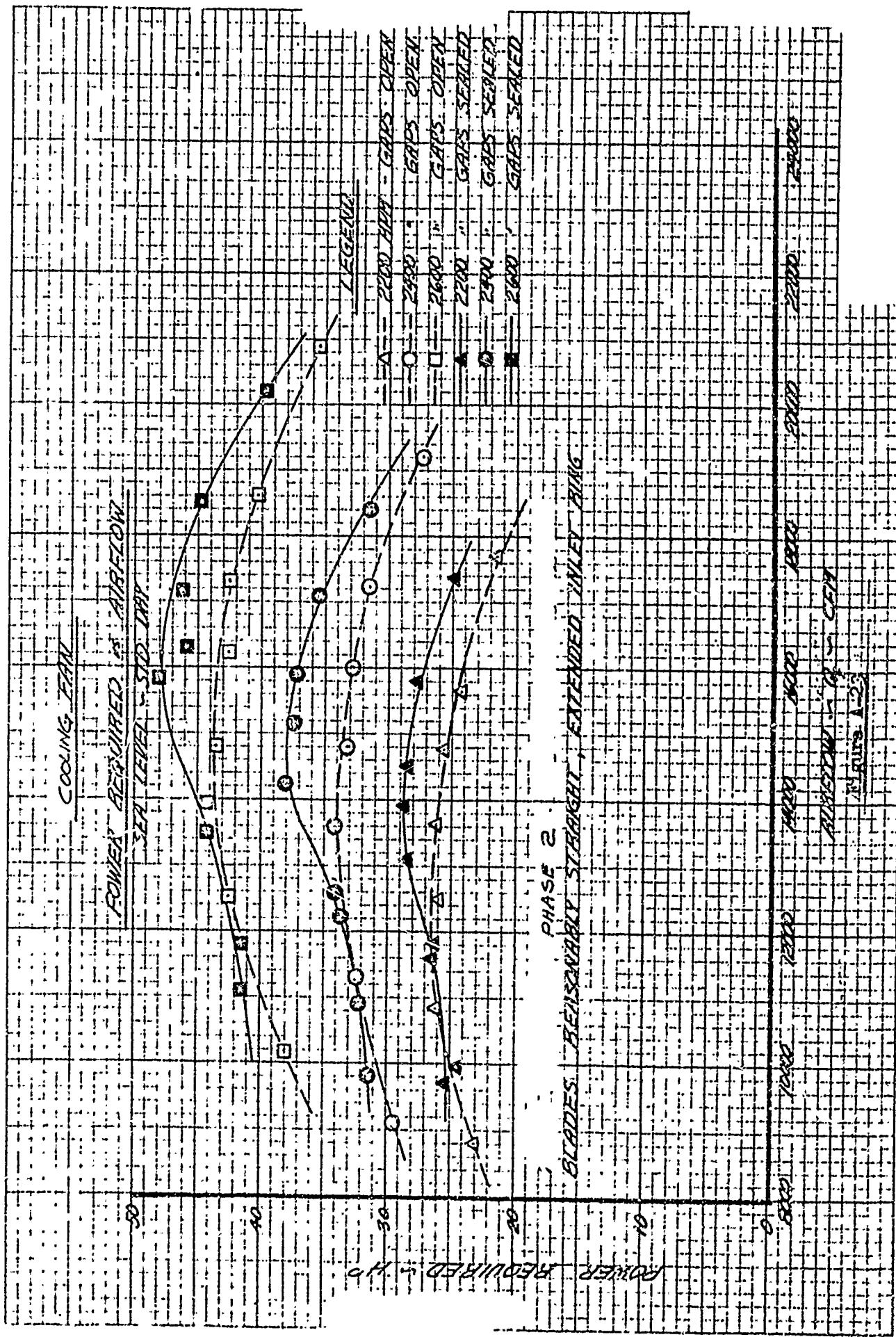


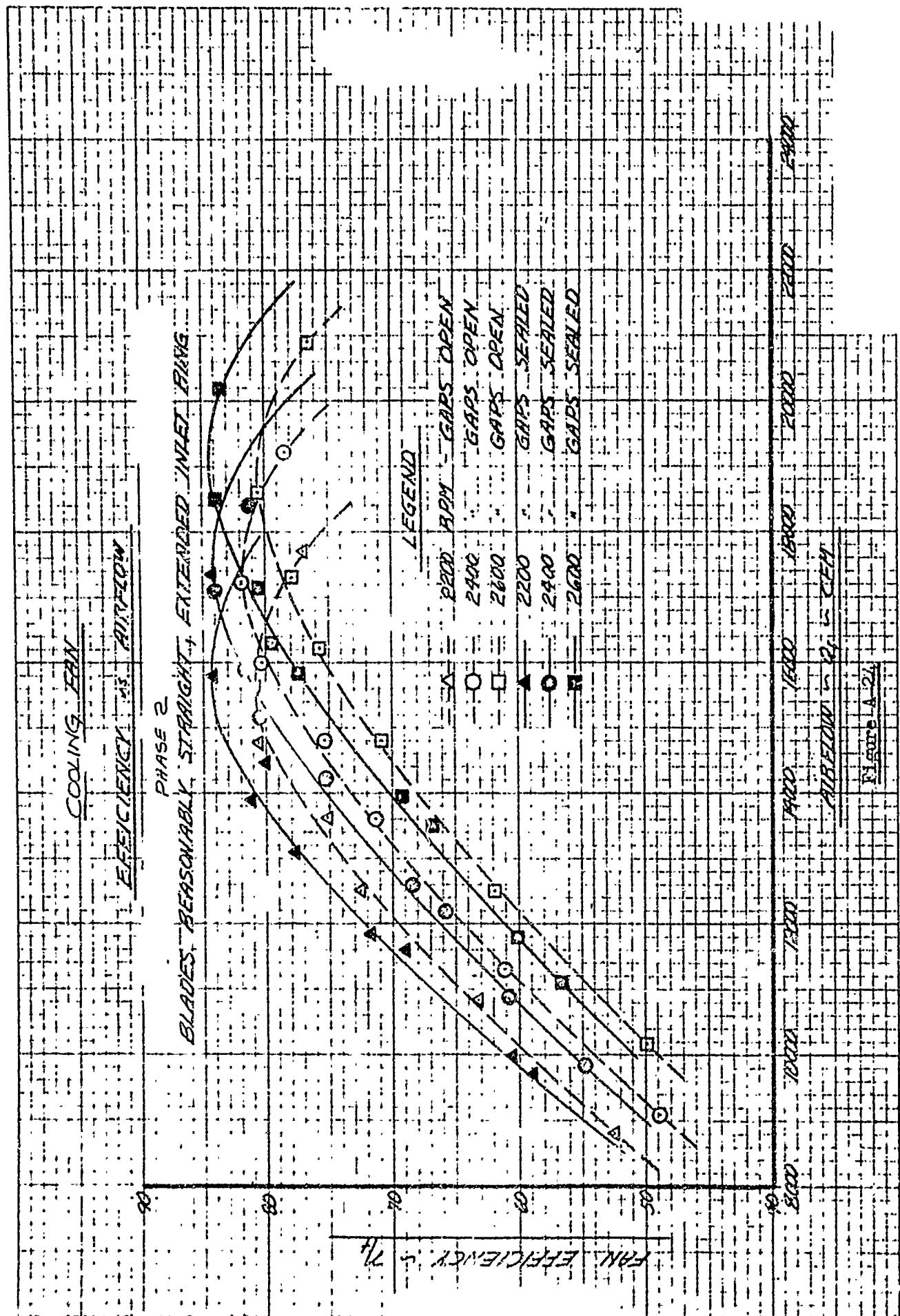
Figure A-12

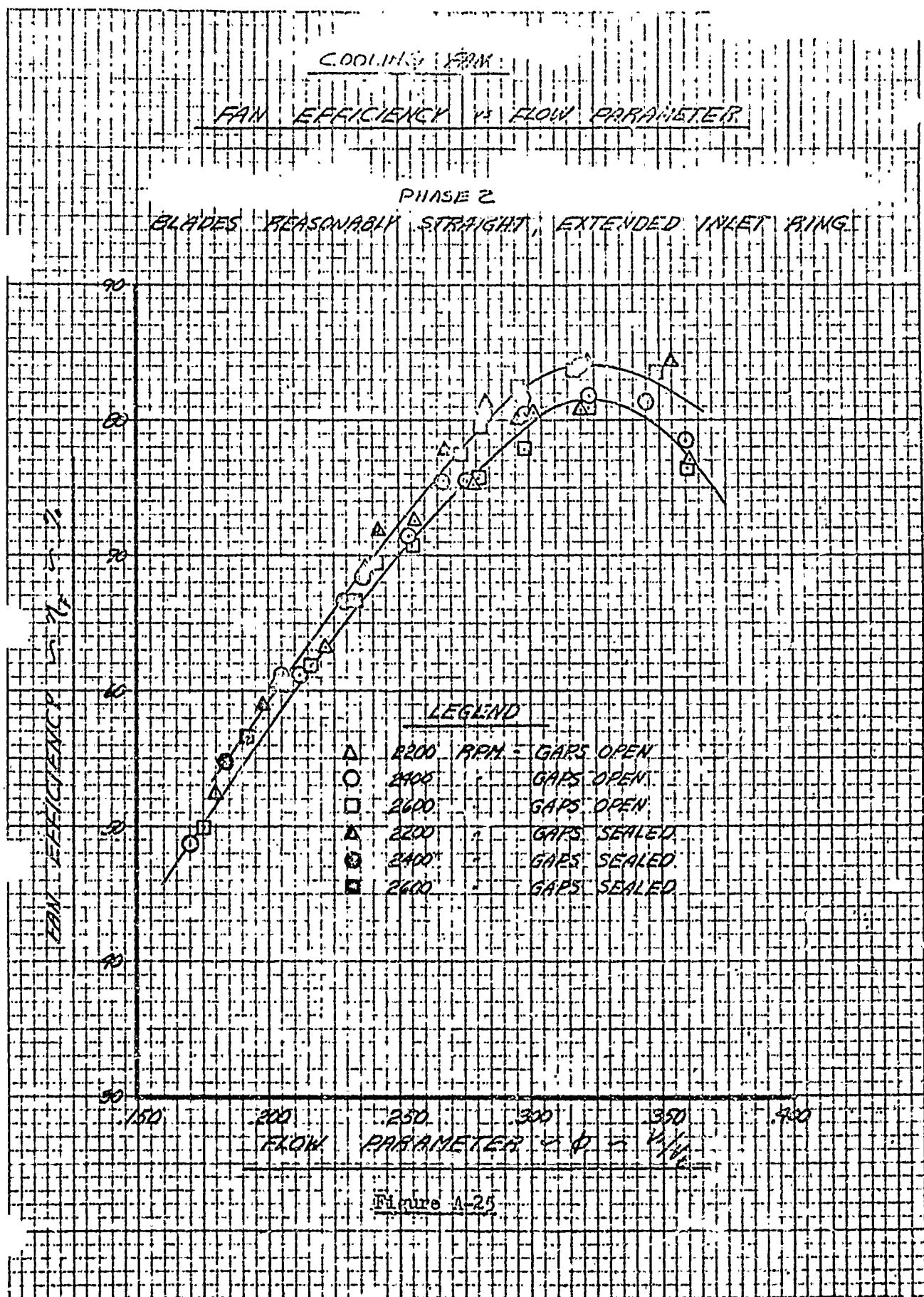


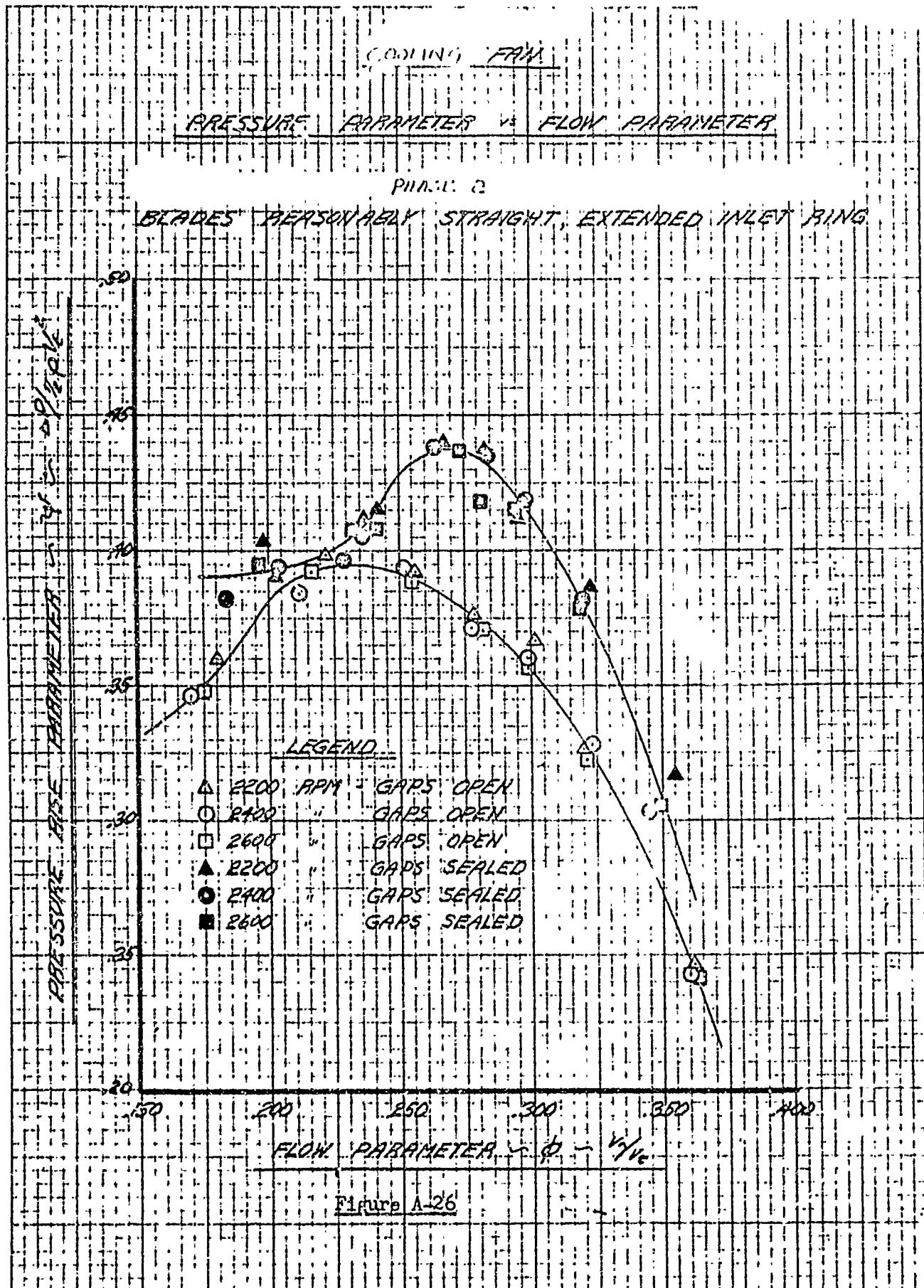


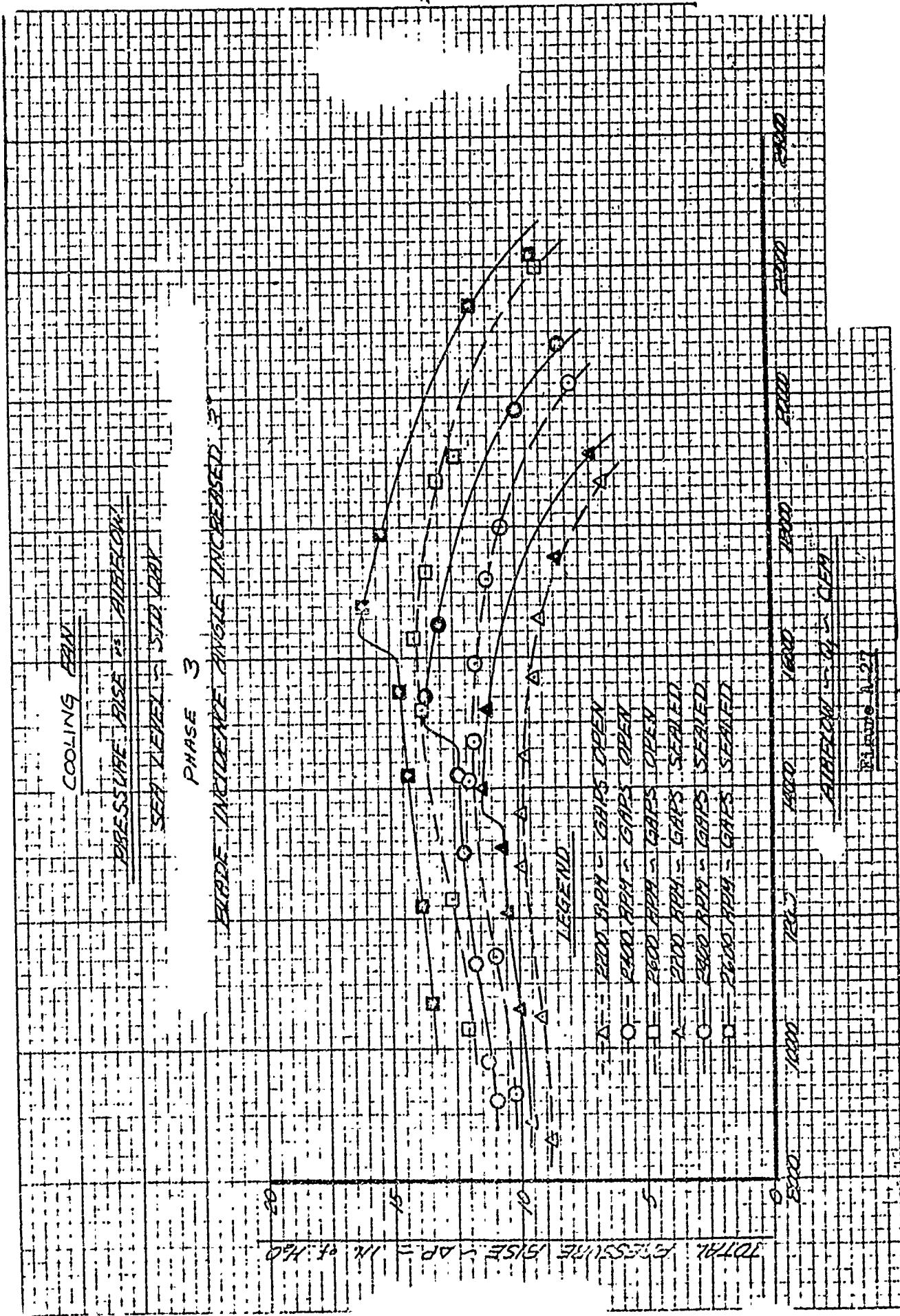


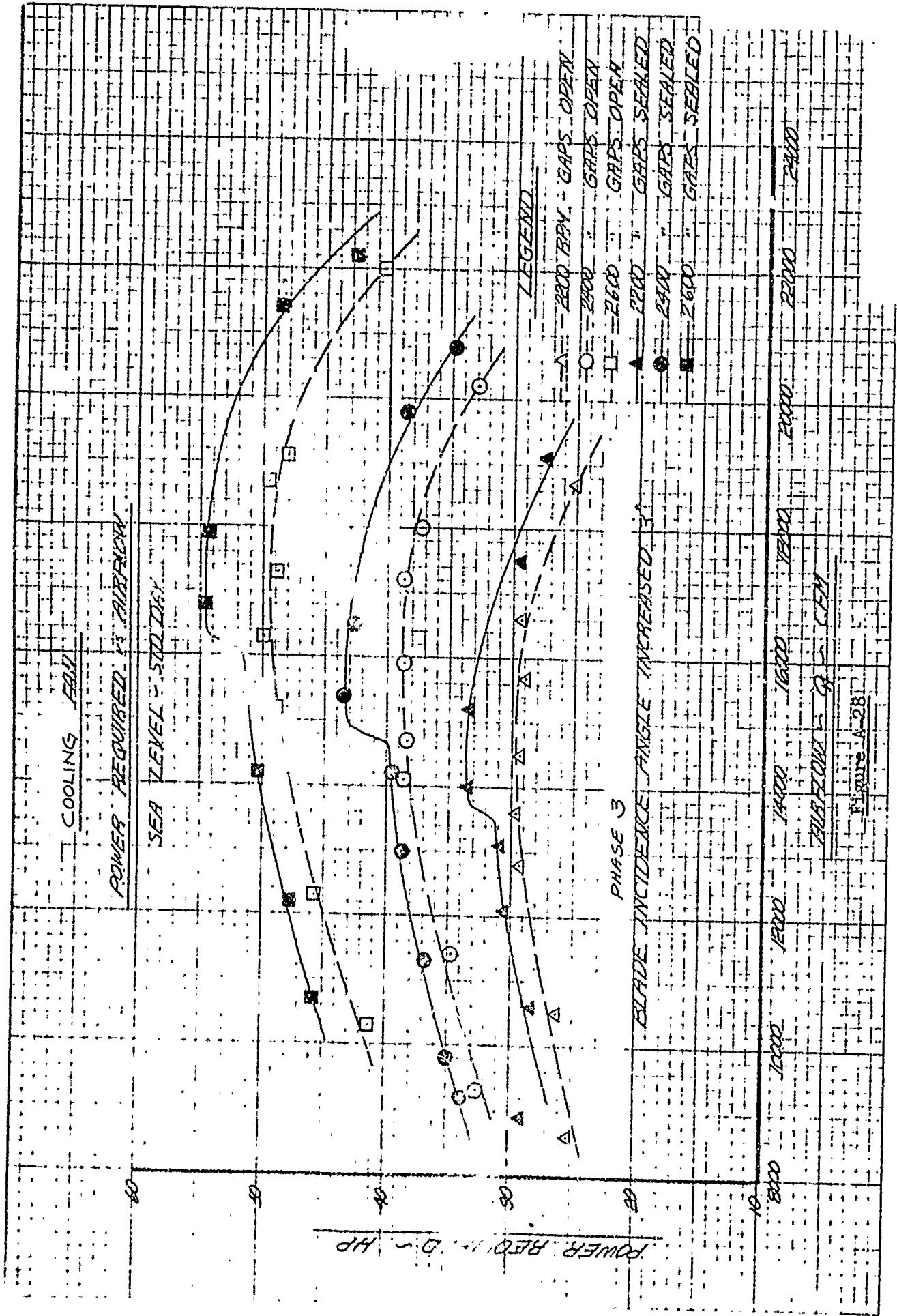


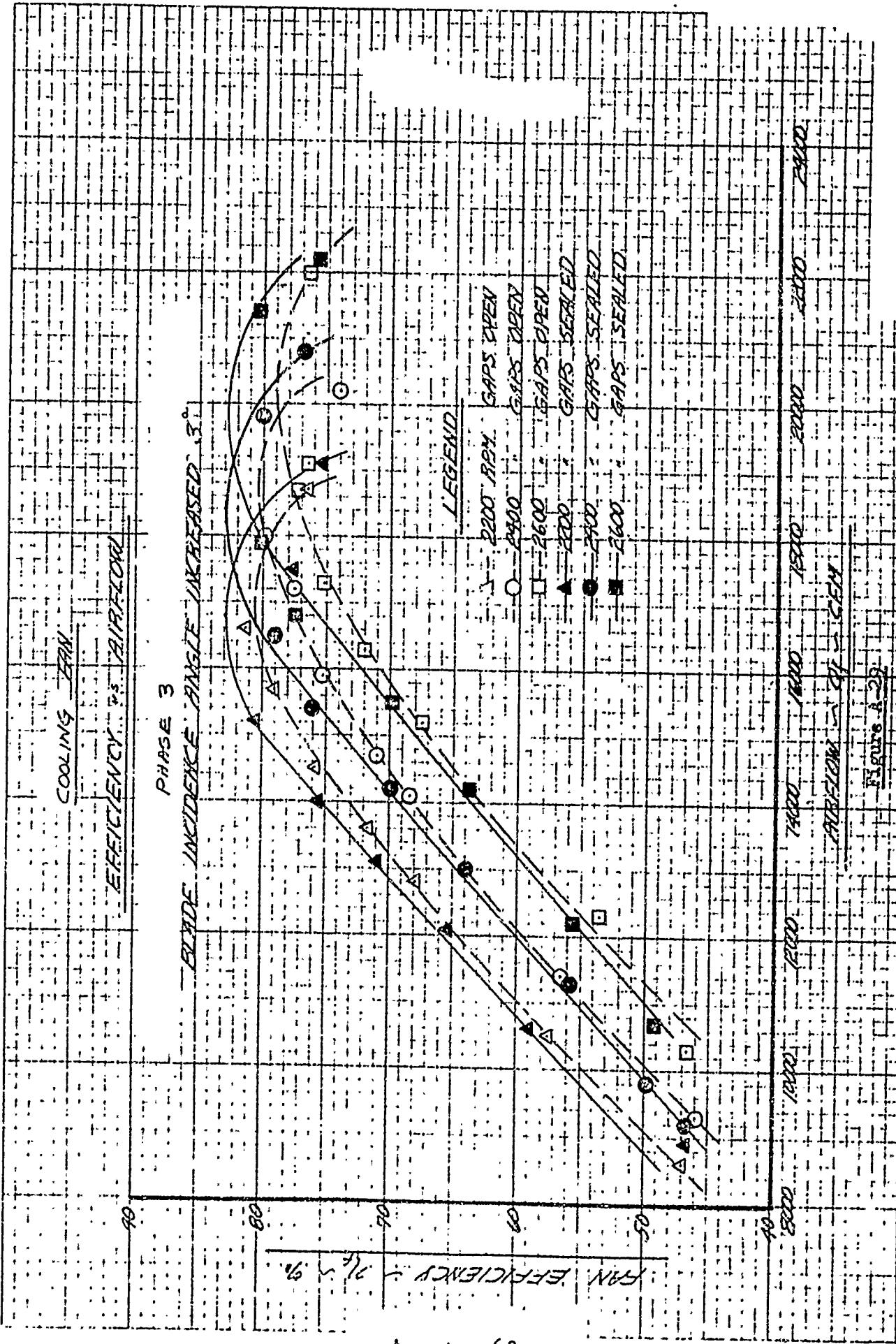


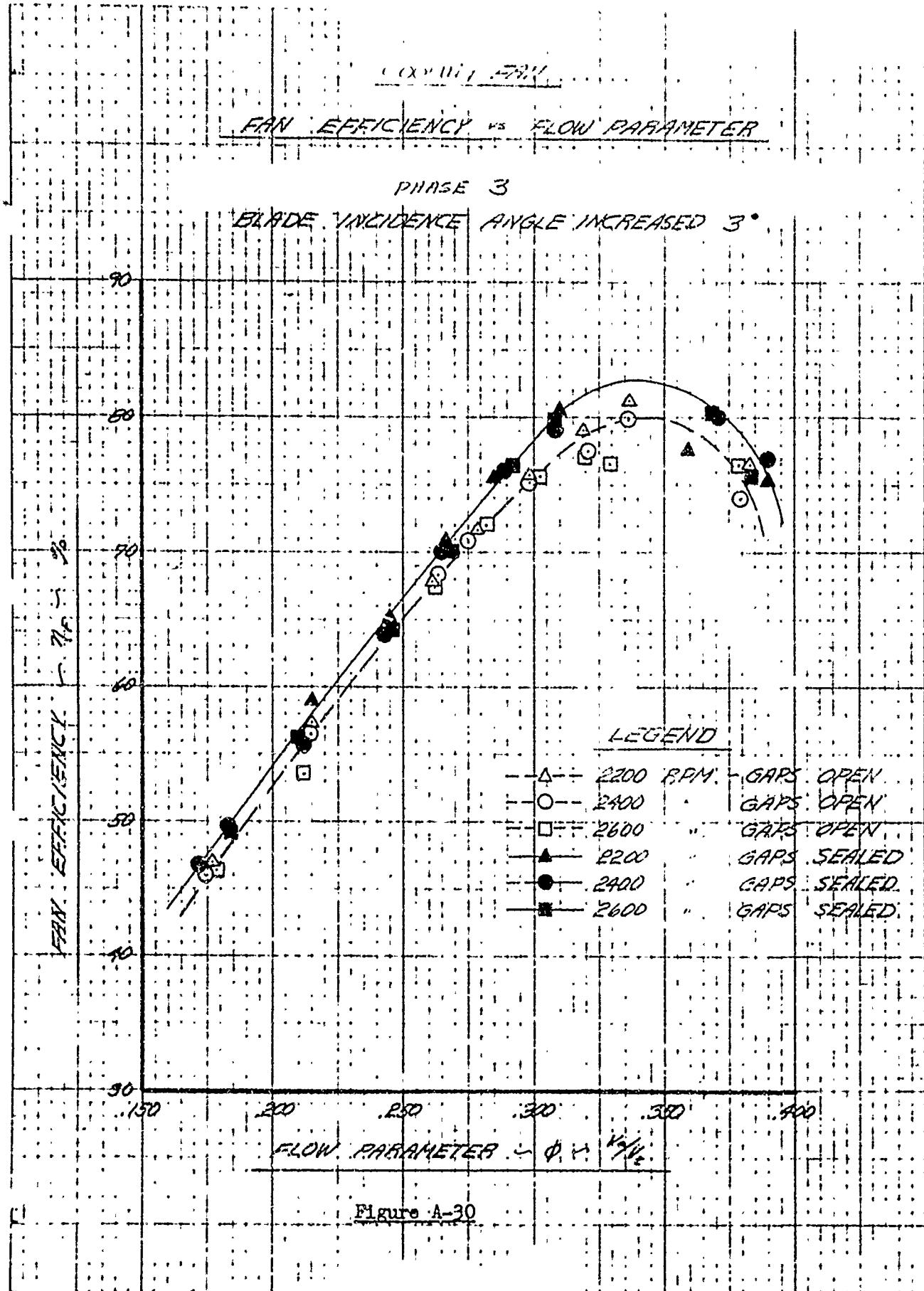












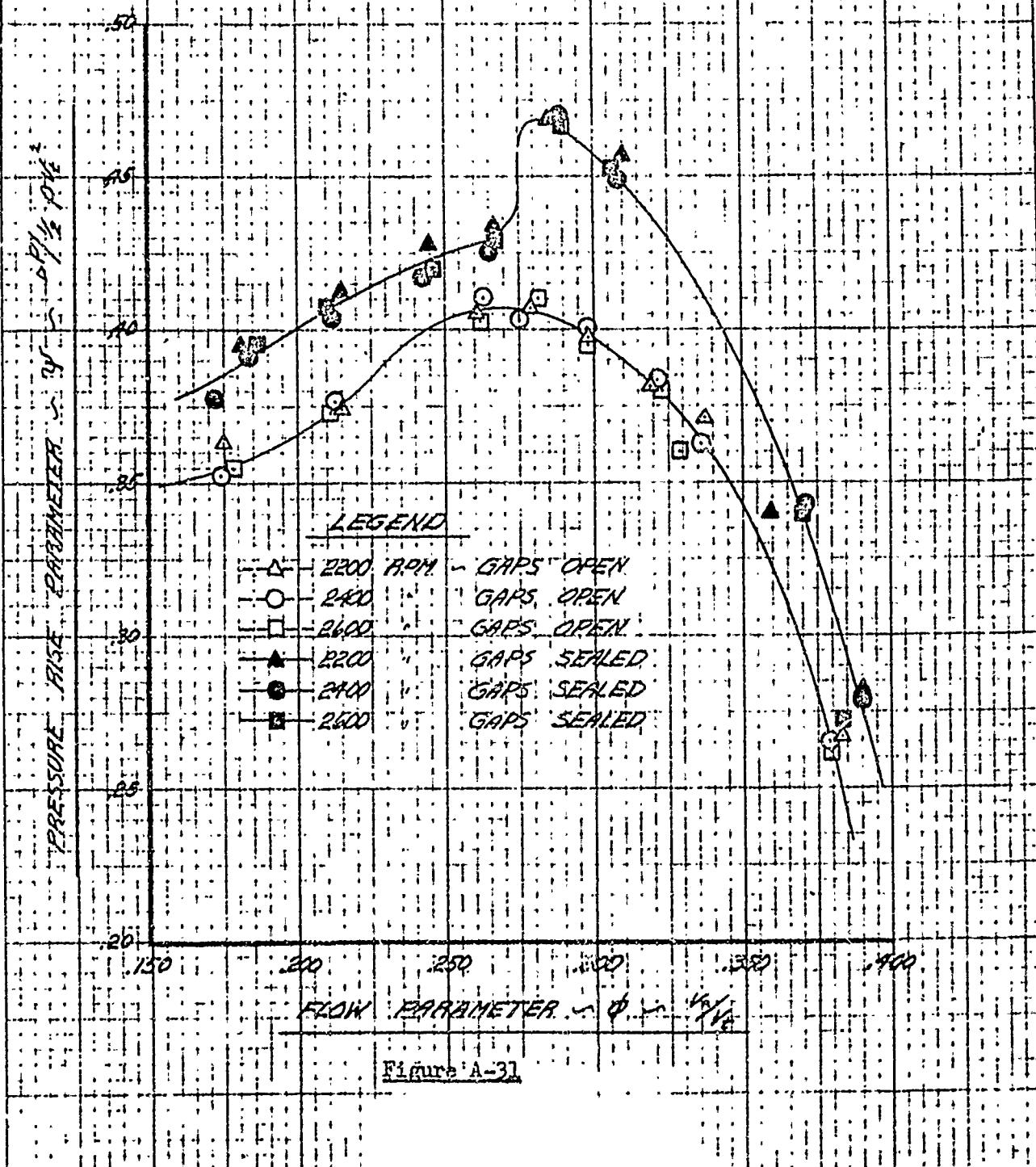
Page No.
Report No.
Model No.

CODING FAN

PRESSURE PARAMETER VS FLOW PARAMETER

PHASE 3

BLADE INCIDENCE ANGLE INCREASED 3°



BLADE NO.	TIP	ROOT
1	23°52'	34°18'
2	23°52'	34°18'
3	23°52'	34°18'
4	23°52'	34°18'
5	23°52'	34°18'
6	23°52'	34°18'
7	23°52'	34°18'
8	23°52'	34°56'
9	23°52'	34°18'
10	23°52'	34°18'
11	23°52'	34°18'
12	23°52'	34°55'
13	22°24'	34°37'
14	23°09'	34°37'
15	23°52'	34°37'
16	23°52'	34°37'
17	23°52'	34°37'
18	23°52'	34°18'
19	23°09'	34°18'
20	23°52'	34°37'
21	23°52'	33°59'
22	23°52'	34°18'
23	23°52'	34°18'
24	23°52'	34°18'
25	23°52'	34°18'
26	23°08'	34°18'
27	22°24'	34°18'
28	23°52'	34°18'
29	23°52'	34°18'
30	23°52'	34°18'
31	23°52'	34°18'
32	23°52'	34°18'

TABLE A-17
Measured Rotor Blade Angles for Fan Tested

Phase 3

APPENDIX I

ILLUSTRATIVE PROBLEM

A-5.0 List of References

<u>Reference No.</u>	<u>Description</u>
A-1	Military Specification, Cooling Requirements of Power Plant Installations, Specification Number MIL-C-8678 (Aer).
A-2	Vertol Aircraft Corporation Report 42-T-32, H-21B (or C) Forward Rotor Transmission Development Test, January 11, 1954.
A-3	Vertol Aircraft Corporation Report 42-T-33, H-21B (or C) Central Transmission Development Test, January 11, 1954.
A-4	Herrig, L. Joseph; Emery, James C. and Erwin, John R.: Systematic Two-Dimensional Cascade Tests of NACA 65 - Series Compressor Blades at Low Speeds, NACA RM L51G31, 1951
A-5	SAE Aeronautical Information Report No. 2, Airplane Heating and Ventilating Equipment Engineering Data, January 1943.
A-6	Curtiss-Wright Corporation, Wright Aeronautical Division, Woodridge, New Jersey, Wright Cyclone Engine R1300-1, -2 and -3 Models Installation Features and Data AED-6F, December 1951.
A-7	Harrison Radiator Division, General Motors Corporation, Lockport, N. Y., Curve AV747 for AP28AU18-01 Oil Cooler.
A-8	Harrison Radiator Division, General Motors Corporation, Lockport, N. Y., Curve AV860.
A-9	Harrison Radiator Division, General Motors Corporation, Lockport, N. Y., Unnumbered Curve, dated 3-9-55.

A-6.0 List of Symbols

<u>Symbols</u>		<u>Subscripts</u>
σ'	Air Density Relative to Standard Sea Level Density	s _l Sea Level
T	Temperature	o Outer Required
P	Pressure	OIL Oil
ΔP	Pressure Drop	REL Released
W	Weight Flow Rate	ax Axial
w	Specific Weight	i Inner Ideal, Inlet
H	Heat Rejection Rate	STATOR Stator
ΔT	Temperature Difference	fan Fan
ITD	Inlet Temperature Difference Between Air and Oil	F Fan
OAT	Outside (Ambient) Air Temperature	d Drag
β	Air Inlet Angle Relative to Blade Section	2 Exit
ω	Rotational Velocity, Radians Per Second	i _{design} ideal (design)
Q	Volumetric Flow Rate	fan root Fan Root
v	Velocity, Feet Per Second	s Stator
D	Diameter	STATOR ROOT Stator Root
θ	Air Turning Angle	FAN TIP Fan Tip
σ'	Solidity	PRO Profile
r	Radius	a Axial
α	Angle of Attack of Blade	m Mean
ϕ	Flow Parameter Incidence Angle of Blade	u Tangential
q	Velocity Head	r
η	Efficiency	T.C. Tip Clearance
X	Blade Station	d _r drag (rotor)
		R rotor

A-6.0 List of Symbols (Continued)

<u>Symbols</u>	<u>Subscripts</u>
Y Blade Ordinate	REQ Required
ρ Air Density	f Fan
K Loss Factor	Sfwd Upstream Static
ψ Pressure Parameter	Tgage Total Gage
	T _{down-stream} Total Downstream
	Corr. Corrected

APPENDIX II

BIBLIOGRAPHY

BIBLIOGRAPHY

B-1 Fans

Venturi Calibration, Rpt. #229-100, Dean & Benson Research, Inc.

Hup-4 Fan Calibration WAD R-1300-3 Engine, Rpt. #22-101, Dean & Benson Research, Inc.

Aerodynamic Design of Axial-Flow Compressors, Volume III, NACA RM E56B03b - August 1, 1956.

Some Effects of Compressibility on the Flow through Fans and Turbines, NACA R-842, W. Perl - 1946.

A General Representation for Axial-Flow Fans and Turbines, NACA R-814, W. Perl - 1945.

Influence of Wall Boundary Layer upon the Performance of an Axial-Flow Fan Rotor, Emanuel Boxer, NACA TN 2291 - February 1951.

Charts of Pressure Rise Obtainable with Airfoil-Type Axial-Flow Cooling Fans, NACA TN 1199, A. Kahane - March 1947.

Effect of Annular Inlet Baffles on Rotating Stall, Blade Vibration and Performance of an Axial-Flow Compressor in a Turbojet Engine, NACA RM E55C25a, Donald F. Johnson, Andre J. Meyer, Jr. and Morgan P. Hanson - October 4, 1955.

Aerodynamic Design of Axial-Flow Compressors, Volume II, NACA RM E56B03a - August 1, 1956.

Blade Design Data for Axial-Flow Fans and Compressors, NACA WR L-635, Seymour M. Bogdonoff and Harriet E. Bogdonoff - July 1945.

Effect of Section Thickness and Trailing-Edge Radius on the Performance of NACA 65-Series Compressor Blades in Cascade at Low Speeds, NACA RM L51J16, L. Joseph Herrig, James C. Emery and John R. Erwin - December 13, 1951.

Cascade Theory and Design of Fan Straighteners, British Publication Index R&M-1885, A. R. Collar - January 1940.

Comparison of NACA 65-Series Compressor, Blade Pressure Distributions and Performance in a Rotor and in Cascade, NACA RM L51H20, Willard R. Westphal and William R. Godwin - November 16, 1951.

Axial-Flow Fan and Compressor Blade Design Data at 52.5° Stagger and Further Verification of Cascade Data by Rotor Tests, NACA TN 1271, Seymour M. Bogdonoff and Eugene F. Hess - April 1947.

Investigation of Performance of Single-Stage Axial-Flow Compressor Using NACA 5509-34 Blade Section, NACA RM E8F30, Harry Mankuta and Donald C. Guentert - September 1948.

BIBLIOGRAPHY (CONTINUED)

B-1 Fans (Continued)

Research on Air-Flow Engine Cooling Fan Drives, ASTIA AD-3839 - November 1952.

Research on Air-Flow Engine Cooling Fan Drives, ASTIA AD-3840 - 1 February 1953.

HUP-2 Helicopter Cooling Fan, Dean and Benson #114, Richard Portofee - November 1952.

Final Tech Report Research on Air-Flow Engine Cooling Fan Drives, ASTIA AD-33 250, University of Virginia - June 10, 1954.

Investigations of an Annular Diffuser-Fan Combination Handling Rotating Flow, NACA RM L9E28, Ira R. Swartz - April 1949.

Performance of Axial-Flow Fan and Compressor Blades Designed for High Loadings NACA TN 1201 Seymour M. Bogdonoff - February 1947.

Ducted Fans - A Nomogram of Analysis, British Publication Index W-47222, J. F. M. Scholes - February 1947.

Investigation of Performance of Typical Inlet Stage of Multi-stage Axial-Flow Compressor, NACA RM E9E13, Jack R. Burtt - July 18, 1949.

Theoretical Determination of Axial Fan Performance, NACA TM 1042, E. Struve - April 1943.

The Calculation of Axial Fans for Aircraft Power Units, British Publication Index GDC/10/13040-1, C. Cordes.

Theory and Design of Axial-Flow Fans or Compressors, USAF AF-TR-5155, F. L. Wattendorf - October, 1944.

Tests of a Single-Stage Axial Flow Fan, NACA R-729, E. B. Bell - 1942.

Investigation of Axial-Flow Fan and Compressor Rotors Designed for Three-Dimensional Flow, NACA TN 1652 - July 1948.

Aerodynamic Design of Axial-Flow Compressors, Volume 1, NACA RM E56B03 - August 1, 1956.

B-2 Cooling System

Power Plant Installation Cooling Study, Part IV - Discussion of Steady State Results, WADC-TR-55-114, R. W. Young - October 1954.

Power Plant Installation Cooling Study, Part I - Introduction WADC-TR-55-414, R. S. Leith and C. M. Robidart - September 1954.

B-2 Cooling System (Continued)

Power Plant Installation Cooling Study, Part V - Optimization of Design Study Installation, WADC-TR-55-414, R. S. Leith, R. W. Young - October 1954.

Power Plant Installation Cooling Study, Part I - Introduction, Part VII - Method of Engine ACC Cooling Analysis and Results, WADC-TR-55-414, R. S. Leith, C. M. Robidart - September 1954.

Power Plant Installation Cooling Study, Part VIII - Summary and Conclusions, WADC-TR-55-414, R. W. Young, R. S. Leith, C. M. Robidart - January 1955.

A Method for the Design of Cooling Systems for Aircraft Power Plant Installations, NACA WR L-491, Kennedy F. Rubert and George S. Knopf - March 1942.

Use of Consolidated Porous Medium for Measurement of Flow Rate and Viscosity of Gases @ Elevated Pressures and Temperatures, NACA TN 2783, Martin B. Bik and J. A. Putnam - September 1952.

High Altitude Cooling, IV - Intercoolers, NACA WR L-774, K. F. Rubert - September 1944.

High Altitude Cooling, I - Resume of the Cooling Problem, NACA WR L-771, Abe Silverstein - September 1944.

High Altitude Cooling, III - Radiators, NACA WR L-773, Jack N. Nielson - September 1944.

High Altitude Cooling, II - Air-Cooled Engines, NACA WR L-772, David T. Williams - September 1944.

Report of Advisory Comm. for Aircraft Equipment Cooling Systems, ASTIA AD-38673, R. O. Clock - 2 March 1953 to 17 April 1953.

Final Report on Exhaust Ejector Cooling Research, AD-52030-C-1 Report No. 1703, W. G. Evans - 19 August 1955.

Heat Transfer Fluids for Aircraft Equipment Cooling System, WADC-TR-54-66, by the Ohio State U. Research Foundation - February 1954.

Aspects of Internal-Flow-System Design for Helicopter Propulsive Units, NACA RM L54F29, John R. Henry - September 14, 1954.

B-3 Cooling Reciprocating Engines

High Altitude Cooling, II - Air Cooled Engines, NACA WR L-772, David T. Williams - September 1944.

The Aerodynamics of the Cooling of Aircraft Reciprocating Engines, Aeronautical Research Council Reports and Memoranda, R&M 2458, A. S. Hartshorn and L. F. Nicholson, London: Her Majesty's Stationery Office - 1956.

B-3 Cooling Reciprocating Engines (Continued)

Full Scale Tests of NACA Cowlings, NACA R-592, Theodore Theodorsen - 1937.

High Altitude Cooling, V - Cowling and Ducting, NACA WR L-775, S. Katzoff - September 1944.

Flight Investigation of the Cooling Characteristics of a Two-Row Radial Engine Installation, II - Cooling-Air Pressure Recovery and Pressure Distribution, NACA TN 1109, John E. Hill - July 1946.

Improved Baffle Designs for the Air Cooled Engine Cylinders, NACA WR L-767, Abe Silverstein - August 1943.

High Altitude Cooling, VI - Axial-Flow Fans and Cooling Power, NACA WR L-776, W. Mutterperl - September 1944.

A Method for Correlating the Cooling Data of Liquid-Cooled Engines and Its Application to the Allison V-3420-11 Engine, NACA WR L-782, George F. Kinghorn - May 1945.

High Altitude Cooling, I - Resume of the Cooling Problem, NACA WR L-771, Abe Silverstein - September 1944.

Flight Investigation of the Cooling Characteristics of a Two-Row Radial Engine Installation Cooling Correlation, NACA TN 1092, Barton E. Bell - July 1946.

An Investigation of Valve-Overlap Scavenging Over a Wide Range of Inlet and Exhaust Pressures, NACA TN 1475, John W. R. Creagh - November 1947.

Effect of Local Boiling and Air Entrainment on Temperatures of Liquid-Cooled Cylinders, NACA TN 1498, A. P. Colburn - March 1948.

Tests to Determine the Effect of Heat on the Pressure Drop through Radiator Tubes, NACA TN 1362, Louis W. Habel - July 1947.

Cylinder-Head Temperatures and Coolant Heat Rejection of a Multi-Cylinder, Liquid Cooled Engine of 1710 cu. in. Displacement, NACA TN 1606, John H. Povolny - June 1948.

Correlation of Single Cylinder Cooling Tests of a P&W R-2800-21 Engine Cylinder with Wind Tunnel Tests of a P&W R-2800-27 Engine, NACA WR E-127, Herman H. Ellerbrock, Jr. - December 1943 (ARR 3L14).

Correlation of Exhaust-Valve Temperatures with Engine Operating Conditions and Valve Design, NACA W E-48, M. A. Zipkin - October 1945 (ARRE 512G).

Correlation of the Characteristics of Single Cylinder and Flight Engines in Tests of High Performance Fuels in an Air Cooled Engine, I - Cooling Characteristics, NACA WR E-271, Robert W. Wilson - October 1945 (MR E5J04).

B-3 Cooling Reciprocating Engines (Continued)

Comparative Cooling of Cylinders of Non-Uniform Fin Width with Tight Fitting Baffles and with Baffles that Provide Constant Flow Path Areas, NACA WR E-85, Oscar W. Schey - April 1944 (ARR E4D21).

Analysis of Cooling Limitations and Effect of Engine Cooling Improvements on Level Flight Cruising Performance of a 4-Engine Heavy Bomber, WR E-275, NACA, Frank E. Marble - March 1946 (MR E6B07).

Cylinder Barrel Cooling with Bonded Preformed Copper Fins, NACA WR E-80, H. H. Foster - May 1941 (ACR).

Cylinder-Head Cooling by Means of a Shield in the Exhaust Passage, NACA WR E-34, H. D. Wilsted - June 1944 (RB E4F23).

Cylinder Temperatures of Two Liquid Cooled Aircraft Cylinders for Various Engine and Coolant Conditions, NACA WR E-146, Eugene J. Manganiello - October 1945 (ARR E5H13).

Effect in Flight of the Propeller Cuffs and Spinner on Pressure Recovery in Front of a Double-Row Radial Aircraft Engine in a Twin-Engine Airplane, NACA WR E-169, Carl Ellisman - March 1944 (MR).

Effect of NACA Injection Impeller and Ducted Head Baffles on Flight Cooling Performance of Double-Row Radial Engine in a 4-Engine Heavy Bomber, NACA WR E-256, Frank E. Marble - April 1945 (MR E5D13).

The Effect of Piston Head Temperature on Knock-Limited Power, NACA WR E-35, Harry S. Imming - July 1944 (ARR E4G13).

Effect of Several Methods of Increasing Knock-Limited Power on Cylinder Temperatures, NACA WR E-36, Harvey A. Cook - September 1944 (ARR E115).

Engine Tests of Pressurized Shunt-Type Cooling Systems for a Liquid Cooled Engine, NACA WR E-125, Eugene J. Manganiello - May 1945 (ARR E5E01).

Heat Transfer Processes in Liquid-Cooled Engine Cylinders, Correlation of Single Cylinder Engine Temperature Under Forced Convection Cooling Conditions, NACA WR E-131, Benjamin Pinkel - November 1945 (ARR E5J31).

Summary Report on the Induction of H_2O to the Inlet Air as a Means of Internal Cooling in Aircraft Engine Cylinders, NACA WR E-79, Addison M. Rotterock - August 1942 (ARR).

An Experimental Investigation of Rectangular Exhaust Gas Ejectors Applicable for Engine Cooling, NACA WR E-224, Eugene J. Manganiello - May 1944 (ARR E4E31).

Relation of Preignition and Knock to Allowable Engine Temperatures, NACA WR E-134, Arnold E. Brermann - July 1943 (ARR 3G14).

B-3 Cooling Reciprocating Engines (Continued)

Operating Temperatures of a Sodium-Cooled Exhaust Valve as Measured by a Thermocouple, NACA WR E-140, J. C. Sanders - December 1943 (ARR 3L06).

Study of the Mixture Distribution of a Double-Row Radial Aircraft Engine, NACA WR E-47, Frank E. Marble - October 1945 (ARR E5105).

Cooling Tests of an Airplane Equipped with NACA Cowling and Wing-Duct Cooling System, NACA TN 813, L. I. Turner - June 1941.

Cooling Tests of an Air Cooled Engine Cylinder with Copper Fins on the Barrel, NACA WR E-103, J. C. Sanders - July 1942 (ACR).

B-4 Cooling Turboshaft Engines

New Developments in Turbo Charging, SAE-PP-250-54, Rudolph Birmann - January 1954.

A Study of Turbine Engine Oil Cooling Problems in High Speed, High Altitude Aircraft, WADC-TR-55-172, George T. Papadopoulos - April 1955.

Influence of Refraction on the Applicability of the Zehnder-Mach Interferometer to Studies of Cooled Boundary Layers, NACA TN 2462, Martin R. Kinsler - September 1951.

Tables of Exact Laminar-Boundary-Layer Solutions when the Wall is Porous and Fluid Properties are Variable, NACA TN 2479, W. Byron Brown and Patrick L. Donoughe - September 1951.

Method for Calculation of Heat Transfer in Laminar Region of Air Flow Around Cylinders of Arbitrary Cross Section (Including Large Temperature Differences and Transpiration Cooling), NACA TN 2733, E. R. G. Eckert and John N. B. Livingood - June 1952.

Use of a Consolidated Porous Medium for Measurement of Flow Rate and Viscosity of Gases at Elevated Pressures and Temperatures, NACA TN 2783, Martin B. Biles and J. A. Putnam - September 1952.

Solutions of Laminar-Boundary-Layer Equations which Result in Specific-Weight-Flow Profiles Locally Exceeding Free-Stream Values, NACA TN 2800, W. Byron Brown and John N. B. Livingood - September 1952.

Radiant-Interchange Configuration Factors, NACA TN 2836, D. C. Hamilton and W. R. Morgan - December 1952.

Laminar Natural-Convection Flow and Heat Transfer of Fluids with and without Heat Sources in Channels with Constant Wall Temperatures, NACA TN 2863, Simon Ostrach - December 1952.

Comparison of Effectiveness of Convection-, Transpiration-, and Film-Cooling Methods with Air as Coolant, NACA TN 3010, E. R. G. Eckert and John N. B. Livingood - October 1953.

B-4 Cooling Turboshaft Engines (Continued)

Combined Natural - and Forced-Convection Laminar Flow and Heat Transfer of Fluids with and without Heat Sources in Channels with Linearly Varying Wall Temperatures, NACA TN 3141, Simon Ostrach - April 1954.

Method for Rapid Determination of Pressure Change for One-Dimensional Flow with Heat Transfer, Friction, Rotation, and Area Change, NACA TN 3150, James E. Hubbartt, Henry O. S lone and Vernon L. Arne - June 1954.

Exact Solutions of Laminar-Boundary-Layer Equations with Constant Property Values for Porous Wall with Variable Temperature, NACA TN 3151, Patrick L. Donoughe and John N. B. Livingood - September 1954.

Heat, Mass, and Momentum Transfer for Flow over a Flat Plate with Blowing or Suction, NACA TN 3208, H. S. Mickley, R. C. Ross, A. L. Squyers and W. E. Stewart - July 1954.

Methods for Rapid Graphical Evaluation of Cooled or Uncooled Turbojet and Turboprop Engine or Component Performance (Effects of Variable Specific Heat Included), NACA TN 3335, Jack B. Esgar and Robert R. Ziemer - January 1955.

Experiments on Turbulent Flow through Channels Having Porous Rough Surfaces with or without Air Injection, NACA TN 3339, E. R. G. Eckert, Anthony J. Diaguila and Patrick L. Donoughe - February 1955.

Experimental Investigation of Air-Flow Uniformity and Pressure Level on Wire Cloth for Transpiration-Cooling Applications, NACA TN 3652, Patrick L. Donoughe and Roy A. McKinnon - January 1956.

Method of Calculating Core Dimensions of Cross Flow Heat Exchanger with Prescribed Gas Flows and Inlet and Exit States, NACA TN 3655, E. R. G. Eckert and Anthony J. Diaguila - April 1956.

Selection of Optimum Configurations for Heat Exchanger with One Dominating Film Resistance, NACA TN 3713, E. R. G. Eckert and T. F. Irvine, Jr. - June 1956.

Analysis of Laminar Incompressible Flow in Semi-Porous Channels, NACA TN 3759, Patrick L. Conaughe - August 1956.

Preliminary Analysis of Problem of Determining Experimental Performance of Air Cooled Turbine, III - Methods for Determining Power and Efficiency, NACA RM E50E18, Herman H. Ellerbrock, Jr. and Robert R. Ziemer - August 1950.

An Experimental Cascade Study of the Effects of a Solidity Reduction on the Two-Dimensional Aerodynamic Characteristics of a Turbine-Rotor Blade Suitable for Air Cooling, NACA RM E52B27 Henry W. Plohr and William J. Nusbaum - May 1952.

B-4 Cooling Turboshaft Engines (Continued)

Investigations of Air Cooled Turbine Rotors for Turbojet Engines, III - Experimental Cooling-Air Impeller Performance and Turbine Rotor Temperatures in Modified J33 Split-Disk Rotor up to Speeds of 10,000 RPM, NACA RM E52C12, Alfred J. Nachtigall, Charles F. Zalabak and Robert R. Ziener - May 1952.

Effects of Turbine Cooling with Compressor Air Bleed on Gas-Turbine Engine Performance, NACA RM E54L20, Jack B. Esgar and Robert R. Ziener - March 1955.

Experimental Investigation of Effect of Cooling Air on Turbine Performance of Two Turbojet Engines, Modified for Air-Cooling, NACA RM E55J19, Gordon T. Smith, John C. Freche and Reeves P. Cochran - January 1956.

B-5 Ducts

The Design and Development of a Thrust Deflector for Use in Research Aircraft, ASTIA AD-72626, P. F. Aslwood - June 1955.

Design of Two-Dimensional Channels with Prescribed Velocity Distributions along the Channel Walls, II - Solution by Green's Function, NACA TN 2595, John D. Stanitz - January 1952.

Design of Two-Dimensional Channels with Prescribed Velocity Distribution along the Channel Walls, I - Relaxation Solution, NACA TN 2593, John D. Stanitz - January 1952.

Analysis of Laminar Forced Convection Heat Transfer in Entrance Region of Flat Rectangular Ducts, NACA TN 3331, E. M. Sparrow, January 1955.

Analysis of Errors Introduced by Several Methods of Weighing Non-Uniform Duct Flows, NACA TN 3400, DeMarquis, D. Wyatt - March 1955.

Wind Tunnel Investigation of Wind Ducts on a Single Engine Pursuit Airplane, NACA WR L-407, W. J. Nelson and K. R. Czarnecki - October 1943.

Pressure Loss In Ducts with Compound Elbows, NACA WR W-39, John R. Weske - February 1943.

Preliminary Investigation of a Submerged Air Scoop Utilizing Boundary-Layer Suction to Obtain Increased Pressure Recovery, NACA TN 3437, Mark R. Nichols and P. Kenneth Pierpont - April 1955.

An Investigation of Diffuser-Resistance Combinations, NACA WR L-329, Charles H. McLellan and Mark R. Nichols - February 1942.

Concerning the Flow on Ring-Shaped Cowlings, Part XIII - the Influence of a Projecting Hub, NACA TM 1361, D. Kuchemann - October 1953.

B-5 Ducts

An Experimental Investigation of the Design Variables for NACA Submerged Duct Entrances, NACA RM A7130, Emmet A. Mossman and Lauros M. Randall - January 8, 1948.

Curves for the Theoretical Skin Friction Loss in Air Intake Ducts, R.A.E. TN Aero 2035, A. B. P. Beeton - February 1950.

An Experimental Investigation of NACA Submerged Duct Entrance, NACA ACR-5120 (Also as) WR W-108A, Charles W. Frick, Wallace F. Davis Lauros M. Randall and Emmet A. Mossman - October 1945.

Essentials of Airplane Duct Design, Aero Digest 1944 - Charles A. Mobley.

Curves for the Theoretical Skin Friction Loss in Air Intake Ducts, British Publication Index, Note Aero 2035, A. Beeton - February 1950.

Design of a Right Angle Bend with Constant Velocities at the Walls, NACA N-21740, British Publication Index, A. S. Thom and W. J. Duncan - 5 February 1952.

Air Admixture to Exhaust Jets, NACA TM 1357, E. Sanger - July 1953.

Experimental and Analytical Investigation of Secondary Flows in Ducts, IAS IAP-PP-593-56, Howard Z. Herzig and Arthur C. Hansen - January 1956.

Suction Slot Ducting Design, British Publication Index, R&M-2580, A. G. Rawcliffe - April 1947.

Some Aerodynamic Properties of a New Type of Aerofoil with Reversed Flow through an Internal Duct, British Publications Index N-32663, D. Kuchemann - May 1954.

Mixing Lengths and Entrainment Ratios in Low-Velocity Jet Pumps, ASTIA AD-23268, J. E. Nowrey and Arnold Kivnick - September 30, 1953.

Detailed Final Report of Research on High Speed Rotary-Fixed Wing Aircraft, Vol. VII-Sample Aircraft Power Plant and Duct Analysis, AD-15012-C-1, McDonnell Aircraft Corp. - 20 December 1950.

Simplified Practice Recommendation - Pipes, Ducts, and Fittings for Warm Air Heating and Air Conditioning, AD-30000-C-1, National Bureau of Standards - 2 August 1954.

Some Gas Turbine Applications to Helicopter Propulsion, ASTIA AD-75982, W. R. Thompson, J. Brown, E. M. F. Burle.

A Survey and Test of Principles Suitable for Use in Design of Ice Detectors for Jet Engine Inlet Ducts, ASTIA AD-509-November 1952.

B-5 Ducts (Continued)

The Development of a Right Angle Turbine Exhaust Duct and Some Notes on the Effects of Size and Shapes on Performance, ASTIA AD-40292, I. H. Johnson and W. A. Abbott - April 1954.

The Effect on Jet Thrusts of Duct Bends Immediately Upstream of a Propelling Nozzle, ASTIA AD19515, P. J. Fletcher and G. W. Crosse - July 1953.

Summary of Metallic Flexible Duct Development Program, ASTIA AD-9915, Boeing Airplane Co., Doct. No. D13688 - 4 March 1953.

Notes on Quantity Requirements and Duct Losses in Practical Applications of Suction Wings, ATI-47-111-C-1, R. C. Pankhurst and R. Hills - 28 August 1947.

A Wind Tunnel Investigation of Entry Loss on Propeller Turbine Installations, ATI-47-107-C-1, J. Seddon and A. Spence - August 1948.

Thermodynamic Analysis of a Gas Flow through a Duct, ASTIA ATI-47-095-C-1, Kellett Aircraft Corp. - 2 July 1946.

Investigation to Determine Effects of Rectangular Vortex Generators on the Static Pressure Drop through a 90° Circular Elbow, NACA RM L53G08, Floyd E. Valentine and Martin R. Copp - 1953.

Aerodynamic Principles for the Design of Jet-Engine Induction Systems, NACA RM A55F16, Wallace F. Davis and Richard Schever - February 1956.

Measurement and Analysis of Turbulent Flow Containing Periodic Flow Fluctuations, NACA RM E53F19, William R. Mickelson and James C. Lawrence - August 1953.

Measurement of Heat-Transfer and Friction Coefficients for Flow of Air in Non-Circular Ducts at High Surface Temperatures, NACA RM E53J07, Warren H. Lowdermilk, Walter F. Weiland, Jr. and John N. B. Livingood - January 1954.

Preliminary Study of Stability of Flow from Two Ducts Discharging into a Common Duct, NACA TN 2417, Albert J. Berlin, D. Richard Messing and Paul B. Richards - July 1951.

Impingement of Droplets in 90° Elbows with Potential Flow, NACA TN 2999, Paul T. Hacker, Rinaldo J. Brun and Bemrose Boyd - September 1953.

Combined Effect of Damping Screens and Stream Convergence on Turbulence, NACA TN 2878, Maurice Tucker - January 1953.

Experimental Investigation of Moving Pressure Disturbances and Shock Waves and Correlation with One-Dimensional Unsteady Flow Theory, NACA TN 1903, Paul W. Huber, Cliff E. Fitton, Jr., and F. Delipino - July 1949.

B-5 Ducts (Continued)

Investigation of Turbulent Flow in a Two-Dimensional Channel, NACA TN 2123, J. Laufer - July 1950.

Principles of Moving Air through Ducts; Book - Flow and Fan, C. Harold Berry, Industrial Press - 1954.

B-6 Inlets

Air Intakes for Aircraft Gas Turbines, Journal R. Ae. S., J. Seddon - October 1952.

An Analysis of Turbojet-Engine-Inlet Matching, NACA TN 3012, De-Marquis D. Wyatt - September 1953.

Analysis of Factors Influencing the Stability Characteristics of Symmetrical Twin Intake Air Induction Systems, NACA TN 2049, Norman J. Martin and Curt A. Holzhauser - March 1950.

Methods and Graphs for the Evaluation of Air Induction Systems, NACA TN 2697, George B. Brajnikoff - April 1952.

Induction System Selection, IAS-PP-594-56, Harry Drell and Thomas A. Sedgwick - January 1956.

Some Internal Flow Characteristics of Several Axisymmetrical NACA i-Series Nose Air Inlets at Zero Flight Speed, NACA RM L54E19a, Carroll R. Bryan and Frank F. Fleming - July 15, 1954.

The Use of Suction to Prevent Shock-Induced Separation in a Nozzle, NACA RM L50K20, James R. Sterrett, Robert W. Dunning and Maurice J. Brevoort - January 1951.

Preliminary Investigation of the Flow in an Annular-Diffuser Tailpipe Combination with an Abrupt Area Expansion and Suction, Injection, and Vortex-Generator Flow Controls, NACA RM L53K30, John R. Henry and Stafford W. Wilbur - February 10, 1954.

An Investigation of Submerged Air Inlets on a 1/4 Scale Model of A Typical Fighter-Type Airplane, NACA RM 48A20, Noel K. Delany - June 2, 1948.

Investigation of Two Short Annular-Diffuser Configurations Utilizing Suction and Injection as a Means of Boundary-Layer Control, NACA RM L54K18, Stafford W. Wilbur and James T. Higginbotham.

Concerning the Flow about Ring-Shaped Cowlings, XII - Two New Classes of Circular Cowls, XIII - the Influence of a Projecting Hub, NACA TM 1360, 1361, Dietrich Kuchemann and Johanna Weber - October 1953.

Preliminary Investigation of a Submerged Air Scoop Utilizing Boundary-Layer Suction to Obtain Increased Pressure Recovery, NACA TN 3437, Mark R. Nichols and P. Kenneth Pierpont - April 1955.

B-6 Inlets (Continued)

Theoretical Performance Characteristics of Sharp-Lip Inlets at Subsonic Speeds, NACA TN 3004, Evan A. Fradenburgh and DeMarquis, D. Wyatt - September 1953.

A Design Study of L. E. Inlets for Unswept Wings, NACA TN 3126, Robert E. Dannenberg - March 1954.

Theoretical Investigation of Submerged Inlets @ Low Speeds, NACA TN 2323, Alvin H. Sacks and John R. Spreiter - August 1951.

Theoretical and Experimental Investigations of Additive Drag, NACA RM E51B13, Merwin Sibulkin - 1951.

Theory of Plane, Symmetrical Inlet Diffusers, NACA TM 1267, W. Brodel - April 1, 1950.

Wind Tunnel Investigation of Carburetor Air Scoops for the XTB2D-1 Airplane with Emphasis on Means for By-passing the Boundary Layer, NACA WR L-751, Mark R. Nichols - June 1944.

A Low Speed Investigation of a Fuselage Side Air Inlet for Use at Transonic Flight Speeds, NACA TN 2684, Mark R. Nichols and Edwin B. Goral - April 1952.

An Experimental Investigation at Low Speeds of the Effects of Lip Shapes on the Drag and Pressure Recovery of a Nose Inlet in a Body of Revolution, NACA TN 3170, James R. Blackaby and Earl C. Watson - April 1954.

The Effect of Screens in Wide Angle Diffusers, NACA Rpt. 949, Schubauer, G. B. & Spangenberg, W. G. - 1949.

An Experimental Investigation of the Design Variables for NACA Submerged Duct Entrances, NACA RM A7130, Emmet A. Mossman and Lauros M. Randall - January 8, 1948.

Investigations of an Annular-Diffuser-Fan Combination Handling Rotating Flow, NACA RM L9B28, Ira A. Schwartz - 1949.

Some Low Speed Characteristics of an Air Induction System Having Scoop Type Inlets with Provisions for Boundary Layer Control, NACA RM A51F15, Earl C. Watson - 1951.

Investigation of Effects of Inlet-Air Velocity Distortion on Performance of Turbojet Engines, NACA RM E50G11, William E. Conrad and Adam E. Sobolewski - 1950.

Wind Tunnel Investigation of Air Inlet and Outlet Openings on a Streamline Body, NACA 1038 (Formerly ACR), John V. Becker - 1951.

Foreign Object Ingestion in Turbojet Engines, SAE-PP-702-56, H. E. Card and R. L. Mathias - January 9-13, 1956.

B-6 Inlets (Continued)

A Survey and Tests of Principles Suitable for Use in the Design of Ice Detectors for Jet Engine Inlet Ducts, ASTIA AD-509 - November 1952.

Ice Protection of Turbojet Engines by Inertia Separation of Water, III - Annular Submerged Inlets, *I Alternate - Duct System, #II - Single Offset Duct System, NACA RM E8A29, *E8A27 ~ May 1948, #E8A28 - June 1948, Vwe Von Glahn.

An Investigation of Aircraft Heaters, XXVII - Distribution of Heat Transfer Rate in the Entrance Section of a Circular Tube, NACA TN 1451, L. M. K. Boelter - July 1948.

Elimination of Rumble from the Cooling Ducts of a Single Engine Pursuit Place, NACA WR A-70, Howard F. Matthews - August 1943.

Foreign - Object Retention and Flow Characteristics of Retractable Engine - Inlet Screens, NACA RM E57A15, Fred W. Steffen and Lewis A. Rodert - July 1957.

B-7 Ejectors

Report of Progress on the Investigation of the Use of Hot Gas Ejectors for Boundary Layer Controls, ASTIA AD-55750, R. V. Deleo and S. E. Rislove - January, February 1955.

Investigation of the Use of Hot Gas Ejectors for Boundary Layer Removal, ASTIA AD-26518, University of Minnesota - 15 December 1953 to 15 February 1954.

Report of Progress on Free Jet and Ejector Studies, ASTIA AD-26378 to AD-26380, University of Minnesota - 15 December 1953 to 15 February 1954.

Report of Progress on the Investigation of the Use of Hot Gas Ejectors for Boundary Layer Control, ASTIA AD-40347, R. V. Deleo and R. D. Wood - 1 July to 1 August 1954.

Report of Progress on the Investigation of the Use of Hot Gas Ejectors for Boundary Layer Control, ASTIA AD-52055, R. V. Deleo, and R. D. Wood - 1 December 1954 to 1 January 1955.

Experimental Data for Four Full Scale Conical Cooling-Air Ejectors, NACA RM E54F02, C. C. Ciepluch and D. B. Fenn - November 1954.

An Experimental Investigation of Rectangular Exhaust Gas Ejectors Applicable for Engine Cooling, NACA WR E-224, Eugene J. Manganiello - May 1944.

Stack Ejectors for Marine Gas Turbine Installation, ASTIA AD-72559, A. L. London - July 1955.

The Design and Performance Calculation of Ejectors and Aspirators, WADC AF-TR-6673, Eugene M. Knoernschild - April 1951.

APPENDIX III

GENERAL TECHNICAL DATA

	Page
C-1 Equivalent Expressions of Measure	A - III - 2
C-2 Thermodynamics Information	A - III - 8
C-3 Greek Alphabet	A - III - 9
C-4 Temperature Conversion Chart, Fahrenheit-Centigrade	
a. - 40 to + 130 degrees Fahrenheit	A - III - 10
b. 0 to + 1900 degrees Fahrenheit	A - III - 11
C-5 Velocity - Velocity Pressure Conversion Chart	A - III - 12
C-6 Psychrometric Chart	A - III - 13

C-1 Equivalent Expressions of Measure

<u>Multiply</u>	<u>By</u>	<u>To Obtain</u>
Atmospheres	76.0	cms. of mercury.
"	29.92	inches of mercury.
"	33.90	feet of water.
"	10,333	kgs. per square meter.
"	14.70	pounds per sq. inch.
"	1.058	tons per sq. foot.
Bars	9.870×10^{-7}	atmospheres.
"	1	dynes per sq. cm.
"	0.01020	kgs. per square meter.
"	2.089×10^{-3}	pounds per sq. foot.
"	1.450×10^{-5}	pounds per sq. inch.
British thermal units	0.2520	kilogram-calories.
" " "	777.5	foot-pounds.
" " "	3.927×10^{-4}	horse-power-hours.
" " "	1054	joules.
" " "	107.5	kilogram-meters.
" " "	2.928×10^{-4}	kilowatt-hours.
B.t.u. per min.	12.96	foot-pounds per sec.
" " "	0.02356	horse-power.
" " "	0.01757	kilowatts.
" " "	17.57	watts.
B.t.u. per sq. ft. per min.	0.1220	watts per square inch.
Centimeters	0.3937	inches.
"	0.01	meters.
"	393.7	mils.
"	10	millimeters.
Centimeters of mercury	0.01316	atmospheres.
" " "	0.4461	feet of water.
" " "	136.0	kgs. per square meter.
" " "	27.85	pounds per sq. foot.
" " "	0.1934	pounds per sq. inch.
Centimeters per second	1.969	feet per minute.
" " "	0.03281	feet per second.
" " "	0.036	kilometers per hour.
" " "	0.6	meters per minute.
" " "	0.02237	miles per hour.
" " "	3.728×10^{-4}	miles per minute.
Cms. per sec. per sec.	0.03281	feet per sec. per sec.
" " " " "	0.036	kms. per hour per sec.
" " " " "	0.02237	miles per hour per sec.
Cubic centimeters	3.531×10^{-5}	cubic feet.
" "	6.102×10^{-2}	cubic inches.
" "	10^{-6}	cubic meters.
" "	1.308×10^{-5}	cubic yards.
" "	2.642×10^{-4}	gallons.
" "	10^{-3}	liters.
" "	2.113×10^{-3}	pints (liq.).
" "	1.057×10^{-3}	quarts (liq.).
Cubic feet	2.832×10^{-4}	cubic cms.
" "	1728	cubic inches.
" "	0.02832	cubic meters.
" "	0.03704	cubic yards.
" "	7.481	gallons

<u>Multiply</u>	<u>By</u>	<u>To Obtain</u>
Cubic feet	28.32	liters.
" "	59.84	pints (liq.).
" "	29.92	quarts (liq.).
Cubic feet per minute	472.0	cubic cms. per sec.
" " "	0.1247	gallons per sec.
" " "	0.4720	liters per second.
" " "	62.4	lbs. of water per min.
Cubic inches	16.39	cubic centimeters.
" "	5.787×10^{-4}	cubic feet.
" "	1.639×10^{-5}	cubic meters.
" "	2.143×10^{-5}	cubic yards.
" "	4.329×10^{-3}	gallons.
" "	1.639×10^{-2}	liters.
" "	0.03463	pints (liq.).
" "	0.01732	quarts (liq.)
Cubic meters	10 ⁶	cubic centimeters.
" "	35.31	cubic feet.
" "	61,023	cubic inches.
" "	1.308	cubic yards.
" "	264.2	gallons.
" "	103	liters.
" "	2113	pints (liq.).
" "	1057	quarts (liq.).
Degrees (angle)	60	minutes.
" "	0.01745	radians.
" "	3600	seconds.
Degrees per second	0.01745	radians per second.
" " "	0.1667	revolutions per min.
" " "	0.002778	revolutions per sec.
Dynes	1.020×10^{-3}	grams.
"	7.233×10^{-5}	poundals.
"	2.248×10^{-6}	pounds.
Dynes per square cm.	1	bars.
Ergs	9.486×10^{-11}	British thermal units.
"	1	dyne-centimeters.
"	7.376×10^{-8}	foot-pounds.
"	1.020×10^{-3}	gram-centimeters.
"	10^{-7}	joules.
"	2.390×10^{-11}	kilogram-calories.
"	1.020×10^{-8}	kilogram-meters.
Ergs per second	5.692×10^{-9}	B.t. units per minute.
" " "	4.426×10^{-6}	foot-pounds per min.
" " "	7.376×10^{-8}	foot-pounds per sec.
" " "	1.341×10^{-10}	horse-power.
" " "	1.434×10^{-9}	kg.-calories per min.
" " "	10^{-10}	kilowatts.
Feet	30.48	centimeters.
"	12	inches.
"	0.3048	meters.
"	.36	varas.
"	1/3	yards.
Feet of water	0.02950	atmospheres.
" " "	0.8826	inches of mercury.

<u>Multiply</u>	<u>By</u>	<u>To Obtain</u>
Feet of water	304.8	kgs. per square meter.
" " "	62.43	pounds per sq. ft.
" " "	0.4335	pounds per sq. inch.
Feet per minute	0.5080	centimeters per sec.
" " "	0.01667	feet per second.
" " "	0.01829	kilometers per hour.
" " "	0.3048	meters per minute.
" " "	0.01136	miles per hour.
Feet per second	30.48	centimeters per sec.
" " "	1.097	kilometers per hour.
" " "	0.5921	nautical miles.
" " "	18.29	meters per minute.
" " "	0.6818	miles per hour.
" " "	0.01136	miles per minute.
Feet per sec. per sec.	30.48	cms. per sec. per sec.
" " " " "	1.097	kms. per hr. per sec.
" " " " "	0.3048	meters per sec. per sec.
" " " " "	0.6818	miles per hr. per sec.
Foot-pounds	1.286×10^{-3}	British thermal units.
" "	1.356×10^7	ergs.
" "	5.050×10^{-7}	horse-power-hours.
" "	1.356	joules.
" "	3.241×10^{-4}	kilogram-calories.
" "	0.1383	kilogram-meters.
" "	3.766×10^{-7}	kilowatt-hours.
Foot-pounds per minute	1.286×10^{-3}	B.t. units per minute.
" " " "	0.01667	foot-pounds per sec.
" " " "	3.030×10^{-5}	horse-power.
" " " "	3.241×10^{-4}	kg.-calories per min.
" " " "	2.260×10^{-5}	kilowatts.
Foot-pounds per second	7.717×10^{-2}	B.t. units per minute
" " " "	1.818×10^{-3}	horse-power.
" " " "	1.945×10^{-2}	kg.-calories per min.
" " " "	1.356×10^{-3}	kilowatts.
Grams	980.7	dynes.
"	15.43	grains (troy).
"	10^{-8}	kilograms.
"	10^8	milligrams.
"	0.03527	ounces.
"	0.03215	ounces (troy).
"	0.07093	poundals.
"	2.205×10^{-3}	pounds.
Gram-calories	3.968×10^{-5}	British thermal units.
Gram-centimeters	9.302×10^{-5}	British thermal units.
" "	980.7	ergs.
" "	7.233×10^{-5}	foot-pounds.
" "	9.807×10^{-5}	joules.
" "	2.344×10^{-8}	kilogram-calories.
" "	10^{-5}	kilogram-meters.
Grams per cm.	5.600×10^{-8}	pounds per inch.
Grams per cu. cm.	62.43	pounds per cubic foot.
" " " "	0.03613	pounds per cubic inch.
" " " "	3.405×10^{-7}	pounds per mil-foot.

<u>Multiply</u>	<u>By</u>	<u>To Obtain</u>
Horse-power	42.44	B.t. units per min.
" "	33,000	foot-pounds per min.
" "	550	foot-pounds per sec.
" "	1.014	horse-power (metric).
" "	10.70	kg.-calories per min.
" "	0.7457	kilowatts.
" "	745.7	watts.
Horse-power (boiler)	33,520	B.t.u. per hour.
" " "	9,804	kilowatts.
Horse-power-hours	2547	British thermal units.
" " "	1.98×10^6	foot-pounds.
" " "	2.684×10^6	joules.
" " "	641.7	kilogram-calories.
" " "	2.737×10^5	kilogram-meters.
" " "	0.7457	kilowatt-hours.
Hours	60	minutes.
"	3600	seconds.
Inches	2.540	centimeters.
"	103	mils.
"	.03	varas.
Inches of mercury	0.03342	atmospheres.
" " "	1.133	feet of water.
" " "	345.3	kgs. per square meter.
" " "	70.73	pounds per square ft.
" " "	0.4912	pounds per square in.
Inches of water	0.002458	atmospheres.
" " "	0.07355	inches of mercury.
" " "	25.40	kgs. per square meter.
" " "	0.5781	ounces per square in.
" " "	5.204	pounds per square ft.
" " "	0.03613	pounds per square in.
Joules	9.486×10^{-4}	British thermal units.
"	107	ergs.
"	0.7376	foot-pounds.
"	2.390×10^{-4}	kilogram-calories.
"	0.1020	kilogram-meters.
"	2.778×10^{-4}	watt-hours.
Kilowatts	56.92	B.t. units per min.
"	4.425×10^4	foot-pounds per min.
"	737.6	foot-pounds per sec.
"	1.341	horse-power.
"	14,34	kg.-calories per min.
"	103	watts.
Kilowatt-hours	3415	British thermal units.
" "	2.655×10^6	foot-pounds.
" "	1.341	horse-power-hours.
" "	3.6×10^6	joules.
" "	860.5	kilogram-calories.
" "	3.671×10^5	kilogram-meters.
Knots	6080	feet.
"	1.853	kilometers.
"	1.152	miles.
"	2027	yards.

<u>Multiply</u>	<u>By</u>	<u>To Obtain</u>
Knots per hour	51.48	centimeters per sec.
" " "	1.689	feet per second.
" " "	1.853	kilometers per hour.
" " "	1.152	miles per hour.
Miles	1.609×10^5	centimeters.
"	5280	feet.
"	1.6093	kilometers.
"	1760	yards.
"	1900.8	varas
Miles per hour	44.70	centimeters per sec.
" " "	88	feet per minute.
" " "	1.467	feet per second.
" " "	1.6093	kilometers per hour.
" " "	0.8684	knots per hour.
" " "	26.82	meters per minute.
Miles per hour per sec.	44.70	cms. per sec. per sec.
" " " " "	1.467	feet per sec. per sec.
" " " " "	1.6093	kms. per hour per sec.
" " " " "	0.4470	M. per sec. per sec.
Miles per minute	2682	centimeters per sec.
" " "	88	feet per second.
" " "	1.6093	kilometers per min.
" " "	0.8684	knots per minute.
" " "	60	miles per hour.
Minutes (angle)	2.909×10^{-4}	radians.
" (")	60	seconds (angle).
Ounces	8	drams.
"	437.5	grains.
"	28.35	grams.
"	0.0625	pounds.
Ounces (fluid)	1.805	cubic inches.
" (")	0.02957	liters.
Ounces (troy)	480	grains (troy).
" (")	31.10	grams.
" (")	20	pennyweights (troy).
" (")	0.08333	pounds (troy).
Poundals	13,826	dynes.
"	14.10	grams.
"	0.03108	pounds.
Pounds	444,823	dynes.
"	7000	grains.
"	453.6	grams.
"	16	ounces.
"	32.17	poundals.
Pounds (troy)	0.8229	pounds (av.).
Pound-feet	1.356×10^7	centimeter-dynes.
" "	13.825	centimeter-grams.
" "	0.1383	meter-kilograms.
Pounds-feet squared	421.3	kgs.-cms. squared.
" " " "	144	pounds-ins. squared.
Pounds-inches squared	2.926	kgs.-cms. squared.
" " " "	6.945×10^{-3}	pounds-feet squared.
Pounds of water	0.01602	cubic feet.

<u>Multiply</u>	<u>By</u>	<u>To Obtain</u>
Pounds of water	27.68	cubic inches.
" " "	0.1198	gallons.
Pounds of wat. per min.	2.669×10^{-4}	cubic feet per sec.
Pounds per cubic foot	0.01602	grams per cubic cm.
" " " "	16.02	kgs. per cubic meter.
" " " "	5.787×10^{-4}	pounds per cubic inch.
" " " "	5.456×10^{-9}	pounds per mil foot.
Pounds per cubic inch	27.68	grams per cubic cm.
" " " "	2.768×10^4	kgs. per cubic meter.
" " " "	1728	pounds per cubic foot.
" " " "	9.425×10^{-6}	pounds per mil foot.
Pound per foot	1.488	kgs. per meter.
Pounds per inch	178.6	grams per cm.
Pounds per square foot	0.01602	feet of water.
" " " "	4.882	kgs. per square meter.
" " " "	6.944×10^{-3}	pounds per sq. inch.
Pounds per square inch	0.06804	atmospheres.
" " " "	2.307	feet of water.
" " " "	2.036	inches of mercury.
" " " "	703.1	kgs. per square meter.
" " " "	144	pounds per sq. foot.
Radians	57.30	degrees.
"	3438	minutes.
"	0.637	quadrants.
Radians per second	57.30	degrees per second.
" " "	0.1592	revolutions per sec.
" " "	9.549	revolutions per min.
Radians per sec. per sec.	573.0	revs. per min. per min.
" " " " "	9.549	revs. per min. per sec.
" " " " "	0.1592	revs. per sec. per sec.
Revolutions	360	degrees.
"	4	quadrants.
"	6.283	radians.
Revolutions per minute	6	degrees per second.
" " "	0.1047	radians per second.
" " "	0.01667	revolutions per sec.
Revs. per min. per min.	1.745×10^{-3}	rads. per sec. per sec.
" " " " "	0.01667	revs. per min. per sec.
" " " " "	2.778×10^{-4}	revs. per sec. per sec.
Revolutions per second	360	degrees per second.
" " "	6.283	radians per second.
" " "	60	revs. per minute.
Revs. per sec. per sec.	6.283	rads. per sec. per sec.
" " " " "	3600	revs. per min. per min.
" " " " "	60	revs. per min. per sec.
Seconds (angle)	4.848×10^{-6}	radians.
Square feet	2.296×10^{-5}	acres.
" "	929.0	square centimeters.
" "	144	square inches.
" "	0.09290	square meters.
" "	3.587×10^{-8}	square miles.
" "	.1296	square varas.
" "	1/9	square yards.

<u>Multiply</u>	<u>By</u>	<u>To Obtain</u>
Square inches	1.273×10^6	circular mils.
" "	6.452	square centimeters.
" "	6.944×10^{-3}	square feet.
" "	10^6	square mils.
" "	645.2	square millimeters.
Temp. (degs. C.) + 273	1	abs. temp. (degs. C.)
" (" ") + 17.8	1.8	temp. (degs. Fahr.)
Temp. (degs. F.) + 460	1	abs. temp. (degs. F.).
" (" ") - 32	5/9	temp. (degs. Cent.).

C-2 Thermodynamics Information

H = Heat from or to an outside reservoir (BTU/#)

U = Internal (molecular) energy (BTU/#)

H = Enthalpy = U + AP v (BTU/#)

where A = Heat equivalent of mechanical energy

$$(\frac{1}{778} \text{ BTU}/\text{ft} \cdot \text{lb.})$$

P = Static pressure (#/sq. ft.)

v = Specific volume (cu. ft./#)

J = Mechanical equivalent of heat = 778 ft. lb./BTU

S = Entropy = the measure of the degradation of energy available for work (BTU/deg/#)

For standard atmospheric air

c_p = 0.241 BTU/deg/# of air (specific heat at constant pressure)

c_v = 0.173 BTU/deg/# of air (specific heat at constant volume)

k = $\frac{c_p}{c_v}$ = 1.4 ratio of specific heats for air

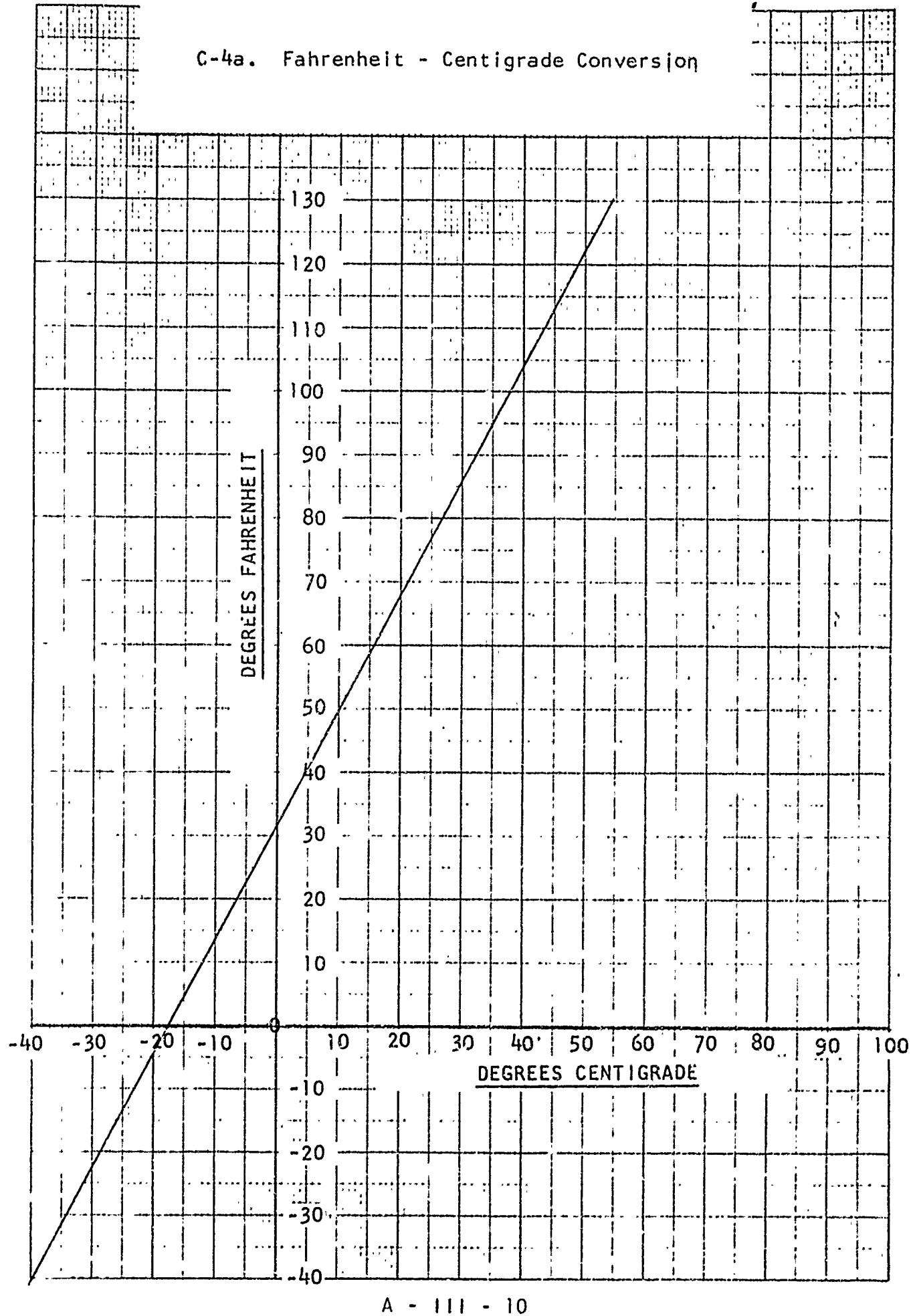
Adiabatic flow systems are those in which external work is performed on or by the fluid without heat transfer.

ISENTROPIC processes are those in which a change of state of the fluid occurs without fluid friction, heat transfer or turbulence. It thus represents an ideal "adiabatic" process. In an isentropic process, the entropy of the fluid remains constant.

C-3 Greek Alphabet

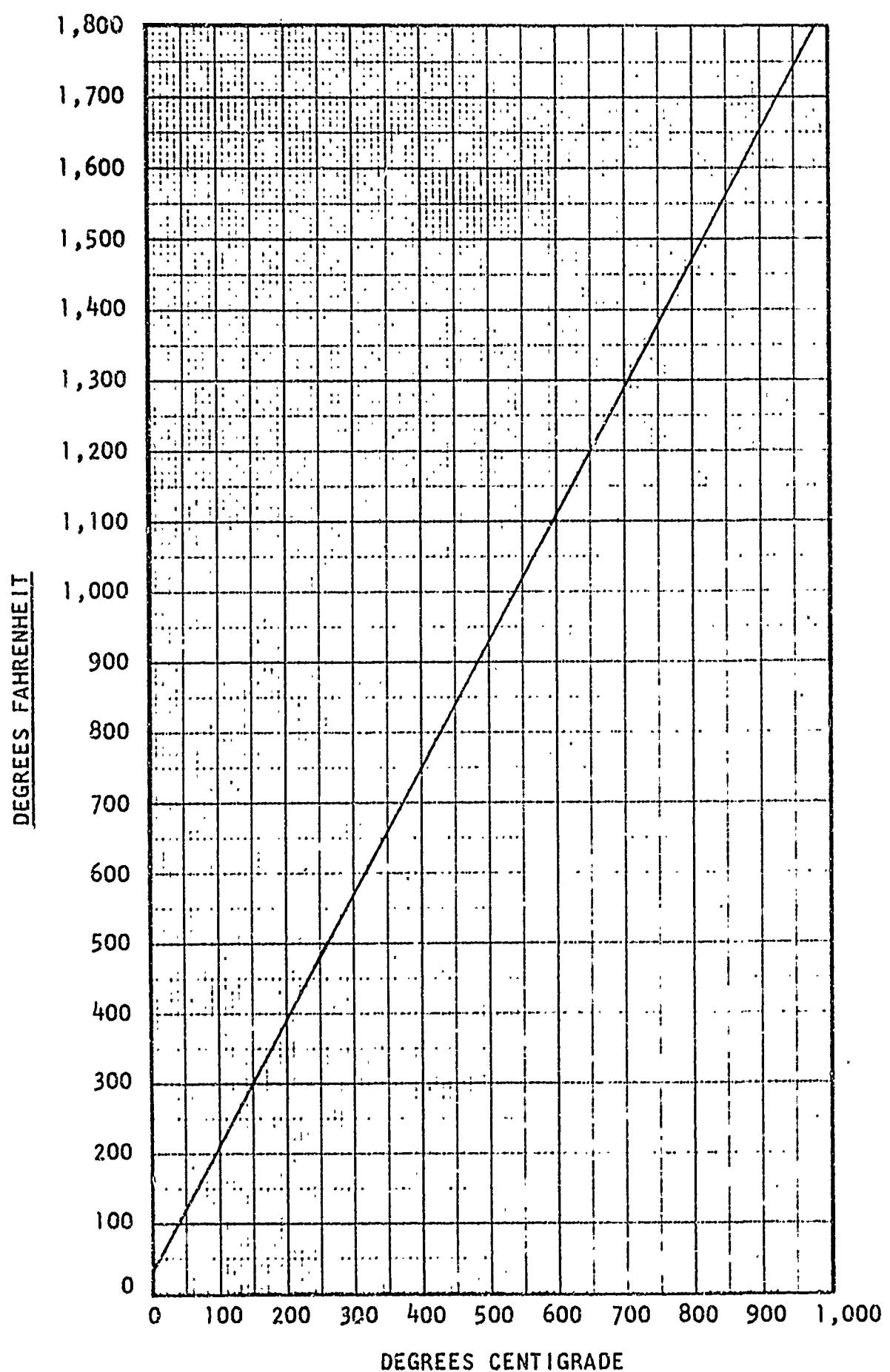
A	α	Alpha
B	β	Beta
Γ	γ	Gamma
Δ	δ	Delta
Ε	ε	Epsilon
Ζ	ζ	Zeta
Η	η	Eta
Θ	θ	Theta
Ι	ι	Iota
Κ	κ	Kappa
Λ	λ	Lambda
Μ	μ	Mu
Ν	ν	Nu
Ξ	ξ	Xi
Ο	ο	Omicron
Π	ϖ	Pi
Ρ	ρ	Rho
Σ	σ	Sigma
Τ	τ	Tau
Υ	υ	Upsilon
Φ	ψ	Phi
Χ	χ	Chi
Ψ	ψ	Psi
Ω	ω	Omega

C-4a. Fahrenheit - Centigrade Conversion

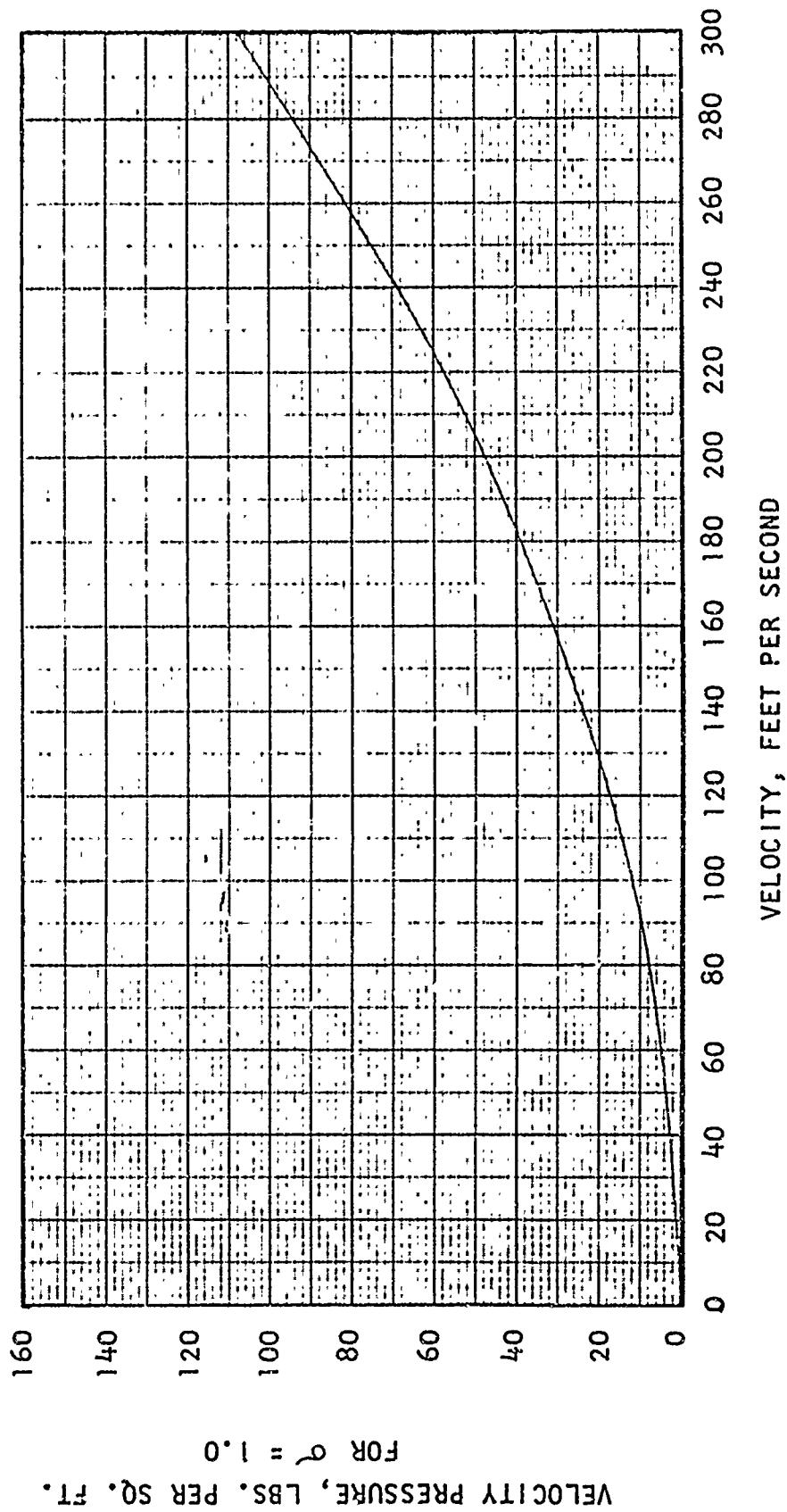


A - III - 10

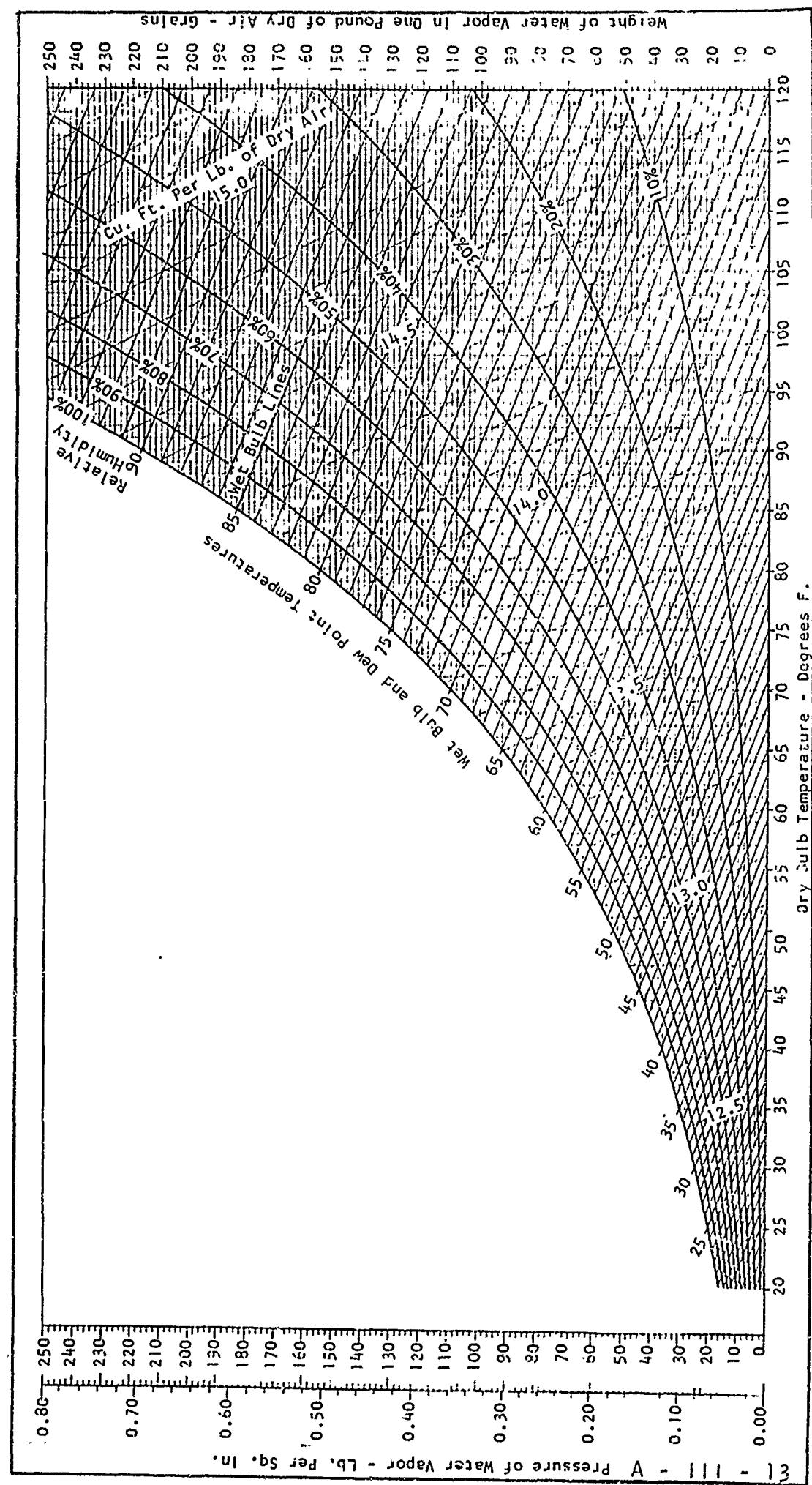
C-4b. Fahrenheit - Centigrade Conversion



C-5. Velocity-Velocity Pressure Conversion



C-6 PSYCHROMETRIC CHART



APPENDIX IV

	Page
D-1 Standard Symbols	A - IV - 2
D-2 Standard Subscripts	A - IV - 4

D-1 Symbols

A	Area Ft ²
A	Area of Surface Exposed to Airflow, Ft ²
A	Area in Plane Perpendicular to Heat Flow Path, Ft ²
A ₁ /A _T	Area Ratio
A ₂ /A ₁	Diffuser Ratio
α	Angle of Attack of Blades, Degrees
α	Diffuser Cone Angle
β	Angle of Velocity Vector from Axial Direction
β	Mixer Entrance Angle
B	Number of Blades
C	Coefficient
C	Blade Chord, Ft
C	Coefficient of Discharge
C _p	Specific Heat BTU/#/ ^o F
C _c	Correction Factor - "Streamline" Factor
D	Diameter, Ft
d	Diameter, Ft
d	Depth of Rectangular Duct, Ft
D	Drag - #
DV	Drag Power Ft#/Sec
e	Factor Representing the Efficiency of the Conversion in a Nozzle
f	Friction Factor
G	Weight Rate of Flow per Unit Area
H	Heat - BTU
H	Heat Absorbed - BTU/Min
H	Heat Transfer - BTU/Hr
h	Film Heat Transfer Coefficient BTU/Hr/Ft ² / ^o F
HP	Horsepower
ITD	Inlet Temperature Difference Between Air and Oil
K	Loss Factor - % of Velocity Head
k	Conductivity of Materials BTU/Hr/Ft ² / ^o F/Inch
k	Ratio of Specific Heats
L	Lift Force, Lbs.
L	Length of Mixing Chamber
L/D	Mixer Length Ratio
L/D ₁	Spacing Ratio
M	Mean Hydraulic Radius = <u>Cross Sectional Area</u> <u>Perimeter</u>
NRS	Normal Rated Speed - RPM
n	Speed - RPM
η	Efficiency

2θ	Included Angle Between Sides of Converging or Diverging Duct
θ	Temperature Correction, $T/518.40 R$
θ	Turning Angle of Air Passing Through Blade Row, Degs.
ϕ	Angle of Incidence of Blade, Degs.
ϕ	Ratio of Fan Axial Velocity to Tangential Velocity
P	Power Input - HP
P	Pressure - Absolute
ΔP	Pressure Loss
P_i/P_o	Primary Pressure Ratio
P_s/P_o	Secondary Pressure Ratio
ρ	Density - Slugs/Ft ³
$\Delta P/q$	Flow Loss Factor - K
Q	Flow - C.F.M.
q	Dynamic Pressure = $1/2 \rho v^2$
R	Gas Constant
R	Reynolds Number
R/D	Radius Ratio
R_i/R_o	Curve Ratio
R	Radius
RPM	Rotational Speed, Revolutions per Minute
S	Peripheral Spacing Between Blades, Ft
T	Thrust Force, Pounds
T	Absolute Temperature °R
t	Temperature °F
Δt	Temperature Difference °F
μ	Fluid Absolute Viscosity - #/Ft-Sec
V	Velocity - Ft/Sec
γ	Fluid Kinematic Viscosity - Ft ² /Sec
W	Weight - Lbs
W	Width of Duct
W	Weight Flow - #/Sec
W	Resultant Velocity Vector
ΔW	Incremental Decrease of Velocity
ω	Fan Rotational Speed, Rad/Sec
w	Density - #/Ft ³ (Specific Weight)
W/d	Aspect Ratio
W''/W'	Weight Flow Ratio
ωR	Fan Linear Velocity - Ft/Sec
X	Thickness of Body or Length of Flow Path, Inches
ψ	Fan Pressure Rise Coefficient
σ'	Solidity Ratio = $\frac{\text{Projected Solid Area}}{\text{Total Area}}$
σ	Density Ratio = $\frac{\text{Density of Air in Duct}}{\text{NACA Std. S.L. Air}}$
σ	Primary Nozzle Angle
δ	Pressure Correction, P/14.7 PSIA

D-2 Subscripts

1	Mixing Chamber
1	Flow
1	Exit - Primary Nozzle
1	Total - Secondary Flow at Entrance to Mixing Chamber
1	Entering Blade Row
2	Exit of Diffuser
2	Outlet
2	Velocity
2	Lift
2	Exit - Mixing Chamber
2	Leaving Blade Row
a	Axial Component
a	Barometric
a	Fan Inlet
a	Dry-Bulb
a	Atmos. Air
AX	Axial
c	Contraction
c	Corrected
c	Bellmouth Entrance
d	Drag
d	Duct
f	Skin-Friction Drag
f	Friction
g	Saturated Vapor
i	Induced
i	Total - Primary Flow
stator	Stator
i	Rotor
i	Inside
i	Inlet
l _o	Design Lift
m	Mean
n	Section Normal ~ Force
o	Fan Outlet
o	Required
o	Ambient
o	Outside
o	Oil
P	Pressure - Oil
PL	Power Loss
P	Pump
p	Partial Vapor

r	Resistance
REL	Actual
s	Specified
S	Static
S.L.	Sea Level
T	Throat of Primary Nozzle
t	Tangential Component
T	Total
V	Velocity
w	Wet-Bulb
x	Test
X	Inlet Air

Single Prime - Primary
Double Prime - Secondary

APPENDIX V

DESCRIPTION AND DEFINITION OF TERMS

(Reprinted from ASME Power Test Code
Reference 6-15, Chapter VI)

(With Standard Air Exception)

E-1.0 Definitions

The following definitions are used in the performance of the work outlined in the wind tunnel tests for fans, Chapter VI.

E-1.1 Fan - Includes all the structural features involved. The fan inlet and outlet shall be unobstructed. If the fan is provided with bearings, it shall be tested on its own shaft in its own bearings. If the contract performance guarantee contemplates that the fan will operate with inlet screens, guide vanes, inlet bearing supports, inlet boxes, diffuser, or dampers in either inlet or outlet, the test shall be made with these appurtenances in place.

E-1.2 Standard Air

Editor's Note: The following standard conditions are used in aircraft in accordance with NACA Report 218.

$$p_0 = 29.921 \text{ in. hg.}$$

$$t_0 = 59.00^\circ\text{F} (15.00^\circ\text{C})$$

$$\rho = 0.002378 \text{ slugs/cu. ft.}$$

$$w_0 = 0.07651 \text{ lbs./cu. ft.}$$

E-1.3 Throttling Device - Consists of a variable obstruction located at a designated point of a test setup to constitute a variable resistance equivalent to that of an external system.

E-1.4.0 The following definitions pertain to a selected setting of the throttling device.

E-1.4.1 Static pressure at a point is the pressure measured by a static connection of a pitot tube pointed upstream at that point.

E-1.4.2 Static pressure at a place of traverse is the arithmetic average of the static pressures at points in the plane of traverse.

APPENDIX V
DESCRIPTION AND DEFINITION OF TERMS
(Continued)

- E-1.4.3 Velocity pressure at a point is the pressure measured by the differential reading of a pitot tube pointed upstream at that point.
- E-1.4.4 Velocity pressure at a plane of traverse is the square of the average of the square roots of the velocity pressures at points in the plane of traverse.
- E-1.4.5 Total pressure at a plane of traverse is the algebraic sum of the velocity pressure at the plane of traverse and the static pressure at the plane of traverse.
- E-1.4.6 Discharge velocity pressure is the pressure corresponding to the calculated average velocity at the fan outlet at specified inlet air density and fan speed.
- E-1.4.7 Fan total pressure is the rise in total pressure between fan inlet and fan outlet at specified inlet air density and fan speed.
- E-1.4.8 Fan static pressure is the fan total pressure minus the discharge velocity pressure at specified inlet air density and fan speed.
- E-1.4.9 Capacity of a fan is the volume rate of flow of air at the fan's inlet at any air density and at specified fan speed.
- E-1.4.10 Power Input is the power supplied to the fan shaft at specified air density and fan speed.
- E-1.4.11 Total efficiency is the ratio of the power output of the fan, based on capacity and fan total pressure, to the shaft power input.
- E-1.4.12 Static efficiency is the ratio of the power output of the fan, based on capacity, and fan static pressure, to the shaft power input.
- E-1.4.13 A traverse is a series of ten or more readings made with a pitot tube or a static tube taken along the diameter of a duct at a selected location.
- E-1.5 Test Run - Pertains to all readings and calculations at any one setting of the throttling device.
- E-1.6 Fan Outlet Area - Determined from the inside dimensions of the fan outlet. The outlet area of a fan furnished with a diffuser is the area at the outlet of the diffuser.
- E-1.7 Fan Inlet Area - Determined from the inside dimensions of the fan inlet. For a fan with inlet boxes, the inlet area is that of the box openings.

APPENDIX V

DESCRIPTION AND DEFINITION OF TERMS
(Continued)

- E-1.8 Straightener Loss - This loss is the pressure drop across the straightener.
- E-1.9 Duct Friction Loss - This loss is the drop in pressure due to the resistance to airflow between points designated.

APPENDIX VI

PROPOSED ENGINE COOLING GROUND AND FLIGHT TEST PROGRAM

HX-XX HELICOPTER

<u>Table of Contents</u>	<u>Page</u>
References	A - VI - 1
I Introduction	A - VI - 2
II Equipment	A - VI - 2
A. Test Vehicle	A - VI - 3
B. Test instrumentation	A - VI - 3 to 6
III Description of Tests	A - VI - 6
A. Natural Frequency Test	A - VI - 6
B. Ground Cooling Tests	A - VI - 6
C. Flight Cooling Tests	A - VI - 6 & 7
IV Results	A - VI - 8
V Conclusions	A - VI - 8

References

- a. Contract No. XX-000.
- b. John Doe Aircraft Corp., Report No. YZ-X-01 dated 10-10-56, "Model Specification HX-XX Helicopter".
- c. MIL-C-8678 Aer Cooling Requirements of Power Plant Installation.
- d. MIL-D-17984 ASG Data Presentation Requirements, Installed Engine Performance and Air Induction Systems.

APPENDIX VI

I. Introduction

1. This report is submitted for review and approval by the Bureau of Aeronautics. It presents the HX-XX Flight Test Engine Cooling Program and natural frequency test in fulfillment of the requirements of the Reference (a) contract as detailed in the Reference (c) and (d) Specifications.
2. The flight portion of the program will be conducted on Aircraft Bu. No. 123456, at the Contractor's facilities. The helicopter shall be of standard configuration as defined by the Reference (b) Model Specification.
3. The primary purpose of the testing outlined herein is to prove the endurance and performance capabilities of the engine cooling fan and aircraft cooling system.
4. These tests will be performed under the cognizance of Project Engineer, Paul Doe, and his assistant, John Smith. Tests will be witnessed by representatives of the Kooler Radiator Co., Ltd., and the Fan Appliance Company.

II. Equipment

A. Test Vehicles

One model HX-XX Helicopter serial number Bu. No. 123456 will be used for these tests. The general description of the helicopter is as follows:

The HX-XX Helicopter is a twin rotor tandem-type, all metal cargo utility-type helicopter, powered by a Zebra R-41XXX single speed supercharged engine.

Normal rated HP at 2500 RPM	- 1000 BHP
Military rated HP at 2700 RPM	- 1200 BHP
Take-off HP at 2700 RPM	- 1200 BHP
Octane rating of Fuel	- MIL-F-5772 (Grade 100-130)
No. of Blades per Rotor	- 4
Rotor Diameter	- 40 ft.
Blade Chord	- 16"
Blade Taper	- None
Blade Twist	- 5°
Swept Disc Area	- 2500 sq. ft.
Design Gross Weight	- 12,000#
Most Fwd CG limit at Design GW	- 34" Fwd of $\frac{1}{2}$ between rotors
Most Aft CG limit at Design GW	- 2" Fwd of $\frac{1}{2}$ between rotors
Normal CG at Design GW	- 18-20" Fwd of $\frac{1}{2}$ between rotors

B. Test Instrumentation

The proposed instrumentation for conducting the flight and ground tests as required under the Contract No. XX-000 on the HX-XX Helicopter is as follows:

1. Equipment

Photo observer, recording oscillograph, and Brown recorder as shown in Figure 1, shall be used for recording all cooling data and will be phased together with run counters.

The engine and necessary temperatures as listed in Table I, will be measured by means of the Brown Automatic Temperature Recorder. The engine cooling air static pressure and total head pick-ups, as listed in Table II, will be measured by means of a manometer board and motion picture camera.

2. Instrumentation Calibration

- a. Airspeed Indicators - The airspeed indicators will be calibrated, using a water manometer as a standard. The position error calibration of the ship's service indicator will be determined, either by flight tests over a measured course, or by using a trailing pitot static bomb, if available.
- b. Altimeter - The sensitive altimeter reading up to 50,000 ft. will be calibrated using a mercury manometer as a standard. A correction will be included for barometric pressure and temperature. Installation will be checked using a trailing bomb, if available.
- c. Manifold Pressure Gage - The manifold pressure gage has a range of 10 to 100" Hg. and will be calibrated using a mercury manometer as a standard. A correction for barometric pressure and temperature will be included.
- d. Tachometer - The engine tachometer with range of 3500 revolutions per minute will be calibrated against a stroboscopic tachometer. Complete range of RPM will be covered.
- e. Temperature Gages - (C.A.T., O.A.T., Mixture, Wet Bulb) - The temperature gages reading from - 50°C to +50°C will be calibrated in kerosene, containing dry ice or a heating element using a glass thermometer as a standard.
- f. Cylinder Head Temperature Gage - Reading from 0 to 350°C will be calibrated using a calibrated potentiometer. ,

TABLE I
ENGINE COOLING - BROWN RECORDER LEGEND

<u>Item No.</u>	<u>Record No.</u>	<u>Thermocouple Reading</u>
1	1	#1 Cylinder Head Temperature
2	2	#2 Cylinder Head Temperature
3	3	#3 Cylinder Head Temperature
4	4	#4 Cylinder Head Temperature
5	5	#5 Cylinder Head Temperature
6	6	#6 Cylinder Head Temperature
7	7	#7 Cylinder Head Temperature
8	8	#8 Cylinder Head Temperature
9	9	#9 Cylinder Head Temperature
10	10	Exhaust Shroud Temperatures
11	11	Flexible Rubber Engine Mount
12	12	Magneto Temperature
13	1	#1 Cylinder Base Temperature
14	2	#2 Cylinder Base Temperature
15	3	#3 Cylinder Base Temperature
16	4	#4 Cylinder Base Temperature
17	5	#5 Cylinder Base Temperature
18	6	#6 Cylinder Base Temperature
19	7	#7 Cylinder Base Temperature
20	8	#8 Cylinder Base Temperature
21	9	#9 Cylinder Base Temperature
22	10	Engine Oil "Into" Engine
23	11	Engine Oil "Out" Engine
24	12	Engine Oil Cooler Oil "Out" Temperature
25	1	#1 Rear Spark Plug Elbow Temperature
26	2	#2 Rear Spark Plug Elbow Temperature
27	3	#3 Rear Spark Plug Elbow Temperature
28	4	#4 Rear Spark Plug Elbow Temperature
29	5	#5 Rear Spark Plug Elbow Temperature
30	6	#6 Rear Spark Plug Elbow Temperature
31	7	#7 Rear Spark Plug Elbow Temperature
32	8	#8 Rear Spark Plug Elbow Temperature
33	9	#9 Rear Spark Plug Elbow Temperature
34	10	Generator Temperature
35	11	Engine Exit Air Temperature
36	12	Carburetor Mixture Temperature
37	1	Fuel Temperature
38	2	Accessory Compartment Temperature
39	3	Accessory Compartment Temperature
40	4	At Air Exit Duct (Engine Compartment)
41	5	Fan Intake Air Temperature
42	6	Fan Exit Air Temperature
43	7	O.A.T.
44	8	Engine Oil Cooler "In" Temperature
45	9	Engine Oil Cooler Air "Out" Temperature
46	10	C.A.T.
47	11	2" Over Voltage Regulator
48	12	Ice Bath
49	1	Inverter Body

TABLE II
PRESSURE PICKUPS

<u>Item No.</u>	<u>Region</u>	<u>Pickups</u>	
		<u>Static</u>	<u>Total</u>
1	Plenum Chamber	1	-
2	Fan - Downstream of Stator	3	3
3	Oil Cooler-Pressure Drop Across	-	3 ea. side
4	Cylinder Baffles Upstream	-	3
5	Cylinder Baffles Downstream	-	3
6	Carburetor Deck	-	3
* 7	Carburetor	Metering Suction Differential (MSD)	

Performance instrumentation outlined in Table III will be located on the photo panel, and/or crew compartment, and will be photographed in phase with the pressure and temperature readings.

TABLE III
PERFORMANCE INSTRUMENTATION

<u>Unit No.</u>	<u>Instrument</u>
1	Airspeed
2	Altimeter
3	Clock
4	Run Counter
5	Attitude Gyro
6	Wet Bulb Temp.
7	Stop Watch
8	M.A.P. Gage
9	Tachometer
10	Yaw Angle Indicator
11	Rate of Pitch
12	Rate of Roll
13	Rate of Yaw
14	Intervalometer
* 15	Fuel Flow

*Require calibrated carburetor; either MSDP or fuel flow may be measured for determination of BSFC.

g. Carburetor - The carburetor to be used during cooling tests is to be calibrated for a complete range of RPM's and BHP's. Operating curves will be provided.

h. Fuel Flow - The fuel flow meter and pump will be calibrated from 100 to 1200 #/hr.

III. Description of Tests

A. Fan Natural Frequency Tests

A series of test conditions shall be investigated to determine the natural frequency of the fan.

1. Fan to be installed in Aircraft Bu. No. 123456 in accordance with production drawing requirements.
2. Perform a bang test to determine the natural frequency of the fan and fan blades. Such test shall be taken on at least two points on the periphery of the fan and fan blades. Two or more readings shall be recorded at each point and the average of all readings shall be used for determination of the natural frequency.
3. The excitations applied during these tests shall be those considered representative of service condition.

B. Ground Cooling Tests (MIL-C-8678)

1. Perform ground runs with rotors engaged at 60% normal rated RPM, rich mixture and with the helicopter pointed upwind, downwind and cross wind (most critical side for cooling). Continue each run until readings are stabilized. Conduct tests in flat pitch with controls neutral and wind speed between 12 - 18 knots.
2. Perform ground runs with rotors engaged at 60% normal rated RPM, rich mixture and with the helicopter pointed cross wind in as little wind as possible (most critical side for cooling). The aircraft is to be run for 10 minutes, then idled for 5 minutes followed by shut down. Shut down temperature shall be measured and recorded.

C. Flight Cooling Tests

1. Hovering out of ground effect at minimum allowable RPM and normal rated RPM with mixture normal and until temperatures stabilize.
2. Level forward flight at sea level while maintaining air speed for minimum power. To be conducted at minimum allowable RPM with mixture control in normal position and run continued until temperatures stabilize.
3. Level forward flight at sea level while maintaining normal rated power and RPM. Mixture control to be in normal position and run continued until temperatures stabilize.

4. Conduct a vertical climb (with zero forward airspeed) between minimum safe altitude and hovering ceiling maintaining normal rated power and RPM to critical altitude. If hover ceiling is above critical altitude, maintain full throttle power at normal rated RPM between critical altitude and hovering ceiling. (Mixture control in normal position.)
5. Repeat test B-2 on ground except, instead of shut down, conduct a climb to service ceiling starting at sea level and maintaining normal rated power and RPM to critical altitude and full throttle at normal rated RPM from critical altitude to service ceiling. To be conducted at airspeed for best rate of climb with mixture control in normal position.
6. Level forward flight at service ceiling developing power as required at normal rated RPM to maintain lowest possible airspeed (to assure maximum power, level flight conditions). Mixture control to be in normal position and run continued until temperatures stabilize.
7. Hover at hovering ceiling at normal rated RPM and normal gross weight with full throttle power available. Mixture control in normal position and run until temperatures stabilize.
8. Level forward flight at critical altitude for normal rated power. Maintain normal rated power at normal rated RPM with mixture control in normal position and run until temperatures stabilize.
9. Level forward flight at an intermediate altitude between critical and service ceiling. Maintain full throttle available power in the low air speed range and repeat at air speed for minimum power. (Conduct at minimum allowable RPM with mixture control in normal position.) Each run continued until temperatures stabilize.
10. The following additional engine cooling tests will be performed:
 - a. Determination of heat rise between free air temperature and carburetor entrance air temperature for the following sea level conditions: Hover, cruise and Vmax at sea level with normal rated RPM and normal mixture position. (Conduct with carburetor air control in "direct" and "alternate" positions.)
 - b. Determination of engine temperatures with variable mixture settings for following conditions: Hover, cruise and Vmax at normal rated RPM with carburetor air control in "direct" position. (Conducted with mixture control in "normal" and "rich" positions.)

IV. Results

A report of the test results will be prepared and submitted within 1 month following completion of testing.

V. Conclusions

It is estimated that approximately 3 hours of ground test operation, 14 hours of flying time and 3,000 engineering man hours will be required to perform this program. The estimated elapsed time to process this test program consists of the following:

1) Time to Instrument Aircraft	-	4 weeks
2) Ground Tests	-	2 weeks
3) Flight Tests	-	8 weeks
4) Data Reduction After Program	-	2 weeks
5) Completion of Test Report After Data is Available	-	<u>2 weeks</u>
Elapsed Time	-	18 weeks

PREPARED BY:

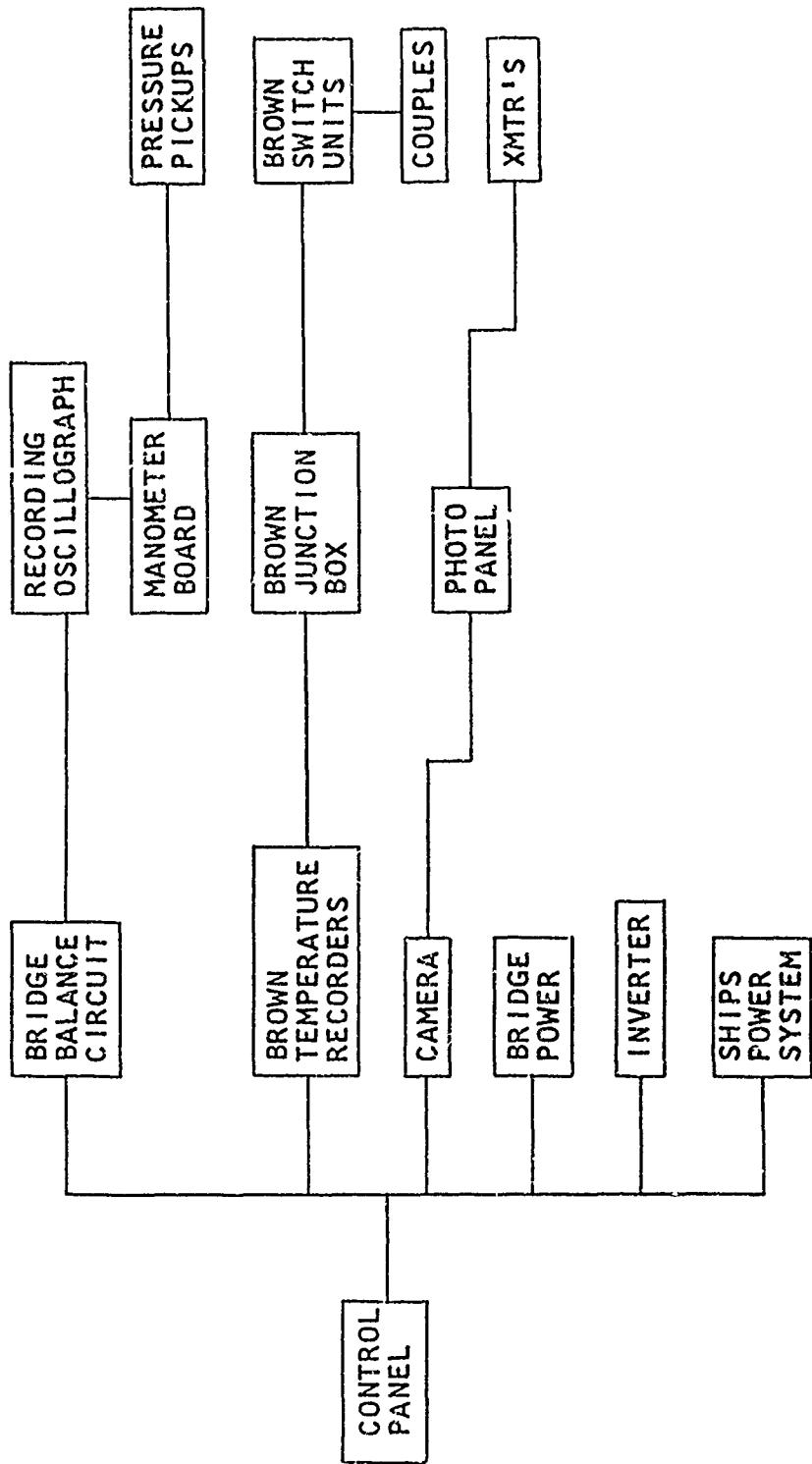
John Smith, Asst. Proj. Engr.
John Doe Aircraft Corp.

APPROVED BY:

Paul Doe, Proj. Engr.

FIGURE 1

BLOCK DIAGRAM - PROPOSED INSTRUMENTATION
FOR SHIP NO. BU 123456



INDEX

Accessory cooling	II-13, A-1-19
Aerodynamic theory	III-6
Air	II-4
Airflow	
pressure drop	I-8
pressure energy diagrams	I-5
quantity (rate)	I-8, II-3, -9
Air pump - also see "ejector" and "fan"	I-9, IV-5
parallel resistances	II-9
power	II-9
Air straighteners	VI-14
Alphabet, Greek	A-III-9
Area, duct	III-8, -9, -15
Axial flow fan - see "fan"	
Barometric pressure	VI-18
Bends, duct	III-19
Bernoulli's theorem	III-6
Bibliography	A-III-1
cooling reciprocating engines	A-III-4
cooling system	A-III-3
cooling turboshaft engines	A-III-7
ducts	A-III-9
ejectors	A-III-14
fans	A-III-2
inlets	A-III-12
Blade design	A-1-21, IV-19
Boundary layer	I-7, III-6
Branches, duct	III-23
British thermal unit	II-4
BSFC	VI-57
Butterfly valve	III-36
Camber	IV-21
Cascade data	IV-15, -25
Clearance loss, fan blade	IV-11

INDEX

Accessory cooling	II-13, A-1-19
Aerodynamic theory	III-6
Air	II-4
Airflow	
pressure drop	I-8
pressure energy diagrams	I-5
quantity (rate)	I-8, II-3, -9
Air pump - also see "ejector" and "fan"	I-9, IV-5
parallel resistances	II-9
power	II-9
Air straighteners	VI-14
Alphabet, Greek	A-III-9
Area, duct	III-8, -9, -15
Axial flow fan - see "fan"	
Barometric pressure	VI-18
Bends, duct	III-19
Bernoulli's theorem	III-6
Bibliography	A-III-1
cooling reciprocating engines	A-III-4
cooling system	A-III-3
cooling turboshaft engines	A-III-7
ducts	A-III-9
ejectors	A-III-14
fans	A-III-2
inlets	A-III-12
Blade design	A-1-21, IV-19
Boundary layer	I-7, III-6
Branches, duct	III-23
British thermal unit	II-4
BSFC	VI-57
Butterfly valve	III-36
Camber	IV-21
Cascade data	IV-15, -25
Clearance loss, fan blade	IV-11

INDEX

Coefficient	
contraction	III-27
discharge	III-27
power loss	III-17
pressure loss	III-40
resistance	III-27
velocity	III-27
Component tests	VI-5
Compound elbows	III-21
Conduction	II-5
Contractions, duct	III-18
Convection	II-5
forced	II-6
natural	II-5
Conversion factors	A-III-2
Cooler weight	II-9
Coolers	V-3
Cooling	
accessories	II-13, A-1-6, -19
airflow, common system	1-5, IV-5
airflow, separate systems	1-5, IV-5
blast	II-7
characteristics, engine	II-7
condition, critical	I-9, II-8, -9, -14
engine external	II-6, A-1-8
engine external, reciprocating	II-6, A-1-8
engine external, turbine	II-7
generators	II-13
oil	II-8, A-1-13, -15
power	II-9
program	A-VI-1
requirements	I-8, II-3, -7, -14, IV-5, A-1-6
system design procedure outline	1-8
Cross-sectional shape of ducts	III-9
Curve ratio, bends	III-19
Cylinder fin cooling	II-7, A-1-8
Cylinder head temperature	II-6, A-1-8
Damper	III-36
Definition of terms	A-V-1
Density	III-39, VI-19, -21
Diverging nozzle	III-25
Drag	
external	III-15
inlets and outlets	III-15
internal	III-15
internal flow system	III-16

INDEX

D	Drag (Continued)	
	momentum	III-15
	power	III-16
	profile	IV-11
	Duct	
↔	access panels	III-73
↔	aerodynamic performance test	VI-47
↔	area selection	III-9
↔	backfire pressure test	VI-50
	bends	III-19
	branches	III-23, -75
	cabin heating	III-73
	connections	III-73
	contractions	III-18
	abrupt	III-18
	conical	III-19
	streamlined	III-19
	cross-sectional shape selection	III-9
	design parameters	III-8, -71
	diffusers	III-24, -25
	ease of fabrication	III-80
	endurance test	VI-50
	exits	III-26
	flexibility	III-71
	flight test	VI-56
	ground test	VI-56
	handling	III-73
	inlets	III-8
	installation requirements	III-71
	losses	I-7, III-8
	materials	III-75
	metal	III-73
	model test	VI-46
	outlets	III-8
	removable	III-73
	rigidity	III-73
	shapes	III-8
	sizes	III-8
	space	III-8, -71
	strength	III-73
	structural test	VI-50
	support	III-71
	systems	I-10
	tests	VI-45
	transition shape selection	III-9
	ventilating	III-73
	weight	III-8, -71, -80

INDEX

Eddy losses	I-7
Efficiency, pump	III-16
Ejector	
aerodynamic performance test	VI-50
area ratio	IV-169
bench test	VI-53
cooling test	VI-59
cylindrical	IV-167
design	I-9, II-18, IV-163, -165
design chart	IV-170
design considerations	IV-175
design considerations, support	IV-175
design considerations, materials	IV-176
design considerations, service	IV-176
design parameters	IV-167
diffuser ratio	IV-169
flight test	VI-56
ground test	VI-56
installation test	VI-53
mixer length ratio	IV-169
molecular weight ratio	IV-170
nomenclature	IV-163
primary flow requirements	IV-167
primary nozzle	IV-170
reciprocating engine exhaust	IV-171
references	IV-177
secondary flow requirements	IV-167
temperature ratio	IV-170
test	I-9
theory	IV-167
turbine compressor bleed air	IV-175
turbine engine exhaust	IV-174
types	IV-165
Elbows	III-19
compound	III-21
end of duct	III-21
losses	III-20
Energy	
internal	II-3, -4
internal, kinetic	II-4
internal potential	II-4
losses	I-8
thermal	II-3
Engine	
accessories	I-9, II-7, A-1-6
cooling characteristics	II-7
cooling test	VI-56, A- VI-1
cylinder fin cooling	II-7, A-1-6, -8
cylinders	" I-8
detonation	II-6

INDEX

P	Engine (Continued)	II-6,-7
	external cooling	II-6,-7
	external temperatures	IV-20
	flywheel inertia requirements	I-8,II-6,-8
	oil	II-10,A-1-6,-13
	oil cooling	II-5,-6
	reciprocating	II-5,-6,-7
	turbine	I-7
	Equation, Bernoulli's	I-7
	Equation of flow continuity	I-7
	Equipment test	VI-58
	Equivalent diameter	III-38
	Equivalent expressions of measure	A-III-2
	Exit design	III-26
	Exits, flapped	I-7
	Expansion, abrupt	III-26
	Expansion losses	III-7
Fan	acceleration test	VI-37
	aerodynamic performance test	VI-8,A-1-34
	assembly	IV-153
	axial flow	IV-6
	aerodynamic theory	IV-7,-12
	design formulae	IV-8
	force diagrams	IV-8
	losses	IV-11
	speed	IV-15,VI-18
	velocity diagrams	IV-8
	axial velocity	IV-15
	balancing	IV-154,VI-5
	bang test	VI-7
	blades	IV-151
	blade airfoil layout	IV-25,A-1-29
	cowlings	IV-154
	design	I-9,II-7,IV-6,-13,-37, A-1-6,-20,-25
	considerations	IV-145
	physical considerations	IV-145
	diameters	IV-15
	diffuser design	IV-35
	disc	IV-151
	drawings	IV-145
	efficiency	IV-23,-27,A-1-27
	endurance testing	VI-37
	entrance design	IV-35
	fabrication processes	IV-146
	flight test	VI-56

INDEX

Fan (Continued)	V1-56
ground test	1-8
horsepower	IV-151
hub	VI-39
inertia testing	IV-22
intermediate spanwise stations	IV-146
materials	VI-7
natural frequency tests	IV-33
operation, off-design	IV-23, VI-16, -27, A-1-27
power required	IV-34
pre-rotation vanes	IV-145
procurement specifications	IV-32
rapid design	IV-32
fan diameters	IV-32
rpm	IV-32
references	IV-161
relief ports	IV-35
rotor assembly	IV-147
rotor blade chord	IV-19
blade design	A-1-21
blade spacing	IV-19
cascade	IV-19
inlet angle	IV-16
pressure rise	IV-17
turning angle	IV-16, -19
velocities	IV-17
shaker test	VI-7
sound test	VI-42
stator parameters	IV-20, A-1-22
test	I-9, IV-37, VI-5, -19, A-1-6
calculation guide	VI-30
report	VI-34
total pressure rise	IV-22, A-1-26
wheel assembly	IV-150
Film, stagnant	II-6
Flight test sample program	A-VI-1
Flow	
continuity equation	III-6
losses	III-7, -9, -37
capacity required	IV-5, -13
laminar	III-15, -37
measurement	III-34, VI-23
nozzle	III-29
orifice	III-27
pressure rise required	IV-5
rotation	III-9, IV-12
theory	III-16
process	II-4
visualization	VI-49
Flowing fluids	II-4
Fluid, compressible	II-4

INDEX

Fluid (Continued)	
in motion	II-4
Flywheel requirements	IV-20
Force diagram	IV-8
Friction factor (coefficient)	III-37, -39
losses	IV-8
Fuel air ratio	I-7, III-37, -38, -39, VI-24 VI-57
Gate valve	III-36
Generator cooling	II-13
Greek alphabet	A-III-9
Heat	
capacity	II-3, -4, -5
rejection	II-4
specific	II-3, -10
specific, water	II-4
transfer	II-4
transfer coefficient	II-6
Humidity	II-4, -6
Hydraulic radius	VI-18 III-38
Impulse and momentum equation	III-6
Induction air	II-7
Inlet temperature difference	II-8, -9, -10
Inlets	
abrupt	III-10
converging	III-11
curved expanding (ram)	III-12
drag	III-15
flush	III-15
losses	III-15
ram	III-16
re-entrant (open-end)	I-7, III-11, -12, -14
scoop	III-10
screens	III-15
straight expanding (ram)	III-13
theory	III-11
velocity	III-17, -18
Installation tests	III-16
Internal flow system	I-9, -11
Internal flow system theory	III-16 III-16

INDEX

Kinetic energy, rotational	IV-12
Laminar flow	III-15,-37
Latent heat of fusion	II-4
Latent heat of vaporization	II-4
Loss	
elbows	III-20
fan	IV-11,-13
fan, inner wall	IV-12
fan, rotational kinetic energy	IV-12
friction	III-27,-37,-38,-39
power	III-16
pressure	III-16,-40
straightener	VI-24
Manometer	VI-16
Materials, duct	III-75
Measure, equivalent expressions	A-III-2
Momentum drag	III-15
Momentum equation	III-6
Nozzle	
converging	III-30,-31
diverging	III-25,-29,-32
end of pipe	III-30
flow	III-29,-30
from plenum	III-26
reentrant	III-29
short pipe	III-29
Offset bends	III-21
Oil cooler pressure drop	II-9,V-3
Oil coolers	II-8,V-3
installation requirements	V-3
Oil cooler weight	II-9
Oil cooling	II-8,-9
engine	II-10,A-1-6,-13
transmission	II-10,A-1-6,-15
Oil temperature	II-8

INDEX

Orifice	111-26
end of pipe	111-30
sharp-edged	111-31
short pipe	111-31
from plenum	111-26
sharp-edged	111-26
smooth-edged	111-27
plates	111-34
Outlet	111-26
design	111-15
drag	111-16, -17
theory	
Pitot tube	VI-14
Power loss	111-16
coefficient	111-17
Power plant	11-5
Pressure	
drop, engine baffle	1-5
oil cooling	1-5
required	11-13, -14
energy increase	1-7
losses	11-3, 111-40
rise, fan rotor	IV-17
required	IV-13
static	1-7, VI-22
total	1-7, VI-25, -26
velocity	1-7, VI-22, -24, A-111-12
traverse	VI-22
Process	
flow	11-4
constant pressure	11-4
throttling	111-35
Profile drag loss	IV-11
Psychrometric chart	A-111-13
Pump - see "air pump"	
Radiation	11-5
Radius ratio, bends	111-19
Ram inlets	1-7, 111-11, -12, -14
recovery	111-14
Reentrant nozzle	111-29
References	1-9, -10, 11-19, 111-81, IV-161, -177, V-8, VI-62, A-1-66, A-111-1
Relief ports, fan	IV-35

INDEX

Requirements, cooling	I-8, II-3, IV-5, A-1-6, -8, -19
Reynolds' number	III-21, -37, -40
Rotation of flow	IV-12
Screens, inlet	III-13
Slots	III-29
Smoke test	VI-48
Solidity, fan blading	IV-8
fan rotor	IV-19
Specifications	I-9, -10, II-19, VI-67
fan procurement	IV-145
Specific heat - see "heat"	
Splitters	III-22
State, change of	II-4
Straighteners	VI-14
Symbols	I-11, II-20, III-83, IV-182, A-1-67, A-IV-1
Temperature	II-3, -4, VI-18
altitude	IV-14
conversion	A-III-10, -11
limits	II-3, -8
Terms, definition of	A-V-1
Testing components	I-10
ejector	I-9
fan	I-9
installation	I-9, -11
Test, sample program	A-VI-1
Thermodynamics information	A-III-8
Throttling device	III-35, VI-14
Tip clearance	IV-11
Transformation section	VI-14
Transitional shapes of ducts	III-9
Transmission	II-8
heat rejection	II-10
oil	I-8, II-8
oil cooling	II-10, A-1-15
Tuft tests	VI-48
Turning vanes	III-22
U-bends	III-21

INDEX

Valve	
butterfly	III-36
gate	III-36
Vanes	
pre-rotation	IV-34
turning	III-22
Vaporization, latent heat of	II-4
Velocity, inlet	III-16
Velocity vector diagram, fan	IV-8
Velocity-velocity pressure conversion	A-III-12
Venturi meter	III-34
Viscosity	III-37
Volumetric flow rate	VI-23
Wake	III-16, IV-8
Wall losses, fan	IV-12
Z-bends	III-21